A Potent and Selective Inhibitor of a Histone Demethylase

Katherine England

New College

DPhil

A Potent and Selective Inhibitor of a Histone Demethylase

Abstract

Katherine England, New College
DPhil Thesis, Hilary 2015

Post-translational modifications (PTMs) to histone proteins play important roles in the regulation of gene expression. Histone lysine demethylases (KDMs) remove methyl groups from N^{ε}-amino methylated lysine residues. There are two classes of human KDMs; the flavin adenosine dinucleotide-dependent demethylases (the KDM1 subfamily) and the 2-oxoglutarate- (2OG) dependent Jumonji C (JmjC) demethylases (KDM2–7). Misregulation and mutation of histone demethylases are associated with multiple human diseases including cancer. Hence potent and selective inhibitors are of interest for investigations into the biological roles of KDMs and their relevance as targets for drug discovery. JmjC KDM inhibitors have been reported in the literature but there are few subfamily selective examples. The aim of the work described in this thesis was to design and synthesise potent and subfamily selective inhibitors of human JmjC KDMs for use as chemical probes.

An aminomethyl pyridine-4-carboxylate series that was derived from a high throughput screening hit delivered a selective, submicromolar KDM2A inhibitor. X-ray crystallographic analyses demonstrated that the aminomethyl pyridine moiety bound the active site iron revealing a novel JmjC KDM inhibitor scaffold.

A known 2,2'-bipyridine-4-carboxylate scaffold was used as a starting point for the identification of a second, novel JmjC KDM inhibitor series that contains a triazolopyridine moiety as a replacement for the bipyridine system. The triazolopyridine core was shown to bind in the 2OG binding site of KDM4A by X-ray crystallography. Optimisation of the triazole substituent gave a selective inhibitor of KDM2A/7B that is significantly more potent (KDM2A IC_{50}: 58 nM, KDM7B IC_{50}: 150 nM) than reported KDM2/7 subfamily selective inhibitors. As for many other JmjC KDM inhibitors, this compound was not found to be efficacious in a cellular assay. A variety of strategies were pursued with the aim of improving the cellular efficacy. However, only a modest effect was observed in the cellular assay (less than 25% inhibition at 100 μM). A biotinylated analogue was immobilised onto streptavidin-coated beads for chemoproteomics experiments and was found to interact with KDM2A in cell lysate.

Overall, this work resulted in the identification of two new scaffolds for JmjC KDM inhibition and in a potent and selective inhibitor of KDM2A/7B.

Acknowledgements

Thanks to Chris and Paul for being great supervisors, and to Opher, Al, Chas and the SGC and its partners for all your help and support. Thanks to Jean-Philippe and Anne-Claude for welcoming me to your lab and all your input and help and to Al and Elizabeth for your hospitality.

Thanks to everyone I've worked with in the CRL and SGC — especially to Tony, Giuseppe, Susanne, Clarence, Stephanie, Aleks, Oleg, Tobias, Verónica, Akane, Duncan, Clarisse, Cyrille, Wendy, Adam, Anne, Martine, Gareth, Jake, Martin, Marina, Sander, Louise, Sarah, Joan, Richard, Rachel, George, Kat, Catherine, Catrine and Vita.

Thanks to everyone else who's encouraged and helped me academically and all my other lab colleagues and friends.

Thanks to my family for their encouragement and to my church family and especially my home group for your support and prayers. Huge thanks to my friends for being with me on this journey — especially Flip, Cyndi, Holly, Jess, Marnie, Priscilla and Elizabeth.

Contents

List of Experiments Done By Others

- The *in vitro* inhibitory activity of compounds was determined by Dr. Anthony Tumber, Dr. Giuseppe Scozzafava and Dr. Louise Walport using AlphaScreen or RapidFire assays.
- Crystallisation experiments and refinement of crystallographic data were carried out by Tobias Krojer.
- Preparative HPLC was performed by Katie Bainbridge.
- NOE experiments were carried out by Dr. Barbara Odell.
- Compounds **171, 176**, **177** and **180** were prepared by Verónica Gómez Pérez.
- Compounds **181**–**216** were prepared by Shanghai Chempartner Co.
- Chiral HPLC was performed by Alistair Farley.
- The cellular efficacy of compounds was determined by Dr. Clarence Yapp and Dr. Stephanie Hatch using an immunofluorescence assay.
- The membrane permeability of compounds **226**, **227** and **307** was assessed using a parallel artificial membrane permeation assay by Brian Linehan.
- Compounds **243**, **245**, **246** and **248**–**251** were prepared by Changchun Discovery Services.
- Protein expression and purification were carried out by Aleksandra Szykowska, Dr. Stanley Ng, Michelle Daniel and Dr. KaHing Che.
- Truncated Full-length FLAG-tagged *KDM2A* plasmid prepared by Dr. Claire Strain-Damerell.
- Full-length FLAG-tagged *KDM2A* plasmid prepared by Dr. Pavel Savitsky.

Abbreviations

2,4-PDCA	2,4-pyridinedicarboxylic acid
2OG	2-oxoglutarate
AD	Alzheimer's disease
ADD	ATRX–DNMT3–DNMT3L
AlphaScreen	amplified luminescent proximity homogeneous assay
app.	apparent
aq	aqueous
ARID	AT-rich interaction domain
ATRX	alpha-thalassemia and mental retardation X-linked syndrome
BLAST	basic local alignment search tool
Boc	*tert*-butyloxycarbonyl
BRCT	breast cancer-associated protein carboxy-terminal
BRD4	bromodomain containing 4
BSA	bovine serum albumin
Cas9	CRISPR associated protein 9
CCD	charge-coupled device
CES	carboxylesterase
*c*log*P*	calculated log*P*
cmpd	compound
cp*	pentamethylcyclopentadienyl
CpG	C-phosphate-G
CRISPR	clustered regularly interspaced short palindromic repeats
crRNA	CRISPR RNA
CTCL	cutaneous T-cell lymphoma
DIBAL	diisobutylaluminium hydride
DIPEA	*N*,*N*-diisopropylethylamine

DMF	*N*,*N*-dimethyl formamide
DMSO	dimethylsulfoxide
DNA	deoxyribonucleic acid
DNMT	DNA methyltransferase
DSBH	double-stranded β-helix
DTT	dithiothreitol
EDTA	ethylenediaminetetraacetic acid
ee	enantiomeric excess
EHMT	euchromatic histone-lysine *N*-methyltransferase
ES	electrospray
et al.	*et alia*
FAD	flavin adenine dinucleotide
FBXL	F-box and leucine-rich repeat
FDH	formaldehyde dehydrogenase
FIH	factor inhibiting HIF
FLAG	DYKDDDDK epitope
GASC1	gene amplified in squamous cell carcinoma 1
h	hour
HDAC	histone deacetylase
HEK-293	human embryonic kidney 293
HEPES	4-(2-hydroxyethyl)piperazine-1-ethanesulfonic acid
HIF	hypoxia-inducible factor
HL-60	human promyelocytic leukaemia
HPLC	high-performance liquid chromatography
HRP	horseradish peroxidase
HTS	high throughput screen
Hz	Hertz
IC_{50}	half maximal inhibitory concentration

ICM	internal coordinate modelling
IF	immunofluorescence
ING	inhibitor of growth
JARID	Jumonji/ARID domain-containing
JmjC	Jumonji C
JMJD	Jumonji domain-containing
KDM	histone lysine demethylase
KIAA1718	name assigned in the Kazusa human cDNA project to the protein subsequently named KDM7A
KOTMS	potassium trimethylsilanolate
LCMS	liquid chromatography–mass spectrometry
LDA	lithium diisopropylamide
LDS	lithium dodecyl sulfate
LipE	lipophilic ligand efficiency
lit.	literature
log*D*	distribution coefficient between *n*-octanol and water
log*P*	partition coefficient between *n*-octanol and water
LSD	lysine-specific demethylase
m/*z*	mass to charge ratio
MES	2-(*N*-morpholino)ethanesulfonic acid
min	minutes
mp	melting point
mRNA	messenger RNA
MS	mass spectrometry
MW	molecular weight
NCBI	National Center for Biotechnology Information
ND	not determined
NFκB	nuclear factor kappa-light-chain-enhancer of activated B cells

NHS	*N*-hydroxysuccinimide
NI	not isolated
NMR	nuclear magnetic resonance
NOE	nuclear Overhauser effect
NOG	*N*-oxalyl glycine
Np	naphthyl
NP-40	nonylphenyl polyethylene glycol
NSCLC	non-small cell lung carcinoma
NuA3	nucleosomal acetyltransferase of histone H3
NUT	nuclear protein in the testis
P65	65 kDa subunit of NFκB
PAMPA	parallel artificial membrane permeation assay
PBMC	peripheral blood mononuclear cells
PBS	phosphate-buffered saline
Pc2	polycomb 2 protein
P_e	effective permeability
PEG	polyethylene glycol
Pent	pentyl
PHD	plant homeodomain
PHD1–3	prolyl hydroxylase domain 1–3 isoforms
PHF	plant homeodomain-like finger
Pip	piperidine
pK_a	acid dissociation constant
PMSF	phenylmethylsulfonyl fluoride
ppm	parts per million
PSA	polar surface area
PTCL	peripheral T-cell lymphoma
PTM	post-translational modification

PTSA	para-toluenesulfonic acid
PWWP	Pro-Trp-Trp-Pro
quant.	quantitative
R&D	research and development
RA	rheumatoid arthritis
R_f	retention factor
RNA	ribonucleic acid
RNAi	RNA interference
SAR	structure–activity relationship
SEM	2-(trimethylsilyl)ethoxymethyl chloride
shRNA	short hairpin RNA
siRNA	short interfering RNA
S_N2	bimolecular nucleophilic substitution
STAB	sodium triacetoxyborohydride
$t_{1/2}$	half-life
T3P	1-propanephosphonic acid cyclic anhydride
TBAF	tetra-*n*-butylammonium fluoride
TBST	tris-buffered saline with 0.1% Tween-20
TET	ten–eleven translocation protein
TFA	trifluoroacetic acid
TFIID	transcription factor II D
TGS	target-guided synthesis
THF	tetrahydrofuran
TLC	thin layer chromatography
TMS	trimethylsilyl
TMSCCH	trimethylsilylacetylene
tosyl	toluenesulfonyl
TPSA	topological polar surface area

tR	retention time
Triton X-100	polyethylene glycol *tert*-octylphenyl ether
Ts	*para*-toluenesulfonyl
TTD	tandem tudor domain
Tween-20	polyethylene glycol sorbitan monolaurate
UTX	ubiquitously transcribed tetratricopeptide repeat, X chromosome
UTY	ubiquitously transcribed tetratricopeptide repeat, Y chromosome
UV	ultraviolet
v/v	volume to volume ratio
WD40	tryptophan and aspartic acid-containing
w/v	mass to volume ratio
w/w	mass to mass ratio
XLMR	X-linked mental retardation
Yng1	inhibitor of growth (ING) family member in yeast

Chapter 1. Introduction

1.1 Challenges in the Development of New Pharmaceuticals

The discovery and development of new drugs is extremely costly; worldwide pharmaceutical research and development (R&D) expenditure exceeded $60 billion in 2010.[1] Bringing drug candidates through the development process accounts for most pharmaceutical R&D expenditure; analysis of data from 13 leading pharmaceutical companies by Paul *et al.*[2] in 2010 showed that Phase II clinical trials accounted for 21% of pharmaceutical R&D expenditure (approximately $40 million per drug candidate in 2010) and Phase III trials accounted for 27% of expenditure (approximately $150 million per drug candidate in 2010). One of the key challenges the pharmaceutical industry faces is the selection of the best targets for drug discovery projects; the reason that most clinical candidates currently fail in Phase II or III trials is due to lack of efficacy (59% of Phase II trials in 2011–2012, and 52% of Phase III trials in 2011–2012 failed because of lack of efficacy, **Figure 1**).[3]

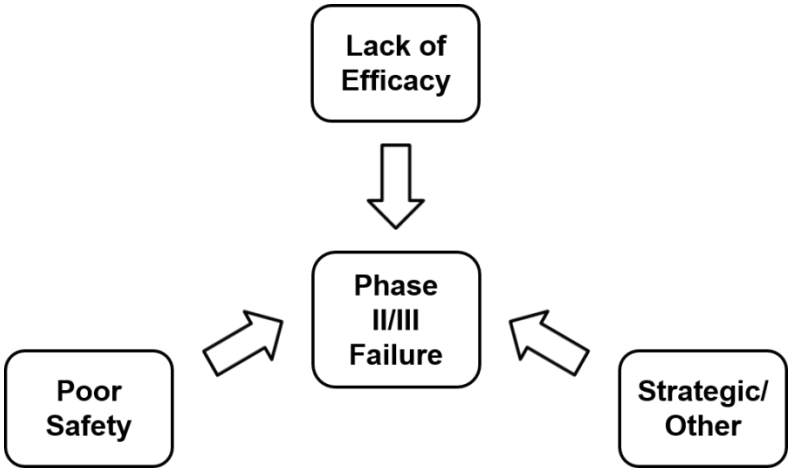

Figure 1 Main reasons for clinical candidates failing in Phase II or III trials.[3]

Reducing the number of compounds entering Phase II and III clinical trials that are not efficacious enough to gain approval as new drugs would result in a dramatic reduction of

unnecessary expenditure. The ultimate success of a pharmaceutical R&D programme rests on the choice of target, which is normally decided very early in the drug discovery process. Selecting targets that are more likely to lead to successful outcomes would significantly reduce the time and economic burden of pursuing unfruitful projects, freeing resources for investment in projects with a greater probability of success.

1.2 Validation of New Targets in Drug Discovery

Several tools are available to study the effect of inhibiting a target in a cellular or *in vivo* system and hence to determine the relevance of the target to disease; for example the gene itself can be silenced through knockdown or knockout studies or one domain of the protein can be inhibited by a small molecule and the biological effects assessed (**Figure 2**).[4, 5] Small molecules that are used as tool compounds for target validation are often referred to as chemical probes.[5] The involvement of a target in disease can also be demonstrated through human genetic association studies; genetic mutations may be associated with disease or have a protective effect.[1]

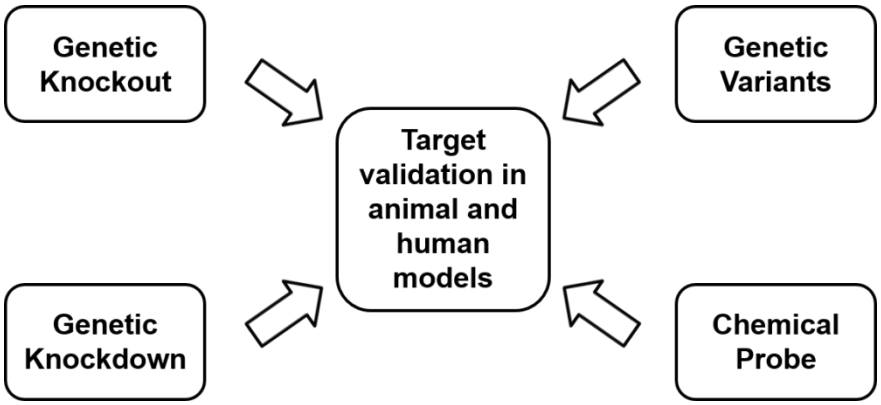

Figure 2 Genetic knockdown or knockout studies, clinically observed human genetic variation and engagement of targets with chemical probes are often used to validate target involvement in disease.[1, 4, 5]

In gene knockdown studies, ribonucleic acid interference (RNAi) technology is used to silence or reduce the expression of a particular gene; short hairpin RNA (shRNA) or short interfering RNA (siRNA) is used to degrade messenger RNA (mRNA) with a complementary nucleotide sequence thus preventing translation of the gene of interest,[4] or

clustered regularly interspaced short palindromic repeats (CRISPR) RNAs (crRNAs) can be used to target deoxyribonucleic acid (DNA) encoding the gene of interest and recruit the CRISPR associated protein 9 (Cas9) protein which degrades the gene.[6] Knockout mice may be generated from embryonic stem cells where the gene of interest has been either deleted or mutated to prevent or disrupt transcription.[7] However, if the gene of interest is important in development, genetic knockout may result in embryonic lethality, limiting its application.[8] Additionally, cells and organisms may adapt to the silencing of a particular gene by upregulating related genes or pathways.[9] Chemical probes provide a valuable and complementary method to genetic knockdown and knockout for target validation; instead of inhibiting the whole protein, small molecule inhibitors can be used to inhibit a selected domain of a multi-domain protein.[10] The degree of inhibition can be modulated by administering the probe for a limited time-frame and in a dose-dependent manner.[10] Small molecule probes and the structure activity relationship (SAR) generated in their discovery also serve as useful starting points for drug discovery programmes. The key properties needed for inhibitors to be useful as chemical probes are potency against the protein of interest, selectivity over other relevant proteins (for example within the same protein family) and cellular activity.[10, 11] Although the potency and selectivity required for a chemical probe will vary according to the nature of the target and its biological role, a consensus has developed in the literature that it is desirable for a probe to inhibit its target at < 100 nM in biochemical assays, at < 1 μM in cellular assays and to be greater than 30- to 100-fold selective over other relevant proteins (**Figure 3**).[5, 12] If new targets can be validated prior to commencing drug discovery programmes, resources could be focused on targets that would have a higher chance of delivering new drugs, increasing the likelihood of successfully bringing new drugs to market.[2]

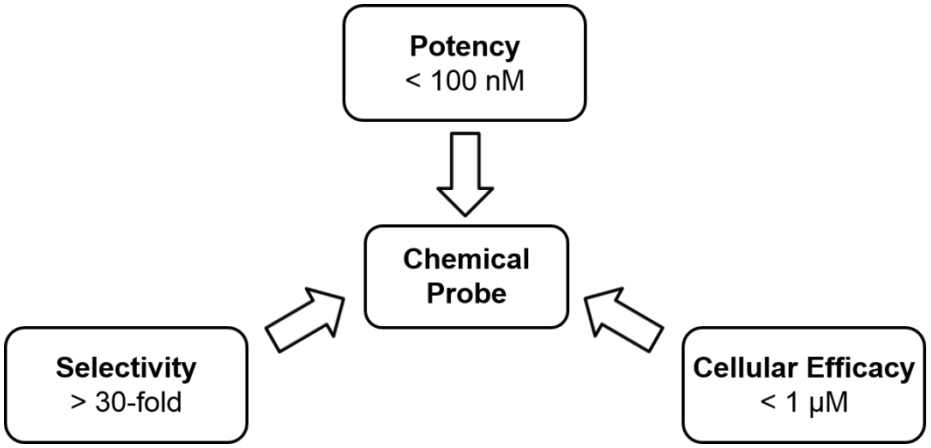

Figure 3 Typical chemical probe criteria.[5, 12]

1.3 Epigenetic Proteins as Drug Targets

The emerging field of epigenetics provides a potentially rich source of targets for drug discovery. Epigenetics (above or beyond genetics)[13, 14] is a broad term and refers to heritable changes in phenotype that are not a result of changes in the DNA sequence.[15] The main processes which are involved in epigenetics are post-translational modifications to histone proteins (see section 1.3.2), post-translational modifications to DNA (most commonly methylation),[16, 17] nucleosome remodelling[18] and gene regulation by non-coding RNAs.[19]

1.3.1 Chromosomal Structure

Chromosomes are comprised of a complex of DNA and histone proteins termed chromatin.[20] Although DNA itself contains the genetic information responsible for encoding proteins, post-translational modifications (PTMs) to DNA and to the histone proteins that DNA wraps around play an important role in the regulation of gene expression. These PTMs are heritable both in mitotic division and in germ-cell producing meiotic division.[21, 22] In chromatin, histone proteins are arranged as octamers comprising two each of H2A, H2B, H3 and H4, and this complex is further stabilised by interactions with histone protein H1.[23] The complex of one octamer of histone proteins and 145–147 base pairs of DNA is termed the nucleosome (**Figure 4**).[24]

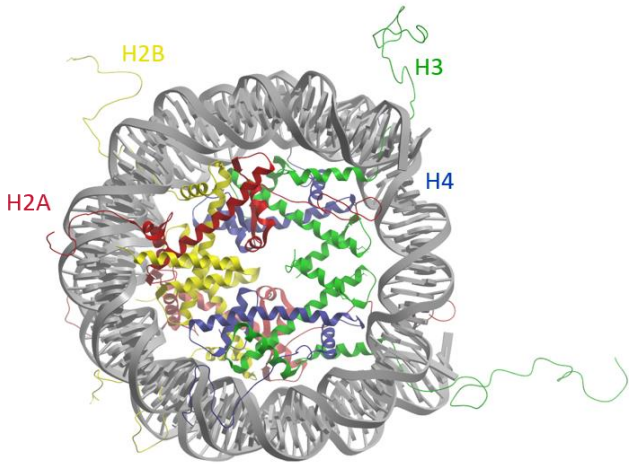

Figure 4 View from a 1.9 Å crystal structure of a 147 base pair DNA fragment (shown in grey) in complex with an octamer of H2A, H2B, H3 and H4 proteins (PDB ID: 1KX5).[25] The *N*-terminal histone tails extend beyond the interior core of the histone octamer.

Important stabilising interactions in the nucleosome are the interaction of the negatively charged DNA phosphate groups with positively charged lysine- and arginine-rich histone proteins[24] and many hydrogen bond interactions, both directly between DNA and histones[24] and also indirectly in water-mediated hydrogen bonds.[25] The nucleosomes package together as chromatin which itself is further compacted as chromosomes.

1.3.2 Post-translational Modifications to Histone Proteins

The *N*-terminal tail regions of the core histone proteins (H2A, H2B, H3 and H4) contain residues which frequently bear PTMs. Histone PTMs are introduced by enzymes termed "writers" and are removed by enzymes termed "erasers".[26] Common modifications are acetylation of lysine residues (introduced by acetyltransferases), methylation of both lysine and arginine residues (introduced by methyltransferases) and phosphorylation of serine and threonine residues (introduced by kinases); these and other established histone PTMs are summarised below (**Table 1**).[27, 28]

Table 1 Examples of PTMs found on histone tails.[27, 28]

PTM	Modified Residues
Acetylation	Kac
Methylation	Kme1, Kme2, Kme3, Rme1, Rme2a, Rme2s
Phosphorylation	Sph, Tph, Yph
Ubiquitination	Kub
Sumoylation	Ksu
Deimination	R modified to citrulline
Proline Isomerization	P-cis modified to P-trans
Tail clipping	Removal of *N*-terminal residues

PTMs to histone proteins can result in changes to chromatin structure and therefore have a direct influence on the accessibility of the neighbouring DNA for transcription. For example, the N^{ε}-amino groups of lysine residues are protonated at physiological pH and the resulting positive charge can form an electrostatic interaction with the phosphate groups of DNA; acetylated lysine residues being uncharged cannot form this interaction and hyperacetylation of histones can therefore result in less compacted chromatin and favour transcription.[29] In addition to their direct effect on chromatin structure, histone tail modifications also influence gene expression through interactions with epigenetic "reader" proteins.

1.3.3 Epigenetic Reader Proteins

Epigenetic reader proteins recognise specific histone tail states. For example the H3K4me3 mark recruits transcription factor II D (TFIID) through its plant homeodomain (PHD)[30] and the H3K36me3 mark recruits DNA methyltransferase 3A (DNMT3A) through its Pro-Trp-Trp-Pro (PWWP) domain.[31] DNMT3A contains a second reader domain which is also found in alpha-thalassemia and mental retardation X-linked syndrome protein (ATRX) and DNA methyltransferase 3L (DNMT3L), termed the ATRX–DNMT3–DNMT3L (ADD) domain.[31] The ADD domain of DNMT3A recognises unmethylated H3K4.[32] The tudor domain of KDM4A binds to H3K4me2/3 and H4K20me2/3.[33] Some of the epigenetic reader proteins and the histone marks they recognise are listed below (**Table 2**).[34]

Table 2 Examples of epigenetic protein reader domains and the PTMs they recognise.[34]

Epigenetic Mark	Reader domains
Acetylated lysine	Bromodomain
Methylated lysine	ADD, Chromodomain, PHD, PWWP, TTD, Tudor, WD40
Methylated arginine	ADD, tudor, WD40
Phosphorylation	14–3–3, tandem BRCT
Unmodified residues	ADD, PHD, WD40

Abbreviations not previously defined are tandem tudor domain (TTD), tryptophan and aspartic acid-containing (WD40) and breast cancer-associated protein carboxy-terminal (BRCT). The 14–3–3 domain is found in the family of 14–3–3 proteins which bind to phosphorylated serine or threonine.[35]

Each nucleosome contains eight histone tails which can each bear several PTMs and these act in concert to regulate gene expression through the recruitment of reader proteins containing other epigenetic domains or which recruit other proteins important in gene regulation.[36] Epigenetically modified histone residues can influence the state of other nearby histone residues through a process known as crosstalk,[37] for example H3K4me3 is recognised by the PHD finger of an inhibitor of growth (ING) family member in yeast (Yng1) which is part of the nucleosomal acetyltransferase of histone H3 (NuA3) histone acetyltransferease complex and acetylates H3K14.[38]

Since the precise effect of histone modifications can be dependent on whether nearby histone residues or DNA bases have been post-translationally modified and on the recruitment of reader proteins it is difficult to correlate specific histone PTMs with specific biological effects; however, in general terms, methylation at H3K4, H3K36 and H3K79 are indicative of transcriptionally active genes while methylation at H3K9, H3K27 and H4K20 are considered repressive.[39]

1.3.4 Reversibility of Covalent Modifications to Histone Proteins

Histone lysine acetylation has long been known to be a reversible epigenetic modification,[14, 40] in contrast, histone methylation was thought to be an irreversible modification which could be altered only by the replacement of the methylated histone

protein with an unmodified one,[41] or by histone tail clipping.[42] The discovery of lysine-specific demethylase 1 (KDM1A or LSD1) in 2004,[43] and lysine-specific demethylase 2A (KDM2A) in 2006,[44] changed this view. Two classes of histone lysine demethylases (KDMs) have been identified which differ in sequence homology and mechanism of demethylation (**Figure 5**).

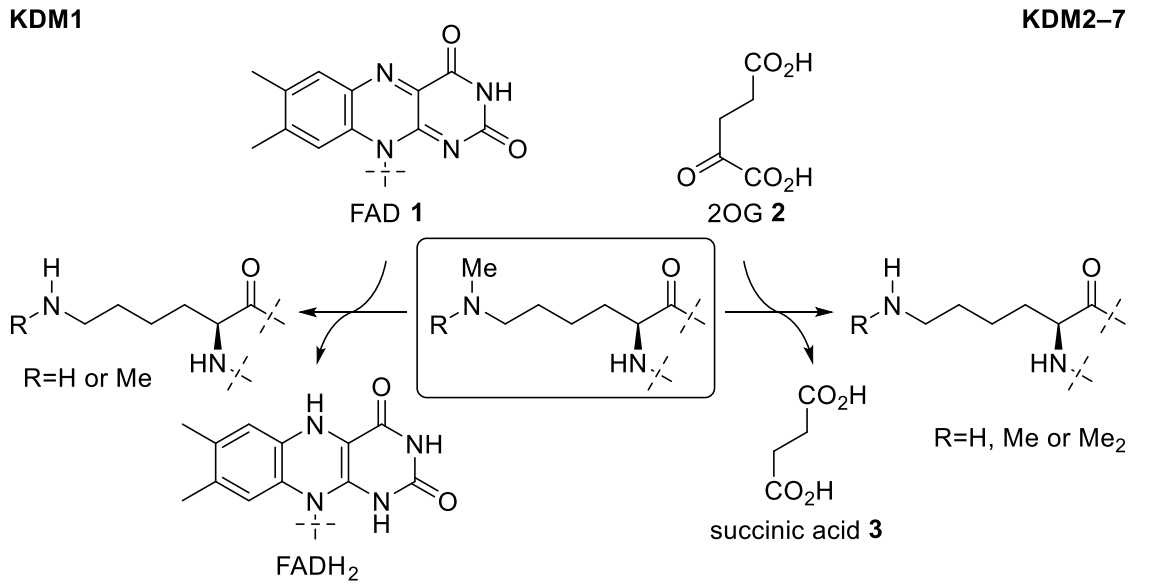

Figure 5 Histone lysine demethylation can be catalysed by the flavin adenine dinucleotide (FAD)-dependent demethylases (KDM1) or the 2-oxoglutarate- (2OG) dependent demethylases (KDM2–7).

The first identified class of KDMs comprises the lysine-specific demethylases 1 and 2 (KDM1A and KDM1B) which contain a catalytic amine-oxidase domain.[28] KDM1A and 1B use FAD as a cofactor in the oxidative demethylation process which proceeds *via* an iminium intermediate which collapses to give the demethylated product and formaldehyde; the involvement of the iminium intermediate limits the substrate scope to mono- and di-methylated lysine (**Figure 5**).[45, 46] The second KDM class is a larger family of about 18 Jumonji C (JmjC) demethylases which in humans are grouped into five subfamilies (KDM2/7, KDM3, KDM4, KDM5 and KDM6)[47] and are part of the large 2-oxoglutarate-(2OG **2**) dependent oxygenase super-family.[48] The JmjC KDMs demethylate lysine residues through an iron(II)-catalysed oxidative process utilising 2OG and oxygen as co-factors and releasing formaldehyde and succinic acid as a by-products (**Figure 7**).[49] The

KDMs are multiple-domain containing proteins which frequently contain other domains capable of interacting with DNA or histone proteins, for example KDM2A contains a zinc finger CxxC domain which recognises non-methylated CpG islands on DNA,[50] and KDM7B contains a PHD domain which binds to H3K4me3.[51]

The JmjC domain is relatively highly conserved between the different JmjC KDMs; a double-stranded β-helix (DSBH) comprised of two beta sheets holds the catalytic iron(II) in place through three iron binding residues (**Figure 6**).

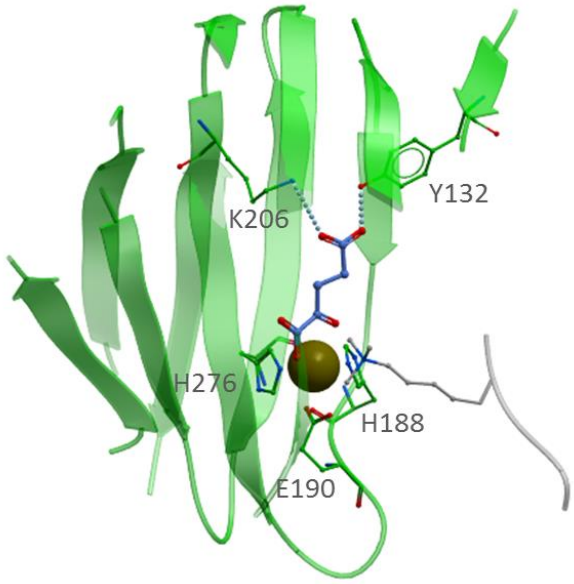

Figure 6 View of the JmjC DSBH from a crystal structure of 2OG **2** (blue sticks) and an H3K9me3 peptide (grey ribbon and sticks) in KDM4A (green ribbon and sticks). The catalytic iron (substituted here by nickel) is bound by residues H276, H188 and E190. 2OG binds to the metal through its C-1 carboxylate and C-2 oxo groups and interacts through its C-5 carboxylate to Y132 and K206. Only the DSBH is shown for clarity. PDB ID: 2Q8C.

The iron binding residues are part of a conserved HXD/E…H motif where two histidines and one carboxylate-containing amino acid coordinate iron. During the catalytic cycle, 2OG binds to iron through its C-1 carboxylate and C-2 oxo groups and to the DSBH through interaction of the C-5 carboxylate with a lysine residue and a hydrogen bond donor (for example tyrosine or serine).[52] The substrate selectivity is determined by differences

both in the JmjC domain itself and other domains found in the JmjC KDMs (for example other histone- or DNA- binding domains).[47]

1.3.5 2OG-Dependent Demethylation

The detection of reaction intermediates spectroscopically has led to the formulation of a consensus mechanism for oxidation of substrates by 2OG-dependent oxygenases.[52-54] The mechanism for demethylation of a methylated lysine substrate by JmjC KDMs is shown below (**Figure 7**). In the resting state, iron(II) is bound by two histidine residues

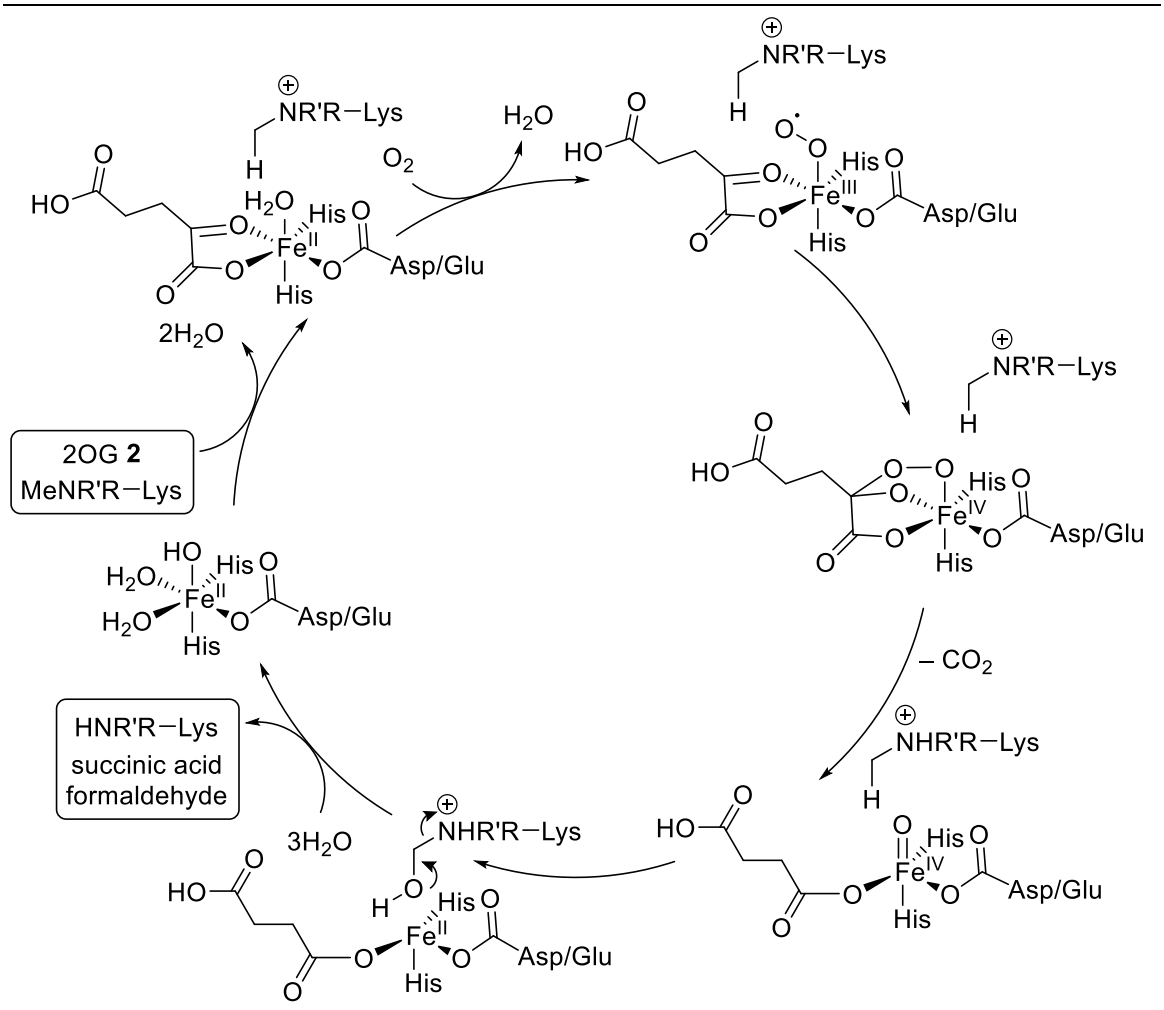

Figure 7 Consensus mechanism for 2OG-dependent histone demethylation.[52-54]

and a carboxylate group (aspartic or glutamic acid) and up to three water molecules of which one or two are displaced by 2OG. Binding of the substrate weakens the bond between iron and the remaining water molecule which is replaced by molecular oxygen to

give an iron(III) species. Oxidative decarboxylation, perhaps *via* a cyclic peroxide species as shown, generates an iron oxo species (Fe^{IV}=O) which reacts with the substrate, likely in a radical process.[55] The resulting hemiaminal then collapses to give the demethylated lysine product, formaldehyde and succinate.[49]

1.4 Epigenetics and Disease

The epigenetic machinery is important in cellular development and survival; knockout studies of histone modifying proteins reveal that the loss of these proteins frequently results in impaired development or embryonic lethality.[56] For example, it has been shown that knockout of KDM2A,[57] KDM2B,[58] and KDM8[59] results in embryonic lethality in mice and that knockout of KDM6A in mice results in embryonic lethality in the case of female embryos.[60] Knockout of KDM3A is not lethal but has been shown to result in downregulation of genes associated with fatty acid metabolism and an obese phenotype was observed in KDM3A knockout mice.[61]

Mutations to histone modifying proteins are associated with multiple human diseases, for example some instances of X-linked mental retardation (XLMR) have been associated with mutations to KDM5C and KDM7B (sometimes in conjunction with cleft lip/cleft palate).[62, 63] Misregulation of histone modifying enzymes has been observed in a large number of disease states, for example in inflammation where reduction in histone deacetylase (HDAC) activity has been observed in synovial tissue samples taken from patients with rheumatoid arthritis[64] and in lung samples taken from patients with chronic obstructive pulmonary disorder;[65] in Alzheimer's disease (AD) where changes in the level of DNA methylation at some CpG islands has been observed in brain tissue samples from patients with AD;[66, 67] and notably in cancers where aberrant epigenetic regulation is frequently observed.[68] The involvement of histone modifying proteins in cancer can be as a result of somatic mutations (for example a translocation involving the bromodomain containing 4 (*BRD4*) and nuclear protein in the testis (*NUT*) genes is associated with NUT midline

carcinoma,[69] and mutations in ubiquitously transcribed tetratricopeptide repeat, X chromosome (*UTX*) have been observed in many cancer tissue samples, particularly in bladder cancers).[70] Abnormal expression levels of histone modifying proteins have also been associated with cancer (for example KDM2A has been found to be overexpressed in lung cancer,[71] KDM4A–C in prostate cancer,[72] KDM4C in breast cancer[73] and KDM5C in prostate, breast and lung cancer),[74] and may be associated with cancer progression (KDM2A was found to be overexpressed in some breast cancer cell lines, however, disease progression was associated with lower expression levels).[75]

1.4.1 Epigenetic Effects of Approved Drugs

Since the discovery of the different epigenetic protein classes, it has been found that some existing drugs are able to modify the epigenome and that these epigenetic effects may contribute to their mechanism of action or to unwanted side-effects.[76, 77] For example sodium valproate **4**, a drug used in the treatment of epilepsy has been found to be an HDAC inhibitor in cellular assays,[78] hydralazine **5**, used to treat hypertension, has been found to result in DNA hypomethylation through down-regulation of DNA methyltransferases DNMT1 and DNMT3A,[79] and methotrexate **6**, a drug used to treat rheumatoid arthritis, has been found to reverse DNA hypomethylation in peripheral blood mononuclear cells (PBMCs) from rheumatoid arthritis patients treated with methotrexate compared to patients not receiving methotrexate (**Figure 8**).[80]

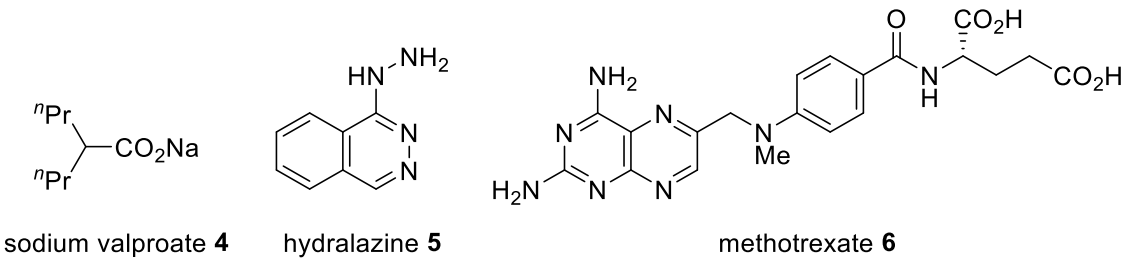

sodium valproate **4** hydralazine **5** methotrexate **6**

Figure 8 Examples of marketed drugs which have been found to exert epigenetic effects.[77]

Sodium valproate **4** and hydralazine **5** have also been used as a combination therapy in the treatment of cervical cancer and cutaneous T-cell lymphoma (CTCL).[81]

1.4.2 Epigenetic Drugs

Research into the importance of epigenetic mechanisms in disease, particularly in cancer, has led to the identification of some previously described antiproliferative agents as epigenetic modulators and several of these have been approved as drugs (**Figure 9**).

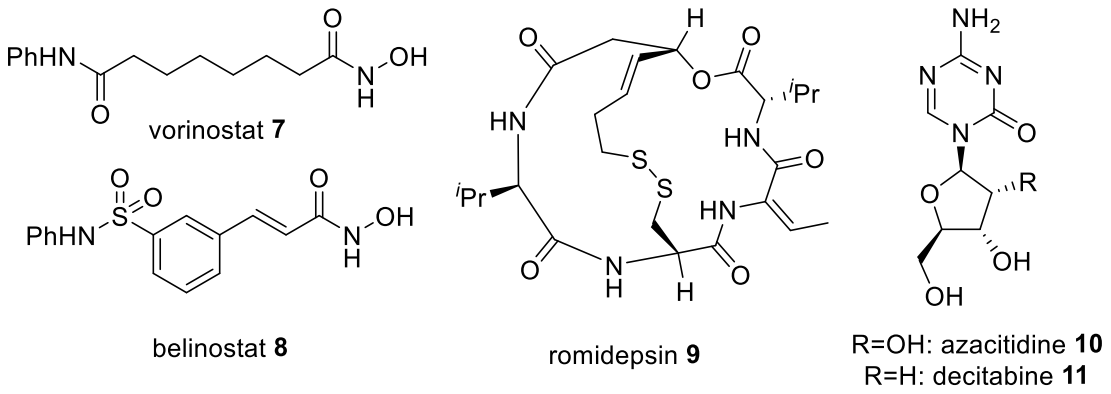

Figure 9 Epigenetic modulators which have been licensed as drugs.

Vorinostat **7** is a class I and II HDAC inhibitor that is licensed for the treatment of CTCL but has also been shown to have an antiproliferative effect on a variety of cell types *in vitro* including non-small cell lung carcinoma (NSCLC) and glioblastoma cells.[82] Belinostat **8** is a class I and II HDAC inhibitor and is licenced as a treatment for peripheral T-cell lymphoma (PTCL).[83, 84] Romidepsin **9**, a bacterial natural product, when reduced to the corresponding dithiol *in vivo* is a class I HDAC inhibitor and is licenced as a treatment for CTCL and PTCL.[84, 85] Azacitidine **10** (an aza analogue of the cytidine nucleoside) and decitabine **11**, its deoxy analogue, are used in the treatment of myeloid leukaemias.[86] They are converted to the 5'-triphosphate derivatives *in vivo* and are incorporated into DNA in place of cytosine nucleotides.[87] Once incorporated into DNA, **10** and **11** block the action of DNA methyltransferases resulting in hypomethylation.[87] In addition to these approved

drugs, clinical trials are ongoing with other epigenetic modulators, predominantly HDAC inhibitors.[88]

1.5 JmjC KDM Inhibitors

The link between the JmjC KDMs and disease, in particular cancer, means that they are of interest as potential targets for drugs. However, potent, selective and cell-active JmjC KDM inhibitors are needed in order to interrogate the precise function of these proteins *in vitro* and *in vivo* and to confirm whether they are appropriate targets for drug discovery programmes.

1.5.1 The JmjC KDM Family

The approximately 18 JmjC KDMs are grouped into five subfamilies (KDM2/7, KDM3, KDM4, KDM5 and KDM6).[47] Calculation of the sequence identity of the JmjC domains using the National Center for Biotechnology Information (NCBI) basic local alignment search tool (BLAST, **Table 3**)[89, 90] shows that whilst there is very high sequence identity within the KDM4 subfamily (74–93%), there is significantly more variation between some other JmjC KDMs (for example KDM6A and 7B have only 19% sequence identity and KDM2A and KDM6B 20% sequence identity).

Table 3 Sequence identity of JmjC domains calculated using the NCBI BLAST search tool for selected JmjC KDMs expressed as percentages.

	2A	**2B**	**3A**	**4A**	**4B**	**4C**	**4D**	**4E**	**5C**	**6A**	**6B**	**7A**	**7B**
2A	100												
2B	79	100											
3A	25	44	100										
4A	29	38	–	100									
4B	29	31	–	84	100								
4C	29	31	–	84	88	100							
4D	28	53	25	74	80	75	100						
4E	24	38	24	74	78	74	93	100					
5C	50	30	35	42	41	40	43	43	100				
6A	31	36	25	31	26	27	31	30	30	100			
6B	20	38	–	35	25	24	30	32	30	79	100		
7A	48	51	29	37	32	32	26	29	33	–	–	100	
7B	55	55	32	37	32	32	28	37	33	19	–	75	100

– represents instances where no significant sequence similarity was found.

Although the JmjC catalytic domains themselves are relatively highly conserved, there are significant differences in the substrate scope of the different JmjC KDMs (**Table 4**).[46] This difference in substrate scope can be exploited in the design of subfamily selective inhibitors through the incorporation of substituents that are able to occupy the substrate binding pocket of one JmjC KDM subfamily better than others.[91]

Table 4 The substrate scope of selected JmjC KDMs grouped by subfamily.

JmjC KDM Family	Enzyme	Substrates
KDM2/7	KDM2A (FBXL11)	H3K36me2/1,[44] P65 subunit of NFκB[92]
	KDM2B (FBXL10)	H3K36me2/1,[93]H3K4me3[94]
	KDM7A (KIAA1718)	H3K9me2, H3K27me2[95]
	KDM7B (PHF8)	H3K9me2/1, H3K27me2, H4K20me1[96]
	PHF2	H3K9me1[97]
KDM3	KDM3A (JMJD1A)	H3K9me2/1[39, 98]
	KDM3B (JMJD1B)	H3K9me2/1[39]
KDM4	KDM4A (JMJD2A)	H3K9me3/2,[72, 99] H3K36me3/2[99]
	KDM4B (JMJD2B)	H3K9me3/2[72]
	KDM4C (JMJD2C, GASC1)	H3K9me3/2,[72, 99] H3K36me3/2[99], Pc2K191me2[100]
	KDM4D (JMJD2D)	H3K9me3/2[101]
	KDM4E (JMJD2E)	H3K9me3/2[102]
KDM5	KDM5B (JARID1B)	H3K4me3/2[103]
	KDM5C (JARID1C)	H3K4me3/2[103]
	KDM5D (JARID1D)	H3K4me3/2[103]
KDM6	KDM6A (UTX)	H3K27me3/2/1[104]
	KDM6B (JMJD3)	H3K27me3/2[104]
	KDM6C (UTY)	H3K27me3/2[105]

Abbreviations not previously defined are F-box and leucine-rich repeat protein (FBXL), 65 kDa subunit (P65) of nuclear factor kappa-light-chain-enhancer of activated B cells (NFκB), plant homeodomain-like finger (PHF), gene amplified in squamous cell carcinoma 1 (GASC1), polycomb 2 protein (Pc2), Jumonji domain-containing protein (JMJD), AT-rich interaction domain (ARID), Jumonji/ARID domain-containing (JARID), ubiquitously transcribed tetratricopeptide repeat, X chromosome (UTX). KIAA1718 is the name assigned in the Kazusa human cDNA project to the protein subsequently named KDM7A.

1.5.2 2OG Mimetic Inhibitors

As for the wider 2OG oxygenase superfamily,[48] most inhibitors of the JmjC KDM demethylases described to date are 2OG mimetics which contain functional groups capable of binding iron(II) and which mimic the hydrogen bonding interactions made by 2OG in the active site. A crystal structure of 2OG in complex with KDM4A is shown below (**Figure 10**) to exemplify the typical interactions formed by 2OG on binding to JmjC KDMs.

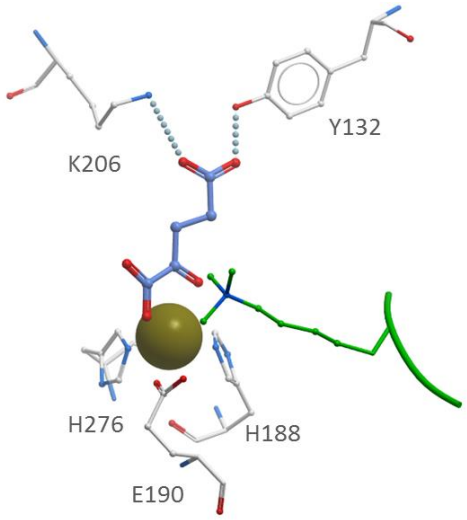

Figure 10 Typical 2OG binding interactions in JmjC KDMs exemplified by a view from a co-crystal structure of 2OG (blue sticks) and an H3K9me3 peptide (green ribbon and sticks) in KDM4A (PDB ID: 2Q8C).[106] 2OG binds to iron (brown sphere, substituted here by nickel) through its C-1 carboxylate and C-2 oxo groups; the C-5 carboxylate typically interacts with a lysine residue and a hydrogen bond donor (for example tyrosine or serine). The substrate binding pocket is adjacent to the 2OG binding site. Key KDM4A residues are shown as grey sticks.

Hypoxia-inducible factor (HIF) is a heterodimeric transcription factor comprised of two subunits (HIFα and HIFβ). HIFα is hydroxylated by the 2OG oxygenases prolyl hydroxylase domain 1–3 (PHD1–3) and factor inhibiting HIF (FIH).[107] Many compounds which were first identified as inhibitors of PHD2 or FIH are structurally related to 2OG and have since been tested against the JmjC KDMs and found to be active.[48] These broad-spectrum 2OG oxygenase inhibitors have provided useful starting points in the search for more potent and selective JmjC KDM inhibitors. Given the significant differences in the nature and scope of the 2OG oxygenase substrates and in the substrate binding sites, a common strategy for imparting selectivity to these broad-spectrum 2OG oxygenase inhibitors is to introduce substituents that can occupy the substrate binding pocket.[91] For example *N*-oxalyl glycine (NOG **12**) is a broad-spectrum 2OG oxygenase inhibitor (**Figure 11A**).[108] NOG derivatives **13–15** which incorporate substituents designed to occupy the lysine binding pocket of KDM4A or KDM4E inhibit the KDM4 subfamily whilst being more selective over other 2OG oxygenases (for example **14** is selective for KDM4E over

PHD2)[101] although their inhibitory effect against KDM4E is somewhat reduced compared to that of NOG.[109-111] The HDAC inhibitor vorinostat **7** has also been found to be a JmjC KDM inhibitor.[110] Presumably the hydroxamic acid moiety coordinates to iron(II); this functional group has also been used as a metal chelator in the design of other JmjC KDM inhibitors. For example **16** and **17** bear a hydroxamic acid moiety to bind to iron(II) and an amino group to occupy the substrate pocket.[112, 113]

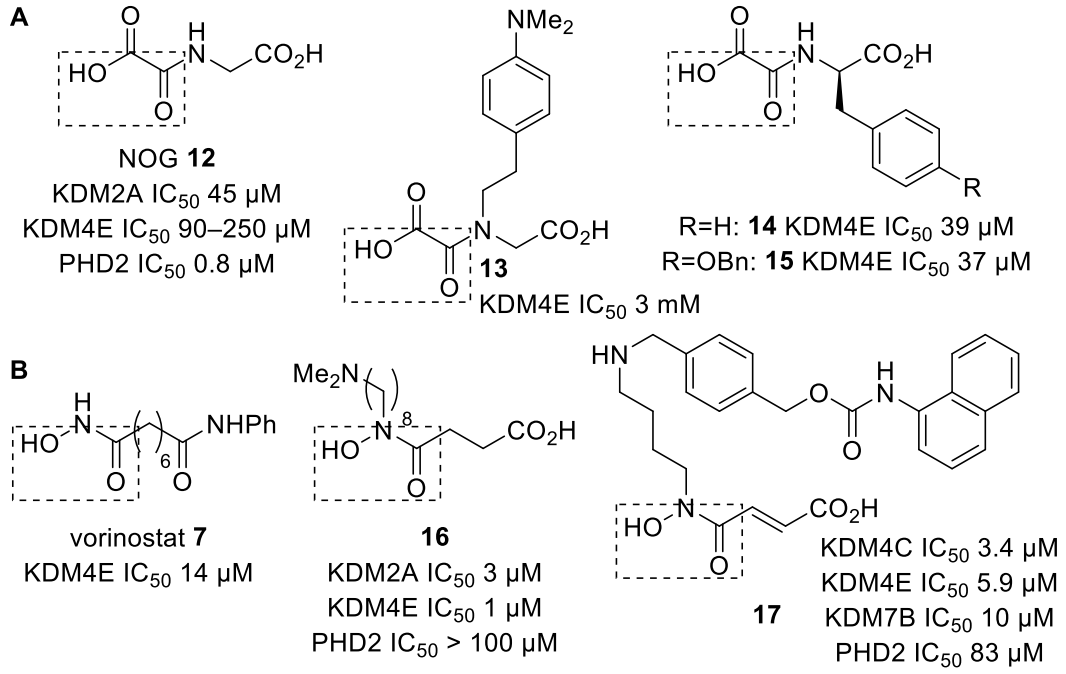

Figure 11 A NOG **12** and selected NOG derivatives **13**–**15** and reported amplified luminescent proximity homogeneous assay (AlphaScreen) half maximal inhibitory concentration (IC_{50}) values; **B** vorinostat **7** and hydroxamic acid derivatives **16** and **17** and reported IC_{50} values from a formaldehyde dehydrogenase (FDH) coupled assay (**7** and **16**) or mass spectrometry (MS) assay (**17**). Iron-chelating groups are highlighted.

Daminozide **18**, a plant growth regular, inhibits the KDM2/7 subfamily in the micromolar range and is more than 100-fold selective over other JmjC KDMs.[114]

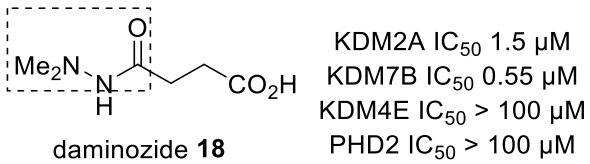

Figure 12 Daminozide **18**, a plant growth regulator, is a KDM2/7 subfamily inhibitor (IC_{50} values are from AlphaScreen assays). The iron-chelating moiety is highlighted.

Heterocycle-containing 2OG mimetics 2,4-pyridinedicarboxylic acid (2,4-PDCA **19**),[110] 4'-(methoxycarbonyl)-2,2'-bipyridine-4-carboxylic acid **20**,[110] and 5-carboxy-8-hydroxyquinoline (IOX1 **21**)[115] have also proved to be useful scaffolds for JmjC KDM inhibition (**Figure 13**). 2,4-PDCA **19** and IOX1 **21** are widely used as broad-spectrum 2OG oxygenase inhibitors.[108, 116] Derivatives of these scaffolds have been prepared with the aim of improving activity and selectivity; although less active against KDM4E than 2,4-PDCA itself, some of the 3-amino derivatives of 2,4-PDCA (for example **22**) are selective for KDM4E over PHD2. The 2,2'-bipyridine-4,4'-carboxylic acid derivative **23** is more than 60-fold more potent against KDM4E (IC_{50}: 110 nM) than the ester **20**.[117]

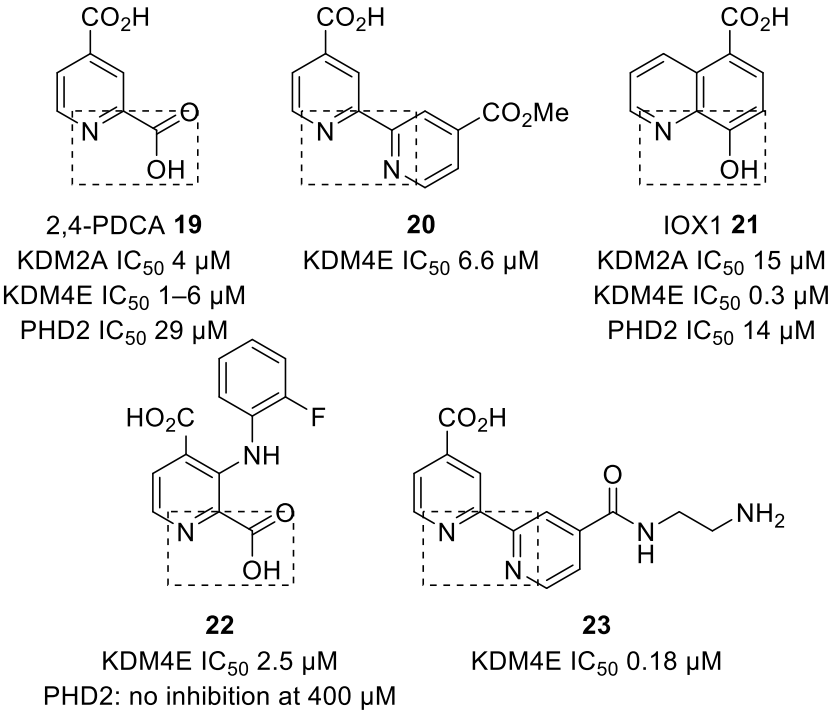

Figure 13 Heterocycle-containing JmjC KDM inhibitors and reported AlphaScreen (**19** and **21**) or FDH assay (**20**, **22** and **23**) IC_{50} values. Iron-chelating groups are highlighted.

Since the work described in this thesis was initiated, other JmjC KDM inhibitors have been reported in the literature (**Figure 14**). Hydroxamic acid derivatives **24** and **25** inhibit the KDM2/7 subfamily in the micromolar range with good selectivity over KDM6 and some selectivity over the KDM4 and KDM5 subfamilies.[118] The pyrimidine derivative (GSK-J1 **26**) is a potent KDM5 and KDM6 subfamily inhibitor and binds to iron(II) through the

pyridine and pyrimidine nitrogen atoms.[119, 120] Despite not containing a carboxylic acid, the pyridylhydrazone **27** is a broad-spectrum JmjC KDM inhibitor which inhibits members of the KDM4, KDM5 and KDM6 subfamilies in the micromolar or submicromolar range and is selective over PHD2 and the methylcytosine oxygenase ten–eleven translocation protein 1 (TET1).[121]

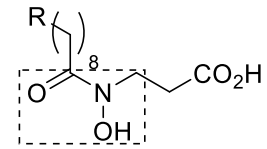

R=^{c}Pr: **24**
KDM2A IC_{50} 6.8 μM
KDM7B IC_{50} 1.2 μM
KDM4C IC_{50} 83 μM
KDM6A IC_{50} > 100 μM

R=Ph: **25**
KDM2A IC_{50} 2.9 μM
KDM7B IC_{50} 23 μM
KDM4C IC_{50} 22 μM
KDM6A IC_{50} > 100 μM

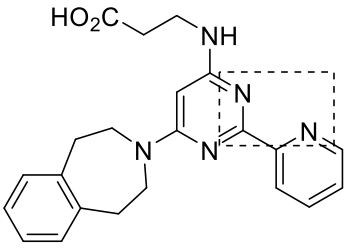

GSK-J1 **26**
KDM4E IC_{50} 20 μM
KDM5B IC_{50} 0.95 μM
KDM6B IC_{50} 0.06 μM

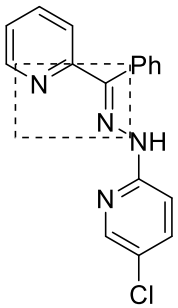

27
KDM4C IC_{50} 1.1 μM
KDM4E IC_{50} 0.34 μM
KDM5A IC_{50} 0.23 μM
KDM6B IC_{50} 0.86 μM
PHD2 IC_{50} > 6 μM

Figure 14 JmjC KDM inhibitors reported since the work described in this thesis was initiated and reported AlphaScreen (**24**–**26**) or enzyme-linked immunosorbent assay (ELISA) IC_{50} values; hydroxamic acid derivatives **24** and **25** are inhibitors of the KDM2/7 subfamily, GSK-J1 **26** is a potent KDM5 and 6 subfamily inhibitor and pyridylhydrazone **27** is a broad-spectrum JmjC KDM inhibitor. Likely iron-chelating groups are highlighted.

A variety of heterocyclic JmjC KDM4 and KDM5 inhibitors have been disclosed in recent oncology-related patent applications (**Figure 15**). Examples of the inhibitors described are bicyclic compound **28**,[122] tricyclic compound **29**,[123] pyrrolopyridine **30**,[124] imidazopyridine **31**,[125] pyrimidone derivative **32**,[126] pyrazolopyridine **33**,[127] and 3-amino-isonicotinic acid derivative **34**.[128]

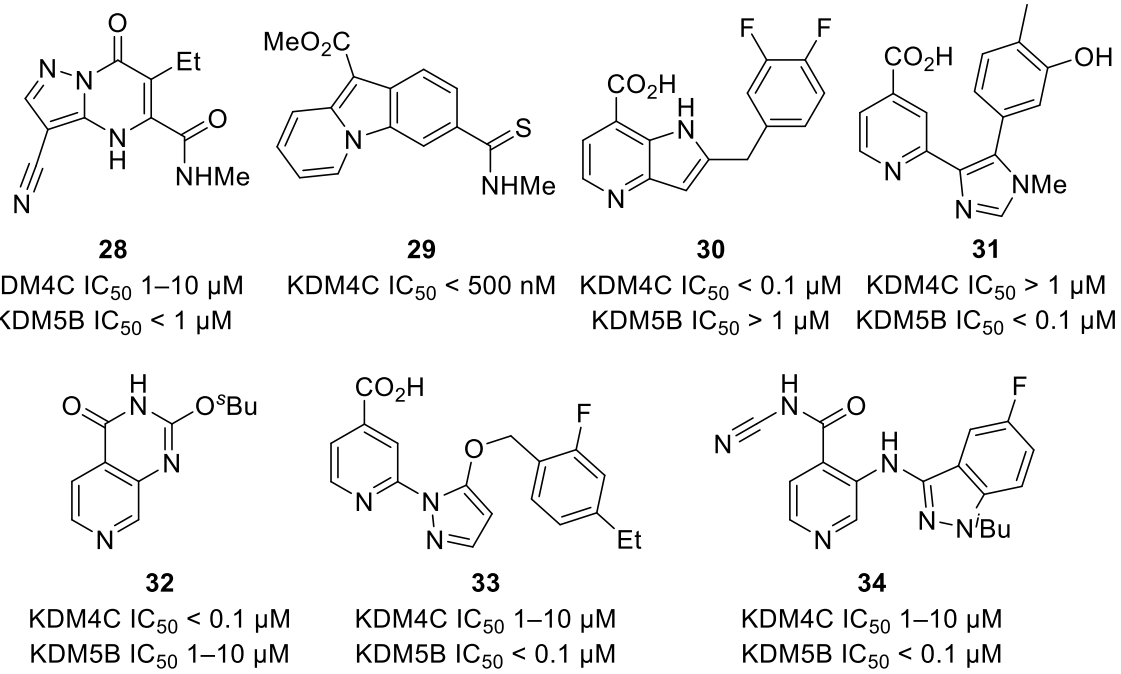

Figure 15 Representative heterocyclic JmjC KDM inhibitors **28**–**34** from recent patent applications and reported IC_{50} data determined by MS based assays (**28**) or fluorescence-based proximity assays (**29**–**34**).

1.5.3 Substrate Mimetics

The approach of inhibiting the JmjC KDMs through compounds that mimic the histone substrate without occupying the 2OG binding pocket is less well explored but has yielded some hits. Compounds **35** and **36** which are inhibitors of the euchromatic histone-lysine *N*-methyltransferases 1 and 2 (EHMT1 and 2), which methylate H3K9 and H3K27,[129, 130] were also found to inhibit the H3K9 and H3K27 demethylase KDM7A but to be selective over H3K4 demethylase KDM5C (**Figure 16**).[131] A co-crystal structure of **36** and 2OG in KDM7A shows that the inhibitor can occupy the same space in KDM7A as the substrate and that 2OG can bind simultaneously.[131]

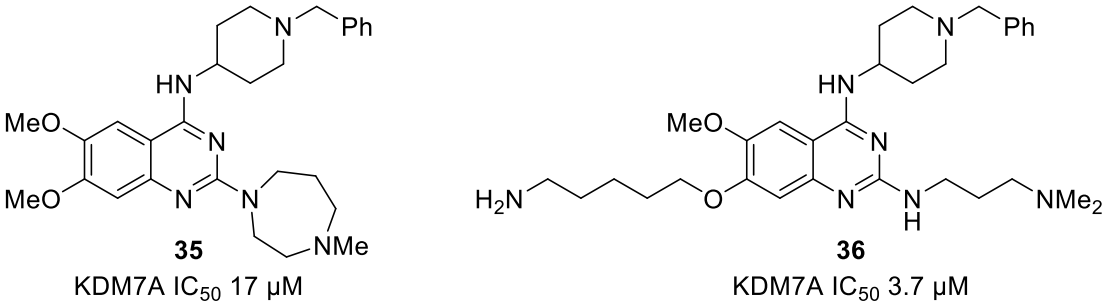

Figure 16 Inhibitors of KDM7A which bind in the substrate binding pocket inhibitor (IC_{50} values are from a MS assay).

1.5.4 Cellular Efficacy

IOX1 **21** is weakly active in cells (KDM4A EC_{50}: 86–100 μM),[116] however, most carboxylic acid-containing JmjC KDM inhibitors do not show significant activity in cell-based assays; this is a major challenge in the development of chemical probes for JmjC KDMs. Several JmjC KDM inhibitors are active in cells as the methyl or ethyl ester prodrugs, presumably due to enhanced membrane permeability of the esters (which can be hydrolysed to the parent drugs intracellularly by esterases)[132] compared to the negatively charged carboxylates.[133] For example, NOG and 2,4-PDCA are used as their methyl esters **37** and **38** in cell-based applications,[108] GSK-J1 **26** is used as its ethyl ester **39**,[119] and **17** is used as its methyl ester (methylstat **40**).[113] Although IOX1 is active in cells as the parent acid, methyl, *n*-butyl and *n*-octyl ester prodrugs of IOX1 have recently been shown to enhance its cellular activity.[116]

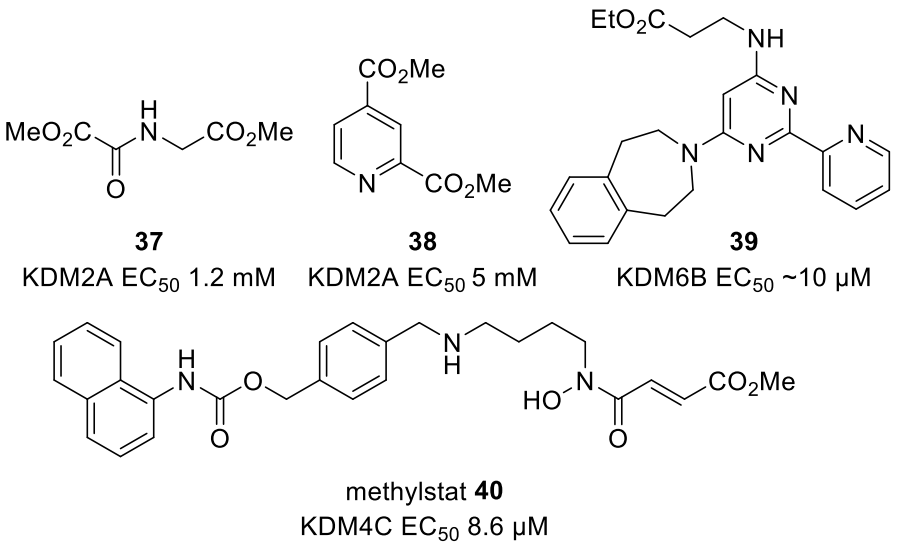

Figure 17 Prodrug esters of JmjC KDM inhibitors which are active in cellular assays.

1.6 Aims

The aim of this project was to design and synthesise potent and selective inhibitors of individual JmjC KDM proteins or subfamilies which would contribute to the tools available to elucidate further the biological role of JmjC KDMs and their relevance as targets for drug discovery. For such inhibitors to be useful as chemical probes, they should be potent (< 100 nM in biochemical assays), selective over other JmjC KDM subfamilies (> 30-fold selective) and active in cellular assays (< 1 μM; see **Figure 3**).

Chapter 2. Optimisation of an Aminomethyl High Throughput Screening Hit for JmjC KDM Inhibition

2.1 Introduction

High throughput screening (HTS) is an expensive but valuable method for the identification of novel ligands for drug discovery targets.[134] After hits have been identified in an HTS, the subsequent optimisation of potency and selectivity typically results in an increase in molecule size and lipophilicity. Larger, more lipophilic molecules are associated with an increased likelihood of problems with solubility, off-target activity and clearance.[135] As drug discovery projects progress, compounds typically become larger and more lipophilic, therefore small, relatively polar hits are preferable to large, lipophilic ones.[136] A number of metrics have been developed to rank hits according to their potency and lipophilicity; one of these is the lipophilic ligand efficiency (LipE)[137] which is defined as:

$$\text{LipE} = \text{p}IC_{50} - \log P$$

In practice, the calculated value of the log*P* is frequently used when the experimental value is not available.

An HTS of 236,000 compounds run at the National Institutes of Health Chemical Genomics Center identified 157 hits as inhibitors of KDM4E; selected hits from the screen are shown in **Figure 18**.[115] Calculation of the LipE scores for the compounds shown above using the reported IC_{50}s and predicted log*P* values (**Figure 18**) shows that hit **42** has a LipE value of 3.6 which represents a very good balance of potency and lipophilicity.[135] Although **42** was not the most active hit identified in the HTS, its low molecular weight (MW: 295.4) and lipophilicity (*c*log*P* 1.8)[138, 139] made it an attractive compound with which to work.

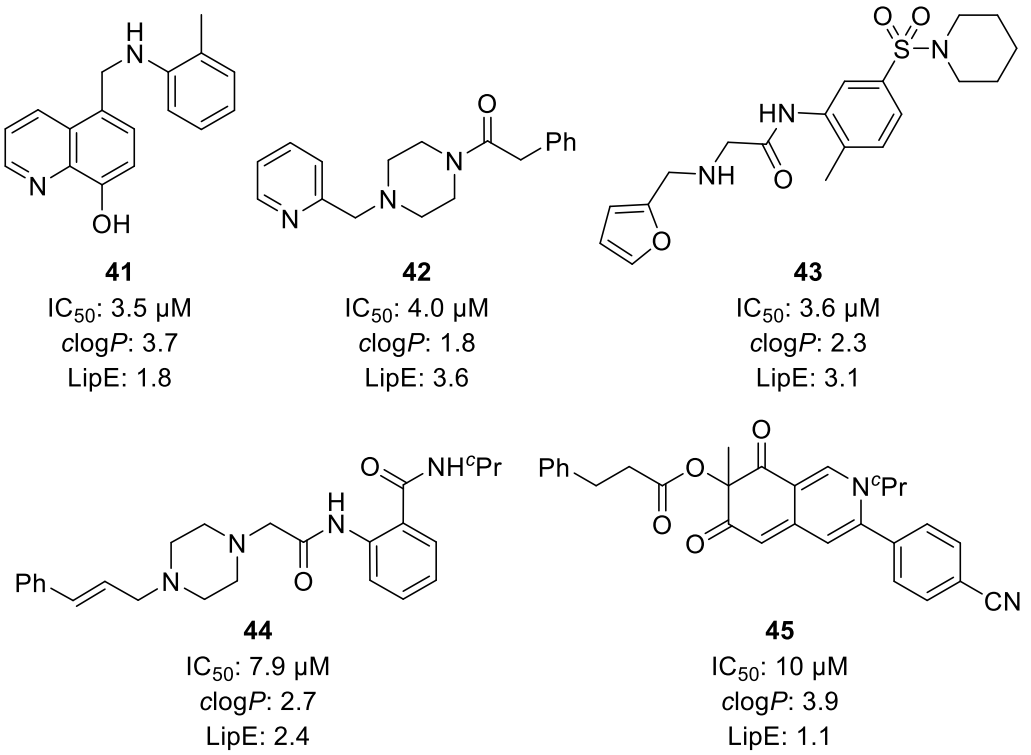

Figure 18 Representative hits from an HTS for KDM4E. The reported inhibitor potencies against KDM4E together with *c*log*P* and LipE scores are shown.

It was hypothesised that hit **42** could adopt a binding mode in KDM4E wherein the pyridine and piperazine lone pairs coordinate to iron(II) in place of 2OG. Many JmjC KDM inhibitors bind to iron(II) through heterocyclic sp^2 nitrogen atoms (for example the bipyridine derivative **23**)[117] and there is also precedence for an sp^3 nitrogen atom binding to the metal; daminozide **18** is known to bind through the carbonyl and dimethylamino groups of the acylhydrazine moiety (**Figure 19**).[114] If **42** is indeed a 2OG mimetic it would be expected that the introduction of a carboxylate group at the C-4 position of the pyridine ring would increase potency against KDM4E because the carboxylate group would be able to occupy the same space in the active site as the 5-carboxy group of 2OG (**Figure 19**). The incorporation of a small, polar carboxylate group would not significantly increase the molecular weight, would result in a decrease in lipophilicity and could potentially have a dramatic effect on potency.

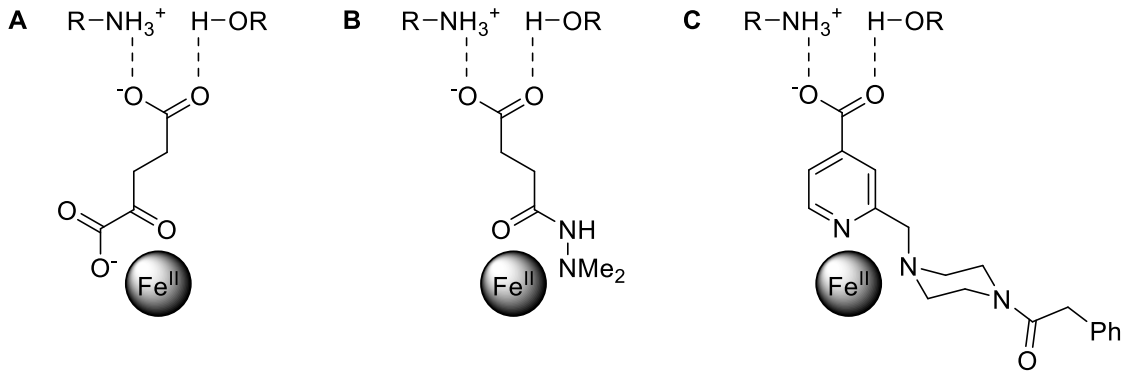

Figure 19 A representation of the key binding interactions formed in JmjC KDMs by **A** 2OG **2**, **B** daminozide **18** and **C** the proposed binding mode of the carboxylate derivative of **42**.

2.2 Synthesis of the Carboxylate Analogue of an HTS Hit

A route to the carboxy analogue of **42** was designed starting from 2,4-PDCA **19** (**Scheme 1**). The diethyl ester **46** was prepared in 79% yield by esterification of 2,4-PDCA **19**. The diethyl ester **46** was submitted to reaction conditions described by Queguiner *et al.*[140] for the reduction of the 2-carboxy group using diisobutylaluminium hydride, which had been reported to proceed in 42% yield. This resulted in a mixture of the desired product, unreacted starting material and the dialdehyde, however, the monoaldehyde was readily separated by chromatography to give aldehyde **47** in 39% yield (**Scheme 1**). Reductive amination of the aldehyde **47** with commercially available 2-phenyl-1-(piperazin-1-

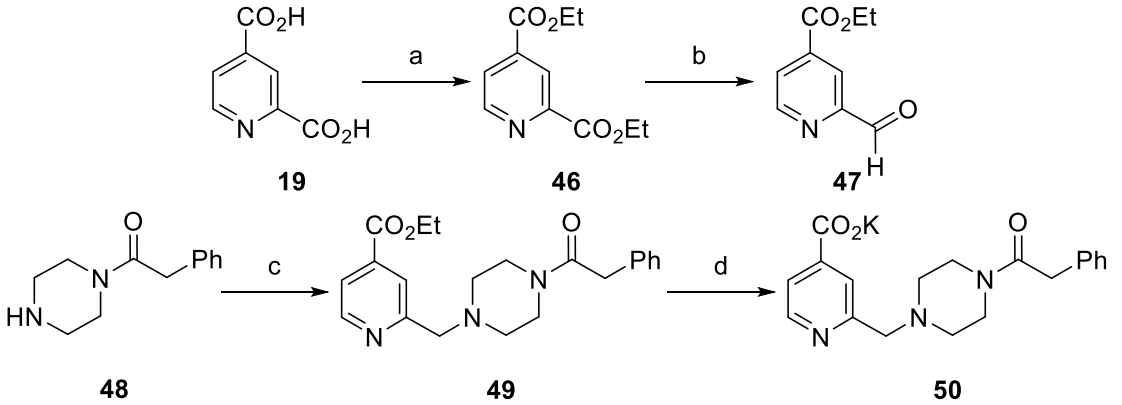

Scheme 1 Synthesis of compound **50**. *Reagents and conditions:* (a) *para*-toluenesulfonic acid (PTSA), EtOH, 80 °C, 79%; (b) diisobutylaluminium hydride (DIBAL), tetrahydrofuran (THF), PhMe, –78 °C, 39%; (c) **47**, sodium triacetoxyborohydride (STAB), CH_2Cl_2, 47%; (d) potassium trimethylsilanolate (KOTMS), MeCN, 69%.

yl)ethanone **48** and sodium triacetoxyborohydride in dichloromethane gave the ethyl ester derivative **49** which was treated with potassium trimethylsilanolate to give the potassium carboxylate **50** (**Scheme 1**).

In vitro screening of inhibitors was carried out by Dr. Anthony Tumber, Dr. Giuseppe Scozzafava and Dr. Louise Walport using an amplified luminescent proximity homogeneous assay (AlphaScreen)[141] or a RapidFire mass spectrometry based assay.[142] The AlphaScreen assay is a fluorescence-based proximity assay; when phthalocyanine-containing donor beads are irradiated at 680 nm, ambient oxygen is excited to the singlet state. The half-life of singlet oxygen in aqueous solution is 4 μsec,[143] and as a result the distance it can diffuse before it decays is limited. The concentration of singlet oxygen decays exponentially with distance from the donor bead surface and at 200 nm is reduced by approximately 97%.[144] If singlet oxygen is formed in close proximity to an appropriately derivatised acceptor bead and therefore within the 200 nm diffusion limit, energy is transferred to thioxene derivatives contained in the acceptor beads resulting in an emission of light at 520–620 nm.[145] In the KDM AlphaScreen assay, demethylation of a biotinylated peptide substrate bearing a methylated lysine residue is detected (**Figure 20**). Biotinylated peptide substrate is used so that it can bind to donor beads through a biotin–streptavidin interaction. An antibody with selectivity for either the methylated lysine substrate or for the product of demethylation is used to couple the substrate to acceptor beads. The donor bead is brought into close proximity with acceptor beads only when the methyl mark of interest is present so that demethylation of the substrate results in a loss or gain of fluorescence which is modulated by the presence of inhibitors.

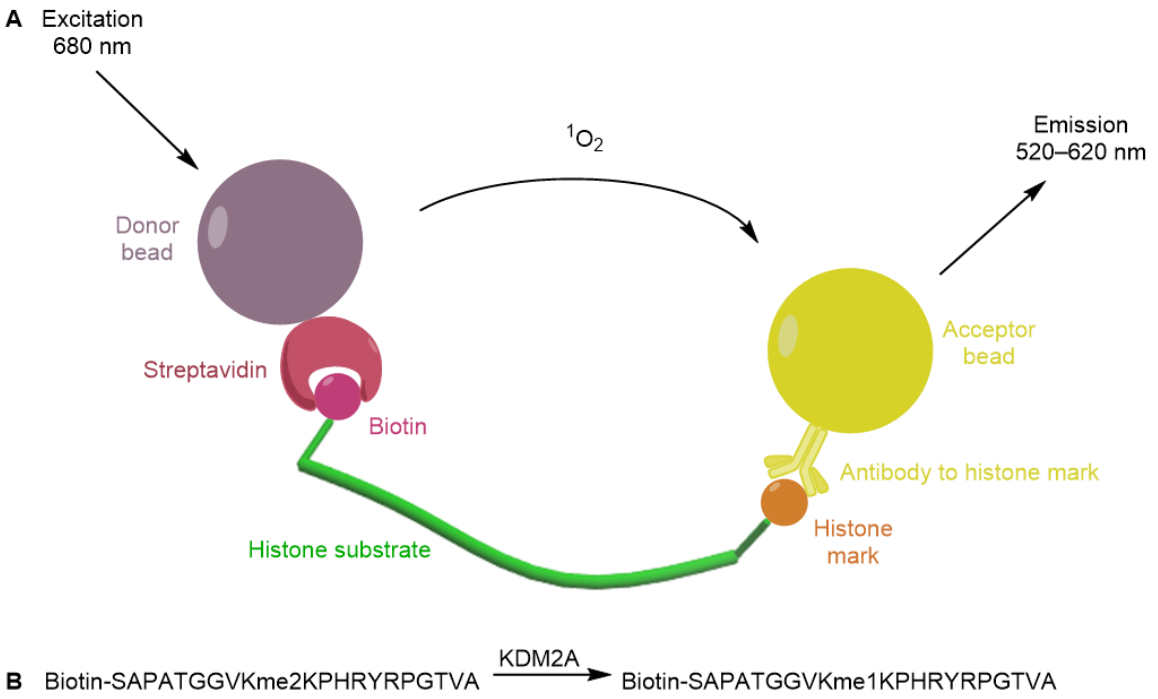

Figure 20 A AlphaScreen method for the detection of JmjC KDM activity. An antibody which is specific to a methylated histone lysine residue of interest is bound to acceptor beads. Biotinylated histone substrate peptide is captured by streptavidin-coated donor beads. When the histone mark of interest is intact, interaction with an immobilised antibody to the histone mark brings the acceptor bead within the diffusion limit of singlet oxygen which is generated upon irradiation at 680 nm. Energy is transferred from singlet oxygen to the acceptor bead causing emission which is detected at 520–620 nm. **B** Representative biotinylated peptide used in the KDM2A AlphaScreen assay (biotin-H3K36(28–48)me2) which binds to the streptavidin-coated donor beads through the biotin moiety. Upon demethylation by KDM2A the biotinylated peptide is recognised by the H3K36me1 antibody on the acceptor beads, the donor and acceptor beads are brought into close proximity and fluorescence is detected.

The RapidFire assay quantifies demethylation of the substrate directly by mass spectrometry.[142, 146] This method does not rely on selective antibodies being available for the methyl mark of interest, can detect several methylation states simultaneously, is amenable to high-throughput applications and unlike the AlphaScreen assay does not suffer from interference by fluorescent molecules. However, the AlphaScreen assay is very sensitive and can generally be performed at lower enzyme concentrations. Both assay methods were used in this project to determine compound potency.

Compound **50** was screened in a panel of seven JmjC KDMs to determine whether the carboxylate group enhanced activity (**Table 5**).

Table 5 Inhibitory effect (IC_{50} value) of **50** against seven JmjC KDMs.

	KDM IC_{50}*						
Cmpd	**2A**[a]	**3A**[b]	**4A**[b]	**4C**[a]	**4E**[a]	**5C**[a]	**6B**[a]
50	1.0 ± 0.13 (12)	>100 (2)	10 ± 0.69 (2)	40 ± 8.3 (2)	62 ± 9.1 (4)	15 ± 2.7 (4)	>100 (6)

*Mean IC_{50} (μM) ± standard error of the mean (number of determinations); determined by determined by the [a]AlphaScreen assay or the [b]RapidFire assay.

Excitingly, this initial work resulted in the identification of a micromolar inhibitor of KDM2A (IC_{50}: 1.0 μM) with 15-fold selectivity over KDM5C, 10- to 60-fold selectivity over KDM4A/C/E and greater than 100-fold selectivity over KDM3A and KDM6B. As a micromolar potency inhibitor of KDM2A, with good physicochemical properties (MW 339.4, *c*log*P* 1.4,[138] LipE score 4.6), compound **50** represented an excellent hit for further medicinal chemistry efforts to optimise subfamily selectivity and potentially deliver a potent and selective tool compound.

2.3 Investigation of the Amide Substituent Structure–Activity Relationship

A small set of amide analogues was designed that could be synthesised in two steps from the aldehyde intermediate **47** and commercially available piperazine amides. The synthetic route developed for the synthesis of **50** was used to prepare these targets efficiently from aldehyde **47** in parallel and in high yield (**Scheme 2**).

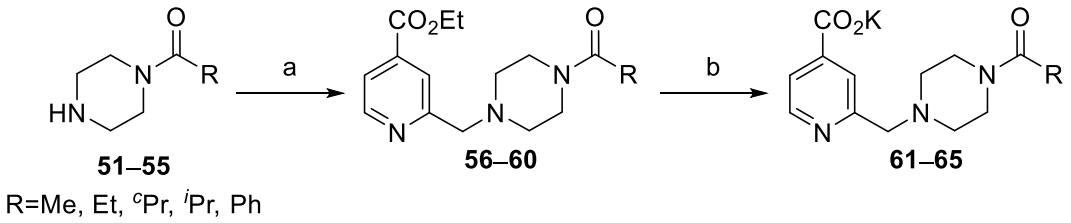

Scheme 2 Synthesis of compounds **61**–**65**. *Reagents and conditions:* (a) **47**, STAB, CH_2Cl_2, 85–100%; (d) KOTMS, MeCN, 58–100%.

Amides **61**–**65** were screened against KDM2A, KDM4C/E and KDM5C (**Table 6**).

Table 6 Inhibitory effect (IC_{50} value) of **61**–**65** against four JmjC KDMs.

		KDM IC_{50}*			
Cmpd	**R**	**2A**	**4C**	**4E**	**5C**
61	Me	11 ± 1.9 (2)	14 ± 3.6 (2)	>100 (2)	5.2 ± 0.70 (2)
62	Et	8.4 ± 2.1 (2)	21 ± 9.0 (2)	>100 (2)	4.4 ± 0.45 (2)
63	^{c}Pr	4.5 ± 1.7 (2)	77 ± 14 (2)	>100 (2)	6.7 ± 0.48 (2)
64	^{i}Pr	4.4 ± 1.2 (2)	19 ± 7.3 (2)	>100 (2)	4.1 ± 1.5 (2)
65	Ph	17 ± 5.0 (2)	18 ± 6.4 (2)	>100 (2)	7.4 ± 3.1 (2)

*Mean IC_{50} (μM) ± standard error of the mean (number of determinations); determined by the AlphaScreen assay.

The small alkyl substituents resulted in enhanced activity against KDM5C (IC_{50}: 4.1–6.7 μM) and a 4- to 11-fold reduction in activity against KDM2A; as a result compounds **61**–**64** were found to be approximately equipotent against KDM2A and KDM5C. The benzamide **65** was found to be more active against KDM5C (IC_{50}: 7.4 μM) than KDM2A (IC_{50}: 17 μM). The degree of selectivity over KDM4C fell from 40-fold for compound **50** to 1.1–17 fold for compounds **61**–**65**, however, selectivity over KDM4E was retained.

2.4 Exploration of Sulfonamide Analogues

Since modification to the amide substituent of the initial series had not resulted in sub-micromolar activity against any of the JmjC KDMs in the screening panel, a series of targets was designed where the amide group was replaced with a sulfonamide. Whilst not changing the polarity of the targets significantly, the tetrahedral geometry of the sulfonamide group positions the sulfonyl groups and the alkyl or aryl substituents in different vectors to the planar geometry of the amide group so the sulfonamide targets would be predicted to have different activities to the amides. The methyl (**72**), ethyl (**73**) and phenyl (**74**) sulfonamides were synthesised from the aldehyde intermediate **47** and commercially available piperazine sulfonamides **66**–**68** (**Scheme 3**).

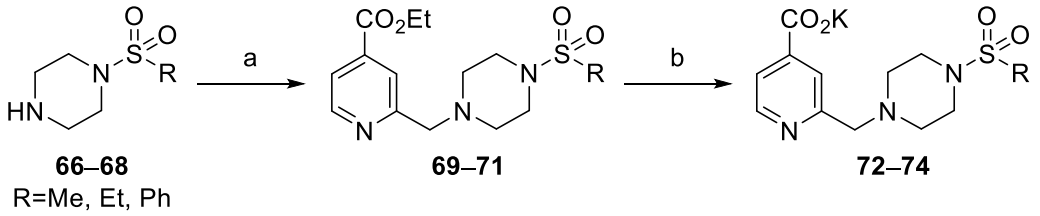

Scheme 3 Synthesis of compounds **72**–**74**. *Reagents and conditions:* (a) **47**, STAB, CH_2Cl_2, 80–96%; (d) KOTMS, MeCN, 97–100%.

Sulfonamides **72**–**74** were tested against KDM2A, KDM4C/E and KDM5C (**Table 7**).

Table 7 Inhibitory effect (IC_{50} value) of **72**–**74** against four JmjC KDMs.

		KDM IC_{50}*			
Cmpd	**R**	**2A**	**4C**	**4E**	**5C**
72	Me	1.9 ± 0.36 (2)	11 ± 2.0 (2)	>100 (2)	6.6 ± 3.2 (2)
73	Et	1.6 ± 0.24 (2)	13 ± 4.4 (2)	>100 (2)	6.6 ± 3.0 (2)
74	Ph	0.93 ± 0.090 (6)	22 ± 16 (4)	>100 (4)	31 ± 4.1 (4)

*Mean IC_{50} (μM) ± standard error of the mean (number of determinations); determined by the AlphaScreen assay.

The sulfonamides were found to be more potent inhibitors of KDM2A than the corresponding amides with the phenyl sulfonamide **74** being the most active (IC_{50}: 0.93 μM), representing an 18-fold improvement in activity compared to the amide analogue **65**. Sulfonamides **72–74** were found to inhibit KDM4C/E and KDM5C in the same order of magnitude as the amide derivatives **61–65**. Consequently the most potent KDM2A inhibitor **74** was found to be more selective than the amide derivatives **61–65** being 24-fold selective for KDM2A over KDM4C, 33-fold selective over KDM5C and more than 100-fold selective over KDM4E.

Due to their promising subfamily selectivity (**Table 7**) it was decided to explore the SAR of the sulfonamide series further. Since other piperazine sulfonamides were not readily available commercially, an alternative route, with sulfonamide formation as the key diversification step, was designed. Since the sulfonamide analogues **72**–**74** had been found to be 5- to 18-fold more potent against KDM2A than the corresponding amides it was

hoped that the sulfonamide analogue of **50** would be a sub-micromolar potency inhibitor of KDM2A.

The unsubstituted piperazine compound **77** was prepared for derivitisation to the sulfonamide analogue of **50** in three steps from aldehyde **47** (**Scheme 4**). Reductive amination of aldehyde **47** and *tert*-butyl piperazine-1-carboxylate gave **75** in quantitative yield. Hydrolysis of ethyl ester **75** with lithium hydroxide gave the lithium salt **76** which was treated with trifluoroacetic acid to give the amino acid **77** which was poorly soluble even in dimethylsulfoxide so was converted to the bis(trifluoroacetic acid) salt. This was taken into a reaction with phenylmethanesulfonyl chloride in a method modified from that described by Milne *et al*. for the preparation of *N*-phenylmethanesulfonyl derivatives of naturally occurring amino acids,[147] however analysis of the reaction by liquid chromatography–mass spectrometry (LCMS) showed that little product had formed; the majority of the phenylmethanesulfonyl chloride had reacted with sodium hydroxide used as a base in the reaction.

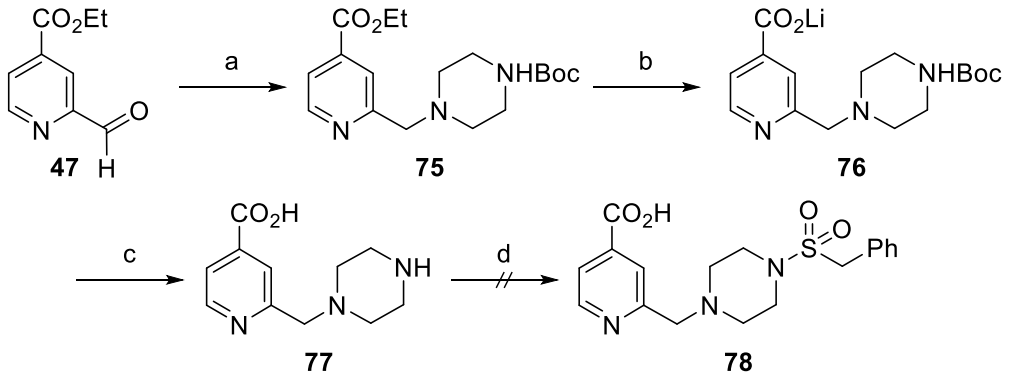

Scheme 4 Attempted synthesis of compound **78**. *Reagents and conditions:* (a) *tert*-butyl piperazine-1-carboxylate, STAB, AcOH, CH_2Cl_2, quant.; (b) LiOH (aq), MeCN, quant.; (c) trifluoroacetic acid (TFA), 48% (d) phenylmethanesulfonyl chloride, NaOH (aq), MeCN, not isolated.

It would likely be possible to optimise the reaction of amine **77** and phenylmethanesulfonyl chloride by the use of an organic base such as trimethylamine; however, it was decided to perform the sulfonamide-forming step earlier in the reaction sequence while the carboxylic

acid was protected as the ether ester. Treating the Boc-protected piperazine derivative **75** with trifluoroacetic acid to remove the Boc group gave ethyl ester **79** (**Scheme 5**). Purification of the ethyl ester **79** by strong cation exchange chromatography led to a degree of transesterification to the methyl ester (20%, determined by nuclear magnetic resonance (NMR) spectroscopy). This was subsequently avoided by the use of ethanol in place of methanol in the eluent. It was anticipated that the ethyl ester **79** could give the target sulfonamide compounds in a one-pot reaction by reaction with sulfonyl chlorides followed by deprotection of the carboxylic ester *in situ* once the sulfonamide formation had gone to completion. This strategy successfully gave **78** in moderate yield (**Scheme 5**).

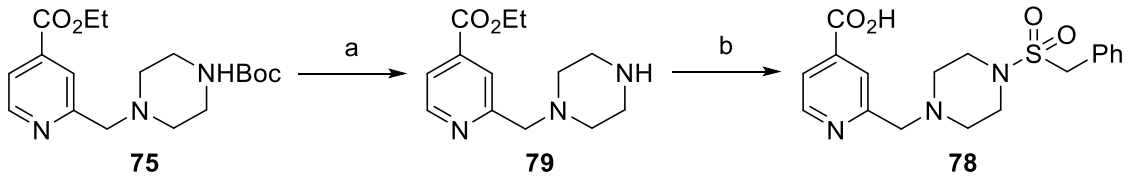

Scheme 5 Synthesis of compound **78**. *Reagents and conditions:* (a) TFA, CH_2Cl_2, 94%; (b) i) phenylmethanesulfonyl chloride, Et_3N, MeCN; ii) LiOH (aq), MeCN, 53%.

Sulfonamide **78** was found to be 2-fold more potent against KDM2A than the amide analogue **50** (0.49 µM versus 1.0 µM), but was less selective over KDM4C (**Table 8**). However, selectivity over the other JmjC KDMs tested was excellent. Compounds **76** and **77** were also screened for activity against the JmjC KDMs. The Boc-protected intermediate **76** was found to inhibit KDM2A and KDM4C in the micromolar range. Removal of the Boc group (compound **77**) resulted in a 31-fold reduction in potency against KDM2A compared to **76** (46 µM versus 1.5 µM) but an 88-fold increase in potency against KDM5C (0.99 µM versus 87 µM); **77** is an interesting lead compound for KDM5C.

Table 8 Inhibitory effect (IC_{50} value) of **76**, **77** and **78** against six JmjC KDMs.

	KDM IC_{50}*					
Cmpd	**2A**	**3A**	**4C**	**4E**	**5C**	**6B**
76	1.5 ± 0.13 (2)	ND	1.7 ± 0.20 (2)	>100 (2)	87 ± 15 (2)	>100 (2)
77	46 ± 33 (2)	>100 (2)	1.3 ± 1.3 (2)	10 ± 1.9 (2)	0.99 ± 0.063 (2)	>100 (2)
78	0.49 ± 0.039 (2)	>100 (2)	0.82 ± 0.13 (2)	>100 (2)	30 ± 1.9 (2)	>100 (2)

*Mean IC_{50} (μM) ± standard error of the mean (number of determinations); determined by the AlphaScreen assay.

Since **78** had been found to be less selective for KDM2A over KDM4C than the benzene sulfonamide derivative **74**, a series of ten halo- and alkyl-substituted targets was designed to explore the SAR of substitution on the phenyl ring. It was also decided to synthesise the phenethyl derivative to investigate the effect of increasing the length of the alkyl chain between the phenyl ring and the sulfonyl group. These targets were synthesised in parallel from **79** with a success rate of 100% and yields from 59–100% (**Scheme 6**).

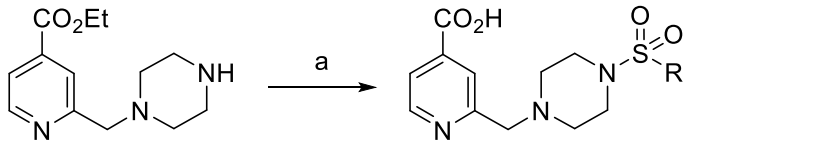

79 **80–89**

R=substituted phenyl, naphthyl or CH_2CH_2Ph

Scheme 6 Synthesis of compounds **80**–**89**. *Reagents and conditions:* (a) i) RSO_2Cl, Et_3N, MeCN; ii) LiOH (aq), MeCN, 59–100%.

The 10 sulfonamides were screened in the JmjC KDM assay panel (**Table 9**).

Table 9 Inhibitory effect (IC_{50} value) of **80–88** against six JmjC KDMs.

		KDM IC_{50}*						KDM2A selectivity over KDM4C
Cmpd	**R**	**2A**	**3A**	**4C**	**4E**	**5C**	**6B**	**(-fold)**
80	*o*-F-phenyl	0.72 ± 0.063 (2)	>100 (2)	0.62 ± 0.23 (2)	>100 (2)	29 ± 2.4 (2)	>100 (2)	0.86
81	*m*-F-phenyl	0.88 ± 0.11 (2)	>100 (2)	2.8 ± 0.70 (2)	>100 (2)	62 ± 11 (2)	>100 (2)	3.2
82	*p*-F-phenyl	0.71 ± 0.049 (2)	>100 (2)	0.72 ± 0.054 (2)	>100 (2)	33 ± 5.0 (2)	>100 (2)	1.0
83	*o*-Cl-phenyl	0.27 ± 0.084 (2)	>100 (2)	0.50 ± 0.092 (2)	>100 (2)	>100 (2)	>100 (2)	1.9
84	*m*-Cl-phenyl	0.64 ± 0.035 (2)	>100 (2)	1.0 ± 0.14 (2)	>100 (2)	76 ± 13 (2)	>100 (2)	1.6
85	*p*-Cl-phenyl	0.81 ± 0.040 (2)	>100 (2)	1.7 ± 0.25 (2)	>100 (2)	42 ± 5.3 (2)	>100 (2)	2.1
86	*p*-tosyl	0.77 ± 0.049 (2)	>100 (2)	1.4 ± 1.6 (2)	>100 (2)	49 ± 4.2 (2)	>100 (2)	1.8
87	1-naphthyl	0.45 ± 0.036 (2)	32 ± 14 (2)	ND	>100 (2)	18 ± 1.1 (2)	25 ± 4.2 (2)	ND
88	2-naphthyl	1.9 ± 0.13 (2)	>100 (2)	0.83 ± 0.59 (2)	>100 (2)	59 ± 5.3 (2)	>100 (2)	0.44
89	CH_2CH_2Ph	0.51 ± 0.046 (2)	>100 (4)	2.5 ± 0.20 (2)	>100 (2)	19 ± 7.6 (2)	>100 (4)	4.9

*Mean IC_{50} (μM) ± standard error of the mean (number of determinations); determined by the AlphaScreen assay.

Introduction of fluoro-, chloro- and methyl-substituents on the phenyl ring (**80–86**) resulted in an increase in activity against both KDM2A and KDM4C with the *ortho*-chlorophenyl compound **83** being the most active against KDM2A (IC_{50}: 0.27 μM) and KDM4C (IC_{50}: 0.50 μM). The 1- and 2-naphthyl derivatives (**87** and **88**) were also found to inhibit KDM2A in the micromolar range, but were not significantly more selective for KDM2A over the other JmjC KDMs tested; in fact **88** was found to be more active against KDM4C (IC_{50}: 0.83 μM) than KDM2A (IC_{50}: 1.9 μM, **Table 9**). The phenethylsulfonyl derivative **89** was also found to be a potent inhibitor of KDM2A (IC_{50}: 0.51 μM) and to be more selective over KDM4C than the other sulfonamide derivatives tested.

A co-crystal was formed when the 1-naphthyl derivative **87** was soaked into crystals of KDM4D. This complex gave a high resolution co-crystal structure (1.9 Å resolution; the crystallisation and refinement of crystallographic data was carried out by Tobias Krojer, **Figure 21**). The X-ray crystal structure confirmed the hypothesis that the isonicotinic acid portion of **87** would occupy the 2OG pocket. **87** indeed binds to the metal in the JmjC domain through the pyridine and piperazine nitrogen atoms, and the carboxylate group interacts with DSBH residues forming an electrostatic interaction with K210 and a hydrogen bond to Y136. The naphthyl moiety extends into the peptide substrate binding pocket and is positioned to form a pi-stacking interaction with Y179. Comparison with a published X-ray crystal structure of KDM4D and a trimethylated H3K9 substrate (PDB ID: 4HON)[148] showed that the sulfonamide-substituted piperazine ring system occupies the same region of the protein as the peptide substrate. A 1.5 Å co-crystal of **83** and

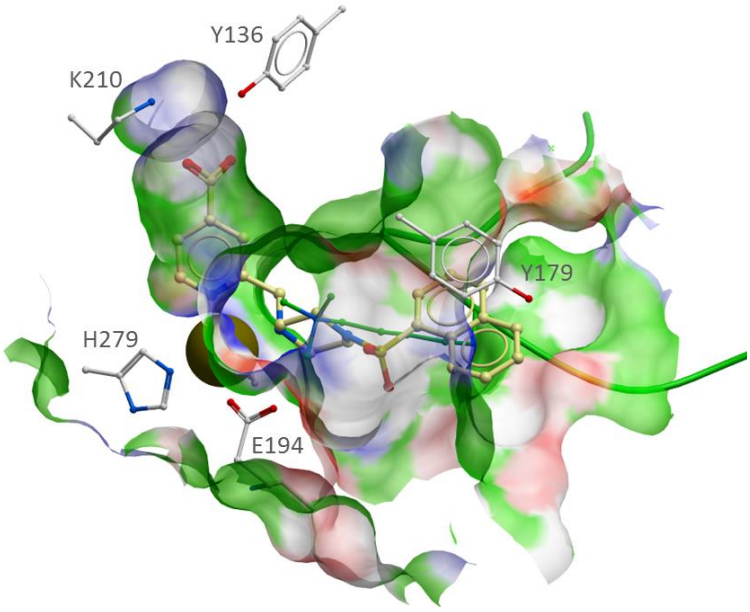

Figure 21 View from a crystal structure of compound **87** (yellow sticks) co-crystallised with KDM4D (key residues shown as grey sticks, unpublished work) overlaid with a view from a crystal structure of an H3K9me3 peptide (green ribbon and sticks) co-crystallised with KDM4D (PDB ID: 4HON). The catalytic iron is substituted by nickel (brown sphere) which is coordinated by H192, E194 and H279.

KDM4D was also obtained (the crystallisation and refinement of crystallographic data was carried out by Tobias Krojer); in this case the isonicotinic acid and piperazine moieties

bind in the same way as **87** but the electron density corresponding to the sulfonamide portion of the inhibitor was not sufficiently defined to determine where it binds in the pocket.

The 1-naphthyl derivative **87** had been found to be a weak inhibitor of KDM6B (IC_{50}: 25 µM) and a co-crystal structure of **87** and KDM6B was also obtained (the crystallisation and refinement of crystallographic data was carried out by Tobias Krojer). An overlay of this structure with the KDM4D structure shows that although the isonicotinic acid and iron-coordinating piperazinyl nitrogen atoms overlay very well in the two structures, the piperazine ring adopts a different conformation in KDM6B which positions the sulfonamide group in a different orientation (**Figure 22**). A tyrosine residue in KDM4D (Y179) is replaced by a glutamine residue in KDM6B (Q1377), removing the possibility of a pi-stacking interaction with the naphthyl ring of **87** at this position. This may partly explain why the naphthyl ring of **87** adopts a different conformation in KDM6B to KDM4D and why the aryl sulfonamides **80–87**, **88** and **89** were found to be weakly active against KDM6B ($IC_{50} \geq 25$ µM).

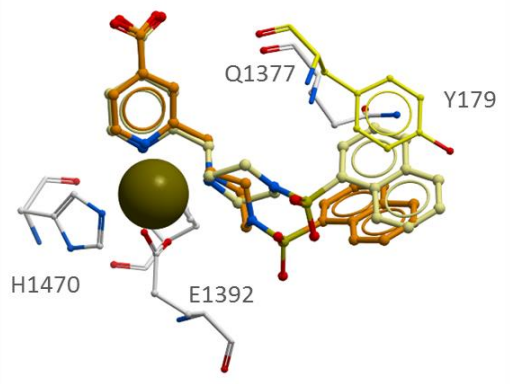

Figure 22 View from a crystal structure of compound **87** (orange sticks) in complex with KDM6B (grey sticks, unpublished work) superimposed with a view from a crystal structure of compound **87** (yellow sticks) in complex with KDM4D (yellow sticks, unpublished work). The catalytic iron is substituted by nickel (brown sphere) which in KDM6B is coordinated by H1470, E1392 and H1390.

2.5 Effect of Modifications to the Aminomethyl Substituent

The aldehyde **47** represented a versatile intermediate for exploring the SAR of the amine substituent. It was proposed to synthesise a series of substituted aminomethyl derivatives for screening in the JmjC KDM assay panel. Secondary and tertiary amines bearing both simple alkyl and aryl substituents and more complex substituents which would be amenable to further derivitisation were designed. Targets were selected that would have a MW < 400 and *c*log*P* < 4 and which could be made in two steps through a reductive amination reaction with aldehyde **47** and commercially available amines followed by ester hydrolysis (**Scheme 7**).

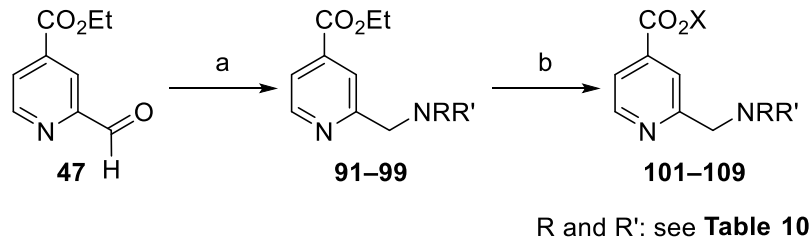

Scheme 7 Synthesis of compounds **101–109**. *Reagents and conditions:* (a) HNRR', STAB, AcOH, CH_2Cl_2, 0–100%; (b) KOTMS, MeCN or LiOH (aq), MeCN, 0–100%.

11 amines were taken into the reductive amination step with aldehyde **47**. No product was isolated from the reactions with methylamine or 4-(benzyloxy)-*N*-methylaniline, however, the other reactions proceeded in 25–100% yield to give nine ethyl ester derivatives **91–99** (**Table 10**). The ethyl esters were deprotected using potassium trimethylsilanolate or lithium hydroxide. The products were either isolated by direct precipitation or purified by reverse phase chromatography to give the carboxylate derivatives **101–109**.

Table 10 Yields and predicted properties of the aminomethyl targets shown in **Scheme 7**.

Amine	Reductive amination		Deprotection					
	Product	**Yield**	**Method**	**X**	**Product**	**Yield**	**MW**	***c*log*P*** [*]
H_2NMe	**90**	NI					166.2	0.02
$HNMe_2$	**91**	84%	KOTMS	K	**101**	86%	180.2	0.37
H_2N^tBu	**92**	69%	LiOH	Li	**102**	89%	208.3	0.99
	**93**	76%	LiOH	H	**103**	36%	220.3	1.1
H_2NPh	**94**	quant.	LiOH	Li	**104**	82%	228.3	2.6
HNMePh	**95**	25%	LiOH	Li	**105**	64%	242.3	2.3
H_2NBn	**96**	93%	LiOH	Li	**106**	quant.	242.3	1.5
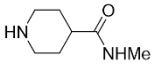	**97**	29%	LiOH		**107**	NI	277.3	0.44
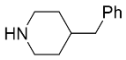	**98**	44%	LiOH	H	**108**	21%	310.4	3.6
$HNBn_2$	**99**	88%	LiOH	Li	**109**[#]	18%	332.4	3.9
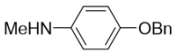	**100**	NI					348.4	4.1

[*]Calculated using ACD labs prediction model,[139] [#]isolated in 75% purity, NI: not isolated.

An alkyne-substituted aminomethyl derivative **110** was also synthesised; the alkynyl group could potentially be used as a handle for derivatisation to 1,2,3-triazoles. This was prepared in a one-pot procedure from the aldehyde **47** and propargylamine (**Scheme 8**).

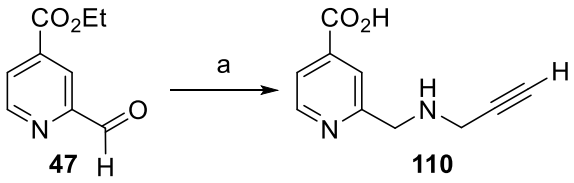

Scheme 8 Synthesis of **110**. *Reagents and conditions:* (a) i) propargylamine, STAB, AcOH, CH_2Cl_2; ii) MeCN, LiOH (aq), 97%.

The resulting aminomethyl derivatives **101**–**106** and **108**–**110** were screened in the JmjC KDM screening panel (**Table 11**).

Table 11 Inhibitory effect (IC_{50} value) of **101**–**106** and **108**–**110** against five JmjC KDMs.

		KDM IC_{50}*						
Cmpd	**NRR'**	**2A**[a]	**3A**[b]	**4A**[b]	**4C**[a]	**4E**	**5C**[a]	**6B**[a]
101	NMe_2	19 ± 7.6 (4)	ND	ND	ND	14 ± 2.1 (2)[a]	ND	>100 (2)
102	HN^tBu	>100 (2)	ND	ND	36 ± 4.8 (2)	ND	71 ± 8.4 (2)	>100 (2)
103		>100 (2)	ND	ND	>100 (2)	ND	48 ± 9.7 (2)	>100 (2)
104	NHPh	3.8 ± 0.36 (2)	ND	ND	16 ± 2.6 (2)	ND	16 ± 1.2 (2)	61 ± 17 (2)
105	NMePh	52 ± 8.6 (2)	ND	ND	18 ± 2.4 (2)	ND	39 ± 7.6 (2)	>100 (2)
106	HNBn	0.45 ± 0.055 (2)	5.3 ± 0.36 (2)	0.58 ± 0.0094 (2)	0.63 ± 0.081 (2)	2.1 ± 0.21 (2)[b]	0.59 ± 0.031 (2)	14 ± 3.0 (2)
108	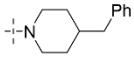	3.3 ± 0.48 (2)	ND	ND	>100 (2)	ND	35 ± 7.3 (2)	>100 (2)
109[#]	NBn_2	12 ± 1.5 (2)	ND	ND	21 ± 14 (2)	ND	35 ± 4.7 (2)	>100 (2)
110	$NHCH_2CCH$	0.64 ± 0.11 (2)	ND	ND	ND	ND	ND	ND

*Mean IC_{50} (μM) ± standard error of the mean (number of determinations); determined by the [a]AlphaScreen assay or the [b]RapidFire assay. [#]isolated in 75% purity

The most active inhibitor of KDM2A in the set of amines was benzyl derivative **106** (IC_{50}: 0.45 μM). Co-crystal structures of **106** with KDM4A and KDM4D were obtained (the crystallisation and refinement of crystallographic data was carried out by Tobias Krojer, **Figure 23**). As would be expected from the high sequence homology of the JmjC domains of KDM4A and KDM4D (74%, **Table 3**), **106** has the same binding mode in both proteins. The crystal structures show that the benzyl substituent can be accommodated by the substrate pocket, occupying the space where the H3K9me3 substrate would normally bind and forming an edge to face interaction with Y175.

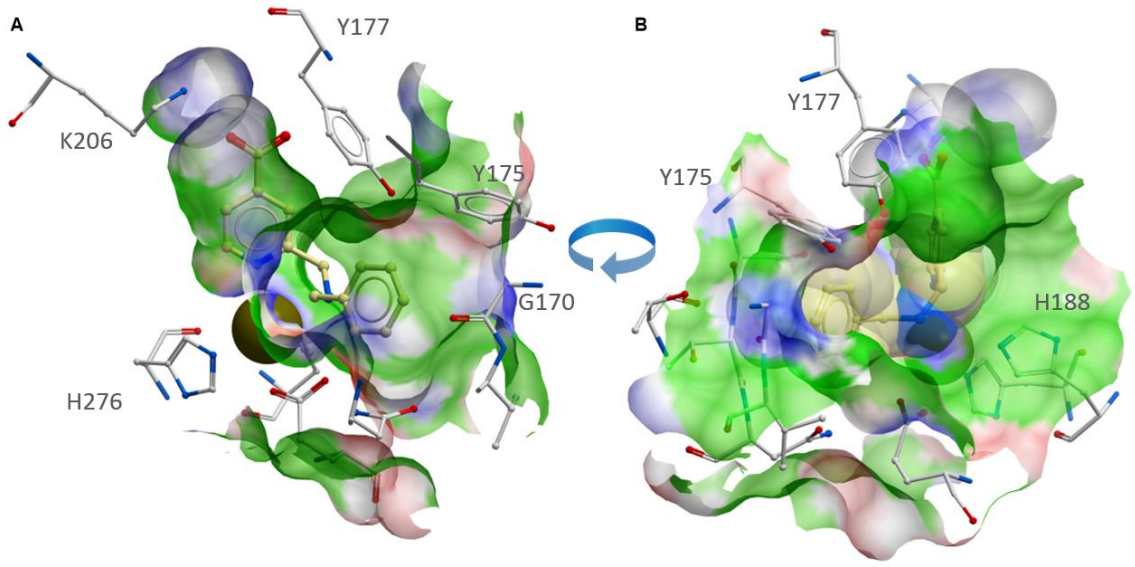

Figure 23 A View from a crystal structure of compound **106** (yellow sticks) in complex with KDM4A (grey sticks, unpublished work). The catalytic iron is substituted by nickel (brown sphere) which is coordinated by H188, E190 and H276. **B** After rotation by 90° about the *y*-axis; compound **106** is shown as yellow sticks and in space-filling representation.

The dibenzyl derivative **109** was found to be more than 30-fold less active than **106** against KDM4A. **109** was docked into the co-crystal structure of **106** with KDM4A using Molsoft internal coordinate modelling (ICM) software.[149] The KDM4A substrate pocket appears

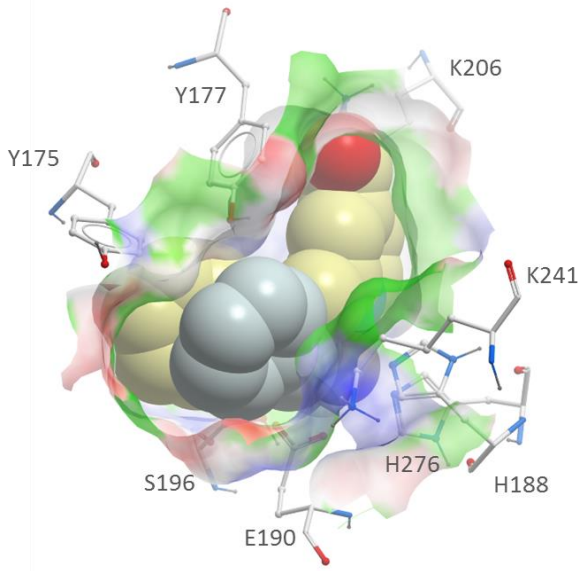

Figure 24 Compound **109** (yellow space-filling display; the additional benzyl group is shown in grey) docked into the crystal structure of compound **106** in complex with KDM4A (grey sticks, unpublished work). The catalytic iron is substituted by nickel (brown sphere) which is coordinated by H188, E190 and H276.

to be able to accommodate the second benzyl ring which might be able to form a cation–pi interaction with K241 (**Figure 24**). The loss in activity may be partly due to the introduction of a second electron withdrawing benzyl group on the aminomethyl nitrogen atom which may reduce its effectiveness as a ligand for iron.

The dimethylamino analogue **101** was found to be a moderately active (double-digit micromolar) inhibitor of KDM2A and KDM4E. Larger substituents that can extend further into the substrate pocket appear to be important to maintain potency. The *tert*-butylamino derivative **102** was found to be a less effective inhibitor of the JmjC KDMs tested (KDM4C IC_{50}: 36 µM, KDM5C IC_{50}: 71 µM, KDM2A, KDM6B: IC_{50} > 100 µM), perhaps due to steric clashes within the substrate binding pocket. Although piperidine **103** is closely related to the piperazine carboxamide and sulfonamide series described above it was found to be much less active against the JmjC KDMs tested indicating that interactions in the KDM active sites formed by substituents on the piperazinyl nitrogen atom are important for potency. Introduction of a benzyl group at the 4-position of the piperidine ring

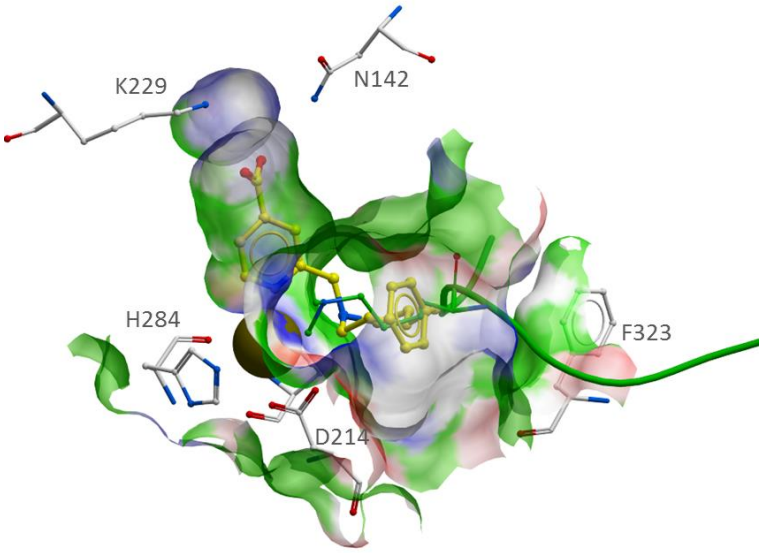

Figure 25 Compound **108** (yellow sticks) docked into the co-crystal structure of 2OG and H3K36me2 in complex with KDM2A (key KDM2A binding residues shown as grey sticks and the substrate shown as a green ribbon and green sticks; PDB ID: 4QX7). The catalytic iron is substituted by nickel (brown sphere) which is coordinated by H212, D214 and H284.

(compound **108**) resulted in a small increase in KDM5C activity and a greater than 30-fold increase in KDM2A activity confirming that substitution at this position is important for potency. **108** was docked into a KDM2A, 2OG and dimethylated H3K36 peptide co-crystal structure after removing the substrates. This showed that the enhancement in activity against KDM2A may be due to the phenyl ring occupying the lipophilic KDM2A substrate pocket (**Figure 25**).

The aniline derivative **104** was found to be less active (KDM2A IC_{50}: 3.8 µM, KDM4C IC_{50}: 16 µM, KDM5C: IC_{50} 16 µM, KDM6B: IC_{50} 61 µM) than the corresponding benzyl derivative **106** (KDM2A IC_{50}: 0.45 µM, KDM4C IC_{50}: 0.63 µM, KDM5C: IC_{50} 0.59 µM, KDM6B: IC_{50} 14 µM). A key factor in this reduction in potency is likely to be the delocalisation of the aniline nitrogen lone pair in the aromatic ring rendering it less available for coordination to iron(II). Introduction of a methyl group on the aniline nitrogen atom (compound **105**) resulted in further loss of potency against the JmjC KDMs tested (KDM2A IC_{50}: 52 µM, KDM4C IC_{50}: 18 µM, KDM5C: IC_{50} 39 µM, KDM6B: IC_{50} > 100 µM).

110 was found to inhibit KDM2A in the micromolar range (IC_{50}: 0.64) and so represents a useful intermediate for derivatisation and could potentially be used in triazole-forming reactions inside the KMD2A active site in a target-guided synthesis (TGS)[150] approach. In TGS, two or more reactants with an affinity for the target protein of interest are incubated with the target. If both reactants bind in the same region of the target, their proximity to one another may facilitate their reaction. A mixture of different reactants can be used concurrently to combine screening and synthesis in one step; only those reactants whose substituents form the most favourable interactions within the active site would react.[150] TGS has been successfully applied to azide–alkyne cycloadditions,[151, 152] indicating that this approach might be of interest for the generation of triazole hits for KDM2A. This

could allow active substituents to be determined without synthesising and purifying each one individually.

2.6 Discussion

A moderately active KDM4E HTS hit has been optimised by the introduction of a carboxylate group in the 4-position of the pyridine ring and by exploration of the substituted piperazine SAR. The binding mode was confirmed through X-ray crystallography. Prior to this work, the only example of a JmjC KDM inhibitor binding to iron through a nitrogen atom that was not part of an aromatic ring system was daminozide **18**, however, this work has demonstrated that the scope of binding motifs capable of binding to iron(II) and acting as JmjC KDM inhibitors is wider and can include secondary and tertiary amino substituents (**Figure 26**).

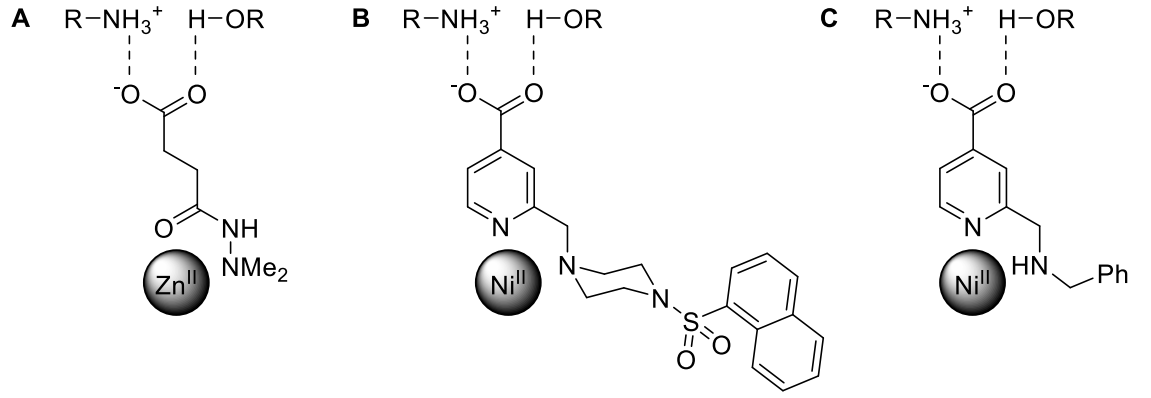

Figure 26 Schematic showing the binding mode of **A** daminozide **18** in complex with KDM7B (from PDB 4DO0), **B 87** in complex with KDM4D (from unpublished crystal structure shown in **Figure 21**) and **C 106** in complex with KDM4A (from unpublished crystal structure **Figure 23**).

Since this work was completed, further aminomethyl substituted pyridine inhibitors, including piperidine **103**, have been disclosed in a patent application (**Figure 27**).[153] Some of these, such as **113** and **114** are potent KDM4C and KDM5C inhibitors. These compounds presumably bind to iron(II) in the same manner as **87** and **106**.

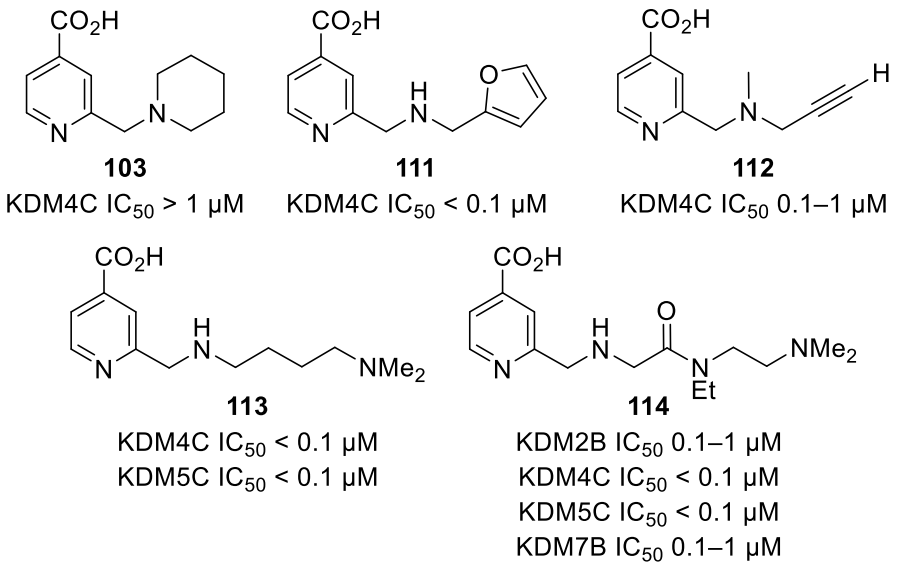

Figure 27 Selected aminomethyl pyridine derivatives reported as inhibitors of JmjC KDMs and reported IC_{50} data determined by fluorescence-based proximity assays.

The amide series **61**–**65** was found to be selective for KDM2A over KDM4E but to inhibit KDM4C and KDM5C in the same range as KDM2A. It was found that replacing the amide functional group with a sulfonamide group resulted in enhanced KDM2A activity and improved selectivity over KDM5C but selectivity over KDM4C was generally found to be poor. The best selectivity over KDM4C was observed with benzene sulfonamide **74** which was 22-fold selective for KDM2A over KDM4C (**Figure 28**). However, introduction of substituents on the benzene ring resulted in an increase in both KDM2A and KDM4C activity so it has proved challenging to introduce selectivity over KDM4C whilst maintaining potency against KDM2A in this series.

The *NH*-piperazine **77** is an interesting lead compound for KDM5C (IC_{50} 0.99 μM); although not selective over the KDM4 subfamily, it was found to be more than 40-fold selective over KDM2A, KDM3A and KDM6B. Its low MW (221.3), low *c*log*P* (–0.32)[138] and high LipE score (6.3) afford considerable scope for further functionalization to improve potency and subfamily selectivity. The piperidinyl analogue **103** was found to be almost 50-fold less active against KDM5C indicating that the piperazinyl nitrogen atom is important for KDM5C activity.

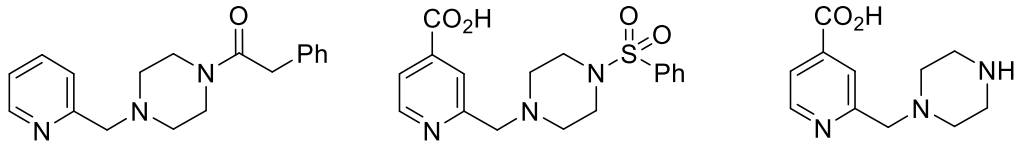

42

74
KDM2A IC_{50} 0.93 μM
KDM4C IC_{50} 22 μM
KDM4E IC_{50} > 100 μM
KDM5C IC_{50} 31 μM

77
KDM2A IC_{50} 46 μM
KDM4C IC_{50} 1.3 μM
KDM4E IC_{50} 10 μM
KDM5C IC_{50} 0.99 μM

Figure 28 KDM4E HTS hit **42** and selected aminomethyl compounds developed from it.

Replacement of the piperazinyl ring system with other amines revealed that the availability of the nitrogen lone pair for coordination to iron(II) is probably an important factor in JmjC KDM activity. The *N*-benzyl derivative **106** demonstrated good activity against KDM2A (IC_{50}: 0.45 μM) but poor selectivity over KDM4C and KDM5C. Co-crystal structures of **106** with both KDM4A and KDM4D demonstrated that the phenyl ring extends into the JmjC KDM substrate pocket so it may be possible to generate inhibitors with subfamily specificity by the introduction of substituents on the phenyl ring that can exploit substrate pocket differences between JmjC KDM family members. The acetylene derivative **110** was found to be a sub-micromolar potency inhibitor of KDM2A (IC_{50}: 0.64 μM) and may be of utility as a reactant in target-guided synthesis.

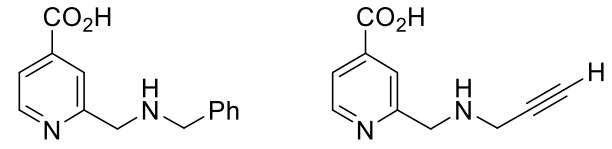

106
KDM2A IC_{50} 0.45 μM
KDM4C IC_{50} 0.63 μM
KDM5C IC_{50} 0.59 μM
KDM6B IC_{50} 14 μM

110
KDM2A IC_{50} 0.64 μM
KDM4C IC_{50} ND
KDM5C IC_{50} ND
KDM6B IC_{50} ND

Figure 29 Two compounds in the aminomethyl series with sub-micromolar potency JmjC KDM activity.

Some of the aminomethyl compounds were tested in cellular assays and the results are described below (Chapter 5).

Chapter 3. Identification of a Triazolopyridine Scaffold for JmjC KDM Inhibition

3.1 Introduction

Most inhibitors of the JmjC KDMs described to date are 2OG mimetics;[91] one such series contains a 2,2'-bipyridine scaffold wherein one of the pyridine rings bears a carboxylate group at the 4-position. Variation of amide substituents at the 4-position of the other pyridine ring led to the discovery of a KDM4 subfamily selective inhibitor **23.**[117] An X-ray crystal structure of compound **23** in complex with KDM4A showed that the pyridyl nitrogen atoms bind to iron(II) in a bidentate manner and that the 4-carboxy group mimics the 5-carboxy group of 2OG (**Figure 30**).[117]

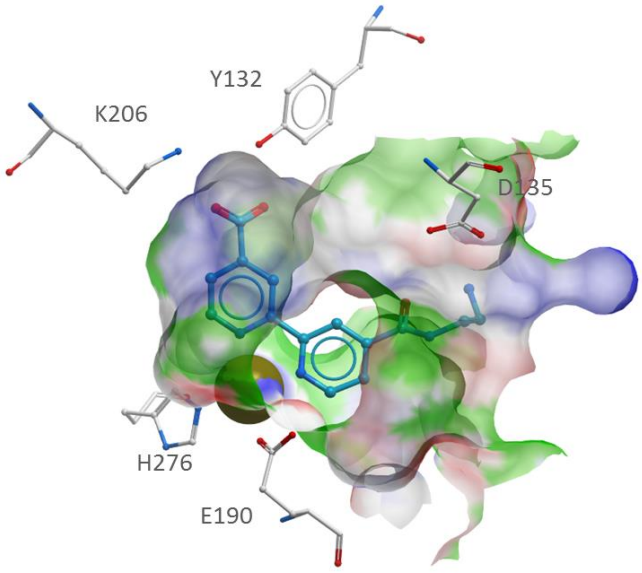

Figure 30 View from a crystal structure of 2,2'-bipyridyl KDM4 inhibitor **23** (blue sticks) in complex with KDM4A showing that the two pyridine nitrogen atoms interact with nickel (brown sphere) that replaces iron in the active site and that the carboxylate group forms hydrogen bonding interactions with K206 and Y132 in place of the 5-carboxy group of 2OG. PDB ID: 3PDQ.

2,2'-Bipyridine compounds are commonly used ligands in organometallic chemistry,[154] however, these ligands frequently have a plane of symmetry between the two pyridine rings. Some of the synthetic approaches to 2,2'-bipyridine compounds that have been

reported in the literature are summarised below (**Figure 31**). Synthesis of 2,2'-bipyridine systems through cross-coupling chemistry is challenging due to the instability of many organometallic 2-pyridine derivatives,[155] and because of the propensity of the 2,2'-bipyridine products to coordinate the transition metal catalyst, which can stall the catalytic cycle.[156] An alternative disconnection wherein one of the pyridine rings is formed in cyclisation or cycloaddition reactions allows access to a variety of non-symmetrically substituted bipyridine products, for example through the Kröhnke pyridine synthesis, however, the scope of suitable pyridine-ring forming reactions is limited by the availability of the appropriately substituted starting materials.[157] Symmetrical 2,2'-bipyridine compounds can be synthesised through metal-catalysed homocoupling of 2-halopyridines (Ullmann coupling)[154, 158] or pyridine derivatives that are unsubstituted in the 2-position using catalytic ferric chloride[159] or Raney nickel[160] (**Figure 31B**). The product scope from homocoupling-type reactions is limited by the plane of symmetry in the products generated and the forcing conditions required for these reactions to proceed.

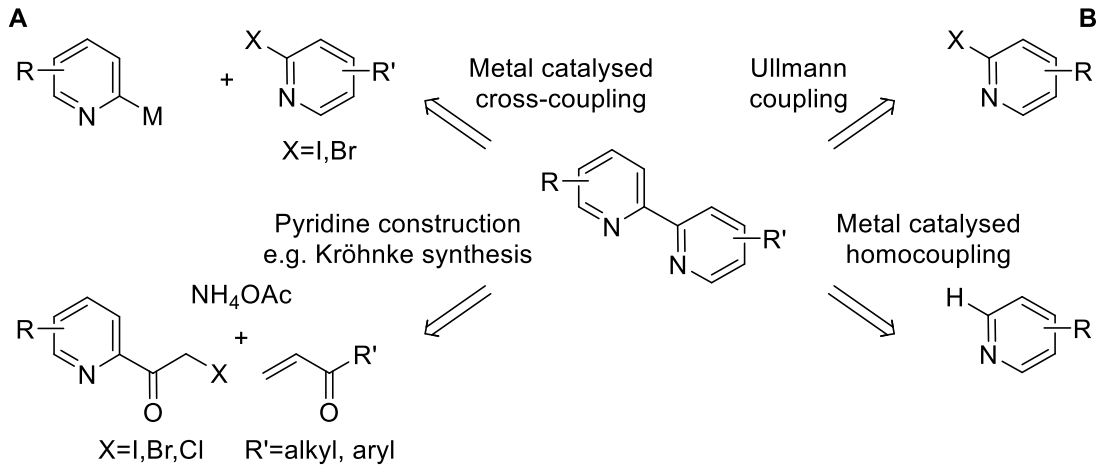

Figure 31 Possible routes to **A** unsymmetrical and **B** symmetrical 2,2'-bipyridine compounds (R=R').

3.2 Design of an Alternative Iron Binding Scaffold

The synthetic challenge of constructing 2,2'-bipyridine systems limits the scope of 2,2'-bipyridine targets that are amenable to chemical synthesis. Thus a new scaffold was

designed based on the 2,2'-bipyridine series where one of the pyridine rings was replaced with a 1,2,3-triazole ring (**Figure 32**).

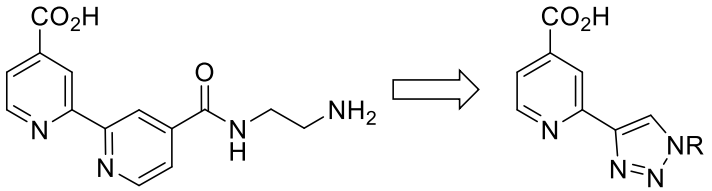

23

Figure 32 Proposed new triazolopyridine scaffold.

It was proposed that the triazole motif in the new scaffold would be able to coordinate iron(II) in place of the second pyridine ring and readily enable the exploration of alternative vectors for compound elaboration through substitution at C5 and N1. This would enable rapid exploration of the SAR with the aim of achieving subfamily selectivity by exploiting differences in the substrate binding pockets of the different JmjC KDM family members.

It was envisaged that the triazole ring could be constructed from an alkyne and a substituted azide using the copper-catalysed click reaction developed by Sharpless *et al.*[161, 162] Click reactions have been defined as facile, single-step reactions which do not generate problematic by-products, have a high thermodynamic driving force and are high yielding; other examples of click reactions are nucleophilic epoxide ring opening and dioxolane formation from 1,3-diols and aldehydes or ketones.[163]

1,2,3-Triazoles have found extensive application in medicinal chemistry, both as linking groups, for example in bioconjugation,[164] and as pharmacophores in their own right, for example in the antibiotics tazobactam **115** and cefatrizine **116** (**Figure 33**).[165]

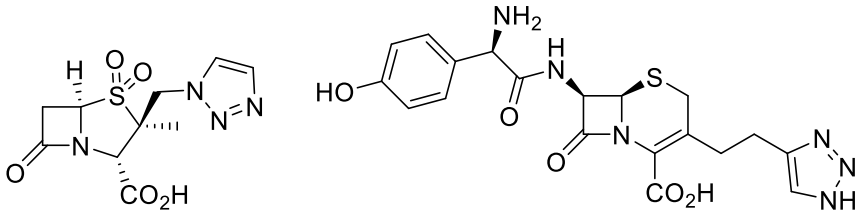

Figure 33 Two 1,2,3-triazole containing antibiotic drugs; Tazobactam and Cefatrizine.

A protected alkyne intermediate **118**, which could be deprotected to give a terminal alkyne for copper-catalysed click reactions, was prepared in excellent yield from the corresponding bromide *via* Sonogashira coupling with trimethylsilylacetylene, using a method reported in the literature (**Scheme 9**).[166]

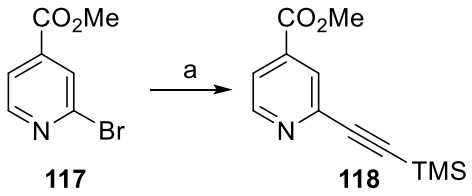

Scheme 9 Synthesis of compound **118**. *Reagents and conditions:* (a) trimethylsilylacetylene (TMSCCH), CuI, $Pd(PPh_3)_4$, Et_3N, THF, 85%.

A small set of triazole derivatives was designed which could be synthesised from the trimethylsilyl- (TMS) protected acetylene derivative **118**. Substituted azides (which were kindly donated by Pfizer) were selected which would generate targets with good lead-like properties (molecular weight 200–350 $gmol^{-1}$, *c*log*P* < 3)[167, 168] and which would be amenable to follow-up using parallel chemistry, for example Suzuki cross-coupling or amide bond formation (**Table 12**).[169]

Table 12 Predicted properties of substituted triazole targets.

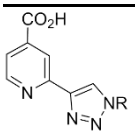	R	MW	*c*log*P**	Hydrogen bond	
				Donors	Acceptors
120		280.3	2.2	1	6
121		292.3	0.5	1	8
122		294.3	2.3	1	6
123		295.3	1.5	3	7
124	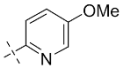	296.3	2.2	1	7
125	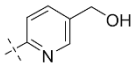	297.3	0.35	2	8
126	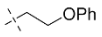	310.3	2.1	1	7
127	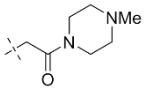	330.3	–0.4	1	9
128	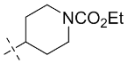	345.4	1.8	1	9
129	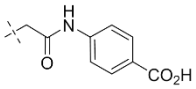	367.3	0.9	3	10
130	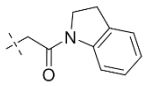	349.4	1.1	1	8

*Calculated using ACD labs prediction model.[139]

3.3 Synthesis of a Small Set of Triazolopyridine Derivatives

The benzyl derivative was prepared initially to pilot the chemistry and determine its suitability for parallel synthesis. *In situ* deprotection of the TMS-protected acetylene derivative **118** with tetrabutylammonium fluoride and reaction with commercially available benzyl azide gave the triazole compound **119** in 69% yield using a method adapted from that of Friscourt *et al.*[170] Deprotection of the methyl ester **119** with potassium trimethylsilanolate gave the carboxylic acid **120** in 87% yield (**Scheme 10**).

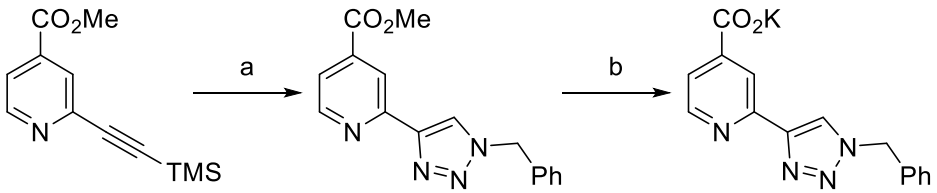

Scheme 10 Synthesis of benzyl substituted triazole **120**. *Reagents and conditions:* (a) benzyl azide, tetra-*n*-butylammonium fluoride (TBAF), CuI, *N*,*N*-diisopropylethylamine (DIPEA), MeOH, 69%; (b) KOTMS, MeCN, 87%.

The assignment of the regiochemistry of the product was assisted by nuclear Overhauser effect (NOE) studies (**Figure 34**). Thus, irradiation at 8.40 ppm (corresponding to the chemical shift observed for the triazole *CH*) resulted in a positive NOE at 8.48 ppm (pyridinyl *C3H*), 7.39 –7.40 (phenyl *CH*) and 5.68 (benzyl CH_2) consistent with a 1,4-substituted 1,2,3-triazole.

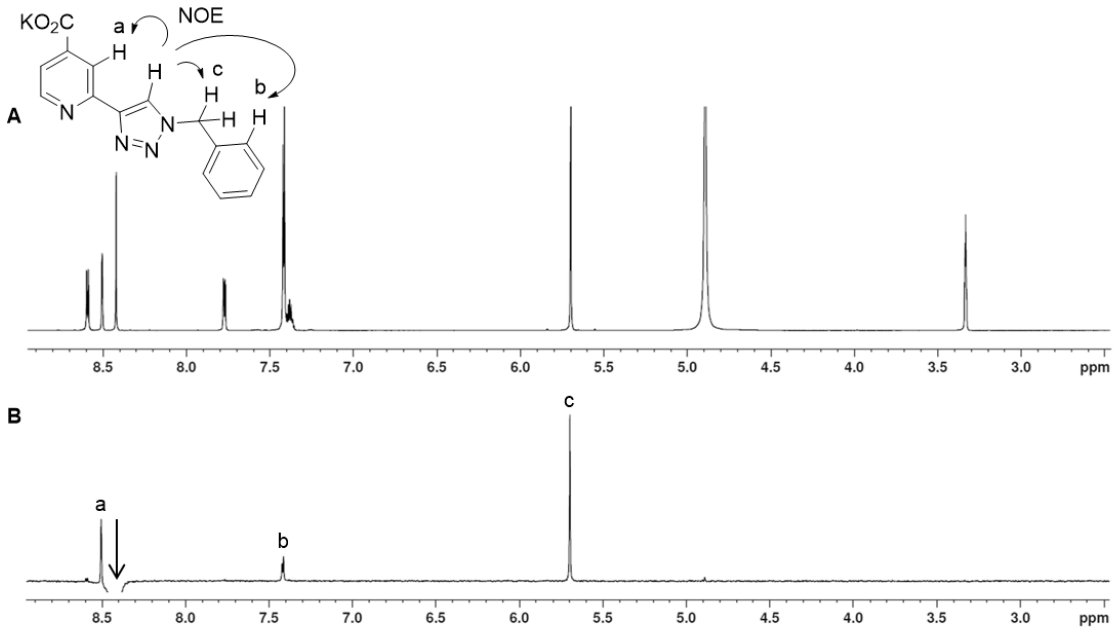

Figure 34 A ^{1}H NMR spectrum of **120**; **B** irradiation of the triazole *CH* signal at 8.40 ppm resulted in enhancement of the pyridinyl *C3H* signal (a), the phenyl *CH* signal (b) and the benzyl CH_2 signal (c).

This procedure was applied in a parallel fashion with a further 10 alkyl and aryl azides (kindly donated by Pfizer). A solution of potassium trimethylsilanolate in acetonitrile was added to the crude products of the copper-catalysed click reaction and the resulting

precipitates purified by preparative high-performance liquid chromatography (HPLC, performed by Katie Bainbridge) to give the target compounds with a success rate of 40% (**Scheme 11**).

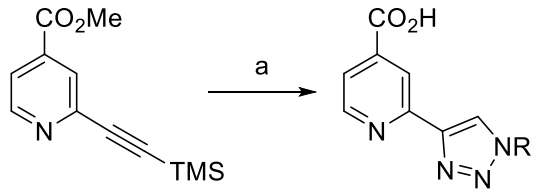

118 **122**, **123**, **126** and **128**
R: see **Table 13**

Scheme 11 Synthesis of substituted triazoles **122**, **123**, **126** and **128** in a one-pot procedure. *Reagents and conditions:* (a) i) RN_3, TBAF, CuI, DIPEA, MeOH; ii) KOTMS, MeCN, 6–50%.

The five resulting substituted triazole derivatives were screened in the JmjC KDM screening panel (**Table 13**). All compounds were found to have a moderate inhibitory effect against KDM2A, KDM3A and KDM5C (IC_{50} < 20 μM where tested). Inhibition of KDM4A/C/E and KDM6B was found to be considerably weaker ($IC_{50} \geq 38$ μM). This represented an improvement in selectivity for KDM2A and KDM5C over KDM4C compared to the aminomethyl pyridine inhibitors described in the previous chapter.

Table 13 Inhibitory effect (IC_{50} value) of substituted triazoles in seven JmjC KDMs

		KDM IC_{50}*						
Cmpd	**R**	**2A**	**3A**	**4A**	**4C**	**4E**	**5C**	**6B**
120		8.3 ± 1.4 (2)	11 ± 3.3 (2)	65 ± 9.1 (4)	40 ± 5.9 (2)	>100 (4)	7.3 ± 1.2 (2)	>100 (4)
122		6.4 ± 0.94 (2)	2.9 ± 0.46 (2)	54 ± 8.3 (4)	38 ± 3.5 (2)	97 ± 23 (2)	6.6 ± 1.2 (2)	79 ± 14 (4)
123		17 ± 4.0 (2)	ND	ND	ND	ND	ND	>100 (2)
126		6.1 ± 0.74 (2)	9.2 ± 2.0 (2)	>100 (4)	>100 (2)	>100 (2)	8.2 ± 0.88 (2)	71 ± 9.4 (4)
128	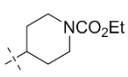	7.3 ± 1.5 (2)	17 ± 5.5 (2)	>100 (4)	>100 (2)	>100 (2)	3.9 ± 0.43 (2)	>100 (4)

*Mean IC_{50} (μM) ± standard error of the mean (number of determinations); determined by the AlphaScreen assay.

3.4 Synthesis of the *NH*-Triazole Derivative

NH-Triazoles are often synthesised from protected triazoles (prepared using suitably substituted azides) because sodium azide is relatively unreactive towards the copper-catalysed click reaction.[171] The pivaloyloxymethyl group was selected as a good protecting group for triazole because it can be readily removed using sodium hydroxide[171] and this would allow the deprotection of both the triazole and the carboxylic acid protecting groups in a one-pot procedure.

The pivaloyloxymethyl-protected triazole **133** was synthesised using a method modified from that developed by Loren *et al*.[171] Azidomethyl pivalate **132** was prepared from chloromethyl pivalate **131** and sodium azide in 74% yield according to the method described in the literature (**Scheme 12**).[171] Employing azidomethyl pivalate in the copper-catalysed click reaction with **118** gave the pivaloyloxymethyl-protected triazole **133** in moderate yield. Deprotection of the carboxylic ester and pivaloyloxymethyl group with sodium hydroxide gave the *NH*-triazole (**Scheme 12**) which was screened in the JmjC KDM assay panel (**Table 14**).

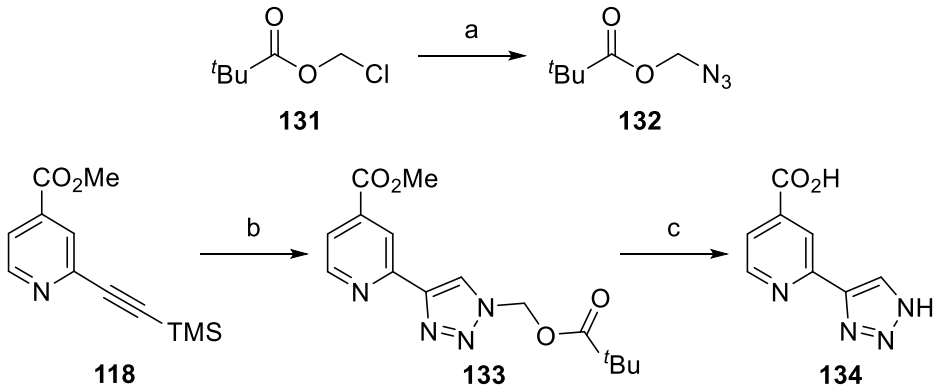

Scheme 12 Synthesis of *NH*-triazole **134**. *Reagents and conditions:* (a) NaN_3, H_2O, 90 °C, 74%; (b) **132**, TBAF, $CuSO_4 \cdot 5H_2O$, (+)-sodium L-ascorbate, DMF, H_2O, 65 °C, 53%; (c) NaOH, H_2O, MeOH, 61%.

In order to assess the impact of replacing a pyridine ring with a the triazole ring, the commercially available unsubstituted 2,2'-bipyridine **135** was also screened in the JmjC KDM assay panel (**Table 14**).

Table 14 Inhibitory effect (IC_{50} value) of the *NH*-triazole **134** and 2,2'-bipyridine **135** against seven JmjC KDMs.

Cmpd		KDM IC_{50}*						
		2A	**3A**	**4A**	**4C**	**4E**	**5C**	**6B**
134	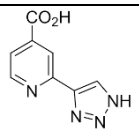	6.6 ± 0.91 (8)	17 ± 3.2 (2)	2.8 ± 1.1 (2)	5.6 ± 1.0 (4)	16 ± 2.7 (4)	11 ± 2.8 (4)	>100 (6)
135	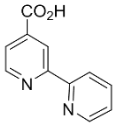	3.6 ± 0.71 (2)	1.2 ± 0.13 (4)	1.1 ± 0.062 (4)	0.46 ± 0.067 (4)	0.33 ± 0.073 (2)	0.53 ± 0.044 (2)	11 ± 1.3 (6)
Potency gain for **135** over **134** (-fold)		1.8	14	2.5	12	49	21	>9

*Mean IC_{50} (μM) ± standard error of the mean (number of determinations); determined by the AlphaScreen assay.

The *NH*-triazole **134** was found to inhibit KDM2A and KDM5C in the same range as the substituted analogues **120, 122, 123, 126** and **128** (IC_{50} < 20 μM) and to be selective over KDM6B (IC_{50} > 100 μM) but not KDM4A/C/E (IC_{50} < 20 μM). The 2,2'-bipyridine **135** was found to inhibit KDM2A, KDM3A, KDM4A/C/E and KDM5C in the single digit micromolar range and to be a moderately active inhibitor of KDM6B (IC_{50} 11 μM).

The inhibitory effect of triazolopyridine **134** was 1.8–49 fold weaker than that of 2,2'-bipyridine **135** against every JmjC KDM screened. Since **134** (*c*logP 0.47)[138] is more polar than **135** (*c*logP 1.5)[138] this could be due to the greater desolvation energy on binding of **134** compared to **135**. Electronic effects may also influence the decreased activity of **134**; 1,2,3-triazole has been shown to be a less effective ligand for platinum(I) than pyridine,[172] and the bite angle of the triazolopyridine scaffold may also be less favourable than that of the 2,2'-bipyridine scaffold. Interestingly, the degree of reduction in potency was KDM-specific; there was a greater than 10-fold reduction in potency against KDM3A, KDM4C/E, KDM5C and KDM6B but a less than 2-fold reduction in potency against KDM2A and KDM4A. These results demonstrate that a degree of JmjC KDM subfamily

selectivity can be achieved through changes in the 2OG mimicking scaffold itself as well as through the introduction of substituents which can bind deeper into the substrate pocket.

3.4.1 Co-crystal Structure of the *NH*-Triazole and KDM4A

In order to verify whether compound **134** binds to JmjC KDMs in the predicted binding mode (as a 2OG mimetic) it was soaked into crystals of KDM4A (the crystallisation and refinement of crystallographic data was carried out by Tobias Krojer; PDB ID: 4URA).[173] The resulting crystal structure confirmed the hypothesis that the triazolopyridine motif would coordinate the metal, and that the carboxylate group would form a salt bridge with K206 and a hydrogen bond with Y132 (**Figure 35**). Comparison with a crystal structure of 2OG and an H3K9me3 peptide in KDM4A (PDB ID: 2Q8C)[106] showed that the triazole ring of **134** partly extends into the *N*-methylated lysine substrate binding pocket. The pyridine nitrogen atom binds in the same position as the 2OG 2-oxo carbonyl but the triazole N occupies a different coordination site to the 2OG C-1 carboxylate positioning the triazole ring in the substrate binding site.

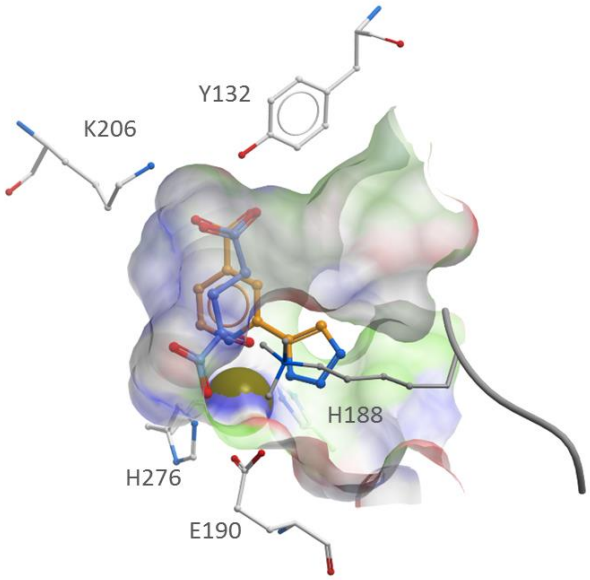

Figure 35 Overlay of a crystal structure of compound **134** (orange sticks) in complex with KDM4A (PDB ID: 4URA) and of 2OG (pale blue sticks) and an H3K9me3 peptide (grey ribbon and sticks) in complex with KDM4A (PDB ID: 2Q8C). The catalytic iron is substituted by nickel (brown sphere) which is coordinated by H188, E190 and H276.

Although the 2OG and iron binding residues in JmjC KDMs are relatively highly conserved,[52] close analogues of 2OG (for example daminozide, **18**, an inhibitor of the KDM2/7 subfamily)[114] do demonstrate a degree of subfamily selectivity, presumably engendered partly by differences in the 2OG binding pockets. It was therefore expected that modifications to the pyridine ring would have an impact on subfamily selectivity. Modifications to the triazole ring substituents will be addressed in the next chapter.

3.5 Effect of Modifications to the Pyridine Ring

Other scaffolds were designed based on the triazolopyridine core wherein the pyridine ring would be replaced with other six-membered heterocycles which would retain a nitrogen atom capable of chelating iron(II) in the JmjC KDM active site but contain heteroatoms or substituted carbon atoms at positions 3-, 5- or 6- of the pyridine ring which might impart further JmjC KDM subfamily selectivity (**Figure 36**).

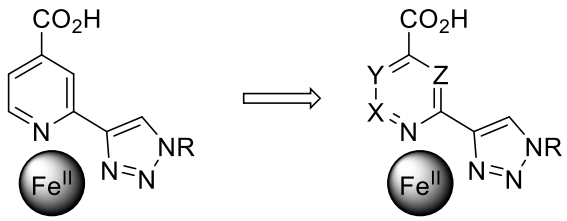

Figure 36 Proposed scaffolds wherein the pyridine ring of **120** and **134** is replaced with other six-membered heterocycles.

It was proposed to synthesise these from the TMS-protected alkynes which would be prepared from the corresponding aryl halides in a route analogous to that used to synthesise the triazolopyridine targets. The number of targets easily accessible through this route was limited by the commercial availability of the aryl halides; the aryl iodides and bromides were not available commercially however a number of suitable aryl chlorides were available (**Figure 37**).

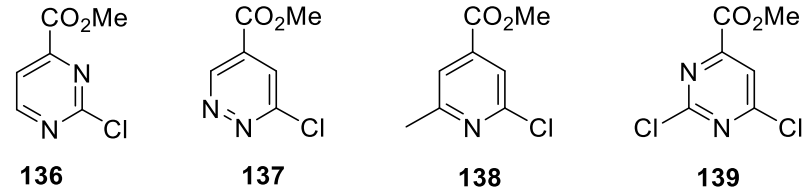

Figure 37 Some commercially available heteroaryl halides bearing a carboxylic ester para- to a nitrogen atom.

Sonogashira cross-couplings with aryl chlorides are in general more challenging than with aryl bromides due to the greater strength of carbon–chlorine bonds in comparison to carbon–bromine bonds.[174] Submitting the pyrimidyl substrate **136** to the reaction conditions used for the 2-bromopyridine derivative **117** gave the cross-coupling product in less than 2% yield. It was therefore necessary to optimise the Sonogashira conditions for the aryl chloride through exploration of the most effective solvent, catalyst and temperature. The addition of 20 mol% of triphenylphosphine, replacement of tetrahydrofuran with *N*,*N*-dimethyl formamide and increasing the reaction temperature from room temperature to 50 °C resulted in a dramatically increased yield of 83% (**Scheme 13**).

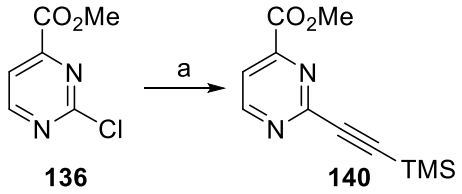

Scheme 13 Synthesis of TMS-protected alkyne **140**. *Reagents and conditions:* (a) TMSCCH, CuI, $Pd(PPh_3)_4$, PPh_3, Et_3N, DMF, 50 °C, 83%.

Application of these conditions to Sonogashira cross-couplings with the other three aryl chlorides **137**–**139** gave two of the corresponding TMS-protected alkynes (**141** and **142**, **Scheme 14**) in 43–72% yield. However, the 2,6-dichloropyrimidine derivative **139** did not give any of the desired product; only the diethylaminopyrimidine derivative **143** was isolated (**Scheme 14**). The diethylamino by-product presumably formed through the displacement of chloride by triethylamine (perhaps *via* an organopalladium intermediate)

to give the quaternary ammonium salt followed by dealkylation upon attack by chloride to give the diethylamino product. It is possible that this side reaction could be avoided if triethylamine was substituted for a more sterically hindered base but this has not been pursued. It was anticipated that the chloride displacement had occurred at the 6-position due to the higher reactivity of the 6-chloro substituent to nucleophilic aromatic substitution; methyl 2,6-dichloropyrimidine-4-carboxylate **139** is known to react with secondary amines such as morpholine regioselectively at the 6-position.[175, 176] Compound **143** was treated with sodium hydroxide to hydrolyse the ester to the carboxylic acid **144**.

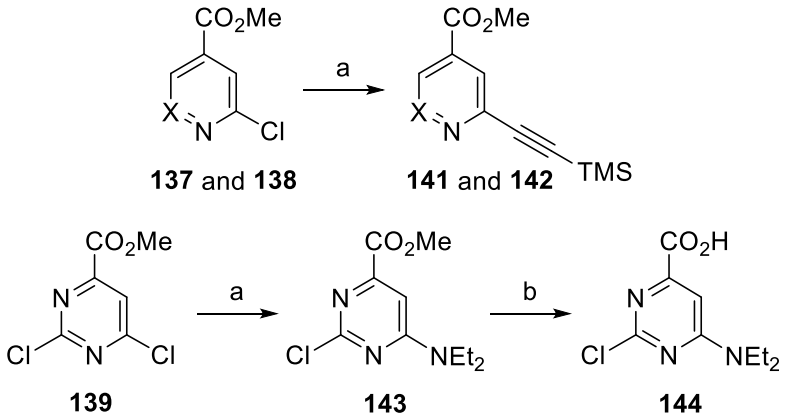

Scheme 14 Synthesis of TMS-protected alkynes **141** and **142** and diamino compound **144**. *Reagents and conditions:* (a) TMSCCH, CuI, $Pd(PPh_3)_4$, PPh_3, Et_3N, DMF, 50 °C; **141**: X=N, 43%; **142**: X=CCH_3, 72%; **143**: 25%; (b) NaOH (aq), MeOH, 73%.

144 was screened for JmjC KDM inhibitory effect but was found to be inactive in those enzymes it was tested against (KDM2A, KDM4C/E and KDM6B, **Table 15**).

Table 15 Inhibitory effect (IC_{50} value) of **144** against four JmjC KDMs.

	KDM IC_{50}*			
Cmpd	**2A**	**4A**	**5C**	**6B**
144	>100 (2)	>100 (2)	>100 (2)	>100 (2)

*Mean IC_{50} (μM) ± standard error of the mean (number of determinations); determined by the AlphaScreen assay.

An NOE experiment was used to assist in the elucidation of the regiochemistry of **144** (**Figure 38**). Thus, irradiation at 6.55 ppm (corresponding to the chemical shift observed

for the pyrimidinyl *C<u>H</u>*) resulted in a positive NOE at 3.48–3.72 (*NC<u>H</u>₂*) indicating that the pyrimidinyl *C<u>H</u>* is in close proximity to the amino group. This result is consistent with displacement of the 6-chloro substituent of **139**.

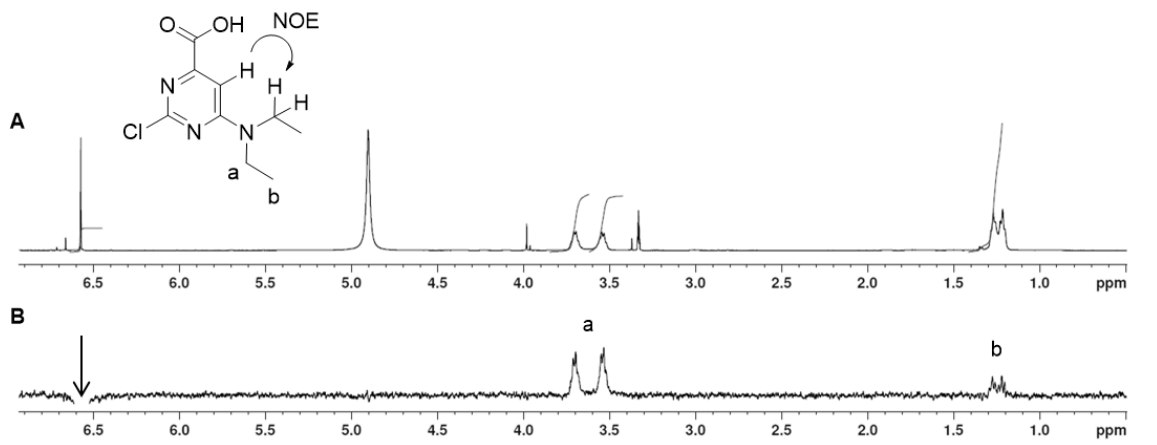

Figure 38 A ^{1}H NMR spectrum of **144**; **B** irradiation at 6.55 ppm resulted in a large enhancement of the *NC<u>H</u>₂* signal (a) and a small enhancement of the *NCH₂C<u>H</u>₃* signal (b).

The resulting TMS-protected alkynes **141** and **142** were submitted to the copper-catalysed click conditions with benzyl azide to give benzyl substituted triazole products. Deprotection with lithium hydroxide either as a one-pot procedure or after isolation of the methyl ester intermediate gave the corresponding targets **145**, **146** and **148** (**Scheme 15**).

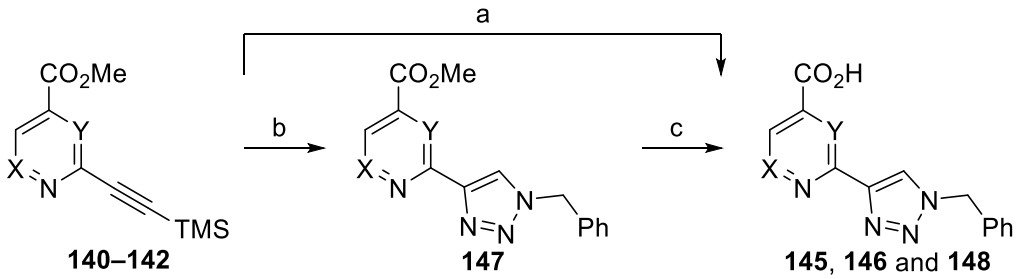

Scheme 15 Synthesis of benzyl substituted triazoles **145**, **146** and **148**. *Reagents and conditions:* (a) for **145** and **146**: i) **140** or **141**, BnN_3, $CuSO_4 \cdot 5H_2O$, sodium L-ascorbate, TBAF, 4:1 DMF:H_2O, RT; ii) LiOH (aq); **145**: X=CH, Y=N, 59%; **146**: X=N, Y=CH, 28%; (b) for **147**, X=CMe, Y=H: **142**, BnN_3, $CuSO_4 \cdot 5H_2O$, (+)-sodium L-ascorbate, TBAF, 4:1 DMF:H_2O, RT, 62%; (c) for **148**, X=CMe, Y=H: **147**, LiOH (aq), THF, 79%;.

The Sonogashira coupling and copper-catalysed click reactions were successfully combined in a one-pot procedure to synthesise the *N*-protected triazole derivatives **149**–

151 which were fully deprotected upon treatment with potassium hydroxide to give **152**–**154** (**Scheme 16**).

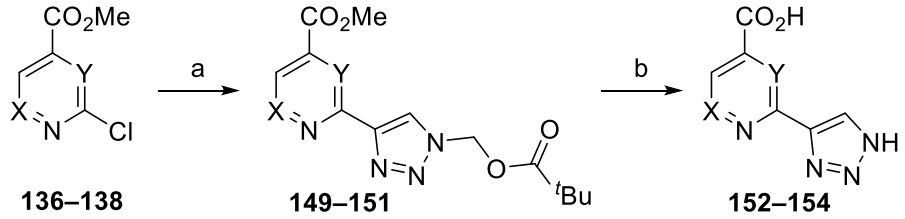

Scheme 16 Synthesis of *NH*-triazoles **152**–**154**. *Reagents and conditions:* (a) i) TMSCCH, CuI, $Pd(PPh_3)_4$, PPh_3, Et_3N, DMF, 50 °C; ii) azidomethyl pivalate, TBAF, CuI, THF, RT; **149**: X=CH, Y=N, 21%; **150**: X=N, Y=CH, 44%; **151**: X=CCH_3, Y=CH, 46%; (b) NaOH, H_2O, MeOH; **152**: X=CH, Y=N, 49%; **153**: X=N, Y=CH, 94%; **154**: X=CCH_3, Y=CH, 41%.

The *NH*- and *N*-benzyl derivatives synthesised through this methodology were screened in the JmjC KDM assay panel (**Table 16**).

Table 16 Inhibitory effect (IC_{50} value) of *NH*- and *N*-benzyltriazole derivatives in five JmjC KDMs.

			KDM IC_{50}*				
Cmpd		**R**	**2A**	**4C**	**4E**	**5C**	**6B**
134	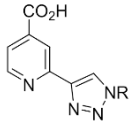	H	6.6 ± 0.91 (8)	5.6 ± 1.0 (4)	16 ± 2.7 (4)	11 ± 2.8 (4)	>100 (6)
120		Bn	8.3 ± 1.4 (2)	40 ± 5.9 (2)	>100 (4)	7.3 ± 1.2 (2)	>100 (4)
152	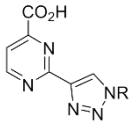	H	72 ± 22 (2)	34 ± 8.7 (2)	>100 (2)	57 ± 9.0 (2)	73 ± 4.5 (2)
145		Bn	>100 (2)	ND	ND	45 ± 12 (2)	>100 (2)
153	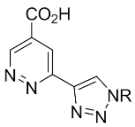	H	21 ± 3.8 (2)	ND	99 ± 12 (2)	17 ± 1.3 (2)	>100 (2)
146		Bn	27 ± 2.6 (4)	ND	ND	4.7 ± 0.75 (2)	>100 (2)
154	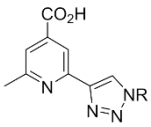	H	22 ± 4.0 (2)	>100 (2)	>100 (2)	>100 (2)	>100 (2)
148		Bn	19 ± 2.9 (4)	ND	ND	46 ± 11 (2)	>100 (4)

*Mean IC_{50} (μM) ± standard error of the mean (number of determinations); determined by the AlphaScreen assay.

Introduction of the methyl group in the 6-position of the pyridine ring resulted in an almost 3-fold reduction in activity against KDM2A from 8.3 μM to 22 μM for the *NH*-triazole

derivative **154**, but a greater reduction in activity against KDM4C/E and KDM5C was observed (from 5.6–16 μM to > 100 μM). These results indicate that the 6-methyl substituent is better tolerated with respect to KDM2A inhibition compared to the other JmjC KDMs tested. Overlaying the 6-methyl pyridine compound **154** with the co-crystal structure of **134** in KDM4A shows that the proximity of a tryptophan residue to the 6-position of the pyridine ring may result in a steric clash with the methyl substituent (**Figure 39**). This finding could provide scope for modifying KDM2A inhibitors by the introduction of a 6-methyl substituent where it is difficult to achieve selectivity over KDM4C/E or KDM5C.

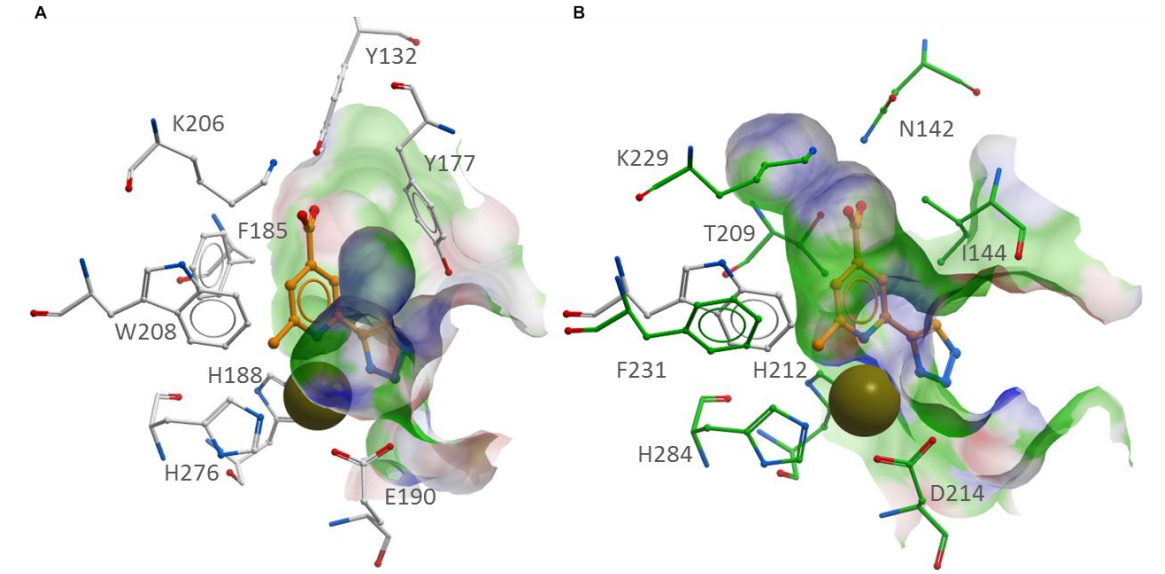

Figure 39 A 6-methyl pyridine **154** (orange sticks) docked into a crystal structure of the pyridine derivative **134** in complex with KDM4A (PDB ID: 4URA). The catalytic iron is substituted by nickel (brown sphere) and key KDM4A residues are shown as grey sticks. There appears to be insufficient space to accommodate the methyl group in the KDM4A binding pocket due to steric clash with W208. **B** 6-methyl pyridine **154** (orange sticks) overlaid with the structure of KDM2A (PDB ID: 4QXZ). The catalytic iron is substituted by nickel (brown sphere) and key KDM2A residues are shown as green sticks. W208 (grey sticks) is replaced with F231 resulting in more space in the pocket for the Me group to occupy.

The pyrimidine derivatives **145** and **152** were found to be less active than the corresponding pyridine derivatives in all the demethylases tested except KDM6B; the *NH*-triazole derivative **152** was found to inhibit KDM6B in the same range as the triazolopyridine **134** (>70 μM). The introduction of a nitrogen atom in the 3-position was

not well tolerated with respect to inhibition of the JmjC KDMs tested; this may be partly due to the electron-withdrawing effect of the second pyrimidinyl nitrogen atom making it a less effective ligand for iron.

Introduction of the pyridazine ring nitrogen atom resulted in a similar reduction in potency as the 6-methyl substituent against KDM2A, KDM4E and KDM6B. However, against KDM5C there was a much smaller loss of activity for the *NH*-triazole derivative **153** and a slight gain in activity for the *N*-benzyl derivative **146** (from 7.3 to 4.7 μM). Pyridine-based inhibitors could potentially be made more selective for KDM5C by introduction of an sp^2 nitrogen atom in the 6-position.

Although the *NH*-triazolopyridine **134** had been found to inhibit KDM2A in the micromolar range with little to no selectivity over KDM4C/E and KDM5C (**Table 14**), modifications to the pyridine ring resulted in gains in subfamily selectivity although generally at the expense of potency.

3.6 Attempted Synthesis of the 1,2,3-Triazole 1,5-Regioisomer

Ruthenium-catalysed azide–alkyne cycloaddition gives access to 1,2,3-triazoles with complementary regioselectivity to the copper-catalysed click reaction (**Figure 40**).

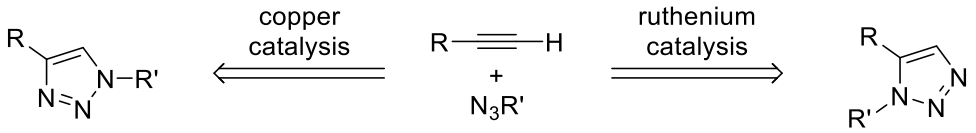

Figure 40 Regioselectivity of the copper- and ruthenium-catalysed azide–alkyne cycloadditions.

It was decided to utilise the ruthenium-catalysed reaction to synthesise the regioisomers of benzyl triazole **120** and phenethyl triazole **122** (**Figure 41**).

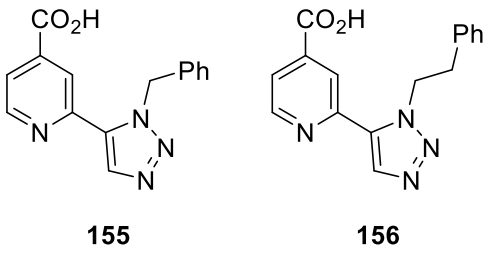

155 **156**

Figure 41 1,5-Substituted triazole targets.

118 was converted to the terminal alkyne **159** in quantitative yield by treatment with potassium fluoride (**Scheme 17**). The terminal alkyne **159** was taken into the ruthenium-catalysed azide–alkyne cycloaddition reaction with cp*Ru(PPh_3)$_2$Cl and benzyl azide or phenethyl azide **158** (which was prepared from the corresponding bromide according to a method described by Shen *et al.*)[177] in a method adapted from that of Boren *et al.*[178] The methyl ester products from the triazole forming reactions were converted to the carboxylic acids with lithium hydroxide (**Scheme 17**).

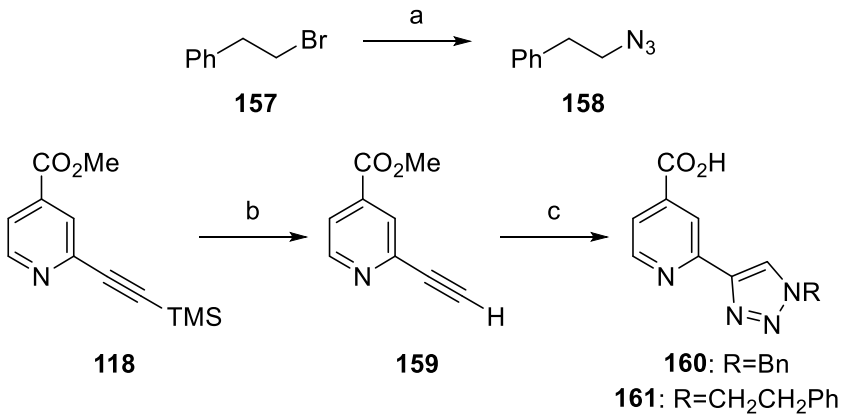

Scheme 17 Attempted synthesis of 1,5-substituted triazole targets **155** and **156**. *Reagents and conditions:* (a) NaN_3, DMSO, 99%; (b) KF, MeOH, quant.; (c) i) cp*Ru(PPh_3)$_2$Cl, RN_3, dioxane, 60 °C; ii) LiOH (aq), MeCN; **160**: R=Bn, 49%; **161**: R=CH_2CH_2Ph, 20%.

In both cases, one of the aromatic *C<u>H</u>* signals was found to overlap with the pyridinyl *C6<u>H</u>* signal by ^{1}H NMR making structural assignment difficult. Therefore, both compounds were converted to the potassium carboxylates by addition of potassium hydroxide to facilitate NOE studies, and allow comparison with the NMR spectra of the previously synthesised 1,4-regioisomer **120**.

NOE experiments and comparison to the ^{1}H and ^{13}C NMR spectra of **120** demonstrated that unfortunately in both cases the 1,4- rather than the desired 1,5-substituted triazoles had been formed (**Figure 42**).

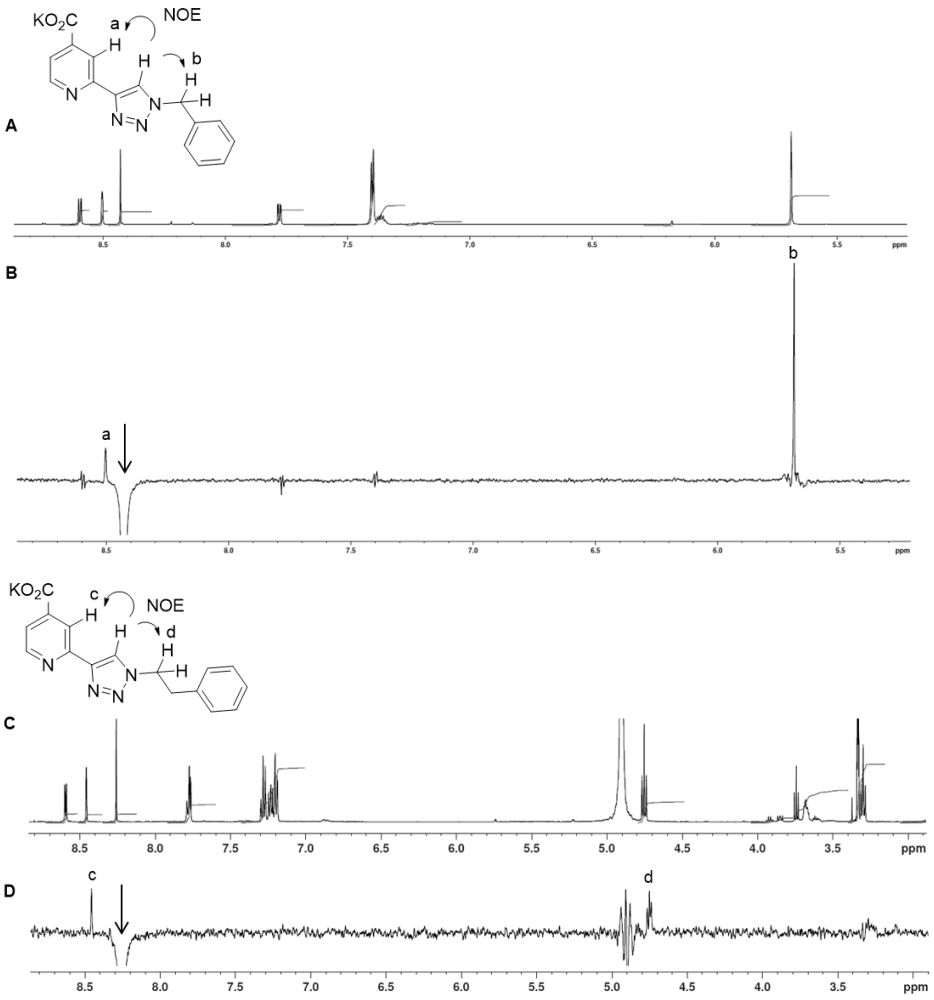

Figure 42 A ^{1}H NMR spectrum of the potassium salt of **160**; **B** irradiation of the triazole *C<u>H</u>* signal at 8.43 ppm resulted in a positive NOE at 8.50 ppm corresponding to the pyridinyl *C3<u>H</u>* (a) and 5.69 ppm corresponding to the benzyl *C<u>H</u>₂* (b); **C** ^{1}H NMR spectrum of the potassium salt of **161**; **D** irradiation of the triazole *C<u>H</u>* signal at 8.26 ppm resulted in a positive NOE at 8.46 ppm corresponding to the pyridinyl *C3<u>H</u>* (c) and 4.75 ppm corresponding to the phenethyl *C<u>H</u>₂* (d).

The 1,5-triazole targets were not isolated from these reactions; it may be that alkyne intermediate **159** contained sufficient levels of copper(I) carried through from the Sonogashira reaction to catalyse the 1,4-triazole formation. It might be possible to form the 1,5-substituted triazole regioisomers by treating **159** with a metal-scavenging resin and

performing the ruthenium-catalysed reaction in scrupulously clean glassware to ensure that no copper was present, however, this has not been pursued.

3.7 Discussion

A novel triazolopyridine JmjC KDM inhibitor scaffold has been identified which binds to JmjC KDMs in the 2OG pocket and coordinates to iron(II) through nitrogen atoms on both the pyridine and triazole rings.

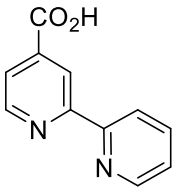

135

KDM2A IC_{50} 3.6 μM
KDM3A IC_{50} 1.2 μM
KDM4A IC_{50} 1.1 μM
KDM4C IC_{50} 0.46 μM
KDM4E IC_{50} 0.33 μM
KDM5C IC_{50} 0.53 μM
KDM6B IC_{50} 11 μM

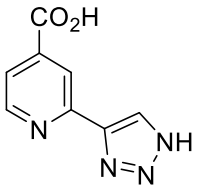

134

KDM2A IC_{50} 6.6 μM
KDM3A IC_{50} 17 μM
KDM4A IC_{50} 2.8 μM
KDM4C IC_{50} 5.6 μM
KDM4E IC_{50} 16 μM
KDM5C IC_{50} 11 μM
KDM6B IC_{50} > 100 μM

Figure 43 Substituting one of the pyridine rings of **135** with a 1,2,3-triazole ring resulted in a different JmjC KDM subfamily selectivity profile.

As for the bipyridine scaffold, exemplified by **135**, this template was found to be most potent against the KDM4 subfamily but to exhibit greater selectivity over KDM6B (**Figure 43**) and was considered an attractive template for medicinal chemistry because structural diversity could be incorporated both by varying the nature of the carboxylate-bearing ring and by substitution on the triazole ring (**Figure 44**).

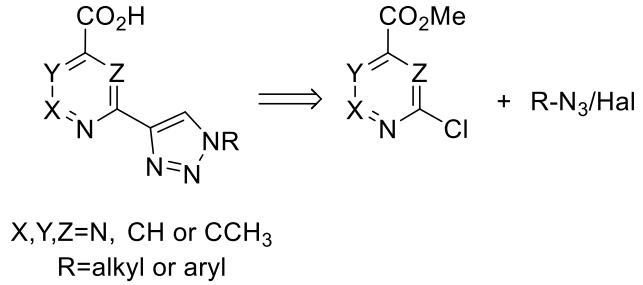

Figure 44 Scope of products accessible through one-pot Sonogashira and triazole-forming chemistry developed for the triazolopyridine series.

Substitution on the triazole ring resulted in compounds that were able to inhibit KDM2A, KDM3A and KDM5C in the same range as the *NH*-triazole **134** but which were found to be selective over the KDM4 subfamily (**Figure 45**).

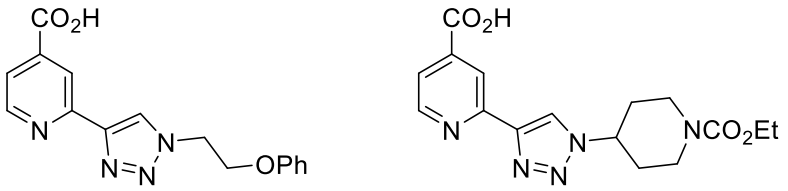

126	**128**
KDM2A IC_{50} 6.1 μM	KDM2A IC_{50} 7.3 μM
KDM3A IC_{50} 9.2 μM	KDM3A IC_{50} 17 μM
KDM4A IC_{50} > 100 μM	KDM4A IC_{50} > 100 μM
KDM4C IC_{50} > 100 μM	KDM4C IC_{50} > 100 μM
KDM4E IC_{50} > 100 μM	KDM4E IC_{50} > 100 μM
KDM5C IC_{50} 8.2 μM	KDM5C IC_{50} 3.9 μM
KDM6B IC_{50} 71 μM	KDM6B IC_{50} > 100 μM

Figure 45 *N*-substituted triazole inhibitors **126** and **128** were found to be more selective for KDM2A, KDM3A and KDM5C over the KDM4 subfamily than the *NH*-triazole inhibitor **134**.

The discovery of the triazolopyridine scaffold has confirmed that a degree of JmjC KDM subfamily selectivity can be achieved through changes in the 2OG mimicking scaffold itself as well as through the introduction of substituents which can access the substrate pocket.

Modifications to the pyridine ring had an effect on subfamily selectivity; introduction of a methyl group at C-6 was found to reduce activity against KDM4C/E and KDM5C and could be used to improve subfamily selectivity for inhibitors of KDM2A, and introduction

of a nitrogen atom at the same position resulted in improved selectivity for KDM5C (**Figure 46**).

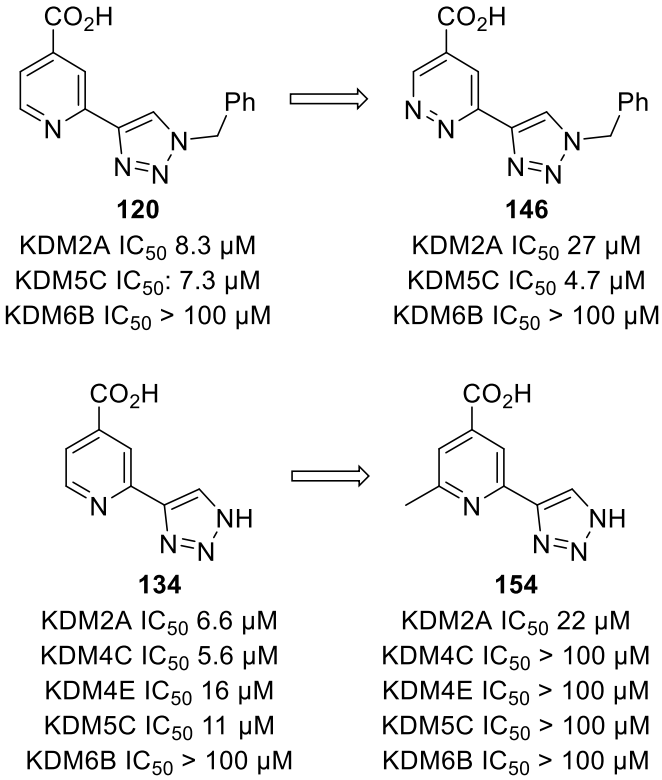

Figure 46 Modification to the 6-position of the pyridine ring had a marked effect on JmjC KDM activity and selectivity.

Chapter 4. Optimisation of the Triazolopyridine Scaffold for KDM2A Inhibition

Some of the work in this chapter has been published[173] and is reproduced in part in this chapter by permission of The Royal Society of Chemistry (RSC).

4.1 Introduction

The discovery of the triazolopyridine scaffold (described in the previous chapter) resulted in a series of micromolar KDM2A inhibitors with good selectivity over the KDM4 subfamily and KDM6 but little selectivity over KDM3A and KDM5C. Although the JmjC domain is characteristic for the JmjC KDM 2OG oxygenases and is relatively conserved between the different JmjC KDMs (see **Table 3**), there is significant variation in the substrate binding pockets. The co-crystal structure of compound **134** with KDM4A showed that the triazole ring extends partly into the substrate binding pocket and it was anticipated that KDM subfamily selectivity for this series of inhibitors might be improved by the introduction of substituents on the triazole ring.

At the time of this work, X-ray crystal structures had not been reported for the JmjC domains of any human KDM3 or 5 subfamily proteins, however, differences in the histone substrate scope for KDM2A (H3K36me2/1),[44] KDM3A/B (H3K9me2/1),[39, 98] and 5A–C (H3K4me3/2)[103] indicated that there was scope to improve the selectivity for KDM2A by the introduction of triazole substituents that would extend further into the histone substrate pocket. Through the synthesis and biological screening of a range of substituted triazoles it was anticipated that KDM2A potency and selectivity could be enhanced by analysis of the SAR of the triazole analogues for the different JmjC KDMs and the design of suitable follow-up analogues which would have more favourable interactions with the substrate

binding pocket of KDM2A than with the substrate binding pockets of the KDM3 and 5 subfamilies.

In order to explore a range of substituted triazole analogues quickly, targets were selected that could be synthesised in fewer than two steps from late-stage intermediates and which would incorporate a range of functional groups in order to introduce chemical diversity into the compounds made.

4.2 *N*-Alkyl and Aryl Substitution of the Triazole Ring

The substituted triazole derivatives had been synthesised through a one-pot silyl deprotection and copper-catalysed click reaction between the TMS-protected alkyne **118** and alkyl or aryl azides (**Scheme 11**). Although a few alkyl or aryl azides are available commercially, the synthesis of further targets would necessitate azide preparation from the corresponding alkyl or aryl halides. The isolation of organic azides is associated with the risk of explosion[179, 180] so it was decided to prepare substituted azides *in situ* without purification from the corresponding halides to reduce the risks associated with handling them and to facilitate the rapid synthesis of different triazole analogues.

Given the interesting selectivity observed for the *NH*-triazole **134**, some simple alkyl and aryl derivatives were designed to investigate the SAR of small triazole substituents. The TMS-protected alkyne **118** was treated with potassium trimethylsilanolate to remove the silyl protecting group and hydrolyse the methyl ester yielding the potassium carboxylate **162** in 81% yield. Reaction with 1.1 equivalents of methyl iodide and 1.2 equivalents of sodium azide in the presence of copper(II) sulfate and (+)-sodium L-ascorbate resulted in formation of the *N*-methyl triazole ring but also resulted in esterification of the carboxylic acid to give the methyl ester **163**. Hydrolysis of the ester with potassium trimethylsilanolate liberated the desired product **164** (**Scheme 18**).

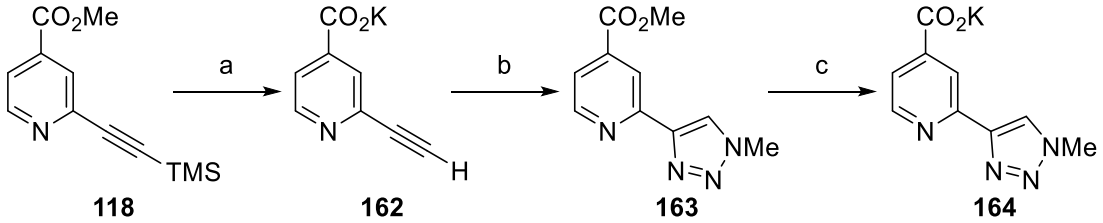

Scheme 18 Synthesis of **164**. *Reagents and conditions:* (a) KOTMS, MeCN, 81%; (b) MeI, NaN_3, $CuSO_4 \cdot 5H_2O$, (+)-sodium L-ascorbate, 4:1 DMF:H_2O, 65 °C, 24%; (c) KOTMS, MeCN, quant.

In order to simplify the synthesis and prepare a variety of analogues more rapidly, a one-pot method was developed which combined *in situ* azide formation with TMS deprotection and copper-catalysed click reaction using a method modified from that developed by Thibault *et al*.[181] This method was successfully applied to both alkyl and aryl halides (with the addition of L-proline as a ligand for copper in the case of *meta*-tolyl iodide) to give **167** and **168** (**Scheme 19**).

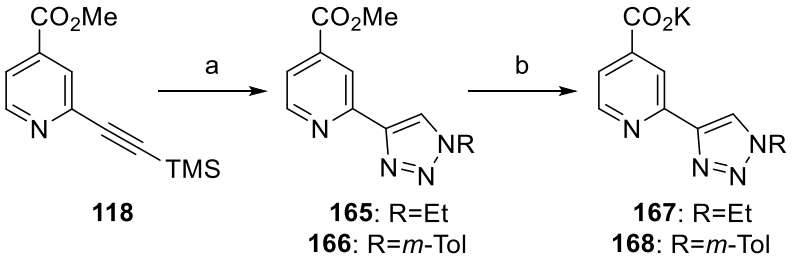

Scheme 19 Synthesis of **167** and **168**. *Reagents and conditions:* for the Et derivative **167** (a) EtI, NaN_3, $CuSO_4 \cdot 5H_2O$, (+)-sodium L-ascorbate, TBAF, 4:1 DMF:H_2O, 65 °C, 77%; (b) KOTMS, MeCN, 59%. For the *m*-tolyl derivative **168** (a) 3-iodotoluene, L-proline, NaN_3, $CuSO_4 \cdot 5H_2O$, (+)-sodium L-ascorbate, TBAF, 4:1 DMF:H_2O, 65 °C, 20%; (b) KOTMS, MeCN, 88%.

The methyl, ethyl and *meta*-tolyl derivatives were screened in the JmjC KDM assay panel (**Table 17**).

Table 17 Inhibitory effect (IC_{50} value) of substituted triazoles **134**, **164**, **167** and **168** against seven JmjC KDMs.

		KDM IC_{50}*						
Cmpd	**R**	**2A**	**3A**	**4A**	**4C**	**4E**	**5C**	**6B**
134	H	6.6 ± 0.91 (8)	17 ± 3.2 (2)	2.8 ± 1.1 (2)	5.6 ± 1.0 (4)	16 ± 2.7 (4)	11 ± 2.8 (4)	>100 (6)
164	Me	16 ± 3.2 (8)	7.8 ± 2.0 (2)	20 ± 4.1 (4)	12 ± 2.8 (4)	46 ± 5.6 (6)	5.7 ± 0.90 (4)	>100 (6)
167	Et	31 ± 5.8 (8)	17 ± 5.5 (2)	ND	6.5 ± 1.1 (4)	39 ± 13 (4)	8.7 ± 0.84 (4)	>100 (4)
168	*m*-tolyl	7.4 ± 0.89 (8)	9.2 ± 2.0 (2)	ND	12 ± 2.8 (4)	24 ± 5.8 (4)	4.3 ± 0.50 (4)	51 ± 4.9 (6)

*Mean IC_{50} (μM) ± standard error of the mean (number of determinations); determined by the AlphaScreen assay.

Activity against KDM2A decreased upon the introduction of small alkyl groups (**164** and **167**) which suggests that the binding energy of the *NH*-substituted triazole may be enhanced due to partial deprotonation of the relatively acidic triazole proton at physiological pH (the triazole is predicted to have a pK_a of 7.9 using ACD labs prediction model).[182] KDM2A activity increased for the *m*-tolyl substituted triazole indicating that the aromatic ring is able to form favourable interactions in the KDM2A substrate pocket. Activity against KDM4A, KDM4C and KDM4E decreased for compounds **164**–**168** compared to the unsubstituted triazole but activity against KDM5C increased indicating that these small substituents are able to form energetically favourable interactions within the KDM5C peptide substrate pocket.

4.3 Synthesis of *N*-Ethyl Derivatives

Hydroxyethyl and acetic acid derivatives were designed to provide synthetic handles that could be readily functionalised after the copper-catalysed click step for the introduction of more complex substituents on the triazole ring. These were prepared from the corresponding bromides using the one-pot method developed for the introduction of the methyl and ethyl substituents (**Scheme 20**). The hydroxyethyl derivative was hydrolysed

to the potassium carboxylate **171** for screening (synthesis of **171** carried out by summer student Verónica Gómez Pérez).

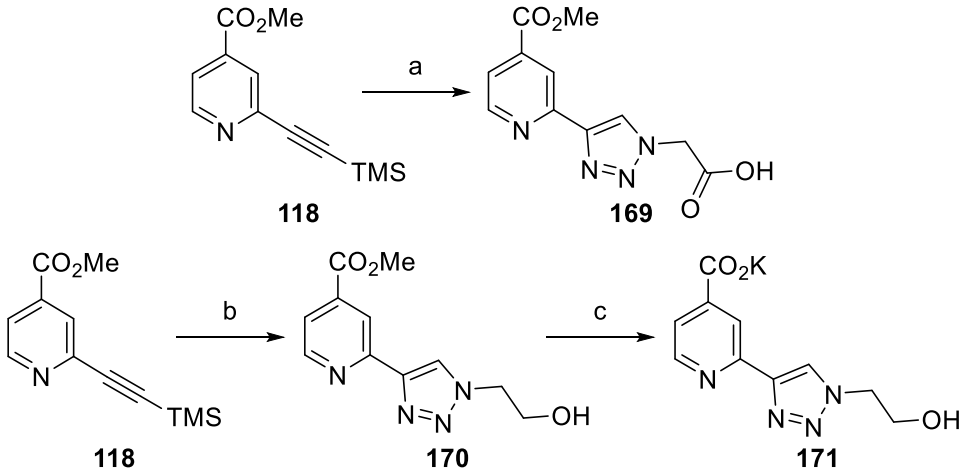

Scheme 20 Synthesis of **169** and **171**. *Reagents and conditions:* (a) bromoacetic acid, NaN_3, $CuSO_4 \cdot 5H_2O$, (+)-sodium L-ascorbate, TBAF, 4:1 DMF:H_2O, 65 °C, 71%; (b) 2-bromoethanol, NaN_3, $CuSO_4 \cdot 5H_2O$, (+)-sodium L-ascorbate, TBAF, 4:1 DMF:H_2O, 65 °C, 73%; (c) KOTMS, MeCN, 90%.

The acetic acid derivative **169** was tested in the screening panel (**Table 18**). It was hypothesised that it might be able to act as a 2OG mimetic by adopting a different binding mode to the isonicotinic acid derivatives, with the triazolopyridine core bound to iron and the carboxylate group mimicking the interactions formed by the 2OG C-1 carboxylate. However, the decrease in activity of **169** compared to the ethyl derivative **167** against the

Table 18 Inhibitory effect (IC_{50} value) of **169** and **171** against four JmjC KDMs.

		KDM IC_{50}*			
Cmpd		**2A**	**4E**	**5C**	**6B**
169	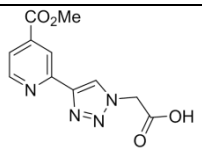	>100 (4)	ND	41 ± 12 (2)	45 ± 77 (2)
171	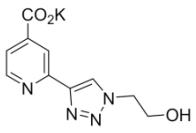	59 ± 10 (6)	47 ± 13 (2)	7.4 ± 1.3 (2)	>100 (2)

*Mean IC_{50} (μM) ± standard error of the mean (number of determinations); determined by the AlphaScreen assay.

JmjC KDMs tested indicates that this scaffold is unlikely to yield good hits for the JmjC KDMs.

Compound **169** was overlaid with the crystal structure of **134** in KDM4A in this potential new binding pose (**Figure 47**). Although the triazolopyridine core could coordinate to the metal, the carboxylate cannot occupy the same space as the carboxylate of **134**. Introduction of a polar atom in the space that would be occupied by the triazole N2 atom may not be favoured; the pyridazine compounds **153** and **146** which contain an sp^2 nitrogen atom at this position resulted in a reduction of potency against all of the demethylases tested except KDM5C.

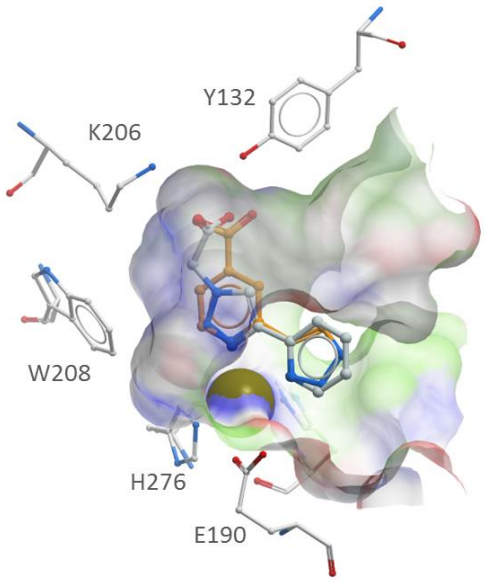

Figure 47 Triazole derivative **169** (grey sticks) docked into a crystal structure of compound **134** (orange sticks) in complex with KDM4A (PDB ID: 4URA).

The hydroxyethyl derivative **171** was found to be essentially equipotent with the ethyl derivative **167** against the four JmjC KDMs tested and to inhibit KDM5C in the single digit micromolar range. Since the polar hydroxyl group was tolerated in this position, the alcohol was used as a synthetic handle for further derivitisation (section 4.3.2).

4.3.1 Acetic Acid Derivatives

Three substituted amides were synthesised from **169** using 1-propanephosphonic acid cyclic anhydride (T3P) as the coupling reagent under microwave irradiation (**Scheme 21**). Aromatic substituents on the triazole ring had generally resulted in good potency against KDM2A whether directly linked to the triazole ring (**123** and **168**) or attached through an alkyl linker (**120**, **122** and **126**) so targets were designed that incorporated aromatic groups. Previous work in the group in the 2,2'-bipyridine series had demonstrated that a 1,2-diamino ethane derivative **23** inhibits KDM4E in the sub-micromolar range,[117] so this motif was incorporated in the triazole series to compare its activity against KDM4E.

The carboxylic acid **169** was found to be poorly soluble in most organic solvents so in the case of the reaction with dibenzylamine, *N*,*N*-dimethylformamide was used as solvent. This modification improved the solubility of the carboxylic acid starting material but the main product isolated was the dimethylamino derivative resulting from the reaction of **169** with dimethylamine. The desired amide was detected by LCMS but was not isolated from the reaction. *N*,*N*-Dimethylformamide is known to be unstable on heating generating dimethylamine and formic acid *via* hydrolysis.[183, 184] Reducing the temperature of the reaction or using an alternative solvent such as *N*,*N*-dimethylacetamide, which is more stable to hydrolysis,[185] could facilitate formation of the desired product but this has not been pursued. The other amide couplings were performed in ethyl acetate and proceeded in good yield despite the poor solubility of the acid starting material **169**. Deprotection with lithium hydroxide or potassium trimethylsilanolate following the amide bond forming reaction gave the carboxylic acids **172**–**174** for biological screening (**Scheme 21**).

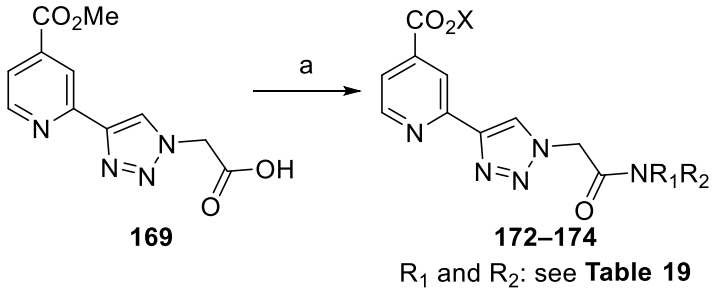

Scheme 21 Synthesis of substituted amides **172**–**174**. *Reagents and conditions:* for **172**, X=Li (a) i) $HNBn_2$, T3P, Et_3N, DMF, 140 °C; ii) LiOH (aq), MeCN, 32%. For **173**, X=K (a) i) 1-(2-aminoethyl)pyrrolidine, T3P, Et_3N, EtOAc, 100 °C; ii) KOTMS, MeCN, 64%. For **174**, X=K (a) i) 4-benzylpiperidine, T3P, Et_3N, EtOAc, 100 °C; ii) KOTMS, MeCN, 78%.

The dimethylamino derivative **172** was found to be moderately active against KDM2A (IC_{50}: 18 µM) and inactive against KDM6B and KDM4E. **172** was found to have interesting selectivity within the KDM4 subfamily; although inactive against KDM4E (IC_{50} > 100 µM), **172** was found to be approximately 100-fold more active against KDM4C (IC_{50} 1.5 µM). This result demonstrates that although the sequence identity between the JmjC domains of KDM4C and KDM4E is high (74%; see **Table 3**), it will nonetheless be possible to design inhibitors with intra-subfamily selectivity. In contrast to the 2,2'-bipyridine analogue **23**, the pyrrolidine derivative **173** was not found to be a potent inhibitor of KDM4E, however, it does show promise as a lead for KDM5C (IC_{50}: 0.95 µM). Of the three amides synthesised, the phenyl-bearing piperidine inhibitor **174** was the most active against KDM2A, likely due to the relatively lipophilic nature of the KDM2A peptide substrate binding pocket, however, this activity was in the same range as that of the best hits from the initial set of triazole derivatives. Due to the poor solubility of the acid **169** and the amide products, this series was not pursued further.

Table 19 Inhibitory effect (IC_{50} value) of amides **172**–**174** against seven JmjC KDMs.

		KDM IC_{50}*						
Cmpd	**NR_1R_2**	**2A**	**3A**	**4A**	**4C**	**4E**	**5C**	**6B**
172	NMe_2	18 ± 1.4 (2)	ND	ND	1.5 ± 0.28 (2)	>100 (2)	51 ± 7.6 (2)	>100 (2)
173	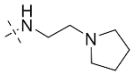	13 ± 3.2 (4)	ND	ND	ND	17 ± 2.6 (2)	0.95 ± 0.086 (4)	>100 (2)
174	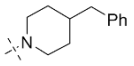	6.1 ± 1.2 (2)	ND	ND	ND	32 ± 6.5 (2)	13 ± 2.6 (2)	>100 (2)

*Mean IC_{50} (μM) ± standard error of the mean (number of determinations); determined by the AlphaScreen assay.

4.3.2 Aminoethyl Derivatives

The hydroxyethyl substituent provided another synthetic handle for derivitisation; activation of the hydroxyl group with methanesulfonyl chloride followed by displacement with *N*-methyl piperazine and deprotection with potassium trimethylsilanolate gave the methyl piperazine derivative **177** for screening (**Scheme 22**, synthesis carried out by Verónica Gómez Pérez).

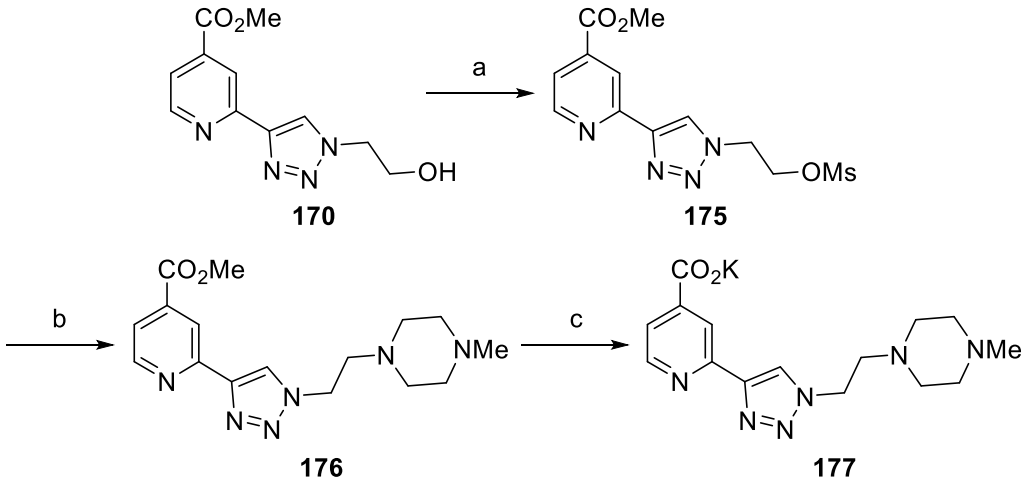

Scheme 22 Synthesis of substituted piperazine **170**–**177**. *Reagents and conditions:* (a) MsCl, DMAP, DIPEA, CH_2Cl_2, quant; (b) *N*-methyl piperazine, Et_3N, MeCN, 80 °C, 58%; (c) KOTMS, MeCN, 45%.

Displacement of the methanesulfonate **175** with *tert*-butyl piperazine-1-carboxylate and methyl ester deprotection gave the Boc derivative **179**. Deprotection with hydrochloric

acid in dioxane yielded the *NH*-piperazine **180** which was synthesised by Verónica Gómez Pérez (**Scheme 23**).

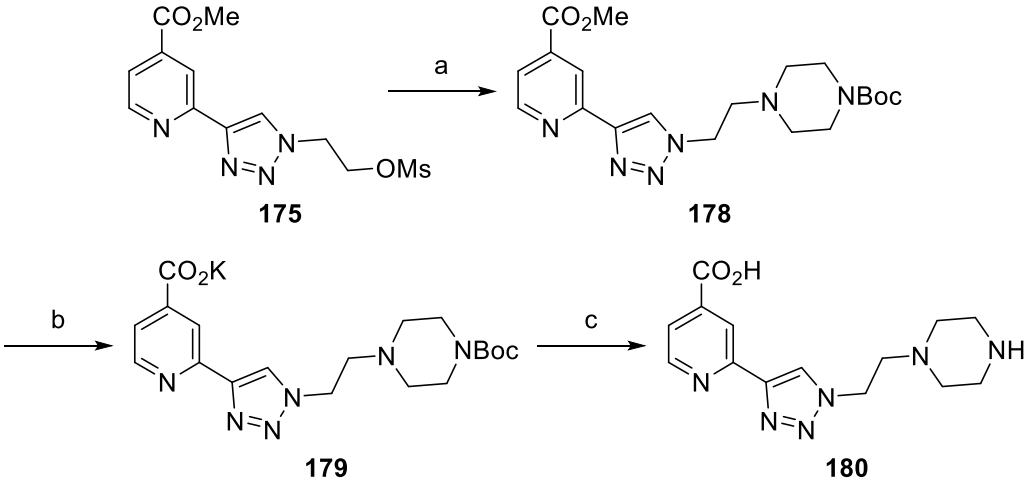

Scheme 23 Synthesis of substituted piperazine **179** and **180**. *Reagents and conditions:* (a) *tert*-butyl piperazine-1-carboxylate, Et_3N, MeCN, 70 °C, 57%; (b) KOTMS, MeCN, quant.; (c) HCl, dioxane.

The derivatives **177**–**180** were tested against four JmjC KDMs (**Table 20**).

Table 20 Inhibitory effect (IC_{50} value) of piperazine derivatives **177**, **179** and **180** against four JmjC KDMs.

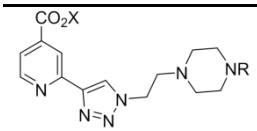

	X	R	KDM IC_{50}*			
			2A	**4E**	**5C**	**6B**
177	K	Me	45 ± 11 (2)	>100 (2)	0.91 ± 0.11 (4)	>100 (4)
179	K	Boc	3.4 ± 0.47 (6)	>100 (2)	1.1 ± 0.27 (2)	>100 (2)
180	H	H	27 ± 4.6 (2)	56 ± 10 (2)	1.8 ± 0.89 (2)	35 ± 3.2 (2)

*Mean IC_{50} (μM) ± standard error of the mean (number of determinations); determined by the AlphaScreen assay.

The *NH*- and *N*-methyl piperazine substituents were not well tolerated with respect to KDM2A inhibition, but the Boc derivative **179** was found to be a single digit micromolar inhibitor of KDM2A. As the protonated forms of the *N*-methyl and *NH*-piperazine compounds will predominate at physiological pH (the conjugate acids of **177** and **180** are predicted to have pK_a values of 8.2 and 9.0 respectively using the ACD labs prediction

model)[182] this indicated that a positively charged group at this position is not optimal for KDM2A inhibition. Conversely, these compounds were found to be potent inhibitors of KDM5C (IC_{50}: 0.91–1.8 μM) with good selectivity over the other JmjC KDMs tested; thus the 4-methyl piperazine derivative **177** is an interesting lead for KDM5C.

4.4 Synthesis of Piperidinyl Triazole Amides

The piperidinyl derivative **128** which was found to inhibit KDM2A in the micromolar range (see previous chapter) was selected as an attractive lead for modification of the piperidine *N*-substituent. A small array of alkyl and aryl-bearing amides was designed to determine if the carbamate group could be replaced with an amide and to explore the SAR of different amide substituents (**Figure 48**).

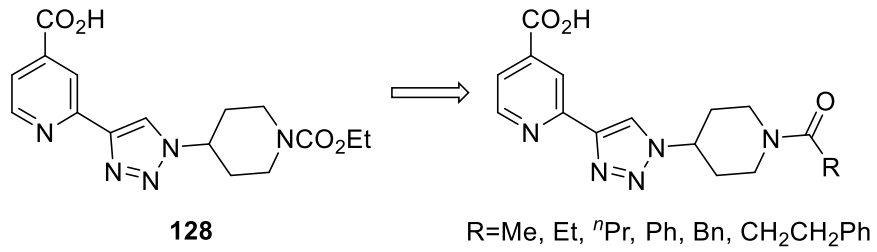

Figure 48 Piperidinyl amide targets designed to follow up hit **128**.

A route to these targets was designed that would use the one-pot TMS deprotection and copper-catalysed click chemistry to generate a late stage piperidine intermediate **185** that could yield a range of amide targets in two steps. The synthesis was carried out by Shanghai Chempartner Co. Boc-protected 4-hydroxypiperidine was transformed to the 4-azido derivative **183** *via* the methanesulfonate **182**, then taken into the copper-catalysed click reaction with the protected alkyne **118**. The Boc group was removed with trifluoroacetic acid to give a late-stage intermediate **185** for functionalization with acid chlorides which, after deprotection of the carboxylic esters, generated the target compounds **187**–**192** for testing (**Scheme 24**).

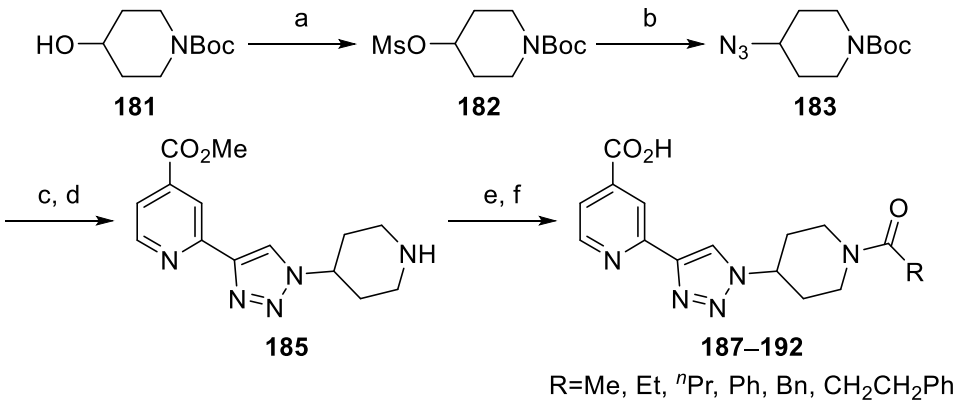

Scheme 24 Synthesis of 4-piperidine derivatives **187**–**192**. *Reagents and conditions:* (a) MsCl, Et_3N, CH_2Cl_2, 59%; (b) NaN_3, DMF, 60 °C, 65%; (c) **118**, TBAF, DIPEA, CuI, MeOH, 56%; (d) TFA, CH_2Cl_2, 73%; (e) RCOCl, Et_3N, CH_2Cl_2; (f) LiOH (aq), MeOH. Synthesis carried out by Shanghai Chempartner Co.

The ethyl, propyl and phenyl substituted amides (**Table 21**, **188**–**190**) were found to be moderately active against KDM2A (6.1–7.2 μM). Gratifyingly, the benzyl (**191**) and phenethyl (**192**) substituted analogues were found to be more active against KDM2A (IC_{50} 3.4 μM and 2.4 μM respectively) than carbamate **128** and to be less active against KDM3A (IC_{50} 27 μM and > 100 μM). **191** and **192** were still selective over the KDM4

Table 21 Inhibitory effect (IC_{50} value) of amides **187**–**192** against seven JmjC KDMs.

		KDM IC_{50}*						
Cmpd	**R**	**2A**	**3A**	**4A**	**4C**	**4E**	**5C**	**6B**
187	Me	7.1 ± 0.28 (2)[a]	ND	ND	ND	ND	ND	ND
188	Et	6.1 ± 1.0 (2)	45 ± 6.9 (2)	ND	14 ± 6.8 (2)	>100 (2)	4.0 ± 0.53 (2)	59 ± 7.8 (2)
189	nPr	7.0 ± 1.1 (2)	>100 (2)	ND	14 ± 3.0 (2)	>100 (2)	5.3 ± 0.44 (2)	>100 (2)
190	Ph	7.2 ± 1.1 (2)	>100 (2)	45 ± 18 (4)	12 ± 2.4 (4)	>100 (2)	3.7 ± 0.12 (2)	37 ± 11 (2)
191	Bn	3.4 ± 0.44 (2)	27 ± 6.1 (2)	35 ± 12 (2)	26 ± 5.7 (2)	>100 (2)	3.9 ± 0.28 (2)	14 ± 1.6 (2)
192		2.4 ± 0.39 (2)	>100 (2)	68 ± 14 (2)	73 ± 13 (2)	>100 (2)	2.8 ± 0.20 (2)	>100 (2)

*Mean IC_{50} (μM) ± standard error of the mean (number of determinations); determined by the AlphaScreen assay unless otherwise stated or by the [a]RapidFire assay.

subfamily and KDM6B ($IC_{50} \geq 14$ μM), however, the 4-piperidine derivatives **188**–**192** were all found to inhibit KDM5C in the same range as KDM2A.

4.4.1 Variation of the Saturated Heterocyclic Ring

Given the differences in substrate selectivity of the KDM5 subfamily (H3K4me3/2) and the KDM2 subfamily (H3K36me2/1), it was anticipated that selectivity for KDM2A over KDM5C could be achieved through further exploration of the histone substrate pocket. Other saturated heterocyclic ring systems were therefore synthesised as alternatives to the 4-piperidine ring to explore different vectors within the pocket. These targets were synthesised from the corresponding Boc-protected amino alcohols **193**–**195** using the same route as for **187**–**192** (**Scheme 25**, synthesis carried out by Shanghai Chempartner Co.). The chiral 3-pyrrolidine and 3-piperidine derivatives were prepared as racemates for initial screening.

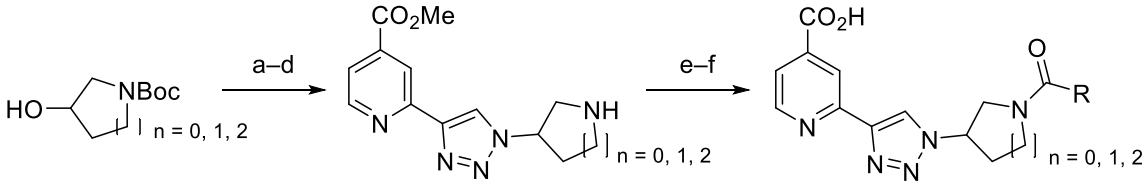

193: n=0
194: n=1
195: n=2

196: n=0
197: n=1
198: n=2

199–216
n=0–2
R=Me, Et, ^{n}Pr, Ph, Bn, CH_2CH_2Ph

Scheme 25 Synthesis of azetidine, pyrrolidine and 3-piperidine derivatives **199**–**216**. *Reagents and conditions*: (a) MsCl, Et_3N, CH_2Cl_2; (b) NaN_3, DMF, 60 °C; (c) **118**, TBAF, DIPEA, CuI, MeOH; (d) TFA, CH_2Cl_2; (e) RCOCl, Et_3N, CH_2Cl_2; (f) LiOH (aq), MeOH. Synthesis carried out by Shanghai Chempartner Co.

The acetyl substituted azetidine **199** manifested sub-micromolar KDM5C activity with selectivity over KDM2A, KDM3A, KDM4E and KDM6B (**Table 22**). Potency against KDM5C was observed to decrease with increasing size of the amide substituent (**199**–**201**). Thus, KDM2A activity increased for the phenyl, benzyl and phenethyl-derivatives (**202**–**204**; IC_{50} 4.2–9.5 μM), but these compounds still suffered from a lack of selectivity

Table 22 Inhibitory effect (IC_{50} value) of amides **199**–**216** against seven JmjC KDMs.

			KDM IC_{50}*						
Cmpd	**n**	**R**	**2A**	**3A**	**4A**	**4C**	**4E**	**5C**	**6B**
199	0	Me	ND	47 ± 9.3 (2)	2.3 ± 0.80 (2)	1.5 ± 0.32 (2)	4.0 ± 0.35 (2)	0.55 ± 0.044 (2)	>100 (2)
200		Et	72 ± 13 (2)	>100 (2)	4.4 ± 1.1 (2)	12 ± 4.2 (2)	>100 (2)	2.5 ± 0.11 (2)	43 ± 43 (2)
201		*n*Pr	43 ± 6.7 (2)	>100 (2)	5.0 ± 1.5 (2)	7.5 ± 1.7 (2)	65 ± 18 (2)	6.1 ± 0.48 (2)	62 ± 59 (2)
202		Ph	4.2 ± 1.0 (2)	26 ± 2.3 (2)	>100 (2)	18 ± 3.0 (2)	49 ± 4.4 (2)	3.9 ± 0.17 (2)	87 ± 3.1 (2)
203		Bn	5.5 ± 1.3 (2)	80 ± 7.1 (2)	ND	33 ± 4.6 (4)	>100 (2)	5.2 ± 0.61 (2)	>100 (2)
204			9.5 ± 2.2 (2)	>100 (2)	5.8 ± 1.7 (2)	7.9 ± 1.1 (4)	25 ± 3.2 (2)	1.0 ± 0.059 (2)	>100 (2)
205	1	Me	30 ± 1.4 (2)[a]	ND	ND	ND	ND	ND	ND
206		Et	88 ± 3.1 (2)[a]	ND	ND	ND	ND	ND	ND
207		*n*Pr	12 ± 1.4 (2)	>100 (4)	ND	22 ± 2.5 (6)	>100 (4)	3.4 ± 0.24 (4)	>100 (2)
208		Ph	0.37 ± 0.045 (2)	ND	ND	ND	ND	ND	ND
209		Bn	0.82 ± 0.093 (2)	52 ± 11 (2)	ND	28 ± 5.9 (2)	>100 (2)	5.0 ± 0.37 (2)	44 ± 32 (2)
210			ND	98 ± 12 (2)	ND	37 ± 6.7 (2)	>100 (2)	1.6 ± 0.14 (2)	72 ± 3.1 (2)
211	2	Me	12 ± 2.1 (2)	38 ± 12 (2)	35 ± 67 (2)	14 ± 3.5 (2)	>100 (2)	2.2 ± 0.17 (2)	84 ± 17 (2)
212		Et	7.8 ± 1.5 (2)	52 ± 11 (2)	ND	15 ± 6.8 (2)	93 ± 14 (2)	3.3 ± 0.19 (2)	48 ± 8.9 (2)
213		*n*Pr	4.6 ± 0.51 (2)	31 ± 8.1 (2)	ND	17 ± 5.7 (2)	92 ± 17 (2)	5.0 ± 0.35 (2)	68 ± 7.9 (2)
214		Ph	0.12 ± 0.013 (6)	46 ± 5.7 (2)	59 ± 76 (2)	16 ± 2.7 (14)	>100 (12)	8.8 ± 1.2 (2)	20 ± 3.6 (8)
215		Bn	1.8 ± 0.18 (2)	21 ± 3.5 (2)	ND	17 ± 8.4 (2)	>100 (2)	7.4 ± 2.4 (2)	12 ± 2.7 (2)
216			0.57 ± 0.057 (2)	42 ± 8.4 (2)	ND	22 ± 25 (4)	>100 (2)	4.1 ± 0.37 (2)	12 ± 1.8 (2)

*Mean IC_{50} (μM) ± standard error of the mean (number of determinations); determined by the AlphaScreen assay unless otherwise stated or by the [a]RapidFire assay.

over KDM5C. The 3-substituted pyrrolidine compounds **205–210** generally showed increased potency against KDM2A (**208** IC_{50}: 370 nM) and improved selectivity over the other KDM representatives. The 3-piperidine series **211–216** resulted in a dramatic increase in KDM2A inhibition with concurrent reduction in KDM5C activity. Excitingly, the most potent KMD2A inhibitor, the benzoyl 3-piperidine derivative **214** (IC_{50}: 120 nM) was found to be more than 50-fold selective for KDM2A over all the other six JmjC KDMs in the panel.

4.4.2 Synthesis of the Two Enantiomers of the Benzoyl 3-Piperidine Derivative

In order to investigate if the activity observed for compound **214** was due to a single stereoisomer, the two enantiomers were synthesised separately from stereoisomerically pure Boc-protected amino alcohols **217** and **222** which were activated as the methanesulfonates **218** and **223** (**Scheme 26**). The methanesulfonates were converted to the corresponding azides, presumably with inversion of configuration in an S_N2-type substitution, and copper-catalysed click reaction with the TMS-protected acetylene derivative **118** in a one-pot procedure gave the triazole derivatives **219** and **224**. Boc deprotection, amide formation and ester hydrolysis gave enantiomers **220** and **227**.

In order to verify the stereochemical integrity of compounds **220** and **227**, they were converted to the methyl ester derivatives **221** and **228** with methyl iodide to enable analysis by chiral HPLC (**Scheme 26**). The enantiomeric excesses (ee) were determined as 98%, confirming that racemisation had not occurred to any significant degree during the synthesis (chiral HPLC performed by Alistair Farley).

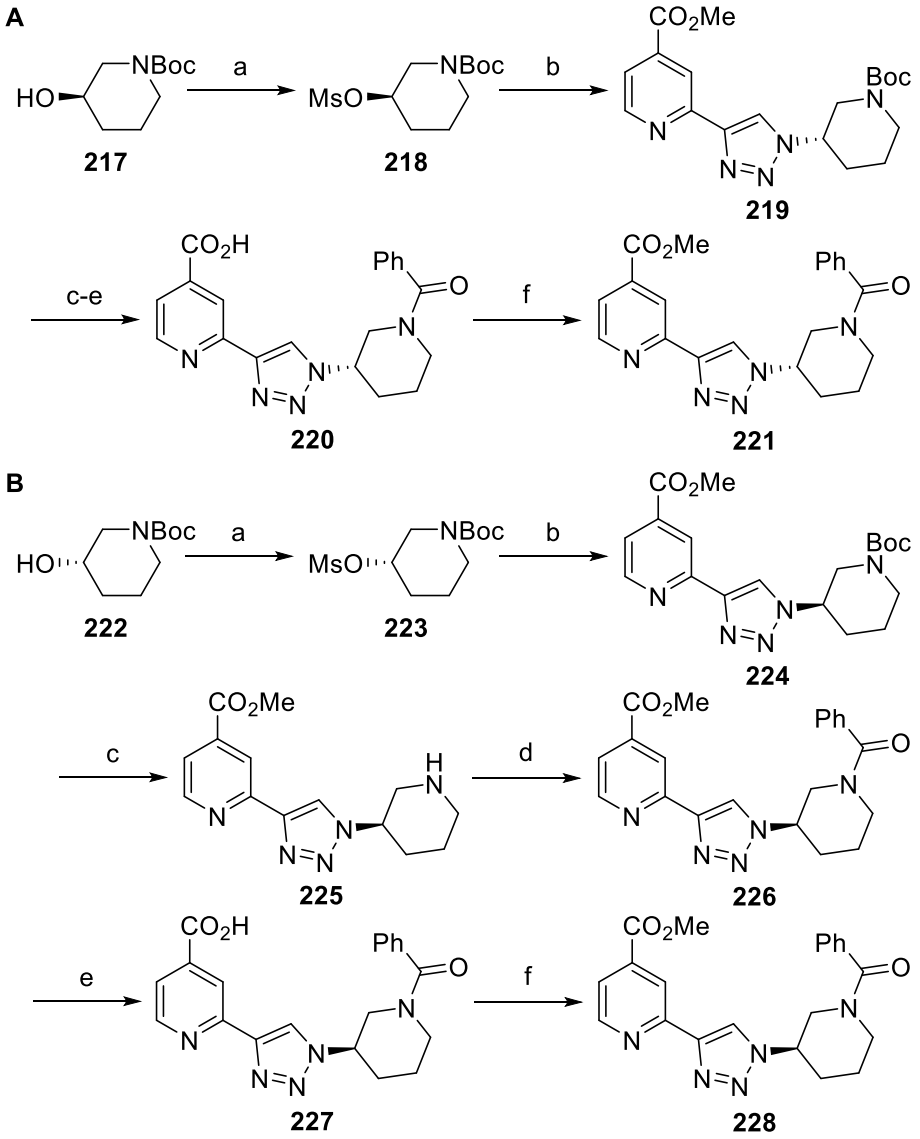

Scheme 26 Synthesis of **220** and **227**, the (*S*)- and (*R*)-enantiomers of compound **214** and conversion to the methyl ester derivatives **221** and **228**. *Reagents and conditions:* **A** For the (*S*)-enantiomer: (a) *tert*-butyl (3*R*)-3-hydroxypiperidine-1-carboxylate, MsCl, Et_3N EtOAc, 98%; (b) i) NaN_3, DMF, 75 °C; ii) **118**, TBAF, DIPEA, CuI, DMF, 34%; (c) TFA, CH_2Cl_2; (d) PhCOCl, Et_3N, MeCN; (e) LiOH (aq), MeCN, 81% over 3 steps; (f) MeI, $NaHCO_3$, DMF, 65%. **B** For the (*R*)-enantiomer: (a) *tert*-butyl (3*S*)-3-hydroxypiperidine-1-carboxylate, MsCl, Et_3N EtOAc, 96%; (b) i) NaN_3, DMF, 75 °C; ii) **118**, TBAF, DIPEA, CuI, DMF, 48%; (c) TFA, CH_2Cl_2, 97%; (d) PhCOCl, Et_3N, MeCN, quant.; (e) LiOH (aq), MeCN, 85%; (f) MeI, $NaHCO_3$, DMF, quant.

The two enantiomers were tested in the JmjC KDM assay panel to determine if they would have different inhibitory effects (**Table 23**). Gratifyingly, the (*R*)-enantiomer **227** was found to be approximately 50-fold more potent (IC_{50}: 58 nM) than the (*S*)-enantiomer **220** indicating that the stereochemistry of the substituted piperidine plays an important role in facilitating binding to KDM2A and that the (*R*)-enantiomer positions the amide substituent

Table 23 Inhibitory effect (IC_{50} value) of the two enantiomers of **214** against eight JmjC KDMs.

Cmpd		KDM IC_{50}*							
		2A	**3A**	**4A**	**4C**	**4E**	**5C**	**6B**	**7B**
220	*S*	3.0 ± 0.35 (2)	ND	ND	>100 (6)	>100 (6)	ND	25 ± 7.2 (2)	ND
227	*R*	0.058 ± 0.018 (2)	>100 (4)	14 ± 4.7 (2)	15 ± 1.7 (4)	>100 (2)	1.6 ± 0.15 (2)	>100 (4)	0.15 ± 0.092 (3)

*Mean IC_{50} (μM) ± standard error of the mean (number of determinations); determined by the AlphaScreen assay.

in a favoured position for binding to KDM2A. Docking of the two enantiomers in a co-crystal structure of KDM2A and a dimethylated lysine substrate shows that the (*R*)-enantiomer can occupy the same space as the H3 substrate and that the phenyl ring may position closer to residue F323, potentially forming a more favourable pi-stacking interaction between the phenyl ring of F323 and the phenyl ring of inhibitor **227** (**Figure 49**).

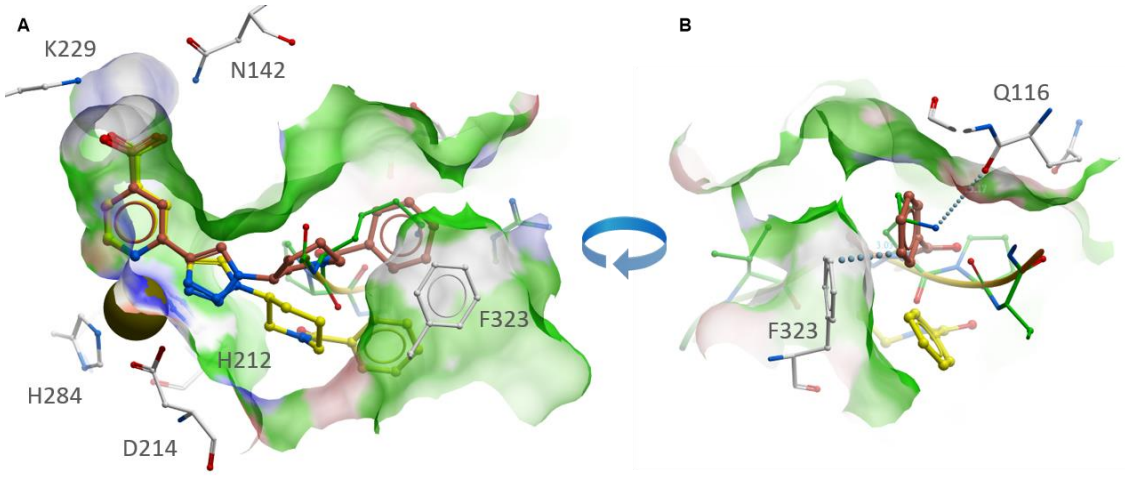

Figure 49 A View from a crystal structure of KDM2A (grey sticks) bound to an H3(A29–Y41)K36me2 peptide (green sticks). The catalytic iron is substituted by nickel (brown sphere). PDB ID: 4QX7. The two enantiomers of **214** were docked into the crystal structure; the (*R*)-enantiomer **227** (brown sticks) overlaps well with the H3 peptide whereas the triazole substituent of the (*S*)-enantiomer **220** (yellow sticks) occupies a different region of the substrate pocket. **B** Rotation by 110° about the *y*-axis shows that the phenyl ring of **227** is slightly closer to F323 than the phenyl ring of **220** which may contribute to its increased potency.

KDM4C and KDM5C activity was also found to increase for the (*R*)-enantiomer relative to the racemic mixture, but inhibitor **227** was still more than 100-fold selective for KDM2A

over KDM4C/4E, 30-fold selective over KDM5C with negligible activity against KDM3A and KDM6B at 100 μM. Since KDM2A is a member of the KDM2/7 subfamily, **227** was also expected to inhibit other KDM2/7 subfamily members. **227** was found to be a potent inhibitor of KDM7B (IC_{50} 150 nM).

4.5 Discussion

The *NH*-triazole derivative **134** was found to be more active against KDM2A (IC_{50}: 6.6 μM) than either the methyl or ethyl derivatives **164** and **167** (IC_{50}: 16 and 31 μM respectively). The reduced activity of **164** and **167** could be due to steric clashes in the active site although this seems unlikely because larger substituents are well tolerated (**Figure 50**). For example the phenethyl derivative **122** (KDM2A IC_{50}: 6.4 μM) was found to be approximately equipotent with **134**, presumably because the phenethyl group forms favourable intermolecular interactions with residues in the active site of KDM2A. Triazole **134** is predicted to have a pK_a of 7.9 (ACD labs prediction model),[182] indicating that it will be partly deprotonated at physiological pH so the slightly enhanced activity of **134** against KDM2A compared to the small alkyl derivatives may be due to it binding as the negatively charged species.

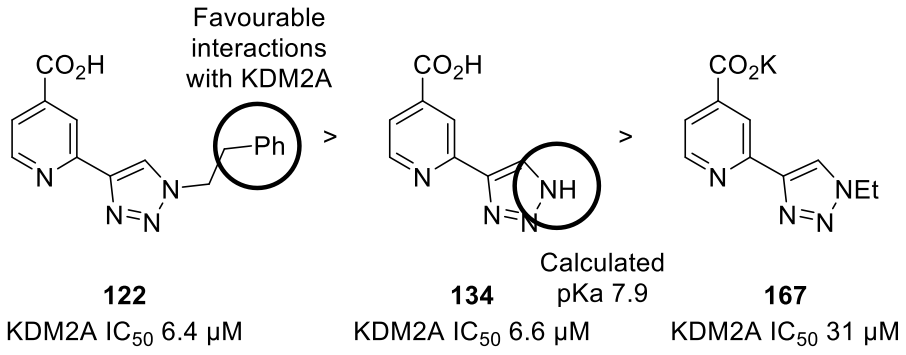

Figure 50 Comparison of the inhibitory activity of triazole derivatives **122**, **134** and **167** against KDM2A.

Polar groups at the 2-position of the ethyl triazole substituents were favoured for KDM5C inhibition but the *NH*- and *N*-methyl piperazine derivatives **177** and **180** were 15- to 49-fold less active against KDM2A than KDM5C indicating that polarity at this position was

not well tolerated with respect to KDM2A inhibition (**Figure 51**). This may be due to the relatively lipophilic peptide substrate binding pocket of KDM2A. **177** and **180** were found to be more active against KDM5C indicating that its substrate binding pocket may be more polar at this position. In contrast, more lipophilic, aryl substituents were favoured for KDM2A inhibition; for example compound **173** which bears a pyrrolidine ring was found to be a relatively weak inhibitor of KDM2A (IC_{50}: 13 µM) but a more potent inhibitor of KDM5C (IC_{50}: 0.95 µM). Conversely, compound **174** which bears a phenyl ring at approximately the same position as the polar tertiary amino substituents of compounds **173** and **177** was found to be a more potent inhibitor of KDM2A (IC_{50}: 6.1 µM) but a weaker inhibitor of KDM5C (IC_{50}: 13 µM).

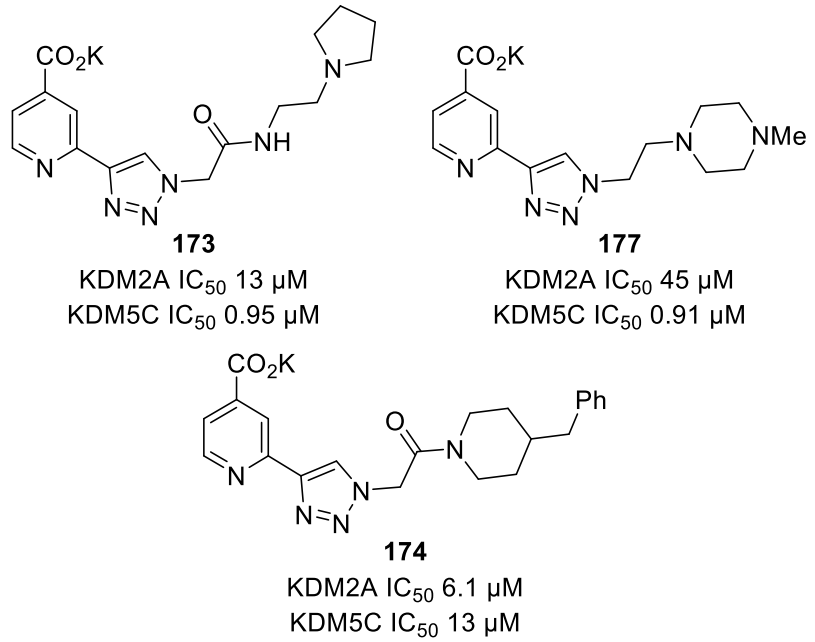

Figure 51 Compounds **173** and **177** which bear a basic amino group were found to be more active against KDM5C than KDM2A whereas compound **174** which bears a phenyl group at a similar position was found to be more active against KDM2A than KDM5C.

Substitution of the carbamate group of piperidine derivative **128** which had been identified as a moderately active inhibitor of KDM2A in the previous chapter (IC_{50}: 7.3 µM) with an amide group was well tolerated (**189** has an IC_{50} of 7.0 µM against KDM2A). The size of the saturated heterocyclic ring and the position of the nitrogen atom within the ring was

varied and resulted in dramatic activity and selectivity changes for the JmjC KDMs tested. A small ring size and small amide substituents resulted in the most potent activity against KDM5C (**199** KDM5C IC_{50}: 0.55 μM). The 3-amino piperidine series proved optimal for KDM2A activity and the benzamide **214** was found to have an IC_{50} of 120 nM against KDM2A. Synthesis of the two enantiomers of **214** identified the (*R*)-enantiomer **227** as a potent and selective inhibitor of KDM2A (IC_{50}: 58 nM) and KDM7B (IC_{50}: 150 nM).

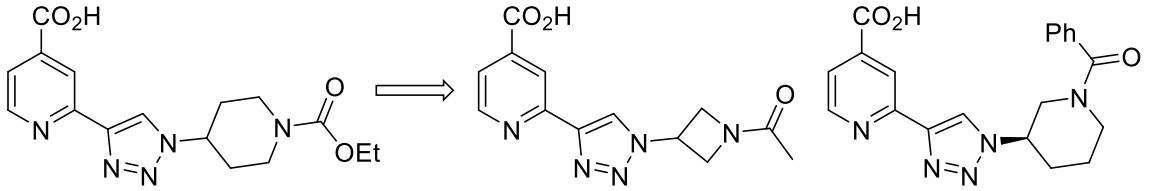

128
KDM2A IC_{50} 7.3 μM
KDM4C IC_{50} > 100 μM
KDM4E IC_{50} > 100 μM
KDM5C IC_{50} 3.9 μM

199
KDM2A IC_{50} ND
KDM4C IC_{50} 1.5 μM
KDM4E IC_{50} 4.0 μM
KDM5C IC_{50} 0.55 μM

227
KDM2A IC_{50} 0.058 μM
KDM4C IC_{50} 15 μM
KDM4E IC_{50} > 100 μM
KDM5C IC_{50} 1.6 μM
KDM7B IC_{50} 0.15 μM

Figure 52 Compounds **199** and **227** was developed from piperidinyl derivative **128**.

Compound **227** was found to be significantly more potent against KDM2A (25- to 100-fold) than other KDM2/7 subfamily selective inhibitors reported in the literature, hydroxamate **24** (KDM2A IC_{50}: 6.8 μM)[118] and daminozide **18** (KDM2A IC_{50}: 1.5 μM).[114] Its potency and selectivity mean that inhibitor **227** will be of interest as a tool compound for the study of KDM2A and KDM7B in biological systems.

Chapter 5. Cell-based Assays and Cellular Permeability

5.1 Introduction

JmjC KDM inhibitors that form interactions in the 2OG binding site usually bear a carboxylate group, which mimics the interactions formed by the 2OG C-1 carboxylate, and other polar atoms which coordinate to iron(II). This class of inhibitor often exhibits poor cellular permeability and activity but inhibitors bearing carboxylic acids have been used as ester prodrugs to improve cellular efficacy (see section 1.5.4). When polar molecules are in aqueous solution, they form stabilising interactions with water molecules through electrostatic and hydrogen bonding interactions.[186] Cell membranes are comprised of a lipid bilayer in complex with other components such as proteins and sterols.[187, 188] Compounds may cross cell membranes by passive diffusion or in processes mediated by transporter proteins.[189] When an equilibrium exists between ionised and uncharged species (as for carboxy-containing 2OG mimetics), the rate of passive diffusion through the cell membrane is strongly influenced by the position of equilibrium, i.e. the pK_a, since passive diffusion is essentially limited to neutral molecules.[189] The KDM2A/7 inhibitor **227** identified in the previous chapter is predicted to have a pK_a of 3.0 (ACD labs prediction model),[182] indicating that it will be found predominantly as the negatively charged species at physiological pH and, as for other JmjC KDM inhibitors, may suffer from poor cell permeability. Prior to passing through the hydrophobic centre of the lipid bilayer in passive diffusion, molecules must also be desolvated; the consequent loss of hydrogen bonding and electrostatic interactions is energetically unfavourable (**Figure 53**).[189] The polar surface area (PSA) can be used as a predictor for the hydrogen bond forming potential of a molecule, and high PSA has been shown to correlate with poor permeability.[190]

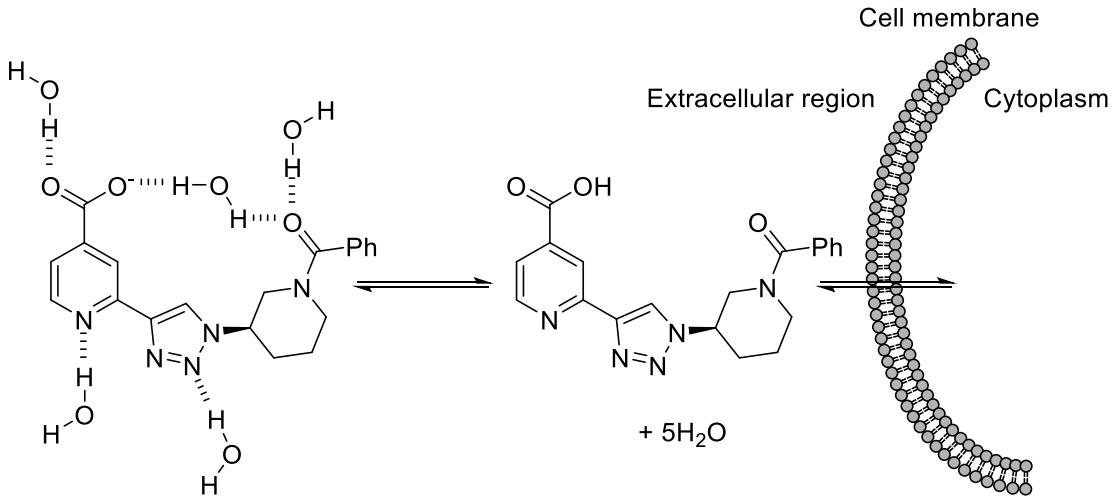

Figure 53 Hydrogen bonding interactions to bulk water must be broken and any charges neutralised before molecules can cross cell membranes in passive diffusion (only selected, representative hydrogen bonding interactions are shown for clarity).

The enhanced cellular activity of the ester prodrugs **37**–**40** (**Figure 17**) is presumably due to improved cellular permeability of the esters compared to the negatively charged carboxylates as would be expected by the resulting increase in pK_a and reduction in PSA compared to the parent carboxylic acids. However, in some instances the esters themselves are also inhibitors of JmjC KDMs, for example the *n*-octyl ester of IOX1.[116]

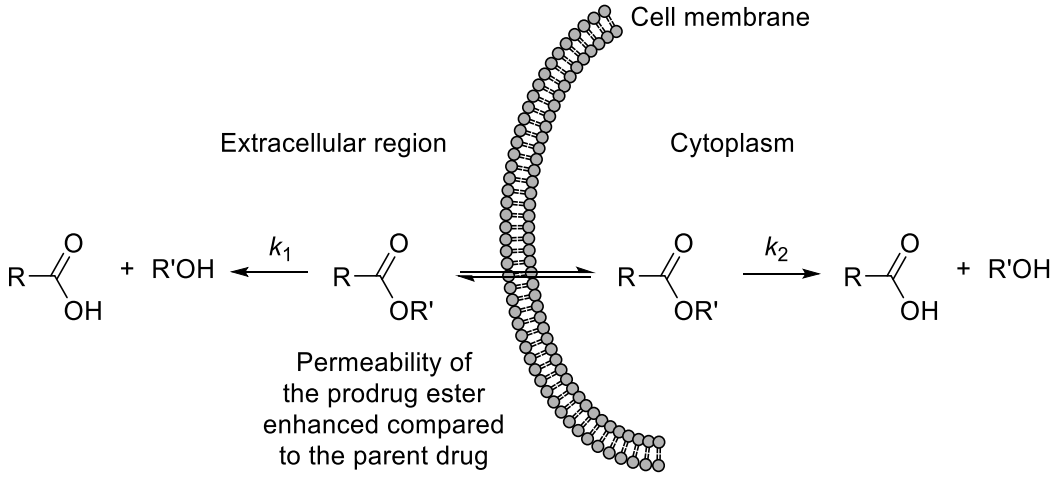

Figure 54 Schematic representation of the hydrolysis of ester prodrugs. Where an ester prodrug is employed to improve cellular permeability, it must be more permeable than the parent drug and the rate of hydrolysis in the extracellular region (for example in the assay buffer conditions), k_1, must be slow enough to prevent significant turnover of the prodrug ester to the acid outside the cell. The rate of hydrolysis inside the cell, k_2, must be sufficiently fast to liberate the parent acid within an appropriate time-frame.

An effective prodrug should be stable in solution, modulate the physicochemical properties of the parent drug appropriately (for example resulting in an improvement in the permeability or solubility of the prodrug compared to the parent drug) and be readily converted to the parent drug once it reaches the desired site of action without releasing harmful by-products (**Figure 54**).[132]

5.2 Cell-Based Activity of JmjC KDM Inhibitors

The potent and selective KDM2A inhibitors identified in chapters 2 and 4 were tested in an immunofluorescence (IF) cellular assay first developed for KDM4A and subsequently developed for other JmjC KDMs (**Figure 55**).[108, 115] Determination of the cellular efficacies of compounds using the IF assay was carried out by Dr. Clarence Yapp and Dr. Stephanie Hatch.

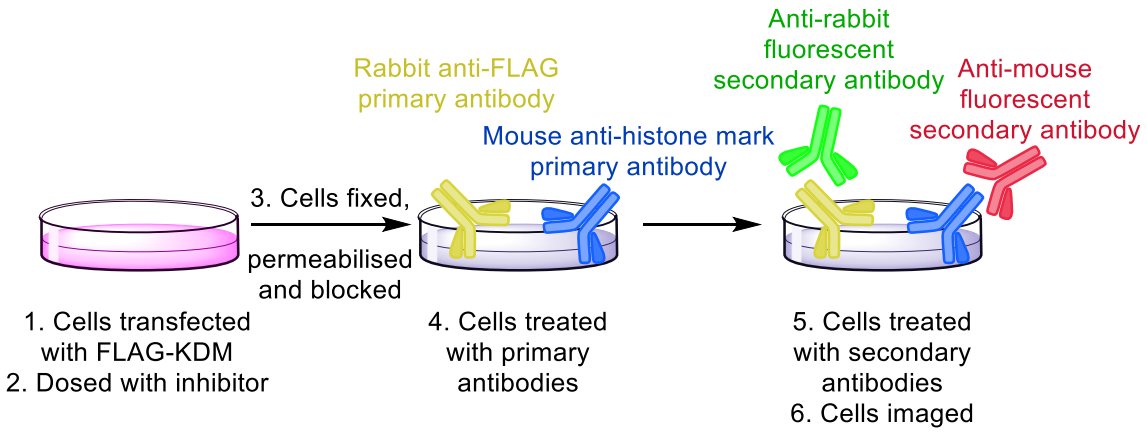

Figure 55 Cellular immunofluorescence (IF) assay for JmjC KDM inhibition. Cells are transiently transfected with DNA encoding the FLAG-tagged JmjC KDM and incubated with the inhibitor for 24 hours (one dose). The cells are fixed and probed with an anti-FLAG antibody to detect transfection efficiency and an antibody to the histone mark of interest to detect the degree of methylation. Secondary antibodies conjugated to fluorescent dyes are added. Fluorescence is quantified upon excitation of the fluorescent antibodies at the appropriate wavelength.

In the IF assay, HeLa cells are transiently transfected with a plasmid encoding for a FLAG-tagged construct of the JmjC KDM of interest and then dosed with inhibitor. After a 24-hour incubation period, the cells are fixed with formalin, permeabilised with 0.5% polyethylene glycol *tert*-octylphenyl ether (Triton X-100) and blocked with a solution of

foetal bovine serum (FBS). Primary antibodies to the FLAG tag and the histone mark of interest are used to probe which cells have been successfully transfected and the degree of methylation remaining on the histone mark of interest. Secondary antibodies, which are conjugated to fluorescent dyes, are used to visualise the extent of antibody labelling in each cell using a fluorescent microscope. By using primary antibodies raised in different species and secondary antibodies bearing dyes that fluoresce at different wavelengths, both the transfection efficiency and histone methylation state can be determined simultaneously. In the KDM2A IF assay, a murine antibody is used to detect the H3K36me2 mark. When KDM2A is overexpressed, extensive demethylation of H3K36me2 occurs and the amount of fluorescence observed is lower. When an inhibitor of KDM2A is present, inhibition of KDM2A occurs and consequently the level of H3K36me2 is increased compared to untreated cells and the fluorescence intensity observed is greater. A negative control may be used where cells are transfected with a plasmid encoding for a catalytically inactive version of KDM2A (a KDM2A iron binding site variant) and the broad-spectrum 2OG oxygenase inhibitor IOX1 **21** can be used as a positive control.

5.3 Cell-Based Activity of 4-Carboxy Pyridine Derivatives

Inhibitors **50** and **227 (Figure 56)** were tested in the IF assay. HeLa cells that had been transfected with a plasmid encoding for either an active form of FLAG-KDM2A or an inactive mutant were dosed with the inhibitors and with IOX1 **21** as a positive control.

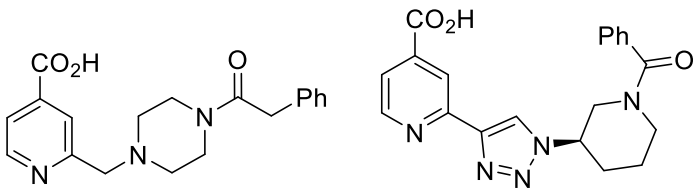

50 **227**

Figure 56 Inhibitors **50** and **227** were tested in the IF assay.

Disappointingly, inhibitors **50** and **227** were not found to inhibit the demethylation of H3K36me2 by KDM2A in the IF assay (**Figure 57**). At 100 μM, the positive control IOX1 **21** resulted in complete inhibition of KDM2A and the fluorescence intensity observed was comparable to that observed in cells that had been transfected with the inactive mutant of *KDM2A* (**Figure 57B**).

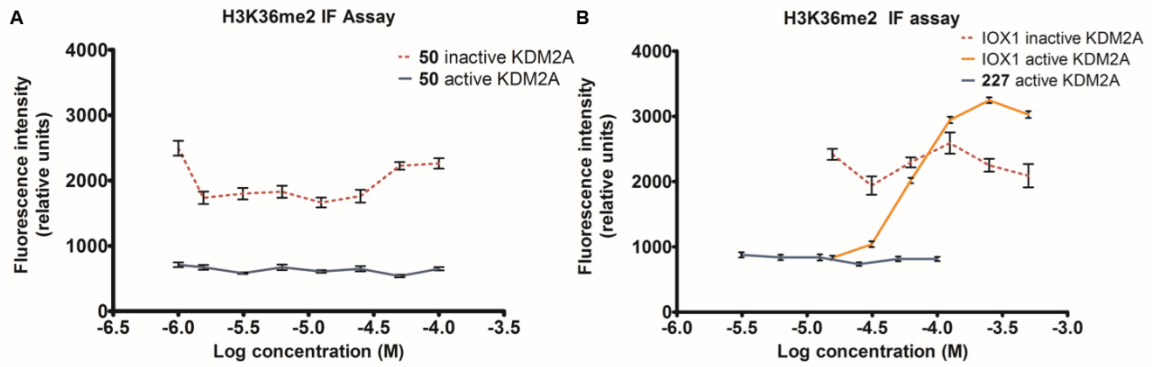

Figure 57 Relative fluorescence intensity observed in cells producing KDM2A or an inactive mutant of KDM2A and dosed once with inhibitor. **A** Cells dosed with **50**. **B** Cells dosed with IOX1 **21** control or **227**. Error bars represent ± 1 standard error of the mean. Assay carried out by Clarence Yapp.

5.4 Synthesis of Prodrug Esters

Since other carboxylate-containing JmjC KDM and 2OG oxygenase inhibitors have enhanced cellular activity when dosed as their ester prodrugs,[48, 113, 116, 119] it was decided to test **226** (the methyl ester prodrug of **227**) and **49** (the ethyl ester prodrug of **50**) in the IF assay. The membrane permeability of compound **227** and its methyl ester **226** was assessed using a parallel artificial membrane permeation assay (PAMPA, assay carried out by Brian Linehan at Boehringer Ingelheim).[191] The membrane permeability of compound **227** in the PAMPA assay was poor (0.41–1.9 × 10^{-6} cms^{-1}), however, the methyl ester **226** had good permeability (45–56 × 10^{-6} cms^{-1}) so it was expected that the methyl and ethyl ester prodrugs **49** and **226** would be more active in the cellular assay than the parent acids **50** and **227** assuming they were hydrolysed as outlined in **Figure 54**.

Table 24 PAMPA data for carboxylate **227** and its methyl ester derivative **226**.

	PAMPA P_e (10^{-6} cms^{-1})		
Cmpd	**pH 7.4**	**pH 6.2**	**pH 5.0**
226	52	45	56
227	0.69	0.41	1.9

Assay carried out by Brian Linehan at Boehringer Ingelheim.

Unfortunately esters **49** and **226** were not active at 100 µM in the IF assay (**Figure 58**) despite being predicted to have better cell permeability.

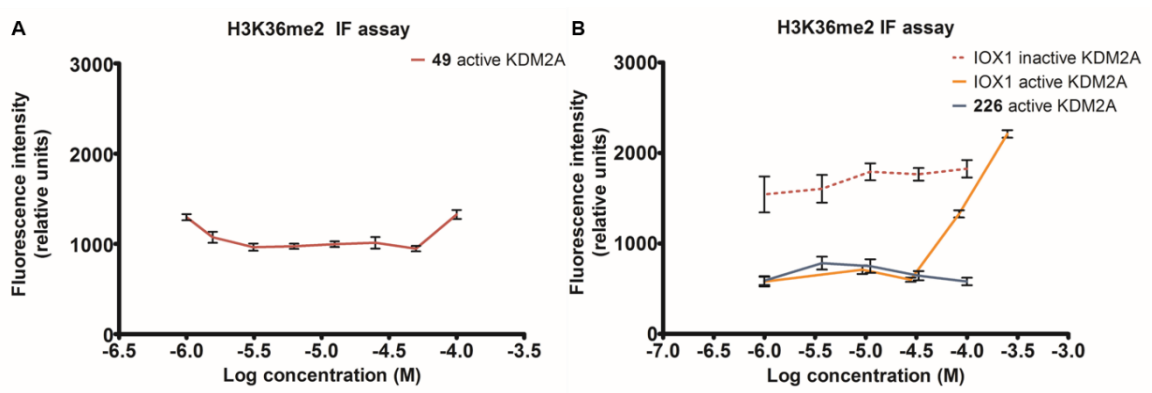

Figure 58 Relative fluorescence intensity observed in cells overexpressing KDM2A or an inactive mutant of KDM2A and dosed once with inhibitor. **A** Cells dosed with ethyl ester **49**. **B** Cells dosed with IOX1 **21** control or methyl ester **226**. Error bars represent ± 1 standard error of the mean. Assay carried out by Clarence Yapp.

The *n*-octyl ester of IOX1 **21** has been shown to be 25-fold more active in cells (KDM4A EC_{50}: 3.8 µM) than the parent drug (KDM4A EC_{50}: 86–100 µM)[116] so the *n*-octyl ester of **227** was prepared by heating the acid **226** in *n*-octanol with catalytic sulfuric acid at 120 °C (**Scheme 27**). LCMS analysis of the reaction mixture showed a 3:1 ratio of the product of amide hydrolysis **230** to the desired product, however, the desired product **229** was obtained in high purity for testing in the IF assay after column chromatography.

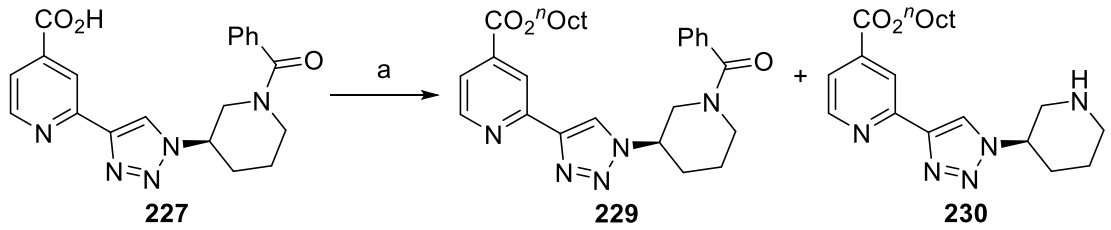

Scheme 27 Synthesis of **229**. *Reagents and conditions:* (a) *n*-octanol, H_2SO_4 (conc.), 120 °C, 14%.

The *n*-octyl ester **229** showed slightly improved cellular efficacy compared to the parent acid **227**, however, the inhibitory effect observed was less than 25% at 100 µM (**Figure 59**).

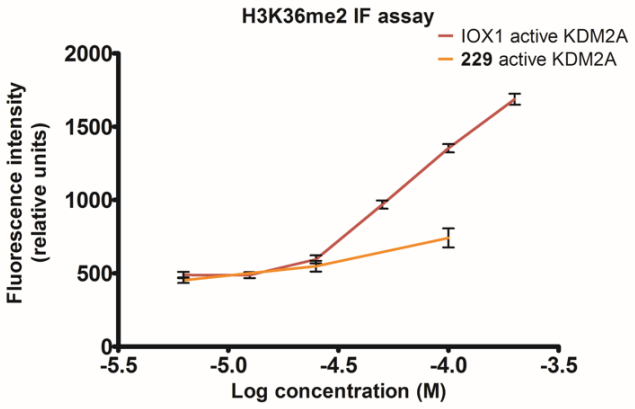

Figure 59 Relative fluorescence intensity observed in cells overexpressing KDM2A and dosed once with IOX1 **21** control or *n*-octyl ester **229**. Error bars represent ± 1 standard error of the mean. Assay carried out by Clarence Yapp.

5.4.1 More Labile Prodrug Esters

The majority of ester prodrugs are hydrolysed by the carboxylesterases CES1 and CES2 but the rate of hydrolysis varies according to the nature of the acyl and alcohol ester substituents.[133] Due to the relatively slow enzymatic hydrolysis of some alkyl esters, a range of more complex esters has been developed, including the acyloxyalkyl esters.[192] The acyloxyalkyl esters are often sufficiently inert to hydrolysis in aqueous solution to be useful as prodrugs but hydrolysed rapidly enough by esterase enzymes to be converted to the active form once in the site of action (i.e. in **Figure 54**, $k_2 > k_1$).

Prodrug esters of the antibiotic nalidixic acid **231** have been reported in the literature which aim to improve dermal absorption compared to the parent drug. The methyl ester prodrug **232** was found to be essentially inert to hydrolysis at 37 °C in both pH 7.4 buffer and in human plasma, however, the acetyloxymethyl ester **233** resulted in a much shorter half-life in human serum (18 minutes) whilst being sufficiently stable in phosphate buffer (half-life 87 hours) to be of interest as a potential prodrug (**Figure 60**).[193]

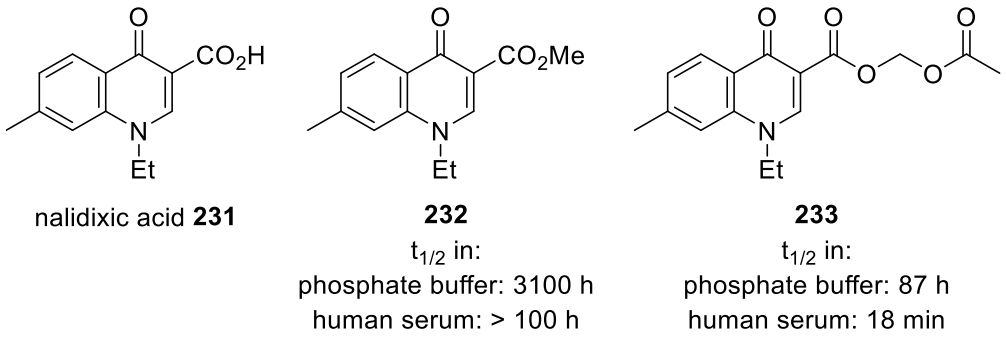

Figure 60 The acetyloxymethyl ester of nalidixic acid **233**, is more useful as a prodrug than the methyl ester **232**, because its half-life in human serum is significantly shorter, resulting in faster turnover to the parent drug **231**.

The PAMPA data for the methyl ester **226** indicates that it is likely to have good cell permeability so the lack of cellular activity could be due to slow hydrolysis to the parent acid after entering the cell. A set of acyloxyalkyl esters **252–261** was prepared through alkylation of the acid **227** with the corresponding acyloxyalkyl chlorides **242–251** (which were available commercially or prepared by Changchun Discovery Services according to a method described by Waranis *et al*.,[194] **Scheme 28**).

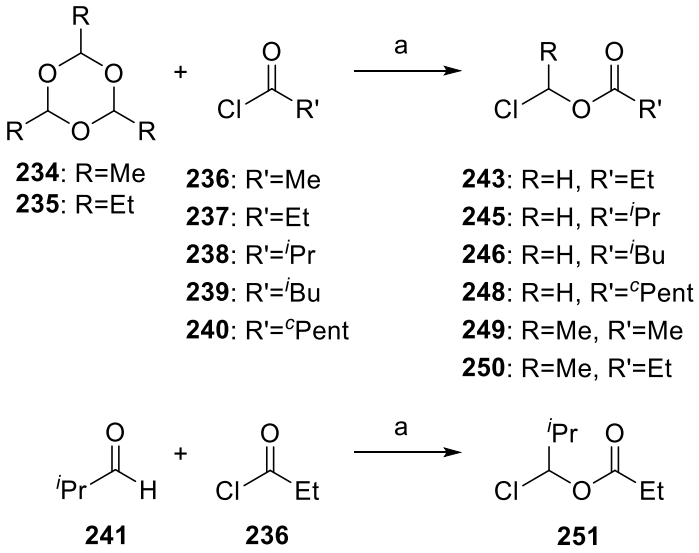

Scheme 28 Synthesis of acyloxyalkyl chlorides **243**, **245**, **246** and **248**–**251**. *Reagents and conditions*: (a) $ZnCl_2$, CH_2Cl_2, 28–71%. Synthesis performed by Changchun Discovery Services.

The reaction between the acid **227** and the acyloxyalkyl chlorides **242**–**250** proceeded at room temperature to give the prodrugs **252–260** but it was necessary to heat the reaction with the more hindered 2-propionyl derivative **251** to 100 °C in order to drive the reaction with acid **227** to completion (**Scheme 29**).

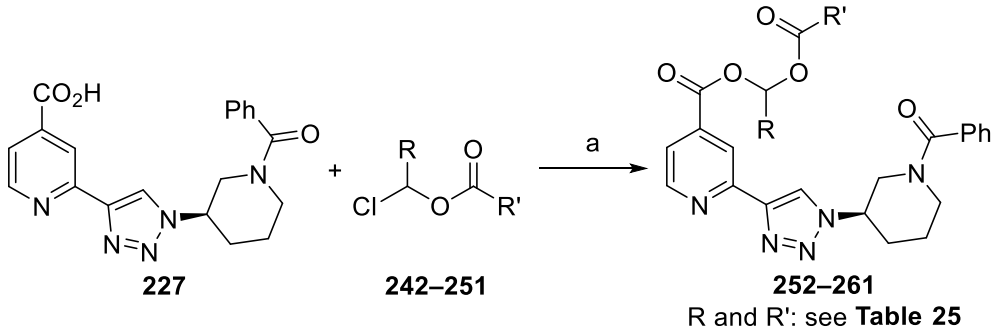

Scheme 29 Synthesis of **252–261**. *Reagents and conditions:* (a) Et_3N, DMF, RT–100 °C, 32–79%.

The acyloxyalkyl esters **252–261** were obtained after column chromatography in 32–79% yield (**Table 25**).

Table 25 Yields and reaction conditions for the formation of acyloxyalkyl esters **252–261**.

Ester Product	Acyloxyalkyl chloride	Acyloxyalkyl Substituents		Reaction	
		R	R'	Temperature	Yield (%)
252	**242**	H	Me	RT	73
253	**243**	H	Et	RT	34
254	**244**	H	^{n}Pr	RT	79
255	**245**	H	^{i}Pr	RT	60
256	**246**	H	^{i}Bu	RT	69
257	**247**	H	^{t}Bu	RT	69
258	**248**	H	^{c}Pent	RT	65
259	**249**	Me	Me	RT	24
260	**250**	Me	Et	RT	71
261	**251**	^{i}Pr	Et	100 °C	32

The acyloxyalkyl esters **252–261** were tested in the IF assay (**Figure 61**).

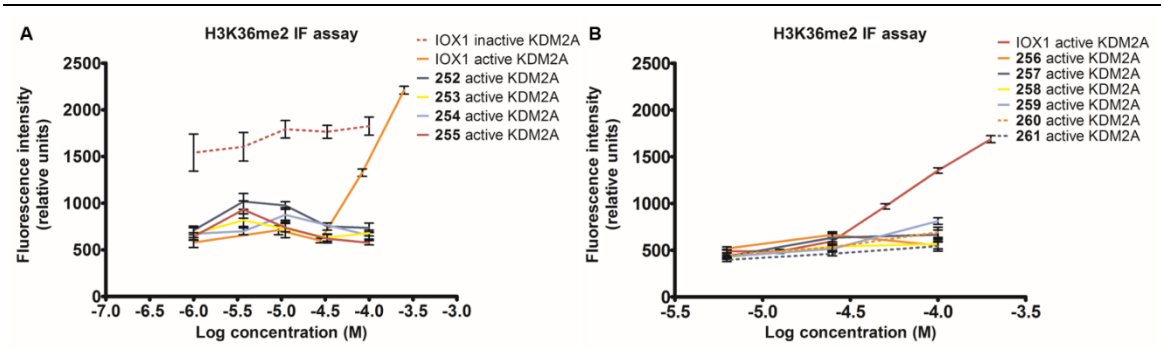

Figure 61 Relative fluorescence intensity observed in cells overexpressing KDM2A or an inactive mutant of KDM2A and dosed once with inhibitor. **A** Cells dosed with IOX1 **21** control and acyloxyalkyl esters **21**, **252**, **253**, **254** and **255**; **B** Cells dosed with IOX1 **21** control and acyloxyalkyl esters **256**, **257**, **258**, **259**, **260** and **261**. Error bars represent ± 1 standard error of the mean. Assay carried out by Clarence Yapp.

No significant inhibition was observed for compounds **252–261**. Compounds **257**, **259** and **260** showed some degree of inhibition, however only at the top concentration (100 µM) where the inhibitory effect observed was less than 25% which is in the same order of magnitude as that observed for the *n*-octyl ester **229**.

5.5 Modulation of the Physicochemical Properties

Compound permeability has been shown to be correlated to the log*D* and inversely correlated with the PSA.[190] Small log*D* values reflect a preference for compounds to

diffuse into an aqueous rather than organic environment and high PSA values indicate that compounds have a high degree of hydrogen bond forming capacity and are consequently likely to be less membrane-permeable.[190, 195, 196]

5.5.1 More Lipophilic Analogues

Since the introduction of a range of prodrug esters had not resulted in significant cellular activity, a set of more lipophilic analogues of **227** was designed which would have a higher log*D* and therefore be expected to be more cell permeable. These targets were prepared in a one-pot procedure from the amino compound **225** and a set of commercially available acyl chlorides to give the protected amides which were treated with lithium hydroxide to liberate the carboxylic acids **262–265** (**Scheme 30**). The sulfonamido analogue **266** was prepared in like manner from **225** and benzensulfonyl chloride.

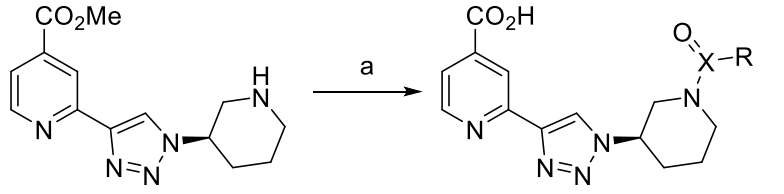

262: X=C, R=1-naphthyl
263: X=C, R=2-naphthyl
264: X=C, R=4-phenylphenyl
265: X=C, R=4-phenoxyphenyl
266: X=SO, R=Ph

Scheme 30 Synthesis of **262–266**. *Reagents and conditions:* for X=C, **262–265**: (a) i) RCOCl, Et_3N, MeCN; ii) LiOH (aq), 13–51%; for X=SO, **266**: (a) i) $PhSO_2Cl$, Et_3N, MeCN; ii) LiOH (aq), 53%.

The resulting five analogues **262–266** were screened against KDM2A and KDM4C (**Table 26**).

Table 26 Inhibitory effect (IC_{50} value) of **262**–**266** against two JmjC KDMs.

			KDM IC_{50}*	
Cmpd	**X**	**R**	**2A**[a]	**4C**[b]
262	C	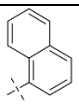	>100 (2)	59 ± 5.0 (2)
263	C	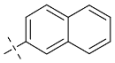	17 ± 2.3 (2)	50 ± 1.7 (2)
264	C	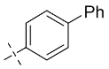	9.9 ± 4.0 (2)	60 ± 2.6 (2)
265	C	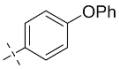	17 ± 30 (2)	ND
266	SO	Ph	>100 (2)	85 ± 2.2 (2)

*Mean IC_{50} (μM) ± standard error of the mean (number of determinations); determined by the [a]AlphaScreen assay or the [b]RapidFire assay.

Amides **262–265** were all found to be more than 170-fold less active against KDM2A than **227**, indicating that the phenyl substituent of **227** likely occupies a relatively narrow area of the substrate binding pocket in KDM2A that cannot accommodate larger substituents. This result is consistent with the results of docking **227** in KDM2A (**Figure 49**). The sulfonamide analogue **266** was found to be inactive against KDM2A at 100 μM. Docking of **266** in a crystal structure of KDM2A indicated that it could be accommodated in the substrate binding pocket (**Figure 62**). The lack of efficacy could be due to the tetrahedral geometry of the sulfonamide group which would place the sulfonamide oxygen atoms in a different position to the amide oxygen atom and the phenyl ring in a different orientation. This might weaken or prevent hydrogen bonding interactions and electrostatic interactions in the substrate binding pocket.

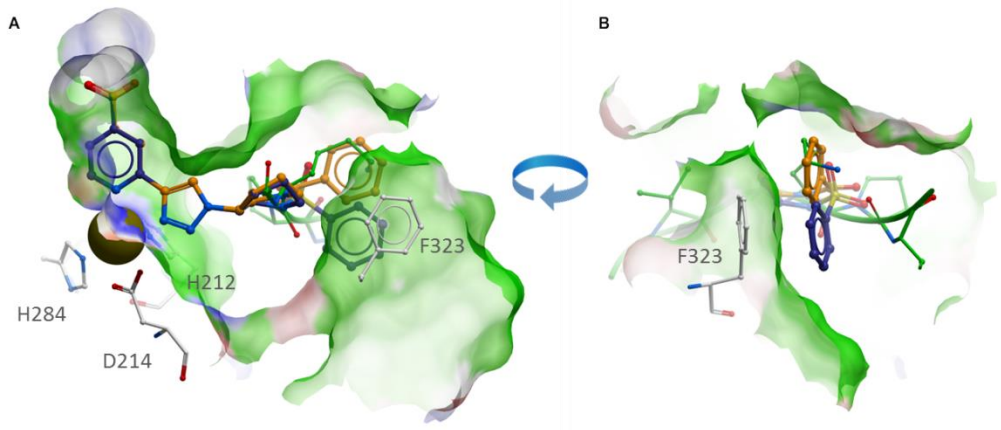

Figure 62 A View from a crystal structure of KDM2A (grey sticks) bound to an H3(A29–Y41)K36me2 peptide (green sticks). The catalytic iron is substituted by nickel (brown sphere). PDB ID: 4QX7. **227** and the sulfonamide analogue **266** were docked into the crystal structure; **227** (orange sticks) overlaps better with the H3 peptide, however, the phenyl ring of **266** (blue sticks) appears to be closer to F323 than the phenyl ring of **227** indicating that it might be capable of forming a favourable pi-stacking interaction, however, the sulfonamide oxygen atoms are in different positions to the amide oxygen atom potentially resulting in the loss of hydrogen bonding interactions with the substrate pocket. **B** Rotation by 110° about the *y*-axis.

5.5.2 Design of Carboxylic Acid Replacements

It was hypothesised that the polar nature of the carboxylate group of **227** was responsible for low cellular permeability and consequently activity so it was proposed to replace the carboxylic acid with other isosteres that could mimic some of the intermolecular interactions formed by the carboxylate in the 2OG binding pocket but reduce the overall polarity of the inhibitor. Common carboxylic acid isosteres including the corresponding hydroxamic acid, tetrazole, sulfonamide and acyl sulfonamide,[197] and other replacements for the carboxylic acid including the hydroxyl, methoxy, hydroxymethyl and aldehyde substituents were considered as possible replacements for the carboxylate group. The pK_a, log*P*, log*D* and topological polar surface area (TPSA)[198] of a set of isonicotinic acid replacements were calculated to determine the likelihood that the acid replacements would be more cell permeable than the parent acid **227** (**Table 27**).

Table 27 Calculated physicochemical properties of isonicotinic acid and a selection of pyridine derivatives.

Cmpd	Structure	*c*log*P**	Carboxylic acid or acid isostere *c*p*K*a*	*c*log*D** (at pH 7.4)	TPSA* (Å^2)
227	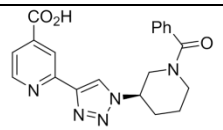	2.5	3.0	–1.3	101
267	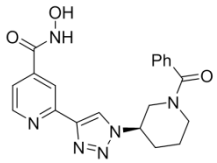	0.74	7.7	0.59	113
268	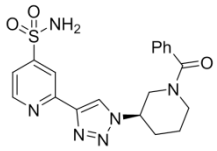	0.81	9.1	0.81	132
269	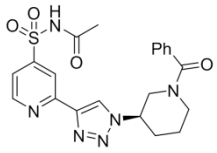	1.2	4.1	–1.5	136
270	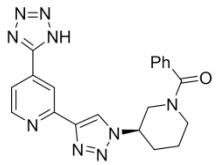	0.50	2.6	–2.1	118
274	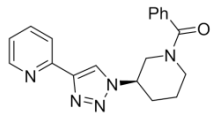	2.6	N/A	2.6	63.9
280	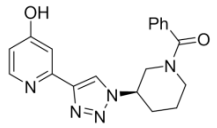	1.9	7.9	1.9	84.1
278	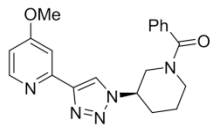	2.5	N/A	2.4	73.1
282	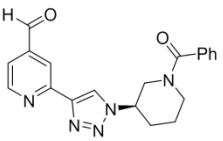	2.4	N/A	2.4	81.0
281	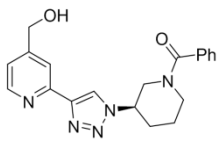	1.4	13	1.4	84.1

*Calculated using ACD labs prediction model.[139, 182]

The potential targets were also docked into a crystal structure of KDM2A which showed that there was likely to be sufficient space in the 2OG binding pocket to accommodate the

functional groups used as carboxylic acid replacements in **268, 274**, **278** and **280**–**282** but that the hydroxamic acid (**267**), acylsulfonamide (**269**) and tetrazole (**270**) moieties would likely be too large to adopt the usual binding mode. Although sulfonamide **268** might be small enough to be accommodated in the 2OG binding pocket its TPSA is significantly higher (132 $Å^2$) than the TPSA of the parent acid **227** (101 $Å^2$). Thus, the energetic cost associated with breaking the hydrogen bonding interactions to the sulfonamide in aqueous solution to allow it to diffuse into cells may be as high as for **227**. Compounds **274**, **278** and **280**–**282** were selected as targets for synthesis; it was expected that they would be accommodated in the active site of KDM2A and their *c*log*D* and TPSA values were expected to correlate with improved membrane permeability compared to **227**.

5.5.3 Synthesis of Carboxylic Acid Replacements

5.5.3.1 Synthesis of Pyridine Derivative 274

The methanesulfonate **223** was heated with sodium azide to give the azide **271** which was used without further purification in a copper-catalysed click triazole-forming reaction with commercially available 2-ethynylpyridine to give **272** (**Scheme 31**). Acid catalysed

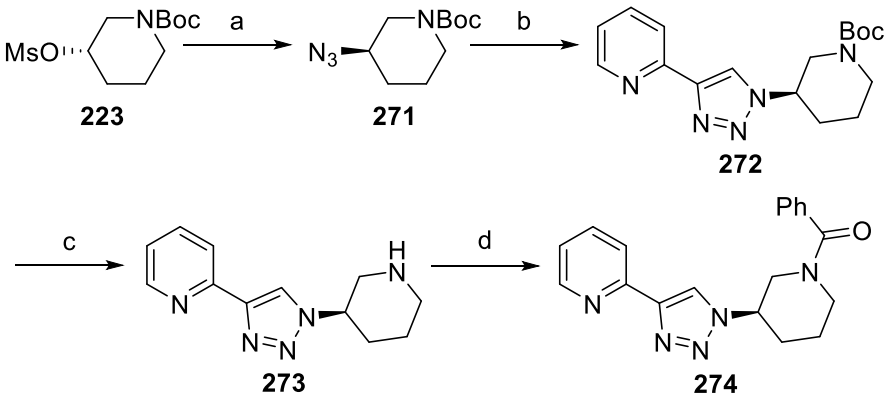

Scheme 31 Synthesis of **274**. *Reagents and conditions:* (a) NaN_3, DMF, 90 °C, 90%; (b) 2-ethynylpyridine, $CuSO_4·5H_2O$, (+)-sodium L-ascorbate, ^tBuOH, H_2O, 65 °C, 71%; (c) TFA, CH_2Cl_2, 51%; (d) $PhCOCl$, Et_3N, MeCN, quant.

removal of the Boc protecting group with trifluoroacetic acid gave **273** and acylation with benzoyl chloride gave the target **274**.

5.5.3.2 Synthesis of Methoxy and Hydroxyl Derivatives 277 and 280

Sonogashira coupling of commercially available 2-chloro-4-methoxypyridine **275** with trimethylsilylacetylene using the conditions optimised for chloride **136** gave **276** in low yield (**Scheme 32**). After purification by flash column chromatography, **276** contained 43% w/w triphenylphosphine oxide but the material was taken on to the copper-catalysed click reaction with the aim of removing the triphenylphosphine oxide later in the synthesis. Acid catalysed deprotection of the Boc protecting group with trifluoroacetic acid gave compound **277** in high purity. Acylation with benzoyl chloride gave the target **278**. Intermediate **277** was also treated with concentrated hydrobromic acid to give the 4-hydroxypyridine derivative **279** which was acylated with benzoyl chloride to give **280**.

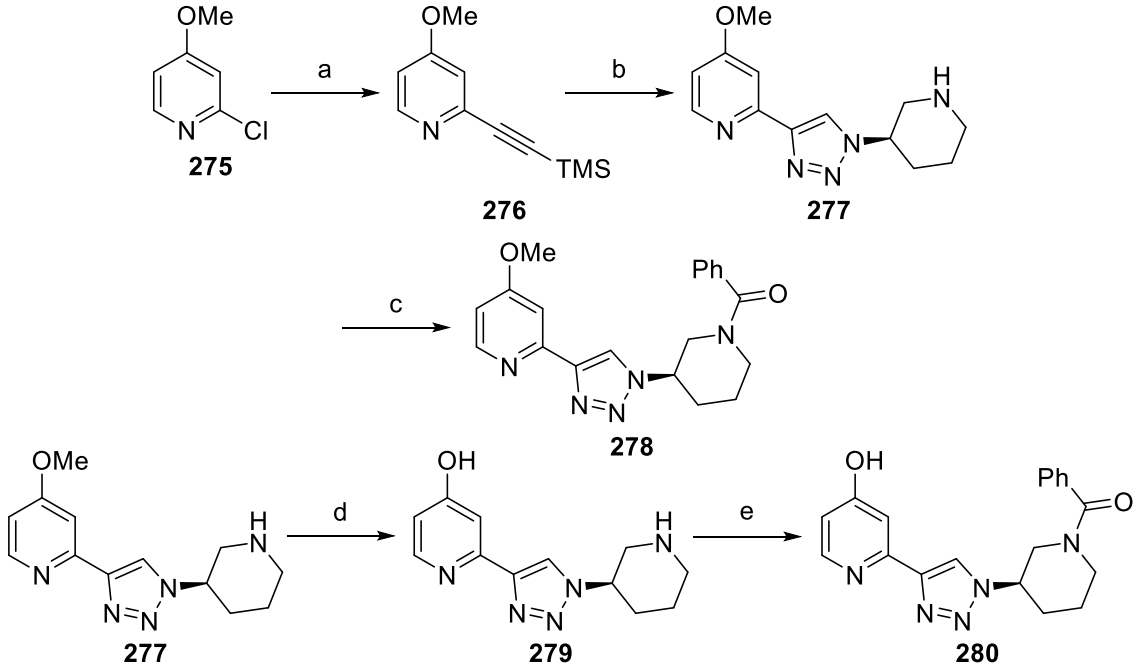

Scheme 32 Synthesis of **278** and **280**. (a) TMSCCH, CuI, $Pd(PPh_3)_4$, PPh_3, Et_3N, DMF, 50 °C, 9%; (b) i) **271**, $CuSO_4 \cdot 5H_2O$, (+)-sodium L-ascorbate, ^tBuOH, H_2O, 65 °C; ii) TFA, CH_2Cl_2, 58%; (c) PhCOCl, Et_3N, MeCN, 91%; (d) HBr (aq), 140 °C, 53%; (e) PhCOCl, Et_3N, MeCN, DMF, 62%.

5.5.3.3 Synthesis of Hydroxymethyl Derivatives 281 and 283 and Aldehyde 282

Activation of the acid **227** with 1,1'-carbonyldiimidazole followed by reduction with sodium borohydride gave the hydroxymethyl compound **281** (**Scheme 33**). Oxidation of

281 with 1,1,1-tris(acetyloxy)-1,1-dihydro-1,2-benziodoxol-3-(1*H*)-one (Dess–Martin periodinane) gave the aldehyde **282**.

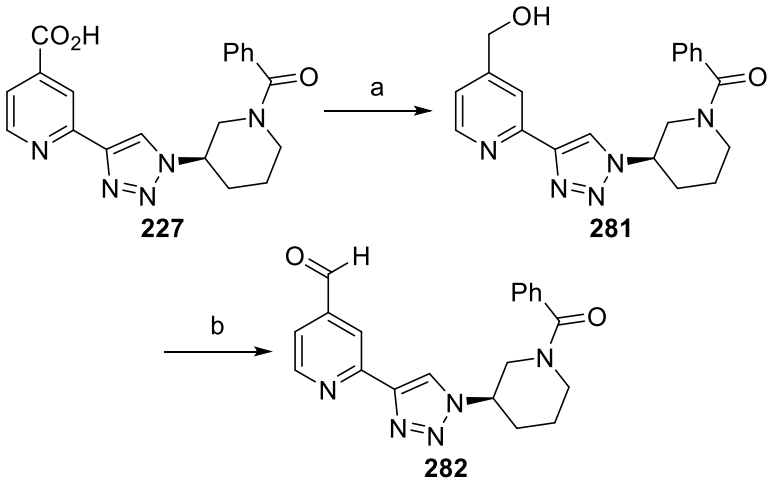

Scheme 33 Synthesis of **281** and **282**. (a) i) 1,1'-carbonyldiimidazole, Et_3N, THF; ii) $NaBH_4$, H_2O, 59%; (b) Dess–Martin periodinane, $CHCl_3$, 40%.

The hydroxymethyl analogue of one of the most potent and selective KDM2A inhibitors in the aminomethyl series, **74**, was also prepared to determine its inhibitory activity. Reduction of the ethyl ester **71** with lithium borohydride gave the hydroxymethyl analogue **283** in good yield (**Scheme 34**).

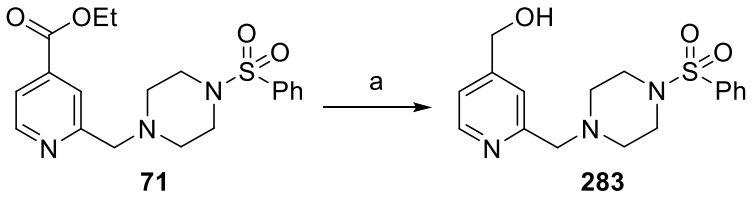

Scheme 34 Synthesis of **283**. (a) $LiBH_4$, EtOH, THF, 40 °C, 77%.

The resulting compounds were tested against KDM2A and some of the other JmjC KDMs from the assay panel (**Table 28**).

Table 28 Inhibitory effect (IC_{50} value) against five JmjC KDMs.

Cmpd	Structure	KDM IC_{50}*				
		2A	**3A**	**4C**	**4E**	**6B**
272	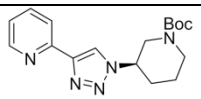	>100 (2)[a]	>100 (2)	>100 (2)	ND	>100 (2)
273	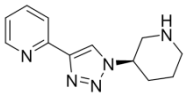	>100 (2)[a]	>100 (2)	>100 (2)	ND	>100 (2)
274	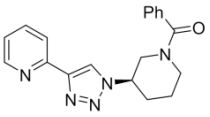	>100 (2)[a]	>100 (2)	>100 (2)	ND	>100 (2)
278	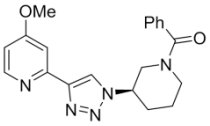	>100 (2)[a]	>100 (2)	>100 (2)	ND	>100 (2)
280	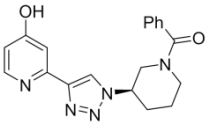	13 ± 1.0 (2)[a]	ND	ND	ND	ND
281	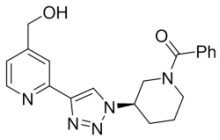	73 ± 9.0 (2)[a]	ND	ND	ND	ND
282	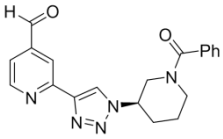	24 ± 6.1 (2)[a]	ND	ND	ND	ND
283	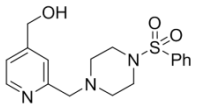	100 ± 27 (2)	ND	>100 (2)	>100 (2)	>100 (2)

*Mean IC_{50} (μM) ± standard error of the mean (number of determinations); determined by the AlphaScreen assay unless otherwise stated or by the [a]RapidFire assay.

The inhibitory activity of these compounds against KDM2A was found to be much reduced compared to that of the acid **227** (KDM2A RapidFire IC_{50}: 0.1 μM, see **Table 30**), for example the pyridine derivative **274** which contains a hydrogen atom in place of the carboxylic acid group resulted in less than 20% inhibition of KDM2A at 100 μM. The 4-hydroxypyridine **280** was found to be the best replacement for the carboxylic acid **227** but was still 130-fold less active against KDM2A (KDM2A IC_{50}: 13 μM).

5.5.4 Intramolecular Hydrogen Bonding

The polarity of the carboxylate was expected to be responsible for the lack of efficacy observed in the cellular assay so it was hypothesised that the introduction of a hydrogen bond donor in one of the positions ortho to the carboxylic acid would improve the activity observed in the cellular assay by improving the permeability of the inhibitor. Since desolvation on crossing the cell membrane through passive diffusion results in loss of hydrogen bonding interactions with the bulk water, it was hypothesised that the energetic cost of desolvation could be reduced by introducing an intramolecular hydrogen bond which could be preserved as the inhibitor crossed the cell membrane.[199] Derivatives of **227** bearing a hydroxyl group capable of forming an intramolecular hydrogen bond to the carboxylic acid were designed as targets (**Figure 63**).

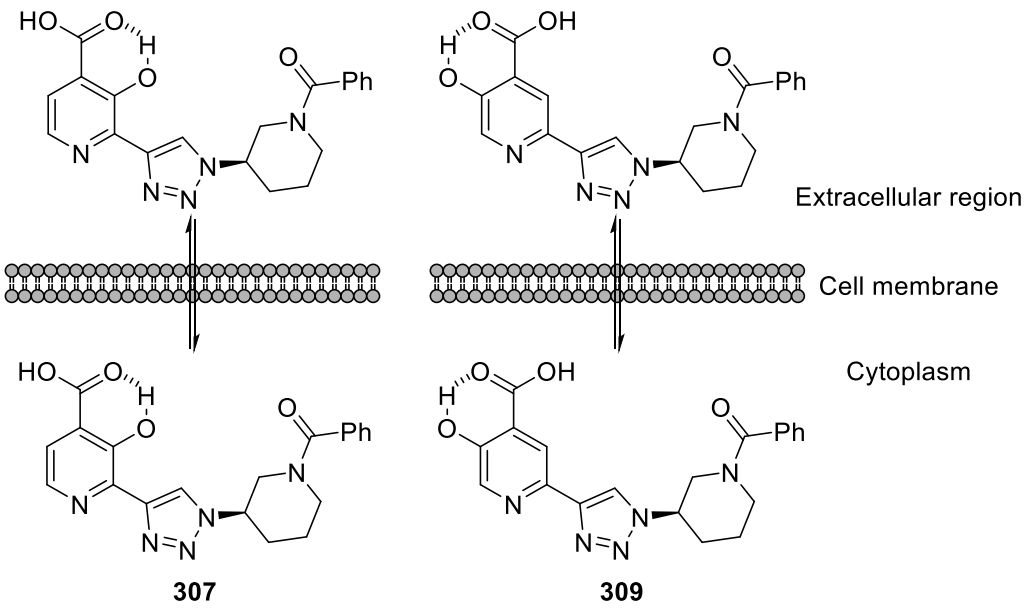

Figure 63 Targets **307** and **309** which were designed to improve membrane permeability compared to **227** by enabling the formation of an intramolecular hydrogen between the carboxylic acid and the hydroxyl group which could be preserved during diffusion through the cell membrane, reducing the energetic desolvation penalty for transmembrane diffusion.

5.5.4.1 Synthetic Route *via* Pyridine *N*-Oxide

It was envisaged that both **307** and **309** could be prepared in a divergent synthesis from 3-hydroxyisonicotinic acid **290** (**Figure 64**). The key step would be a Polonovski-type

reaction[200] of a pyridine *N*-oxide **293** with acetic anhydride. It was anticipated that treatment of **293** with acetic anhydride would proceed to give a mixture of the two pyridone regioisomers **286** and **287** which could be converted to the corresponding TMS-protected acetylene derivatives **284** and **289** *via* the trifluoromethanesulfonates **285** and **288** and then submitted to the same reaction sequence as for the synthesis of **227** from TMS-protected acetylene **118** to give **307** and **309**.

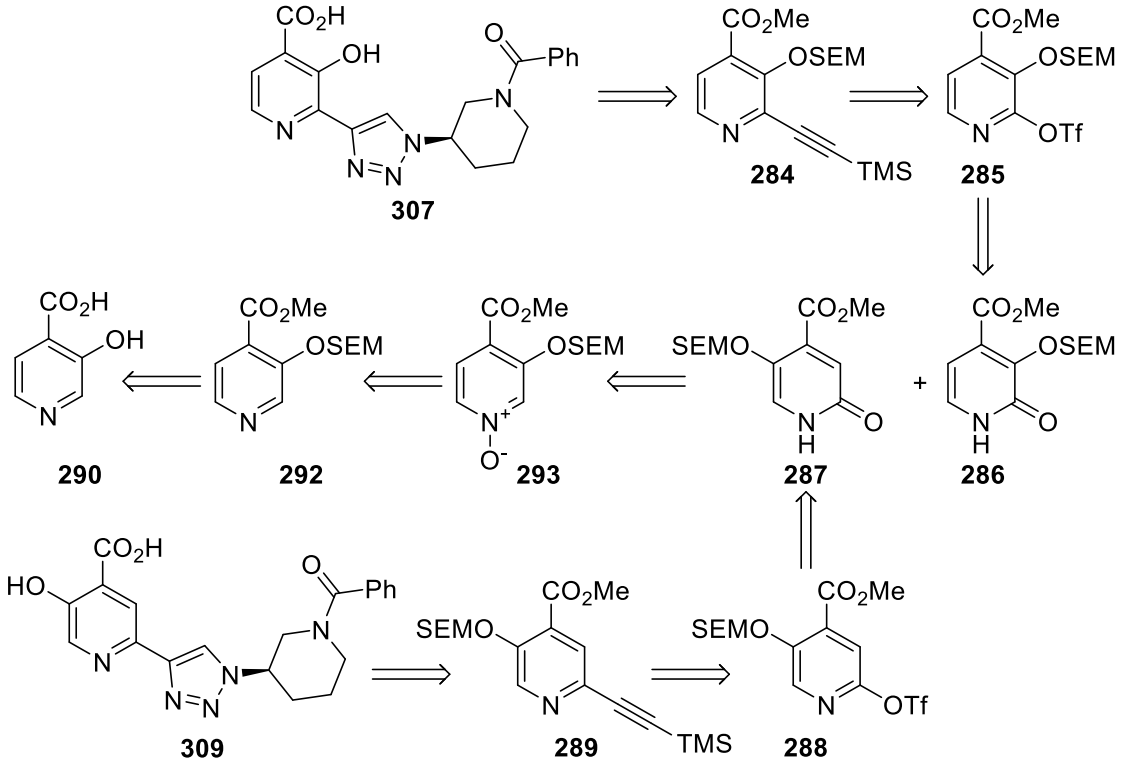

Figure 64 Proposed route to **307** and **309** from a common *N*-oxide intermediate **293**.

The hydroxyisonicotinate **290** was converted to the methyl ester **291** according to a method reported by Hansen *et al.* (**Scheme 35**).[201] Protection of the hydroxyl group with 2-(trimethylsilyl)ethoxymethyl chloride (SEM-Cl) gave **292** which was converted to the *N*-oxide **293** with *meta*-chloroperbenzoic acid. The Polonovski-type rearrangement appeared to occur regioselectively; on reaction with acetic anhydride only one product was isolated which had a molecular weight consistent with loss of the SEM protecting group and acylation of the pyridine *N*-oxide followed by rearrangement to give an acylpyridone derivative. The aromatic region was found to contain only two doublets which would

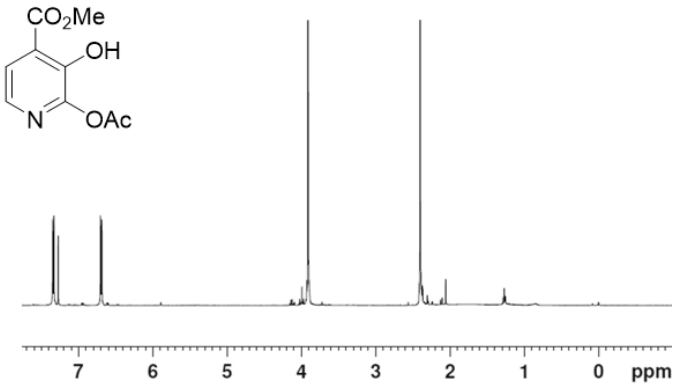

Figure 65 ^{1}H NMR spectrum of **294**. The two doublets found in the aromatic region at 6.69 and 7.34 ppm (*J* 7.0) are consistent with a 1,2,3-substituted pyridine product.

indicate that the Polonovski-type rearrangement had occurred to give a product that was substituted at the 2-position.

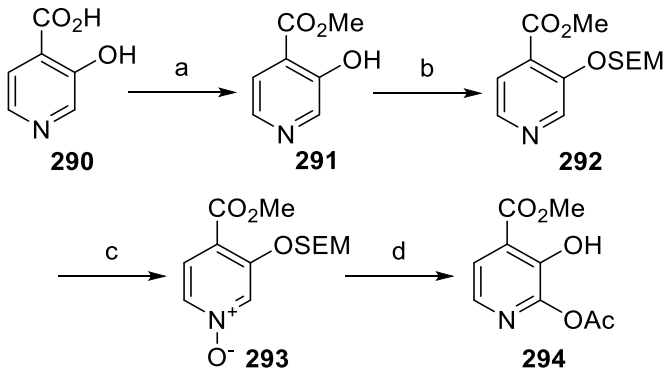

Scheme 35 Synthesis of **294**. *Reagents and conditions:* (a) MeOH, H_2SO_4, 65 °C, 56%; (b) SEM-Cl, NaH, THF, 63%; (c) *meta*-chloroperbenzoic acid (mCPBA), CH_2Cl_2, 41%; (d) Ac_2O, Et_3N, 140 °C, 33%.

Since the reaction only gave one regioisomer and the SEM protecting group was not stable to the reaction conditions, an alternative route was designed to synthesise the hydroxyl targets **307** and **309**.

5.5.4.2 Synthetic Route Employing Lithiation Chemistry

An alternative route to targets **307** and **309** from two commercially available 2-bromopyridine compounds (**295** and **298**) was designed (**Scheme 36**). The key step would be directed ortho-metalation (DOM)[202] of **295** and **298** followed by carboxylation with carbon dioxide. It was hypothesised that in both cases deprotonation with lithium

diisopropylamide (LDA) would be directed ortho to the methoxy group resulting in lithiation at the 4-position of the pyridine ring and on quenching with carbon dioxide would generate intermediates **296** and **299** which could be converted to the targets **307** and **309** using the route previously described for the synthesis of **227** from **118**.

Deprotonation of **295** and **298** with LDA at –78 °C and quenching of the lithiated species with dry ice in a procedure adapted from that described by Manteau *et al.*[203] for reaction of the corresponding 2-chlorotrifluoromethoxy pyridine compounds gave **296** and **299** in moderate yield (**Scheme 36**). No evidence of the products resulting from rearrangement of the organolithium intermediates was seen; the moderate yields were due to the isolation of significant amounts of starting material. Although the recovery of **295** and **298** could be due to insufficient LDA for deprotonation to go to completion, the recovery of starting material is likely due to water present on the surface of the dry ice which would quench the organolithium intermediate to regenerate starting material. **296** and **299** were converted to the methyl esters **297** and **300** by heating in methanol with sulfuric acid at 65 °C (**Scheme 36**).

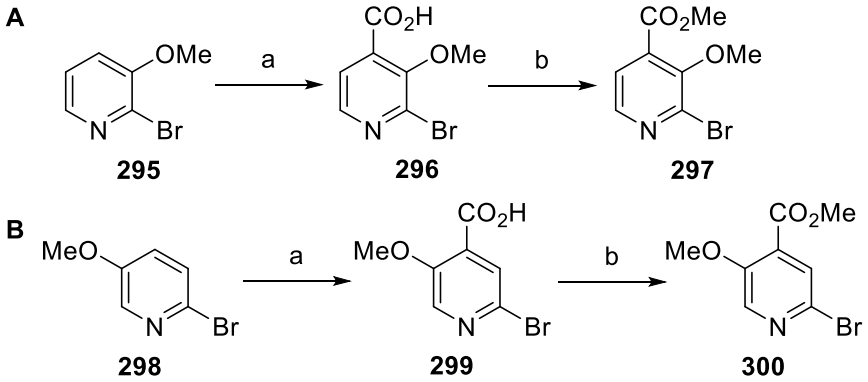

Scheme 36 Synthesis of intermediates **297** and **300**. *Reagents and conditions:* **A** for **297** (a) i) $H(^{i}Pr)_2N$, BuLi, THF, –78 °C; ii) CO_2 (s), –78 °C, 21%; (b) H_2SO_4, MeOH, 65 °C, 91%. **B** for **300** (a) i) $H(^{i}Pr)_2N$, BuLi, THF, –78 °C; ii) CO_2 (s), –78 °C, 56%; (b) H_2SO_4, MeOH, 65 °C, 90%.

Bromide **300** was submitted to the Sonogashira conditions for the conversion of bromide **117** to acetylene derivative **118** (**Scheme 37**). Analysis of the reaction mixture by LCMS

showed that it contained mostly starting material bromide **300**. A small amount of desired product **301** had formed but the major reaction product was the reduced material **302** (entry 1, **Table 29**).

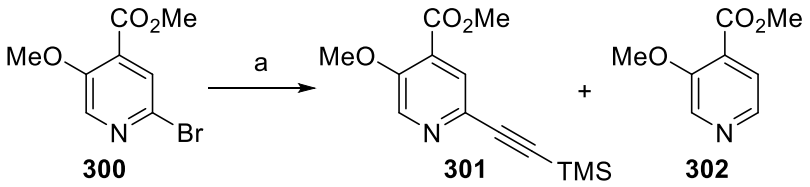

Scheme 37 Optimisation of the Sonogashira coupling of **300**. *Reagents:* (a) TMSCCH, CuX, $Pd(PPh_3)_4$ or $Pd(dppf)Cl_2$, Et_3N or DIPEA, THF, PPh_3; see **Table 29** for conditions.

The reaction was optimised by systematically varying the reaction temperature, source of copper, catalyst, base, solvent and amount of trimethylsilylacetylene used (**Table 29**). Increasing the amount of trimethylsilylacetylene, increasing the reaction temperature to 80 °C, changing the solvent to *N*,*N*-dimethylformamide and adding 20 mol% triphenylphosphine resulted in complete conversion to the desired product by LCMS (entry 12, **Table 29**).

Table 29 Proportion of starting material bromide **300**, reduced product **302** and Sonogashira coupling product **301** formed in different reaction conditions (by LCMS).

Entry	CuX	Temp (°C)	Solvent	Catalyst	Base	Equiv. PPh_3	Equiv. TMSCCH	Proportion by LCMS		
								300	302	301
1	CuI	50	THF	$Pd(PPh_3)_4$	Et_3N	0	2.2	90	7	2
2	CuI	70	THF	$Pd(PPh_3)_4$	Et_3N	0	2.2	85	6	9
3	CuI	50	DMF	$Pd(PPh_3)_4$	Et_3N	0	2.2	82	9	9
4	CuI	50	DMF	$Pd(PPh_3)_4$	Et_3N	0.2	2.2	91	6	3
5	CuI	50	DMF	$Pd(dppf)Cl_2$	Et_3N	0	10	91	4	5
6	CuI	50	DMF	$Pd(PPh_3)_4$	DIPEA	0.2	10	87	5	7
7	CuBr	50	DMF	$Pd(PPh_3)_4$	Et_3N	0.2	10	79	6	16
8	CuI	90	DMF	$Pd(PPh_3)_4$	Et_3N	0.2	10	13	9	78
9	CuI	80	DMF	$Pd(PPh_3)_4$	Et_3N	0	10	17	3	80
10	CuBr	80	DMF	$Pd(PPh_3)_4$	Et_3N	0	10	0	4	96
11	CuI	80	DMF	$Pd(PPh_3)_4$	Et_3N	0.2	10	0	4	96
12	CuBr	80	DMF	$Pd(PPh_3)_4$	Et_3N	0.2	10	0	0	100

The optimised Sonogashira coupling conditions were applied to both **297** and **300** to give the TMS-protected alkyne derivatives **301** and **303** which were reacted with Boc-protected azidopiperidine **271** to give triazole derivatives **304** and **305** (**Scheme 38**).

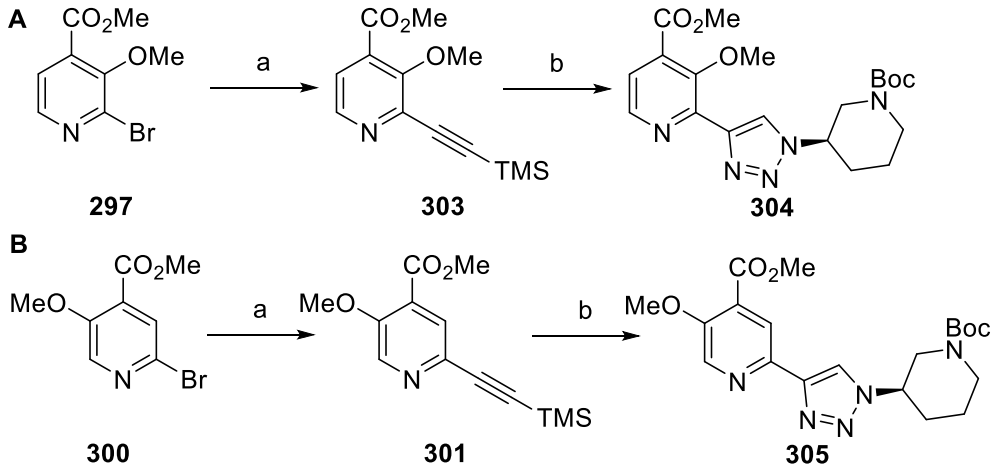

Scheme 38 Synthesis of compounds **304** and **305**. *Reagents and conditions:* **A** for **304** (a) TMSCCH, CuBr, $Pd(PPh_3)_4$, PPh_3, Et_3N, DMF, 80 °C, 56%; (b) **271**, TBAF, $CuSO_4 \cdot 5H_2O$, (+)-sodium L-ascorbate, ^tBuOH, H_2O, 65 °C, 78%. **B** for **305** (a) TMSCCH, CuBr, $Pd(PPh_3)_4$, PPh_3, Et_3N, DMF, 80 °C, 84%; (b) **271**, TBAF, $CuSO_4 \cdot 5H_2O$, (+)-sodium L-ascorbate, ^tBuOH, H_2O, 65 °C, 66%.

Deprotection of the methyl ester, methyl ether and Boc protecting groups was achieved in one step by heating **304** and **305** in concentrated hydrobromic acid to give **306** and **308**. Reaction with benzoyl chloride gave the target compounds **307** and **309** (**Scheme 39**).

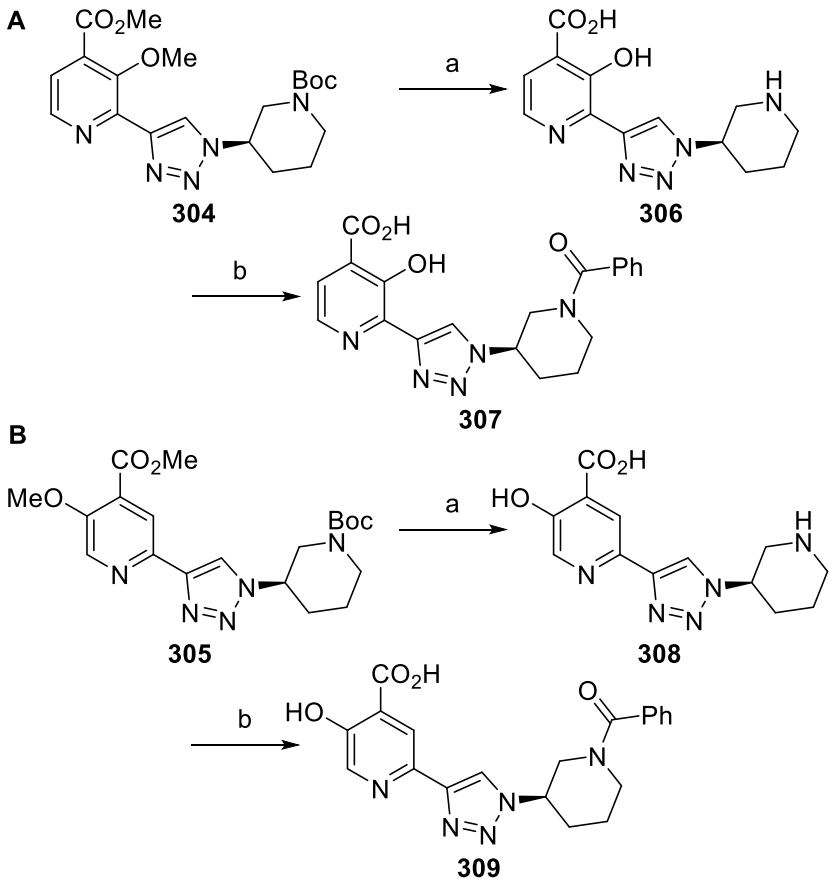

Scheme 39 Synthesis of **307** and **309**. *Reagents and conditions:* **A** for **307** (a) HBr (aq), 90 °C, 52%; (b) PhCOCl, Et_3N, DMF, 44%. **B** for **309** (a) HBr (aq), 90 °C, 78%; (b) PhCOCl, Et_3N, DMF, 43%.

The methyl ester and Boc protecting groups were also removed selectively over the methyl ether protecting group in a one-pot procedure by treating **304** and **305** with lithium hydroxide to hydrolyse the methyl esters followed by acidifying with trifluoroacetic acid to remove the Boc groups to give the methoxy compounds **310** and **311** (**Scheme 40**). The *NH*-piperidine compound **312** was also prepared through hydrolysis of methyl ester **225**.

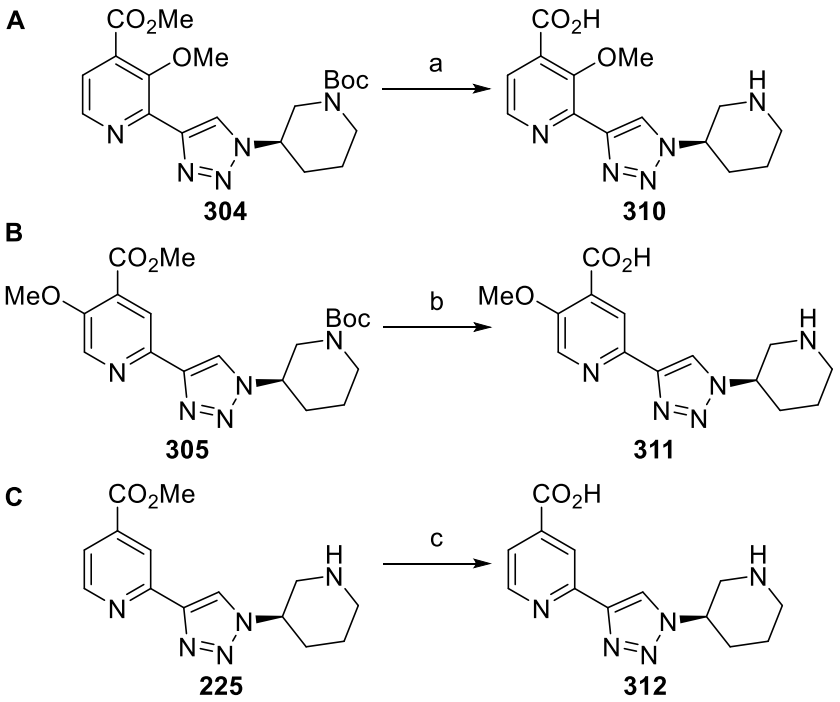

Scheme 40 Synthesis of *NH*-piperidine compounds **310**–**312**. *Reagents and conditions:* (a) i) LiOH (aq), MeCN; ii) TFA, 54%; (b) i) LiOH (aq), MeCN; ii) TFA, 27%; (c) LiOH (aq), MeCN, quant.

5.5.4.3 Biological Activity of Hydroxy- Derivatives 307 and 309

The parent compound **227** and the two hydroxy- derivatives **307** and **309** were screened against KDM2A using the RapidFire assay (**Table 30**). The *NH*-piperidine compounds **306**, **308**, **310**, **311** and **312** were also tested to determine the effect of introducing a methoxy group on the pyridine ring on the inhibitory potency against KDM2A.

Table 30 Inhibitory effect (IC_{50} value) of **227** and **306**–**312** against KDM2A.

Cmpd	KDM2A IC_{50}*	Fold change compared to 227
227	0.10 ± 0.0033 (12)	1
306	1.4 ± 0.14 (4)	14
307	0.16 ± 0.0066 (4)	1.6
308	69 ± 3.8 (4)	690
309	21 ± 1.3 (4)	210
310	15 ± 3.2 (2)	150
311	>100 (2)	>1000
312	>100 (2)[a]	>1000

*Mean IC_{50} (μM) ± standard error of the mean (number of determinations); determined by the RapidFire assay unless otherwise stated or by the [a]AlphaScreen assay.

Gratifyingly, the 3-hydroxy substituent (compound **307**) was well tolerated with respect to KDM2A inhibition and **307** was found to be approximately equipotent with **227** against KDM2A (IC_{50}: 0.16 µM). The 5-hydroxy substituent (compound **309**) was found to be a much weaker inhibitor of KDM2A (IC_{50}: 21 µM). The *NH*-piperidine derivatives **310** – **312** were found to be less active against KDM2A, although the 3-hydroxy derivative **310** was found to be more potent against KDM2A (IC_{50}: 15 µM) than the 5-hydroxy derivative **311** (IC_{50}: >100 µM). Although examination of the crystal structure of a complex of KDM2A with 2OG[204] indicates that the space available to accommodate the *ortho*-hydroxy groups in the 2OG binding pocket appears to be similar in the 3- and 5-positions, it is possible that the 2OG binding pocket is more flexible in the region occupied by the C3 pyridine substituent resulting in more favourable binding interactions with **307** and greater inhibitory activity against KDM2A compared to **309** (**Figure 66**).

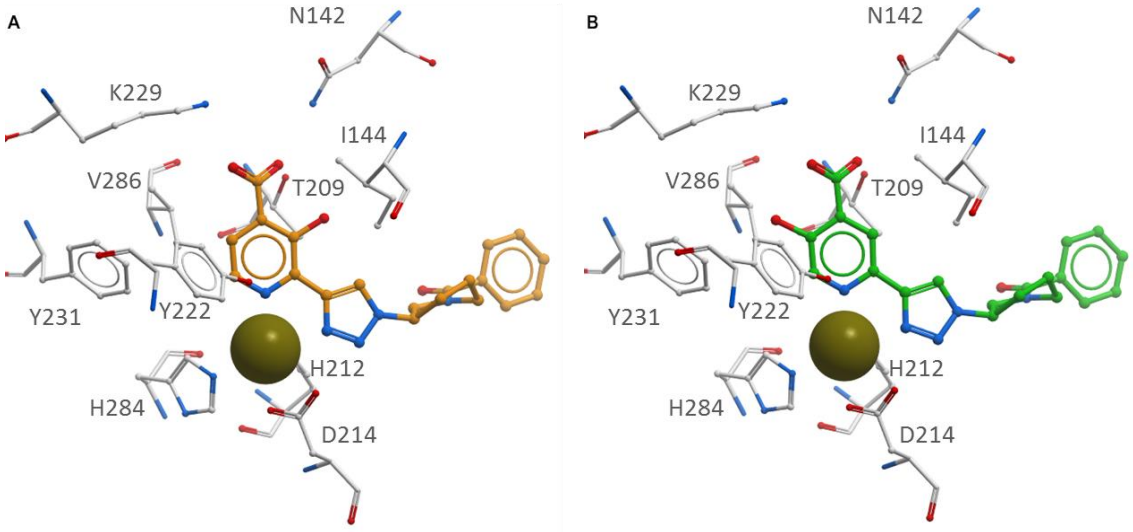

Figure 66 Compounds **A 307** (orange sticks) and **B 309** (green sticks) docked into the co-crystal structure of 2OG and H3K36me2 in complex with KDM2A (key KDM2A binding residues shown as grey sticks; PDB ID: 4QX7). The catalytic iron is substituted by nickel (brown sphere) which is coordinated by H212, D214 and H284.

The 3-hydroxy derivative **307** was tested in the IF assay but disappointingly no inhibition was observed at 100 µM (**Figure 67**).

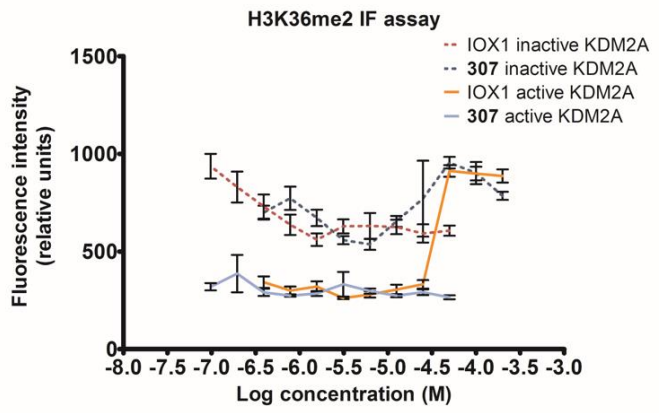

Figure 67 Relative fluorescence intensity observed in cells overexpressing KDM2A or an inactive mutant of KDM2A and dosed once with inhibitor. Cells dosed with IOX1 **21** control and 3-hydroxy compound **307**. Error bars represent ± 1 standard error of the mean. Assay carried out by Stephanie Hatch.

Submitting this compound to the PAMPA assay showed that the introduction of the hydroxyl group did not improve the permeability in the PAMPA screen; **307** was found to be less permeable than **227** at pH 7.4, 6.2 and 5.0 (**Table 31**).

Table 31 PAMPA data for carboxylate **227** and the 3-hydroxy substituted analogue **307**.

	PAMPA P_e (10^{-6} cms^{-1})		
	pH 7.4	**pH 6.2**	**pH 5.0**
227	0.69	0.41	1.9
307	0.40	0.20	0.20

Assay carried out by Brian Linehan at Boehringer Ingelheim.

5.6 Discussion

Although carboxylic acids **50** and **227** have been shown to be potent inhibitors of KDM2A, they did not result in inhibition of KDM2A at 100 µM concentration in the IF assay. It was hypothesised that this lack of cellular efficacy was due to poor cell permeability, and a number of strategies were employed to improve cell penetration (**Figure 68**).

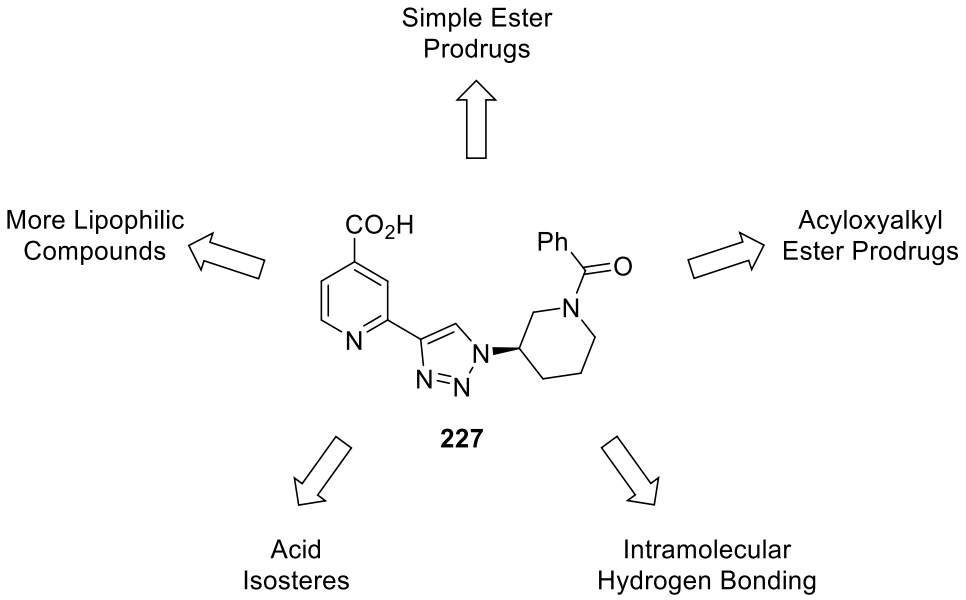

227

Figure 68 Strategies employed to improve the cellular efficacy of **227**.

Simple ester prodrugs of the aminomethyl pyridine compound **50** (ethyl ester **49**), and of the triazolopyridine compound **227** (methyl and *n*-octyl esters **226** and **229**) did not result in significant efficacy in the IF assay; the most potent inhibitor was *n*-octyl ester **229** which resulted in KDM2A inhibition of approximately 25% at 100 μM. Of the acyloxyalkyl prodrug esters, **257**, **259** and **260** showed a similar degree of inhibitory effect at 100 μM to **229**. This weak cellular activity is not significant enough for **229**, **257**, **259** and **260** to be useful as prodrugs in cellular studies of KDM2A.

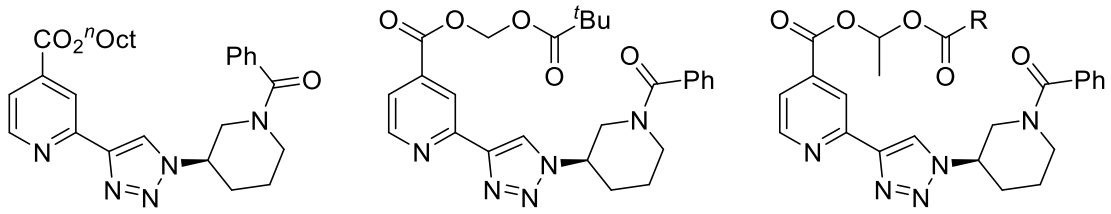

229 **257** R=Me: **259** R=Et: **260**

Figure 69 Prodrug esters found to result in weak inhibition of KDM2A in the IF assay.

Modulating the physicochemical properties of **227** by increasing the lipophilicity of the amide substituent or replacing the carboxylic acid with less polar groups resulted in a loss

of inhibitory activity against KDM2A *in vitro* so these compounds were not tested in the cellular assay (**Figure 70**).

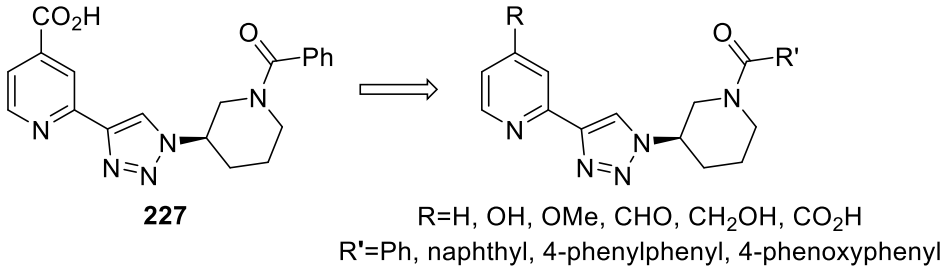

Figure 70 More lipophilic analogues of **227** were designed and synthesised in order to reduce the polarity of **227** and improve membrane permeability.

Ortho-hydroxy derivatives of **227**, compounds **307** and **309** were synthesised. **307** was found to be a potent inhibitor of KDM2A (IC_{50}: 0.16 µM) but this compound had poor PAMPA permeability and did not show an inhibitory effect in the IF assay at 100 µM (**Figure 71**).

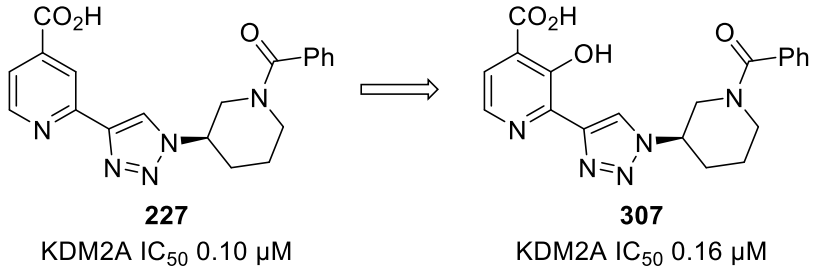

Figure 71 Introduction of a hydroxyl group at the 3-position of the pyridine ring of **307** was well tolerated with respect to KDM2A inhibition but did not result in cellular efficacy.

Chapter 6. Investigation of the Interaction with KDM2A in a Cellular Context

6.1 Introduction

Whilst the results from the AlphaScreen and RapidFire assays had demonstrated that **227** is a potent and selective inhibitor of KDM2A/7B *in vitro* (**Chapter 4**), **227** and its prodrug esters had not been found to inhibit the demethylation of H3K36me2 by KDM2A in the IF assay. Thus, it was decided to pursue a "chemical proteomics" (chemoproteomics)[205] approach as an orthogonal method for determining the engagement of **227** with KDM2A in a cellular environment. In affinity-based chemoproteomic profiling, inhibitors are immobilised onto agarose or magnetic beads (**Figure 72**).[206] The inhibitor must bear a functional group or tag that can covalently react or form a strong affinity-based interaction with suitably functionalised beads. For example an amino-substituted inhibitor can be immobilised onto *N*-hydroxysuccinimide- (NHS) activated beads or a biotin-substituted inhibitor can be immobilised onto avidin- or streptavidin-functionalised beads.[207] The biotin–streptavidin interaction is extremely strong (the K_d at pH 7.0 is 4×10^{-14} M) and the half-life at pH 7.0 is 2.9 days so the interaction is essentially irreversible on the timescale of a typical chemoproteomics experiment.[208] The immobilised inhibitor, the "bait", is then incubated with a cell lysate. Proteins with a high affinity for the bait bind to it and can be separated from the residual cell lysate by washing the beads.[209] Any proteins that remain bound after washing are eluted from the beads either specifically (by the addition of free inhibitor) or non-specifically (for example by the addition of detergent, sodium chloride or urea).[209] The resulting eluate is analysed by mass spectrometry or western blotting to determine which proteins from the cell lysate have bound to the bait.[207]

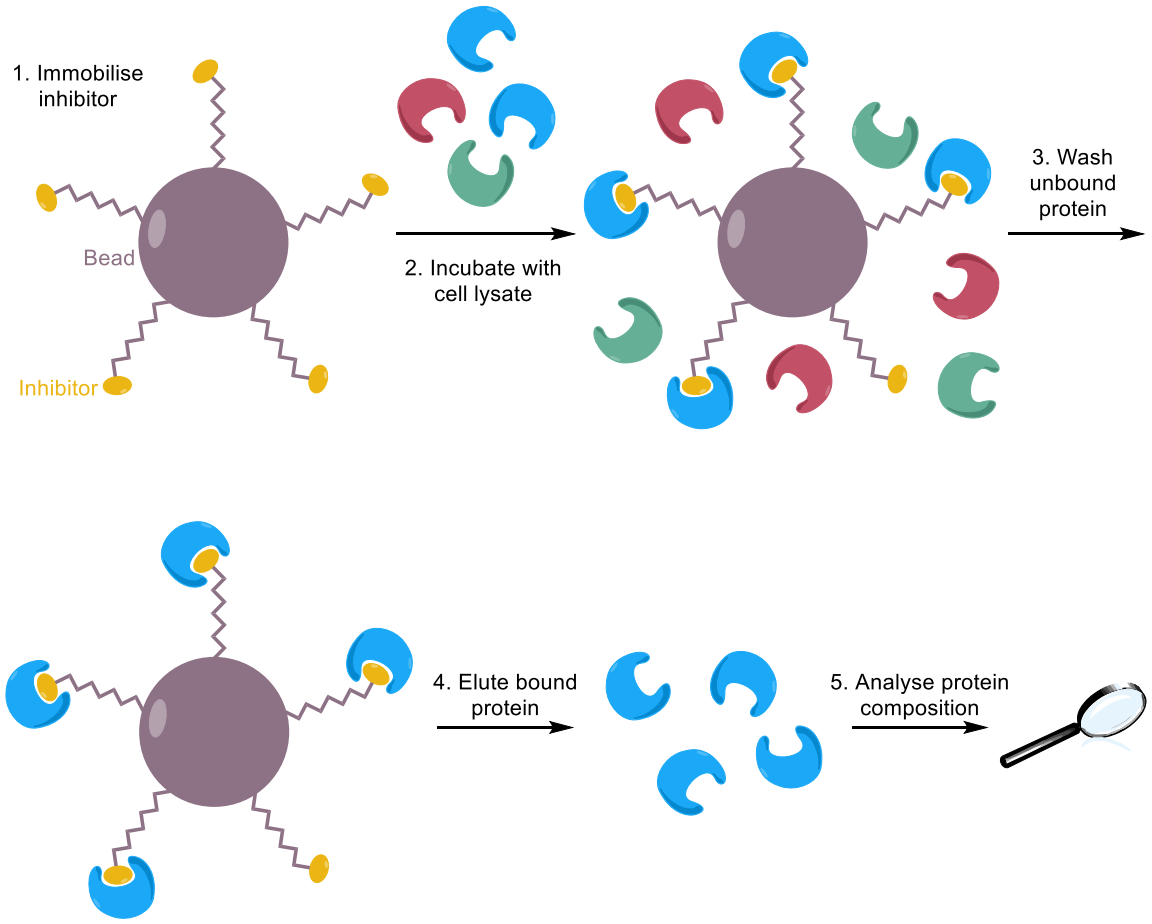

Figure 72 Principle of affinity-based profiling. The inhibitor is functionalised to facilitate immobilisation onto beads. The immobilised inhibitor is incubated with cell lysate, unbound proteins are washed away and bound proteins are eluted and analysed by mass spectrometry or western blotting.[207]

Chemoproteomics had previously been used to demonstrate the interaction of the potent KDM6 inhibitor GSK-J1 **26** with KDM6B in human embryonic kidney 293 (HEK-293) and human promyelocytic leukaemia (HL-60) cell lysates.[119] GSK-J3 **313**, an analogue of GSK-J1 bearing an amino group was chemically immobilised onto NHS-activated sepharose beads through the formation of an amide bond (**Figure 73**). Incubation of the immobilised probe with cell lysates and analysis by western blotting and mass spectrometry demonstrated that KDM6A and KDM6B in cell lysates can bind to immobilised GSK-J3. The binding was found to be specific; it could be inhibited through the addition of the free inhibitor GSK-J1 **26**.[119]

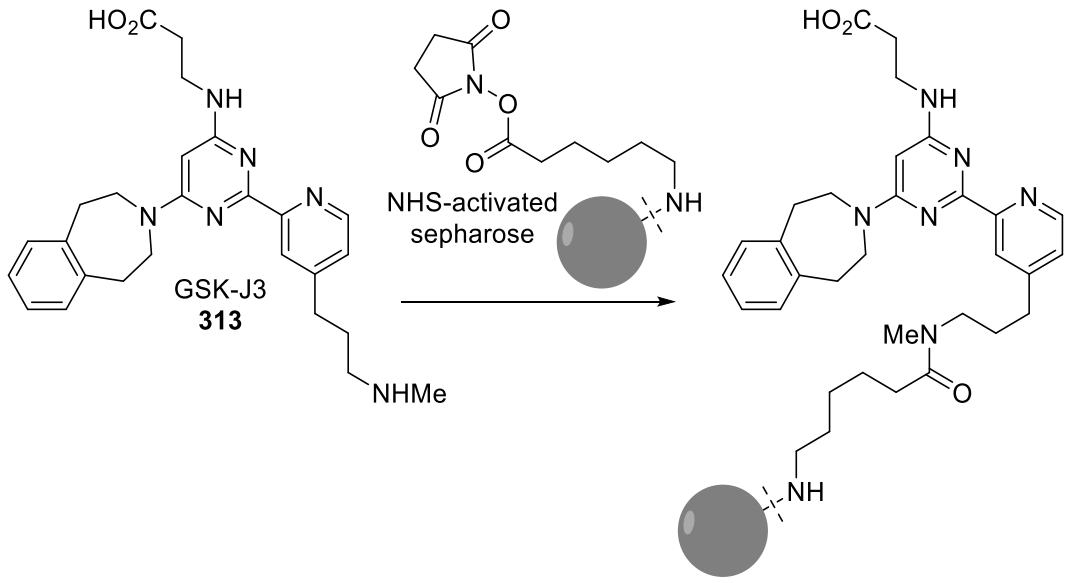

Figure 73 GSK-J3 **313**, an amino-substituted version of GSK-J1 **26** has been described and used to demonstrate binding of KDM6B with GSK-J3 beads in cell lysates.[119]

It was decided to prepare analogues of **227** bearing functional groups that would allow immobilisation onto solid supports. These compounds would be used to prepare immobilised versions of **227** for use in chemoproteomics experiments.

6.2 Immobilisation onto Beads

In comparison with the binding mode of triazolopyridine compound **134** in KDM4A (**Figure 35**), **227** would be expected to bind to iron(II) through the triazolopyridine motif. Docking **227** in a KDM2A crystal structure (**Figure 49**) had shown that the phenyl ring may occupy the peptide substrate binding site of KDM2A and therefore to be closer to the surface of the protein than the triazolopyridine core. Hence the phenyl ring was expected to provide the best attachment point for further functionalization. Naphthyl (**262** and **263**) and biphenyl (**264**) replacements for the phenyl ring had been found to result in a dramatic reduction in KDM2A inhibition (see section 5.5.1). This may be because the peptide substrate pocket of KDM2A is too narrow to accommodate these larger aromatic ring systems, thus it was hypothesised that smaller, more flexible substituents might be better tolerated.

Ether targets **315** and **317** were designed to investigate the best attachment point on the phenyl ring and mimic the effect of introducing a polyethylene glycol (PEG) linker (**Figure 74**).

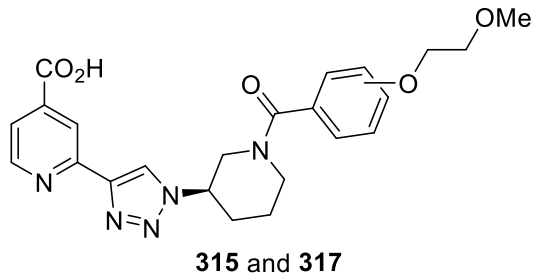

Figure 74 Methoxyethyl targets **315** and **317**.

Two commercially available benzoic acid derivatives **314** and **316** were converted to the acyl chlorides by reaction with oxalyl chloride. Reaction with the *NH*-piperidine compound **225** and deprotection of the methyl ester in a one-pot procedure gave the target compounds **315** and **317** (**Scheme 41**).

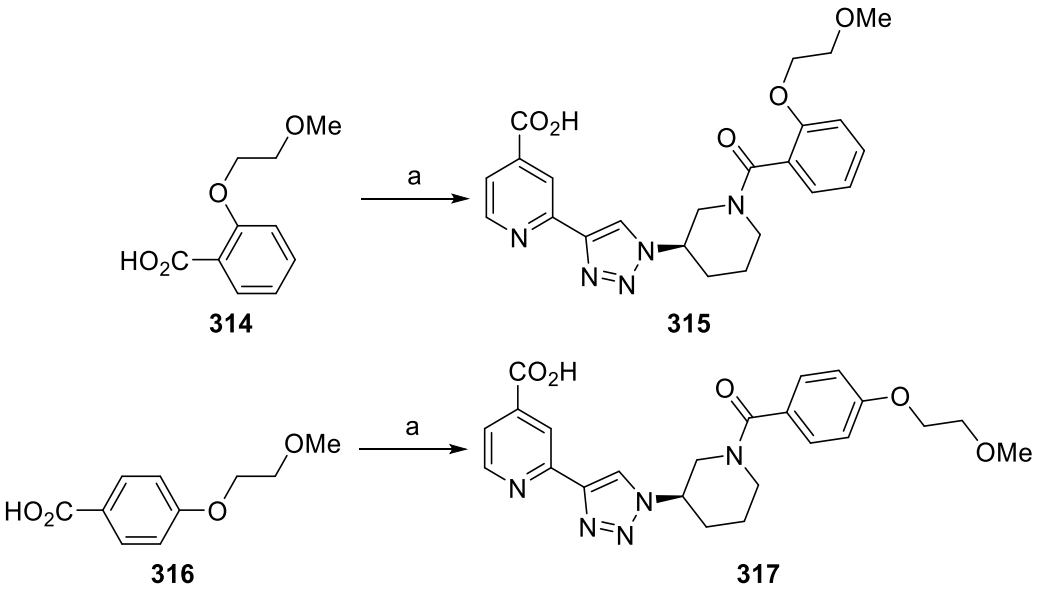

Scheme 41 Synthesis of **315** and **317**. *Reagents and conditions:* (a) i) $(COCl)_2$, DMF, CH_2Cl_2; ii) **225**, Et_3N, MeCN; iii) LiOH; for **315**:18%, for **317**:19%.

315 and **317** were both found to inhibit KDM2A in the micromolar range, with the ortho-substituted **315** being more potent than para-substituted **317** (**Table 32**).

Table 32 Inhibitory effect (IC_{50} value) of **315** and **317** against KDM2A.

Cmpd	Substitution	KDM2A IC_{50}*
315	*o*-	0.35 ± 0.0073 (2)
317	*p*-	2.0 ± 0.097 (2)

*Mean IC_{50} (μM) ± standard error of the mean (number of determinations); determined by the RapidFire assay.

Since the introduction of both the ortho- and para-substituents did not result in a dramatic reduction in potency against KDM2A, it was decided to use the phenyl ring of **227** as an attachment point for immobilisation onto solid support. It was envisaged that copper-catalysed click chemistry could be used to introduce a PEG-linked biotin moiety at each of the three positions of the phenyl ring from the corresponding propargyl ethers which could be prepared from **225** and propargyl ether substituted benzoic acids (**Figure 75**).

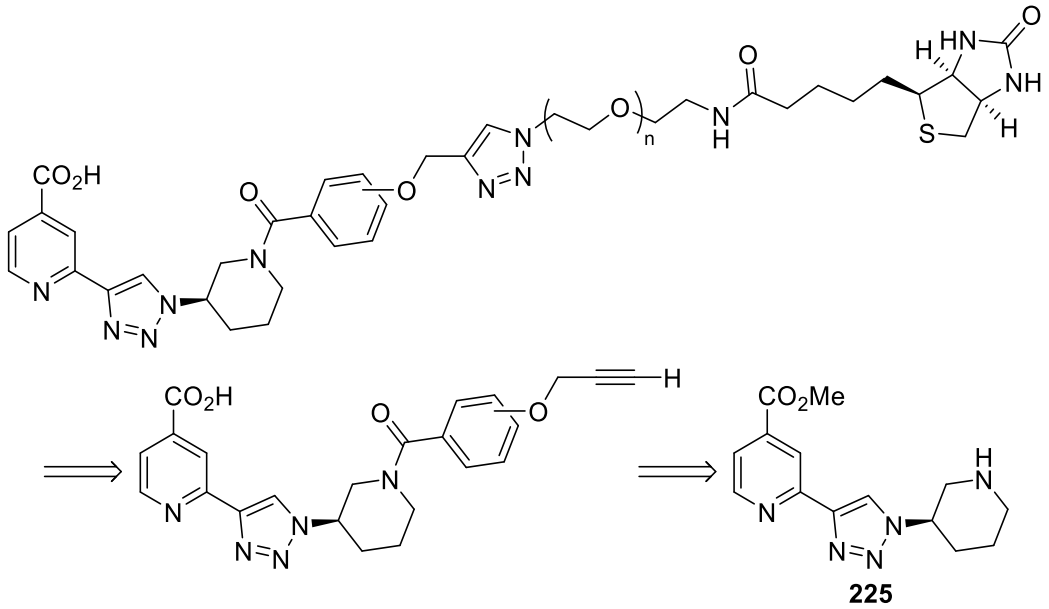

Figure 75 Proposed synthesis of biotinylated derivatives of **227**.

The propargyl ethers **320**, **323** and **325** were synthesised from the corresponding commercially available hydroxybenzoic acid derivatives **318**, **321** and **324**. Etherification of **318** and **321** with propargyl bromide according to a method modified from that reported by Peschke *et al.*[210] gave intermediates **319**[162] and **322**[163] (**Scheme 42**). Hydrolysis with

lithium hydroxide yielded the carboxylic acids **320**,[211] and **323**.[163] The synthesis of **325**[163] was performed as a one-pot reaction from **324** in 95% yield.

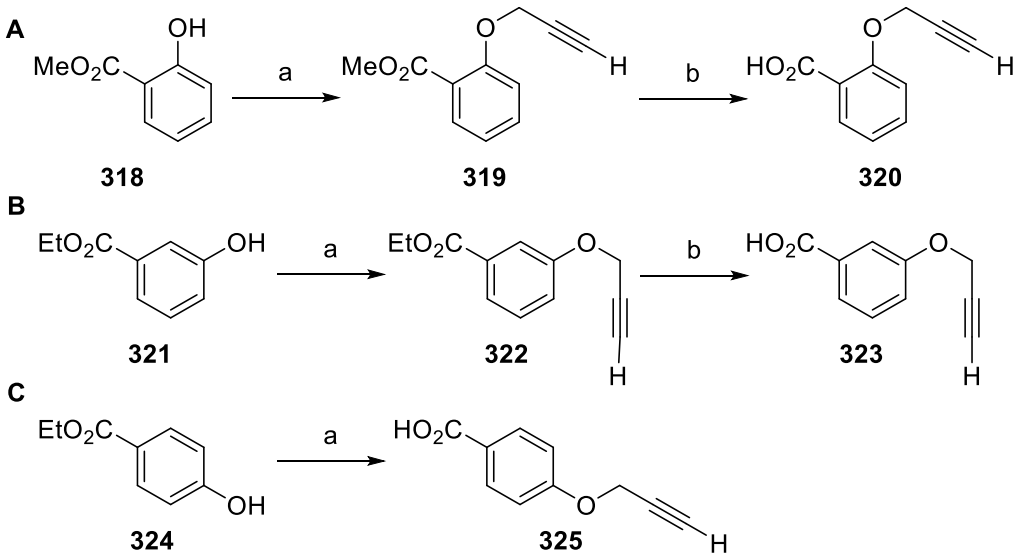

Scheme 42 Synthesis of propargyl ethers **320**, **323** and **325**. *Reagents and conditions:* **A** for **320** (a) propargyl bromide, K_2CO_3, DMF, 90%; (b) LiOH, MeOH, THF, H_2O, 80%. **B** for **323** (a) propargyl bromide, K_2CO_3, DMF, 92%; (b) LiOH, MeOH, THF, H_2O, 99%. **C** for **325** (a) i) propargyl bromide, K_2CO_3, DMF; ii) LiOH, 95%.

The resulting carboxylic acids **320**, **323** and **325** were converted to the acyl chlorides for reaction with **225** using the same conditions as employed in the synthesis of **315** and **317** to give **326**–**328** (**Scheme 43**).

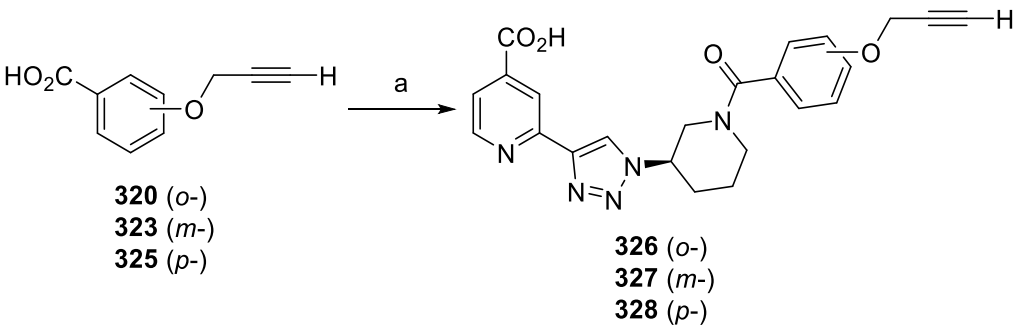

Scheme 43 Synthesis of **326**–**328**. *Reagents and conditions:* (a) i) $(COCl)_2$, DMF, CH_2Cl_2; ii) **225**, Et_3N, MeCN, iii) LiOH; for **326**: 46%, for **327**: 40%, for **328**: 29%.

Propargyl ether derivatives **326**–**328** were tested against KDM2A using the RapidFire assay and were found to be potent inhibitors of KDM2A (IC_{50}: 220–380 nM, **Table 33**). Thus it was decided that these were suitable intermediates for the attachment of biotin.

Table 33 Inhibitory effect (IC_{50} value) of **326**–**328** against KDM2A.

Cmpd	Substitution	KDM2A IC_{50}*
326	*o*-	0.25 ± 0.020 (2)
327	*m*-	0.22 ± 0.0082 (2)
328	*p*-	0.38 ± 0.0082 (2)

*Mean IC_{50} (μM) ± standard error of the mean (number of determinations); determined by the RapidFire assay.

The methyl ester intermediate **329** was also prepared from the benzoic acid **320** and the piperidine derivative **225** (**Scheme 44**).

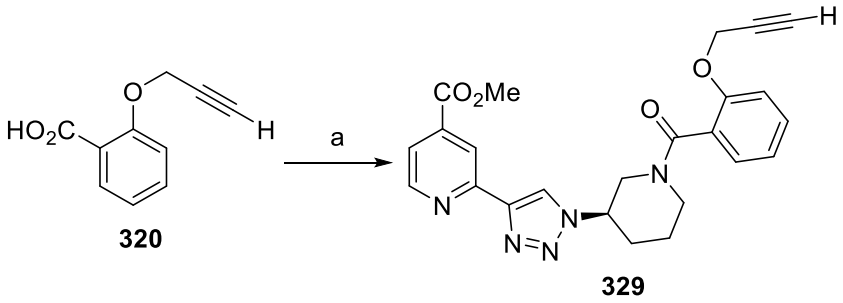

320 **329**

Scheme 44 Synthesis of **329**. *Reagents and conditions:* (a) i) $(COCl)_2$, DMF, CH_2Cl_2; ii) **225**, Et_3N, MeCN, 90%.

6.3 Synthesis of Biotinylated Analogues

A PEG-linked biotin moiety was introduced in a copper-catalysed click reaction between the resulting propargyl ethers **327**–**329** and a commercially available azido biotin reagent to give **330**–**332** (**Scheme 45**).

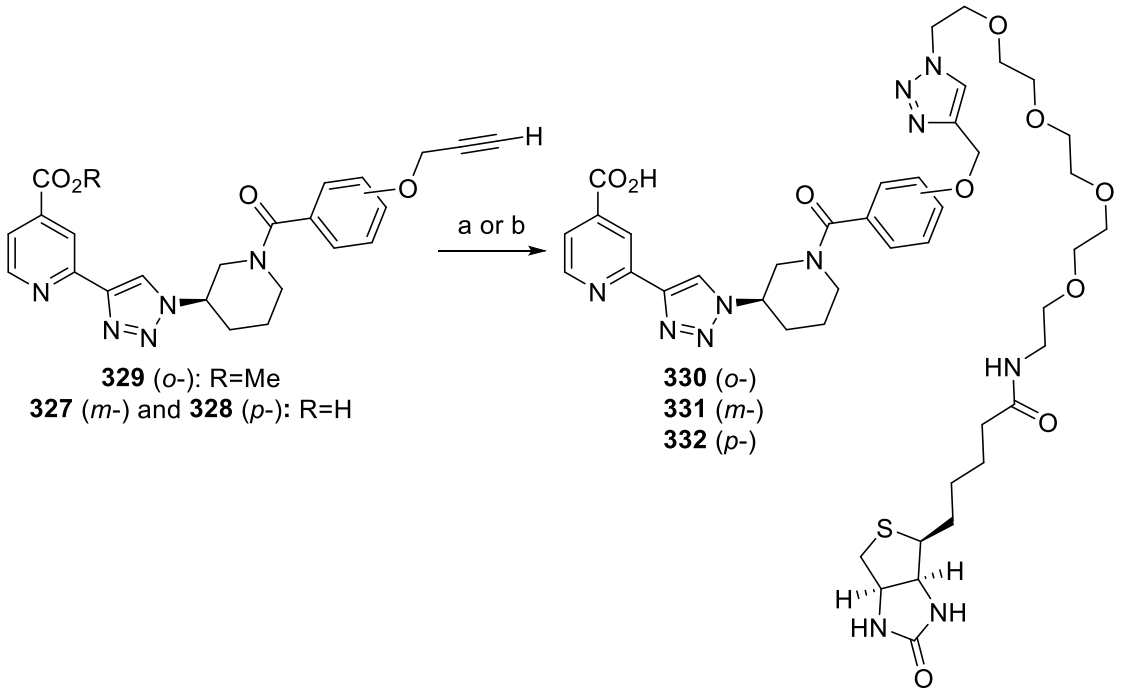

Scheme 45 Synthesis of **330**–**332**. *Reagents and conditions:* (a) i) biotin-$NHCH_2CH_2(PEG)_4N_3$, $CuSO_4 \cdot 5H_2O$, (+)-sodium L-ascorbate, DMF, 70 °C; ii) LiOH (aq), MeCN, 38%; for **330**: 38%; or (b) $CuSO_4 \cdot 5H_2O$, (+)-sodium L-ascorbate, DMF, 70 °C; for **331**: 44%, for **332**: quant.

The inhibitory activity of biotinylated compounds **330**–**332** was determined against KDM2A *in vitro* (**Table 34**).

Table 34 Inhibitory effect (IC_{50} value) of **330**, **331** and **332** against KDM2A.

Cmpd	Substitution	KDM2A IC_{50}*
330	*o*-	0.36 ± 0.012 (2)
331	*m*-	1.3 ± 0.040 (2)
332	*p*-	1.8 ± 0.047 (2)

*Mean IC_{50} (μM) ± standard error of the mean (number of determinations); determined by the RapidFire assay.

Ortho-substituted compound **330** was found to be the most potent biotinylated inhibitor of KDM2A (IC_{50}: 360 nM) and was selected for immobilisation onto streptavidin-coupled magnetic beads. Un-derivatised biotin was also immobilised onto beads and used as a negative control. The beads were incubated at 4 °C for 2 hours with a 125 nM solution of a truncated version of KDM2A (which was expressed and purified by Aleksandra Szykowska) in buffer (50 mM 4-(2-hydroxyethyl)piperazine-1-ethanesulfonic acid

(HEPES), 60 mM NaCl). After washing with 50 mM HEPES, 60 mM NaCl three times and eluting with lithium dodecyl sulfate (LDS) loading buffer (141 mM tris(hydroxymethyl)aminomethane (tris base) pH 8.5, 2% w/v LDS, 10% v/v glycerol, 5 mM dithiothreitol (DTT), 0.51 mM ethylenediaminetetraacetic acid (EDTA), 0.22 mM Brilliant Blue G, 0.175 mM phenolsulfonphthalein), the level of KDM2A that had bound to the beads was detected by western blotting.[212]

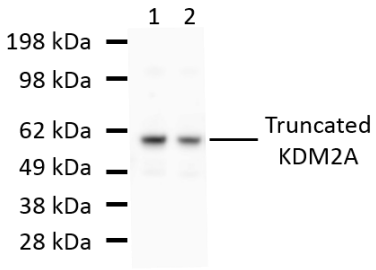

Figure 76 Biotin functionalised control beads (lane 1) and **330** functionalised beads (lane 2) were used to capture KDM2A from a 125 nM solution in 50 mM HEPES, 60 mM NaCl. A western blot probed with an anti-KDM2A antibody (ab31739) shows that the **330** functionalised beads did not bind more KDM2A than the biotin functionalised beads. KDM2A was expressed and purified by Aleksandra Szykowska.

Unfortunately the **330** functionalised beads did not result in any increase in the amount of KDM2A binding compared to the biotin functionalised control beads.

Biotinylated compound **330** was docked into a crystal structure of a complex of biotin and streptavidin.[213] This docked structure indicated that when **330** is bound to streptavidin, the PEG linker is likely too short for the bait to be exposed sufficiently beyond the surface of streptavidin for KDM2A to bind concurrently (**Figure 77**). Hence it was proposed that a longer PEG linker might be required to allow concurrent binding of streptavidin and KDM2A.

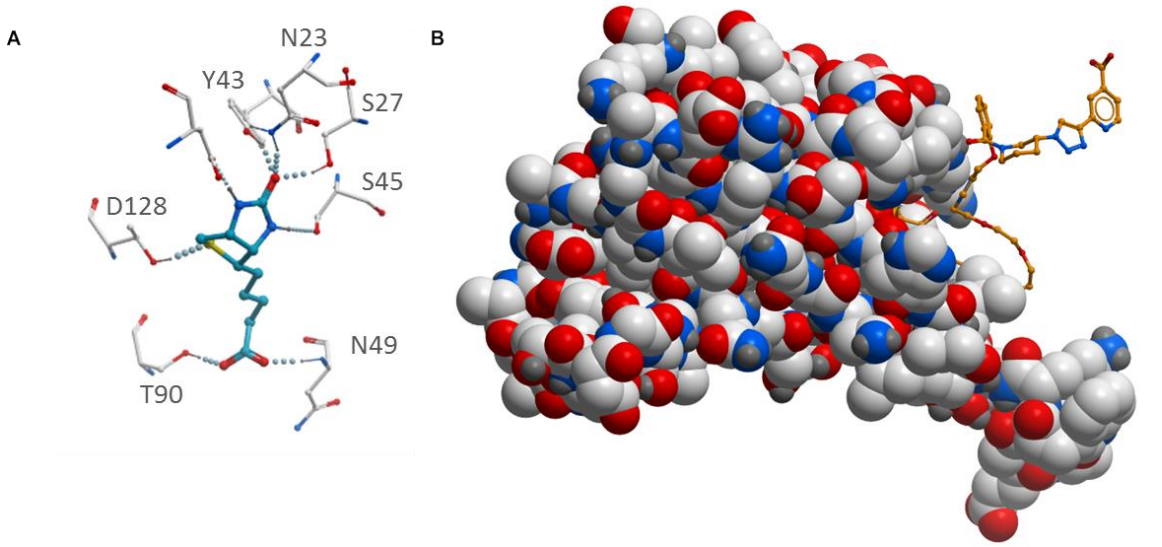

Figure 77 A View from a crystal structure of biotin (blue sticks) in complex with streptavidin (grey sticks) showing some of the key hydrogen bonding interactions (PDB ID: 3RY2). **B** Compound **330** (orange sticks) docked into the crystal structure of biotin in complex with streptavidin (streptavidin is shown in space filling representation; PDB ID: 3RY2).

6.4 Synthesis of Biotinylated Inhibitors with Longer PEG Linkers

Biotinylated versions of **227** with longer PEG linkers (**333**–**336**) were therefore prepared from **329** using the conditions developed for the synthesis of **330** (**Scheme 46**).

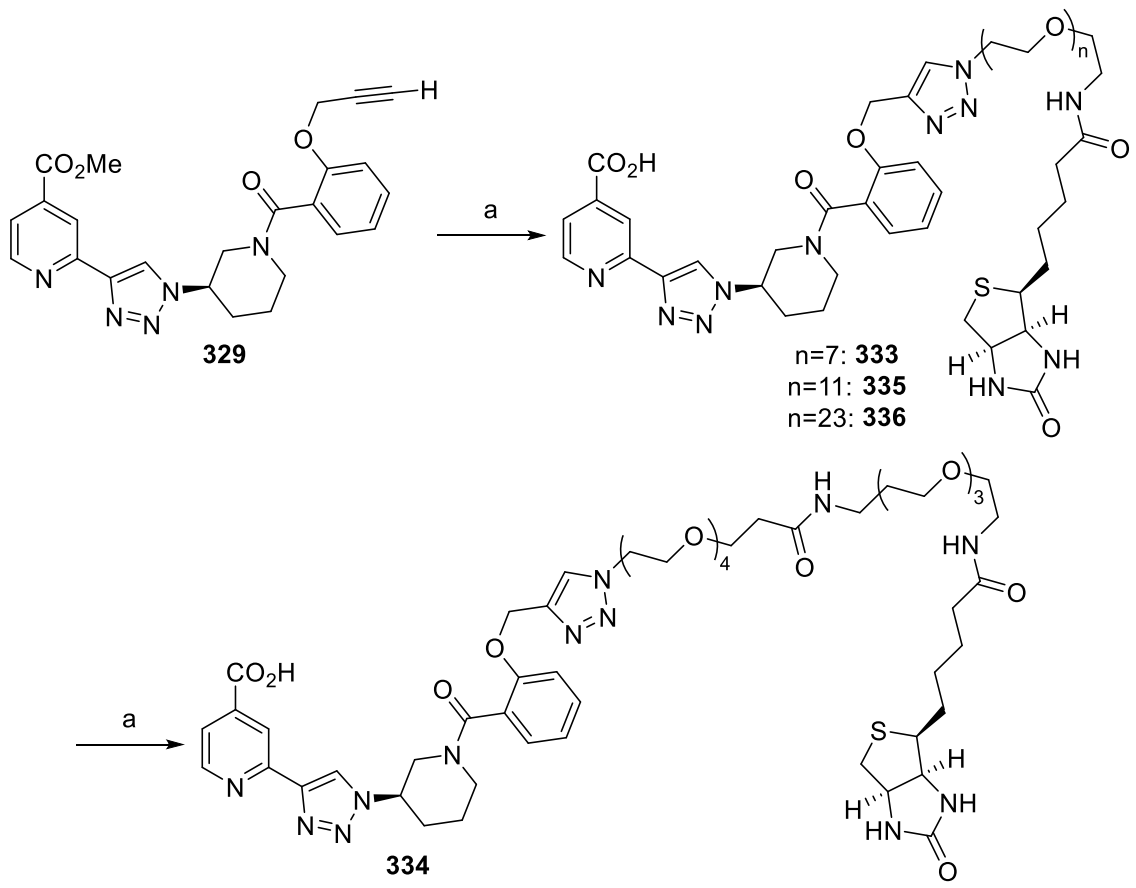

Scheme 46 Synthesis of **333**–**336**. *Reagents and conditions:* (a) i) biotin-$NHCH_2CH_2(PEG)_nN_3$ or biotin-$NHCH_2CH_2(PEG)_3CH_2NHCOCH_2CH_2(PEG)_4N_3$, $CuSO_4{\cdot}5H_2O$, (+)-sodium L-ascorbate, ^{t}BuOH, H_2O, 70 °C; ii) LiOH (aq), MeCN; for **333**: 59%, for **334**: 54%, for **335**: 35%, for **336**: 59%.

Biotinylated compounds **333**–**336** were tested against KDM2A using the RapidFire assay (**Table 35**).

Table 35 Inhibitory effect (IC_{50} value) of **330** and **333**–**336** against KDM2A.

Cmpd	Nature of linker	KDM2A IC_{50}*
330	4 × PEG	0.36 ± 0.012 (2)
333	7 × PEG	0.75 ± 0.055 (2)
334	(4 × PEG)[$(CH_2)_2CONHCH_2$](3 × PEG)	1.1 ± 0.073 (2)
335	11 × PEG	1.4 ± 0.084 (2)
336	23 × PEG	2.0 ± 0.14 (2)

*Mean IC_{50} (μM) ± standard error of the mean (number of determinations); determined by the RapidFire assay.

The inhibitory activity of the biotinylated compounds **330** and **333**–**336** was found to decrease slightly as the length of the PEG linker increased (from 0.36 μM for **330** to 2.0

µM for **336**). Compounds **330** and **333**–**336** were immobilised onto streptavidin-coated magnetic beads and incubated with a solution of a truncated version of KDM2A as for **330**. The level of KDM2A that had bound to the beads was detected by western blotting (**Figure 78**).

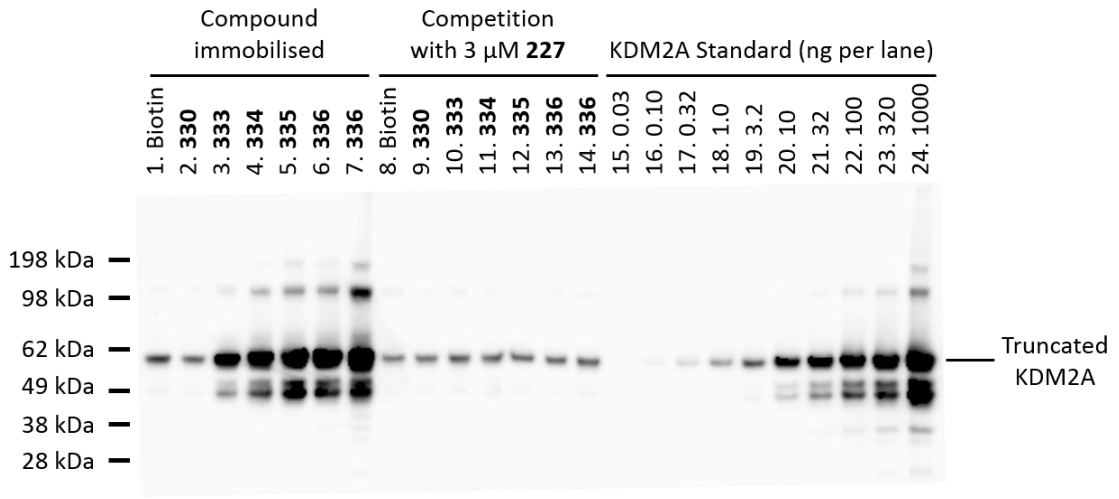

Figure 78 Biotin functionalised control beads and **330** and **333**–**336** functionalised beads were prepared by incubating 1.3 nmol of the biotinylated compound with magnetic beads and were used to capture KDM2A from a 125 nM solution of KDM2A in 50 mM HEPES, 60 mM NaCl (lanes 1–6) and from a 125 nM solution of KDM2A in 50 mM HEPES, 60 mM NaCl containing 3 µM **227** (lanes 8–13). **336** functionalised beads which had been prepared by incubating 13 nmol of **336** with magnetic beads were also incubated with 125 nM KDM2A (lanes 7 and 14). A western blot probed with an anti-KDM2A antibody (ab31739) shows that the **333**–**336** functionalised beads bind more KDM2A than the biotin functionalised beads and that this effect is reversed upon the addition of free inhibitor **227** to the solution. 0.03–1000 ng of KDM2A was loaded as a standard for qualitative assessment of KDM2A levels (lanes 15–24). KDM2A was expressed and purified by Aleksandra Szykowska.

Interestingly, it was found that the **333**–**336** functionalised beads bound significantly more KDM2A than the **330** functionalised beads and that the amount of KDM2A bound increased as the linker length increased. Competition with **227** reduced the amount of KDM2A binding to the **333**–**336** functionalised beads, but not to the **330** functionalised beads, indicating that some KDM2A bound non-specifically to the beads but that the extra signal observed in lanes 3–7 was due to specific binding of KDM2A to the triazolopyridine portion of **333**–**336**. These results confirmed the hypothesis that the PEG linker of **330** was

too short to allow binding to both streptavidin and KDM2A concurrently. **336** was selected for further chemoproteomics experiments in cell lysates.

6.5 Optimisation of Cell Lysis Conditions for KDM2A

HeLa cells were harvested and lysed in lysis buffer containing 100 mM KCl, 50 mM HEPES pH 8.0, 0.1% v/v nonylphenyl polyethylene glycol (NP-40), 10% v/v glycerol, 1 mM phenylmethylsulfonyl fluoride (PMSF), 1 mM DTT and 0.02% v/v protease inhibitor cocktail.[214] After lysis, DNA was digested using DNAse I for 1 hour at 4 °C and the soluble fraction separated by centrifugation. The insoluble fraction was taken up in lysis buffer containing 500 mM KCl and incubated with DNAse I for a further hour at 4 °C and the soluble fraction separated by centrifugation. It was found that the soluble fraction that had been obtained after lysis with 100 mM KCl did not contain a significant quantity of KDM2A, but the soluble fraction after treatment with 500 mM KCl resulted in a higher concentration of KDM2A (**Figure 79**). Presumably the interaction between KDM2A and histones or DNA is not disrupted sufficiently when 100 mM KCl is used for KDM2A to be found in the soluble fraction, but at 500 mM KCl, KDM2A dissociates and is found in the soluble fraction.

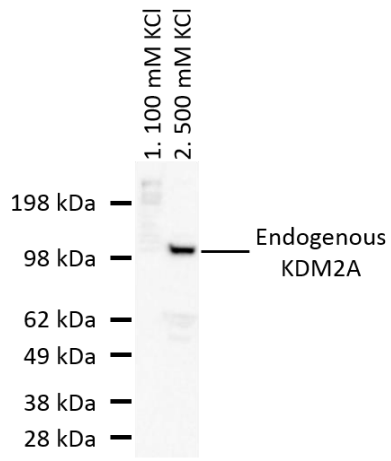

Figure 79 A western blot probed with an anti-KDM2A antibody (ab31739) shows that HeLa cell lysate prepared with 100 mM KCl contains little KDM2A (lane 1) but treatment with 500 mM KCl resulted in KDM2A being detected (lane 2).

6.6 Optimisation of Buffer Conditions for KDM2A Binding

336 functionalised beads were incubated with 125 nM KDM2A as before but other buffer components or cell lysate were added in order to investigate the effect on binding with KDM2A. **336** functionalised beads were incubated with 125 nM KDM2A in 50 mM HEPES and 60 mM NaCl buffer, in lysis buffers containing 100 mM or 500 mM KCl and in lysis buffer containing 500 mM KCl with 5–100% HeLa cell lysate (**Figure 80**).

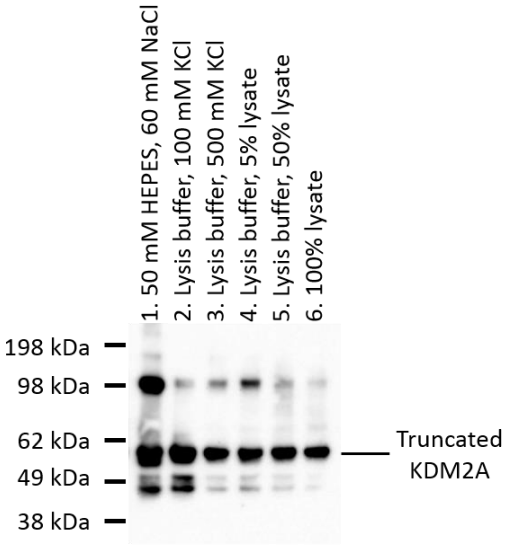

Figure 80 336 functionalised beads were used to capture KDM2A from a 125 nM solution of KDM2A in: 50 mM HEPES, 60 mM NaCl (lane 1); lysis buffer containing 100 mM KCl (lane 2); lysis buffer containing 500 mM KCl (lane 3); lysis buffer containing 500 mM KCl and 5% cell lysate (lane 4); lysis buffer containing 500 mM KCl and 5% cell lysate (lane 5); cell lysate (lane 6). Western blot probed with an anti-KDM2A antibody (ab31739). KDM2A was expressed and purified by Aleksandra Szykowska

It was found that the amount of KDM2A bound to the **336** functionalised beads was dependent on the composition of the KDM2A solution; less KDM2A bound when the KCl concentration was 500 mM than 100 mM (lanes 2 and 3). However, the presence of cell lysate did not affect the amount of KDM2A binding significantly (lanes 4–6).

Since a greater than 100 mM KCl concentration was required for KDM2A to be extracted from nucleosomes into the soluble fraction after cell lysis and a KCl concentration of less than 500 mM was required for efficient binding with **336** functionalised beads, it was decided to perform the cell lysis at 500 mM KCl and dilute the resulting lysate 5-fold with

dilution buffer (50 mM HEPES pH 8.0, 0.1% v/v NP-40, 10% v/v glycerol, 1 mM PMSF, 1 mM DTT and 0.02% v/v protease inhibitor cocktail) to give a final concentration of 100 mM KCl for the pulldown experiment.

6.7 Optimisation of Incubation Time and Temperature for KDM2A Binding

HeLa cells were transiently transfected with a FLAG-tagged version of full-length *KDM2A* (plasmid prepared by Dr. Pavel Savitsky) using Lipofectamine 2000 as the transfection reagent to increase the intracellular KDM2A concentration sufficiently for detection in the pulldown experiment. **336** functionalised beads were incubated with the resulting cell lysate (which had been prepared with 500 mM KCl lysis buffer and diluted 5-fold with dilution buffer) at 4 °C or at room temperature for 2 or 22 hours and the amount of KDM2A that bound to the beads was determined by western blot (**Figure 81**).

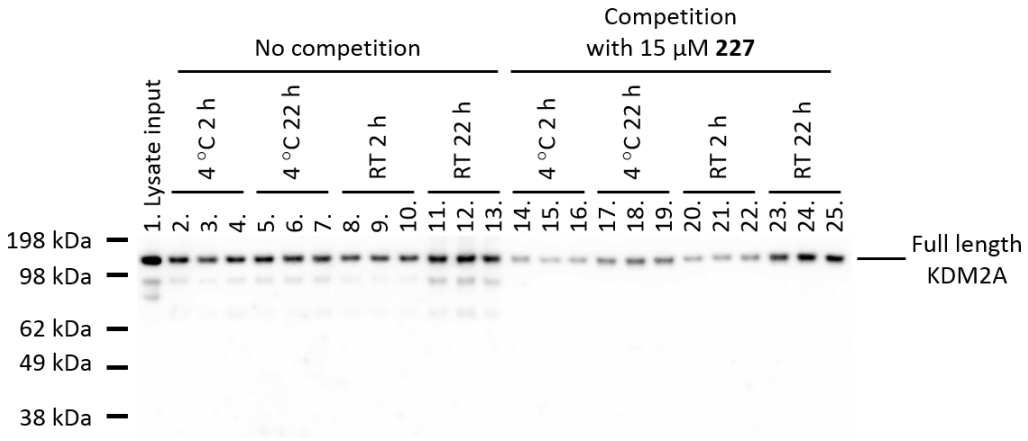

Figure 81 HeLa cells were transiently transfected with *KDM2A* and the lysate which had been diluted 5-fold (lane 1) incubated with **336** functionalised beads in triplicate ± 15 µM **227** as a competitor. A western blot probed with an anti-KDM2A antibody (ab31739) shows that the amount of KDM2A pulled down on incubation at 4 °C and RT for 2 hours is similar (lanes 2–4 and 8–10); slightly more KDM2A is pulled down on incubation at RT for 22 hours (lanes 11–13). The degree to which the presence of 15 µM **227** inhibits binding of KDM2A has a marked time dependence; competition with **227** is more effective at 4 °C than at RT and when the incubation time is shorter (lanes 14–19).

The amount of protein bound to the **336** functionalised beads was not found to vary significantly with the incubation time or temperature, however, the effectiveness of 15 µM **227** in inhibiting binding showed strong time- and temperature-dependence. Competition

with **227** was found to be most effective when the incubation was performed at 4 °C for 2 hours. The incubation step in subsequent experiments was carried out at 4 °C for 2 hours in order to maximise the window between the amount of KDM2A binding with and without competition.

6.8 Dosing Cells with Inhibitor

HeLa cells were transiently transfected with a FLAG-tagged truncated version of *KDM2A* (plasmid prepared by Dr. Claire Strain-Damerell). After transfection, the cells were dosed for 2 hours with a 400 µM solution of either **227** or its prodrugs **226** and **257** or with DMSO as a control. After dosing, the cells were washed four times with phosphate-buffered saline (PBS) then harvested, lysed and the soluble fractions diluted 5-fold with dilution buffer and used in the pulldown experiment with **336** functionalised beads in triplicate. Analysis by western blot (**Figure 82**) showed that the amount of KDM2A binding to the **336** functionalised beads from lysate from cells that had been dosed with **226**, **227** and **257** was reduced compared to the lysate from undosed cells.

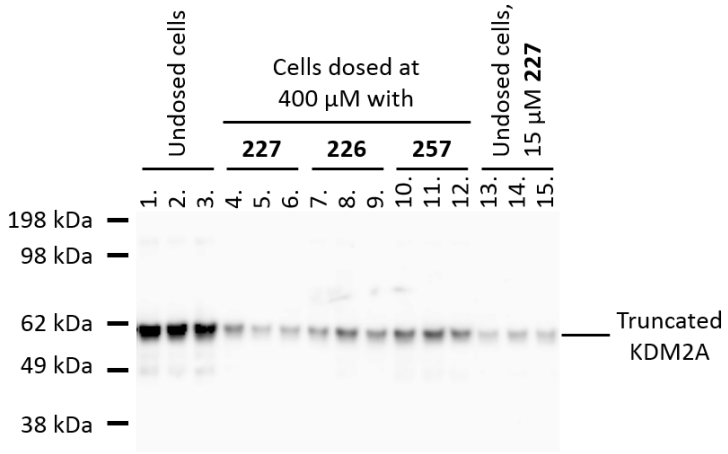

Figure 82 336 functionalised beads were used to capture KDM2A from lysate from cells that had been transfected with FLAG-tagged truncated *KDM2A* and treated with: DMSO (lanes 1–3); **227** (lanes 4–6); **226** (lanes 7–9); **257** (lanes 10–12) and where 15 µM **227** was added to the lysate to competitively inhibit binding (lanes 13–15). Western blot probed with an anti-KDM2A antibody (ab31739).

Interestingly, dosing with **227** was more effective at reducing binding of KDM2A to **336** functionalised beads than dosing with the prodrugs **226** and **257**. This would indicate that

the concentration of **227** in the cell lysate was higher on dosing with **227** than with its two prodrugs **226** and **257**, perhaps as a result of incomplete intracellular hydrolysis of **226** and **257** to **227** under these conditions. Dosing cells with 400 µM **227** (lanes 4–6) was almost as effective in reducing binding of KDM2A to the beads as adding 15 µM **227** to the undosed lysate (lanes 13–15). These results suggest that **227** is able to penetrate HeLa cells at 400 µM and that the resulting **227** present in the cell lysate binds to KDM2A, preventing it from binding to immobilised **336**.

6.9 Dosing Cells with a Dilution Series of Inhibitor

In order to investigate the concentration range at which **227** can permeate cells, HeLa cells that had been transiently transfected with a FLAG-tagged version of full-length *KDM2A* (plasmid prepared by Dr. Pavel Savitsky) were dosed with 50-400 µM **227**. The resulting cells were washed four times with PBS then harvested, lysed, the soluble fractions diluted 5-fold with dilution buffer and used in the pulldown experiment with **336** functionalised beads (**Figure 83**).

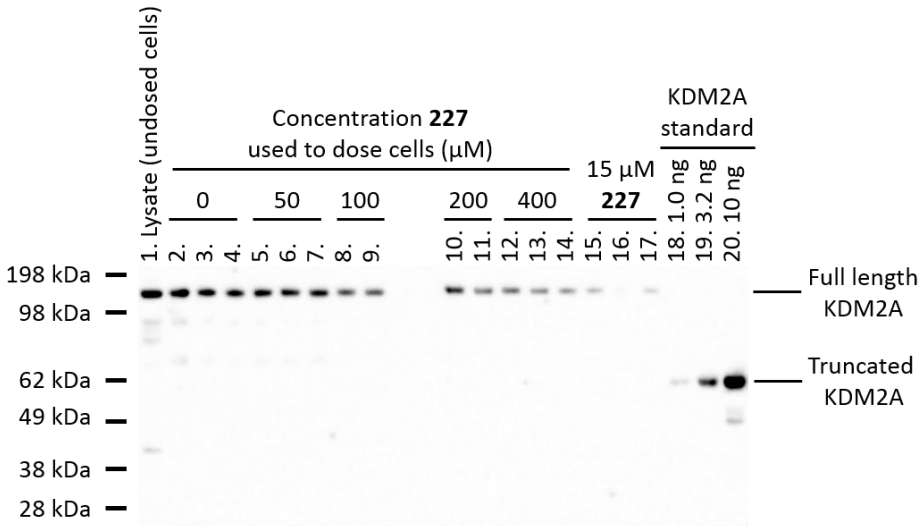

Figure 83 336 functionalised beads were used to capture KDM2A from lysate from cells that had been transfected with FLAG-tagged *KDM2A* and treated with: DMSO (lanes 2–4 and 15–17) or 50–400 µM **227** (lanes 5–14). 15 µM **227** was added to DMSO-treated lysate to competitively inhibit binding (lanes 15–17). 1.0–10 ng of KDM2A was loaded as a standard (lanes 18–20). KDM2A was expressed and purified by Aleksandra Szykowska. Western blot probed with an anti-KDM2A antibody (ab31739).

It was found that the amount of KDM2A binding to **336** functionalised beads from cell lysate that had been dosed with **227** at 50 μM was approximately equal to that from undosed lysate indicating that **227** is poorly cell permeable at 50 μM, however, a greater reduction in signal was observed when cells had been dosed at higher concentrations.

Although western blot densitometry is a semi-quantitative method,[215, 216] integration of the bands corresponding to the recombinant protein standard (**Figure 78**, lanes 17–21) showed an approximately linear relationship between the optical density and the mass of protein at the optical density range observed in the pulldown experiments with cell lysates (**Figure 84**).

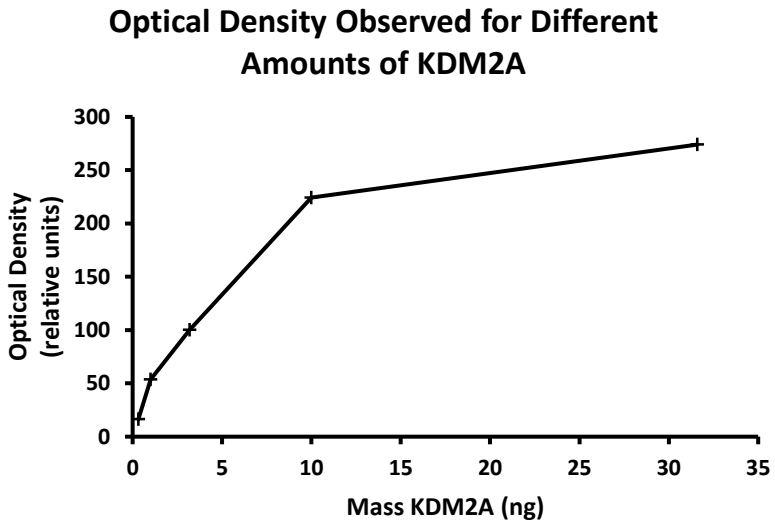

Figure 84 The optical density of the KDM2A bands corresponding to recombinant protein standard (**Figure 78**, lanes 17–21) was calculated; there is an approximately linear relationship between the optical density and the mass of protein at the range observed for the mass of protein binding to **336** functionalised beads (0–10 ng) but partial saturation of the signal is observed above 10 ng of protein.

Therefore, the optical density of the KDM2A bands from the pulldown experiment with lysate from dosed cells (**Figure 83**) was calculated in order to quantify the effect of dosing with **227**. The mean amount of KDM2A binding on competition with **227** at 15 μM (lanes 15–17) was subtracted from the amount binding from each of the pulldown experiments with undosed cell lysate (lanes 2–4), the mean value calculated and normalised to 100 units

to give the maximum level of specific binding observed (**Figure 85**). This was repeated for the results from dosed cell lysate to determine how effective dosing the cells with **227** was in reducing the amount of KDM2A bound compared to competition with **227** at 15 μM (**Figure 85**).

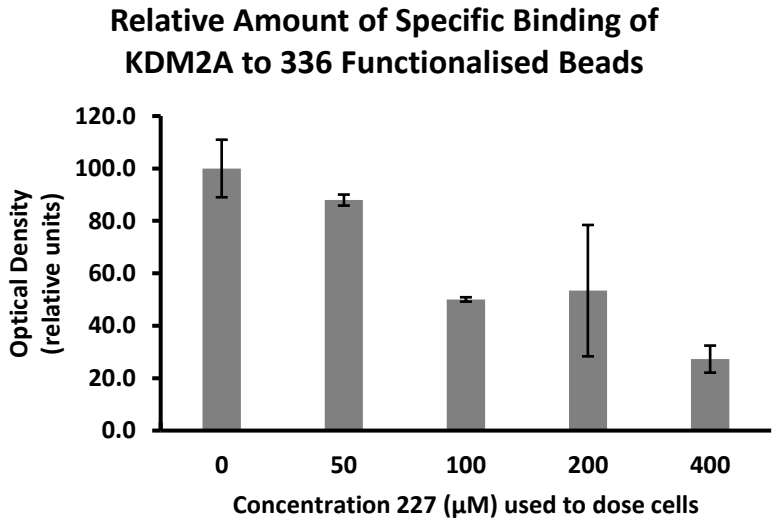

Figure 85 The optical density of the KDM2A bands from the western blot shown in **Figure 83** was calculated and the mean optical density corresponding to the amount of KDM2A bound to beads when **227** was added as a competitor was subtracted to approximate the amount of specific binding. Error bars represent ± 1 standard error of the mean.

It was found that treatment of HeLa cells with 100 μM **227** resulted in approximately 50% reduction in the amount of KDM2A specifically binding to **336** functionalised beads and that treatment with 400 μM **227** resulted in approximately 70% reduction.

6.10 Discussion

Biotinylated versions of **227** were prepared for immobilisation on streptavidin-coated beads. It was found that a PEG linker of greater than 4–7 PEG units between the bait and the biotin moiety was required for the resulting compound to be able to bind to streptavidin and KDM2A concurrently.

336 (containing a 23 PEG unit linker) was used in chemoproteomics experiments with lysates from cells that had been transiently transfected with *KDM2A*. KDM2A was found

to bind to the **336** functionalised beads indicating that even in the presence of the many other proteins found in cell lysate the inhibitor is able to bind to the desired target. This interaction could be competitively inhibited by the presence of 15 μM **227** indicating that it is a specific interaction with the triazolopyridine portion of **336** rather than a nonspecific interaction, for example with the PEG linker or the streptavidin-coated beads themselves.

On dosing transfected cells with the acid **227** and two prodrug esters **226** and **257** at 400 μM it was found that the acid resulted in a greater reduction in the amount of KDM2A binding to **336** functionalised beads than the two prodrug esters. This would suggest that the concentration of **227** in the lysate from **227**-treated cells was higher than in the lysate from the prodrug-treated cells. This may be due to slow hydrolysis of the prodrug esters in HeLa cells.

Transfected cells were also dosed with **227** at 0–400 μM. After dosing at 50 μM, the amount of KDM2A pulled down was approximately the same as for the undosed cells, however, at 100–400 μM there was a 50–70% reduction in the amount of KDM2A pulled down. This would suggest that **227** has some cell permeability at 100 μM but this appears to be insufficient to inhibit the demethylation of H3K36me2 by KDM2A in the cellular IF assay (**Figure 57A**).

Chapter 7. Summary

Few chemical probes have been discovered for JmjC KDMs, which play important roles in multiple human diseases. Such probes constitute useful tools to elucidate further the biological roles of the JmjC KDMs and their interesting potential as targets for drug discovery. As a result of the conserved nature of the iron and 2OG binding sites of the JmjC KDMs, attaining selectivity is challenging. The aim of this project was to design and synthesise potent and selective inhibitors of individual JmjC KDM proteins or subfamilies.

A hit from a KDM4E HTS screen was optimised through the introduction of a carboxylate group and through SAR exploration. A novel mode of JmjC KDM inhibition involving metal chelation by the tertiary amine of the aminomethyl pyridine moiety was revealed by X-ray crystallography (**Figure 21**). Submicromolar potency inhibitors in this series were identified for KDM2A, KDM4A/C and KDM5C (**Figure 86**); the sulfonamide derivative **74** was found to be greater than 20-fold selective for KDM2A over the other JmjC KDMs tested whereas the less selective *N*-benzyl derivative **106** was shown to be a potent inhibitor of KDM2A, KDM4A/C and KDM5C.

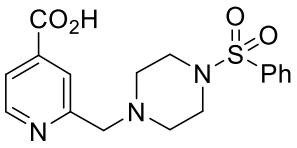

74
KDM2A IC_{50} 0.93 μM
KDM4C IC_{50} 22 μM
KDM4E IC_{50} > 100 μM
KDM5C IC_{50} 31 μM

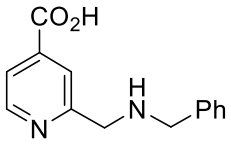

106
KDM2A IC_{50} 0.45 μM
KDM3A IC_{50} 5.3 μM
KDM4A IC_{50} 0.58 μM
KDM4C IC_{50} 0.63 μM
KDM4E IC_{50} 2.1 μM
KDM5C IC_{50} 0.59 μM
KDM6B IC_{50} 14 μM

Figure 86 Submicromolar potency inhibitors discovered in the aminomethyl pyridine series.

A novel triazolopyridine scaffold was also identified which was shown to bind to KDM4A in the 2OG binding pocket, coordinating iron(II) through its pyridine and triazole ring nitrogen atoms with the triazole ring partly extending into the *N*-methylated lysine substrate binding pocket (**Figure 35**). A flexible synthetic route was developed that allowed variation of both the pyridine ring and of the substituents on the triazole ring (**Figure 44**). Exploration of the SAR of the triazole substituents demonstrated that JmjC KDM subfamily selectivity in the triazolopyridine series could be achieved through selection of appropriate substituents on the triazole ring. Submicromolar inhibitors in the triazolopyridine series were identified for KDM2A/7B (**227**) and KDM5C (**177** and **199**) through optimisation of the triazole substituents (**Figure 87**).

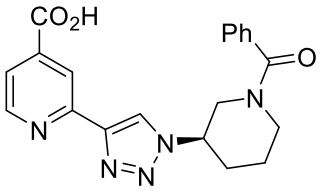

227

KDM2A IC_{50} 0.058 μM

KDM3A IC_{50} > 100 μM

KDM4A IC_{50} 14 μM

KDM4C IC_{50} 15 μM

KDM4E IC_{50} > 100 μM

KDM5C IC_{50} 1.6 μM

KDM6B IC_{50} > 100 μM

KDM7B IC_{50} 0.15 μM

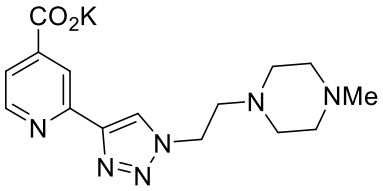

177

KDM2A IC_{50} 45 μM

KDM4E IC_{50} > 100 μM

KDM5C IC_{50} 0.91 μM

KDM6B IC_{50} > 100 μM

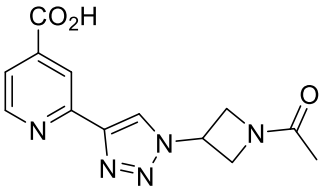

199

KDM2A IC_{50} ND

KDM4C IC_{50} 1.5 μM

KDM4E IC_{50} 4.0 μM

KDM5C IC_{50} 0.55 μM

Figure 87 Submicromolar potency inhibitors identified for KDM2A and KDM5C.

Although triazolopyridine **227** was found to be a potent inhibitor of KDM2A *in vitro*, it was not found to inhibit the demethylation of H3K36me2 by KDM2A in a cellular IF-based assay (**Figure 57**). A variety of strategies were pursued with the aim of increasing the cellular efficacy of **227** (**Figure 88**).

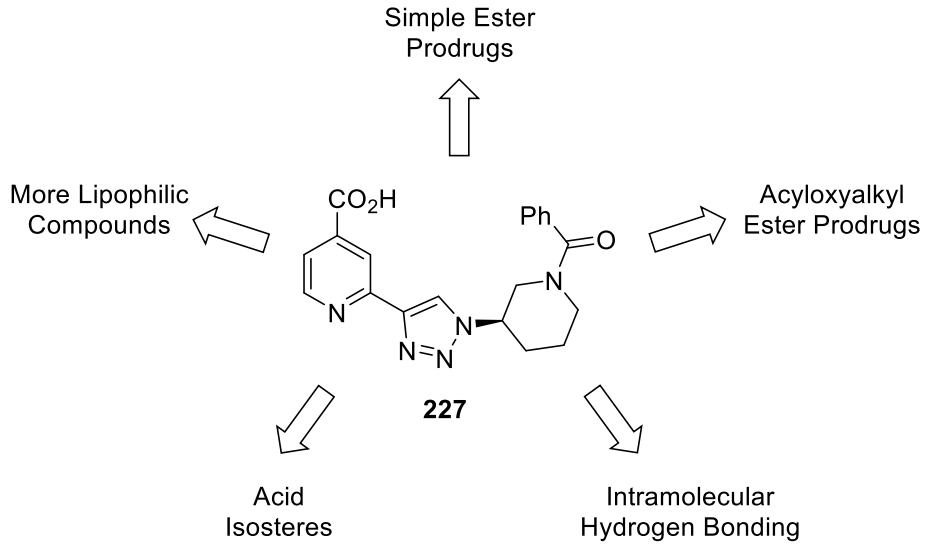

Figure 88 Strategies employed to improve the cellular efficacy of **227**.

Since simple alkyl ester prodrugs of JmjC KDM inhibitors such as NOG **12**, 2,4-PDCA **19**, IOX1 **21** and GSK-J1 **26** are used in cell-based applications to improve cellular permeability the ethyl ester of **50** (aminomethyl pyridine compound **49**), and the methyl and *n*-octyl esters of **227** (triazolopyridine compounds **226** and **229**), were also synthesised and tested in the cellular IF assay. These were not found to result in significant efficacy in the IF assay; the largest effect was seen with the *n*-octyl ester **229** which resulted in approximately 25% inhibition of H3K36me2 demethylation at 100 μM (**Figure 59**). It was hypothesised that the lack of efficacy observed could be due to slow intracellular hydrolysis of the prodrugs so acyloxyalkyl ester prodrugs of **227** were prepared (**252**–**261**) which would be expected to be hydrolysed more rapidly. These resulted in only 25% or less inhibition of H3K36me2 demethylation at 100 μM in the IF assay (**Figure 61**). The physicochemical properties of **227** were also modified in an attempt to improve cellular permeability. More lipophilic analogues (**262**–**265**) were prepared but were found to be much weaker inhibitors of KDM2A than **227** (KDM2A $IC_{50} \geq 10$ μM). The carboxylate group of **227** was replaced with less polar acid isosteres (**Table 28**) but these were also found to be much less active than **227**. The 4-hydroxypyridine derivative **280** was found to retain the most activity against KDM2A (IC_{50}: 13 μM), however, this constitutes a 130-

fold reduction in potency compared to carboxylic acid **227**. *Ortho*-hydroxy derivatives **307** and **309** were also prepared with the aim of improving cellular permeability through the formation of an intramolecular hydrogen bond with the carboxylate group (**Figure 63**). Introduction of a hydroxyl group at the 3- position of the pyridine ring, compound **307**, was found to result in a less than 2-fold reduction in potency against KDM2A (IC_{50}: 0.16 µM) but no inhibition of H3K36me2 demethylation at 100 µM was observed in the IF assay (**Figure 67**).

A chemoproteomics approach was pursued to investigate the engagement of **227** with KDM2A in a cellular environment. A biotin moiety was attached to **227** through a PEG linker to enable immobilisation of **227** onto streptavidin-coated beads for pulldown experiments (**Figure 89**). The attachment point and PEG linker length were optimised to maintain potency against KDM2A and allow concurrent binding to streptavidin. **336** was selected for use in pulldown experiments with cell lysates from HeLa cells that had been transiently transfected with *KDM2A*.

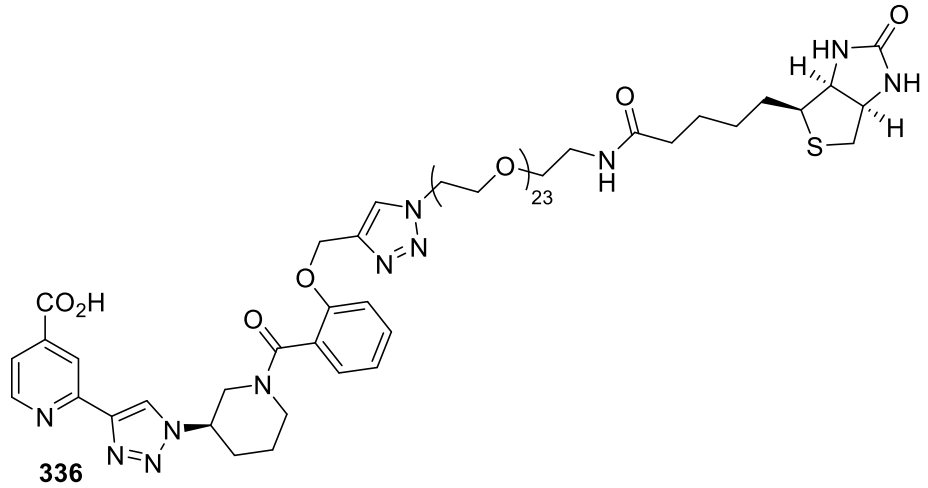

336

Figure 89 Biotinylated analogue of **227** used in chemoproteomics experiments.

It was found by western blot that KDM2A was able to bind to **336** functionalised beads indicating that even in the presence of the many other proteins found in cell lysate the inhibitor is able to bind to the desired target. This interaction was shown to be a specific

interaction; when **227** was added to the cell lysate it was able to competitively inhibit the interaction of KDM2A with the **336** functionalised beads (**Figure 81**). The use of cell lysate from HeLa cells that had been treated with **227** prior to cell lysis also resulted in a reduction in the amount of KDM2A binding to the **336** functionalised beads (**Figure 83**). Dosing cells with 100 μM **227** resulted in an approximately 50% reduction in the amount of KDM2A binding to the **336** functionalised beads indicating that **227** has some cell permeability at 100 μM; however, this appears to be insufficient to inhibit the demethylation of H3K36me2 by KDM2A in the cellular IF assay.

In conclusion, a new JmjC KDM inhibitor scaffold has been discovered through the incorporation of an alternative triazolopyridine iron(II) binding motif to the known 2,2'-bipyridine scaffold. A number of analogues were synthesised leading to the potent and selective KDM2A/7B inhibitor **227** which is significantly more potent than other KDM2/7 selective inhibitors reported in the literature to date, hydroxamate **24** and daminozide **18**. Although **227** was not found to be active in the cellular IF assay, it will be of utility in the investigation of the function of KDM2A/7B in *in vitro* applications and was found to engage KDM2A in cell lysate. Other triazolopyridine derivatives (**177** and **199**) show promise as KDM5C inhibitors.

Experimental Details

7.1 General Experimental Details

Reagents and solvents were used without further purification and were obtained, unless otherwise stated, from Sigma Aldrich, Alfa Aesar, Acros, Fluorochem or Enamine. 2,2'-bipyridine **135** was purchased from Synthon Chemicals and azido biotin reagents were purchased from Iris Biotech. Reactions involving moisture-sensitive reagents were carried out under a nitrogen atmosphere using standard vacuum line techniques. Dry DMF and THF were purchased from Sigma Aldrich in SureSeal® bottles. Toluene was dried by evaporation of 25% v/v of HPLC grade toluene. Brine refers to a saturated aqueous solution of sodium chloride. Water was purified by an Elix® UV-10 system. *In vacuo* refers to the use of a Büchi® rotary evaporator to remove solvent. Microwave experiments were carried out using a Biotage Initiator 8.

Analytical thin layer chromatography (TLC) was carried out on Merck silica gel 60 F254 aluminium supported thin layer chromatography sheets. Visualisation was by absorption of ultraviolet (UV light, λmax 254 nm) and thermal development after dipping in a solution of 1% aq $KMnO_4$. R_f values are quoted to the nearest 0.05.

Flash Column chromatography was carried out either using Kieselgel 60 silica in a glass column or using pre-packed Redisep® or SNAP® cartridges on a CombiFlash Companion or Biotage SP4 automated flash column chromatography platform. Reverse phase chromatography was carried out using a C18 Redisep® cartridge. Strong cation exchange chromatography was carried out using sulfonic acid functionalised silica gel.

Melting points were determined using a Leica Galen III hot stage melting point apparatus and microscope or a Stuart SMP40 melting point apparatus.

Infrared spectra were recorded on a Bruker Tensor 27 spectrometer as a thin film using a diamond attenuated total reflection module. Selected characteristic absorption maxima (ν_{max}) are reported in wavenumbers (cm^{-1}).

NMR spectra were recorded on a Bruker DPX200 (200 MHz), Bruker AV400 (400 MHz), Varian Mercury 400 MHz (400MHz) or Bruker AVII 500 (500 MHz) in the deuterated solvent stated using the solvent as internal deuterium lock. Coupling constants (*J*) are expressed in Hz and are recorded to the nearest 0.5 Hz. Identical coupling constants are averaged in each spectrum and reported to the nearest 0.5 Hz. The ^1H NMR chemical shift data for each signal are given as δ_H in units of parts per million (ppm) relative to tetramethylsilane where δ(tetramethylsilane) = 0.00 ppm. The number of protons (n) for a given resonance signal is indicated by nH. When peak multiplicities are reported, the following abbreviations are used: s (singlet); br s (broad singlet); d (doublet); t (triplet); q (quartet); quin (quintet); dd (doublet of doublets); ddd (doublet of doublet of doublets);

dddd (doublet of doublet of doublet of doublets); td (triplet of doublets); spt (septet); or m (multiplet). ^{13}C NMR spectra were recorded using the PENDANT or DEPT Q pulse sequences with broadband proton decoupling. The chemical shift data for each signal are given as δ in units of parts per million (ppm) relative to tetramethylsilane where δ_C (tetramethylsilane) = 0.00 ppm. ^{1}H and ^{13}C spectra were assigned using 2D NMR experiments including COSY and HSQC. ^{19}F NMR were recorded using a broadband proton decoupling pulse sequence and chemical shift data for each signal are given as δ in units of parts per million (ppm) relative to $CFCl_3$ where δ_F ($CFCl_3$) = 0.00 ppm.

Mass spectra were recorded using a Waters LCT Premier or Micromass Platform 1 spectrometer, operating in the positive or negative ion mode or a Waters MALDI Micro MX, from solutions of methanol or acetonitrile. *m*/*z* values are reported in Daltons and followed by their percentage abundance in parentheses. High resolution mass spectra (HRMS) were recorded using Bruker MicroTOF internally calibrated with polyalanine or a Waters MALDI Micro MX.

Analytical reverse-phase LCMS was used to determine the purity of the synthesized compounds either using a WATERS sunfire C18 column (system A; used unless otherwise stated), a Gemini-NX C18 110Å column (system B), a WATERS sunfire C18 column (system C), an Xbridge C18 column (system D) or a Merk Millipore Chromolith Performance RP-18e column (system E). System A used electrospray ionization, operating in the positive ion mode; separation was achieved using a linear gradient of solvent A (water + 0.01% CF_3CO_2H) and solvent B (acetonitrile + 0.01% CF_3CO_2H), eluting at a flow rate of 1 mL/min and monitoring at 254 nm: 0% B over 2 min, 0% B to 100% B over 16 min and 100% B over 2 min. System B used electrospray ionization, operating in the positive or negative ion mode; separation was achieved using a linear gradient of solvent A (water + 0.1% HCO_2H) and solvent B (acetonitrile + 0.1% HCO_2H), eluting at a flow rate of 1.5 mL/min and monitoring at 225 nm: 5% B to 95% B over 3 min and 95% B over 1 min. System C used electrospray ionization, operating in the positive or negative ion mode; separation was achieved using a linear gradient of solvent A (water + 0.01% CF_3CO_2H) and solvent B (acetonitrile + 0.01% CF_3CO_2H), eluting at a flow rate of 2.5 mL/min and monitoring at 210, 254 and 280 nm: 5% B to 95% B over 2 min and 95% B over 1.5 min. System D used electrospray ionization, operating in the positive ion mode; separation was achieved using a linear gradient of solvent A (water + 0.05% CF_3CO_2H) and solvent B (acetonitrile + 0.05% CF_3CO_2H), eluting at a flow rate of 1.8 mL/min and monitoring at 254 and 280 nm: 5% B to 95% B over 1.2 min and 95% B over 1.5 min. System E used electrospray ionization, operating in the positive or negative ion mode; separation was achieved using a linear gradient of solvent A (water + 0.01% CF_3CO_2H) and solvent B (acetonitrile + 0.01% CF_3CO_2H), eluting at a flow rate of 1 mL/min and monitoring at 254 nm: 2% B over 2 min, 2% B to 100% B over 8 min and 100% B over 1 min. HPLC tR are quoted to the nearest 0.1 min. Preparative HPLC purification was carried out using a Gemini-NX C18 110Å column at ambient temperature; detection was by ELSD–MS; the flow rate was 18 mL/min. The

mobile phase used was A: water + 0.1% HCO_2H, B: MeCN + 0.1% HCO_2H; gradient (time/min, %B) (0–1, 5%), (1–7, 5–98%), (7–9, 98%), (9–9.1, 98–5%), (9.1–10, 5%).

Elemental analyses were recorded by the elemental analysis service of London Metropolitan University.

Enantiomeric excesses were determined by HPLC analysis employing a Chiralpak® amylose tris(3,5-dimethylphenyl) carbamate (Chiralpak® AD) analytical column. Separation was achieved using 80:20 hexane–isopropanol, eluting at a flow rate of 0.8 mL/min and monitoring at 254 nm and by comparing the samples to a 1:1 mixture of each enantiomer.

Specific optical rotations were recorded on a Perkin-Elmer 241 polarimeter with a water jacketed 10 cm cell at 20 °C. The light source was maintained at 589 nm. Specific rotations are denoted $[\alpha]_D^{20}$ and are given in implied units of 10^{-1} deg cm^2 g^{-1} and concentrations in g/100 mL.

7.2 Synthesis of Compounds

Diethyl pyridine-2,4-dicarboxylate 46[217]

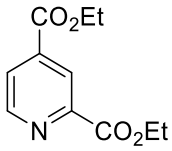

para-Toluene sulfonic acid (11.37 g, 190.2 mmol) was added to a suspension of pyridine-2,4-dicarboxylic acid (5.27 g, 185.1 mmol) in ethanol (100 mL) and the resulting suspension stirred at room temperature for 10 min. A colourless solution formed that was heated at 80 °C for 16 h. The ethanol was removed *in vacuo*, 60 mL water added followed by 60 mL saturated sodium carbonate solution and the resulting suspension extracted with diethyl ether (3 × 80 mL). The organic layers were combined, dried over sodium sulfate and concentrated *in vacuo* to give **46** as a colourless oil (5.00 g, 79% yield). R_f 0.80 (diethyl ether); ν_{max} (film) 2984 (C–H), 2940 (C–H), 1725 (C=O); δ_H (400 MHz, $CDCl_3$) 1.43 (3H, t, *J* 7.0, *C<u>H</u>₃*), 1.46 (3H, t, *J* 7.0, *C<u>H</u>₃*), 4.45 (2H, q, *J* 7.0, *PyC4CO₂C<u>H</u>₂CH₃*), 4.51 (2H, q, *J* 7.0, *PyC2CO₂C<u>H</u>₂CH₃*), 8.03 (1H, dd, *J* 5.0, 1.5, *PyC5<u>H</u>*), 8.64 (1H, dd, *J* 1.5, 1.0, *PyC3<u>H</u>*), 8.91 (1H, dd, *J* 5.0, 1.0, *PyC6<u>H</u>*) [*consistent with literature*]; δ_C (100 MHz, $CDCl_3$) 14.2 and 14.3 (2 × *<u>C</u>H₃*), 62.2 (*PyC4CO₂<u>C</u>H₂CH₃*), 62.3 (*PyC2CO₂<u>C</u>H₂CH₃*), 124.3 (*Py<u>C</u>3H*), 125.9 (*Py<u>C</u>5H*), 139.0 (*Py<u>C</u>4*), 149.3 (*Py<u>C</u>2*), 150.6 (*Py<u>C</u>6H*), 164.3 (*PyC4<u>C</u>O₂Et*), 164.6 (*PyC2<u>C</u>O₂Et*); *m/z* (MS, ES^+) 469 (100%, M_2Na^+); LCMS tR 13.2 min (99%).

Ethyl 2-formylisonicotinate 47[140]

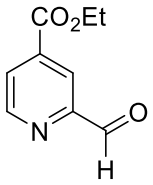

Diisobutylaluminum hydride (1 M in tetrahydrofuran, 22.4 mL, 22.4 mmol) was added dropwise over 30 min to a solution of diethyl pyridine-2,4-dicarboxylate **46** (5.00 g, 22.4 mmol) in toluene (150 mL) at –78 °C under an atmosphere of nitrogen and the resulting solution stirred at –78 °C for 30 min. Further diisobutylaluminum hydride (22.4 mL, 22.4 mmol) was added dropwise over 10 min and the resulting solution stirred at –78 °C for a further 2 h. Acetic acid (10 mL) was added dropwise over 5 min followed by diethyl ether (75 mL) and the reaction mixture allowed to warm to room temperature then filtered, washing with diethyl ether (2 × 10 mL). The filtrate was concentrated *in vacuo* to give a yellow solid that was purified by flash column chromatography (1:4 → 1:1 diethyl ether–cyclohexane) to give **47** as an off-white solid (1.56 g, 39%). R_f 0.50 (2:1 diethyl ether–cyclohexane); mp 58–61 °C [*lit. mp 63* °C]; ν_{max} (film) 3077 (C–H), 2986 (C–H), 2851 (C–H), 1723 (C=O, ester), 1709 (C=O, aldehyde) [*consistent with literature*]; δ_H (400 MHz, $CDCl_3$) 1.44 (3H, t, *J* 7.0, *C*<u>*H*</u>$_3$), 4.46 (2H, q, *J* 7.0, *C*<u>*H*</u>$_2$), 8.10 (1H, dd, *J* 5.0, 1.5, *PyC5*<u>*H*</u>), 8.49 (1H, app. s, *PyC3*<u>*H*</u>), 8.95 (1H, d, *J* 5.0, *PyC6*<u>*H*</u>), 10.15 (1H, s, *C*<u>*H*</u>*O*) [*consistent with literature*]; δ_C (100 MHz, $CDCl_3$) 14.2 (<u>*C*</u>H_3), 62.3 (<u>*C*</u>H_2), 120.9 (*Py*<u>*C*</u>*3H*), 127.0 (*Py*<u>*C*</u>*5H*), 139.2 (*Py*<u>*C*</u>*4*), 151.0 (*Py*<u>*C*</u>*6H*), 153.7 (*Py*<u>*C*</u>*2*), 164.2 (<u>*C*</u>O_2*Et*), 192.6 (<u>*C*</u>*HO*); LCMS tR 15.9 min (95%); *m/z* (MS, ES^+) 333 (100%, MH^+).

Ethyl 2-{(4-(2-phenylacetyl)piperazin-1-yl)methyl}isonicotinate 49

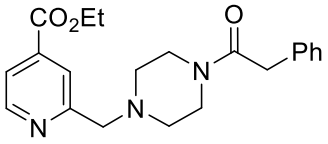

2-Phenyl-1-(piperazin-1-yl)ethanone (56 mg, 0.28 mmol) was added to a solution of ethyl 2-formylisonicotinate (45 mg, 0.25 mmol) in dichloromethane (2 mL) and the resulting solution stirred at room temperature for 10 min. Sodium triacetoxyborohydride (80 mg, 0.38 mmol) was added and the resulting suspension stirred at room temperature for 72 h. The reaction mixture was purified by flash column chromatography (ethyl acetate) to give **49** as an opaque colourless oil (43 mg, 47%). R_f 0.20 (ethyl acetate); ν_{max} (film) 2934 (C–H), 2813 (C–H), 2767 (C–H), 1725 (C=O, ester), 1641 (C=O, amide); δ_H (400 MHz, $CDCl_3$) 1.39 (3H, t, *J* 7.0, *CH*$_2$*C*<u>*H*</u>$_3$), 2.28–2.32 and 2.44–2.48 (2 × 2H, m, 2 × *piperazinyl C*<u>*H*</u>$_2$), 3.43–3.48 (2H, m, *piperazinyl C*<u>*H*</u>$_2$), 3.65–3.69 (4H, m, *C*<u>*H*</u>$_2$*Py* and *piperazinyl C*<u>*H*</u>$_2$), 3.71 (2H, s, *C*<u>*H*</u>$_2$*Ph*), 4.39 (2H, q, *J* 7.0, *C*<u>*H*</u>$_2$*CH*$_3$), 7.18–7.32 (5H, m, *Ph*), 7.70 (1H, dd, *J* 5.0, 1.5, *PyC5*<u>*H*</u>), 7.88 (1H, app. s, *PyC3*<u>*H*</u>), 8.68 (1H, d, *J* 5.0, *PyC6*<u>*H*</u>); δ_C (100 MHz, $CDCl_3$) 14.2 (*CH*$_2$<u>*C*</u>H_3), 41.0 (<u>*C*</u>H_2*Ph*), 41.6 (*piperazinyl* <u>*C*</u>H_2), 46.0 (*piperazinyl* <u>*C*</u>H_2), 52.8 and 53.0 (2 × *piperazinyl* <u>*C*</u>H_2), 61.8 (<u>*C*</u>H_2*CH*$_3$), 64.0 (<u>*C*</u>H_2*Py*), 121.4 (*Py*<u>*C*</u>*5H*), 122.4

(*PyC3H*), 126.8 (1 × *PhCH*), 128.5 (2 × *PhCH*), 128.7 (2 × *PhCH*), 135.0 (*ipso-Ph*), 138.3 (*PyC4*), 150.1 (*PyC6H*), 159.2 (*PyC2*), 165.2 (*CO₂Et*), 169.4 (*CON*); *m/z* (MS, ES^+) 390 (100%, MNa^+); LCMS tR 9.6 min (100%); accurate mass: found 368.1967, calc. for $C_{21}H_{26}N_3O_3^+$ 368.1969.

Potassium 2-{[4-(phenylacetyl)piperazin-1-yl]methyl} isonicotinate 50

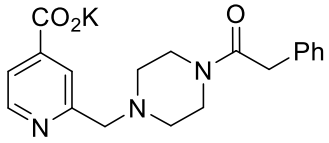

Potassium trimethylsilanolate (13 mg, 0.10 mmol) was added to a solution of ethyl 2-{(4-(2-phenylacetyl)piperazin-1-yl)methyl}isonicotinate **49** (24 mg, 0.07 mmol) in acetonitrile (4 mL) and the resulting suspension stirred at room temperature for 16 h. The resulting precipitate was filtered, washed with acetonitrile (2 × 3 mL) and dried under vacuum to give **50** as a white gum (17 mg, 69%). R_f 0.50 (8:2 dichloromethane–methanol); ν_{max} (film) 3028 (C–H), 2922 (C–H), 2817 (C–H), 1596 (C=O, amide), 1548 (CO_2K); δ_H (400 MHz, CD_3OD) 2.31–2.37 and 2.26–2.52 (4H, m, 2 × *piperazinyl CH₂*), 3.55–3.60 (2H, m, *piperazinyl CH₂*), 3.64–3.69 (4H, m, *piperazinyl CH₂* and *CH₂Ph*), 3.79 (2H, s, *CH₂Py*), 7.22–7.36 (5H, m, *Ph*), 7.72 (1H, dd, *J* 5.0, 1.5, *PyC5H*), 7.93 (1H, app. s, *PyC3H*), 8.50 (1H, d, *J* 5.0, *PyC6H*); δ_C (100 MHz, CD_3OD) 40.3 (*CH₂Ph*), 42.0 (*piperazinyl CH₂*), 46.3 (*piperazinyl CH₂*), 52.8 (*piperazinyl CH₂*), 53.0 (*piperazinyl CH₂*), 63.4 (*CH₂Py*), 122.3 (*PyC5H*), 123.4 (*PyC3H*), 126.9 (1 × *PhCH*), 128.7 (2 × *PhCH*), 128.8 (2 × *PhCH*), 135.4 (*ipso Ph*), 147.5 (*PyC4*), 148.7 (*PyC6H*), 158.1 (*PyC2*), 171.1 and 171.6 (*CO₂K* and *CON*); *m/z* (MS, ES^-) 338 (100%, $[M–K]^-$); LCMS tR 8.5 min (90%); accurate mass: found 362.1476, calc. for $C_{19}H_{21}N_3NaO_3^+$ 362.1475.

Ethyl 2-[(4-acetylpiperazin-1-yl)methyl]isonicotinate 56

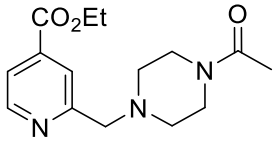

A solution of ethyl 2-formylisonicotinate **47** (45 mg, 0.25 mmol) in dichloromethane (2 mL) was added to 1-(piperazin-1-yl)ethanone (49 mg, 0.38 mmol) and the resulting solution stirred at room temperature for 15 min. Sodium triacetoxyborohydride (80 mg, 0.38 mmol) was added and the resulting suspension stirred at room temperature for 16 h. The reaction mixture was purified by flash column chromatography (dichloromethane → 90:10 dichloromethane–methanol) to give **56** as a colourless oil (62 mg, 85%). R_f 0.10 (ethyl acetate); ν_{max} (film) 2982 (C–H), 2935 (C–H), 2813 (C–H), 1724 (C=O, ester), 1643 (C=O, amide); δ_H (400 MHz, $CDCl_3$) 1.41 (3H, t, *J* 7.0, *CH₃CH₂O*), 2.07 (3H, s, *CH₃CON*), 2.46–2.54 (4H, m, 2 × *piperazinyl CH₂*), 3.47–3.51 (2H, m, *piperazinyl CH₂*), 3.62–3.67 (2H, m, *piperazinyl CH₂*), 3.73 (2H, s, *CH₂Py*), 4.41 (2H, q, *J* 7.0, *CH₃CH₂O*), 7.73 (1H, dd, *J* 5.0, 1.5, *PyC5H*), 7.93 (1H, app. s, *PyC3H*), 8.71 (1H, d, *J* 5.0, *PyC6H*); δ_C (100 MHz, $CDCl_3$) 14.2 (*CH₃CH₂O*), 21.3 (*CH₃C=O*), 41.2 (*piperazinyl CH₂*), 46.1 (*piperazinyl*

CH_2) 52.8 and 53.2 (2 × *piperazinyl C*H_2), 61.8 (*C*H_3*C*H_2*O*), 64.0 (*C*H_2*Py*), 121.4 (*PyC5H*), 122.4 (*PyC3H*), 138.3 (*PyC4*), 150.1 (*PyC6H*), 159.1 (*PyC2*), 165.2 (*CO*$_2$*Et*), 168.9 (*CON*); *m/z* (MS, ES$^+$) 605 (100%, M_2Na^+); LCMS tR 7.7 min (86%); accurate mass: found 292.1652, calc. for $C_{15}H_{22}N_3O_3^+$ 292.1656.

Ethyl 2-[(4-propionylpiperazin-1-yl)methyl]isonicotinate 57

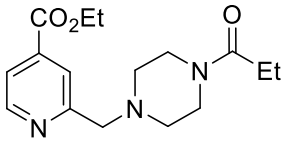

A solution of ethyl 2-formylisonicotinate **47** (45 mg, 0.25 mmol) in dichloromethane (2 mL) was added to 1-(piperazin-1-yl)propanone (54 mg, 0.38 mmol) and the resulting solution stirred at room temperature for 15 min. Sodium triacetoxyborohydride (80 mg, 0.38 mmol) was added and the resulting suspension stirred at room temperature for 16 h. The reaction mixture was purified by flash column chromatography (dichloromethane → 90:10 dichloromethane–methanol) to give **57** as a colourless oil (74 mg, 97%). R_f 0.15 (ethyl acetate); ν_{max} (film) 2980 (C–H), 2938 (C–H), 2813 (C–H), 1725 (C=O, ester), 1644 (C=O, amide); δ_H (400 MHz, $CDCl_3$) 1.12 (3H, t, *J* 7.5, *CH*$_3$*CH*$_2$*C=O*), 1.40 (3H, t, *J* 7.0, *CH*$_3$*CH*$_2$*O*), 2.32 (2H, q, *J* 7.5, *CH*$_3$*CH*$_2$*C=O*), 2.46–2.53 (4H, m, 2 × *piperazinyl CH*$_2$), 3.46–3.51 (2H, m, *piperazinyl CH*$_2$), 3.63–3.68 (2H, m, *piperazinyl CH*$_2$), 3.73 (2H, s, *CH*$_2$*Py*), 4.41 (2H, q, *J* 7.0, *CH*$_3$*CH*$_2$*O*), 7.73 (1H, d, *J* 5.0, *PyC5H*), 7.93 (1H, s, *PyC3H*), 8.71 (1H, d, *J* 5.0, *PyC6H*); δ_C (100 MHz, $CDCl_3$) 9.4 (*CH*$_3$*CH*$_2$*C=O*), 14.1 (*CH*$_3$*CH*$_2$*O*), 26.4 (*CH*$_3$*CH*$_2$*C=O*), 41.3 (*piperazinyl CH*$_2$), 45.2 (*piperazinyl CH*$_2$), 52.9 and 53.3 (2 × *piperazinyl CH*$_2$), 61.8 (*CH*$_3$*CH*$_2$*O*), 64.0 (*CH*$_2$*Py*), 121.4 (*PyC5H*), 122.5 (*PyC3H*), 138.3 (*PyC4*), 150.0 (*PyC6H*), 159.0 (*PyC2*), 165.1 (*CO*$_2$*Et*), 172.3 (*CON*); *m/z* (MS, ES$^+$) 633 (100%, M_2Na^+); LCMS tR 8.1 min (96%); accurate mass: found accurate mass: found 306.1805, calc. for $C_{16}H_{24}N_3O_3^+$ 306.1812.

Ethyl 2-[(4-(cyclopropanecarbonyl)piperazin-1-yl]methyl)isonicotinate 58

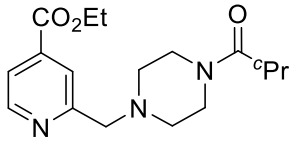

A solution of ethyl 2-formylisonicotinate **47** (45 mg, 0.25 mmol) in dichloromethane (2 mL) was added to cyclopropyl(piperazin-1-yl)methanone (59 mg, 0.38 mmol) and the resulting solution stirred at room temperature for 15 min. Sodium triacetoxyborohydride (80 mg, 0.38 mmol) was added and the resulting suspension stirred at room temperature for 16 h. The reaction mixture was purified by flash column chromatography (dichloromethane → 90:10 dichloromethane–methanol) to give **58** as a colourless oil (92 mg contaminated with 10% w/w acetic acid, quant.). R_f 0.20 (ethyl acetate); ν_{max} (film) 3007 (C–H), 2938 (C–H), 2813 (C–H), 1724 (C=O, ester), 1637 (C=O, amide); δ_H (400 MHz, $CDCl_3$) 0.71–0.77 (2H, m, *^{c}Pr*), 0.94–0.99 (2H, m, *^{c}Pr*), 1.41 (4H, t, *J* 7.0,

C<u>H</u>₃CH₂O), 1.67–1.74 (1H, m, *C<u>H</u>C=O*), 2.46–2.60 (4H, m, 2 × *piperazinyl C<u>H₂</u>*), 3.63–3.74 (4H, m, 2 × *piperazinyl C<u>H₂</u>*), 3.76 (2H, s, *C<u>H₂</u>Py*), 4.41 (2H, q, *J* 7.0, *CH₃C<u>H₂</u>O*), 7.75 (1H, dd, *J* 5.0, 1.5, *PyC5<u>H</u>*), 7.95 (1H, app. s, *PyC3<u>H</u>*), 8.72 (1H, d, *J* 5.0, *PyC6<u>H</u>*); δ_C (100 MHz, $CDCl_3$) 7.4 (*ᶜPr* 2 × *<u>C</u>H₂*), 10.8 (*ᶜPr <u>C</u>H*), 14.1 (*<u>C</u>H₃CH₂O*), 41.9 (*piperazinyl <u>C</u>H₂*), 45.2 (*piperazinyl <u>C</u>H₂*), 52.8 and 53.3 (2 × *piperazinyl <u>C</u>H₂*), 61.8 (*CH₃<u>C</u>H₂O*), 63.7 (*<u>C</u>H₂Py*), 121.5 (*Py<u>C</u>5H*), 122.6 (*Py<u>C</u>3H*), 138.4 (*Py<u>C</u>4*), 149.9 (*Py<u>C</u>6H*), 158.8 (*Py<u>C</u>2*), 165.1 (*<u>C</u>O₂Et*), 172.0 (*<u>C</u>ON*); *m/z* (MS, ES^+) 657 (100%, M_2Na^+); LCMS tR 8.3 min (91%); accurate mass: found 318.1811, calc. for $C_{17}H_{24}N_3O_3^+$ 318.1812.

Ethyl 2-[(4-isobutyrylpiperazin-1-yl)methyl]isonicotinate 59

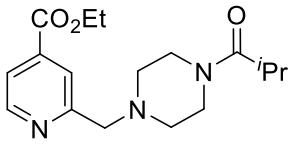

A solution of ethyl 2-formylisonicotinate **47** (45 mg, 0.25 mmol) in dichloromethane (2 mL) was added to 2-methyl-1-(piperazin-1-yl)propan-1-one (59 mg, 0.38 mmol) and the resulting solution stirred at room temperature for 15 min. Sodium triacetoxyborohydride (80 mg, 0.38 mmol) was added and the resulting suspension stirred at room temperature for 16 h. The reaction mixture was purified by flash column chromatography (dichloromethane → 90:10 dichloromethane–methanol) to give **59** as a colourless oil (76 mg contaminated with 9% w/w acetic acid, 87%). R_f 0.20 (ethyl acetate); ν_{max} (film) 2971 (C–H), 2934 (C–H), 2812 (C–H), 1726 (C=O, ester), 1642 (C=O, amide); δ_H (400 MHz, $CDCl_3$) 1.10 (6H, d, *J* 7.0, *CH(C<u>H</u>₃)₂*), 1.40 (3H, t, *J* 7.0, *C<u>H</u>₃CH₂O*), 2.47–2.55 (4H, m, 2 × *piperazinyl C<u>H₂</u>*), 2.76 (1H, sep, *J* 7.0, *C<u>H</u>(CH₃)₂*), 3.52–3.56 (2H, m, *piperazinyl C<u>H₂</u>*), 3.63–3.68 (2H, m, *piperazinyl C<u>H₂</u>*), 3.74 (2H, s, *C<u>H₂</u>Py*), 4.41 (2H, q, *J* 7.0, *CH₃C<u>H₂</u>O*), 7.74 (1H, dd, *J* 5.0, 1.5, *PyC5<u>H</u>*), 7.94 (1H, app. s, *PyC3<u>H</u>*), 8.71 (1H, d, *J* 5.0, *PyC6<u>H</u>*); δ_C (100 MHz, $CDCl_3$) 14.1 (*<u>C</u>H₃CH₂O*), 19.3 (*CH(<u>C</u>H₃)₂*), 29.9 (*<u>C</u>H(CH₃)₂*), 41.4 (*piperazinyl <u>C</u>H₂*), 45.1 (*piperazinyl <u>C</u>H₂*), 52.9 and 53.4 (2 × *piperazinyl <u>C</u>H₂*), 61.8 (*CH₃<u>C</u>H₂O*), 63.7 (*<u>C</u>H₂Py*), 121.5 (*Py<u>C</u>5H*), 122.6 (*Py<u>C</u>3H*), 138.4 (*Py<u>C</u>4*), 149.9 (*Py<u>C</u>6H*), 158.8 (*Py<u>C</u>2*), 165.1 (*<u>C</u>O₂Et*), 175.4 (*<u>C</u>ON*); *m/z* (MS, ES^+) 661 (100%, M_2Na^+); LCMS tR 8.5 min (92%); accurate mass: found 320.1958, calc. for $C_{17}H_{26}N_3O_3^+$ 320.1969.

Ethyl 2-[(4-benzoylpiperazin-1-yl)methyl]isonicotinate 60

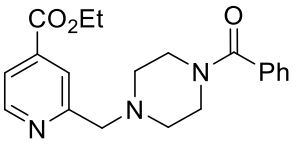

A solution of ethyl 2-formylisonicotinate **47** (45 mg, 0.25 mmol) in dichloromethane (2 mL) was added to 1 phenyl(piperazin-1-yl)methanone hydrochloride (86 mg, 0.38 mmol) followed by triethylamine (53 µL, 0.38 mmol) and the resulting suspension stirred at room temperature for 15 min. Sodium triacetoxyborohydride (80 mg, 0.38 mmol) was added and the resulting suspension

stirred at room temperature for 16 h. The reaction mixture was purified by flash column chromatography (dichloromethane → 90:10 dichloromethane–methanol) to give **60** as a colourless oil (98 mg contaminated with 9% acetic acid w/w, quant.). R_f 0.30 (ethyl acetate); ν_{max} (film) 2983 (C–H), 2936 (C–H), 2814 (C–H), 1723 (C=O, ester), 1631 (C=O, amide); δ_H (400 MHz, $CDCl_3$) 1.40 (3H, t, *J* 7.0, *C<u>H</u>₃CH₂O*), 2.41–2.67 (4H, m, 2 × *piperazinyl C<u>H</u>₂*), 3.38–3.53 (2H, m, *piperazinyl C<u>H</u>₂*), 3.77 (2H, *C<u>H</u>₂Py*), 3.74–3.87 (2H, m, *piperazinyl C<u>H</u>₂*), 4.40 (2H, q, *J* 7.0, *CH₃C<u>H</u>₂O*), 7.35–7.44 (5H, m, *Ph*), 7.74 (1H, dd, *J* 5.0, 1.5, *PyC5<u>H</u>*), 7.94 (1H, app. s, *PyC3<u>H</u>*), 8.71 (1H, d, *J* 5.0, *PyC6<u>H</u>*); δ_C (100 MHz, $CDCl_3$) 14.1 (*<u>C</u>H₃CH₂O*), 41.9 (*piperazinyl <u>C</u>H₂*), 47.5 (*piperazinyl <u>C</u>H₂*), 52.8 and 53.3 (2 × *piperazinyl <u>C</u>H₂*), 61.8 (*CH₃<u>C</u>H₂O*), 63.7 (*<u>C</u>H₂Py*), 121.6 (*Py<u>C</u>5H*), 122.6 (*Py<u>C</u>3H*), 126.9 (2 × *Ph<u>C</u>H*), 128.4 (2 × *Ph<u>C</u>H*), 129.6 (*Ph<u>C</u>H*), 135.5 (*Ph ipso-C)*, 138.4 (*Py<u>C</u>4*), 149.9 (*Py<u>C</u>6H*), 158.7 (*Py<u>C</u>2*), 165.0 (*<u>C</u>O₂Et*), 170.3 (*<u>C</u>ON*); *m/z* (MS, ES^+) 354 (100%, MH^+); LCMS tR 9.2 min (66%); accurate mass: found 318.1811, calc. for $C_{17}H_{24}N_3O_3^+$ 318.1812.

Potassium 2-[(4-acetylpiperazin-1-yl)methyl]isonicotinate 61

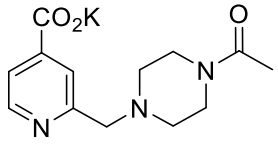

Potassium trimethylsilanolate (25 mg, 0.20 mmol) was added to a solution of ethyl 2-[(4-acetylpiperazin-1-yl)methyl]isonicotinate **56** (38 mg, 0.13 mmol) in acetonitrile (5 mL) and the resulting suspension stirred at room temperature for 16 h. The resulting precipitate was filtered, washed with acetonitrile (2 × 2 mL) and dried under vacuum to give **61** as a white solid (29 mg, 75%). mp 280–282 °C; ν_{max} (film) 2947 (C–H), 2846 (C–H), 2816 (C–H), 1616 (C=O, amide), 1551 (CO_2K); δ_H (500 MHz, CD_3OD) 2.11 (3H, s, *C<u>H</u>₃*), 2.50–2.53 and 2.54–2.58 (4H, m, 2 × *piperazinyl C<u>H</u>₂*), 3.57–3.61 (2H, m, *piperazinyl C<u>H</u>₂*), 3.62–3.66 (2H, m, *piperazinyl C<u>H</u>₂*), 3.74 (2H, s, *C<u>H</u>₂Py*), 7.74 (1H, dd, *J* 5.0, 1.5, *PyC5<u>H</u>*), 7.98 (1H, app. s, *PyC3<u>H</u>*), 8.53 (1H, dd, *J* 5.0, 0.5, *PyC6<u>H</u>*); δ_C (125 MHz, CD_3OD) 21.3 (*<u>C</u>H₃*), 42.8 (*piperazinyl <u>C</u>H₂*), 47.5 (*piperazinyl <u>C</u>H₂*), 54.1 and 54.4 (2 × *piperazinyl <u>C</u>H₂*), 64.7 (*<u>C</u>H₂Py*), 123.5 (*Py<u>C</u>5H*), 124.6 (*Py<u>C</u>3H*), 148.7 (*Py<u>C</u>4*), 149.9 (*Py<u>C</u>6H*), 159.4 (*Py<u>C</u>2*), 171.7 and 172.8 (*<u>C</u>O₂K* and *<u>C</u>ON*); LCMS tR 3.5 min (86%); *m/z* (MS, ES^-) 262 (100%, $[M–K]^-$); accurate mass: found 286.1166, calc. for $C_{13}H_{17}N_3NaO_3^+$ 286.1162.

Potassium 2-[(4-propionylpiperazin-1-yl)methyl]isonicotinate 62

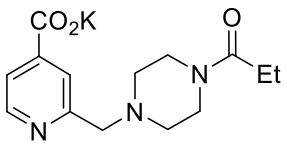

Potassium trimethylsilanolate (32 mg, 0.25 mmol) was added to a solution of ethyl 2-[(4-propionylpiperazin-1-yl)methyl]isonicotinate **57** (50 mg, 0.16 mmol) in acetonitrile (5 mL) and the

resulting suspension stirred at room temperature for 16 h. The volatiles were removed *in vacuo* to give a yellow gum that was washed with acetonitrile (2 × 2 mL) to give **62** as a yellow gum (53 mg, quant.). ν_{max} (film) 2978 (C–H), 2941 (C–H), 2818 (C–H), 1597 (C=O, amide), 1548 (CO_2K); δ_H (400 MHz, CD_3OD) 1.11 (3H, t, *J* 7.5, *C<u>H</u>₃CH₂C=O*), 2.41 (2H, q, *J* 7.5, *CH₃C<u>H</u>₂C=O*), 2.49–2.57 (4H, m, 2 × *PipC<u>H</u>₂*), 3.56–3.61 (2H, m, *PipC<u>H</u>₂*), 3.61–3.67 (2H, m, *PipC<u>H</u>₂*), 3.73 (2H, s, *C<u>H</u>₂Py*), 7.74 (1H, d, *J* 5.0, *PyC5<u>H</u>*), 7.97 (1H, s, *PyC3<u>H</u>*), 8.52 (1H, d, *J* 5.0, *PyC6<u>H</u>*); δ_C (125 MHz, CD_3OD) 10.1 (*<u>C</u>H₃CH₂*), 27.4 (*CH₃<u>C</u>H₂*), 42.9 (*Pip<u>C</u>H₂*), 46.7 (*Pip<u>C</u>H₂*), 54.2 and 54.5 (2 × *Pip<u>C</u>H₂*), 64.7 (*<u>C</u>H₂Py*), 123.5 (*Py<u>C</u>5H*), 124.6 (*Py<u>C</u>3H*), 148.7 (*Py<u>C</u>4*), 149.9 (*Py<u>C</u>6H*), 159.4 (*Py<u>C</u>2*), 172.8 and 175.0 (*<u>C</u>O₂K* and *<u>C</u>ON*); *m/z* (MS, ES^-) 276 (100%, $[M–K]^-$); LCMS tR 6.2 min (96%); accurate mass: found 300.1321, calc. for $C_{14}H_{19}N_3NaO_3^+$ 300.1319.

Potassium 2-[(4-(cyclopropanecarbonyl)piperazin-1-yl)methyl]isonicotinate 63

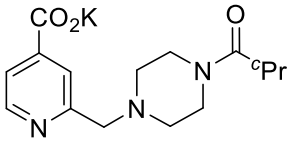

Potassium trimethylsilanolate (58 mg, 0.45 mmol) was added to a solution of ethyl 2-[(4-(cyclopropanecarbonyl)piperazin-1-yl)methyl]isonicotinate **58** (38 mg, 0.13 mmol) in acetonitrile (5 mL) and the resulting suspension stirred at room temperature for 16 h. The reaction mixture was filtered, the filtrate concentrated *in vacuo* to give a colourless gum that was washed with acetonitrile (3 × 4 mL) and dried under vacuum to give **63** as a white gum (35 mg, contaminated with 5% acetic acid w/w, 58%). ν_{max} (film) 3011 (C–H), 2917 (C–H), 2819 (C–H), 1597 (C=O, amide), 1548 (CO_2K); δ_H (200 MHz, CD_3OD) 0.76–0.95 (4H, m, 2 × *^{c}PrC<u>H</u>₂*), 1.90–2.04 (1H, m, *^{c}PrC<u>H</u>*), 2.47–2.68 (4H, m, 2 × *piperazinyl C<u>H</u>₂*), 3.60–3.73 (2H, m, *piperazinyl C<u>H</u>₂*), 3.76 (2H, s, *C<u>H</u>₂Py*), 3.79–3.92 (2H, m, *piperazinyl C<u>H</u>₂*), 7.77 (1H, dd, *J* 5.0, 1.5, *PyC5<u>H</u>*), 8.01 (1H, app. s, *PyC3<u>H</u>*), 8.56 (1H, dd, *J* 5.0, 0.5, *PyC6<u>H</u>*); δ_C (125 MHz, CD_3OD) 8.0 (2 × *^{c}Pr<u>C</u>H₂*), 11.8 (*^{c}Pr<u>C</u>H*), 43.5 (*piperazinyl <u>C</u>H₂*), 46.7 (*piperazinyl <u>C</u>H₂*), 54.2 and 54.7 (2 × *piperazinyl <u>C</u>H₂*), 64.7 (*<u>C</u>H₂Py*), 123.5 (*Py<u>C</u>5H*), 124.6 (*Py<u>C</u>3H*), 148.7 (*Py<u>C</u>4*), 149.9 (*Py<u>C</u>6H*), 159.4 (*Py<u>C</u>2*), 172.8 and 174.5 (*<u>C</u>O₂K* and *<u>C</u>ON*); *m/z* (MS, ES^-) 288 (100%, $[M–K]^-$); LCMS tR 6.6 min (96%); accurate mass: found 312.1313, calc. for $C_{15}H_{19}N_3NaO_3^+$ 312.1319.

Potassium 2-[(4-isobutyrylpiperazin-1-yl)methyl]isonicotinate 64

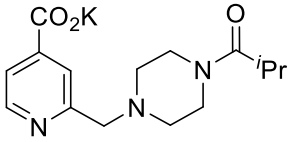

Potassium trimethylsilanolate (40 mg, 0.32 mmol) was added to a solution of ethyl 2-[(4-isobutyrylpiperazin-1-yl)methyl]isonicotinate **59** (46 mg, contaminated with 9% acetic acid by mass, 0.13 mmol) in acetonitrile (5 mL) and the resulting suspension stirred at room temperature for 16 h. The volatiles were removed *in vacuo* to give a gum that was washed with acetonitrile (3

× 1 mL) to give **64** as a white gum (37 mg, contaminated with 4% acetic acid by mass, 82%). ν_{max} (film) 2970 (C–H), 2934 (C–H), 2872 (C–H), 2816 (C–H), 1598 (C=O, amide), 1549 (CO_2K); δ_H (400 MHz, CD_3OD) 1.06–1.12 (6H, m, *CH(C<u>H</u>$_3$)$_2$*), 2.47–2.57 (4H, m, 2 × *piperazinyl C<u>H</u>$_2$*), 2.89–2.99 (1H, m, *C<u>H</u>(CH$_3$)$_2$*), 3.60–3.67 (4H, m, 2 × *piperazinyl C<u>H</u>$_2$*), 3.71 (2H, s, *C<u>H</u>$_2$Py*), 7.71–7.75 (1H, m, *PyC5<u>H</u>*), 7.96 (1H, s, *PyC3<u>H</u>*.), 8.50–8.54 (1H, m, *PyC6<u>H</u>*); δ_C (100 MHz, CD_3OD) 19.9 (*CH(C<u>H</u>$_3$)$_2$*), 31.1 (*C<u>H</u>(CH$_3$)$_2$*), 43.0, 46.7 (2 × *piperazinyl C<u>H</u>$_2$*), 54.2, 54.8 (2 × *piperazinyl C<u>H</u>$_2$*), 64.7 (*C<u>H</u>$_2$Py*), 123.5 (*PyC<u>5</u>H*), 124.6 (*PyC<u>3</u>H*), 148.7 (*PyC<u>4</u>*), 149.9 (*PyC<u>6</u>H*), 159.4 (*PyC<u>2</u>*), 172.7 and 177.9 (*C<u>O</u>$_2$K* and *C<u>O</u>N*); *m/z* (MS, ES$^-$) 290 (100%, $[M–K]^-$); LCMS tR 6.9 min (98%); accurate mass: found 314.1474, calc. for $C_{15}H_{21}N_3NaO_3^+$ 314.1475.

Potassium 2-[(4-benzoylpiperazin-1-yl)methyl]isonicotinate 65

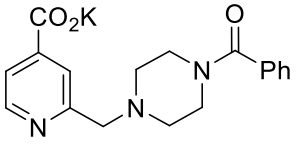

Potassium trimethylsilanolate (52 mg, 0.41 mmol) was added to a solution of ethyl 2 2-[(4-benzoylpiperazin-1-yl)methyl]isonicotinate **60** (63 mg, contaminated with 9% acetic acid w/w, 0.16 mmol) in acetonitrile (5 mL) and the resulting suspension stirred at room temperature for 16 h. The reaction mixture was filtered, the filtrate concentrated *in vacuo* to give a colourless gum that was washed with acetonitrile (3 × 4 mL) and dried under vacuum to give **65** as a white gum (36 mg, contaminated with 5% acetic acid w/w, 58%). ν_{max} (film) 2917 (C–H), 2818 (C–H), 1597 (C=O, amide), 1548 (CO_2K); δ_H (200 MHz, CD_3OD) 2.45–2.74 (4H, m, 2 × *piperazinyl C<u>H</u>$_2$*), 3.46–3.60 (2H, m, *piperazinyl C<u>H</u>$_2$*), 3.77 (2H, s, *C<u>H</u>$_2$Py*), 3.80–3.91 (2H, m, *piperazinyl C<u>H</u>$_2$*), 7.40–7.54 (5H, m, *Ph*), 7.76 (1H, dd, *J* 5.0, 1.5, *PyC5<u>H</u>*), 8.00 (1H, app. s, *PyC3<u>H</u>*), 8.55 (1H, dd, *J* 5.0, 0.5, *PyC6<u>H</u>*); δ_C (125 MHz, CD_3OD) 43.4 (*piperazinyl C<u>H</u>$_2$*), 48.6–49.7 (CD_3OD and *piperazinyl C<u>H</u>$_2$*), 55.0 (2 × *piperazinyl C<u>H</u>$_2$*), 64.6 (*C<u>H</u>$_2$Py*), 123.5 (*PyC<u>5</u>H*), 124.5 (*PyC<u>3</u>H*), 128.2 (2 × *PhC<u>H</u>*), 129.9 (2 × *PhC<u>H</u>*), 131.2 (*PhC<u>H</u>*), 137.0 (*Ph ipso-C*), 148.7 (*PyC<u>4</u>*), 149.9 (*PyC<u>6</u>H*), 159.4 (*PyC<u>2</u>*), 172.6 and 172.8 (*C<u>O</u>$_2$K* and *C<u>O</u>N*); *m/z* (MS, ES$^-$) 324 (100%, $[M–K]^-$); LCMS tR 7.8 min (95%); accurate mass: found 348.1314, calc. for $C_{18}H_{19}N_3NaO_3^+$ 348.1319.

Ethyl 2-[(4-(methylsulfonyl)piperazin-1-yl)methyl]isonicotinate 69

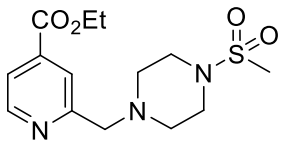

A solution of ethyl 2-formylisonicotinate (45 mg, 0.25 mmol) in dichloromethane (2 mL) was added to 1-(methylsulfonyl)piperazine (62 mg, 0.38 mmol) and the resulting solution stirred at room temperature for 15 min. Sodium triacetoxyborohydride (80 mg, 0.38 mmol) was added and the resulting suspension stirred at room temperature for 16 h. The reaction mixture was purified by flash column chromatography (dichloromethane → 90:10 dichloromethane–methanol) to give **69**

as a colourless oil (74 mg contaminated with 6% acetic acid w/w, 85%). R_f 0.30 (ethyl acetate); ν_{max} (film) 2984 (C–H), 2934 (C–H), 2821 (C–H), 1724 (C=O); δ_H (400 MHz, $CDCl_3$) 1.41 (3H, t, *J* 7.0, *C<u>H</u>₃CH₂O*), 2.62–2.67 (4H, m, 2 × *piperazinyl C<u>H</u>₂*), 2.78 (3H, s, *C<u>H</u>₃SO₂*), 3.25–3.31 (4H, m, 2 × *piperazinyl C<u>H</u>₂*), 3.78 (2H, s, *C<u>H</u>₂Py*), 4.42 (2H, q, *J* 7.0, *CH₃C<u>H</u>₂O*), 7.75 (1H, dd, *J* 5.0, 1.0, *PyC5<u>H</u>*), 7.92 (1H, app. s, *PyC3<u>H</u>*), 8.73 (1H, d, *J* 5.0, *PyC6<u>H</u>*); δ_C (100 MHz, $CDCl_3$) 14.2 (*<u>C</u>H₃CH₂O*), 34.1 (*<u>C</u>H₃SO₂*), 45.6 (2 × *piperazinyl <u>C</u>H₂*), 52.3 (2 × *piperazinyl <u>C</u>H₂*), 61.9 (*CH₃<u>C</u>H₂O*), 63.5 (*<u>C</u>H₂Py*), 121.6 (*Py<u>C</u>5H*), 122.5 (*Py<u>C</u>3H*), 138.4 (*Py<u>C</u>4*), 150.1 (*Py<u>C</u>6H*), 158.7 (*Py<u>C</u>2*), 165.1 (*<u>C</u>O₂Et*); *m/z* (MS, ES^+) 328 (100%, MH^+); LCMS tR 8.2 min (91%); accurate mass: found 328.1316, calc. for $C_{14}H_{22}N_3O_4S^+$ 328.1326.

Ethyl 2-[(4-(ethylsulfonyl)piperazin-1-yl)methyl]isonicotinate 70

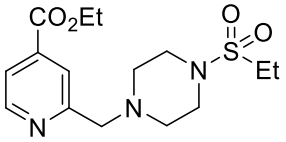

A solution of ethyl 2-formylisonicotinate (45 mg, 0.25 mmol) in dichloromethane (2 mL) was added to 1-(ethylsulfonyl)piperazine (68 mg, 0.38 mmol) and the resulting solution stirred at room temperature for 15 min. Sodium triacetoxyborohydride (80 mg, 0.38 mmol) was added and the resulting suspension stirred at room temperature for 16 h. The reaction mixture was purified by flash column chromatography (dichloromethane → 90:10 dichloromethane–methanol) to give **70** as a colourless oil (86 mg contaminated with 4% acetic acid, 96%). R_f 0.30 (ethyl acetate); ν_{max} (film) 2984 (C–H), 2941 (C–H), 2818 (C–H), 1725 (C=O); δ_H (400 MHz, $CDCl_3$) 1.33–1.44 (6H, m, *C<u>H</u>₃CH₂O* and *C<u>H</u>₃CH₂SO₂*), 2.61 (4H, s, 2 × *piperazinyl C<u>H</u>₂*), 2.95 (2H, q, *J* 7.0, *C<u>H</u>₂SO₂*), 3.35 (4H, s, 2 × *piperazinyl C<u>H</u>₂*), 3.77 (2H, s, *C<u>H</u>₂Py*), 4.42 (2H, q, *J* 7.0, *CH₃C<u>H</u>₂O*), 7.75 (1H, d, *J* 5.0, *PyC5<u>H</u>*), 7.92 (1H, s, *PyC3<u>H</u>*), 8.73 (1H, d, *J* 5.0, *PyC6<u>H</u>*); δ_C (100 MHz, $CDCl_3$) 7.7 (*<u>C</u>H₃CH₂SO₂*), 14.2 (*<u>C</u>H₃CH₂O*), 43.6 (*<u>C</u>H₂SO₂*), 45.6 (2 × *piperazinyl <u>C</u>H₂*), 52.8 (2 × *piperazinyl <u>C</u>H₂*), 61.9 (*CH₃<u>C</u>H₂O*), 63.7 (*<u>C</u>H₂Py*), 121.6 (*Py<u>C</u>5H*), 122.5 (*Py<u>C</u>3H*), 138.4 (*Py<u>C</u>4*), 150.1 (*Py<u>C</u>6H*), 158.8 (*Py<u>C</u>2*), 165.1 (*<u>C</u>O₂Et*); *m/z* (MS, ES^+) 364 (100%, MNa^+); LCMS tR 8.6 min (100%); accurate mass: found 342.1468, calc. for $C_{15}H_{24}N_3O_4S^+$ 342.1482.

Ethyl 2-[(4-(phenylsulfonyl)piperazin-1-yl)methyl]isonicotinate 71

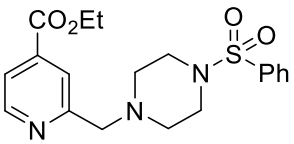

A solution of ethyl 2-formylisonicotinate (45 mg, 0.25 mmol) in dichloromethane (2 mL) was added to 1-(phenylsulfonyl)piperazine (86 mg, 0.38 mmol) and the resulting solution stirred at room temperature for 15 min. Sodium triacetoxyborohydride (80 mg, 0.38 mmol) was added and the resulting suspension stirred at room temperature for 16 h. The reaction mixture was purified by flash column chromatography (dichloromethane → 90:10 dichloromethane–methanol) to give **71**

as a colourless oil (84 mg contaminated with 8% acetic acid w/w, 80%). R_f 0.55 (ethyl acetate); ν_{max} (film) 2983 (C–H), 2853 (C–H), 2819 (C–H), 1724 (C=O); δ_H (400 MHz, $CDCl_3$) 1.39 (3H, t, *J* 7.0, *C<u>H</u>₃CH₂O*), 2.57–2.63 (4H, m, 2 × *piperazinyl C<u>H₂</u>*), 3.03–3.11 (4H, m, 2 × *piperazinyl C<u>H₂</u>*), 3.71 (2H, s, *C<u>H₂</u>Py*), 4.39 (2H, q, *J* 7.0, *CH₃C<u>H₂</u>O*), 7.50–7.63 (3H, m, 3 × *Ph*), 7.70–7.77 (3H, m, *PyC5<u>H</u>* and 2 × *Ph*), 7.82 (1H, s, *PyC3<u>H</u>*), 8.69 (1H, d, *J* 5.0, *PyC6<u>H</u>*); δ_C (100 MHz, $CDCl_3$) 14.1 (*<u>C</u>H₃CH₂O*), 45.8 (2 × *piperazinyl <u>C</u>H₂*), 52.2 (2 × *piperazinyl <u>C</u>H₂*), 61.8 (*CH₃<u>C</u>H₂O*), 63.5 (*<u>C</u>H₂Py*), 121.5 (*Py<u>C</u>5H*), 122.5 (*Py<u>C</u>3H*), 127.8 (2 × *Ph<u>C</u>H*), 129.0 (2 × *Ph<u>C</u>H*), 132.8 (*Ph<u>C</u>H*), 135.3 (*ipso-Ph*), 138.3 (*Py<u>C</u>4*), 150.1 (*Py<u>C</u>6H*), 158.7 (*Py<u>C</u>2*), 165.0 (*<u>C</u>O₂Et*); *m/z* (MS, ES^+) 801 (100%, M_2Na^+); LCMS tR 10.2 min (95%); accurate mass: found 390.1470, calc. for $C_{19}H_{24}N_3O_4S^+$ 390.1482.

Potassium 2-[(4-(methylsulfonyl)piperazin-1-yl)methyl]isonicotinate 72

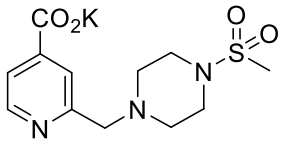

Potassium trimethylsilanolate (36 mg, 0.28 mmol) was added to a solution of ethyl 2-[(4-(methylsulfonyl)piperazin-1-yl]methyl)isonicotinate **69** (47 mg, 94% w/w, 0.13 mmol) in acetonitrile (5 mL) and the resulting suspension stirred at room temperature for 16 h. The resulting precipitate was filtered, washed with acetonitrile (2 × 2 mL) and dried under vacuum to give **72** as a white solid (44 mg, 97%). mp 265–268 °C; ν_{max} (film) 2923 (C–H), 2850 (C–H), 2824 (C–H), 1602 and 1551 (CO_2K); δ_H (400 MHz, CD_3OD) 2.61–2.71 (4H, m, 2 × *piperazinyl C<u>H₂</u>*), 2.87 (3H, s, *C<u>H</u>₃SO₂*), 3.26–3.32 (4H, m, 2 × *piperazinyl C<u>H₂</u>*), 3.76 (2H, s, *C<u>H₂</u>Py*), 7.74 (1H, dd, *J* 5.0, 1.5, *PyC5<u>H</u>*), 7.98 (1H, app. s, *PyC3<u>H</u>*), 8.53 (1H, d, *J* 5.0, *PyC6<u>H</u>*); δ_C (125 MHz, CD_3OD) 34.0 (*<u>C</u>H₃SO₂*), 47.0 (2 × *piperazinyl <u>C</u>H₂*), 53.8 (2 × *piperazinyl <u>C</u>H₂*), 64.5 (*<u>C</u>H₂Py*), 123.5 (*Py<u>C</u>5H*), 124.5 (*Py<u>C</u>3H*), 148.7 (*Py<u>C</u>4*), 149.9 (*Py<u>C</u>6H*), 159.5 (*Py<u>C</u>2*), 172.8 (*<u>C</u>O₂K*); *m/z* (MS, ES^-) 298 (100%, $[M–K]^-$); LCMS tR 6.4 min (95%); accurate mass: found 300.1018, calc. for $C_{12}H_{18}N_3O_4S^+$ 300.1013.

Potassium 2-[(4-(ethylsulfonyl)piperazin-1-yl)methyl]isonicotinate 73

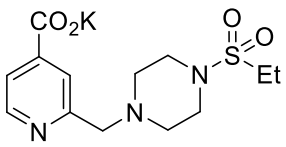

Potassium trimethylsilanolate (43 mg, 0.34 mmol) was added to a solution of ethyl 2-[(4-(ethylsulfonyl)piperazin-1-yl)methyl]isonicotinate **70** (62 mg, 96% w/w, 0.17 mmol) in acetonitrile (5 mL) and the resulting suspension stirred at room temperature for 16 h. The resulting precipitate was filtered, washed with acetonitrile (2 × 2 mL) and dried under vacuum to give **73** as a white solid (62 mg, quant.). mp 232–234 °C; ν_{max} (film) 2922 (C–H), 2825 (C–H), 2807 (C–H), 1601 and 1551 (CO_2K); δ_H (400 MHz, CD_3OD) 1.34 (3H, t, *J* 7.5, *C<u>H</u>₃CH₂*), 2.59–2.63 (4H, m, 2

× *piperazinyl C<u>H</u>₂*), 3.07 (2H, q, *J* 7.5, *CH₃C<u>H</u>₂*), 3.32–3.37 (4H, m, 2 × *piperazinyl C<u>H</u>₂*), 3.75 (2H, s, *C<u>H</u>₂Py*), 7.74 (1H, dd, *J* 5.0, 1.5, *PyC5<u>H</u>*), 7.97 (1H, app. s, *PyC3<u>H</u>*), 8.53 (1H, dd, *J* 5.0, 0.5, *PyC6<u>H</u>*); δ_C (125 MHz, CD_3OD) 8.1 (*<u>C</u>H₃CH₂*), 44.5 (*CH₃<u>C</u>H₂*), 46.9 (2 × *piperazinyl <u>C</u>H₂*), 54.2 (2 × *piperazinyl <u>C</u>H₂*), 64.5 (*<u>C</u>H₂Py*), 123.5 (*Py<u>C</u>5H*), 124.5 (*Py<u>C</u>3H*), 148.7 (*Py<u>C</u>4*), 149.9 (*Py<u>C</u>6H*), 159.4 (*Py<u>C</u>2*), 172.8 (*<u>C</u>O₂K*); *m/z* (MS, ES^-) 312 (100%, $[M–K]^-$); LCMS tR 7.0 min (97%); accurate mass: found 314.1163, calc. for $C_{13}H_{20}N_3O_4S^+$ 314.1169.

Potassium 2-[(4-(phenylsulfonyl)piperazin-1-yl)methyl]isonicotinate 74

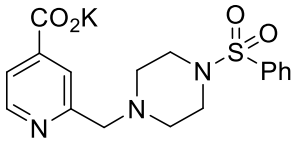

Potassium trimethylsilanolate (43 mg, 0.34 mmol) was added to a solution of ethyl 2-[(4-(phenylsulfonyl)piperazin-1-yl)methyl]isonicotinate **71** (58 mg, 92% w/w, 0.14 mmol) in acetonitrile (5 mL) and the resulting suspension stirred at room temperature for 16 h. The reaction mixture was filtered, washing with acetonitrile (2 × 2 mL) and the filtrate concentrated *in vacuo* to give **74** as a white gum (44 mg, 80%). ν_{max} (film) 2919 (C–H), 2855 (C–H), 2823 (C–H), 1598 and 1549 (CO_2K); δ_H (400 MHz, CD_3OD) 2.57 (4H, s, *piperazinyl C<u>H</u>₂*), 3.04 (4H, s, *piperazinyl C<u>H</u>₂*), 3.67 (2H, s, *C<u>H</u>₂Py*), 7.57–7.81 (6H, m, *PyC5<u>H</u>* and 5 × *Ph*), 7.85 (1H, s, *PyC3<u>H</u>*), 8.47 (1H, d, *J* 5.0, *PyC6<u>H</u>*); δ_C (100 MHz, CD_3OD) 47.5 (2 × *piperazinyl <u>C</u>H₂*), 53.5 (2 × *piperazinyl <u>C</u>H₂*), 64.3 (*<u>C</u>H₂Py*), 123.4 (*Py<u>C</u>5H*), 124.3 (*Py<u>C</u>3H*), 129.1 (2 × *Ph<u>C</u>H*), 130.5 (2 × *Ph<u>C</u>H*), 134.4 (*Ph<u>C</u>H*), 137.0 (*ipso-Ph*), 148.6 (*Py<u>C</u>4*), 149.8 (*Py<u>C</u>6H*), 159.4 (*Py<u>C</u>2*), 172.7 (*<u>C</u>O₂K*); *m/z* (MS, ES^-) 360 (100%, $[M–K]^-$); LCMS tR 8.9 min (95%); accurate mass: found 362.1177, calc. for $C_{17}H_{20}N_3O_4S^+$ 362.1169.

***tert*-Butyl 4-[(4-(ethoxycarbonyl)pyridin-2-yl)methyl]piperazine-1-carboxylate 75**

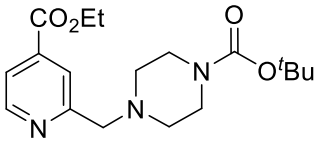

tert-Butyl piperazine-1-carboxylate (1.15 g, 6.20 mmol) was added to a solution of ethyl 2-formylisonicotinate **47** (735 mg, 4.10 mmol) in dichloromethane (20 mL) and the resulting solution stirred at room temperature for 1 h. Glacial acetic acid (3 drops) was added followed by sodium triacetoxyborohydride (1.31 g, 6.20 mmol) and the resulting suspension stirred at room temperature for 16 h. The reaction mixture was diluted with water (20 mL), neutralised with saturated aq sodium bicarbonate and extracted with dichloromethane (2 × 20 mL). The organic layers were washed with brine (20 mL) then combined, dried over magnesium sulfate and concentrated *in vacuo* to give **75** as a colourless oil (1.44 g, quant.). R_f 0.30 (97.5:2.5 dichloromethane–methanol); ν_{max} (film) 2978 (C–H), 2934 (C–H), 2814 (C–H), 1727 (C=O, ester), 1692 (C=O, carbamate); δ_H (400 MHz, $CDCl_3$) 1.35–1.46 (12H, *C<u>H</u>₃CH₂O* and *^{t}Bu*), 2.42–2.48 (4H, m, 2 × *piperazinyl C<u>H</u>₂*), 3.42–3.48

(4H, m, 2 × *piperazinyl* C$\underline{H_2}$), 3.72 (2H, s, C$\underline{H_2}$*Py*), 4.39 (2H, q, *J* 7.0, $CH_3C\underline{H_2}O$), 7.71 (1H, dd, *J* 5.0, 1.5, *PyC5*$\underline{H}$), 7.92 (1H, app. s, *PyC3*$\underline{H}$), 8.69 (1H, d, *J* 5.0, *PyC6*$\underline{H}$); δ_C (125 MHz, $CDCl_3$) 14.1 ($\underline{C}H_3CH_2O$), 28.3 ($C(\underline{C}H_3)_3$), 42.8 and 43.8 (broad, 2 × *piperazinyl* $\underline{C}H_2$), 52.9 (2 × *piperazinyl* $\underline{C}H_2$), 61.8 ($CH_3\underline{C}H_2O$), 64.1 ($\underline{C}H_2Py$), 79.6 ($\underline{C}(CH_3)_3$), 121.4 (*Py*$\underline{C}$*5H*), 122.5 (*Py*$\underline{C}$*3H*), 138.2 (*Py*$\underline{C}$*4*), 150.0 (*Py*$\underline{C}$*6H*), 154.7 ($\underline{C}ON$), 159.1 (*Py*$\underline{C}$*2*), 165.2 ($\underline{C}O_2Et$); *m/z* (MS, ES^+) 350 (100%, MH^+); LCMS tR 9.6 min (90%); accurate mass: found 372.1891, calc. for $C_{18}H_{27}N_3NaO_4^+$ 372.1894.

Lithium 2-[(4-(*tert*-butoxycarbonyl)piperazin-1-yl)methyl]isonicotinate 76

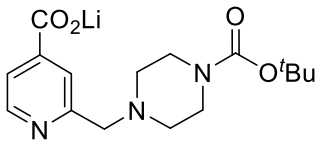

Lithium hydroxide (1 M, aq, 0.20 mL, 0.20 mmol) was added to a solution of *tert*-butyl 4-[(4-(ethoxycarbonyl)pyridin-2-yl)methyl]piperazine-1-carboxylate **75** (70 mg, 0.20 mmol) in acetonitrile (1.0 mL) and water (0.8 mL) and the resulting solution stirred at room temperature for 16 h. The reaction mixture was concentrated *in vacuo* and the residue washed with cyclohexane (3 × 1 mL) to give **76** as a yellow solid (68 mg, quant.). mp 151–154 °C; ν_{max} (film) 2976 (C–H), 2932 (C–H), 1671 (C=O, carbamate), 1601 and 1551 (CO_2Li); δ_H (400 MHz, CD_3OD) 1.46 (9H, s, ^tBu), 2.45–2.52 (4H, m, 2 × *piperazinyl* C$\underline{H_2}$), 3.44–3.51 (4H, m, 2 × *piperazinyl* C$\underline{H_2}$), 3.71 (2H, s, C$\underline{H_2}$*Py*), 7.74 (1H, d, *J* 5.0, *PyC5*$\underline{H}$), 7.97 (1H, s, *PyC3*$\underline{H}$), 8.52 (1H, d, *J* 5.0, *PyC6*$\underline{H}$); δ_C (100 MHz, CD_3OD) 28.8 ($C(\underline{C}H_3)_3$), 44.3 and 45.3 (broad, 2 × *piperazinyl* $\underline{C}H_2$), 54.2 (2 × *piperazinyl* $\underline{C}H_2$), 64.9 ($\underline{C}H_2Py$), 81.3 ($\underline{C}(CH_3)_3$), 123.5 (*Py*$\underline{C}$*5H*), 124.6 (*Py*$\underline{C}$*3H*), 148.5 (*Py*$\underline{C}$*4*), 149.8 (*Py*$\underline{C}$*6H*), 156.5 ($\underline{C}ON$), 159.4 (*Py*$\underline{C}$*2*), 172.6 ($\underline{C}O_2Li$); *m/z* (MS, ES^+) 322 (100%, MH^+); LCMS tR 8.6 min (94%); accurate mass: found 344.1577, calc. for $C_{16}H_{23}N_3NaO_4^+$ 344.1581.

2-(Piperazin-1-ylmethyl)isonicotinic acid bis(trifluoroacetate) monohydrate 77

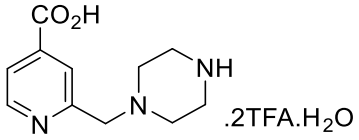

A solution of lithium 2-[(4-(*tert*-butoxycarbonyl)piperazin-1-yl)methyl]isonicotinate **76** (61 mg, 0.19 mmol) in trifluoroacetic acid (1.0 mL) was stirred at room temperature for 16 h. The reaction mixture was concentrated *in vacuo* and the residue purified by strong cation exchange chromatography, washing with methanol and eluting with methanolic ammonia (5% v/v solution of conc. ammonia in methanol) to give an off-white solid that was taken up in acetonitrile (1 mL). Trifluoroacetic acid (35 µL, 0.46 mmol) was added, the resulting suspension filtered and the filtrate concentrated *in vacuo* to give **77** as a beige gum (43 mg, 48%). ν_{max} (film) 2852 (C–H), 2518 ([N–H]$^+$), 1666 (CO_2H); δ_H (400 MHz, CD_3OD) 3.11–3.22 (4H, m, 2 × *piperazinyl* C$\underline{H_2}$), 3.39–3.48 (4H, m, 2 × *piperazinyl* C$\underline{H_2}$), 4.22 (2H, s, C$\underline{H_2}$*Py*), 7.98 (1H, d, *J* 5.0, *PyC5*$\underline{H}$), 8.13 (1H, s,

PyC3H), 8.79 (1H, d, *J* 5.0, *PyC6H*); δ_C (100 MHz, CD_3OD) 43.8 (2 × *piperazinyl* *C*H_2), 50.7 (2 × *piperazinyl* *C*H_2), 62.2 (*C*H_2*Py*), 124.7 (*PyC5H*), 125.3 (*PyC3H*), 142.7 (*PyC4*), 150.3 (*PyC6H*), 156.4 (*PyC2*), 167.1 (*C*O_2*H*); *m/z* (MS, ES^+) 222 (100%, MH^+); LCMS tR 1.9 min (99%); accurate mass: found 222.1232, calc. for $C_{11}H_{16}N_3O_2^+$ 222.1237; elemental analysis: $C_{15}H_{19}F_6N_3O_7$ requires C, 38.55; H, 4.1; N, 9.0%; found C, 38.4; H, 3.9; N, 9.1%.

2-{[4-(Benzylsulfonyl)piperazin-1-yl]methyl}isonicotinic acid trifluoroacetate 78

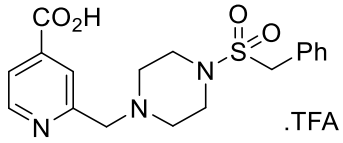

Triethylamine (32 µL, 0.23 mmol) was added to a suspension of ethyl 2-(piperazin-1-ylmethyl)isonicotinate **79** (37 mg, 0.15 mmol) and phenylmethanesulfonyl chloride (43 mg, 0.23 mmol) in acetonitrile (1 mL) and the resulting solution stirred at room temperature for 6 h. The reaction mixture was diluted with water (0.5 mL) and lithium hydroxide added (1 M, aq, 3.0 mL, 3.0 mmol). The resulting solution was stirred at room temperature for 3 h. The reaction mixture was acidified to pH 1 with trifluoroacetic acid then concentrated *in vacuo* and purified by reverse phase chromatography (C18 column, eluting with 0.1% trifluoroacetic acid in water → 0.1% trifluoroacetic acid in acetonitrile) to give **78** as an off-white solid (39 mg, 53%). mp 250–254 °C; ν_{max} (film) 2450 (br, OH), 1661 (CO_2H); δ_H (400 MHz, CD_3OD) 3.29–3.36 (4H, m, 2 × *piperazinyl* *C*H_2), 3.43–3.50 (4H, m, 2 × *piperazinyl* *C*H_2), 4.46 (2H, s), 4.55 (2H, s), 7.39–7.44 (3H, m, 3 × *Ph*), 7.45–7.52 (2H, m, 2 × *Ph*), 7.95 (1H, d, *J* 5.0, *PyC5H*), 8.01 (1H, s, *PyC3H*), 8.83 (1H, d, *J* 5.0, *PyC6H*); δ_C (100 MHz, CD_3OD) 44.2 (2 × *piperazinyl* *C*H_2), 53.7 (2 × *piperazinyl* *C*H_2), 58.0 (*C*H_2*Ph*), 61.2 (*C*H_2*Py*), 124.9 (*PyC5H*), 125.1 (*PyC3H*), 130.0 (2 × *PhCH*), 130.1 (1 × *PhCH*), 130.3 (*ipso-Ph*), 132.2 (2 × *PhCH*), 141.6 (*PyC4*), 152.1 (*PyC6H*), 152.2 (*PyC2*), 167.2 (*C*O_2*H*); *m/z* (MS, ES^+) 376 (100%, MH^+); LCMS tR 9.1 min (99%); accurate mass: found 398.1140, calc. for $C_{18}H_{21}N_3NaO_4S^+$ 398.1145.

Ethyl 2-(piperazin-1-ylmethyl)isonicotinate 79

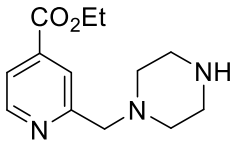

Trifluoroacetic acid (1.75 mL, 22.90 mmol) was added to a solution of *tert*-butyl 4-[(4-(ethoxycarbonyl)pyridin-2-yl]methyl)piperazine-1-carboxylate **75** (1.00 g, 2.86 mmol) in dichloromethane (10 mL) and the resulting solution stirred at room temperature for 60 h. The reaction mixture was concentrated *in vacuo*, azeotroping with ethyl acetate (3 × 10 mL) to give a brown oil that was purified by strong cation exchange chromatography, washing with ethanol and eluting with ethanolic ammonia (5% conc. ammonia in ethanol) to give **79** as a brown oil (740 mg, 90%). ν_{max} (film) 3302 (N–H), 2940 (C–H), 2819 (C–H), 1725 (C=O); δ_H (400 MHz, $CHCl_3$) 1.41

(3H, t, *J* 7.0, *$CH_2C\underline{H}_3$*), 2.42–2.55 (4H, m, 2 × *piperazinyl $C\underline{H}_2$*), 2.88–2.95 (4H, m, 2 × *piperazinyl $C\underline{H}_2$*), 3.70 (2H, s, *$C\underline{H}_2Py$*), 4.40 (2H, q, *J* 7.0, *$C\underline{H}_2CH_3$*), 7.71 (1H, d, *J* 5.0, *PyC5H*), 7.93 (1H, s, *PyC3H*), 8.69 (1H, d, *J* 5.0, *PyC6H*); δ_C (100 MHz, $CHCl_3$) 14.2 (*$CH_2\underline{C}H_3$*), 45.8 (2 × *piperazinyl $\underline{C}H_2$*), 54.5 (2 × *piperazinyl $\underline{C}H_2$*), 61.7 (*$\underline{C}H_2Py$*), 64.9 (*$\underline{C}H_2CH_3$*), 121.2 (*Py$\underline{C}5H$*), 122.5 (*Py$\underline{C}3H$*), 138.1 (*Py$\underline{C}4$*), 150.0 (*Py$\underline{C}6H$*), 159.7 (*Py$\underline{C}2$*), 165.3 (*$\underline{C}O_2Et$*); *m/z* (MS, ES^+) 250 (100%, MH^+); LCMS tR 7.4 min (91%); accurate mass: found 250.1553, calc. for $C_{13}H_{20}N_3O_2^+$ 250.1550.

2-({4-[(2-Fluorophenyl)sulfonyl]piperazin-1-yl}methyl)isonicotinic acid trifluoroacetate 80

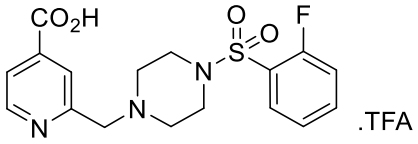

Triethylamine (21 µL, 0.15 mmol) was added to a suspension of ethyl 2-(piperazin-1-ylmethyl)isonicotinate **79** (25 mg, 0.10 mmol) and 2-fluorobenzenesulfonyl chloride (20 µL, 0.15 mmol) in acetonitrile (1 mL) and the resulting solution stirred at room temperature for 16 h. Lithium hydroxide was added (1 M, aq, 1.0 mL, 1.0 mmol) and the resulting solution stirred at room temperature for 3 h. The reaction mixture was acidified to pH 1 with trifluoroacetic acid then concentrated *in vacuo* and purified by reverse phase chromatography (C18 column, eluting with 0.1% trifluoroacetic acid in water → 0.1% trifluoroacetic acid in 3:2 acetonitrile–water) to give **80** as an off-white solid (46 mg, 93%). mp 153–157 °C; ν_{max} (film) 2447 (br, OH), 1657 (CO_2H); δ_H (400 MHz, CD_3OD) 3.39–3.46 (4H, m, 2 × *piperazinyl $C\underline{H}_2$*), 3.46–3.54 (4H, m, 2 × *piperazinyl $C\underline{H}_2$*), 4.53 (2H, s, *$C\underline{H}_2Py$*), 7.32–7.43 (2H, m, *PhC3H* and *PhC4H*), 7.68–7.76 (1H, m, *PhC6H*), 7.81–7.87 (1H, m, *PhC5H*), 7.89 (1H, d, *J* 5.0, *PyC5H*), 7.96 (1H, s, *PyC3H*), 8.76 (1H, d, *J* 5.0, *PyC6H*); δ_C (125 MHz, CD_3OD) 44.6 (2 × *piperazinyl $\underline{C}H_2$*), 53.3 (2 × *piperazinyl $\underline{C}H_2$*), 61.5 (*$\underline{C}H_2Py$*), 118.7 (d, *J* 22.0, *Ph$\underline{C}3H$*), 124.5 (*Py$\underline{C}5H$*), 124.8 (*Py$\underline{C}3H$*), 125.8 (d, *J* 14.5, *Ph$\underline{C}1$*), 126.2 (d, *J* 4.0, *Ph$\underline{C}6H$*), 132.4 (s, *Ph$\underline{C}5H$*), 137.5 (d, *J* 8.5, *Ph$\underline{C}4H$*), 141.7 (*Py$\underline{C}4$*), 151.7 (*Py$\underline{C}6H$*), 153.6 (*Py$\underline{C}2$*), 160.4 (d, *J* 255.0, *Ph$\underline{C}2$*), 167.2 (*$\underline{C}O_2H$*); δ_F (500 MHz, CD_3OD) –109.4 (*Ar$\underline{F}$*), –76.8 (*$\underline{F}_3CO_2$*); *m/z* (MS, ES^+) 380 (100%, MH^+); LCMS tR 9.1 min (100%); accurate mass: found 380.1061, calc. for $C_{17}H_{19}FN_3O_4S^+$ 380.1075.

2-({4-[(3-Fluorophenyl)sulfonyl]piperazin-1-yl}methyl)isonicotinic acid trifluoroacetate 81

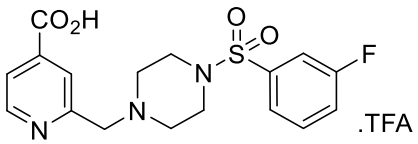

Triethylamine (21 µL, 0.15 mmol) was added to a suspension of ethyl 2-(piperazin-1-ylmethyl)isonicotinate **79** (25 mg, 0.10 mmol) and 3-fluorobenzenesulfonyl chloride (20 µL, 0.15 mmol) in acetonitrile (1 mL) and the resulting solution stirred at room temperature for 16 h. Lithium hydroxide (1 M, aq, 1.0 mL, 1.0 mmol) was added and the resulting solution stirred at room temperature for 3 h. The reaction mixture was acidified to pH 1 with trifluoroacetic acid then

concentrated *in vacuo* and purified by reverse phase chromatography (C18 column, eluting with 0.1% trifluoroacetic acid in water → 0.1% trifluoroacetic acid in 3:2 acetonitrile–water) to give **81** as beige solid (47 mg, 95%). mp 208–211 °C; ν_{max} (film) 2616 (br, OH), 2518 (br, OH), 1708 (CO_2H); δ_H (400 MHz, CD_3OD) 3.33–3.41 (4H, m, 2 × *piperazinyl C<u>H</u>₂*), 3.41–3.50 (4H, m, 2 × *piperazinyl C<u>H</u>₂*), 4.54 (2H, s, *PyC<u>H</u>₂*), 7.48–7.55 (1H, m, 1 × *Ph*), 7.58–7.64 (1H, m, 1 × *Ph*), 7.64–7.75 (2H, m, 2 × *Ph*), 7.93 (1H, d, *J* 5.0, *PyC5<u>H</u>*), 7.99 (1H, s, *PyC3<u>H</u>*), 8.78 (1H, d, *J* 5.0, *PyC6<u>H</u>*); δ_C (125 MHz, CD_3OD) 45.0 (2 × *piperazinyl <u>C</u>H₂*), 53.1 (2 × *piperazinyl <u>C</u>H₂*), 61.5 (*<u>C</u>H₂Py*), 116.2 (d, *J* 25.0, *Ph<u>C</u>2H*), 122.0 (d, *J* 21.0, *Ph<u>C</u>4H*), 124.7 (*Py<u>C</u>5H*), 124.9 (*Py<u>C</u>3H*), 125.2 (d, *J* 4.0, *Ph<u>C</u>6H*), 133.1 (d, *J* 7.5, *Ph<u>C</u>5H*), 138.9 (d, *J* 6.5, *Ph<u>C</u>1*), 141.7 (*Py<u>C</u>4*), 151.8 (*Py<u>C</u>6H*), 153.5 (*Py<u>C</u>2*), 164.2 (d, *J* 251.0, *Ph<u>C</u>3H*), 167.3 (*<u>C</u>O₂*); δ_F (500 MHz, CD_3OD) –111.3 (*Ar<u>F</u>*), –76.8 (*<u>F</u>₃CO₂*); *m/z* (MS, ES^+) 380 (100%, MH^+); LCMS tR 9.5 min (100%); accurate mass: found 380.1062, calc. for $C_{17}H_{19}FN_3O_4S^+$ 380.1075.

2-({4-[(4-Fluorophenyl)sulfonyl]piperazin-1-yl}methyl)isonicotinic acid trifluoroacetate 82

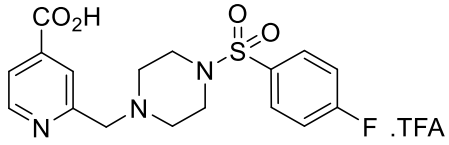

Triethylamine (21 µL, 0.15 mmol) was added to a suspension of ethyl 2-(piperazin-1-ylmethyl)isonicotinate **79** (25 mg, 0.10 mmol) and 4-fluorobenzenesulfonyl chloride (29 mg, 0.15 mmol) in acetonitrile (1 mL) and the resulting solution stirred at room temperature for 16 h. Lithium hydroxide (1 M, aq, 1.0 mL, 1.0 mmol) was added and the resulting solution stirred at room temperature for 3 h. The reaction mixture was acidified to pH 1 with trifluoroacetic acid then concentrated *in vacuo* and purified by reverse phase chromatography (C18 column, eluting with 0.1% trifluoroacetic acid in water → 0.1% trifluoroacetic acid in 3:2 acetonitrile–water) to give **82** as an off-white solid (45 mg, 91%). mp 256–261 °C; ν_{max} (film) 2384 (br, OH), 1678 (CO_2H); δ_H (400 MHz, CD_3OD) 3.28–3.41 (4H, m, 2 × *piperazinyl C<u>H</u>₂*), 3.43–3.53 (4H, m, 2 × *piperazinyl C<u>H</u>₂*), 4.55 (2H, s, *C<u>H</u>₂Py*), 7.36–7.46 (2H, m, 2 × *Ph [ortho to F]*), 7.86–7.96 (3H, m, *PyC5<u>H</u>* and 2 × *Ph [meta to F]*), 8.00 (1H, s, *PyC3<u>H</u>*), 8.78 (1H, d, *J* 5.0, *PyC6<u>H</u>*); δ_C (100 MHz, CD_3OD) 44.7 (2 × *piperazinyl <u>C</u>H₂*), 53.0 (2 × *piperazinyl <u>C</u>H₂*), 61.2 (*<u>C</u>H₂Py*), 117.9 (d, *J* 23.0, 2 × *Ph [ortho to F]*), 124.8 (*Py<u>C</u>3H*), 125.0 (*Py<u>C</u>5H*), 132.2 (d, *J* 9.5, 2 × *Ph [meta to F]*), 132.7 (d, *J* 2.5, 1 × *Ph [para to F]*), 141.7 (*Py<u>C</u>4*), 151.9 (*Py<u>C</u>6H*), 152.6 (*Py<u>C</u>2*), 167.2 (*<u>C</u>O₂H*), 167.3 (d, *J* 255.0, 1 × *Ph [ipso to F]*); δ_F (500 MHz, CD_3OD) –106.4 (*Ar<u>F</u>*), –76.9 (*<u>F</u>₃CO₂*); *m/z* (MS, ES^+) 380 (100%, MH^+); LCMS tR 9.3 min (98%); accurate mass: found 380.1065, calc. for $C_{17}H_{19}FN_3O_4S^+$ 380.1075.

2-({4-[(2-Chlorophenyl)sulfonyl]piperazin-1-yl}methyl)isonicotinic acid trifluoroacetate 83

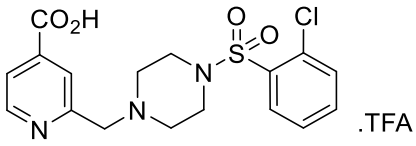

Triethylamine (21 μL, 0.15 mmol) was added to a suspension of ethyl 2-(piperazin-1-ylmethyl)isonicotinate **79** (25 mg, 0.10 mmol) and 2-chlorobenzenesulfonyl chloride (32 mg, 0.15 mmol) in acetonitrile (1 mL) and the resulting solution stirred at room temperature for 16 h. Lithium hydroxide (1 M, aq, 1.0 mL, 1.0 mmol) was added and the resulting solution stirred at room temperature for 3 h. The reaction mixture was acidified to pH 1 with trifluoroacetic acid then concentrated *in vacuo* and purified by reverse phase chromatography (C18 column, eluting with 0.1% trifluoroacetic acid in water → 0.1% trifluoroacetic acid in 3:2 acetonitrile–water) to give **83** as an off-white solid (48 mg, 94%). mp 124–127 °C; ν_{max} (film) 2441 (br, OH), 1691 (CO_2H); δ_H (400 MHz, CD_3OD) 3.39–3.45 (4H, m, 2 × *piperazinyl* C<u>H</u>$_2$), 3.62–3.68 (4H, m, 2 × *piperazinyl* C<u>H</u>$_2$), 4.57 (2H, s, C<u>H</u>$_2$*Py*), 7.52–7.58 (1H, m, *PhC5H*), 7.64–7.70 (2H, m, *PhC3H* and *PhC4H*), 7.95 (1H, dd, *J* 5.0, 1.5, *PyC5H*), 8.02 (1H, app. s, *PyC3H*), 8.08–8.11 (1H, m, *PhC6H*), 8.82 (1H, d, *J* 5.0, *PyC6H*); δ_C (100 MHz, CD_3OD) 44.2 (2 × *piperazinyl* C<u>H</u>$_2$), 53.6 (2 × *piperazinyl* C<u>H</u>$_2$), 61.4 (C<u>H</u>$_2$*Py*), 124.8 (*PyC5H*), 125.0 (*PyC3H*), 128.9 (*PhC5H*), 133.4 (*PhC6H*), 133.5 (*PhC2*), 133.8 (*PhC3H*), 136.1 (*PhC4H*), 136.8 (*PhC1*), 141.7 (*PyC4*), 152.0 (*PyC6H*), 152.9 (*PyC2*), 167.3 (C<u>O</u>$_2$*H*); *m/z* (MS, ES^+) 396 (100%, MH^+); LCMS tR 9.4 min (98%); accurate mass: found 396.0771, calc. for $C_{17}H_{19}ClN_3O_4S^+$ 396.0779.

2-({4-[(3-Chlorophenyl)sulfonyl]piperazin-1-yl}methyl)isonicotinic acid trifluoroacetate 84

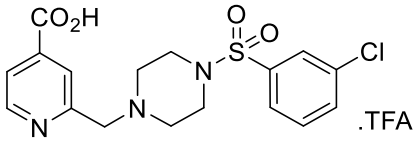

Triethylamine (21 μL, 0.15 mmol) was added to a suspension of ethyl 2-(piperazin-1-ylmethyl)isonicotinate **79** (25 mg, 0.10 mmol) and 3-chlorobenzenesulfonyl chloride (21 μL, 0.15 mmol) in acetonitrile (1 mL) and the resulting solution stirred at room temperature for 16 h. Lithium hydroxide (1 M, aq, 1.0 mL, 1.0 mmol) was added and the resulting solution stirred at room temperature for 3 h. The reaction mixture was acidified to pH 1 with trifluoroacetic acid then concentrated *in vacuo* and purified by reverse phase chromatography (C18 column, eluting with 0.1% trifluoroacetic acid in water → 0.1% trifluoroacetic acid in 3:2 acetonitrile–water) to **84** as a beige solid (48 mg, 94%). mp 208–216 °C; ν_{max} (film) 2612 (br, OH), 2520 (br, OH), 1632 (CO_2H); δ_H (400 MHz, CD_3OD) 3.36–3.44 (4H, m, 2 × *piperazinyl* C<u>H</u>$_2$), 3.47–3.55 (4H, m, 2 × *piperazinyl* C<u>H</u>$_2$), 4.59 (2H, s, C<u>H</u>$_2$*Py*), 7.62–7.71 (1H, m, *PhC5H*), 7.73–7.79 (2H, m, *PhC4H* and *PhC6H*), 7.83–7.87 (1H, m, *PhC2H*), 7.93 (1H, dd, *J* 5.0, 1.5, *PyC5H*), 7.99 (1H, app. s, *PyC3H*), 8.78 (1H, d, *J* 5.0, *PyC6H*); δ_C (100 MHz, CD_3OD) 44.6 (2 × *piperazinyl* C<u>H</u>$_2$), 53.0 (2 × *piperazinyl* C<u>H</u>$_2$), 61.0 (C<u>H</u>$_2$*Py*), 124.9 (*PyC5H*), 124.9 (*PyC3H*), 127.5 (*PhC6H*), 128.8 (*PhC2H*), 132.6 (*PhC5H*),

135.1 (*PhC4H*), 136.9 (*PhC3*), 138.5 (*PhC1*), 141.6 (*PyC4*), 152.0 (*PyC6H*), 152.3 (*PyC2*), 167.1 (*CO₂H*); *m/z* (MS, ES^+) 396 (100%, MH^+); LCMS tR 10.0 min (95%); accurate mass: found 396.0775, calc. for $C_{17}H_{19}ClN_3O_4S^+$ 396.0779.

2-({4-[(4-Chlorophenyl)sulfonyl]piperazin-1-yl}methyl)isonicotinic acid trifluoroacetate 85

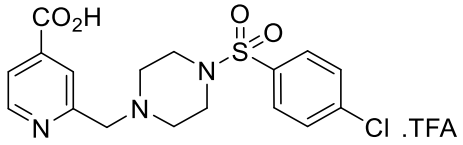

Triethylamine (21 µL, 0.15 mmol) was added to a suspension of ethyl 2-(piperazin-1-ylmethyl)isonicotinate **79** (25 mg, 0.10 mmol) and 4-chlorobenzenesulfonyl chloride (32 mg, 0.15 mmol) in acetonitrile (1 mL) and the resulting solution stirred at room temperature for 16 h. Lithium hydroxide (1 M, aq, 1.0 mL, 1.0 mmol) was added and the resulting solution stirred at room temperature for 3 h. The reaction mixture was acidified to pH 1 with trifluoroacetic acid then concentrated *in vacuo* and purified by reverse phase chromatography (C18 column, eluting with 0.1% trifluoroacetic acid in water → 0.1% trifluoroacetic acid in 3:2 acetonitrile–water) to give **85** as an off-white solid (51 mg, quant.). mp 227–230 °C; ν_{max} (film) 2435 (br, OH), 1678 (CO_2H); δ_H (400 MHz, CD_3OD) 3.33–3.39 (4H, m, 2 × *piperazinyl CH₂*), 3.44–3.49 (4H, m, 2 × *piperazinyl CH₂*), 4.55 (2H, s, *CH₂Py*), 7.68 (2H, d, *J* 8.5, 2 × *PhCH*), 7.82 (2H, d, *J* 8.5, 2 × *PhCH*), 7.93 (1H, dd, *J* 5.0, 1.0, *PyC5H*), 8.00 (1H, app. s, *PyC3H*), 8.78 (1H, d, *J* 5.0, *PyC6H*); δ_C (100 MHz, CD_3OD) 44.7 (2 × *piperazinyl CH₂*), 53.0 (2 × *piperazinyl CH₂*), 61.2 (*CH₂Py*), 124.8 (*PyC5H*), 125.0 (*PyC3H*), 130.8 (2 × *PhCH*), 131.1 (2 × *PhCH*), 135.3 (*PhC1*), 141.4 and 141.7 (*PyC4* and *PhC4*), 152.0 (*PyC6H*), 152.6 (*PyC2*), 167.2 (*CO₂H*); *m/z* (MS, ES^+) 396 (100%, MH^+); LCMS tR 9.9 min (95%); accurate mass: found 396.0772, calc. for $C_{17}H_{19}ClN_3O_4S^+$ 396.0779.

2-({4-[(4-Methylphenyl)sulfonyl]piperazin-1-yl}methyl)isonicotinic acid trifluoroacetate 86

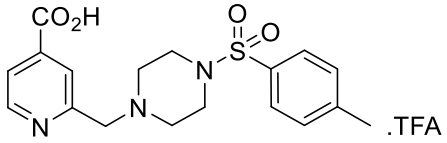

Triethylamine (21 µL, 0.15 mmol) was added to a suspension of ethyl 2-(piperazin-1-ylmethyl)isonicotinate **79** (25 mg, 0.10 mmol) and 4-tosyl chloride (29 mg, 0.15 mmol) in acetonitrile (1 mL) and the resulting solution stirred at room temperature for 16 h. Lithium hydroxide (1 M, aq, 1.0 mL, 1.0 mmol) was added and the resulting solution stirred at room temperature for 3 h. The reaction mixture was acidified to pH 1 with trifluoroacetic acid then concentrated *in vacuo* and purified by reverse phase chromatography (C18 column, eluting with 0.1% trifluoroacetic acid in water → 0.1% trifluoroacetic acid in 3:2 acetonitrile–water) to give **86** as an off-white solid (39 mg, 80%). mp 270–275 °C; ν_{max} (film) 2448 (br, OH), 1672 (CO_2H); δ_H (400 MHz, CD_3OD) 2.46 (3H, s, *Me*), 3.28–3.40 (4H, m, 2 × *piperazinyl CH₂*), 3.45–3.54 (4H, m, 2 × *piperazinyl CH₂*), 4.58 (2H, s, *CH₂Py*), 7.47 (2H, d, *J* 8.0, *PhC3H* and *PhC5H*), 7.71 (2H, d, *J*

8.0, *PhC2H* and *PhC6H*), 7.93 (1H, dd, *J* 5.0, 1.5, *PyC5H*), 7.99 (1H, app. s, *PyC3H*), 8.79 (1H, d, *J* 5.0, *PyC6H*); δ_C (100 MHz, CD_3OD) 21.7 (*Me*), 44.6 (2 × *piperazinyl* $\underline{C}H_2$), 53.1 (2 × *piperazinyl* $\underline{C}H_2$), 61.0 ($\underline{C}H_2Py$), 124.9 (*PyC5H*), 125.0 (*PyC3H*), 129.2 (*PhC2H* and *PhC6H*), 131.4 (*PhC3H* and *PhC5H*), 133.4 (*PhC1*), 141.6 and 146.4 (*PhC4* and *PyC4*), 152.0 (*PyC6H*), 152.2 (*PyC2*), 167.1 ($\underline{C}O_2H$); *m/z* (MS, ES^+) 376 (100%, MH^+); LCMS tR 9.5 min (96%); accurate mass: found 376.1312, calc. for $C_{18}H_{22}N_3O_4S^+$ 376.1326.

2-{[4-(1-Naphthylsulfonyl)piperazin-1-yl]methyl}isonicotinic acid trifluoroacetate 87

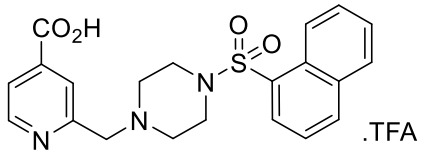

Triethylamine (21 µL, 0.15 mmol) was added to a suspension of ethyl 2-(piperazin-1-ylmethyl)isonicotinate **79** (25 mg, 0.10 mmol) and 1-naphthalenesulfonyl chloride (34 mg, 0.15 mmol) in acetonitrile (1 mL) and the resulting solution stirred at room temperature for 16 h. Lithium hydroxide (1 M, aq, 1.0 mL, 1.0 mmol) was added and the resulting solution stirred at room temperature for 3 h. The reaction mixture was acidified to pH 1 with trifluoroacetic acid then concentrated *in vacuo* and purified by reverse phase chromatography (C18 column, eluting with 0.1% trifluoroacetic acid in water → 0.1% trifluoroacetic acid in 3:2 acetonitrile–water) to give **87** as an off-white solid (35 mg, 67%). mp 168–171 °C; ν_{max} (film) 2410 (br, OH), 1671 (CO_2H); δ_H (400 MHz, CD_3OD) 3.34–3.42 (4H, m, 2 × *piperazinyl* $C\underline{H}_2$), 3.45–3.59 (4H, m, 2 × *piperazinyl* $C\underline{H}_2$), 4.51 (2H, s, *PyC*$\underline{H}_2$), 7.41–7.74 (3H, m, 3 × *Np*), 7.90 (1H, d, *J* 4.5, *PyC5H*), 7.94 (1H, s, *PyC3H*), 8.02–8.07 (1H, m, 1 × *Np*), 8.22–8.27 (2H, m, 2 × *Np*), 8.67–8.72 (1H, m, 1 × *Np*), 8.74 (1H, d, *J* 4.5, *PyC6H*); δ_C (100 MHz, CD_3OD) 44.1 (2 × *piperazinyl* $\underline{C}H_2$), 53.2 (2 × *piperazinyl* $\underline{C}H_2$), 61.1 ($\underline{C}H_2Py$), 124.8 (*PyC5H*), 124.9 (*PyC3H*), 125.6 (1 × *NpCH*), 125.9 (1 × *NpCH*), 128.4 (1 × *NpCH*), 129.7 (1 × *NpCH*), 130.1 (1 × *NpCC*), 130.5 (1 × *NpCH*), 132.4 (1 × *NpCH*), 133.0 (1 × *NpCC*), 136.1 ($SO_2\underline{C}$), 136.7 (1 × *NpCH*), 140.9 (*PyC4*), 151.9 (*PyC6H*), 152.5 (*PyC2*), 167.2 ($\underline{C}O_2H$); *m/z* (MS, ES^+) 412 (100%, MH^+); LCMS tR 10.2 min (62%); accurate mass: found 412.1315, calc. for $C_{21}H_{22}N_3O_4S^+$ 412.1326.

2-{[4-(2-Naphthylsulfonyl)piperazin-1-yl]methyl}isonicotinic acid trifluoroacetate 88

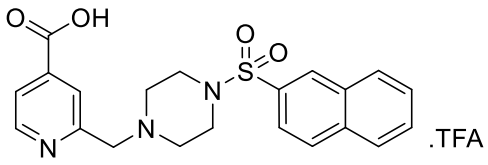

Triethylamine (21 µL, 0.15 mmol) was added to a suspension of ethyl 2-(piperazin-1-ylmethyl)isonicotinate **79** (25 mg, 0.10 mmol) and 2-naphthalenesulfonyl chloride (34 mg, 0.15 mmol) in acetonitrile (1 mL) and the resulting solution stirred at room temperature for 16 h. Lithium hydroxide (1 M, aq, 1.0 mL, 1.0 mmol) was added and the resulting solution stirred at room temperature for 3 h. The reaction mixture was acidified to pH 1 with trifluoroacetic acid then

concentrated *in vacuo* and purified by reverse phase chromatography (C18 column, eluting with 0.1% trifluoroacetic acid in water → 0.1% trifluoroacetic acid in 3:2 acetonitrile–water) to give **88** as a white solid (34 mg, 65%). mp 158–163 °C; ν_{max} (film) 2840 (br, OH), 1656 (CO_2H); δ_H (400 MHz, CD_3OD) 3.43 (8H, br. s, 4 × *piperazinyl* C<u>H</u>$_2$), 4.51 (2H, s, *C*<u>*H*</u>$_2$*Py*), 7.64–7.76 (2H, m, 2 × *Np*), 7.80 (1H, d, *J* 9.0, 1 × *Np*), 7.88 (1H, d, *J* 4.5, *PyC5*<u>*H*</u>), 7.97 (1H, s, *SO*$_2$*CC*<u>*H*</u>), 8.02 (1H, d, *J* 8.0, 1 × *Np*), 8.07–8.15 (2H, m, 2 × *Np*), 8.44 (1H, s, *PyC3*<u>*H*</u>), 8.72 (1H, d, *J* 4.5, *PyC6*<u>*H*</u>); δ_C (100 MHz, CD_3OD) 45.0 (2 × *piperazinyl* <u>*C*</u>*H*$_2$), 53.1 (2 × *piperazinyl* <u>*C*</u>*H*$_2$), 61.3 (<u>*C*</u>*H*$_2$*Py*), 123.9 (1 × *Np*<u>*C*</u>*H*), 124.7 (*Py*<u>*C*</u>*5H*), 125.0 (1 × *Np*<u>*C*</u>*H*), 129.2 (1 × *Np*<u>*C*</u>*H*), 129.3 (1 × *Np*<u>*C*</u>*H*), 130.6 (1 × *Np*<u>*C*</u>*H*), 130.6 (*Py*<u>*C*</u>*3H*), 130.7 (1 × *Np*<u>*C*</u>*H*), 131.0 (1 × *Np*<u>*C*</u>*H*), 133.8 and 133.8 (2 × *Np*<u>*C*</u>*C*), 136.8 (*SO*$_2$<u>*C*</u>), 141.7 (*Py*<u>*C*</u>*4*), 151.8 (*Py*<u>*C*</u>*6H*), 153.0 (*Py*<u>*C*</u>*2*), 167.4 (<u>*C*</u>*O*$_2$*H*); *m/z* (MS, ES^+) 412 (100%, MH^+); LCMS tR 10.4 min (92%); accurate mass: found 412.1314, calc. for $C_{21}H_{22}N_3O_4S^+$ 412.1326.

2-({4-[(2-Phenylethyl)sulfonyl]piperazin-1-yl}methyl)isonicotinic acid trifluoroacetate 89

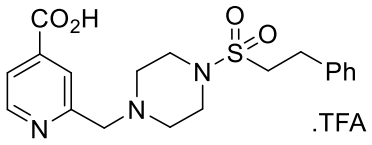

Triethylamine (21 μL, 0.15 mmol) was added to a suspension of ethyl 2-(piperazin-1-ylmethyl)isonicotinate **79** (25 mg, 0.10 mmol) and 2-phenylethanesulfonyl chloride (31 mg, 0.15 mmol) in acetonitrile (1 mL) and the resulting solution stirred at room temperature for 16 h. Lithium hydroxide (1 M, aq, 1.0 mL, 1.0 mmol) was added and the resulting solution stirred at room temperature for 3 h. The reaction mixture was acidified to pH 1 with trifluoroacetic acid then concentrated *in vacuo* and purified by reverse phase chromatography (C18 column, eluting with 0.1% trifluoroacetic acid in water → 0.1% trifluoroacetic acid in 3:2 acetonitrile–water) to give **89** as a brown oil (56 mg, quant.). ν_{max} (film) 2586 (br, OH), 1667 (CO_2H); δ_H (400 MHz, CD_3OD) 2.99–3.13 (2H, m, *SO*$_2$*CH*$_2$*C*<u>*H*</u>$_2$), 3.35–3.48 (6H, m, 2 × *piperazinyl* C<u>*H*</u>$_2$ and *SO*$_2$*C*<u>*H*</u>$_2$*CH*$_2$), 3.50–3.74 (4H, m, 2 × *piperazinyl* C<u>*H*</u>$_2$), 4.59 (2H, s, *PyC*<u>*H*</u>$_2$), 7.12–7.37 (5H, m, *Ph*), 7.94 (1H, d, *J* 4.5, *PyC5*<u>*H*</u>), 8.03 (1H, s, *PyC3*<u>*H*</u>), 8.83 (1H, d, *J* 4.5, *PyC6*<u>*H*</u>); δ_C (125 MHz, CD_3OD) 30.5 (*SO*$_2$*CH*$_2$<u>*C*</u>*H*$_2$), 43.8 (2 × *piperazinyl* <u>*C*</u>*H*$_2$), 52.6 (*SO*$_2$<u>*C*</u>*H*$_2$*CH*$_2$), 53.5 (2 × *piperazinyl* <u>*C*</u>*H*$_2$), 61.3 (<u>*C*</u>*H*$_2$*Py*), 124.9 (*Py*<u>*C*</u>*5H*), 125.1 (*Py*<u>*C*</u>*3H*), 128.0 (1 × *Ph*), 129.5 (*ipso-Ph*), 129.7 (2 × *Ph*), 129.9 (2 × *Ph*), 139.6 (*Py*<u>*C*</u>*4*), 152.0 (*Py*<u>*C*</u>*6H*), 152.6 (*Py*<u>*C*</u>*2*), 167.2 (<u>*C*</u>*O*$_2$*H*); *m/z* (MS, ES^+) 390 (100%, MH^+); LCMS tR 9.8 min (100%); accurate mass: found 390.1477, calc. for $C_{19}H_{24}N_3O_4S^+$ 390.1482.

Ethyl 2-[(dimethylamino)methyl]isonicotinate 91

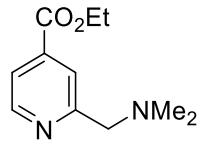

Dimethylamine (0.15 mL of a 2 M solution in tetrahydrofuran, 0.30 mmol) was added to a solution of ethyl 2-formylisonicotinate **47** (36 mg, 0.20 mmol) in dichloromethane (1.5 mL) and the resulting solution stirred at room temperature for 15 min. Sodium triacetoxyborohydride (64 mg, 0.30 mmol) was added and the resulting suspension stirred at room temperature for 16 h. The reaction mixture was purified by flash column chromatography (ethyl acetate → 95:5 dichloromethane–methanol) to give **91** as a yellow oil (35 mg, 84%). R_f 0.40 (95:5 dichloromethane–methanol); ν_{max} (film) 2979 (C–H), 2942 (C–H), 2821 (C–H), 2773 (C–H), 1726 (C=O); δ_H (400 MHz, $CDCl_3$) 1.42 (3H, t, *J* 7.0, *CH₂CH₃*), 2.32 (6H, s, *NMe₂*), 3.68 (2H, *CH₂Py*), 4.42 (2H, q, *J* 7.0, *CH₂CH₃*), 7.74 (1H, dd, *J* 5.0, 1.5, *PyC5H*), 7.94 (1H, app. s, *PyC3H*), 8.71 (1H, d, *J* 5.0, *PyC6H*); δ_C (100 MHz, $CDCl_3$) 14.2 (*CH₂CH₃*), 45.5 (*N(CH₃)₂*), 61.7 (*CH₂CH₃*), 65.4 (*CH₂Py*), 121.3 (*PyC5H*), 122.4 (*PyC3H*), 138.3 (*PyC4*), 150.0 (*PyC6H*), 160.1 (*PyC2*), 165.3 (*CO₂Et*); *m/z* (MS, ES^+) 209 (100%, MH^+); LCMS tR 7.6 min (89%); accurate mass: found 209.1281, calc. for $C_{11}H_{17}N_2O_2^+$ 209.1285**.**

Ethyl 2-[(*tert*-butylamino)methyl]isonicotinate 92

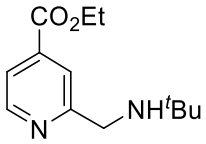

A solution of ethyl 2-formylisonicotinate **47** (45 mg, 0.25 mmol) in dichloromethane (2 mL) was added to *tert*-butylamine (39 µL, 0.38 mmol). Glacial acetic acid (1 drop) was added and the resulting suspension stirred at room temperature for 15 min. Sodium triacetoxyborohydride (80 mg, 0.38 mmol) was added and the resulting suspension stirred at room temperature for 16 h. The reaction mixture was diluted with water (5 mL), extracted with dichloromethane (2 × 5 mL), the organic layers combined, concentrated *in vacuo* and purified by flash column chromatography (98:2 dichloromethane–methanol → 88:12 dichloromethane–methanol) to give **92** as a yellow oil (41 mg, 69%). R_f 0.30 (95:5 dichloromethane–methanol); ν_{max} (film) 2965 (C–H), 2907 (C–H), 2871 (C–H), 1726 (C=O); δ_H (400 MHz, $CDCl_3$) 1.22 (9H, s, *^tBu*), 1.40 (3H, t, *J* 7.0, *CH₃CH₂O*), 4.00 (2H, s, *CH₂Py*), 4.28 (1H, s, *NH*), 4.40 (2H, q, *J* 7.0, *CH₃CH₂O*), 7.71 (1H, d, *J* 5.0, *PyC5H*), 7.88 (1H, s, *PyC3H*), 8.67 (1H, d, *J* 5.0, *PyC6H*); δ_C (100 MHz, $CDCl_3$) 14.2 (*CH₃CH₂O*), 28.7 (*C(CH₃)₃*), 47.8 (*CH₂Py*), 51.2 (*C(CH₃)₃*), 61.7 (*CH₃CH₂O*), 121.1 (*PyC5H*), 121.7 (*PyC3H*), 138.2 (*PyC4*), 149.7 (*PyC6H*), 160.7 (*PyC2*), 165.1 (*CO₂Et*); *m/z* (MS, ES^+) 237 (100%, MH^+); LCMS tR 7.9 min (96%); accurate mass: found 237.1602, calc. for $C_{13}H_{21}N_2O_2^+$ 237.1598.

Ethyl 2-[(benzylamino)methyl]isonicotinate 93

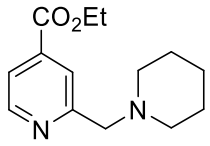

A solution of ethyl 2-formylisonicotinate **47** (45 mg, 0.25 mmol) in dichloromethane (2 mL) was added to piperidine (38 μL, 0.38 mmol). Glacial acetic acid (1 drop) was added and the resulting suspension stirred at room temperature for 15 min. Sodium triacetoxyborohydride (80 mg, 0.38 mmol) was added and the resulting suspension stirred at room temperature for 16 h. The reaction mixture was diluted with water (5 mL), extracted with dichloromethane (2 × 5 mL), the organic layers combined, concentrated *in vacuo* and purified by flash column chromatography (98:2 dichloromethane–methanol → 89:11 dichloromethane–methanol) to give **93** as a colourless oil (47 mg, 76%). R_f 0.45 (95:5 dichloromethane–methanol); ν_{max} (film) 2935 (C–H), 2854 (C–H), 2800 (C–H), 1727 (C=O); δ_H (400 MHz, $CDCl_3$) 1.38–1.48 (5H, m, *C<u>H</u>₃CH₂O* and *PipC4<u>H</u>₂*), 1.56–1.64 (4H, m, *PipC3<u>H</u>₂* and *PipC5<u>H</u>₂*), 2.41–2.48 (4H, m, *PipC2<u>H</u>₂* and *PipC6<u>H</u>₂*), 3.67 (2H, s, *C<u>H</u>₂Py*), 4.40 (2H, q, *J* 7.0, *CH₃C<u>H</u>₂O*), 7.69 (1H, dd, *J* 5.0, 1.5, *PyC5<u>H</u>*), 7.94 (1H, app. s, *PyC3<u>H</u>*), 8.69 (1H, d, *J* 5.0, *PyC6<u>H</u>*); δ_C (100 MHz, $CDCl_3$) 14.2 (*<u>C</u>H₃CH₂O*), 24.1 (*Pip<u>C</u>4H₂*), 25.8 (*Pip<u>C</u>3H₂* and *Pip<u>C</u>5H₂*), 54.7 (*Pip<u>C</u>2H₂* and *Pip<u>C</u>6H₂*), 61.7 (*CH₃<u>C</u>H₂O*), 65.1 (*<u>C</u>H₂Py*), 121.0 (*Py<u>C</u>5H*), 122.4 (*Py<u>C</u>3H*), 138.0 (*Py<u>C</u>4*), 149.8 (*Py<u>C</u>6H*), 160.3 (*Py<u>C</u>2*), 165.4 (*<u>C</u>O₂Et*); *m/z* (MS, ES^+) 271 (100%, MH^+); LCMS tR 7.9 min (100%); accurate mass: found 249.1605, calc. for $C_{14}H_{21}N_2O_2^+$ 249.1598.

Ethyl 2-[(phenylamino)methyl]isonicotinate 94

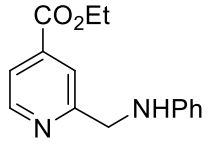

A solution of ethyl 2-formylisonicotinate **47** (45 mg, 0.25 mmol) in dichloromethane (2 mL) was added to aniline (35 μL, 0.38 mmol). Glacial acetic acid (1 drop) was added and the resulting suspension stirred at room temperature for 15 min. Sodium triacetoxyborohydride (80 mg, 0.38 mmol) was added and the resulting suspension stirred at room temperature for 16 h. The reaction mixture was diluted with water (5 mL), extracted with dichloromethane (2 × 5 mL), the organic layers combined, concentrated *in vacuo* and purified by flash column chromatography (dichloromethane → 94:6 dichloromethane–methanol) to give **94** as a yellow oil (64 mg, quant.). R_f 0.70 (95:5 dichloromethane–methanol); ν_{max} (film) 2982 (C–H), 2936 (C–H), 2905 (C–H), 1724 (C=O); δ_H (400 MHz, $CDCl_3$) 1.41 (3H, t, *J* 7.0, *C<u>H</u>₃CH₂O*), 4.41 (2H, q, *J* 7.0, *CH₃C<u>H</u>₂O*), 4.54 (2H, s, *C<u>H</u>₂Py*), 6.67–6.77 (3H, m, *PhC2<u>H</u>*, *PhC4<u>H</u>* and *PhC6<u>H</u>*), 7.16–7.22 (2H, m, *PhC3<u>H</u>* and *PhC5<u>H</u>*), 7.75 (1H, dd, *J* 5.0, 1.5, *PyC5<u>H</u>*), 7.92 (1H, app. s, *PyC3<u>H</u>*), 8.74 (1H, d, *J* 5.0, *PyC6<u>H</u>*) δ_C (100 MHz, $CDCl_3$) 14.1 (*<u>C</u>H₃CH₂O*), 49.3 (*<u>C</u>H₂Py*), 61.8 (*CH₃<u>C</u>H₂O*), 113.1 (*Ph<u>C</u>2H* and *Ph<u>C</u>6H*), 117.8 (*Ph<u>C</u>4H*), 120.9 (*Py<u>C</u>3H*), 121.3 (*Py<u>C</u>5H*), 129.2 (*Ph<u>C</u>3H* and *Ph<u>C</u>5H*), 138.4

(*PyC4*), 147.6 (*ipso-Ph*), 149.9 (*PyC6H*), 159.8 (*PyC2*), 165.1 (*CO₂Et*); *m/z* (MS, ES⁺) 257 (100%, MH⁺); LCMS tR 14.5 min (99%); accurate mass: found 279.1104, calc. for $C_{15}H_{16}N_2NaO_2^+$ 279.1104.

Ethyl 2-{[methyl(phenyl)amino]methyl}isonicotinate 95

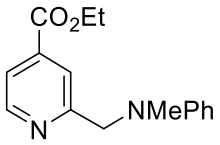

A solution of ethyl 2-formylisonicotinate **47** (45 mg, 0.25 mmol) in dichloromethane (2 mL) was added to *N*-methylaniline (43 µL, 0.38 mmol). Glacial acetic acid (1 drop) was added and the resulting suspension stirred at room temperature for 15 min. Sodium triacetoxyborohydride (80 mg, 0.38 mmol) was added and the resulting suspension stirred at room temperature for 16 h. The reaction mixture was diluted with water (5 mL), extracted with dichloromethane (2 × 5 mL), the organic layers combined, concentrated *in vacuo* and purified by flash column chromatography (dichloromethane → 94:6 dichloromethane–methanol) to give **95** as a yellow oil (17 mg, 25%). R_f 0.80 (95:5 dichloromethane–methanol); ν_{max} (film) 2982 (C–H), 2935 (C–H), 2904 (C–H), 1725 (C=O); δ_H (400 MHz, $CDCl_3$) 1.39 (3H, t, *J* 7.0, *CH₃CH₂O*), 3.16 (3H, s, *CH₃N*), 4.40 (2H, q, *J* 7.0, *CH₃CH₂O*), 4.72 (2H, s, *CH₂Py*), 6.74–6.80 (3H, m, *Ph*), 7.22–7.30 (2H, m, *Ph*), 7.75 (1H, d, *J* 5.0, *PyC5H*), 7.79 (1H, s, *PyC3H*), 8.76 (1H, d, *J* 5.0, *PyC6H*); δ_C (100 MHz, $CDCl_3$) 14.1 (*CH₃CH₂O*), 39.3 (*CH₃N*), 59.1 (*CH₂Py*), 61.7 (*CH₃CH₂O*), 112.5 (2 × *Ph*), 117.1 (1 × *Ph*), 120.1 (*PyC3H*), 121.2 (*PyC5H*), 129.2 (2 × *Ph*), 138.6 (*PyC4*), 149.3 (*ipso-Ph*), 150.2 (*PyC6H*), 161.0 (*PyC2*), 165.2 (*CO₂Et*); *m/z* (MS, ES⁺) 271 (100%, MH⁺); LCMS tR 15.5 min (99%); accurate mass: found 293.1260, calc. for $C_{16}H_{18}N_2NaO_2^+$ 293.1260.

Ethyl 2-[(benzylamino)methyl]isonicotinate 96

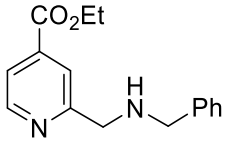

A solution of ethyl 2-formylisonicotinate **47** (45 mg, 0.25 mmol) in dichloromethane (2 mL) was added to benzylamine (42 µL, 0.38 mmol). Glacial acetic acid (1 drop) was added and the resulting suspension stirred at room temperature for 15 min. Sodium triacetoxyborohydride (80 mg, 0.38 mmol) was added and the resulting suspension stirred at room temperature for 16 h. The reaction mixture was diluted with water (5 mL), extracted with dichloromethane (2 × 5 mL), the organic layers combined, concentrated *in vacuo* and purified by flash column chromatography (dichloromethane → 92:8 dichloromethane–methanol) to give **96** as a yellow oil (63 mg, 93%). R_f 0.40 (95:5 dichloromethane–methanol); ν_{max} (film) 3027 (C–H), 2982 (C–H), 2906 (C–H), 1725 (C=O); δ_H (400 MHz, $CDCl_3$) 1.43 (3H, t, *J* 7.0, *CH₃CH₂O*), 2.47 (1H, s, *NH*), 3.88 (2H, s, *CH₂Ph*), 4.02 (2H, s, *CH₂Py*), 4.42 (2H, q, *J* 7.0, *CH₃CH₂O*), 7.24–7.41 (5H, m, *Ph*), 7.74 (1H, d, *J* 5.0,

PyC5H), 7.90 (1H, s, *PyC3H*), 8.72 (1H, d, *J* 5.0, *PyC6H*); δ_C (100 MHz, $CDCl_3$) 14.2 (*C*H_3*C*H_2*O*), 53.4 (*C*H_2*Ph*), 54.2 (*C*H_2*Py*), 61.7 (*CH*$_3$*C*H_2*O*), 121.1 (*PyC5H*), 121.5 (*PyC3H*), 127.0 (1 × *PhCH*), 128.2 (2 × *PhCH*), 128.4 (2 × *PhCH*), 138.1, 139.7 (*ipso-Ph* and *PyC4*), 150.0 (*PyC6H*), 160.8 (*PyC2*), 165.2 (*CO*$_2$*Et*); *m/z* (MS, ES^+) 271 (100%, MH^+); LCMS tR 9.2 min (97%); accurate mass: found 271.1443, calc. for $C_{16}H_{19}N_2O_2^+$ 271.1441.

Ethyl 2-[(4-(methylcarbamoyl)piperidin-1-yl)methyl]isonicotinate 97

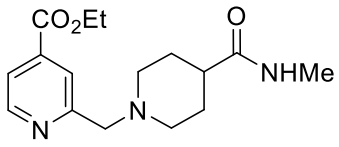

A solution of ethyl 2-formylisonicotinate **47** (45 mg, 0.25 mmol) in dichloromethane (2 mL) was added to piperidine-4-carboxylic acid methylamide (54 mg, 0.38 mmol). Glacial acetic acid (1 drop) was added and the resulting suspension stirred at room temperature for 15 min. Sodium triacetoxyborohydride (80 mg, 0.38 mmol) was added and the resulting suspension stirred at room temperature for 16 h. The reaction mixture was diluted with water (5 mL), extracted with dichloromethane (2 × 5 mL), the organic layers combined, concentrated *in vacuo* and purified by flash column chromatography (96:4 dichloromethane–methanol → 90:10 dichloromethane–methanol) to give **97** as a white solid (22mg, 29%). R_f 0.25 (95:5 dichloromethane–methanol); mp 170–172 °C; ν_{max} (film) 3295 (N–H), 2935 (C–H), 2807 (C–H), 2763 (C–H), 1727 (C=O, ester), 1640 (C=O, amide); δ_H (400 MHz, $CDCl_3$) 1.40 (3H, t, *J* 7.0, *C*H_3*C*H_2*O*), 1.77–1.85 (4H, m, 2 × *PipC*H_2), 2.04–2.16 (3H, m, *CHCO* and *PipC*H_2), 2.79 (3H, d, *J* 5.0, *C*H_3*N*), 2.91–2.97 (2H, m, *PipC*H_2), 3.70 (2H, s, *C*H_2*Py*), 4.41 (2H, q, *J* 7.0, *CH*$_3$*C*H_2*O*), 5.70 (1H, br. s, *NH*), 7.71 (1H, dd, *J* 5.0, 1.5, *PyC5H*), 7.94 (1H, app. s, *PyC3H*), 8.68 (1H, d, *J* 5.0, *PyC6H*); δ_C (100 MHz, $CDCl_3$) 14.2 (*C*H_3*C*H_2*O*), 26.2 (*C*H_3*N*), 28.8 (2 × *PipC*H_2), 43.1 (*CHCO*), 53.3 (2 × *PipC*H_2), 61.7 (*CH*$_3$*C*H_2*O*), 64.4 (*C*H_2*Py*), 121.2 (*PyC5H*), 122.3 (*PyC3H*), 138.2 (*PyC4*), 149.8 (*PyC6H*), 159.9 (*PyC2*), 165.3 (*CO*$_2$*Et*), 175.5 (*NC*=*O*); *m/z* (MS, ES^+) 306 (100%, MH^+); LCMS tR 7.7 min (99%); accurate mass: found 306.1808, calc. for $C_{16}H_{24}N_3O_3^+$ 306.1812.

Ethyl 2-[(4-benzylpiperidin-1-yl)methyl]isonicotinate 98

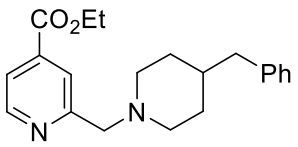

A solution of ethyl 2-formylisonicotinate **47** (45 mg, 0.25 mmol) in dichloromethane (2 mL) was added to 4-benzylpiperidine (67 µL, 0.38 mmol). Glacial acetic acid (1 drop) was added and the resulting suspension stirred at room temperature for 15 min. Sodium triacetoxyborohydride (80 mg, 0.38 mmol) was added and the resulting suspension stirred at room temperature for 16 h. The reaction mixture was diluted with water (5 mL), extracted with dichloromethane (2 × 5 mL), the organic layers combined, concentrated *in vacuo* and purified by flash column chromatography

(97:3 dichloromethane–methanol → 92:8 dichloromethane–methanol) to give **98** as a yellow oil (37 mg, 44%). R_f 0.30 (95:5 dichloromethane–methanol); ν_{max} (film) 2920 (C–H), 2848 (C–H), 2803 (C–H), 1727 (C=O); δ_H (400 MHz, $CDCl_3$) 1.31–1.46 (5H, m, *C<u>H</u>₃CH₂O* and 2 × *Pip*), 1.48–1.68 (3H, m, *C<u>H</u>CH₂Ph* and 2 × *Pip*), 2.00–2.09 (2H, m, 2 × *Pip*), 2.54 (2H, d, *J* 7.0, *C<u>H</u>₂Ph*), 2.88 (2H, app. d, *J* 11.5, 2 × *Pip*), 3.70 (2H, s, *C<u>H</u>₂Py*), 4.42 (2H, q, *J* 7.0, *CH₃C<u>H</u>₂O*), 7.08–7.22 (3H, m, 3 × *Ph*), 7.24–7.30 (2H, m, 2 × *Ph*), 7.71 (1H, dd, *J* 5.0, 1.5, *PyC5<u>H</u>*), 7.95 (1H, app. s, *PyC3<u>H</u>*), 8.70 (1H, d, *J* 5.0, *PyC6<u>H</u>*); δ_C (100 MHz, $CDCl_3$) 14.2 (*<u>C</u>H₃CH₂O*), 32.0 (2 × *Pip <u>C</u>H₂*), 37.7 (*<u>C</u>HCH₂Ph*), 43.1 (*<u>C</u>H₂Ph*), 54.0 (2 × *Pip <u>C</u>H₂*), 61.7 (*CH₃<u>C</u>H₂O*), 64.6 (*<u>C</u>H₂Py*), 121.1 (*Py<u>C</u>5H*), 122.4 (*Py<u>C</u>3H*), 125.7 (*Ph*), 128.1 (2 × *Ph*), 129.1 (2 × *Ph*), 138.1 and 140.6 (*ipso-Ph* and *Py<u>C</u>4*), 149.9 (*Py<u>C</u>6H*), 160.2 (*Py<u>C</u>2*), 165.4 (*<u>C</u>O₂Et*); *m/z* (MS, ES^+) 339 (100%, MH^+); LCMS tR 10.8 min (90%); accurate mass: found 339.2070, calc. for $C_{21}H_{27}N_2O_2^+$ 339.2067.

Ethyl 2-[(dibenzylamino)methyl]isonicotinate 99

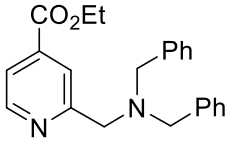

A solution of ethyl 2-formylisonicotinate **47** (45 mg, 0.25 mmol) in dichloromethane (2 mL) was added to dibenzylamine (73.1 µL, 0.38 mmol). Glacial acetic acid (1 drop) was added and the resulting suspension stirred at room temperature for 15 min. Sodium triacetoxyborohydride (80 mg, 0.38 mmol) was added and the resulting suspension stirred at room temperature for 16 h. The reaction mixture was diluted with water (5 mL), extracted with dichloromethane (2 × 5 mL), the organic layers combined, concentrated *in vacuo* and purified by flash column chromatography (dichloromethane–methanol → 94:6 dichloromethane–methanol) to give the title compound as a white gum (79 mg, 88% yield). R_f 0.85 (95:5 dichloromethane–methanol); ν_{max} (film) 3028 (C–H), 2982 (C–H), 2926 (C–H), 2800 (C–H), 1727 (C=O); δ_H (400 MHz, $CDCl_3$) 1.48 (3H, t, *J* 7.0, *C<u>H</u>₃CH₂O*), 3.68 (4H, s, 2 × *C<u>H</u>₂Ph*), 3.86 (2H, s, *C<u>H</u>₂Py*), 4.46 (2H, q, *J* 7.0, *CH₃C<u>H</u>₂O*), 7.24–7.30 (2H, m, *Ph*), 7.33–7.39 (4H, m, *Ph*), 7.44–7.49 (4H, m, *Ph*), 7.72 (1H, d, *J* 5.0, *PyC5<u>H</u>*), 8.21 (1H, s, *PyC3<u>H</u>*), 8.68 (1H, d, *J* 5.0, *PyC6<u>H</u>*); δ_C (100 MHz, $CDCl_3$) 14.2 (*<u>C</u>H₃CH₂O*), 58.3 (2 × *<u>C</u>H₂Ph*), 59.4 (*<u>C</u>H₂Py*), 61.6 (*CH₃<u>C</u>H₂O*), 121.0 (*Py<u>C</u>5H*), 122.0 (*Py<u>C</u>3H*), 127.0 (2 × *Ph<u>C</u>H*), 128.3 (4 × *Ph<u>C</u>H*), 128.8 (4 × *Ph<u>C</u>H*), 138.1, 138.9 (2 × *ipso Ph* and *Py<u>C</u>4*), 149.5 (*Py<u>C</u>6H*), 161.4 (*Py<u>C</u>2*), 165.3 (*<u>C</u>O₂Et*); *m/z* (MS, ES^+) 361 (100%, MH^+); LCMS tR 11.8 min (90%); accurate mass: found 361.1904, calc. for $C_{23}H_{25}N_2O_2^+$ 361.1911.

Potassium 2-[(dimethylamino)methyl]isonicotinate 101

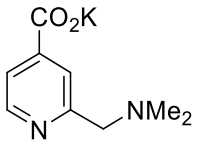

Potassium trimethylsilanolate (25 mg, 0.19 mmol) was added to a solution of ethyl 2-[(dimethylamino)methyl]isonicotinate **91** (26 mg, 0.13 mmol) in acetonitrile (4 mL) and the resulting suspension stirred at room temperature for 16 h. The resulting precipitate was filtered, washed with acetonitrile (2 × 2 mL) and dried under vacuum to give **101** as a brown gum (23 mg, 86%). R_f 0.10 (70:30:1 dichloromethane–methanol–acetic acid); ν_{max} (film) 2974 (C–H), 2948 (C–H), 2827 (C–H), 2777 (C–H), 1602 and 1546 (CO_2K); δ_H (400 MHz, CD_3OD) 2.28 (6H, s, *NMe*$_2$), 3.64 (2H, s, *C*$\underline{H}_2$*Py*), 7.73 (1H, dd, *J* 5.0, 1.5, *PyC5*$\underline{H}$), 7.90 (1H, app. s, *PyC3*$\underline{H}$), 8.52 (1H, d, *J* 5.0, *PyC6*$\underline{H}$); δ_C (125 MHz, CD_3OD) 45.7 (*N*(*C*$\underline{H}_3$)$_2$), 65.9 (*C*$\underline{H}_2$*Py*), 123.5 (*PyC*$\underline{5}$*H*), 124.9 (*PyC*$\underline{3}$*H*), 148.6 (*PyC4*), 149.9 (*PyC*$\underline{6}$*H*), 159.3 (*PyC2*), 172.7 (*C*$\underline{O}_2$*K*); *m/z* (MS, ES^-) 179 (100%, $[M–K]^-$); LCMS tR 2.0 min (93%); accurate mass: found 181.0967, calc. for $C_9H_{13}N_2O_2^+$ 181.0972.

Lithium 2-[(*tert*-butylamino)methyl]isonicotinate 102

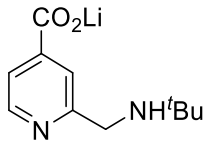

Lithium hydroxide (1 M, aq, 0.13 mL, 0.13 mmol) was added to a solution of ethyl 2-[(*tert*-butylamino)methyl]isonicotinate **92** (30 mg, 0.13 mmol) in tetrahydrofuran (0.6 mL) and water (0.5 mL) and the resulting suspension stirred at room temperature for 16 h. Acetonitrile (2 mL) was added, the volatiles evaporated, the residue washed with dichloromethane (3 × 1 mL) then dried under vacuum to give **102** as a white solid (24 mg, 89%). mp 220–242 °C (dec); ν_{max} (film) 2970 (C–H), 1581 and 1544 (CO_2Li); δ_H (400 MHz, CD_3OD) 1.27 (9H, s, *t Bu*), 4.03 (2H, s, *C*$\underline{H}_2$*Py*), 7.72 (1H, d, *J* 4.5, *PyC5*$\underline{H}$), 7.85 (1H, s, *PyC3*$\underline{H}$), 8.56 (1H, d, *J* 4.5, *PyC6*$\underline{H}$); δ_C (125 MHz, CD_3OD) 28.0 (*C*(*C*$\underline{H}_3$)$_3$), 48.1 (*C*$\underline{H}_2$*Py*), 53.6 (*C*$\underline{(}$*CH*$_3$)$_3$), 123.4 (*PyC*$\underline{5}$*H*), 123.6 (*PyC*$\underline{3}$*H*), 148.5 (*PyC4*), 150.1 (*PyC*$\underline{6}$*H*), 158.9 (*PyC2*), 172.4 (*C*$\underline{O}_2$*Li*); *m/z* (MS, ES^-) 207 (100%, $[M–Li]^-$); LCMS tR 6.7 min (76%); accurate mass: found 231.1107, calc. for $C_{11}H_{16}N_2NaO_2^+$ 231.1104.

2-(Piperidin-1-ylmethyl)isonicotinic acid trifluoroacetate 103

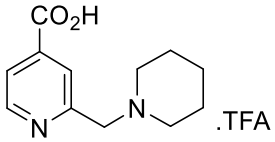

Lithium hydroxide (1 M, aq, 0.16 mL, 0.16 mmol) was added to a solution of ethyl 2-(piperidin-1-ylmethyl)isonicotinate **93** (40 mg, 0.16 mmol) in tetrahydrofuran (0.6 mL) and water (0.5 mL) and the resulting suspension stirred at room temperature for 16 h. Acetonitrile (2 mL) was added, the volatiles evaporated, the residue washed with dichloromethane (3 × 1 mL) then dried under vacuum

and purified by reverse phase HPLC (0.1% trifluoroacetic acid in water → 0.1% trifluoroacetic acid in acetonitrile) to give **103** as a white gum (19 mg, 36%). ν_{max} (film) 2937 (C–H), 2857 (C–H), 2821 (C–H), 1599 (CO_2H); δ_H (400 MHz, CD_3OD) 1.46–2.01(6H, m, *PipC3H*$_2$, *PipC4H*$_2$ and *PipC5H*$_2$), 2.98–3.16 and 3.45–3.62 (2H, m and 2H, m, *PipC2H*$_2$ and *PipC6H*$_2$), 4.47–4.56 (2 H, m, *CH*$_2$*Py*), 7.89–7.97 and 7.98–8.04 (1H, m and 1H, m, *PyC5H* and *PyC3H*), 8.78–8.89 (1H, m, *PyC6H*); δ_C (100 MHz, CD_3OD) 22.8 (*PipC4H*$_2$), 24.1 (*PipC3H*$_2$ and *PipC5H*$_2$), 55.0 (*PipC2H*$_2$ and *PipC6H*$_2$), 61.4 (*CH*$_2$*Py*), 124.8 and 125.0 (*PyC5H* and *PyC3H*), 141.5 (*PyC4*), 152.2 and 152.6 (*PyC2* and *PyC6H*), 167.2 (*CO*$_2$*H*); *m/z* (MS, ES^-) 219 (100%, $[M–H]^-$); LCMS tR 6.8 min (99%); accurate mass: found 243.1104, calc. for $C_{12}H_{16}N_2NaO_2^+$ 243.1104.

Lithium 2-[(phenylamino)methyl]isonicotinate 104

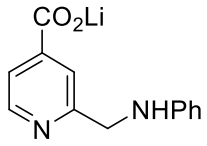

Lithium hydroxide (1 M, aq, 0.14 mL, 0.14 mmol) was added to a solution of ethyl 2-[(phenylamino)methyl]isonicotinate **94** (30 mg, 0.14 mmol) in tetrahydrofuran (0.6 mL) and water (0.5 mL) and the resulting suspension stirred at room temperature for 16 h. Acetonitrile (2 mL) was added, the volatiles evaporated, the residue washed with dichloromethane (3 × 1 mL) then dried *in vacuo* to give **104** as an orange gum (27 mg, 82%). ν_{max} (film) 2961 (C–H), 1601 and 1550 (CO_2Li); δ_H (400 MHz, CD_3OD) 4.46 (2H, s, *CH*$_2$*Py*), 6.56–6.62 (3H, m, *Ph*), 7.02–7.09 (2H, m, *Ph*), 7.69 (1H, d, *J* 5.0, *PyC5H*), 7.92 (1H, s, *PyC3H*), 8.51 (1H, d, *J* 5.0, *PyC6H*); δ_C (100 MHz, CD_3OD) 50.2 (*CH*$_2$*Py*), 114.1 (*PhC2H* and *PhC6H*), 118.2 (*PhC4H*), 122.5 (*PyC3H*), 123.1 (*PyC5H*), 130.1 (*PhC3H* and *PhC5H*), 148.7 (*PyC4*), 149.8 (*PyC6H* and *ipso-Ph*), 161.8 (*PyC2*), 172.9 (*CO*$_2$*Li*); *m/z* (MS, ES^-) 227 (100%, $[M–Li]^-$); LCMS tR 10.0 min (97%); accurate mass: found 251.0792, calc. for $C_{13}H_{12}N_2NaO_2^+$ 251.0791.

Lithium 2-{[methyl(phenyl)amino]methyl}isonicotinate 105

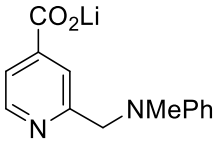

Lithium hydroxide (1 M, aq, 0.06 mL, 0.06 mmol) was added to a solution of ethyl 2-{[methyl(phenyl)amino]methyl}isonicotinate **95** (17 mg, 0.06 mmol) in tetrahydrofuran (0.6 mL) and water (0.5 mL). The resulting suspension was stirred at room temperature for 16 h and then heated to 40 °C for 3 h. Acetonitrile (2 mL) was added, the volatiles evaporated, the residue washed with dichloromethane (3 × 1 mL) then dried *in vacuo* to give **105** as a yellow gum (10 mg, 64%). ν_{max} (film) 1596 and 1548 (CO_2Li); δ_H (400 MHz, CD_3OD) 3.13 (3H, s, *CH*$_3$), 4.65 (2H, s, *CH*$_2$*Py*), 6.57–6.75 (3H, m, *Ph*), 7.08–7.17 (2H, m, *Ph*), 7.69 (1H, d, *J* 4.5, *PyC5H*), 7.75 (1H, s, *PyC3H*), 8.53 (1H, d, *J* 4.5, *PyC6H*); δ_C (125 MHz, CD_3OD) 39.7 (*CH*$_3$), 59.6 (*CH*$_2$*Py*), 113.7 (*PhC2H* and

Ph<u>C</u>6H), 118.0 (*Ph<u>C</u>4H*), 122.2 (*Py<u>C</u>3H*), 123.2 (*Py<u>C</u>5H*), 130.2 (*Ph<u>C</u>3H* and *Ph<u>C</u>5H*), 148.8 (*Py<u>C</u>4*), 150.1 (*Py<u>C</u>6H*), 150.8 (*ipso-Ph*), 161.4 (*Py<u>C</u>2*), 172.8 (*<u>C</u>O₂Li*); *m/z* (MS, ES⁻) 241 (100%, [M–Li]⁻); LCMS tR 11.4 min (90%); accurate mass: found 265.0952, calc. for $C_{14}H_{14}N_2NaO_2^+$ 265.0947.

Lithium 2-[(benzylamino)methyl]isonicotinate 106

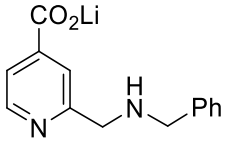

Lithium hydroxide (1 M, aq, 0.11 mL, 0.11 mmol) was added to a solution of ethyl 2-[(benzylamino)methyl]isonicotinate **96** (30 mg, 0.11 mmol) in tetrahydrofuran (0.6 mL) and water (0.5 mL) and the resulting suspension stirred at room temperature for 16 h. Acetonitrile (2 mL) was added, the volatiles evaporated, the residue washed with dichloromethane (3 × 1 mL) then dried *in vacuo* to give **106** as a yellow gum (30 mg, quant.). ν_{max} (film) 2849 (C–H), 1598 and 1550 (CO_2Li); δ_H (400 MHz, CD_3OD) 3.80 (2H, s, *C<u>H₂</u>Ph*), 3.93 (2H, s, *C<u>H₂</u>Py*), 7.21–7.39 (5H, m, *Ph*), 7.69–7.73 (1H, m, *PyC5<u>H</u>*), 7.87 (1H, s, *PyC3<u>H</u>*), 8.52–8.55 (1H, m, *PyC6<u>H</u>*); δ_C (100 MHz, CD_3OD) 53.9 (*<u>C</u>H₂Ph*), 54.5 (*<u>C</u>H₂Py*), 123.3 (*Py<u>C</u>5H*), 123.6 (*Py<u>C</u>3H*), 128.5 (1 × *Ph<u>C</u>H*), 129.7 (2 × *Ph<u>C</u>H*), 129.8 (2 × *Ph<u>C</u>H*), 140.4 (*ipso-Ph*), 148.6 (*Py<u>C</u>4*), 150.1 (*Py<u>C</u>6H*), 160.3 (*Py<u>C</u>2*), 172.7 (*<u>C</u>O₂Li*); *m/z* (MS, ES⁻) 241 (100%, [M–Li]⁻); LCMS tR 7.9 min (82%); accurate mass: found 265.0947, calc. for $C_{14}H_{14}N_2NaO_2^+$ 265.0947.

2-[(4-benzylpiperidin-1-yl)methyl]isonicotinic acid trifluoroacetate 108

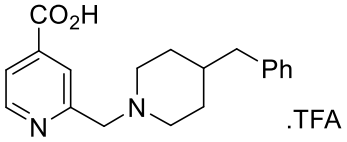

Lithium hydroxide (1 M, aq, 0.10 mL, 0.10 mmol) was added to a solution of ethyl 2-[(4-benzylpiperidin-1-yl)methyl]isonicotinate **98** (33 mg, 0.10 mmol) in tetrahydrofuran (0.6 mL) and water (0.5 mL) and the resulting suspension stirred at room temperature for 16 h. Acetonitrile (2 mL) was added, the volatiles evaporated, the residue washed with dichloromethane (3 × 1 mL) then purified by reverse phase HPLC (0.1% trifluoroacetic acid in water → 0.1% trifluoroacetic acid in acetonitrile) to give **108** as a yellow gum (9 mg, 21%). ν_{max} (film) 2925 (C–H), 1604 (CO_2H); δ_H (400 MHz, CD_3OD) 1.50–1.65 (2H, m, 2 × *Pip*), 1.86–1.99 (3H, m, 3 × *Pip*), 2.59–2.71 (2H, m, *C<u>H₂</u>Ph*), 3.01–3.14 (2H, m, 2 × *Pip*), 3.47–3.61 (2H, m, 2 × *Pip*), 4.51 (2H, s, *C<u>H₂</u>Py*), 7.17–7.22 (3H, m, 3 × *Ph*), 7.26–7.32 (2H, m, 2 × *Ph*), 7.95 (1H, d, *J* 5.0, *PyC5<u>H</u>*), 8.00 (1H, s, *PyC3<u>H</u>*), 8.85 (1H, d, *J* 5.0, *PyC6<u>H</u>*); δ_C (125 MHz, $CDCl_3$) 30.5 (2 × *Pip <u>C</u>H₂*), 36.9 (*<u>C</u>HCH₂Ph*), 43.1 (*<u>C</u>H₂Ph*), 54.8 (2 × *Pip <u>C</u>H₂*), 61.7 (*<u>C</u>H₂Py*), 124.8 (*Py<u>C</u>5H*), 124.9 (*Py<u>C</u>3H*), 127.6, 129.7 and 130.3 (5 × *Ph*), 140.6 and 141.6 (*ipso-Ph* and *Py<u>C</u>4*), 152.2 (*Py<u>C</u>6H*), 152.7 (*Py<u>C</u>2*), 167.2

(*C*O_2*H*); *m/z* (MS, ES^-) 309 (100%, $[M–H]^-$); LCMS tR 9.9 min (97%); accurate mass: found 333.1583, calc. for $C_{19}H_{22}N_2NaO_2^+$ 333.1573.

Lithium 2-[(dibenzylamino)methyl]isonicotinate 109

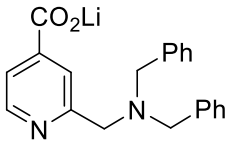

Lithium hydroxide (1 M, aq, 0.11 mL, 0.11 mmol) was added to a solution of ethyl 2-[(dibenzylamino)methyl]isonicotinate **99** (40 mg, 0.11 mmol) in tetrahydrofuran (0.6 mL) and water (0.5 mL) and the resulting suspension stirred at room temperature overnight. Further lithium hydroxide (1 M, aq, 0.01 mL, 0.01 mmol) was added and the resulting suspension stirred at room temperature overnight. Acetonitrile (2 mL) was added, the volatiles evaporated, the residue washed with cyclohexane (3 × 1 mL) then dried *in vacuo* to **109** as a white gum (9 mg, 75% pure by LCMS, 18%). ν_{max} (film) 1549 (CO_2Li); δ_H (400 MHz, CD_3OD) 3.58 (4H, s, 2 × *C*$\underline{H}_2$*Ph*), 3.71 (2H, s, *C*$\underline{H}_2$*Py*), 7.19–7.25 (2H, m, *Ph*), 7.28–7.35 (4H, m, *Ph*), 7.37–7.46 (4H, m, *Ph*), 7.68 (1H, d, *J* 5.0, *PyC5*$\underline{H}$), 8.18 (1H, s, *PyC3*$\underline{H}$), 8.44 (1H, d, *J* 5.0, *PyC6*$\underline{H}$) *m/z* (MS, ES^-) 331 (100%, $[M–Li]^-$); LCMS tR 10.1 min (75%); accurate mass: found 355.1417, calc. for $C_{21}H_{20}N_2NaO_2^+$ 355.1417.

2-[(Prop-2-yn-1-ylamino)methyl]isonicotinic acid 110

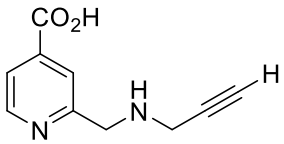

A solution of ethyl 2-formylisonicotinate **47** (45 mg, 0.25 mmol) in dichloromethane (0.5 mL) was added to prop-2-yn-1-amine (24 µL, 0.38 mmol). Glacial acetic acid (1 drop) was added and the resulting suspension stirred at room temperature for 30 min. Sodium triacetoxyborohydride (80 mg, 0.38 mmol) was added and the resulting suspension stirred at room temperature for 16 h. The reaction mixture was acidified to pH 1 with trifluoroacetic acid and purified by reverse phase chromatography (C18 column, eluting with 0.1% trifluoroacetic acid in water → 0.1% trifluoroacetic acid in acetonitrile) to give the ethyl ester as a brown gum that was taken up in acetonitrile (1 mL). Lithium hydroxide (1 M, aq, 1.0 mL, 1.0 mmol) was added and the resulting solution stirred at room temperature for 16 h. The reaction mixture was acidified with hydrochloric acid (1 M, aq, 1.1 mL) then purified on a 10 g strong cation exchange column, washing with methanol (100 mL) then eluting with methanolic ammonia (2 M, 100 mL) to give **110** as a brown gum (53 mg, quant.). ν_{max} (film) 2800 (C–H), 1590 and 1546 (CO_2H); δ_H (400 MHz, CD_3OD) 2.90 (1H, t, *J* 2.5, *C*≡*C*$\underline{H}$), 3.71 (2H, d, *J* 2.5, *C*$\underline{H}_2$*C*≡*C*), 4.21 (2H, s, *C*$\underline{H}_2$*Py*), 7.73 (1H, dd, *J* 5.0, 1.5 Hz, *PyC5*$\underline{H}$), 7.84 (1H, s), 8.58 (1H, d, *J* 5.0, *PyC6*$\underline{H}$); δ_C (100 MHz, CD_3OD) 37.8 (*C*$\underline{H}_2$*C*≡*C*), 52.8 (*C*$\underline{H}_2$*Py*), 76.1 (*C*≡*C*$\underline{H}$), 79.0 (*C*$\underline{}$≡*CH*), 123.6 (*Py*$\underline{C}$*3H*), 123.8 (*Py*$\underline{C}$*5H*), 148.3 (*Py*$\underline{C}$*4*), 150.5

(*PyC6H*), 157.1 (*PyC2*), 172.3 (*CO₂H*); *m/z* (MS, ES⁻) 189 (100%, [M–H]⁻); LCMS tR 0.7 min (100%); accurate mass: found 191.0815, calc. for $C_{10}H_{11}N_2O_2^+$ 191.0815.

Methyl 2-[(trimethylsilyl)ethynyl]isonicotinate 118[218]

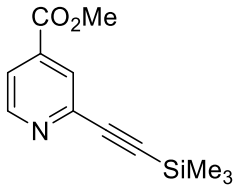

A solution of methyl 2-bromopyridine-4-carboxylate (5.40 g, 25.0 mmol), copper(I) iodide (571 mg, 3.00 mmol), tetrakis(triphenylphosphine)palladium (722 mg, 0.63 mmol) and triethylamine (87.1 mL, 130 mmol) in tetrahydrofuran (43.5 mL) was evacuated and refilled with nitrogen (× 5) then trimethylsilylacetylene (7.6 mL, 55.0 mmol) was added and the resulting solution stirred at room temperature for 16 h. The reaction mixture was concentrated *in vacuo* to give a black gum that was taken up in dichloromethane (40 mL) and filtered. The filtrate was concentrated *in vacuo* and purified by flash column chromatography (9:1 heptane–ethyl acetate) to give **118** as an orange oil (4.94 g, 85%). R_f 0.20 (9:1 heptane–ethyl acetate); ν_{max} (film) 2963 (C–H), 1726 (C=O); δ_H (400 MHz, $CDCl_3$) 0.26 (9H, s, 3 × *SiCH₃*), 3.94 (3H, s, *CO₂CH₃*), 7.75 (1H, dd, *J* 5.0, 2.0, *PyC5H*), 7.97–7.99 (1H, m, PyC3H), 8.70 (1H, dd, *J* 5.0, 1.0, *PyC6H*) [*consistent with literature*]; δ_C (100 MHz, $CDCl_3$) 0.00 (3 × *SiCH₃*), 53.2 (*CO₂CH₃*), 96.7 (*CSi(CH₃)₃*), 103.3 (*CCSi(CH₃)₃*), 122.4 (*PyC5H*), 126.9 (*PyC3H*), 138.0 (*PyC4*), 144.5 (*PyC2*), 151.1 (*PyC6H*), 165.3 (*CO₂CH₃*); *m/z* (MS, ES^+) 234 (100%, MH^+); LCMS tR 5.9 min (100%); accurate mass: found 234.0947, calc. for $C_{12}H_{16}NO_2Si^+$ 234.0945.

Methyl 2-(1-benzyl-1*H*-1,2,3-triazol-4-yl)isonicotinate 119

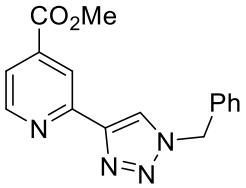

A solution of tetrabutylammonium fluoride in tetrahydrofuran (1 M, 1.25 mL, 1.25 mmol) was added to a suspension of methyl 2-[(trimethylsilyl)ethynyl]isonicotinate **118** (291 mg, 1.25 mmol), benzyl azide (166 mg, 1.25 mmol), diisopropylethylamine (44 μL, 0.25 mmol) and copper(I) iodide (24 mg, 0.13 mmol) in methanol (2.5 mL) and the resulting suspension stirred at room temperature for 16 h. The reaction mixture was diluted with water (5 mL) then extracted with dichloromethane (3 × 5 mL). The organic layers were combined, evaporated and purified by flash column chromatography (2:1 heptane–ethyl acetate) to give **119** as a tan solid (255 mg, 69%). R_f 0.20 (9:1 heptane–ethyl acetate); mp 158–160 °C; ν_{max} (film) 3135 (C–H), 3067 (C–H), 2954 (C–H), 1724 (C=O); δ_H (400 MHz, $CDCl_3$) 3.95 (3H, s, *OCH₃*), 5.57 (2H, s, *CH₂*), 7.30–7.39 (5H, m, *Ph*), 7.73 (1H, dd, *J* 5.13, 1.71, *PyC5H*), 8.05 (1H, s, *TriCH*), 8.65 (1H, dd, *J* 5.13, 0.98, *PyC6H*), 8.68 (1H, dd, *J* 1.71, 0.98, *PyC3H*); δ_C (100 MHz, $CDCl_3$) 52.8 (*CO₂CH₃*), 54.5 (*CH₂Ph*), 119.6 (*PyC3H*),

122.0 (*TriCH*), 122.4 (*PyC5H*), 128.4 (*PhC2H* and *PhC6H*), 129.0 (*PhC4H*), 129.3 (*PhC3H* and *PhC5H*), 134.3 (*PhC1*), 138.5 (*PyC4*), 148.2 (*TriCC*), 150.2 (*PyC6*), 151.5 (*PyC2*), 165.6 (*CO$_2$CH$_3$*); *m/z* (MS, ES$^+$) 295 (100%, MH$^+$); LCMS tR 14.5 min (98%); accurate mass: found 317.0998, calc. for $C_{16}H_{14}N_4NaO_2^+$ 317.1009.

Potassium 2-(1-benzyl-1*H*-1,2,3-triazol-4-yl)-isonicotinate 120

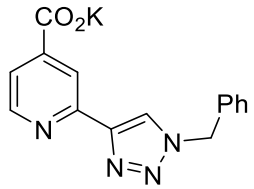

Potassium trimethylsilanolate (24 mg, 0.19 mmol) was added to a solution of methyl 2-(1-benzyl-1*H*-1,2,3-triazol-4-yl)isonicotinate **118** (50 mg, 0.17 mmol) in acetonitrile (2 mL) and the resulting suspension stirred overnight at for 16 h. The resulting precipitate was filtered, washed with acetonitrile (2 × 2 mL) and dried under vacuum at 30 °C for 16 h to give **120** as an off-white solid (47 mg, 87%). R_f 0.55 (2:8 2 M methanolic ammonia–dichloromethane); mp 148–151 °C; ν_{max} (film) 1609 and 1549 (CO_2K); δ_H (400 MHz, CD_3OD) 5.68 (2H, s, *CH$_2$Ph*), 7.33–7.43 (5H, m, *Ph*), 7.76 (1H, dd, *J* 5.0, 1.5, *PyC5H*), 8.40 (1H, s, *TriCH*), 8.49 (1H, dd, *J* 1.5, 0.5, *PyC3H*), 8.58 (1H, dd, *J* 5.0, 0.5, *PyC6H*); δ_C (100 MHz, CD_3OD) 55.2 (*CH$_2$Ph*), 121.4 (*PyC3H*), 123.9 (*TriCH*), 124.2 (*PyC5H*), 129.3 (2 × *PhCH*), 129.8 (*PhCH*), 130.2 (2 × *PhCH*), 136.8 (*PhC1*), 149.1, 149.2, 150.6 (*PyC6H*), 151.4, 172.5 (*CO$_2$K*); *m/z* (MS, ES$^+$) 281 (100%, MH$^+$); LCMS tR 12.4 min (99%); accurate mass: found 303.0840, calc. for $C_{15}H_{12}N_4NaO_2^+$ 303.0852.

2-(1-Phenethyl-1*H*-1,2,3-triazol-4-yl)isonicotinic acid 122

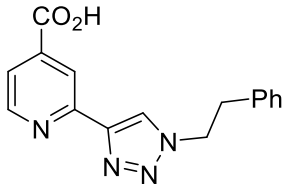

A solution of tetrabutylammonium fluoride (1 M in tetrahydrofuran, 0.20 mL, 0.20 mmol) was added to a suspension of methyl 2-[(trimethylsilyl)ethynyl]isonicotinate **118** (47 mg, 0.20 mmol), 1-phenethyl azide (29 mg, 0.20 mmol), diisopropylethylamine (7 μL, 0.04 mmol) and copper(I) iodide (4 mg, 0.02 mmol) in methanol (1 mL) and the resulting suspension stirred at room temperature for 16 h. The reaction mixture was diluted with water (5 mL) then extracted with dichloromethane (3 × 5 mL). The organic layers were combined, evaporated and concentrated *in vacuo*. Potassium trimethylsilanolate (28 mg, 0.22 mmol) was added as a solution in acetonitrile (2 mL) and the resulting suspension stirred at room temperature for 2 h. The precipitate was filtered and washed with acetonitrile (2 × 2 mL) then dried under vacuum at 30°C for 16 h and purified by reverse phase HPLC (0.1% formic acid in water → 0.1% formic acid in acetonitrile) to give **122** as a beige solid (21 mg, 32%). *m/z* (MS, ES$^+$) 295 (100%, MH$^+$); LCMS (system B) tR 2.9 min (225 nm: 84%; ELSD: 98%).

2-[1-(3-Amino-4-methylphenyl)-1*H*-1,2,3-triazol-4-yl]isonicotinic acid 123

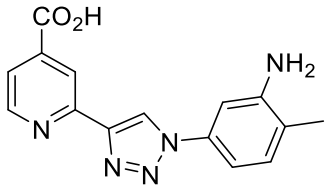

A solution of tetrabutylammonium fluoride (1 M in tetrahydrofuran, 0.20 mL, 0.20 mmol) was added to a suspension of methyl 2-[(trimethylsilyl)ethynyl]isonicotinate **118** (47 mg, 0.20 mmol), 3-amino-4-methylphenyl azide (30 mg, 0.20 mmol), diisopropylethylamine (7 μL, 0.04 mmol) and copper(I) iodide (4 mg, 0.02 mmol) in methanol (1 mL) and the resulting suspension stirred at room temperature for 16 h. The reaction mixture was diluted with water (5 mL) then extracted with dichloromethane (3 × 5 mL). The organic layers were combined, evaporated and concentrated *in vacuo*. Potassium trimethylsilanolate (28 mg, 0.22 mmol) was added as a solution in acetonitrile (2 mL) and the resulting suspension stirred at room temperature for 2 h. The precipitate was filtered and washed with acetonitrile (2 × 2 mL) then dried under vacuum at 30°C for 16 h and purified by reverse phase HPLC (0.1% formic acid in water → 0.1% formic acid in acetonitrile) to give **123** as a beige solid (4 mg, 6%). *m/z* (MS, ES^+) 296 (100%, MH^+); LCMS (system B) tR 2.6 min (225 nm: 96%; ELSD: 100%).

2-[1-(2-phenoxyethyl)-1*H*-1,2,3-triazol-4-yl]isonicotinic acid 126

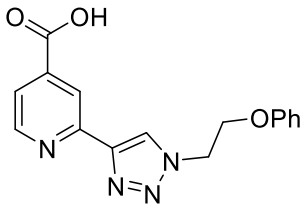

A solution of tetrabutylammonium fluoride (1 M in tetrahydrofuran, 0.20 mL, 0.20 mmol) was added to a suspension of methyl 2-[(trimethylsilyl)ethynyl]isonicotinate **118** (47 mg, 0.20 mmol), 2-phenoxyethyl azide (33 mg, 0.20 mmol), diisopropylethylamine (7 μL, 0.04 mmol) and copper(I) iodide (4 mg, 0.02 mmol) in methanol (1 mL) and the resulting suspension stirred at room temperature for 16 h. The reaction mixture was diluted with water (5 mL) then extracted with dichloromethane (3 × 5 mL). The organic layers were combined, evaporated and concentrated *in vacuo*. Potassium trimethylsilanolate (28 mg, 0.22 mmol) was added as a solution in acetonitrile (2 mL) and the resulting suspension stirred at room temperature for 2 h. The precipitate was filtered and washed with acetonitrile (2 × 2 mL) then dried under vacuum at 30°C for 16 h and purified by reverse phase HPLC (0.1% formic acid in water → 0.1% formic acid in acetonitrile) to give **126** as a beige solid (35 mg, 50%). *m/z* (MS, ES^+) 311 (100%, MH^+); LCMS (system B) tR 2.9 min (225 nm: 96%; ELSD: 100%).

2-{1-[1-(Ethoxycarbonyl)piperidin-4-yl]-1*H*-1,2,3-triazol-4-yl}isonicotinic acid 128

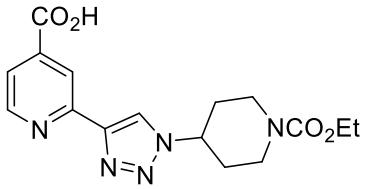

A solution of tetrabutylammonium fluoride (1 M in tetrahydrofuran, 0.20 mL, 0.20 mmol) was added to a suspension of methyl 2-[(trimethylsilyl)ethynyl]isonicotinate **118** (47 mg, 0.20 mmol), ethyl 4-azidopiperidine-1-carboxylate (40 mg, 0.20 mmol), diisopropylethylamine (7 μL, 0.04 mmol) and copper(I) iodide (4 mg, 0.02 mmol) in methanol (1 mL) and the resulting suspension stirred at room temperature for 16 h. The reaction mixture was diluted with water (5 mL) then extracted with dichloromethane (3 × 5 mL). The organic layers were combined, evaporated and concentrated *in vacuo*. Potassium trimethylsilanolate (28 mg, 0.22 mmol) was added as a solution in acetonitrile (2 mL) and the resulting suspension stirred at room temperature for 2 h. The precipitate was filtered and washed with acetonitrile (2 × 2 mL) then dried under vacuum at 30°C for 16 h and purified by reverse phase HPLC (0.1% formic acid in water → 0.1% formic acid in acetonitrile) to give **128** as a brown solid (11 mg, 14%). *m/z* (MS, ES^+) 346 (100%, MH^+); LCMS (system B) tR 2.9 min (225 nm: 99%; ELSD: 100%).

Azidomethyl pivalate 132[171]

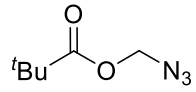

Chloromethyl pivalate (0.86 mL, 6.0 mmol) was added to a solution of sodium azide (429 mg, 6.6 mmol) in water (3.5 mL) and the resulting solution heated at 90 °C for 16 h. The solution was diluted with water (15 mL) then extracted with dichloromethane (2 × 20 mL). The organic layers were combined, dried over sodium sulfate and concentrated *in vacuo* to give **132** as a colourless liquid (698 mg, 74%). ν_{max} (film) 2975 (C–H), 2104 (N_3), 1739 (C=O) [*lit. values: 2976, 2104, 1739*]; δ_H (400 MHz, $CDCl_3$) 1.26 (9H, s, 3 × *C*H$_3$), 5.14 (2H, s, *C*H$_2$) [*consistent with lit.*]; δ_C (100 MHz, $CDCl_3$) 27.0 (3 × *C*H$_3$), 39.0 (*C*Me$_3$), 74.4 (*C*H$_2$), 178.1 (*C*O^t*Bu*) [*consistent with lit.*].

Methyl 2-(1-{[(2,2-dimethylpropanoyl)oxy]methyl}-1*H*-1,2,3-triazol-4-yl)isonicotinate 133

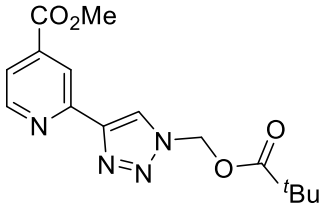

A solution of tetrabutylammonium fluoride in water (75% w/w, 85 μL, 0.24 mmol) was added dropwise over 5 min to a mixture of methyl 2-[(trimethylsilyl)ethynyl]isonicotinate **118** (57 mg, 0.24 mmol), azidomethyl pivalate **132** (42 mg, 0.27 mmol), copper(II) sulfate pentahydrate (3 mg, 0.01 mmol) and (+)-sodium L-ascorbate (5 mg, 0.03 mmol) in 1 mL of a 4:1 mixture of *N*,*N*-

dimethylformamide–water. The resulting suspension was heated at 65 °C for 16 h. The reaction mixture was diluted with brine (15 mL) and extracted with ethyl acetate (2 × 20 mL). The organic layers were washed with brine (2 × 15 mL) then combined, dried over sodium sulfate and concentrated *in vacuo* to give a brown oil that was purified by flash column chromatography (10% → 30% ethyl acetate in cyclohexane) to give **133** as a white solid (41 mg, 53%). R_f 0.40 (2:1 cyclohexane–ethyl acetate); mp 78–81 °C; ν_{max} (film) 2962 (C–H), 2873 (C–H), 1724 (2 × C=O); δ_H (400 MHz, $CDCl_3$) 1.20 (9H, s, *C(C<u>H</u>₃)₃*), 3.98 (3H, s, *OC<u>H</u>₃*), 6.32 (2H, s, *C<u>H</u>₂*), 7.80 (1H, dd, *J* 5.0, 1.5, *PyC5<u>H</u>*), 8.42 (1H, s, *TriC<u>H</u>*), 8.70 (1H, dd, *J* 1.5, 1.0, *PyC3<u>H</u>*), 8.74 (1H, dd, *J* 5.0, 1.0, *PyC6<u>H</u>*); δ_C (100 MHz, $CDCl_3$) 26.8 (*C(<u>C</u>H₃)₃*), 38.8 (*<u>C</u>(CH₃)₃*), 52.7 (*O<u>C</u>H₃*), 69.8 (*<u>C</u>H₂*), 119.7 (*Py<u>C</u>3H*), 122.2 (*Py<u>C</u>5H*), 123.7 (*Tri<u>C</u>H*), 138.4 (*Py<u>C</u>4*), 148.3, 150.3 (*Py<u>C</u>6H*), 150.9, 165.4 (*<u>C</u>O₂Me*), 177.6 (*<u>C</u>O^{t}Bu*); *m/z* (MS, ES^+) 319 (100%, MH^+); LCMS tR 15.2 min (99%); accurate mass: found 341.1209, calc. for $C_{15}H_{18}N_4NaO_4^+$ 341.1220.

2-(1*H*-1,2,3-Triazol-4-yl)isonicotinic acid 134

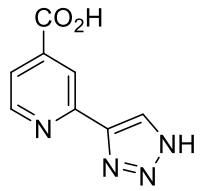

Sodium hydroxide (1 M, aq, 0.6 mL, 0.6 mmol) was added to a solution of methyl 2-(1-{[(2,2-dimethylpropanoyl)oxy]methyl}-1*H*-1,2,3-triazol-4-yl)isonicotinate **133** (80 mg, 0.25 mmol) in methanol (0.6 mL). The resulting suspension was stirred at room temperature for 16 h. The reaction mixture was concentrated *in vacuo*, diluted with water (10 mL), acidified to pH 1 with hydrochloric acid (1 M, aq) and extracted with ethyl acetate (3 × 10 mL). The organic layers were combined, dried over sodium sulfate and concentrated *in vacuo* to give **134** as a white solid (29 mg, 61%). mp 298–300 °C; ν_{max} (film) 2769 (br, OH), 2636 (br, OH), 1722 (CO_2H); δ_H (500 MHz, $(CD_3)_2SO$) 7.77 (1H, dd, *J* 5.0, 1.5, *PyC5<u>H</u>*), 8.39 (1H, s, *Tri*), 8.42–8.49 (1H, m, *PyC3<u>H</u>*), 8.80 (1H, d, *J* 5.0, *PyC6<u>H</u>*); δ_C (125 MHz, Py-d_5) 120.8 (*Py<u>C</u>3H*), 123.1 (*Py<u>C</u>5H*), 130.8 (*Tri<u>C</u>H*), 141.6, 147.6, 151.2 (*Py<u>C</u>6H*), 152.4, 168.3 (*<u>C</u>O₂H*); *m/z* (MS, ES^-) 189 (100%, $[M–H]^-$); LCMS tR 8.2 min (100%); accurate mass: found 189.0421, calc. for $C_8H_5N_4O_2^-$ 189.0418.

Methyl 2-[(trimethylsilyl)ethynyl]pyrimidine-4-carboxylate 140

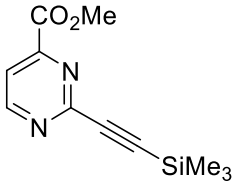

A solution of methyl 2-chloropyrimidine-4-carboxylate (173 mg, 1.00 mmol), copper(I) iodide (23 mg, 0.12 mmol), triphenylphosphine (53 mg, 0.20 mmol), tetrakis(triphenylphosphine)palladium (69 mg, 0.06 mmol) and triethylamine (3.30 mL, 23.7 mmol) in *N*,*N*-dimethylformamide (1.65 mL) was evacuated and refilled with nitrogen (× 5) then trimethylsilylacetylene (0.31 mL, 2.20

mmol) was added and the resulting solution heated at 50 °C for 3.5 h. The reaction mixture was concentrated *in vacuo* to give a black gum that was purified by flash column chromatography (4% → 20% ethyl acetate in cyclohexane) to give **140** as a beige solid (194 mg, 83%). R_f 0.30 (4:1 cyclohexane–ethyl acetate); mp 88–91 °C; ν_{max} (film) 2958 (C–H), 2900 (C–H), 1732 (C=O); δ_H (400 MHz, $CDCl_3$) 0.26 (9H, s, *Si(C<u>H</u>₃)₃*), 4.00 (3H, s, *OC<u>H</u>₃*), 7.89 (1H, d, *J* 5.0, *pyrimidinyl C5<u>H</u>*), 8.92 (1H, d, *J* 5.0, *pyrimidinyl C6<u>H</u>*); δ_C (100 MHz, $CDCl_3$) 0.0 (*Si(<u>C</u>H₃)₃*), 54.1 (*O<u>C</u>H₃*), 96.8 (*C≡<u>C</u>Si*), 102.3 (*<u>C</u>≡CSi*), 119.9 (*pyrimidinyl <u>C</u>5H*), 153.3 (*pyrimidinyl <u>C</u>2*), 155.7 (*pyrimidinyl <u>C</u>4*), 159.9 (*pyrimidinyl <u>C</u>6H*), 164.6 (*<u>C</u>O₂Me*); LCMS tR 16.0 min (94%); *m/z* (MS, ES^+) 257 (100%, MNa^+); accurate mass: found 257.0719, calc. for $C_{11}H_{14}N_2NaO_2Si^+$ 257.0717.

Methyl 6-[(trimethylsilyl)ethynyl]pyridazine-4-carboxylate 141

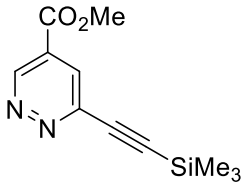

A solution of methyl 2-chloropyridazine-4-carboxylate (173 mg, 1.00 mmol), copper(I) iodide (23 mg, 0.12 mmol), triphenylphosphine (53 mg, 0.20 mmol), tetrakis(triphenylphosphine)palladium (69 mg, 0.06 mmol) and triethylamine (3.30 mL, 23.7 mmol) in *N*,*N*-dimethylformamide (1.65 mL) was evacuated and refilled with nitrogen (× 5) then trimethylsilylacetylene (0.31 mL, 2.20 mmol) was added and the resulting solution heated at 50 °C for 3.5 h. The reaction mixture was concentrated *in vacuo* to give a black gum that was purified by flash column chromatography (4% → 20% ethyl acetate in cyclohexane) to give the **141** as a beige solid (100 mg, 43%). R_f 0.30 (4:1 cyclohexane–ethyl acetate); mp 88–91 °C; ν_{max} (film) 3042 (C–H), 2959 (C–H), 2900 (C–H), 1728 (C=O); δ_H (400 MHz, $CDCl_3$) 0.30 (9H, s, *Si(C<u>H</u>₃)₃*), 4.01 (3H, s, *OC<u>H</u>₃*), 8.05 (1H, d, *J* 1.5, *pyridazinyl C5<u>H</u>*), 9.54 (1H, app. s, *pyridazinyl C3<u>H</u>*); δ_C (100 MHz, $CDCl_3$) 0.0 (*Si(<u>C</u>H₃)₃*), 53.9 (*O<u>C</u>H₃*), 100.3 (*C≡<u>C</u>Si*), 102.9 (*<u>C</u>≡CSi*), 127.7 (*pyridazinyl <u>C</u>4*), 129.5 (*pyridazinyl <u>C</u>5H*), 147.9 (*pyridazinyl <u>C</u>3H*), 149.1 (*pyridazinyl <u>C</u>6*), 164.3 (*<u>C</u>O₂Me*); LCMS tR 16.1 min (78%); *m/z* (MS, ES^+) 257 (100%, MNa^+); accurate mass: found 257.0719, calc. for $C_{11}H_{14}N_2NaO_2Si^+$ 257.0717.

Methyl 2-methyl-6-[(trimethylsilyl)ethynyl]isonicotinate 142

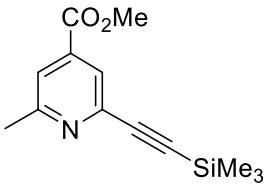

A solution of methyl 2-chloro-6-methylisonicotinate (186 mg, 1.00 mmol), copper(I) iodide (23 mg, 0.12 mmol), triphenylphosphine (53 mg, 0.20 mmol), tetrakis(triphenylphosphine)palladium (69 mg, 0.06 mmol) and triethylamine (3.30 mL, 23.7 mmol) in *N*,*N*-dimethylformamide (1.65 mL) was evacuated and refilled with nitrogen (× 5) then trimethylsilylacetylene (0.31 mL, 2.20 mmol) was added and the resulting solution heated at 50 °C for 3.5 h. The reaction mixture was

concentrated *in vacuo* to give a black gum that was purified by flash column chromatography (4% → 20% ethyl acetate in cyclohexane) to give **142** as a yellow solid (179 mg, 72%). R_f 0.60 (4:1 cyclohexane–ethyl acetate); mp 83–86 °C; ν_{max} (film) 2957 (C–H), 2900 (C–H), 2163 (C≡C), 1734 (C=O); δ_H (400 MHz, $CDCl_3$) 0.26 (9H, s, *Si(C<u>H</u>₃)₃*), 2.61 (3H, s, *PyC<u>H</u>₃*), 3.94 (3H, s, *OC<u>H</u>₃*), 7.63 (1H, s), 7.81 (1H, s); δ_C (100 MHz, $CDCl_3$) 0.0 (*Si(<u>C</u>H₃)₃*), 24.9 (*Py<u>C</u>H₃*), 53.1 (*O<u>C</u>H₃*), 96.1 (*C≡<u>C</u>Si*), 103.4 (*<u>C</u>≡CSi*), 122.3 (*Py<u>C</u>3H*), 124.2 (*Py<u>C</u>5H*), 138.2 (*Py<u>C</u>4*), 143.6 (*Py<u>C</u>6*), 160.4 (*Py<u>C</u>2*), 165.5 (*<u>C</u>O₂Me*); LCMS tR 18.3 min (95%); *m/z* 248 (100%, MH^+); accurate mass: found 270.0919, calc. for $C_{13}H_{17}NNaO_2Si^+$ 270.0921.

2-Chloro-6-(diethylamino)pyrimidine-4-carboxylic acid 144

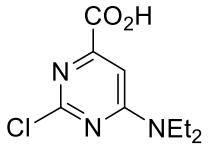

Sodium hydroxide (1 M, aq, 0.5 mL, 0.5 mmol) was added to a solution of methyl 2-chloro-6-(diethylamino)pyrimidine-4-carboxylate **143** (29 mg, 0.12 mmol) in methanol (0.5 mL) and the resulting solution heated at room temperature for 16 h. The methanol was removed *in vacuo*, the residue acidified to pH 3 with 10% citric acid and extracted with ethyl acetate (3 × 5 mL). The organic layers were combined, dried over sodium sulfate, concentrated *in vacuo* and the residue purified by strong cation exchange chromatography, washing with methanol and eluting with methanolic ammonia (2 M) to give **144** as a colourless gum (20 mg, 73%). R_f 0.90 (7:3 dichloromethane–methanol); ν_{max} (film) 2977 (C–H), 2933 (C–H), 1592 (CO_2H); δ_H (400 MHz, CD_3OD) 1.15–1.30 (6H, m, 2 × *C<u>H</u>₃*), 3.48–3.72 (4H, m, 2 × *C<u>H</u>₂*), 6.55 (1H, s, *pyrimidyl C5<u>H</u>*); δ_C (100 MHz, CD_3OD) 13.1 and 13.8 (2 × *<u>C</u>H₃*; rotamers), 43.9 and 44.6 (2 × *<u>C</u>H₂*; rotamers), 95.8 (*pyrimidyl <u>C</u>5H*), 150.0, 160.3, 165.6, 165.8; *m/z* (MS, ES^-) 228 (100%, $[M(^{35}Cl)–H]^-$); LCMS tR 12.0 min (96%); accurate mass: found 228.0554, calc. for $C_9H_{11}{}^{35}ClN_3O_2^-$ 228.0545.

2-(1-Benzyl-1*H*-1,2,3-triazol-4-yl)pyrimidine-4-carboxylic acid 145

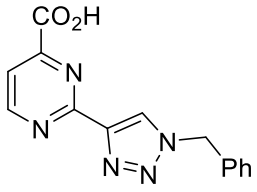

A solution of tetrabutylammonium fluoride in tetrahydrofuran (1 M, 0.30 mL, 0.30 mmol) was added dropwise to a suspension of methyl 2-[(trimethylsilyl)ethynyl]pyrimidine-4-carboxylate **140** (70 mg, 0.30 mmol), benzyl azide (44 mg, 0.30 mmol), copper(II) sulfate pentahydrate (4 mg, 0.02 mmol) and (+)-sodium L-ascorbate (7 mg, 0.03 mmol) in 2 mL of a 4:1 mixture of *N*,*N*-dimethylformamide–water and the reaction mixture stirred at room temperature for 72 h. The volatiles were removed *in vacuo* and the residue purified by flash column chromatography (2:3 ethyl acetate–cyclohexane → ethyl acetate) to give a white solid that was taken up in tetrahydrofuran (0.9 mL). Lithium hydroxide (1 M, aq, 0.90 mL, 0.90 mmol) was added and the

resulting solution stirred at room temperature for 3 h. The volatiles were removed *in vacuo*, the residue acidified to pH 1 with hydrochloric acid (1 M, aq) and extracted with dichloromethane (3 × 3 mL). The organic layers were combined and concentrated *in vacuo* to give **145** as a white solid (50 mg, 59%). R_f 0.15 (95:5 dichloromethane–methanol); mp 191–193 °C; ν_{max} (film) 2923 (C–H), 2853 (C–H), 1744 (CO_2H); δ_H (400 MHz, $(CD_3)_2SO$) 5.71 (2H, s, *C<u>H</u>₂*), 7.32–7.42 (5H, m, *Ph*), 7.88 (1H, d, *J* 5.0, *pyrimidinyl C5<u>H</u>*), 8.92 (1H, s, *Tri*), 9.10 (1H, d, *J* 5.0, *pyrimidinyl C6<u>H</u>*); δ_C (125 MHz, $CD_3)_2SO$) 53.1 (*<u>C</u>H₂*), 119.0 (*pyrimidinyl <u>C</u>5H*), 127.1 (1 × *Ph<u>C</u>H*), 128.1 (2 × *Ph<u>C</u>H*), 128.9 (2 × *Ph<u>C</u>H*), 131.5 (*ipso-Ph*), 135.8 (*Tri<u>C</u>H*), 146.1, 156.2, 158.9, 160.2 (*pyrimidinyl <u>C</u>6H*), 165.3 (*<u>C</u>O₂H*); *m/z* (MS, ES^-) 280 (100%, $[M–H]^-$); LCMS tR 12.3 min (87%); accurate mass: found 280.0844, calc. for $C_{14}H_{10}N_5O_2^-$ 280.0840.

6-(1-Benzyl-1*H*-1,2,3-triazol-4-yl)pyridazine-4-carboxylic acid 146

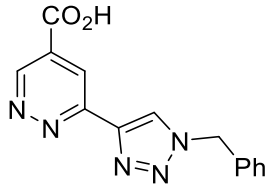

A solution of tetrabutylammonium fluoride in tetrahydrofuran (1 M, 0.15 mL, 0.15 mmol) was added dropwise to a suspension of methyl 6-[(trimethylsilyl)ethynyl]pyridazine-4-carboxylate **141** (35 mg, 0.15 mmol), benzyl azide (24 mg, 0.165 mmol), copper(II) sulfate pentahydrate (2 mg, 0.01 mmol) and (+)-sodium L-ascorbate (3 mg, 0.02 mmol) in 1 mL of a 4:1 mixture of *N*,*N*-dimethylformamide–water and the reaction mixture stirred at room temperature for 72 h. The volatiles were removed *in vacuo* and the residue purified by flash column chromatography (2:3 ethyl acetate–cyclohexane → ethyl acetate) to give a yellow solid that was taken up in tetrahydrofuran (0.45 mL). Lithium hydroxide (1 M, aq, 0.45 mL, 0.45 mmol) was added and the resulting suspension stirred at room temperature for 72 h. The volatiles were removed *in vacuo*, the residue diluted with water (1 mL), acidified to pH 1 with hydrochloric acid (1 M, aq) and extracted with dichloromethane (3 × 3 mL). The organic layers were combined, dried over sodium sulfate and concentrated *in vacuo* to give **146** as a white solid (12 mg, 28%). R_f 0.10 (95:5 dichloromethane–methanol); mp 244–247 °C; ν_{max} (film) 2446 (br, OH), 1698 (CO_2H); δ_H (400 MHz, $(CH_3)_2SO$) 5.74 (2H, s, *C<u>H</u>₂*), 7.32–7.44 (5H, m, *Ph*), 8.50 (1H, d, *J* 2.0, *pyridazinyl C5<u>H</u>*), 9.08 (1H, s, *TriC<u>H</u>*), 9.49 (1H, d, *J* 2.0, *pyridazinyl C3<u>H</u>*); δ_C (100 MHz, $(CH_3)_2SO$) 53.3 (*<u>C</u>H₂*), 122.1 (*pyridazinyl <u>C</u>5H*), 124.5 (*Tri<u>C</u>H*), 128.1 (2 × *Ph<u>C</u>H*), 128.3 (*Ph<u>C</u>H*), 128.9 (2 × *Ph<u>C</u>H*), 129.7 (*pyridazinyl <u>C</u>4*), 135.7 (*ipso-Ph*), 144.0 (*Tri<u>C</u>C*), 148.8 (*pyridazinyl <u>C</u>3H*), 153.8 (*pyridazinyl <u>C</u>6*), 164.9 (*<u>C</u>O₂H*); *m/z* (MS, ES^+) 282 (100%, MH^+); LCMS tR 12.3 min (100%); accurate mass: found 304.0799, calc. for $C_{14}H_{11}N_5NaO_2^+$ 304.0805.

Methyl 2-(1-benzyl-1*H*-1,2,3-triazol-4-yl)-6-methylisonicotinate 147

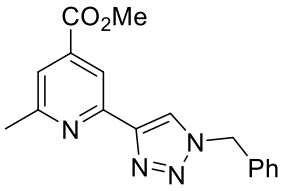

A solution of tetrabutylammonium fluoride in tetrahydrofuran (1 M, 0.30 mL, 0.30 mmol) was added dropwise to a suspension of methyl 2-methyl-6-[(trimethylsilyl)ethynyl]isonicotinate **142** (74 mg, 0.30 mmol), benzyl azide (44 mg, 0.30 mmol), copper(II) sulfate pentahydrate (4 mg, 0.02 mmol) and (+)-sodium L-ascorbate (7 mg, 0.03 mmol) in 2 mL of a 4:1 mixture of *N*,*N*-dimethylformamide–water and the reaction mixture stirred at room temperature for 72 h. The volatiles were removed *in vacuo* and the residue purified by flash column chromatography (1:4 ethyl acetate–cyclohexane → 2:1 ethyl acetate–cyclohexane) to give the **147** as a white solid (57 mg, 62%). R_f 0.25 (1:2 ethyl acetate–cyclohexane); mp 135–140 °C; ν_{max} (film) 3033 (C–H), 2952 (C–H), 1729 (C=O); δ_H (400 MHz, $CDCl_3$) 2.60 (3H, s, *PyC*<u>*H*</u>$_3$), 3.96 (3H, s, *OC*<u>*H*</u>$_3$), 5.60 (2H, s, *C*<u>*H*</u>$_2$), 7.32–7.42 (5H, m, *Ph*), 7.63–7.64 (1H, m, *PyC5*<u>*H*</u>), 8.08 (1H, s, *TriC*<u>*H*</u>), 8.49–8.50 (1H, m, *PyC3*<u>*H*</u>); δ_C (100 MHz, $CDCl_3$) 24.5 (Py<u>*C*</u>H_3), 52.6 (*O*<u>*C*</u>H_3), 54.4 (<u>*C*</u>H_2), 116.7 (*Py*<u>*C*</u>*3H*), 121.6 (*Py*<u>*C*</u>*5H*), 122.2 (*Tri*<u>*CH*</u>), 128.2 (2 × *Ph*), 128.8 (1 × *Ph*), 129.2 (2 × *Ph*), 134.4 (*ipso-Ph*), 138.5, 148.4, 150.7, 159.4, 165.8 (<u>*C*</u>O_2*Me*) LCMS tR 15.2 min (99%); *m/z* (MS, ES^+) 309 (100%, MH^+); accurate mass: found 331.1163, calc. for $C_{17}H_{16}N_4NaO_2^+$ 331.1165.

2-(1-Benzyl-1*H*-1,2,3-triazol-4-yl)-6-methylisonicotinic acid 148

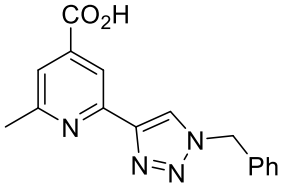

Lithium hydroxide (1 M, aq, 0.20 mL, 0.20 mmol) was added to a solution of methyl 2-(1-benzyl-1*H*-1,2,3-triazol-4-yl)-6-methylisonicotinate **147** (20 mg, 0.07 mmol) in tetrahydrofuran (0.4 mL) and water (0.2 mL) and the resulting solution stirred at room temperature for 16 h, the volatiles removed *in vacuo* and the residue acidified to pH 1 with hydrochloric acid (1 M, aq). The resulting precipitate was filtered, washing with hydrochloric acid (1 M, aq) to give **148** as a white solid (15 mg, 79%). R_f 0.25 (95:5 dichloromethane–methanol); mp 254–258 °C (sub); ν_{max} (film) 3149 (C–H), 3054 (C–H), 3001 (C–H), 1700 (C=O); δ_H (400 MHz, $(CD_3)_2SO$) 2.57 (3H, s, *PyC*<u>*H*</u>$_3$), 5.67 (2H, s, *C*<u>*H*</u>$_2$), 7.29–7.47 (5H, m, *Ph*), 7.63 (1H, s, *Ar*<u>*H*</u>), 8.23 (1H, s, *Ar*<u>*H*</u>), 8.72 (1H, s, *Ar*<u>*H*</u>); δ_C (100 MHz, $CD_3)_2SO$) 24.1 (*Py*<u>*C*</u>H_3), 53.1 (<u>*C*</u>H_2), 115.6 (*Ar*<u>*C*</u>*H*), 121.3 (*Ar*<u>*C*</u>*H*), 123.7 (*Ar*<u>*C*</u>*H*), 128.1 (2 × *Ph*<u>*C*</u>*H*), 128.3 (1 × *Ph*<u>*C*</u>*H*), 128.9 (2 × *Ph*<u>*C*</u>*H*), 135.9 (*ipso-Ph*), 139.5, 147.0, 150.3, 159.5, 166.2 (<u>*C*</u>O_2*H*); *m/z* (MS, ES^-) 293 (100%, $[M–H]^-$); LCMS tR 12.6 min (100%); accurate mass: found 317.1003, calc. for $C_{16}H_{14}N_4NaO_2^+$ 317.1009.

Methyl 2-(1-{[(2,2-dimethylpropanoyl)oxy]methyl}-1*H*-1,2,3-triazol-4-yl)pyrimidine-4-carboxylate 149

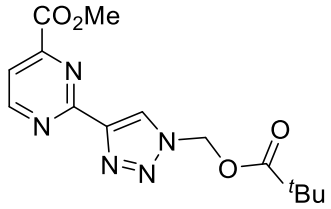

A mixture of methyl 2-chloropyrimidine-4-carboxylate (173 mg, 1.00 mmol), copper(I) iodide (23 mg, 0.12 mmol), triphenylphosphine (53 mg, 0.20 mmol) and tetrakis(triphenylphosphine)palladium (69 mg, 0.06 mmol) was placed in a sealed vial which was evacuated and refilled with nitrogen (× 4) then triethylamine (3.3 mL, 23.7 mmol), *N*,*N*-dimethylformamide (1.65 mL) and trimethylsilylacetylene (0.31 mL, 2.20 mmol) were added and the resulting solution heated at 50 °C for 9 h. The reaction mixture was allowed to cool to room temperature then azidomethyl pivalate **132** (173 mg, 1.10 mmol) and further copper(I) iodide (23 mg, 0.12 mmol) were added. A solution of tetrabutylammonium fluoride in tetrahydrofuran (1 M, 1.0 mL, 1.0 mmol) was added dropwise over 5 min and the resulting suspension stirred at room temperature for 16 h. The reaction mixture was concentrated *in vacuo* to give a black gum that was purified by flash column chromatography (cyclohexane → 1:1 cyclohexane–ethyl acetate) to give **149** as a beige solid (83 mg contaminated with 20% w/w triphenylphosphine oxide, 21%). R_f 0.20 (2:1 cyclohexane–ethyl acetate); mp 158-161 °C; ν_{max} (film) 3105 (C–H), 2973 (C–H), 1739 (2 × C=O); δ_H (400 MHz, CD_3OD) 1.22 (9H, s, *C(C<u>H</u>₃)₃*), 4.05 (3H, s, *OC<u>H</u>₃*), 6.44 (2H, s, *C<u>H</u>₂*), 7.99 (1H, d, *J* 5.0, *pyrimidinyl C5<u>H</u>*), 8.93 (1H, s, *Tri<u>C</u>H*), 9.12 (1H, d, *J* 5.0, *pyrimidinyl C6<u>H</u>*); δ_C (125 MHz, (CD_3OD) 27.3 (*C(<u>C</u>H₃)₃*), 39.9 (*<u>C</u>(CH₃)₃*), 53.9 (*O<u>C</u>H₃*), 71.6 (*<u>C</u>H₂*), 120.8 (*pyrimidyl <u>C</u>5H*), 129.2 (*Tri<u>C</u>H*), 147.9, 157.0, 160.4, 161.5 (*pyrimidyl <u>C</u>6H*), 165.9 (*<u>C</u>O₂Me*), 178.7 (*<u>C</u>O^{t}Bu*); *m/z* (MS, ES^+) 661 (100%, M_2Na^+); LCMS tR 13.4 min (86%); accurate mass: found 342.1167, calc. for $C_{14}H_{17}N_5NaO_4^+$ 342.1173.

Methyl 6-(1-{[(2,2-dimethylpropanoyl)oxy]methyl}-1*H*-1,2,3-triazol-4-yl)pyridazine-4-carboxylate 150

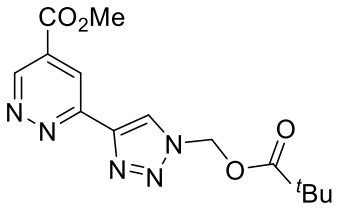

A solution of methyl 6-chloropyridazine-4-carboxylate (173 mg, 1.00 mmol), copper(I) iodide (23 mg, 0.12 mmol), triphenylphosphine (53 mg, 0.20 mmol), tetrakis(triphenylphosphine)palladium (69 mg, 0.06 mmol) and triethylamine (3.3 mL, 23.7 mmol) in *N*,*N*-dimethylformamide (1.65 mL) was evacuated and refilled with nitrogen (× 5) then trimethylsilylacetylene (0.31 mL, 2.20 mmol) was added and the resulting solution heated at 50 °C for 4 h. The reaction mixture was allowed to

cool to room temperature then azidomethyl pivalate **132** (173 mg, 1.10 mmol) and further copper(I) iodide (23 mg, 0.12 mmol) were added. A solution of tetrabutylammonium fluoride in tetrahydrofuran (1 M, 1.0 mL, 1.0 mmol) was added dropwise over 5 min and the resulting suspension stirred at room temperature overnight. The reaction mixture was concentrated *in vacuo* to give a black gum that was purified by flash column chromatography (9:1 → 1:1 cyclohexane–ethyl acetate) to give **150** as a yellow solid (139 mg, 44%). R_f 0.20 (2:1 cyclohexane–ethyl acetate); mp 110–116 °C; ν_{max} (film) 3089 (C–H), 3031 (C–H), 2977 (C–H), 1750 (C=O, carbamate), 1731 (C=O, ester); δ_H (400 MHz, $CDCl_3$) 1.21 (9H, s, *C(CH₃)₃*), 4.04 (3H, s, *OCH₃*), 6.36 (2H, s, *CH₂*), 8.70 (1H, s, *TriCH*), 8.83 (1H, d, *J* 2.0, *pyridazinyl C5H*), 9.60 (1H, d, *J* 2.0, *pyridazinyl C3H*); δ_C (100 MHz, $CDCl_3$) 26.8 (*C(CH₃)₃*), 38.8 (*C(CH₃)₃*), 53.2 (*OCH₃*), 69.9 (*CH₂*), 122.9 (*pyridazinyl C5H*), 124.5 (*TriCH*), 128.5, 145.2, 148.8 (*pyridazinyl C3H*), 153.9, 164.0 (*CO₂Me*), 177.5 (*CO^{t}Bu*); *m/z* (MS, ES^+) 661 (100%, M_2Na^+); LCMS tR 14.2 min (85%); accurate mass: found 342.1172, calc. for $C_{14}H_{17}N_5NaO_4^+$ 342.1173.

Methyl 2-(1-{[(2,2-dimethylpropanoyl)oxy]methyl}-1*H*-1,2,3-triazol-4-yl)-6-methylisonicotinate 151

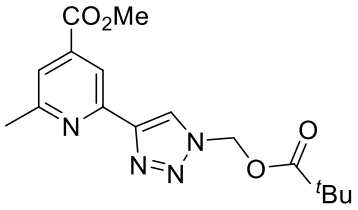

A mixture of methyl 2-chloro-6-methylisonicotinate (186 mg, 1.00 mmol), copper(I) iodide (23 mg, 0.12 mmol), triphenylphosphine (53 mg, 0.20 mmol) and tetrakis(triphenylphosphine)palladium (69 mg, 0.06 mmol) was placed in a sealed vial which was evacuated and refilled with nitrogen (× 4) then triethylamine (3.3 mL, 23.7 mmol), *N*,*N*-dimethylformamide (1.65 mL) and trimethylsilylacetylene (0.31 mL, 2.20 mmol) were added and the resulting solution heated at 50 °C for 9 h. The reaction mixture was allowed to cool to room temperature then azidomethyl pivalate **132** (173 mg, 1.10 mmol) and further copper(I) iodide (23 mg, 0.12 mmol) were added. A solution of tetrabutylammonium fluoride in tetrahydrofuran (1 M, 1.0 mL, 1.0 mmol) was added dropwise over 5 min and the resulting suspension stirred at room temperature for 16 h. The reaction mixture was concentrated *in vacuo* to give a black gum that was purified by flash column chromatography (cyclohexane → 4:1 cyclohexane–ethyl acetate) to give **151** as a beige solid (152 mg, 46%). R_f 0.45 (2:1 cyclohexane–ethyl acetate); mp 134–136 °C; ν_{max} (film) 3151 (C–H), 2979 (C–H), 2876 (C–H), 1753 (C=O, carbamate), 1724 (C=O, ester); δ_H (400 MHz, $CDCl_3$) 1.20 (9H, s, *C(CH₃)₃*), 2.64 (3H, s, *PyCH₃*), 3.96 (3H, s, *OCH₃*), 6.30 (2H, s, *CH₂*), 7.65–7.67 (1H, m, *PyC3H*), 8.41 (1H, s, *TriCH*), 8.47–8.49 (1H, m, *PyC5H*); δ_C (100 MHz, $CDCl_3$) 24.5 (*PyCH₃*), 26.8 (*C(CH₃)₃*), 38.8 (*C(CH₃)₃*), 52.6 (*OCH₃*), 69.8 (*CH₂*), 116.7 (*PyC5H*), 121.8 (*PyC3H*), 123.7 (*TriCH*), 138.5, 148.5, 150.2, 159.6, 165.7 (*CO₂Me*), 177.7 (*CO^{t}Bu*); *m/z* (MS,

ES^+) 333 (100%, MH^+); LCMS tR 15.9 min (95%); accurate mass: found 355.1372, calc. for $C_{16}H_{20}N_4NaO_4^+$ 355.1377.

2-(1*H*-1,2,3-Triazol-4-yl)pyrimidine-4-carboxylic acid 152

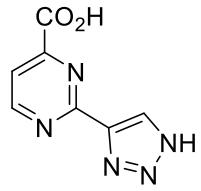

A solution of sodium hydroxide (1 M, 1.0 mL, 1.0 mmol) was added to a solution of methyl 2-(1-{[(2,2-dimethylpropanoyl)oxy]methyl}-1*H*-1,2,3-triazol-4-yl)pyrimidine-4-carboxylate **149** (62 mg, 0.19 mmol) in methanol (1 mL) and the resulting solution stirred at room temperature for 16 h. The volatiles were removed *in vacuo*, the residue diluted with water (5 mL), washed with diethyl ether (2 × 5 mL) then acidified to pH 1 with hydrochloric acid (1 M, aq) and extracted with ethyl acetate (3 × 10 mL). The organic layers were combined, dried (sodium sulfate) and concentrated *in vacuo* to give a solid that was triturated with dichloromethane (3 × 3 mL) to give **152** as a yellow solid (18 mg, 49%). mp 237–292 °C (sub); ν_{max} (film) 2915 (br, OH), 2791 (br, OH), 2633 (C–H), 1742 (C=O); δ_H (400 MHz, CD_3OD) 8.00 (1H, d, *J* 5.0, *pyrimidyl C5H*), 8.63 (1H, s, *Tri*), 9.11 (1H, d, *J* 5.0, *pyrimidyl C6H*); δ_C (125 MHz, $(CD_3)_2SO$) 119.3 (*pyrimidyl C5H*), 134.6 (*TriCH*), 145.1, 156.3, 158.9, 160.2 (*pyrimidyl C6H*), 165.2 (CO_2H); *m/z* (MS, ES^+) 192 (100%, MH^+); LCMS tR 8.0 min (99%); accurate mass: found 190.0373, calc. for $C_7H_4N_5O_2^-$ 190.0370.

6-(1*H*-1,2,3-Triazol-4-yl)pyridazine-4-carboxylic acid 153

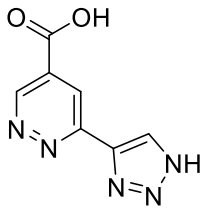

A solution of sodium hydroxide (1 M, 0.25 mL, 0.25 mmol) was added to a solution of methyl 6-(1-{[(2,2-dimethylpropanoyl)oxy]methyl}-1*H*-1,2,3-triazol-4-yl)pyridazine-4-carboxylate **150** (32 mg, 0.10 mmol) in methanol (0.25 mL). The resulting suspension was stirred at room temperature for 16 h. The reaction mixture was concentrated *in vacuo*, diluted with water (5 mL), acidified to pH 1 with hydrochloric acid (1 M, aq), washed with dichloromethane (3 × 5 mL) then extracted with ethyl acetate (3 × 5 mL). The organic layers were combined, dried over sodium sulfate and concentrated *in vacuo* to give a yellow gum that was purified by flash column chromatography (dichloromethane → 80:20:1 dichloromethane–methanol–acetic acid) to give **153** as a yellow solid (18 mg, 94%). R_f 0.20 (80:20:1 dichloromethane–methanol–acetic acid); mp 198–201 °C; ν_{max} (film) 2920 (C–H), 2853 (C–H), 1716 (CO_2H); δ_H (400 MHz, CD_3OD) 8.57 (1H, s, *ArH*), 8.70 (1H, s, *ArH*), 9.54 (1H, d, *J* 2.0, *pyridazinyl C3H*); δ_C (125 MHz, Py-d_5) 124.7 (*ArCH*), 131.6 (*ArCH*), 133.6, 146.5, 151.0 (*pyridazinyl C3H*), 156.5, 168.8 (CO_2H); *m/z* (MS, ES^-) 190

(100%, $[M–H]^–$); LCMS tR 8.0 min (97%); accurate mass: found 190.0367, calc. for $C_7H_4N_5O_2^–$ 190.0370.

2-Methyl-6-(1*H*-1,2,3-triazol-4-yl)isonicotinic acid 154

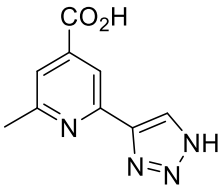

A solution of sodium hydroxide (1 M, 1.0 mL, 1.0 mmol) was added to a solution of methyl 2-(1-{[(2,2-dimethylpropanoyl)oxy]methyl}-1*H*-1,2,3-triazol-4-yl)-6-methylisonicotinate **151** (67 mg, 0.20 mmol) in methanol (7 mL) and the resulting solution stirred at room temperature for 16 h. The volatiles were removed *in vacuo*, the residue diluted with water (1 mL), acidified to pH 1 with hydrochloric acid (1 M) and extracted with ethyl acetate (3 × 3 mL). The organic layers were combined, dried (sodium sulfate) and concentrated *in vacuo* to give a solid that was triturated with dichloromethane (3 × 3 mL) to give **154** as a beige solid (17 mg, 41%). R_f 0.30 (7:3 dichloromethane–methanol); mp 250–320 °C (sub); ν_{max} (film) 2895 (br, OH), 2790 (br, OH), 1715 (C=O); δ_H (400 MHz, $(CD_3)_2SO$) 2.61 (3H, s, *C*H*₃*), 7.67 (1H, s, *ArH*), 8.21 (1H, s, *ArH*), 8.43 (1H, s, *ArH*); δ_C (100 MHz, $(CD_3)_2SO$) 24.0 (*PyCH₃*), 116.3 (*ArCH*), 121.6 (*ArCH*), 128.5 (*ArCH*), 139.7, 154.8, 159.5, 166.1 (*CO₂H*); *m/z* (MS, $ES^–$) 203 (100%, $[M–K]^–$); LCMS tR 8.2 min (95%); accurate mass: found 203.0578, calc. for $C_9H_7N_4O_2^–$ 203.0574.

2-Phenylethyl azide 158[177]

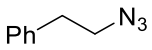

2-Phenylethyl bromide (1.11 mL, 8.11 mmol) was added to a suspension of sodium azide (580 mg, 8.92 mmol) in dimethylsulfoxide (15 mL) and the resulting mixture stirred at room temperature for 16 h. The reaction mixture was diluted with water (25 mL) and extracted with diethyl ether (3 × 20 mL). The organic layers were washed with brine (20 mL) then combined, dried over sodium sulfate and concentrated *in vacuo* to give **158** as a pale yellow oil (1.18 g, 99%). ν_{max} (film) 2091 (azide); δ_H (400 MHz, $CDCl_3$) 3.00 (2H, t, *J* 7.5, *CH₂CH₂Ph*), 3.59 (2H, t, *J* 7.5, *CH₂CH₂Ph*), 7.32–7.51 (5H, m, *Ph*) [*consistent with lit.*]; δ_C (100 MHz, $CDCl_3$) 35.1 (*CH₂CH₂Ph*), 52.2 (*CH₂CH₂Ph*), 126.6 (*PhC4H*), 128.4 and 128.6 (*PhC2H*, *PhC3H*, *PhC5H*, and *PhC6H*), 137.9 (*ipso-Ph*); *m/z* (MS, FI^+) 147 (100%, M^+); LCMS tR 10.1 min (89%).

Methyl 2-ethynylisonicotinate 159[218]

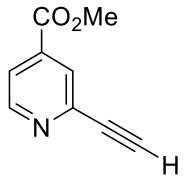

Potassium fluoride (44 mg, 0.75 mmol) was added to a solution of methyl 2-[(trimethylsilyl)ethynyl]isonicotinate **118** (58 mg, 0.25 mmol) in methanol (1 mL) and the resulting suspension stirred at room temperature for 16 h. The volatiles were removed *in vacuo* and the residue taken up in dichloromethane (5 mL). The resulting suspension was filtered, washing with dichloromethane (2 × 2 mL). The filtrate was concentrated *in vacuo* to give **159** as a beige solid (42 mg, quant.) R_f 0.50 (4:1 cyclohexane–ethyl acetate); mp 63–66 °C; ν_{max} (film) 3267 (C–H, alkynyl), 2955 (C–H), 2114 (C≡C), 1730 (C=O); δ_H (400 MHz, $CDCl_3$) 3.24 (1H, s, C≡C*H*), 3.97 (3H, s, *CO₂CH₃*), 7.81–7.84 (1H, m, *PyC5H*), 8.03 (1H, app. s, *PyC3H*), 8.75 (1H, app. d, *J* 5.0, *PyC6H*) [*consistent with literature*]; δ_C (100 MHz, $CDCl_3$) 52.9 (*CO₂CH₃*), 78.3 (C≡CH), 82.1 (C≡CH), 122.5 (*PyC5H*), 126.7 (*PyC3H*), 137.8 and 143.3 (*PyC2* and *PyC4*), 150.8 (*PyC6H*), 164.8 (*CO₂CH₃*); *m/z* (MS, ES^+) 162 (100%, MH^+); LCMS (system E) tR 5.9 min (95%).

2-(1-Benzyl-1*H*-1,2,3-triazol-4-yl)isonicotinic acid 160

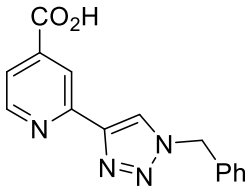

(Pentamethylcyclopentadienyl)bis(triphenylphosphine)ruthenium(II) chloride (4.8 mg, 0.006 mmol) was placed in a sealed vial and degassed dioxane added (1 mL). A degassed solution of benzyl azide (43 mg, 94% w/w, 0.30 mmol) and methyl 2-ethynylisonicotinate **159** (48 mg, 0.30 mmol) in dioxane (2 mL) was added and the resulting suspension heated at 60 ºC for 16 h. The reaction mixture was diluted with water (5 mL) and extracted with dichloromethane (3 × 5 mL). The organic layers were combined, concentrated *in vacuo* and purified by flash column chromatography (15% ethyl acetate in cyclohexane → 25% ethyl acetate in cyclohexane) to give an off-white solid that was taken up in acetonitrile (1 mL). Lithium hydroxide (1 M, aq, 1.0 mL, 1.0 mmol) was added and the resulting solution stirred at room temperature for 16 h. The reaction mixture was acidified to pH 1 with trifluoroacetic acid and the resulting precipitate filtered, washed with dilute trifluoroacetic acid (2 × 2 mL) and dried under vacuum to give **160** as an off-white solid (41 mg, 49%). mp 272–278 °C; ν_{max} (film) 1717 (C=O); δ_H (400 MHz, $(CD_3)_2SO$) 5.68 (2H, s, *CH₂Ph*), 7.29–7.45 (5H, m, *Ph*), 7.75 (1H, dd, *J* 5.0, 1.5, *PyC5H*), 8.43 (1H, s, *ArCH*), 8.70–8.82 (2H, m, *ArCH* and *PyC6H*); δ_C (100 MHz, $(CD_3)_2SO$) 53.2 (*CH₂Ph*), 118.3 (*ArCH*), 121.9 (*PyC5H*), 123.9 (*ArCH*), 128.1 (2 × *PhC2H*), 128.3 (*PhC4H*), 128.9 (2 × *PhC2H*), 135.9, 139.3, 146.9, 150.8 (*PyC6H*), 151.0, 166.1 (*CO₂H*); *m/z* (MS, ES^+) 281 (100%, MH^+); LCMS tR 13.8 min

(96%); accurate mass: found 303.0854, calc. for $C_{15}H_{12}N_4NaO_2^+$ 303.0852. Regiochemistry assigned by NOE.

2-[1-(2-Phenylethyl)-1*H*-1,2,3-triazol-4-yl] isonicotinic acid 161

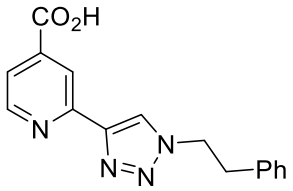

(Pentamethylcyclopentadienyl)bis(triphenylphosphine)ruthenium(II) chloride (4.8 mg, 0.006 mmol) was placed in a sealed vial and degassed dioxane added (1 mL). A degassed solution of 2-phenylethyl azide **158** (49 mg, 0.33 mmol) and methyl 2-ethynylisonicotinate **159** (48 mg, 0.30 mmol) in dioxane (2 mL) was added and the resulting suspension heated at 60 ºC for 72 h. The reaction mixture was diluted with water (5 mL) and extracted with dichloromethane (3 × 5 mL). The organic layers were combined, concentrated *in vacuo* and purified by flash column chromatography (10% ethyl acetate in cyclohexane → 35% ethyl acetate in cyclohexane) to give an off-white solid that was taken up in acetonitrile (1 mL). Lithium hydroxide (1 M, aq, 1.0 mL, 1.0 mmol) was added and the resulting solution stirred at room temperature for 16 h. The reaction mixture was acidified to pH 1 with trifluoroacetic acid and the resulting precipitate filtered, washed with dilute trifluoroacetic acid (2 × 2 mL) and dried under vacuum to give **161** as a white solid (24 mg, 20%). mp 270–276 °C; ν_{max} (film) 1720 (C=O); δ_H (400 MHz, $(CD_3)_2SO$) 3.24 (2H, t, *J* 7.0, *CH₂CH₂Ph*), 4.71 (2H, t, *J* 7.0, *CH₂CH₂Ph*), 7.11–7.34 (5H, m, *Ph*), 7.74 (1H, dd, *J* 5.0, 1.5, *PyC5H*), 8.41 (1H, s, *ArCH*), 8.63 (1H, s, *ArCH*), 8.76 (1H, d, *J* 5.0, *PyC6H*); δ_C (100 MHz, $(CD_3)_2SO$) 35.5 (*CH₂CH₂Ph*), 50.7 (*CH₂CH₂Ph*), 118.2 (*ArCH*), 121.7 (*PyC5H*), 123.7 (*ArCH*), 126.6 (*PhC4H*), 128.5 (2 × *PhCH*), 128.7 (2 × *PhCH*), 137.6, 139.2, 146.4, 150.8 (*PyC6H*), 151.1, 166.0 (*CO₂H*); *m/z* (MS, ES^+) 295 (100%, MH^+); LCMS (system E) tR 4.6 min (99%); accurate mass: found 317.1017, calc. for $C_{16}H_{14}N_4NaO_2^+$ 317.1009. Regiochemistry assigned by NOE.

Potassium 2-ethynylisonicotinate 162

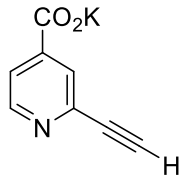

Potassium trimethylsilanolate (141 mg, 1.10 mmol) was added to a solution of methyl 2-[(trimethylsilyl)ethynyl]isonicotinate **118** (233 mg, 1.00 mmol) in acetonitrile (40 mL) and the resulting suspension stirred at room temperature for 16 h. The resulting precipitate was filtered, washed with acetonitrile (2 × 5 mL) and dried under vacuum to give **162** as a beige solid (150 mg, 81%). R_f 0.30 (8:2 dichloromethane–methanol); mp 370–372 °C; ν_{max} (film) 3214 (alkynyl C–H), 2105 (C≡C), 1619, 1541 (CO_2K); δ_H (400 MHz, $(CD_3)_2SO$) 4.24 (1H, s, C≡CH), 7.68 (1H, dd, *J* 5.0, 1.5, *PyC5H*), 7.81 (1H, app. s, *PyC3H*), 8.48 (1H, d, *J* 5.0, *PyC6H*); δ_C (100 MHz, $(CD_3)_2SO$)

79.3 (C≡CH), 83.7 (C≡CH), 123.3 (*PyC5H*), 127.0 (*PyC3H*), 141.3, 148.9, 149.7 (*PyC6H*), 166.1 (*CO₂K*); *m/z* (MS, ES⁻) 146 (100%, [M–K]⁻); LCMS tR 8.9 min (85%); accurate mass: found 146.0243, calc. for $C_8H_4NO_2^-$ 146.0248.

Methyl 2-(1-methyl-1*H*-1,2,3-triazol-4-yl)isonicotinate 163

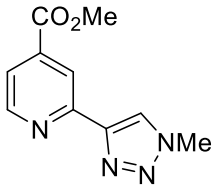

Methyl iodide (20.5 µL, 0.33 mmol) was added to a solution of potassium 2-ethynylisonicotinate **162** (56 mg, 0.30 mmol), sodium azide (23 mg, 0.36 mmol), copper(II) sulfate pentahydrate (4 mg, 0.02 mmol) and (+)-sodium L-ascorbate (7 mg, 0.03 mmol) in 2 mL of a 4:1 mixture of *N*,*N*-dimethylformamide–water. The resulting solution was heated at 65 °C for 16 h. The reaction mixture was diluted with brine (10 mL) and extracted with ethyl acetate (2 × 10 mL). The organic layers were washed with brine (2 × 10 mL) then combined, dried over sodium sulfate and concentrated *in vacuo*. The residue was washed with hexane (10 mL) to give **163** as a brown solid (16 mg, 24%). mp 108–110°C; ν_{max} (film) 2954 (C–H), 1729 (C=O); δ_H (400 MHz, $CDCl_3$) 3.97 (3H, s, *OMe*), 4.18 (3H, s, *NMe*), 7.76–7.79 (1H, m, *PyC5H*), 8.15 (1H, s, *ArCH*), 8.68–8.73 (2H, m, *ArCH* and *PyC6H*); δ_C (100 MHz, $CDCl_3$) 36.9 (*NCH₃*), 52.7 (*OCH₃*), 119.4 (*ArCH*), 121.9 (*PyC5H*), 123.3 (*ArCH*), 138.3, 148.0, 150.2 (*PyC6H*), 151.3, 165.5 (*CO₂Me*); *m/z* (MS, ES⁺) 219 (100%, MH⁺); LCMS tR 10.7 min (88%); accurate mass: found 241.0692, calc. for $C_{10}H_{10}N_4NaO_2^+$ 241.0696.

Potassium 2-(1-methyl-1*H*-1,2,3-triazol-4-yl)isonicotinate 164

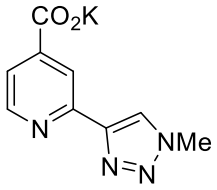

Methyl 2-(1-methyl-1*H*-1,2,3-triazol-4-yl)isonicotinate **163** (12 mg, 0.06 mmol) was dissolved in acetonitrile (4 mL), potassium trimethylsilanolate (11 mg, 0.08 mmol) was added and the resulting suspension stirred at room temperature for 16 h, the volatiles removed *in vacuo*, the residue taken up in methanol (2 mL) then filtered and washed with methanol (2 × 2 mL). The filtrate was concentrated *in vacuo* to give an orange solid that was washed with acetonitrile (3 × 2 mL) then dried under vacuum to give **164** as a yellow solid (14 mg, quant.). mp 255–261 °C; ν_{max} (film) 2957 (C–H), 2922 (C–H), 2852 (C–H), 1636 and 1614 (CO_2K); δ_H (400 MHz, CD_3OD) 4.18 (3H, s, *Me*), 7.76 (1H, dd, *J* 5.0, 1.5, *PyC5H*), 8.38 (1H, s, *ArCH*), 8.47 (1H, s, *ArCH*), 8.59 (1H, d, *J* 5.0, *PyC6H*); δ_C (125 MHz, CD_3OD) 37.2 (*CH₃*), 121.2 (*ArCH*), 123.8 (*PyC5H*), 125.2 (*ArCH*), 128.4, 148.9, 150.5 (*PyC6H*), 151.3, 172.4 (*CO₂K*); *m/z* (MS, ES⁻) 203 (100%, [M–K]⁻); LCMS tR 9.2 min (97%); accurate mass: found 203.0572, calc. for $C_9H_7N_4O_2^-$ 203.0574.

Methyl 2-(1-ethyl-1*H*-1,2,3-triazol-4-yl)isonicotinate 165

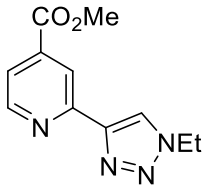

A solution of tetrabutylammonium fluoride in tetrahydrofuran (1 M, 0.50 mL, 0.50 mmol) was added to a solution of methyl 2-[(trimethylsilyl)ethynyl]isonicotinate **118** (117 mg, 0.50 mmol), ethyl iodide (44 μL, 86 mg, 0.55 mmol), copper(II) sulfate pentahydrate (6 mg, 0.03 mmol), sodium azide (39 mg, 0.60 mmol) and (+)-sodium L-ascorbate (11 mg, 0.06 mmol) in 2 mL of a 4:1 mixture of *N*,*N*-dimethylformamide–water. The resulting solution was heated at 65 °C for 60 h. The reaction mixture was diluted with brine (15 mL) and extracted with ethyl acetate (2 × 12 mL). The organic layers were combined, dried over sodium sulfate and concentrated *in vacuo* to give a brown oil which was purified by flash column chromatography (15% ethyl acetate in 30–40 petroleum ether → ethyl acetate) to give **165** as a brown solid (89 mg, 77%). R_f 0.20 (2:1 30–40 petroleum ether–ethyl acetate). mp 106–107 °C; ν_{max} (film) 3144 (C–H), 2985 (C–H), 2954 (C–H), 1731 (C=O); δ_H (400 MHz, $CDCl_3$) 1.62 (3H, t, *J* 7.5, *CH*$_2$*C*$\underline{H}_3$), 3.97 (3H, s, *OC*$\underline{H}_3$), 4.50 (2H, q, *J* 7.5, *C*$\underline{H}_2$*CH*$_3$), 7.77 (1H, dd, *J* 5.0, 1.5, *PyC5*$\underline{H}$), 8.17 (1H, s, *ArC*$\underline{H}$), 8.69–8.72 (2H, m, *ArC*$\underline{H}$ and *PyC6*$\underline{H}$); δ_C (100 MHz, $CDCl_3$) 15.4 (*CH*$_2$*C*$\underline{H}_3$), 45.5 (*C*$\underline{H}_2$*CH*$_3$), 52.7 (*CO*$_2$*C*$\underline{H}_3$), 119.5 (*Ar*$\underline{C}$*H*), 121.7 (*Ar*$\underline{C}$*H*), 121.8 (*Py*$\underline{C}$*5H*), 138.4, 147.8, 150.2 (*Py*$\underline{C}$*6H*), 151.5, 165.5 (*C*$\underline{O}_2$*Me*); *m/z* (MS, ES^+) 487 (100%, M_2Na^+); accurate mass: found 255.0850, calc. for $C_{11}H_{12}N_4NaO_2^+$ 255.0852.

Methyl 2-[1-(3-methylphenyl)-1*H*-1,2,3-triazol-4-yl]isonicotinate 166

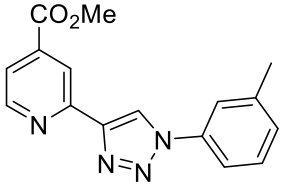

A solution of tetrabutylammonium fluoride in tetrahydrofuran (1 M, 0.5 mL, 0.5 mmol) was added to a solution of methyl 2-[(trimethylsilyl)ethynyl]isonicotinate **118** (117 mg, 0.5 mmol), 3-iodotoluene (71 μL, 120 mg, 0.55 mmol), L-proline (12 mg, 0.10 mmol), copper(II) sulfate pentahydrate (6 mg, 0.03 mmol), sodium azide (39 mg, 0.60 mmol) and (+)-sodium L-ascorbate (11 mg, 0.06 mmol) in 2 mL of a 9:1 mixture of dimethylsulfoxide–water. The resulting solution was heated at 65 °C for 16 h. The reaction mixture was poured into ammonium hydroxide (1% w/w solution, aq, 0.5 mL) diluted with ethyl acetate (10 mL), washed with brine (3 × 10 mL) and the aqueous layers back-extracted with ethyl acetate (10 mL). The organic layers were combined, dried over sodium sulfate and concentrated *in vacuo* to give a brown oil which was purified by flash column chromatography (9:1 hexane–ethyl acetate) to give **166** as a brown solid (30 mg, 20%). R_f 0.35 (2:1 hexane–ethyl acetate); mp 143–145 °C; ν_{max} (film) 3149 (C–H), 2961 (C–H), 2924 (C–H), 1718 (C=O); δ_H (400 MHz, $CDCl_3$) 2.48 (3H, s, *C*$\underline{H}_3$*Ph*), 4.01 (3H, s, *C*$\underline{H}_3$*O*), 7.28

(1H, app. d, *J* 8.0, *PhC4H*) 7.44 (1H, app. t, *J* 8.0, *PhC5H*), 7.60 (1H, ddd, *J* 8.0, 1.0, 0.5, *PhC6H*), 7.67 (1H, app. s, *PhC2H*), 7.82 (1H, dd, *J* 5.0, 1.5, *PyC5H*), 8.61 (1H, s, *TriCH*), 8.76 (1H, dd, *J* 5.0, 1.0, *PyC6H*), 8.79 (1H, dd, *J* 1.5, 1.0, *PyC3H*); δ_C (100 MHz, $CDCl_3$) 21.4 (*C*H_3*Ph*), 52.7 (*C*H_3*O*), 117.5 (*PhC6H*), 119.7 (*PyC3H*), 120.4 (*TriCH*), 121.2 (*PhC2H*), 122.1 (*PyC5H*), 129.6 and 129.7 (*PhC4H* and *PhC5H*), 136.8, 138.4, 140.1, 148.2, 150.3 (*PyC6H*), 151.1, 165.5 (*C*O_2*Me*); *m/z* (MS, ES^+) 611 (100%, M_2Na^+); LCMS tR 16.2 min (100%); accurate mass: found 317.1010, calc. for $C_{16}H_{14}N_4NaO_2^+$ 317.1009.

Potassium 2-(1-ethyl-1*H*-1,2,3-triazol-4-yl)isonicotinate 167

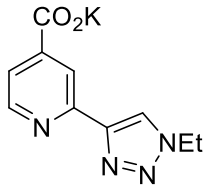

Potassium trimethylsilanolate (14 mg, 0.11 mmol) was added to a solution of methyl 2-(1-ethyl-1*H*-1,2,3-triazol-4-yl)isonicotinate **165** (23 mg, 0.10 mmol) in acetonitrile (2 mL) and the resulting suspension stirred at room temperature for 60 h. The resulting precipitate was filtered, washed with acetonitrile (2 × 3 mL) and dried under vacuum to give **167** as a beige solid (15 mg, 59%). R_f 0.45 (7:3 dichloromethane–methanol); mp 162–164 °C; ν_{max} (film) 2980 (C–H), 2935 (C–H), 1602 and 1548 (CO_2K); δ_H (500 MHz, $(CD_3)_2SO$) 1.50 (3H, t, *J* 7.5, *CH*$_2$*CH*$_3$), 4.45 (2H, q, *J* 7.5, *CH*$_2$*CH*$_3$), 7.61 (1H, dd, *J* 5.0, 1.5, *PyC5H*), 8.37 (1H, s, *ArCH*), 8.50 (1H, dd, *J* 5.0, 0.5, *PyC6H*), 8.58 (1H, s, *ArCH*); δ_C (125 MHz, $(CD_3)_2SO$) 15.4 (*C*H_3*CH*$_2$), 44.7 (*CH*$_3$*C*H_2), 119.1 (*ArCH*), 122.4 (*ArCH*), 125.3 (*PyC5H*), 128.9, 147.8, 148.9 (*PyC6H*), 149.7, 166.6 (*C*O_2*K*); *m/z* (MS, ES^-) 217 (100%, $[M–K]^-$); LCMS tR 9.4 min (98%); accurate mass: found 217.0733, calc. for $C_{10}H_9N_4O_2^-$ 217.0731.

Potassium 2-[1-(3-methylphenyl)-1*H*-1,2,3-triazol-4-yl]isonicotinate 168

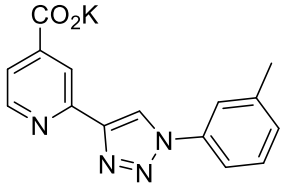

Potassium trimethylsilanolate (15 mg, 0.12 mmol) was added to a solution of methyl 2-[1-(3-methylphenyl)-1*H*-1,2,3-triazol-4-yl]isonicotinate **166** (21 mg, 0.07 mmol) in acetonitrile (4 mL) and the resulting suspension stirred at room temperature for 16 h. The resulting precipitate was filtered, washed with acetonitrile (2 × 3 mL) and dried under vacuum to give **168** as a yellow solid (20 mg, 88%). R_f 0.15 (9:1 dichloromethane–methanol); mp 198–200 °C; ν_{max} (film) 3060 (C–H), 2978 (C–H), 2918 (C–H), 2852 (C–H), 1601, 1548 (CO_2K); δ_H (500 MHz, $(CD_3)_2SO$) 2.43 (3H, s, *CH*$_3$), 7.32 (1H, d, *J* 8.0, *PhC4H*), 7.49 (1H, t, *J* 8.0, *PhC5H*), 7.67 (1H, dd, *J* 5.0, 1.5, *PyC5H*), 7.83 (1H, d, *J* 8.0, *PhC6H*), 7.90 (1H, s, *PhC2H*), 8.44–8.46 (1H, m, *PyC3H*), 8.56 (1H, dd, *J* 5.0, 1.0, *PyC6H*), 9.25 (1H, s, *TriCH*); δ_C (125 MHz, $(CD_3)_2SO$) 21.0 (*C*H_3), 117.2 (*PhC6H*), 119.6 (*PyC3H*), 120.6 (*PhC2H*), 120.9 (*TriCH*), 122.9 (*PyC5H*), 129.3 (*PhC4H*), 129.7 (*PhC5H*), 136.6,

139.7, 148.8, 149.1 (*PyC6H* and *ArC*), 150.0, 166.5 (*CO_2K*); *m/z* (MS, ES^-) 279 (100%, $[M–K]^-$); LCMS tR 13.7 min (100%); accurate mass: found 303.0854, calc. for $C_{15}H_{12}N_4NaO_2^+$ 303.0852.

{4-[4-(Methoxycarbonyl)pyridin-2-yl]-1*H*-1,2,3-triazol-1-yl}acetic acid 169

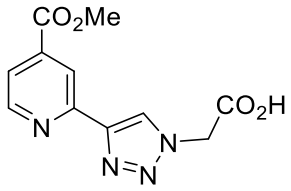

A solution of methyl 2-[(trimethylsilyl)ethynyl]isonicotinate **118** (117 mg, 0.50 mmol), bromoacetic acid (70 mg, 0.50 mmol), copper(II) sulfate pentahydrate (6 mg, 0.03 mmol), sodium azide (49 mg, 0.75 mmol) and (+)-sodium L-ascorbate (11 mg, 0.06 mmol) in 2 mL of a 4:1 mixture of *N*,*N*-dimethylformamide–water was heated at 65 °C for 15 min. A solution of tetrabutylammonium fluoride in tetrahydrofuran (1 M, 0.50 mL, 0.50 mmol) was added dropwise over 5 min and the resulting solution heated at 65 °C for 16 h. The reaction mixture was diluted with brine (15 mL) and extracted with ethyl acetate (2 × 15 mL). The organic layers were washed with brine (2 × 15 mL) then combined, concentrated *in vacuo* and purified by flash column chromatography (dichloromethane → 95:5:1 dichloromethane–methanol–acetic acid) to give **169** as a white solid (93 mg, 71%). R_f 0.25 (80:20 dichloromethane–methanol). mp 226–227 °C; ν_{max} (film) 2961 (C–H), 2923 (C–H), 2852 (C–H), 1734 (C=O, ester), 1619 (CO_2H); δ_H (400 MHz, $(CD_3)_2SO$) 3.94 (3H, s, *C*H$_3$), 4.83 (2H, s, *C*H$_2$), 7.76 (1H, dd, *J* 5.0, 1.5, *PyC5H*), 8.44 (1H, d, *J* 1.0, 0.5, *PyC3H*), 8.50 (1H, s, *TriH*), 8.81 (1H, dd, *J* 5.0, 0.5, *PyC6H*); δ_C (100 MHz, $(CD_3)_2SO$) 52.9 (*C*H$_3$), 53.8 (*C*H$_2$), 117.8 (*PyC3H*), 121.1 (*PyC5H*), 124.8 (*TriCH*), 137.8, 145.8, 150.9 (*PyC6H*), 151.6, 165.0 (*CO$_2$Me*), 168.5 (*CO$_2$H*); *m/z* (MS, ES^-) 261 (100%, $[M−H]^-$); LCMS tR 10.5 min (98%); accurate mass: found 261.0632, calc. for $C_{11}H_9N_4O_4^-$ 261.0629.

Methyl 2-[1-(2-hydroxyethyl)-1*H*-1,2,3-triazol-4-yl]isonicotinate 170

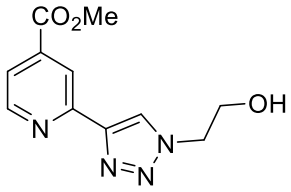

A solution of methyl 2-[(trimethylsilyl)ethynyl]isonicotinate **118** (373 mg, 1.60 mmol), 2-bromoethanol (125 µL, 1.76 mmol), copper(II) sulfate pentahydrate (20 mg, 0.08 mmol), sodium azide (125 mg, 1.92 mmol) and (+)-sodium L-ascorbate (32 mg, 0.16 mmol) in 6 mL of a 4:1 mixture of *N*,*N*-dimethylformamide–water was heated at 40 °C for 10 min. A solution of tetrabutylammonium fluoride in tetrahydrofuran (1 M, 1.60 mL, 1.60 mmol) was added dropwise over 10 min and the resulting solution heated at 65 °C for 6 h. The reaction mixture was diluted with brine (15 mL) and extracted with ethyl acetate (3 × 15 mL). The organic layers were combined, concentrated *in vacuo* and purified by flash column chromatography (ethyl acetate →

95:5 dichloromethane–methanol) to give **170** as an off-white solid (290 mg, 73% yield). R_f 0.30 (ethyl acetate); mp 135–139 °C; ν_{max} (film) 3328 (br., O–H), 2956 (C–H), 2880 (C–H), 1729 (C=O); δ_H (500 MHz, $CDCl_3$) 3.99 (3H, s, *Me*), 4.14–4.18 (2H, m, *C<u>H</u>₂O*), 4.57–4.61 (2H, m, *C<u>H</u>₂N*), 7.77 (1H, br. s, *PyC5<u>H</u>*), 8.30 (1H, s, *ArC<u>H</u>*), 8.62 (1H, s, *ArC<u>H</u>*), 8.67 (1H, br. s, *PyC6<u>H</u>*); δ_C (125 MHz, $CDCl_3$) 52.8 (*Me*), 52.9 (*C<u>H</u>₂N*), 61.2 (*C<u>H</u>₂O*), 119.6 (*Ar<u>C</u>H*), 121.9 (*Py<u>C</u>5H*), 123.7 (*Ar<u>C</u>H*), 138.4, 147.4, 150.0 (*Py<u>C</u>6H*), 151.1, 165.4 (*<u>C</u>O₂Me*); *m/z* (MS, ES^+) 519 (100%, M_2Na^+); LCMS tR 9.8 min (100%); accurate mass: found 271.0804, calc. for $C_{11}H_{12}N_4NaO_3^+$ 271.0802.

Potassium 2-[1-(2-hydroxyethyl)-1*H*-1,2,3-triazol-4-yl] isonicotinate 171

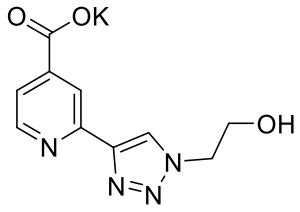

Potassium trimethylsilanolate (18 mg, 0.14 mmol) was added to a solution of methyl 2-[1-(2-hydroxyethyl)-1*H*-1,2,3-triazol-4-yl]isonicotinate **170** (23 mg, 0.09 mmol) in acetonitrile (2 mL) and the resulting suspension stirred at room temperature for 16 h, the volatiles removed *in vacuo*, the residue washed with acetonitrile (2 × 2 mL) and dried *in vacuo* to give **171** as an off-white solid (22 mg, 90%). δ_H (500 MHz, MeOD) 3.97–4.01 (2H, m, *C<u>H</u>₂O*), 4.55–4.59 (2H, m, *C<u>H</u>₂N*), 7.75 (1H, dd, *J* 5.0, 1.5, *PyC5<u>H</u>*), 8.46 (1H, s, *ArC<u>H</u>*), 8.50 (1H, s, *ArC<u>H</u>*), 8.59 (1H, d, *J* 5.0, *PyC6<u>H</u>*); δ_C (125 MHz, MeOD) 54.0 (*<u>C</u>H₂N*), 61.6 (*<u>C</u>H₂O*), 121.2 (*Ar<u>C</u>H*), 123.7 (*Py<u>C</u>5H*), 124.9 (*Ar<u>C</u>H*), 148.6, 148.9, 150.5 (*Py<u>C</u>6H*), 151.5, 172.4 (*<u>C</u>O₂K*); *m/z* (MS, ES^-) 233 (100%, $[M–K]^-$).

Lithium 2-{1-[2-(dimethylamino)-2-oxoethyl]-1*H*-1,2,3-triazol-4-yl} isonicotinate 172

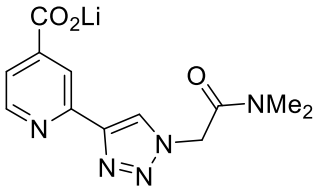

A solution of {4-[4-(methoxycarbonyl)pyridin-2-yl]-1*H*-1,2,3-triazol-1-yl}acetic acid **169** (37 mg, 0.14 mmol), dibenzylamine (118 µL, 0.60 mmol), 1-propanephosphonic acid cyclic anhydride (357 µL of a 50% w/w solution in ethyl acetate, 0.60 mmol) and triethylamine (84 µL, 0.60 mmol) in 0.5 mL of *N*,*N*-dimethylformamide was heated at 110 °C under microwave irradiation for 30 min then at 130 °C for 2 h and 140 °C for 4 h. The reaction mixture was diluted with brine (5 mL), extracted with ethyl acetate (3 × 4 mL), the organic layers combined, concentrated *in vacuo* and purified by flash column chromatography (neat dichloromethane → 1:1 dichloromethane–ethyl acetate) to give a yellow gum (R_f 0.70 in 1:1 dichloromethane–ethyl acetate) that was taken up in 1 mL of a 1:1 mixture of acetonitrile–water. Lithium hydroxide (1 M, aq, 45 µL) was added and the resulting suspension stirred at room temperature for 16 h then concentrated *in vacuo* to give **172** as a yellow gum. (11 mg, 32%). ν_{max} (film) 2931 (C–H), 2855 (C–H), 1645 and 1604 (CO_2Li);

δ_H (400 MHz, CD_3OD) 3.00 (3H, s, 2 × C<u>H</u>$_3$; rotamers), 3.17 (3H, s, 2 × C<u>H</u>$_3$; rotamers), 5.54 (2H, s, C<u>H</u>$_2$), 7.75–7.79 (1H, m, *PyC5<u>H</u>*), 8.41 (1H, s, *ArC<u>H</u>*), 8.52 (1H, s, *ArC<u>H</u>*), 8.60 (1H, d, *J* 4.5, *PyC6<u>H</u>*); δ_C (100 MHz, CD_3OD) 36.3 and 36.9 (2 × <u>C</u>H$_3$; rotamers), 52.3 (<u>C</u>H$_2$), 121.3 (*Ar<u>C</u>H*), 123.9 (*Py<u>C</u>5H*), 126.2 (*Ar<u>C</u>H*), 148.8, 148.9, 150.6 (*Py<u>C</u>6H*), 151.5, 167.8 (*<u>C</u>ON*), 172.5 (*<u>C</u>O$_2$Li*); *m/z* (MS, ES^+) 276 (100%, MH^+); LCMS tR 8.5 min (90%); accurate mass: found 298.0913, calc. for $C_{12}H_{13}N_5NaO_3^+$ 298.0911.

Potassium 2-[1-(2-oxo-2-{[2-(pyrrolidin-1-yl)ethyl]amino}ethyl)-1*H*-1,2,3-triazol-4-yl] isonicotinate 173

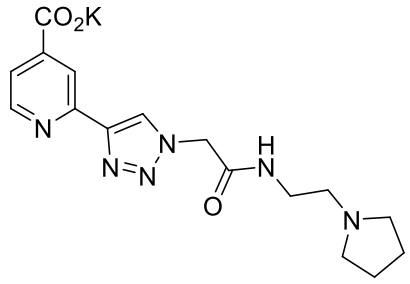

A suspension of {4-[4-(methoxycarbonyl)pyridin-2-yl]-1*H*-1,2,3-triazol-1-yl}acetic acid **169** (52 mg, 0.20 mmol), 1-(2-aminoethyl)pyrrolidine (28 µL, 0.22 mmol), 1-propanephosphonic acid cyclic anhydride (131 µL of a 50% w/w solution in ethyl acetate, 0.22 mmol) and triethylamine (31 µL, 0.224 mmol) in 1 mL of ethyl acetate was heated at 100 °C under microwave irradiation for 15 min. The reaction mixture was loaded onto a strong cation exchange cartridge (10 g) which was washed with methanol (120 mL) then extracted with methanolic ammonia (120 mL of a 5% v/v solution of conc. ammonia in methanol). The resulting gum was purified by flash column chromatography (dichloromethane → 90:10:1 dichloromethane–methanol–conc. ammonia) to give a beige solid that was taken up in acetonitrile (4 mL). Potassium trimethylsilanolate (39 mg, 0.30 mmol) was added and the resulting suspension stirred at room temperature for 16 h. The volatiles were removed *in vacuo*, the residue washed with acetonitrile (3 × 2 mL) then taken up in methanol (2 mL) and filtered, washing with methanol (2 × 2 mL). The filtrate was concentrated *in vacuo* to give **173** as a beige solid (49 mg, 64%). mp 143–150 °C; ν_{max} (film) 3284 (br, N–H), 2963 (C–H), 2803 (C–H), 1662 (C=O, amide), 1600 and 1548 (CO_2K); δ_H (500 MHz, CD_3OD) 1.78–1.83 (4H, m, *pyrrolidinyl C3<u>H</u>$_2$* and *C4<u>H</u>$_2$*), 2.56–2.60 (4H, m, *pyrrolidinyl C2<u>H</u>$_2$* and *C5<u>H</u>$_2$*), 2.64 (2H, t, *J* 7.0, *CONHCH$_2$C<u>H</u>$_2$*), 3.41 (2H, t, *J* 7.0, *CONHC<u>H</u>$_2$CH$_2$*), 4.93 (*C<u>H</u>$_2$CON* and *CD$_3$OD*), 7.77 (1H, dd, *J* 5.0, 1.5, *PyC5<u>H</u>*), 8.49 (1H, s, *Tri*), 8.51 (1H, dd, *J* 1.5, 1.0, *PyC3<u>H</u>*), 8.61 (1H, dd, *J* 5.0, 1.0, *PyC6<u>H</u>*); δ_C (125 MHz, CD_3OD) 24.4 (*pyrrolidinyl <u>C</u>3H$_2$* and *<u>C</u>4H$_2$*), 39.6 (*CONH<u>C</u>H$_2$CH$_2$*), 50.0 (*<u>C</u>H$_2$CON*), 55.1 (*pyrrolidinyl <u>C</u>2H$_2$* and *<u>C</u>5H$_2$*), 56.1 (*CONHCH$_2$<u>C</u>H$_2$*), 121.4 (*ArC<u>H</u>*), 123.9 (*Py<u>C</u>5H*), 125.9 (*ArC<u>H</u>*), 148.9, 149.0, 150.7 (*Py<u>C</u>6H*), 151.4, 168.0 (*<u>C</u>ON*), 172.5 (*<u>C</u>O$_2$K*); *m/z* (MS, ES^-) 343 (100%, $[M–K]^-$); LCMS tR 6.9 min (78%); accurate mass: found 343.1528, calc. for $C_{16}H_{19}N_6O_3^-$ 343.1524.

Potassium 2-{1-[2-(4-benzylpiperidin-1-yl)-2-oxoethyl]-1*H*-1,2,3-triazol-4-yl} isonicotinate 174

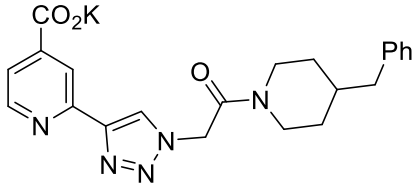

A suspension of {4-[4-(methoxycarbonyl)pyridin-2-yl]-1*H*-1,2,3-triazol-1-yl}acetic acid **169** (52 mg, 0.20 mmol), 4-benzylpiperidine (39 µL, 0.22 mmol), 1-propanephosphonic acid cyclic anhydride (131 µL of a 50% w/w solution in ethyl acetate, 0.22 mmol) and triethylamine (31 µL, 0.224 mmol) in 1 mL of ethyl acetate was heated at 100 °C under microwave irradiation for 15 min. The reaction mixture was diluted with water (5 mL) then extracted with ethyl acetate (3 × 5 mL). The organic layers were combined and concentrated *in vacuo*. The resulting gum was purified by flash column chromatography (dichloromethane → ethyl acetate) to give a brown solid that was taken up in acetonitrile (4 mL). Potassium trimethylsilanolate (39 mg, 0.30 mmol) was added and the resulting suspension stirred at room temperature for 16 h. The volatiles were removed *in vacuo*, the residue washed with acetonitrile (3 × 2 mL) then taken up in methanol (2 mL) and filtered, washing with methanol (2 × 2 mL). The filtrate was concentrated *in vacuo* to give **174** as a beige solid (69 mg, 78%). mp 143–150 °C; ν_{max} (film) 2921 (C–H), 1622 (C=O, amide), 1602 and 1548 (CO_2K); δ_H (500 MHz, $(CH_3)_2SO$) 1.08–1.29 (2H, m) and 1.51–1.79 (2H, m); 2 × *PipC*$\underline{H_2}$, 1.81–1.90 (1H, m, *PipC*$\underline{H}$), 2.58 (2H, d, *J* 7.5, *C*$\underline{H_2}$*Ph*), 3.75–4.40 (4H, m, 2 × *PipC*$\underline{H_2}$*N*), 5.38–5.49 (2H, m, *C*$\underline{H_2}$*CON*), 7.14–7.22 (3H, m, 3 × *Ph*), 7.25–7.32 (2H, m, 2 × *Ph*), 7.62 (1H, dd, *J* 5.0, 1.5, *PyC5*$\underline{H}$), 8.35 (1H, s, *Tri*), 8.37–8.38 (1H, m, *PyC3*$\underline{H}$), 8.48 (1H, d, *J* 5.0, *PyC6*$\underline{H}$); δ_C (125 MHz, $(CH_3)_2SO$) 31.0 (br., 2 × *Pip*$\underline{C}$$\underline{H_2}$), 36.5 (*Pip*$\underline{C}$*H*), 41.5 (2 × *Pip*$\underline{C}$$\underline{H_2}$*N*), 41.8 ($\underline{C}$$\underline{H_2}$*Ph*), 50.3 ($\underline{C}$$\underline{H_2}$*CON*), 118.9 (*Ar*$\underline{C}$*H*), 121.9 (*Py*$\underline{C}$*5H*), 124.0 (*Ar*$\underline{C}$*H*), 125.3 (1 × *Ph*$\underline{C}$*H*), 127.7 (2 × *Ph*$\underline{C}$*H*), 128.5 (2 × *Ph*$\underline{C}$*H*), 139.5 (*ipso-Ph*), 147.3, 148.3 (*Py*$\underline{C}$*6H*), 149.3, 149.9, 163.4 ($\underline{C}$*ON*), 166.5 ($\underline{C}$$\underline{O_2}$*H*); *m/z* (MS, ES^-) 404 (100%, $[M–K]^-$); LCMS tR 13.9 min (79%); accurate mass: found 404.1726, calc. for $C_{22}H_{22}N_5O_3^-$ 404.1728.

Methyl 2-(1-{2-[(methylsulfonyl)oxy]ethyl}-1*H*-1,2,3-triazol-4-yl)isonicotinate 175

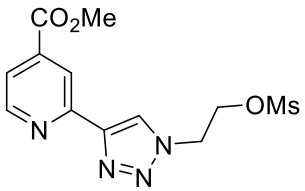

Methanesulfonyl chloride (23 µL, 0.30 mmol) was added dropwise to a suspension of methyl 2-[1-(2-hydroxyethyl)-1*H*-1,2,3-triazol-4-yl]isonicotinate **170** (50 mg, 0.20 mmol), 4-(dimethylamino)pyridine (24 mg, 0.20 mmol) and diisopropylethylamine (70 µL, 0.40 mmol) in dichloromethane (2 mL) and the resulting solution stirred at room temperature for 2 h. The reaction mixture was diluted with water (10 mL), extracted with ethyl acetate (2 × 20 mL), the organic

layers washed with brine (10 mL) then combined, dried over magnesium sulfate and concentrated *in vacuo* to give **175** as a yellow solid (152 mg, contaminated with 11% 4-(dimethylamino)pyridine w/w, quant.). R_f 0.30 (3:2 ethyl acetate–dichloromethane); mp 135–139 °C; ν_{max} (film) 3015 (C–H), 2947 (C–H), 2933 (C–H), 1730 (C=O); δ_H (400 MHz, $CDCl_3$) 2.98 (3H, s, *SO₂CH₃*), 3.98 (3H, s, *CO₂CH₃*), 4.71 (2H, t, *J* 5.0, *CH₂O*), 4.81 (2H, t, *J* 5.0, *CH₂N*), 7.80 (1H, d, *J* 4.5, *PyC5H*), 8.30 (1H, s, *ArCH*), 8.69 (1H, s, *ArCH*), 8.74 (1H, d, *J* 4.5, *PyC6H*); δ_C (125 MHz, $CDCl_3$) 37.7 (*SO₂CH₃*), 49.6 (*CH₂N*), 53.4 (*CO₂CH₃*), 66.8 (*CH₂O*), 119.5 (*ArCH*), 122.1 (*PyC5H*), 123.5 (*ArCH*), 138.4, 148.1, 150.3 (*PyC6H*), 150.9, 165.4 (*CO₂Me*); *m/z* (MS, ES^+) 675 (100%, $[M_2Na]^+$); LCMS tR 11.6 min (77%); accurate mass: found 349.0592, calc. for $C_{12}H_{14}N_4NaO_5S^+$ 349.0577.

Methyl 2-{1-[2-(4-methylpiperazin-1-yl)ethyl]-1*H*-1,2,3-triazol-4-yl}isonicotinate 176

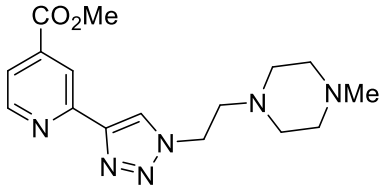

A suspension of methyl 2-(1-{2-[(methylsulfonyl)oxy]ethyl}-1*H*-1,2,3-triazol-4-yl)isonicotinate **175** (60 mg, 0.18 mmol), methyl piperazine (23 µL, 0.18 mmol) and triethylamine (26 µL, 0.20 mmol) in acetonitrile (1 mL) was heated at 80 °C for 5 h then diluted with water and extracted with ethyl acetate. The organic layers were combined, dried over magnesium sulfate and concentrated *in vacuo* to give a brown oil that was purified by flash column chromatography (5% methanol in dichloromethane–ethyl acetate → 30% methanol in dichloromethane) to give **176** as a brown foam (35 mg, 58%). δ_H (400 MHz, $CDCl_3$) 2.41 (3H, s, *NCH₃*), 2.53–2.73 (8H, m, 4 × *piperazinyl CH₂*), 2.93 (2H, t, *J* 6.0, *TriCH₂CH₂*), 3.98 (3H, s, *OCH₃*), 4.55 (2H, t, *J* 6.0, *TriCH₂CH₂*), 7.79 (1H, dd, *J* 5.0, 1.5, *PyC5H*), 8.26 (1H, s, *ArCH*), 8.71 (1H, s, *ArCH*), 8.73 (1H, d, *J* 5.0, *PyC6H*); δ_C (100 MHz, $CDCl_3$) 45.3 (*NCH₃*), 47.8, 52.1, 52.7 (*OCH₃*), 54.6, 57.1, 119.5 (*ArCH*), 121.9 (*PyC5H*), 122.8 (*ArCH*), 138.4, 147.7, 150.2 (*PyC6H*), 151.5, 165.5 (*CO₂Me*); *m/z* (MS, ES^+) 683 (100%, M_2Na^+).

Potassium 2-{1-[2-(4-methylpiperazin-1-yl)ethyl]-1*H*-1,2,3-triazol-4-yl}isonicotinate 177

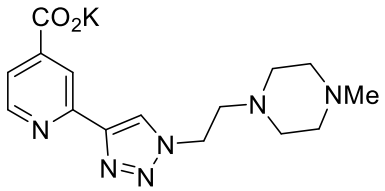

Potassium trimethylsilanolate (18 mg, 0.14 mmol) was added to a solution of methyl 2-{1-[2-(4-methylpiperazin-1-yl)ethyl]-1*H*-1,2,3-triazol-4-yl}isonicotinate **176** (30 mg, 0.09 mmol) in acetonitrile (4 mL) and the resulting suspension stirred at room temperature for 16 h, the volatiles removed *in vacuo*, the residue taken up in methanol (2 mL) to give a suspension that was filtered. The filtrate was concentrated *in vacuo* to give **177** as a yellow solid (15 mg, 45%). δ_H (500 MHz,

MeOD) 2.27 (3H, s, *NCH₃)*, 2.37–2.73 (8H, m, 4 × *piperazinyl CH₂*), 2.91 (2H, t, *J* 6.0, *TriCH₂CH₂*), 4.62 (2H, t, *J* 6.0, *TriCH₂CH₂*), 7.76 (1H, dd, *J* 5.0, 1.5, *PyC5H*), 8.49 (2H, s, 2 × *ArCH*), 8.61 (1H, d, *J* 5.0, *PyC6H*); δ_C (125 MHz, MeOD) 45.0 (*CH₃N*), 48.9, 52.5, 54.8, 57.3, 120.2 (*ArCH*), 122.7 (*ArCH*), 123.7 (*ArCH*), 147.5, 147.8, 149.5 (*PyC6H*), 150.4, 171.4 (*CO₂K*); *m/z* (MS, ES^+) 355 (100%, MH^+).

tert-Butyl 4-(2-{4-[4-(methoxycarbonyl)pyridin-2-yl]-1*H*-1,2,3-triazol-1-yl}ethyl)piperazine-1-carboxylate 178

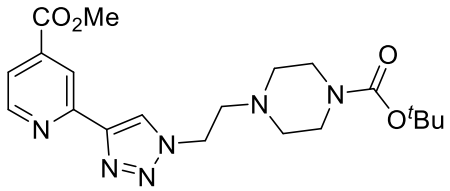

A suspension of methyl 2-(1-{2-[(methylsulfonyl)oxy]ethyl}-1*H*-1,2,3-triazol-4-yl)isonicotinate **175** (250 mg, 0.77 mmol), *tert*-butyl piperazine-1-carboxylate (157 mg, 0.84 mmol) and triethylamine (0.11 mL, 0.79 mmol) in acetonitrile (6 mL) was heated at 70 °C for 90 h then diluted with water (15 mL) and extracted with dichloromethane (3 × 15 mL). The organic layers were combined, dried over sodium sulfate and concentrated *in vacuo* to give an orange oil that was purified by flash column chromatography (1:1 dichloromethane–ethyl acetate → ethyl acetate) to give **178** as a brown foam (182 mg, 57% yield). R_f 0.15 (ethyl acetate); ν_{max} (film) 2976 (C–H), 2953 (C–H), 2817 (C–H), 1732 (C=O, ester), 1687 (C=O, carbamate); δ_H (400 MHz, $CDCl_3$) 1.45 (9H, s, *Boc*), 2.44–2.50 (4H, m, 2 × *piperazinyl CH₂*), 2.90 (2H, t, *J* 6.0, *TriCH₂CH₂*), 3.40–3.45 (4H, m, 2 × *piperazinyl CH₂*), 3.98 (3H, s, *Me*), 4.55 (2H, t, *J* 6.0, *TriCH₂CH₂*), 7.78 (1H, d, *J* 4.5, *PyC5H*), 8.27 (1H, s, *ArCH*), 8.70–8.75 (2H, m, *ArCH* and *PyC6H*); δ_C (100 MHz, $CDCl_3$) 28.4 (*C(CH₃)₃*), 43.3 (2 × *piperazinyl CH₂*), 47.8 (*TriCH₂CH₂*), 52.7 (*Me*), 52.9 (2 × *piperazinyl CH₂*), 57.5 (*TriCH₂CH₂*), 79.7 (*C(CH₃)₃*), 119.5 (*ArCH*), 121.8 (*PyC5H*), 122.9 (*ArCH*), 138.3, 147.7, 150.2 (*PyC6H*), 151.4, 154.6 (*NC=O*), 165.5 (*CO₂Me*); *m/z* (MS, ES^+) 439 (100%, MNa^+); LCMS tR 9.7 min (100%); accurate mass: found 439.2052, calc. for $C_{20}H_{28}N_6NaO_4^+$ 439.2064.

Potassium 2-(1-{2-[4-(*tert*-butoxycarbonyl)piperazin-1-yl]ethyl}-1*H*-1,2,3-triazol-4-yl)isonicotinate 179

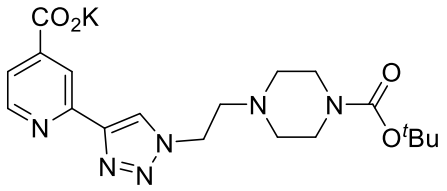

Potassium trimethylsilanolate (19 mg, 0.15 mmol) was added to a solution of *tert*-butyl 4-(2-{4-[4-(methoxycarbonyl)pyridin-2-yl]-1*H*-1,2,3-triazol-1-yl}ethyl)piperazine-1-carboxylate **178** (42 mg, 0.10 mmol) in acetonitrile (6.5 mL) and the resulting suspension stirred at room temperature for 16 h, the volatiles removed *in vacuo*, the residue washed with acetonitrile (3 × 5 mL) then taken up in methanol (5 mL) and filtered, washing with methanol (2 × 5 mL). The filtrate was

concentrated *in vacuo* to give **179** as a yellow solid (47 mg, quant.). R_f 0.10 (8:2 dichloromethane–methanol); mp 155–158 °C; ν_{max} (film) 2975 (C–H), 2932 (C–H), 2816 (C–H), 1686 (C=O, carbamate), 1629 and 1550 (CO_2K); δ_H (500 MHz, MeOD) 1.47 (9H, s, *Boc*), 2.49–2.54 (4H, m, 2 × *piperazinyl* C$\underline{H}_2$), 2.93 (2H, t, *J* 6.0, *TriCH*$_2$C$\underline{H}_2$), 3.42–3.46 (4H, m, 2 × *piperazinyl* C$\underline{H}_2$), 4.65 (2H, t, *J* 6.0, *TriC*$\underline{H}_2$*CH*$_2$), 7.79 (1H, dd, *J* 5.0, 1.5, *PyC5*$\underline{H}$), 8.52 (1H, dd, *J* 1.5, 1.0, *PyC3*$\underline{H}$), 8.53 (1H, s, *TriC*$\underline{H}$), 8.63 (1H, dd, *J* 5.0, 1.0, *PyC6*$\underline{H}$); δ_C (125 MHz, MeOD) 28.7 (*C*($\underline{C}$*H*$_3$)$_3$), 44.3 and 45.2 (broad, 2 × *piperazinyl* $\underline{C}$*H*$_2$), 48.6 (*Tri*$\underline{C}$*H*$_2$*CH*$_2$), 53.9 (2 × *piperazinyl* $\underline{C}$*H*$_2$), 58.4 (*TriCH*$_2$$\underline{C}$*H*$_2$), 81.2 ($\underline{C}$(*CH*$_3$)$_3$), 121.2 (*Py*$\underline{C}$*3H*), 123.7 (*Tri*$\underline{C}$*H*), 124.8 (*Py*$\underline{C}$*5H*), 148.6, 148.9, 150.6 (*Py*$\underline{C}$*6H*), 151.5, 156.4 (*CON*), 172.4 ($\underline{C}$*O*$_2$*K*); *m/z* (MS, ES^-) 401 (100%, $[M–K]^-$); LCMS tR 8.8 min (100%); accurate mass: found 401.1950, calc. for $C_{19}H_{25}N_6O_4^+$ 401.1943.

2-{1-[2-(Piperazin-1-yl)ethyl]-1*H*-1,2,3-triazol-4-yl}isonicotinic acid hydrochloride 180

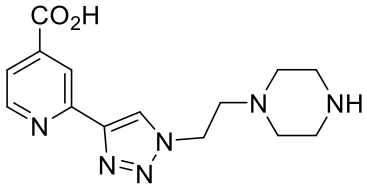

Hydrochloric acid (1 mL of a 4 M solution in dioxane) was added to potassium 2-(1-{2-[4-(*tert*-butoxycarbonyl)piperazin-1-yl]ethyl}-1*H*-1,2,3-triazol-4-yl)isonicotinate **179** (20 mg, 0.045 mmol) at 0 °C and the resulting mixture allowed to warm to room temperature over 16 h, the volatiles removed *in vacuo* and the residue washed with diethyl ether to give **180** as a white solid. δ_H (500 MHz, D_2O) 3.57–3.63 (4H, m, 2 × *piperazinyl* C$\underline{H}_2$), 3.64–3.70 (4H, m, 2 × *piperazinyl* C$\underline{H}_2$), 3.86–3.95 (2H, m, C$\underline{H}_2$), 4.99–5.10 (2H, m, C$\underline{H}_2$), 8.10 (1H, br. s, *ArC*$\underline{H}$), 8.50 (1H, br. s, *ArC*$\underline{H}$), 8.75 (1H, br. s, *ArC*$\underline{H}$), 8.81 (1H, br. s, *ArC*$\underline{H}$); *m/z* (MS, ES^+) 303 (100%, MH^+).

***tert*-Butyl 4-[(methylsulfonyl)oxy]piperidine-1-carboxylate 182[219]**

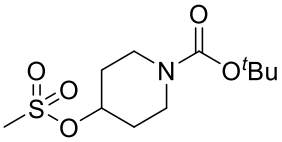

Methanesulfonyl chloride (2.04 g, 17.9 mmol) was added to a solution of *tert*-butyl 4-hydroxypiperidine-1-carboxylate (3.00 g, 14.9 mmol) and triethylamine (1.4 mL, 10.0 mmol) in dichloromethane (75 mL) at 0 °C and the resulting mixture stirred at room temperature for 1 h. The reaction mixture was diluted with dichloromethane (200 mL), washed with sodium hydrogencarbonate (2 M, aq, 80 mL) and brine (80 mL). The organic layer was dried over sodium sulfate and concentrated *in vacuo* to give **182** as a pale yellow oil that was used in the next step without further purification (4.1 g, 60% pure, 59%). LCMS (system C) tR 1.3 min (214nm: 60%); *m/z* 302 (MNa^+).

***tert*-Butyl 4-azidopiperidine-1-carboxylate 183**

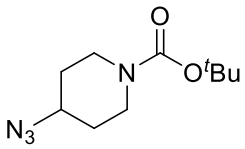

Sodium azide (2.39 g, 36.7 mmol) was added to a solution of *tert*-butyl 4-[(methylsulfonyl)oxy]piperidine-1-carboxylate **182** (4.1 g, 60% pure, 8.8 mmol) in *N*,*N*-dimethylformamide (26 mL) and the resulting suspension heated at 60 °C for 16 h. The reaction mixture was diluted with ethyl acetate (300 mL), washed with sodium hydrogencarbonate (2 M, aq, 100 mL) and brine 100 mL). The organic layer was dried over sodium sulfate and concentrated *in vacuo* to give **183** as a brown oil that was used in the next step without further purification (3.28 g, 65%). LCMS (system C) tR 1.5 min (214nm: 66%); *m/z* 171 ([M–56]$^+$).

Methyl 2-{1-[1-(*tert*-butoxycarbonyl)piperidin-4-yl]-1*H*-1,2,3-triazol-4-yl}isonicotinate 184

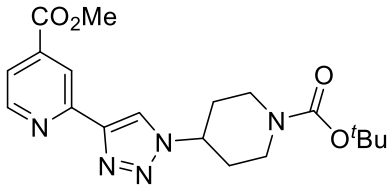

Diisopropylethylamine (0.46 mL, 2.66 mmol), copper(I) iodide (253 mg, 1.33 mmol) and a solution of tetrabutylammonium fluoride in tetrahydrofuran (0.9 M, 15.0 mL, 13.3 mmol) were added to a solution of methyl 2-[(trimethylsilyl)ethynyl]isonicotinate **183** (3.1 g, 13.3 mmol) and *tert*-butyl 4-azidopiperidine-1-carboxylate (3.01 g, 13.3 mmol) in methanol (30 mL). The reaction mixture was stirred at room temperature for 16 h then diluted with water (50 mL) and extracted with dichloromethane (3 × 80 mL). The organic layers were combined, concentrated *in vacuo* and purified by flash column chromatography (2:1 heptane–ethyl acetate) to give **184** as a pale yellow solid (2.9 g, 56%) LCMS (system D) tR 1.7 min (254nm: 100%); *m/z* 388 (MH$^+$).

Methyl 2-[1-(piperidin-4-yl)-1*H*-1,2,3-triazol-4-yl]isonicotinate trifluoroacetate 185

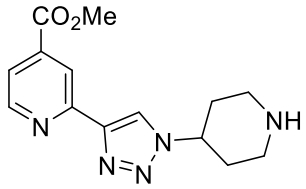

Trifluoroacetic acid (3.0 mL, 38.9 mmol) was added to a solution of methyl 2-{1-[1-(*tert*-butoxycarbonyl)piperidin-4-yl]-1*H*-1,2,3-triazol-4-yl}isonicotinate **184** (330 mg, 0.85 mmol) in dichloromethane (10 mL) and the reaction mixture stirred at room temperature for 2 h. The reaction mixture was concentrated *in vacuo* to give **185** as a brown oil (251 mg, 73%). LCMS (system C) tR 0.9 min (254nm: 100%); *m/z* 288 (MH$^+$).

Methyl 2-[1-(1-acetylpiperidin-4-yl)-1*H*-1,2,3-triazol-4-yl]isonicotinate 186

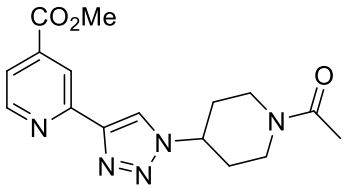

Acetyl chloride (0.075 mL, 1.05 mmol) was added to a solution of methyl 2-[1-(piperidin-4-yl)-1*H*-1,2,3-triazol-4-yl]isonicotinate trifluoroacetate **185** (251 mg, 0.63 mmol) and triethylamine (0.365 mL, 2.62 mmol) in dichloromethane (15 mL) at 0 °C. The reaction mixture was stirred at room temperature for 2 h then concentrated *in vacuo*, diluted with water (50 mL) and extracted with ethyl acetate (3 × 60 mL). The organic layers were combined and concentrated *in vacuo*. The residue was recrystallized from a 1:10 mixture of ethyl acetate–petroleum ether to give **186** as a pale yellow solid (260 mg, quant.). LCMS (system D) tR 1.4 min (254nm: 98%); *m/z* 330 (MH^+).

2-[1-(1-Acetylpiperidin-4-yl)-1*H*-1,2,3-triazol-4-yl]isonicotinic acid 187

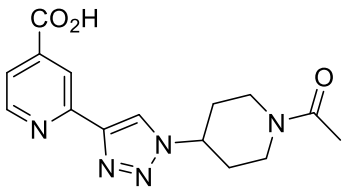

Lithium hydroxide (76 mg, 3.19 mmol) was added to a solution of methyl 2-[1-(1-acetylpiperidin-4-yl)-1*H*-1,2,3-triazol-4-yl]isonicotinate **186** (221 mg, 0.67 mmol) in methanol (6 mL) and water (3 mL) and the resulting solution stirred at room temperature for 2 h. The methanol was removed *in vacuo* and the residue acidified to pH 2 with hydrochloric acid (1 M, aq) and the resulting precipitate filtered, washing with water and diethyl ether (50 mL). The precipitate was dried *in vacuo* to give **187** as a grey solid (150 mg, 71%). LCMS (system D) tR 1.0 min (280nm: 100%); *m/z* 316 (MH^+); δ_H (400 MHz, $(CD_3)_2SO$) 1.82–1.95 (1H, m, *PipCH*), 1.99–2.07 (4H, m, *Me* and *PipCH*), 2.08–2.22 (2H, m, 2 × *PipCH*), 2.74–2.81 (1H, m, *PipCH*), 3.23–3.29 (1H, m, *PipCH*), 3.93–3.96 (1H, m, *PipCH*), 4.45–4.49 (1H, m, *PipCH*), 4.83–4.90 (1H, m, *PipCH*), 7.75 (1H, dd, *J* 5.0, 1.5, *PyC5H*), 8.42 (1H, s, *ArH*), 8.77–8.79 (2H, m, 2 × *ArH*).

2-[1-(1-Propionylpiperidin-4-yl)-1*H*-1,2,3-triazol-4-yl]isonicotinic acid 188

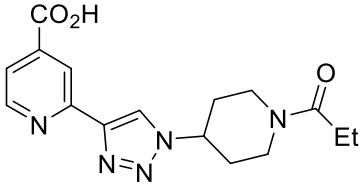

Synthesised as described above for **187** to give **188** as a white solid. LCMS (system D) tR 0.9 min (280nm: 100%); *m/z* 330 (MH^+).

2-[1-(1-Butyrylpiperidin-4-yl)-1*H*-1,2,3-triazol-4-yl]isonicotinic acid 189

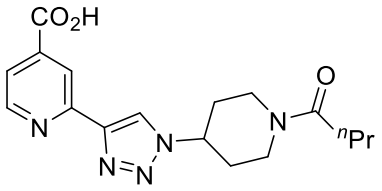

Synthesised as described above for **187** to give **189** as a white solid. LCMS (system D) tR 1.0 min (280nm: 100%); *m/z* 344 (MH^+).

2-[1-(1-Benzoylpiperidin-4-yl)-1*H*-1,2,3-triazol-4-yl]isonicotinic acid 190

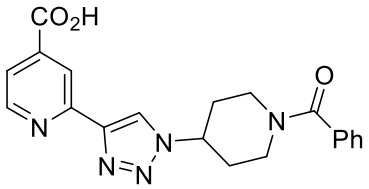

Synthesised as described above for **187** to give **190** as a white solid. LCMS (system C) tR 1.4 min (280nm: 100%); *m/z* 378 (MH^+).

2-[1-(1-Phenylacetylpiperidin-4-yl)-1*H*-1,2,3-triazol-4-yl]isonicotinic acid 191

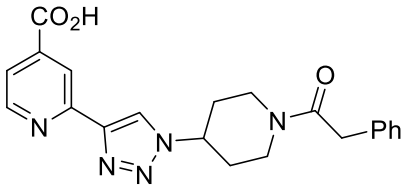

Synthesised as described above for **187** to give **191** as a white solid. LCMS (system C) tR 1.5 min (280nm: 100%); *m/z* 392 (MH^+).

2-[1-(1-Phenylpropanoylpiperidin-4-yl)-1*H*-1,2,3-triazol-4-yl]isonicotinic acid 192

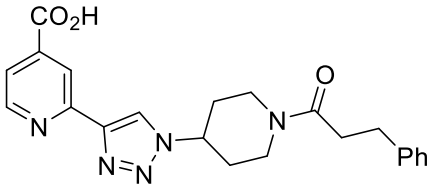

Synthesised as described above for **187** to give **192** as a white solid. LCMS (system C) tR 1.6 min (280nm: 100%); *m/z* 406 (MH^+).

2-[1-(1-Acetylazetidin-3-yl)-1*H*-1,2,3-triazol-4-yl]isonicotinic acid 199

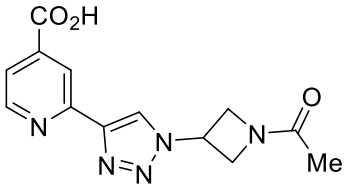

Synthesised as described above for **187** to give **199** as a white solid. LCMS (system D) tR 1.0 min (280nm: 100%); *m/z* 288 (MH^+).

2-[1-(1-Propionylazetidin-3-yl)-1*H*-1,2,3-triazol-4-yl]isonicotinic acid 200

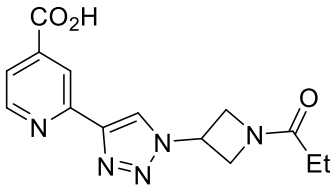

Synthesised as described above for **187** to give **200** as a white solid. LCMS (system D) tR 1.1 min (280nm: 100%); *m/z* 302 (MH^+).

2-[1-(1-Butyrylazetidin-3-yl)-1*H*-1,2,3-triazol-4-yl]isonicotinic acid 201

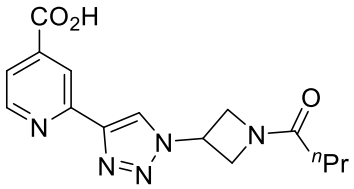

Synthesised as described above for **187** to give **201** as a white solid. LCMS (system D) tR 1.2 min (280nm: 99%); *m/z* 316 (MH^+).

2-[1-(1-Benzoylazetidin-3-yl)-1*H*-1,2,3-triazol-4-yl]isonicotinic acid 202

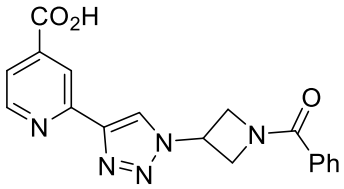

Synthesised as described above for **187** to give **202** as a white solid. LCMS (system D) tR 1.4 min (280nm: 100%); *m/z* 350 (MH^+).

2-[1-(1-Phenylacetylazetidin-3-yl)-1*H*-1,2,3-triazol-4-yl]isonicotinic acid 203

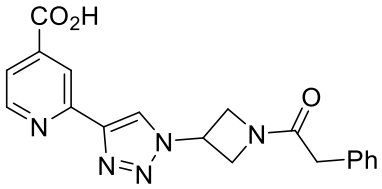

Synthesised as described above for **187** to give **203** as a white solid. LCMS (system D) tR 1.4 min (280nm: 100%); *m/z* 364 (MH^+).

2-[1-(1-Phenylpropanoylazetidin-3-yl)-1*H*-1,2,3-triazol-4-yl]isonicotinic acid 204

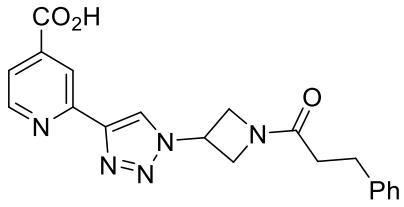

Synthesised as described above for **187** to give **204** as a white solid. LCMS (system D) tR 1.5 min (280nm: 100%); *m/z* 378 (MH^+).

2-[1-(1-Acetylpyrrolidin-3-yl)-1*H*-1,2,3-triazol-4-yl]isonicotinic acid 205

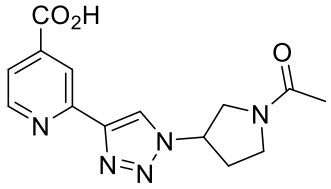

Synthesised as described above for **187** to give **205** as a white solid. LCMS (system C) tR 1.0 min (280nm: 100%); *m/z* 302 (MH^+).

2-[1-(1-Propionylpyrrolidin-3-yl)-1*H*-1,2,3-triazol-4-yl]isonicotinic acid 206

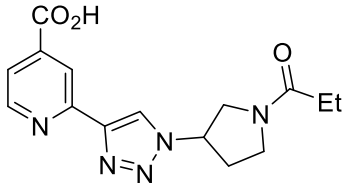

Synthesised as described above for **187** to give **206** as a white solid. LCMS (system C) tR 1.2 min (280nm: 100%); *m/z* 316 (MH^+).

2-[1-(1-Butyrylpyrrolidin-3-yl)-1*H*-1,2,3-triazol-4-yl]isonicotinic acid 207

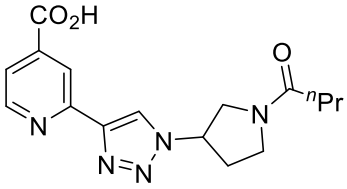

Synthesised as described above for **187** to give **207** as a white solid. LCMS (system D) tR 1.4 min (280nm: 100%); *m/z* 330 (MH^+).

2-[1-(1-Benzoylpyrrolidin-3-yl)-1*H*-1,2,3-triazol-4-yl]isonicotinic acid 208

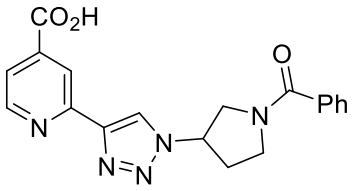

Synthesised as described above for **187** to give **208** as a white solid. LCMS (system C) tR 1.4 min (280nm: 96%); *m/z* 364 (MH^+).

2-[1-(1-Phenylacetylpyrrolidin-3-yl)-1*H*-1,2,3-triazol-4-yl]isonicotinic acid 209

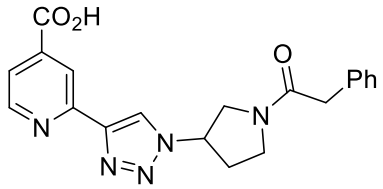

Synthesised as described above for **187** to give **209** as a white solid. LCMS (Method C): tR 1.4 min (280nm: 99%); *m/z* (ES^-) 376 (100%, $[M–H]^-$).

2-[1-(1-Phenylpropanoylpyrrolidin-3-yl)-1*H*-1,2,3-triazol-4-yl]isonicotinic acid 210

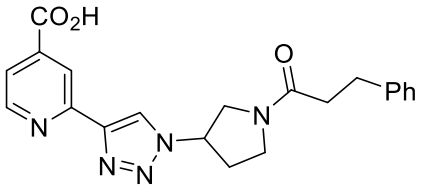

Synthesised as described above for **187** to give **210** as a white solid. LCMS (system C) tR 1.5 min (280nm: 100%); *m/z* 392 (MH^+).

2-[1-(1-Acetylpiperidin-3-yl)-1*H*-1,2,3-triazol-4-yl]isonicotinic acid 211

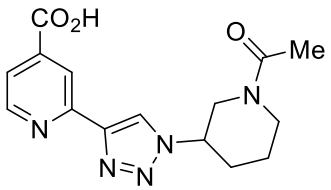

Synthesised as described above for **187** to give **211** as a yellow solid. LCMS (system C) tR 1.2 min (280nm: 100%); *m/z* 316 (MH^+).

2-[1-(1-Propionylpiperidin-3-yl)-1*H*-1,2,3-triazol-4-yl]isonicotinic acid 212

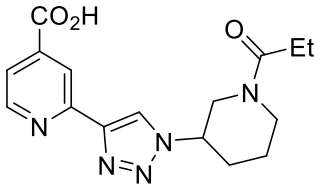

Synthesised as described above for **187** to give **212** as a yellow solid. LCMS (system C) tR 1.3 min (280nm: 100%); *m/z* 330 (MH^+).

2-[1-(1-Butyrylpiperidin-3-yl)-1*H*-1,2,3-triazol-4-yl]isonicotinic acid 213

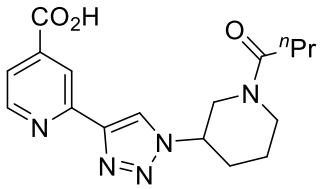

Synthesised as described above for **187** to give **213** as a yellow solid. LCMS (system C) tR 1.4 min (280nm: 100%); *m/z* 344 (MH^+).

2-[1-(1-Benzoylpiperidin-3-yl)-1*H*-1,2,3-triazol-4-yl]isonicotinic acid 214

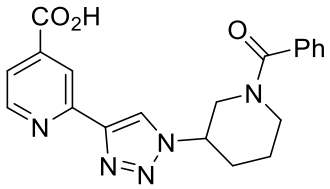

Synthesised as described above for **187** to give **214** as a white solid. LCMS (system C) tR 1.5 min (280nm: 100%); *m/z* 378 (MH^+).

2-[1-(1-Phenylacetylpiperidin-3-yl)-1*H*-1,2,3-triazol-4-yl]isonicotinic acid 215

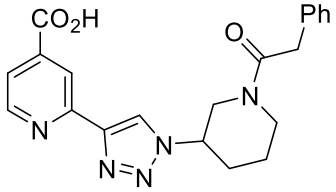

Synthesised as described above for **187** to give **215** as a yellow solid. LCMS (system C) tR 1.5 min (280nm: 100%); *m/z* 392 (MH^+).

2-[1-(1-Phenylpropanoylpiperidin-3-yl)-1*H*-1,2,3-triazol-4-yl]isonicotinic acid 216

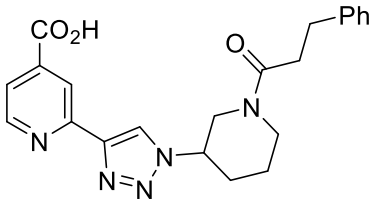

Synthesised as described above for **187** to give **216** as a white solid. LCMS (system C) tR 1.6 min (280nm: 100%); *m/z* 406 (MH^+).

***tert*-Butyl (3*R*)-3-[(methylsulfonyl)oxy]piperidine-1-carboxylate 218[220]**

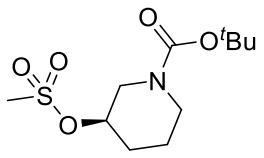

Methanesulfonyl chloride (0.19 mL, 2.40 mmol) was added dropwise over 5 min to a solution of *tert*-butyl (3*R*)-3-hydroxypiperidine-1-carboxylate (403 mg, 2.00 mmol) and triethylamine (0.56

mL, 4.00 mmol) in ethyl acetate (5.5 mL) at –5 °C and the resulting suspension stirred at –5 °C for 1 h. Water was added (6 mL), the layers separated and the organic layer washed with hydrochloric acid (1 M, aq, 2 mL) followed by sodium hydrogencarbonate (saturated, aq, 6 mL). The organic layer was dried over sodium sulfate and concentrated *in vacuo* to give **218** as a white solid (546 mg, 98%). mp 91–96 °C; ν_{max} (film) 2975 (C–H), 2937 (C–H), 2866 (C–H), 1688 (C=O); δ_H (400 MHz, $CDCl_3$) 1.45 (9H, s, *C(C<u>H</u>)₃*), 1.48–1.85 (2H, m, *PipC5<u>H</u>₂*), 1.86–2.00 (2H, m, *PipC4<u>H</u>₂*), 3.04 (3H, s, *SC<u>H</u>₃*), 3.24–3.47 (2H, m, *PipC6<u>H</u>₂*), 3.55–3.67 (2H, m, *PipC2<u>H</u>₂*), 4.66–4.74 (1H, m, *PipC3<u>H</u>*) [*consistent with lit.*]; δ_C (100 MHz, $CDCl_3$) 21.6 (*Pip<u>C</u>5H₂*), 28.3 (*C(<u>C</u>H)₃*), 30.4 (*Pip<u>C</u>4H₂*), 38.7 (*S<u>C</u>H₃*), 42.8–44.6 (*Pip<u>C</u>6H₂*), 46.5–48.9 (*Pip<u>C</u>2H₂*), 75.3 (*Pip<u>C</u>3H*), 80.1 (*<u>C</u>(CH)₃*), 154.6 (*<u>C</u>=O*) [*consistent with lit.*]; *m/z* (MS, EI^+) 279 (100%, $[M]^+$); elemental analysis: $C_{11}H_{21}NO_5S$ requires C, 47.3; H, 7.6; N, 5.0%; found C, 47.15; H, 7.7; N, 5.1%; $[\alpha]_D^{20}$ +0.4 (*c* 1.0 in $CHCl_3$) [*consistent with lit.*].

Methyl 2-{1-[(3*S*)-1-(*tert*-butoxycarbonyl)piperidin-3-yl]-1*H*-1,2,3-triazol-4-yl}isonicotinate 219

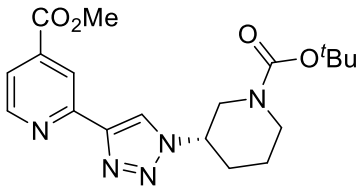

Sodium azide (186 mg, 2.86 mmol) was added to a solution of *tert*-butyl (3*R*)-3-[(methylsulfonyl)oxy]piperidine-1-carboxylate **218** (400 mg, 1.43 mmol) in *N*,*N*-dimethylformamide (5 mL) and the resulting suspension heated at 75 °C for 5 h. The reaction mixture was cooled to room temperature then diisopropylethylamine (45 µL, 0.26 mmol), copper(I) iodide (25 mg, 0.13 mmol) and methyl 2-ethynylisonicotinate (210 mg, 1.30 mmol) were added. The reaction mixture was stirred at room temperature for 16 h then diluted with brine (20 mL) and extracted with ethyl acetate (2 × 20 mL). The organic layers were washed with brine (20 mL) then combined, evaporated and purified by flash column chromatography (dichloromethane → 4:1 dichloromethane–ethyl acetate) to give **219** as a white foam (202 mg, contaminated with 16% *N*,*N*-dimethylformamide w/w, 34%). R_f 0.50 (3:2 dichloromethane–ethyl acetate); ν_{max} (film) 2952 (C–H), 2864 (C–H), 1732 (C=O, ester), 1676 (C=O, carbamate); δ_H (400 MHz, $CDCl_3$) 1.42 (9H, s, *C(C<u>H</u>)₃*), 1.56–1.70 (1H, m, *PipC5<u>H</u>*), 1.76–1.87 (1H, m, *PipC5<u>H</u>*), 2.08–2.20 (1H, m, *PipC4<u>H</u>*), 2.24–2.34 (1H, m, *PipC4<u>H</u>*), 2.97–3.07 (1H, m), 3.30–3.46 (1H, m), 3.85–3.92 (1H, m), 3.93 (3H, s, *CO₂C<u>H</u>₃*), 4.18–4.37 (1H, m), 4.52–4.61 (1H, m, *PipC3<u>H</u>*), 7.74 (1H, d, *J* 4.0, *PyC5<u>H</u>*), 8.26 (1H, s, *Ar<u>H</u>*), 8.64–8.68 (2H, m, *Ar<u>H</u>* and *PyC6<u>H</u>*); δ_C (100 MHz, $CDCl_3$) 23.3 (*Pip<u>C</u>5H₂*), 28.2 (*C(<u>C</u>H)₃*), 30.6 (*Pip<u>C</u>4H₂*), 43.9 and 48.7 (*Pip<u>C</u>2H₂* and *Pip<u>C</u>6H₂*), 52.6 (*CO₂<u>C</u>H₃*), 56.5 (*Pip<u>C</u>3H*), 80.4 (*<u>C</u>(CH)₃*), 119.3 (*Ar<u>C</u>H*), 121.2 (*Ar<u>C</u>H*), 121.8 (*Py<u>C</u>5H*), 138.3, 147.1, 149.9 (*Py<u>C</u>6H*), 151.1, 162.4 and 165.3 (2 × *<u>C</u>O₂*); *m/z* (MS, ES^+) 410 (100%, MNa^+); LCMS tR 15.5 min (96%); accurate mass: found 410.1789, calc. for $C_{19}H_{25}N_5NaO_4^+$ 410.1799; $[\alpha]_D^{20}$ +0.573 (*c* 1.0 in $CHCl_3$).

2-{1-[(3*S*)-1-Benzoylpiperidin-3-yl]-1*H*-1,2,3-triazol-4-yl}isonicotinic acid hemitrifluoroacetate 220

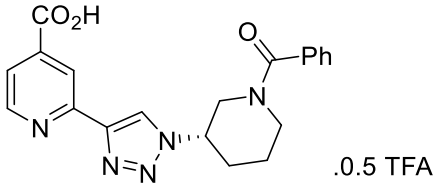

Trifluoroacetic acid (120 µL, 0.20 mmol) was added to a solution of methyl 2-{1-[(3*S*)-1-(*tert*-butoxycarbonyl)piperidin-3-yl]-1*H*-1,2,3-triazol-4-yl}isonicotinate **219** (100 mg, 84% w/w, 0.17 mmol) in dichloromethane (0.5 mL) and the resulting solution stirred at room temperature for 16 h. The reaction mixture was concentrated *in vacuo* then dissolved in acetonitrile (2 mL). Benzoyl chloride (30 µL, 0.26 mmol) and triethylamine (0.22 mL, 0.73 mmol) were added and the resulting solution stirred at room temperature for 2.5 h. Lithium hydroxide (1 M, aq, 2.0 mL, 2.0 mmol) was added and the resulting solution stirred at room temperature for 2 h. The reaction mixture was acidified to pH 1 with trifluoroacetic acid then concentrated *in vacuo* and purified by reverse phase chromatography (C18 column, eluting with 0.1% trifluoroacetic acid in water → 0.1% trifluoroacetic acid in 3:2 acetonitrile–water) to give **220** as an off-white solid (70 mg, 81%). mp 254–263 °C; ν_{max} (film) 2944 (C–H), 2866 (C–H), 2450 (br, OH), 1629 (C=O, amide), 1569 (C=O, acid); δ_H (500 MHz, $(CD_3)_2SO$) 1.57–2.00 (2H, m, *PipC5H*$_2$), 2.16–2.35 (2H, m, *PipC4H*$_2$), 3.06–4.68 (4H, m, *PipC2H*$_2$ and *PipC6H*$_2$), 4.77–4.85 (1H, m, *PipC3H*), 7.35–7.52 (5H, m, *Ph*), 7.77 (1H, d *J* 4.0, *PyC5H*), 8.44 (1H, s, *ArH*), 8.68–8.90 (2H, m, *ArH* and *PyC6H*); δ_C (125 MHz, $(CD_3)_2SO$) 23.7 (*PipC5H*$_2$), 29.9 (*PipC4H*$_2$), 45.9 and 47.0 (*PipC2H*$_2$ and *C6H*$_2$), 55.9 (*PipC3H*), 118.3 (*ArCH*), 121.8 (*PyC5H*), 122.6 (*ArCH*), 126.7 (2 × *PhCH*), 128.5 (2 × *PhCH*), 129.3 (*ipso-Ph*), 129.6 (*PhCH*), 135.8, 139.2, 146.4, 150.8 (*PyC6H*), 166.0 (*CO*$_2$*H*), 169.4 (*CON*); *m/z* (MS, ES^+) 400 (100%, MNa^+); LCMS (system E) tR 3.9 min (95%); accurate mass: found 400.1372, calc. for $C_{20}H_{19}N_5NaO_3^+$ 400.1380.

Methyl 2-{1-[(3*S*)-1-benzoylpiperidin-3-yl]-1*H*-1,2,3-triazol-4-yl}isonicotinate 221

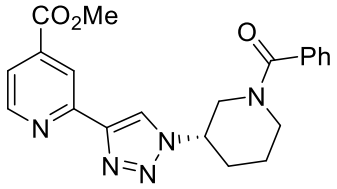

Methyl iodide (4.6 µL, 0.073 mmol) was added to a suspension of 2-{1-[(3*S*)-1-benzoylpiperidin-3-yl]-1*H*-1,2,3-triazol-4-yl}isonicotinic acid hemitrifluoroacetate **220** (29 mg, 0.067 mmol) and sodium hydrogencarbonate (16.9 mg, 0.20 mmol) in *N*,*N*-dimethylformamide (0.5 mL) and the resulting suspension stirred at room temperature for 16 h. Further methyl iodide (4.6 µL, 0.073 mmol) was added and the resulting suspension stirred at room temperature for 16 h. Further methyl iodide (4.6 µL, 0.073 mmol) was added and the resulting suspension stirred at room temperature for 6 h. Ethyl acetate (5 mL) was added and the resulting suspension washed with brine (5 × 5 mL).

The aqueous layers were back-extracted with ethyl acetate (5 mL). The organic layers were combined, dried over sodium sulfate, concentrated *in vacuo* and purified by flash column chromatography (dichloromethane → 6% methanol in dichloromethane) to give **221** as a white foam (17 mg, 65%). ν_{max} (film) 2951 (C–H), 2862 (C–H), 1732 (C=O, ester), 1633 (C=O, amide); δ_H (400 MHz, $(CD_3)_2SO$) 1.56–2.01 (2H, m, *PipC5*$\underline{H_2}$), 2.16–2.37 (2H, m, *PipC4*$\underline{H_2}$), 3.02–3.90 (3H, m), 3.94 (3H, s, *OC*$\underline{H_3}$), 3.97–4.69 (1H, m), 4.73–4.90 (1H, m, *PipC3*$\underline{H}$), 7.32–7.55 (5H, m, *Ph*), 7.79 (1H, d *J* 4.0, *PyC5*$\underline{H}$), 8.45 (1H, s, *Ar*$\underline{H}$), 8.67–8.95 (2H, m, *Ar*$\underline{H}$ and *PyC6*$\underline{H}$); δ_C (125 MHz, CD_3OD) 23.9–25.1 (*Pip*$\underline{C}$*5H*$_2$), 31.5 (*Pip*$\underline{C}$*4H*$_2$), 43.4 and 47.9 (*Pip*$\underline{C}$*2H*$_2$ and $\underline{C}$*6H*$_2$), 53.5 (*O*$\underline{C}$*H*$_3$), 58.0 (*Pip*$\underline{C}$*3H*), 120.5, 123.4, 123.9, 128.1 (2 × *Ph*$\underline{C}$*H*), 129.9 (2 × *Ph*$\underline{C}$*H*), 131.4 (*Ph*$\underline{C}$*H*), 136.8, 140.3, 148.2, 151.8 (*Py*$\underline{C}$*6H*), 152.4, 166.7 ($\underline{C}O_2H$), 173.1 ($\underline{C}ON$); *m/z* (MS, ES^+) 392 (100%, MH^+); LCMS (system E) tR 6.8 min (100%); $[\alpha]_D^{20}$ +0. 643 (*c* 0.9 in CH_3OH).

tert-Butyl (3*S*)-3-[(methylsulfonyl)oxy]piperidine-1-carboxylate 223[220]

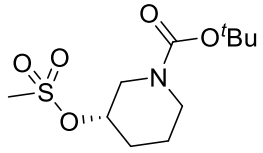

Methanesulfonyl chloride (5.0 mL, 64.6 mmol) was added dropwise over 5 min to a solution of *tert*-butyl (3*S*)-3-hydroxypiperidine-1-carboxylate (10.79 g, 53.6 mmol) and triethylamine (15.0 mL, 108 mmol) in ethyl acetate (100 mL) at –5 °C and the resulting suspension stirred at –5 °C for 1 h. Water was added (100 mL), the mixture allowed to warm to room temperature, the layers separated and the organic layer washed with hydrochloric acid (1 M, aq, 55 mL) followed by sodium hydrogencarbonate (saturated, aq, 100 mL). The organic layer was dried over sodium sulfate and concentrated *in vacuo* to give **223** as a white solid (14.44 g, 96%). mp 92–97 °C; ν_{max} (film) 2975 (C–H), 2937 (C–H), 2866 (C–H), 1687 (C=O); δ_H (400 MHz, $CDCl_3$) 1.43 (9H, s, *C(C*$\underline{H}$*)*$_3$), 1.46–1.82 (2H, m, *PipC5*$\underline{H_2}$), 1.82–1.99 (2H, m, *PipC4*$\underline{H_2}$), 3.03 (3H, s, *SC*$\underline{H_3}$), 3.24–3.48 (2H, m, *PipC6*$\underline{H_2}$), 3.53–3.67 (2H, m, *PipC2*$\underline{H_2}$), 4.64–4.74 (1H, m, *PipC3*$\underline{H}$) [*consistent with lit.*]; δ_C (100 MHz, $CDCl_3$) 21.5 (*Pip*$\underline{C}$*5H*$_2$), 28.2 (*C(*$\underline{C}$*H)*$_3$), 30.3 (*Pip*$\underline{C}$*4H*$_2$), 38.7 (*S*$\underline{C}$*H*$_3$), 42.6–44.6 (*Pip*$\underline{C}$*6H*$_2$), 46.6–48.7 (*Pip*$\underline{C}$*2H*$_2$), 75.3 (*Pip*$\underline{C}$*3H*), 80.0 ($\underline{C}$*(CH)*$_3$), 154.6 ($\underline{C}$*=O*) [*consistent with lit.*]; *m/z* (MS, EI^+) 279 (100%, $[M]^+$); elemental analysis: $C_{11}H_{21}NO_5S$ requires C, 47.3; H, 7.6; N, 5.0%; found C, 47.5; H, 7.7; N, 5.1%; $[\alpha]_D^{20}$ −0.4 (*c* 1.0 in $CHCl_3$) [*consistent with lit.*].

Methyl 2-{1-[(3*R*)-1-(*tert*-butoxycarbonyl)piperidin-3-yl]-1*H*-1,2,3-triazol-4-yl}isonicotinate 224

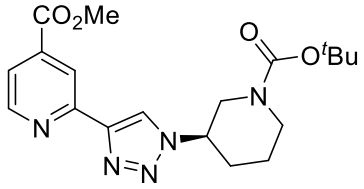

Sodium azide (1.54 g, 23.7 mmol) was added to a solution of *tert*-butyl (3*S*)-3-[(methylsulfonyl)oxy]piperidine-1-carboxylate **223** (3.35 g, 12.0 mmol) in *N*,*N*-dimethylformamide (25 mL) and the resulting suspension heated at 75 °C for 6 h. The reaction mixture was cooled to room temperature then diisopropylethylamine (0.33 mL, 1.89 mmol), copper(I) iodide (180 mg, 0.96 mmol) and a solution of tetrabutylammonium fluoride in tetrahydrofuran (1 M, 12.0 mL, 12.0 mmol) were added. A solution of methyl 2-[(trimethylsilyl)ethynyl]isonicotinate (2.32 g, 9.94 mmol) in *N*,*N*-dimethylformamide (10 mL) was added dropwise over 20 min. The reaction mixture was stirred at room temperature for 16 h then diluted with brine (100 mL) and extracted with ethyl acetate (3 × 100 mL). The organic layers were washed with brine (2 × 100 mL) then combined, dried over sodium sulfate, concentrated *in vacuo* and purified by flash column chromatography (cyclohexane → 55% ethyl acetate in cyclohexane) to give **224** as an orange foam (1.84 g, 48%). R_f 0.50 (3:1 ethyl acetate–cyclohexane); ν_{max} (film) 3154 (C–H), 2955 (C–H), 2928 (C–H), 2868 (C–H), 1726 (C=O, ester), 1683 (C=O, carbamate); δ_H (400 MHz, CD_3OD) 1.44 (9H, s, *C(C*<u>*H*</u>*)₃*), 1.61–1.75 (1H, m, *PipC5*<u>*H*</u>), 1.83–1.95 (1H, m, *PipC5*<u>*H*</u>), 2.19–2.23 (2H, m, *PipC4*<u>*H*</u>*₂*), 3.13–3.28 (1H, m), 3.41–3.56 (1H, m), 3.65–3.94 (2H, m), 3.98 (3H, s, *CO₂C*<u>*H*</u>*₃*), 4.09–4.34 (1H, m), 4.62–4.75 (1H, m, *PipC3*<u>*H*</u>), 7.80 (1H, dd, *J* 5.0, 1.5, *PyC5*<u>*H*</u>), 8.52 (1H, s, *Ar*<u>*H*</u>), 8.58 (1H, s, *Ar*<u>*H*</u>), 8.72 (1H, d, *J* 5.0, *PyC6*<u>*H*</u>); δ_C (100 MHz, CD_3OD) 23.8–24.8 (*PipC*<u>*C*</u>*5H₂*), 28.7 (*C(*<u>*C*</u>*H)₃*), 30.8–31.7 (*PipC*<u>*C*</u>*4H₂*), 44.1–45.6 and 48.4–49.8 (*PipC*<u>*C*</u>*2H₂* and *PipC*<u>*C*</u>*6H₂*), 53.5 (*CO₂*<u>*C*</u>*H₃*), 58.1 (*PipC*<u>*C*</u>*3H*), 81.8 (<u>*C*</u>*(CH)₃*), 120.3 (*Ar*<u>*C*</u>*H*), 123.3 (*PyC*<u>*C*</u>*5H*), 123.7 (*Ar*<u>*C*</u>*H*), 140.2, 148.1, 151.8 (*PyC*<u>*C*</u>*6H*), 152.4, 166.7 (2 × <u>*C*</u>*O₂*); *m/z* (MS, ES^+) 388 (100%, MH^+); LCMS tR 15.4 min (98%); accurate mass: found 410.1785, calc. for $C_{19}H_{25}N_5NaO_4^+$ 410.1799; $[\alpha]_D^{20}$ −0.526 (*c* 1.0 in $CHCl_3$).

Methyl 2-{1-[(3*R*)-piperidin-3-yl]-1*H*-1,2,3-triazol-4-yl}isonicotinate 225

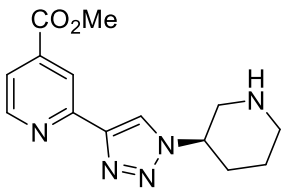

Trifluoroacetic acid (2.0 mL, 25.6 mmol) was added to a solution of methyl 2-{1-[(3*R*)-1-(*tert*-butoxycarbonyl)piperidin-3-yl]-1*H*-1,2,3-triazol-4-yl}isonicotinate **224** (1.10 g, 2.84 mmol) in dichloromethane (4 mL) and the resulting solution stirred at room temperature for 16 h. The reaction mixture was concentrated *in vacuo* then purified on a 10 g strong cation exchange column,

washing with methanol (100 mL) then eluting with methanolic ammonia (2 M, 100 mL) to give **225** as an orange gum (789 mg, 97%). R_f 0.45 (9:1 dichloromethane–2 M methanolic ammonia); ν_{max} (film) 3138 (C–H), 2951 (C–H), 2822 (C–H), 1720 (C=O); δ_H (400 MHz, CD_3OD) 1.65–1.78 (1H, m, *PipC5H*), 1.86–1.94 (1H, m, *PipC5H*), 2.06–2.18 (1H, m, *PipC4H*), 2.29–2.39 (1H, m, *PipC4H*), 2.64–2.75 (1H, m, *PipC6H*), 3.00–3.08 (2H, m, *PipC6H* and *PipC2H*), 3.37–3.44 (1H, m, *PipC2H*), 3.98 (3H, s, CH_3), 4.61–4.70 (1H, m, *PipC3H*), 7.81 (1H, d, *J* 5.0, *PyC5H*), 8.51 (1H, s, *ArH*), 8.56 (1H, s, *ArH*), 8.72 (1H, d, *J* 5.0, *PyC6H*); δ_C (100 MHz, CD_3OD) 26.2 (*PipC5H*$_2$), 32.2 (*PipC4H*$_2$), 46.3 (*PipC6H*$_2$), 52.1 (*PipC2H*$_2$), 53.5 (CH_3), 59.4 (*PipC3H*), 120.4 (*ArCH*), 123.3 (*ArCH*), 123.4 (*PyC5H*), 140.2, 148.1, 151.8 (*PyC6H*), 152.5, 166.7 (CO_2Me); *m/z* (MS, ES^+) 288 (100%, MH^+); LCMS (system E) tR 2.8 min (97%); accurate mass: found 310.1263, calc. for $C_{14}H_{17}N_5NaO_2^+$ 310.1274; $[\alpha]_D^{20}$ +0.004 (*c* 1.0 in CH_3OH).

Methyl 2-{1-[(3*R*)-1-benzoylpiperidin-3-yl]-1*H*-1,2,3-triazol-4-yl}isonicotinate 226

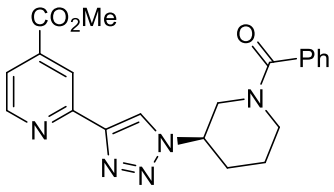

Benzoyl chloride (242 µL, 2.09 mmol) was added to a solution of methyl 2-{1-[(3*R*)-piperidin-3-yl]-1*H*-1,2,3-triazol-4-yl}isonicotinate **225** (599 mg, 2.09 mmol) and triethylamine (0.30 mL, 2.09 mmol) in acetonitrile (15 mL) and the resulting solution stirred at room temperature for 1.5 h. The reaction mixture was diluted with water (20 mL), basified to pH 10 with sodium hydrogencarbonate (saturated, aq) and extracted with dichloromethane (2 × 20 mL). The organic layers were combined, dried over sodium sulfate then concentrated *in vacuo* to give **226** as a beige foam (856 mg, quant.). ν_{max} (film) 2951 (C–H), 2862 (C–H), 1729 (C=O, ester), 1629 (C=O, amide); δ_H (200 MHz, $(CD_3)_2SO$) 1.49–2.00 (2H, m, *PipC5H*$_2$), 2.08–2.40 (2H, m, *PipC4H*$_2$), 3.03–3.85 (3H, m), 3.94 (3H, s, OCH_3), 4.00–4.69 (1H, m), 4.71–4.93 (1H, m, *PipC3H*), 7.35–7.51 (5H, m, *Ph*), 7.78 (1H, dd *J* 5.0, 1.5, *PyC5H*), 8.44 (1H, app. s, *ArH*), 8.74–8.91 (2H, m, *ArH* and *PyC6H*); δ_C (125 MHz, CD_3OD) 23.9–25.1 (*PipC5H*$_2$), 31.4 (*PipC4H*$_2$), 43.3 and 47.7 (*PipC2H*$_2$ and *C6H*$_2$), 53.4 (OCH_3), 58.0 (*PipC3H*), 120.3, 123.2, 123.8, 128.0 (2 × *PhCH*), 129.8 (2 × *PhCH*), 131.3 (*PhCH*), 136.7, 140.1, 148.1, 151.7 (*PyC6H*), 152.2, 166.6 (CO_2H), 173.0 (*CON*); *m/z* (MS, ES^+) 392 (100%, MH^+); LCMS tR 13.5 min (95%); accurate mass: found 414.1525, calc. for $C_{21}H_{21}N_5NaO_3^+$ 414.1537; $[\alpha]_D^{20}$ −0. 659 (*c* 0.9 in CH_3OH).

2-{1-[(3*R*)-1-Benzoylpiperidin-3-yl]-1*H*-1,2,3-triazol-4-yl}isonicotinic acid hemitrifluoroacetate 227

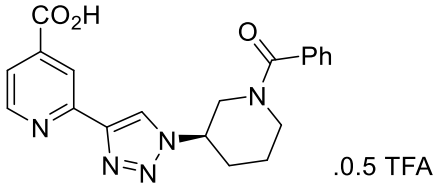

Lithium hydroxide (1 M, aq, 2.0 mL, 2.0 mmol) was added to a solution of methyl 2-{1-[(3*R*)-1-benzoylpiperidin-3-yl]-1*H*-1,2,3-triazol-4-yl}isonicotinate **226** (700 mg, 1.79 mmol) in acetonitrile (10 mL) and the resulting solution stirred at room temperature for 3 h. The reaction mixture was concentrated *in vacuo* and taken up in 10 mL of an 8:2 mixture of water–acetonitrile. 0.4 mL of trifluoroacetic acid was added and the resulting precipitate filtered, washing with water (2 × 10 mL). The precipitate was dried *in vacuo* to give **227** as a white solid (664 mg, 85%). mp 264–250 °C; ν_{max} (film) 2944 (C–H), 2866 (C–H), 2322 (br, OH), 1628 (C=O, amide), 1568 (C=O, acid); δ_H (500 MHz, $(CD_3)_2SO$) 1.58–2.02 (2H, m, *PipC5H*$_2$), 2.17–2.35 (2H, m, *PipC4H*$_2$), 3.07–4.67 (4H, m, *PipC2H*$_2$ and *PipC6H*$_2$), 4.77–4.87 (1H, m, *PipC3H*), 7.35–7.53 (5H, m, *Ph*), 7.77 (1H, app. s, *PyC5H*), 8.44 (1H, s, *ArH*), 8.66–8.92 (2H, m, *ArH* and *PyC6H*); δ_C (125 MHz, $(CD_3)_2SO$) 23.7 (*PipC5H*$_2$), 29.9 (*PipC4H*$_2$), 45.9 and 47.0 (*PipC2H*$_2$ and *PipC6H*$_2$), 55.9 (*PipC3H*), 118.3 (*ArCH*), 121.9 (*PyC5H*), 122.6 (*ArCH*), 126.8 (2 × *PhCH*), 128.5 (2 × *PhCH*), 129.6 (*ipso-Ph* and *PhCH*), 135.8, 139.2, 146.4, 150.8 (*PyC6H*), 166.0 (*CO*$_2$*H*), 169.4 (*CON*); *m/z* (MS, ES$^-$) 376 (100%, $[M–H]^-$); LCMS tR 11.7 min (99%); accurate mass: found 400.1377, calc. for $C_{20}H_{19}N_5O_3Na^+$ 400.1380; elemental analysis: $C_{20}H_{19}N_5O_3$.0.5 $C_2HF_3O_2$ requires C, 58.1; H, 4.5; N, 16.1%; found C, 57.9; H, 4.7; N, 15.8%.

Methyl 2-{1-[(3*R*)-1-benzoylpiperidin-3-yl]-1*H*-1,2,3-triazol-4-yl}isonicotinate 228

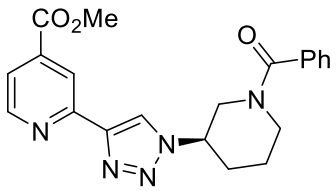

Methyl iodide (13.8 µL, 0.22 mmol) was added to a suspension of 2-{1-[(3*R*)-1-benzoylpiperidin-3-yl]-1*H*-1,2,3-triazol-4-yl}isonicotinic acid hemitrifluoroacetate **227** (87 mg, 0.20 mmol) and sodium hydrogencarbonate (50.7 mg, 0.60 mmol) in *N*,*N*-dimethylformamide (0.9 mL) and the resulting suspension stirred at room temperature for 16 h. Further methyl iodide (13.8 µL, 0.22 mmol) was added and the resulting suspension stirred at room temperature for 16 h. Further methyl iodide (13.8 µL, 0.22 mmol) was added and the resulting suspension stirred at room temperature for 6 h. Ethyl acetate (5 mL) was added and the resulting suspension washed with brine (5 × 5 mL). The aqueous layers were back-extracted with ethyl acetate (5 mL). The organic layers were combined, dried over sodium sulfate, concentrated *in vacuo* and purified by flash column chromatography (dichloromethane → 6% methanol in dichloromethane) to give **228** as an off-

white gum (80 mg, quant.). ν_{max} (film) 2951 (C–H), 2863 (C–H), 1731 (C=O, ester), 1632 (C=O, amide); δ_H (400 MHz, $(CD_3)_2SO$) 1.54–1.98 (2H, m, *PipC5H₂*), 2.14–2.36 (2H, m, *PipC4H₂*), 3.05–3.75 (3H, m), 3.92 (3H, s, *OCH₃*), 4.01–4.70 (1H, m), 4.73–4.88 (1H, m, *PipC3H*), 7.34–7.52 (5H, m, *Ph*), 7.75 (1H, dd *J* 5.0, 1.5, *PyC5H*), 8.43 (1H, app. s, *ArH*), 8.68–8.89 (2H, m, *ArH* and *PyC6H*); δ_C (125 MHz, CD_3OD) 24.2–25.2 (*PipC5H₂*), 31.6 (*PipC4H₂*), 43.4 and 47.9 (*PipC2H₂* and *PipC6H₂*), 53.5 (*OCH₃*), 58.0 (*PipC3H*), 120.4, 123.3, 123.8, 128.1 (2 × *PhCH*), 129.9 (2 × *PhCH*), 131.4 (*PhCH*), 136.8, 140.2, 148.1, 151.8 (*PyC6H*), 152.4, 166.7 (*CO₂H*), 173.1 (*CON*); *m/z* (MS, ES^+) 392 (100%, MH^+); LCMS (system E) tR 6.8 min (99%); $[\alpha]_D^{20}$ −0. 697 (*c* 0.9 in CH_3OH).

Octyl 2-{1-[(3*R*)-1-benzoylpiperidin-3-yl]-1*H*-1,2,3-triazol-4-yl}isonicotinate 229

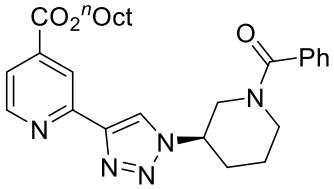

Concentrated sulfuric acid (1 drop) was added to a solution of 2-{1-[(3*R*)-1-benzoylpiperidin-3-yl]-1*H*-1,2,3-triazol-4-yl}isonicotinic acid hemitrifluoroacetate **227** (50 mg, 0.10 mmol) in *n*-octanol (0.8 mL) and the resulting mixture heated at 120 °C for 16 h. The volume was reduced *in vacuo* and the residue purified by flash column chromatography (dichloromethane → 1% 0.4 M ammonia in tetrahydrofuran in ethyl acetate) to give **229** as a colourless gum (9 mg, 14%). R_f 0.35 (ethyl acetate); ν_{max} (film) 2927 (C–H), 2856 (C–H), 1727 (C=O, amide), 1635 (C=O, ester); δ_H (500 MHz, $CDCl_3$) 0.80–0.95 (3H, m, *CH₃*), 1.20–1.50 (10H, m, 5 × *n-OctCH₂*), 1.59–2.08 (4H, m, *PipC5H₂* and *OCH₂CH₂*), 2.19–2.51 (2H, m, *PipC4H₂*), 3.05–3.30 (1H, m, *PipCH*), 3.49–3.60 (1H, m, *PipCH*), 3.72–4.28 (2H, m, 2 × 1H, m, *PipCH*), 4.38 (2H, t, *J* 7.0, *OCH₂CH₂*), 4.55–4.99 (1H, m, *PipC3H*), 7.43 (5H, s, *Ph*), 7.80 (1H, dd, *J* 5.0, 1.5, *PyC5H*), 8.15–8.38 (1H, m, *ArH*), 8.69–8.71 (1H, m, *ArH*), 8.72 (1H, d, *J* 5.0, *PyC6H*); δ_C (125 MHz, $CDCl_3$) 14.1 (*CH₃*), 22.6 (1 × *n-OctCH₂*), 23.2–24.7 (*PipC5H₂*), 25.9 (1 × *n-OctCH₂*), 28.6 (1 × *n-OctCH₂*), 29.1 (1 × *n-OctCH₂*), 29.2 (1 × *n-OctCH₂*), 29.7 (*PipC4H₂*), 31.1 (*OCH₂*), 31.8 (1 × *n-OctCH₂*), 46.8 and 47.7 (*PipC2H₂* and *PipC6H₂*), 56.6 (*PipC3H*), 66.1 (*OCH₂*), 119.5 (*ArCH*), 121.5 (*ArCH*), 122.1 (*PyC5H*), 126.9 (2 × *PhCH*), 128.7 (2 × *PhCH*), 130.1 (*PhCH*), 135.2, 138.9, 147.4, 150.0 (*PyC6H*), 151.0, 165.0 (*C=O*), 170.9 (*C=O*); *m/z* (MS, ES^+) 490 (100%, MH^+); LCMS (system E) tR 7.2 min (100%); accurate mass: found 512.2632, calc. for $C_{28}H_{35}N_5O_3Na^+$ 512.2632; $[\alpha]_D^{20}$ –0.181 (*c* 0.2 in CH_3OH).

Chloromethyl propanoate 243[221]

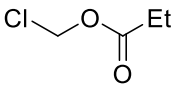

1,3,5-Trioxane (1.8 g, 59.4 mmol) was added to a suspension of propanoyl chloride (5.0 mL, 54 mmol), thionyl chloride (1.5 mL, 20 mmol) and zinc (II) chloride (1.1 g, 8.1 mmol) in chloroform

(20 mL). The reaction mixture was heated at 80 °C for 6 h then poured into ice-water and the resulting mixture stirred for 10 min. The organic layer was washed with water then sodium carbonate and dried over calcium chloride and concentrated *in vacuo* to give **243** as a colourless oil (2.0 g, 48%). δ_H (400 MHz, $CDCl_3$) 1.16 (3H, t, *J* 7.5, $C\underline{H}_3CH_2$), 2.40 (2H, q, *J* 7.5, $CH_3C\underline{H}_2$), 5.69 (2H, s, $OC\underline{H}_2$) [*consistent with lit*].

Chloromethyl 2-methylpropanoate 245[221]

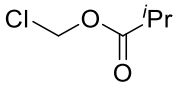

Synthesised as described above for **243** to give **245** as a colourless oil (49%). δ_H (400 MHz, $CDCl_3$) 1.20 (6H, d, *J* 7.0, $CH(C\underline{H}_3)_2$), 2.61 (1H, m, $C\underline{H}(CH_3)_2$), 5.70 (2H, s, $OC\underline{H}_2$) [*consistent with lit.*].

Chloromethyl 3-methylbutanoate 246[222]

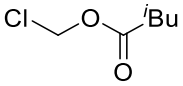

Synthesised as described above for **243** to give **246** as a brown oil (59%). δ_H (400 MHz, $CDCl_3$) 0.96 (6H, d, *J* 7.0, $CH(C\underline{H}_3)_2CH_2$), 2.13 (1H, m, $C\underline{H}(CH_3)_2CH_2$), 2.24 (2H, d, *J* 7.0, $CH(CH_3)_2C\underline{H}_2$), 5.68 (2H, s, $OC\underline{H}_2$) [*consistent with lit.*].

Chloromethyl cyclopentanecarboxylate 248[223]

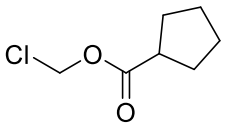

Synthesised as described above for **243** to give **248** as a brown oil (71%). δ_H (400 MHz, $CDCl_3$) 1.56–1.86 (8H, m, 4 × $C\underline{H}_2$), 2.79 (1H, m, $C\underline{H}$), 5.70 (2H, s, $OC\underline{H}_2$) [*consistent with lit.*].

1-Chloroethyl acetate 249[224]

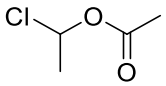

Synthesised as described above for **243** to give **249** as a colourless oil (32%). δ_H (400 MHz, $CDCl_3$) 1.77 (3H, d, *J* 6.0, $C\underline{H}_3CH$), 2.10 (3H, s, $C\underline{H}_3CO_2$), 6.50 (1H, q, *J* 6.0, $CH_3C\underline{H}$) [*consistent with lit.*].

1-Chloroethyl propionate 250[221]

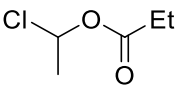

Synthesised as described above for **243** to give **250** as a colourless oil (28%). δ_H (400 MHz, $CDCl_3$) 1.17 (3H, t, *J* 7.5, $C\underline{H}_3CH_2$), 1.79 (3H, d, *J* 6.0, $CH_3C\underline{H}$), 2.39 (2H, q, *J* 7.5, $CH_3C\underline{H}_2$), 6.56 (1H, q, *J* 6.0, $CH_3C\underline{H}$) [*consistent with lit.*].

1-Chloro-2-methylpropyl propionate 251[221]

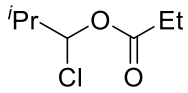

Synthesised as described above for **243** to give **251** as a colourless oil (46%). δ_H (400 MHz, $CDCl_3$) 1.03–1.06 (6H, m, *CH(CH*$_3$*)*$_2$), 1.17 (3H, t, *J* 7.5, *CH*$_3$*CH*$_2$), 2.15 (1H, m, *CH(CH*$_3$*)*$_2$), 2.40 (2H, q, *J* 7.5, *CH*$_3$*CH*$_2$), 6.30 (1H, d, *J* 4.5, *CHCO*) [*consistent with lit.*].

(Acetyloxy)methyl 2-{1-[(3*R*)-1-benzoylpiperidin-3-yl]-1*H*-1,2,3-triazol-4-yl}isonicotinate 252

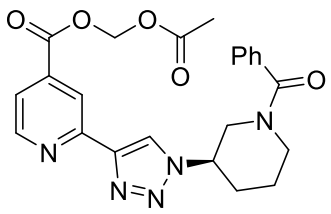

Chloromethyl acetate (15 µL, 0.16 mmol) was added to a solution of 2-{1-[(3*R*)-1-benzoylpiperidin-3-yl]-1*H*-1,2,3-triazol-4-yl}isonicotinic acid hemitrifluoroacetate **227** (50 mg, 0.10 mmol) and triethylamine (41 µL, 0.29 mmol) in *N*,*N*-dimethylformamide (0.5 mL) and the resulting mixture stirred at room temperature for 16 h. Further chloromethyl acetate (15 µL, 0.16 mmol) was added and the reaction mixture stirred at room temperature for 2.5 h. The volatile components were removed *in vacuo* and the residue purified by flash column chromatography (35% → 80% ethyl acetate in dichloromethane) to give **252** as a colourless gum (33 mg, 73%). R_f 0.40 (ethyl acetate); ν_{max} (film) 3062 (C–H), 2946 (C–H), 2865 (C–H), 1748 (C=O, amide), 1632 (C=O, ester); δ_H (400 MHz, $CDCl_3$) 1.58–2.07 (2H, m, *PipC5H*$_2$), 2.16 (3H, s, *CH*$_3$), 2.21–2.51 (2H, m, *PipC4H*$_2$), 3.02–4.32 (4H, m, *PipC2H*$_2$ and *PipC6H*$_2$), 4.51–4.79 (1H, m, *PipC3H*), 6.02 (2H, s, *CH*$_2$*O*), 7.42 (5H, s, *Ph*), 7.80 (1H, dd, *J* 5.0, 1.5, *PyC5H*), 8.14–8.38 (1H, m, *ArH*), 8.71 (1H, s, *ArH*), 8.74 (1H, d, *J* 5.0, *PyC6H*); δ_C (100 MHz, $CDCl_3$) 20.5 (*CH*$_3$), 24.1 (*PipC5H*$_2$), 30.8 (*PipC4H*$_2$), 46.6 and 47.6 (*PipC2H*$_2$ and *PipC6H*$_2$), 56.4 (*PipC3H*), 79.9 (*CH*$_2$*O*), 119.4 (*ArCH*), 121.4 (*ArCH*), 121.9 (*PyC5H*), 126.8 (2 × *PhCH*), 128.5 (2 × *PhCH*), 129.9 (*PhCH*), 135.1, 137.2, 147.1, 150.2 (*PyC6H*), 151.2, 163.6 (*C*=*O*), 169.3 (*C*=*O*), 170.6 (*C*=*O*); *m/z* (MS, ES^+) 472 (100%, MNa^+); LCMS tR 13.8 min (97%); accurate mass: found 472.1583, calc. for $C_{23}H_{23}N_5NaO_5^+$ 472.1591; $[\alpha]_D^{20}$ –0.681 (*c* 1.0 in $CHCl_3$).

(Propanoyloxy)methyl 2-{1-[(3*R*)-1-benzoylpiperidin-3-yl]-1*H*-1,2,3-triazol-4-yl}isonicotinate 253

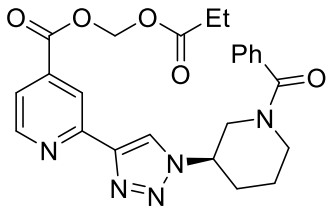

Chloromethyl propionate **243** (20 mg, 0.16 mmol) was added to a solution of 2-{1-[(3*R*)-1-benzoylpiperidin-3-yl]-1*H*-1,2,3-triazol-4-yl}isonicotinic acid hemitrifluoroacetate **227** (50 mg, 0.10 mmol) and triethylamine (41 µL, 0.29 mmol) in *N*,*N*-dimethylformamide (0.5 mL) and the resulting mixture stirred at room temperature for 16 h. The volatile components were removed *in vacuo* and the residue purified by flash column chromatography (35% → 80% ethyl acetate in dichloromethane) to give **253** as a colourless gum (16 mg, 34%). R_f 0.45 (ethyl acetate); ν_{max} (film) 2986 (C–H), 2944 (C–H), 2866 (C–H), 1750 (C=O, amide), 1633 (C=O, ester); δ_H (400 MHz, $CDCl_3$) 1.18 (3H, t, *J* 8.0, *C*$\underline{H}_3$*C*H_2), 1.60–2.13 (2H, m, *PipC5*$\underline{H}_2$), 2.21–2.49 (2H, m, *PipC4*$\underline{H}_2$), 2.44 (2H, q, *J* 8.0, *CH*$_3$*C*$\underline{H}_2$), 3.03–4.33 (4H, m, *PipC2*$\underline{H}_2$ and *PipC6*$\underline{H}_2$), 4.55–4.75 (1H, m, *PipC3*$\underline{H}$), 7.42 (5H, s, *Ph*), 7.81 (1H, dd, *J* 5.0, 2.0, *PyC5*$\underline{H}$), 8.13–8.38 (1H, m, *Ar*$\underline{H}$), 8.69–8.77 (2H, m, *Ar*$\underline{H}$ and *PyC6*$\underline{H}$); δ_C (125 MHz, $CDCl_3$) 8.6 (*C*$\underline{H}_3$*C*H_2), 23.3–24.8 (*Pip*$\underline{C}$*5*H_2), 27.2 (*CH*$_3$$\underline{C}$*H*$_2$), 31.0 (*Pip*$\underline{C}$*4*$H_2$), 46.5–48.3 (*Pip*$\underline{C}$*2*$H_2$ and *Pip*$\underline{C}$*6*H_2), 56.2–57.5 (*Pip*$\underline{C}$*3H*), 80.1 ($\underline{C}$*H*$_2$*O*), 119.9 (*Ar*$\underline{C}$*H*), 121.7 (*Ar*$\underline{C}$*H*), 122.2 (*Py*$\underline{C}$*5H*), 126.9 (2 × *Ph*$\underline{C}$*H*), 128.7 (2 × *Ph*$\underline{C}$*H*), 130.1 (*Ph*$\underline{C}$*H*), 135.1, 137.7, 146.9, 150.0 (*Py*$\underline{C}$*6H*), 151.1, 163.7 ($\underline{C}$*=O*), 170.9 ($\underline{C}$*=O*), 172.9 ($\underline{C}$*=O*); *m/z* (MS, ES^+) 486 (100%, MNa^+); LCMS tR 14.7 min (99%); accurate mass: found 486.1742, calc. for $C_{24}H_{25}N_5O_5Na^+$ 486.1748; $[\alpha]_D^{20}$ –0.414 (*c* 0.35 in $CHCl_3$).

(Butanoyloxy)methyl 2-{1-[(3*R*)-1-benzoylpiperidin-3-yl]-1*H*-1,2,3-triazol-4-yl}isonicotinate 254

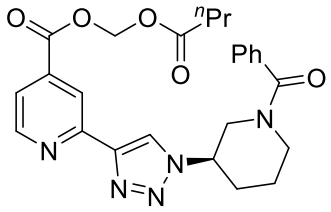

Chloromethyl butyrate (20 µL, 0.16 mmol) was added to a solution of 2-{1-[(3*R*)-1-benzoylpiperidin-3-yl]-1*H*-1,2,3-triazol-4-yl}isonicotinic acid hemitrifluoroacetate **227** (50 mg, 0.10 mmol) and triethylamine (41 µL, 0.29 mmol) in *N*,*N*-dimethylformamide (0.5 mL) and the resulting mixture stirred at room temperature for 16 h. Further chloromethyl butyrate (20 µL, 0.16 mmol) was added and the reaction mixture stirred at room temperature for 2.5 h. The volatile components were removed *in vacuo* and the residue purified by flash column chromatography (35% → 80% ethyl acetate in dichloromethane) to give **254** as a colourless gum (38 mg, 79%). R_f 0.50 (ethyl acetate); ν_{max} (film) 2964 (C–H), 2938 (C–H), 2874 (C–H), 1748 (C=O, amide), 1632

(C=O, ester); δ_H (400 MHz, $CDCl_3$) 0.85–1.04 (2 H, m), 0.96 (2H, t, *J* 7.5, *C*$\underline{H_3}$), 1.60–1.76 (2H, m, *CH*$_3$*C*$\underline{H_2}$*CH*$_2$), 1.82–2.11 (2H, m, *PipC5*$\underline{H_2}$), 2.19–2.49 (5H, m, *CH*$_3$*CH*$_2$*C*$\underline{H_2}$ and *PipC4*$\underline{H_2}$), 3.00–4.36 (4H, m, *PipC2*$\underline{H_2}$ and *PipC6*$\underline{H_2}$), 6.04 (2H, s, *C*$\underline{H_2}$*O*), 7.37–7.47 (5H, m, *Ph*), 7.80 (1H, dd, *J* 5.0, 1.5, *PyC5*$\underline{H}$), 8.11–8.45 (1H, m, *Ar*$\underline{H}$), 8.62–8.83 (2H, m, *Ar*$\underline{H}$ and *PyC6*$\underline{H}$); δ_C (125 MHz, $CDCl_3$) 13.3 (*C*$\underline{H_3}$), 17.9 (*CH*$_3$*C*$\underline{H_2}$*CH*$_2$), 24.2 (*Pip*$\underline{C}$*5H*$_2$), 30.9 (*Pip*$\underline{C}$*4H*$_2$), 35.6 (*CH*$_3$*CH*$_2$*C*$\underline{H_2}$), 46.5–47.8 (*Pip*$\underline{C}$*2H*$_2$ and *Pip*$\underline{C}$*6H*$_2$), 56.5 (*Pip*$\underline{C}$*3H*), 79.9 (*C*$\underline{H_2}$*O*), 119.5 (*Ar*$\underline{C}$*H*), 121.4 (*Ar*$\underline{C}$*H*), 122.0 (*Py*$\underline{C}$*5H*), 126.8 (2 × *Ph*$\underline{C}$*H*), 128.5 (2 × *Ph*$\underline{C}$*H*), 130.0 (*Ph*$\underline{C}$*H*), 135.1, 137.3, 147.1, 150.2 (*Py*$\underline{C}$*6H*), 151.2, 163.7 (*C*$\underline{}$*=O*), 170.7 (*C*$\underline{}$*=O*), 172.0 (*C*$\underline{}$*=O*); *m/z* (MS, ES^+) 500 (100%, MNa^+); LCMS tR 15.6 min (99%); accurate mass: found 500.1909, calc. for $C_{25}H_{27}N_5O_5Na^+$ 500.1904; $[\alpha]_D^{20}$ –0.731 (*c* 1.0 in $CHCl_3$).

(Isobutyryloxy)methyl 2-{1-[(3*R*)-1-benzoylpiperidin-3-yl]-1*H*-1,2,3-triazol-4-yl}isonicotinate 255

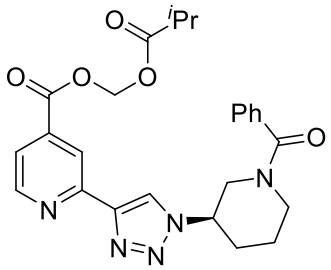

Chloromethyl 2-methylpropanoate **245** (22 mg, 0.16 mmol) was added to a solution of 2-{1-[(3*R*)-1-benzoylpiperidin-3-yl]-1*H*-1,2,3-triazol-4-yl}isonicotinic acid hemitrifluoroacetate **227** (50 mg, 0.10 mmol) and triethylamine (41 µL, 0.29 mmol) in *N*,*N*-dimethylformamide (0.5 mL) and the resulting mixture stirred at room temperature for 16 h. The volatile components were removed *in vacuo* and the residue purified by flash column chromatography (35% → 80% ethyl acetate in dichloromethane) to give **255** as a colourless gum (38 mg, 60%). R_f 0.50 (ethyl acetate); ν_{max} (film) 2977 (C–H), 2939 (C–H), 2874 (C–H), 1752 (C=O, ester), 1633 (C=O, amide); δ_H (400 MHz, $CDCl_3$) 1.20 (6H, d, *J* 7.0, *(C*$\underline{H_3}$*)*$_2$*CH*), 1.59–2.11 (2H, m, *PipC5*$\underline{H_2}$), 2.19–2.49 (2H, m, *PipC4*$\underline{H_2}$), 2.64 (1H, spt, *J* 7.0, *(CH*$_3$*)*$_2$*C*$\underline{H}$), 2.99–4.37 (4H, m, *PipC2*$\underline{H_2}$ and *PipC6*$\underline{H_2}$), 4.49–4.77 (1H, m, *PipC3*$\underline{H}$), 6.04 (2H, s, *C*$\underline{H_2}$*O*), 7.42 (5H, s, *Ph*), 7.80 (1H, dd, *J* 5.0, 1.5, *PyC5*$\underline{H}$), 8.12–8.39 (1H, m, *Ar*$\underline{H}$), 8.65–8.79 (2H, m, *Ar*$\underline{H}$ and *PyC6*$\underline{H}$); δ_C (125 MHz, $CDCl_3$) 18.6 (*(*$\underline{C}$*H*$_3$*)*$_2$*CH*) 23.3–24.7 *Pip*$\underline{C}$*5H*$_2$), 31.0 (*Pip*$\underline{C}$*4H*$_2$), 33.7 (*(CH*$_3$*)*$_2$$\underline{C}$*H*), 46.2–48.2 (*Pip*$\underline{C}$*2H*$_2$ and *Pip*$\underline{C}$*6H*$_2$), 56.1–57.6 (*Pip*$\underline{C}$*3H*), 80.2 (*C*$\underline{H_2}$*O*), 119.7 (*Ar*$\underline{C}$*H*), 121.6 (*Ar*$\underline{C}$*H*), 122.1 (*Py*$\underline{C}$*5H*), 126.9 (2 × *Ph*$\underline{C}$*H*), 128.6 (2 × *Ph*$\underline{C}$*H*), 130.1 (*Ph*$\underline{C}$*H*), 135.1, 137.5, 147.2, 150.2 (s), 151.3 (*Py*$\underline{C}$*6H*), 163.7 (*C*$\underline{}$*=O*), 170.9 (*C*$\underline{}$*=O*), 175.5 (*C*$\underline{}$*=O*); *m/z* (MS, ES^+) 478 (100%, MH^+); LCMS tR 15.6 min (99%); accurate mass: found 500.1898, calc. for $C_{25}H_{27}N_5O_5Na^+$ 500.1904; $[\alpha]_D^{20}$ −0.319 (*c* 0.5 in CH_3OH).

[(3-Methylbutanoyl)oxy]methyl 2-{1-[(3*R*)-1-benzoylpiperidin-3-yl]-1*H*-1,2,3-triazol-4-yl} isonicotinate 256

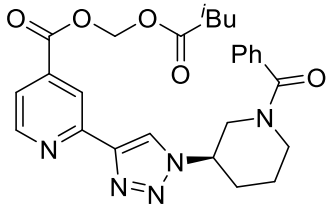

Chloromethyl 3-methylbutanoate **246** (24 mg, 0.16 mmol) was added to a solution of 2-{1-[(3*R*)-1-benzoylpiperidin-3-yl]-1*H*-1,2,3-triazol-4-yl}isonicotinic acid hemitrifluoroacetate **227** (50 mg, 0.10 mmol) and triethylamine (41 µL, 0.29 mmol) in *N*,*N*-dimethylformamide (0.5 mL) and the resulting mixture stirred at room temperature for 16 h. The volatile components were removed *in vacuo* and the residue purified by flash column chromatography (50% → 100% ethyl acetate in dichloromethane) to give **256** as a colourless gum (34 mg, 71%). R_f 0.50 (ethyl acetate); ν_{max} (film) 2959 (C–H), 2872 (C–H), 1748 (C=O, amide), 1632 (C=O, ester); δ_H (500 MHz, $CDCl_3$) 0.96 (6H, d, *J* 6.9, *(C<u>H</u>₃)₂CHCH₂*), 1.60–1.97 (2H, m, *PipC5<u>H</u>₂*), 2.09–2.18 (1 H, m, *(CH₃)₂C<u>H</u>CH₂*), 2.24–2.48 (4H, m *PipC4<u>H</u>₂* and *(CH₃)₂CHC<u>H</u>₂*), 3.02–4.31 (4H, m, *PipC2<u>H</u>₂* and *PipC6<u>H</u>₂*), 4.55–4.74 (1H, m, *PipC3<u>H</u>*), 6.03 (2H, s, *C<u>H</u>₂O*), 7.41 (5H, s, *Ph*), 7.79 (1H, dd, *J* 5.0, 1.5, *PyC5<u>H</u>*), 8.13–8.36 (1H, m, *Ar<u>H</u>*), 8.70 (1H, s, *Ar<u>H</u>*), 8.73 (1H, d, *J* 5.0, *PyC6<u>H</u>*); δ_C (125 MHz, $CDCl_3$) 22.2 (*(<u>C</u>H₃)₂CHCH₂*), 24.3 (*Pip<u>C</u>5H₂*), 25.4 (*(CH₃)₂<u>C</u>HCH₂*), 31.0 (*Pip<u>C</u>4H₂*), 42.8 (*(CH₃)₂CH<u>C</u>H₂*), 46.8 and 47.6 (*Pip<u>C</u>2H₂* and *Pip<u>C</u>6H₂*), 56.6 (*Pip<u>C</u>3H*), 79.9 (*<u>C</u>H₂O*), 119.6 (*Ar<u>C</u>H*), 121.5 (*Ar<u>C</u>H*), 122.0 (*Py<u>C</u>5H*), 126.9 (2 × *Ph<u>C</u>H*), 128.6 (2 × *Ph<u>C</u>H*), 130.1 (*Ph<u>C</u>H*), 135.1, 137.4, 147.2, 150.2 (*Py<u>C</u>6H*), 151.3, 163.7 (*<u>C</u>=O*), 170.8 (*<u>C</u>=O*), 171.4 (*<u>C</u>=O*); *m/z* (MS, ES^+) 492 (100%, MH^+); LCMS (system E) tR 5.7 min (100%); accurate mass: found 514.2046, calc. for $C_{26}H_{29}N_5O_5Na^+$ 514.2061; $[\alpha]_D^{20}$ –0.614 (*c* 1.0 in $CHCl_3$).

[(2,2-Dimethylpropanoyl)oxy]methyl 2-{1-[(3*R*)-1-benzoylpiperidin-3-yl]-1*H*-1,2,3-triazol-4-yl} isonicotinate 257

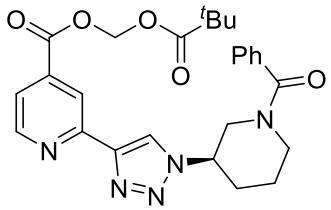

Chloromethyl pivalate (23 µL, 0.16 mmol) was added to a solution of 2-{1-[(3*R*)-1-benzoylpiperidin-3-yl]-1*H*-1,2,3-triazol-4-yl}isonicotinic acid hemitrifluoroacetate **227** (50 mg, 0.10 mmol) and triethylamine (41 µL, 0.29 mmol) in *N*,*N*-dimethylformamide (0.5 mL) and the resulting mixture stirred at room temperature for 16 h. The volatile components were removed *in vacuo* and the residue purified by flash column chromatography (50% → 100% ethyl acetate in dichloromethane) to give **257** as a white solid (34 mg, 69%). R_f 0.50 (ethyl acetate); mp 56–62 °C; ν_{max} (film) 2974 (C–H), 2872 (C–H), 1750 (C=O, amide), 1632 (C=O, ester); δ_H (500 MHz, $CDCl_3$)

1.23 (9H, s, *(C<u>H</u>3)3C*), 1.60–2.00 (2H, m, *PipC5<u>H</u>2*), 2.19–2.48 (2H, m, *PipC4<u>H</u>2*), 3.01–4.29 (4H, m, *PipC2<u>H</u>2* and *PipC6<u>H</u>2*), 4.52–4.75 (1H, m, *PipC3<u>H</u>*), 6.03 (2H, s, *C<u>H</u>2O*), 7.41 (5H, s, *Ph*), 7.79 (1H, dd, *J* 5.0, 1.5, *PyC5<u>H</u>*), 8.12–8.38 (1H, m, *Ar<u>H</u>*), 8.70 (1H, s, *Ar<u>H</u>*), 8.73 (1H, d, *J* 5.0, *PyC6<u>H</u>*); δ_C (125 MHz, $CDCl_3$) 24.3 (*Pip<u>C</u>5H2*), 26.8 (*(<u>C</u>H3)3C*), 31.0 (*Pip<u>C</u>4H2*), 38.8 (*(CH3)3<u>C</u>*), 46.8 and 47.6 (*Pip<u>C</u>2H2* and *Pip<u>C</u>6H2*), 56.5 (*Pip<u>C</u>3H*), 80.4 (*<u>C</u>H2O*), 119.7 (*Ar<u>C</u>H*), 121.5 (*Ar<u>C</u>H*), 122.1 (*Py<u>C</u>5H*), 126.9 (2 × *Ph<u>C</u>H*), 128.6 (2 × *Ph<u>C</u>H*), 130.1 (*Ph<u>C</u>H*), 135.1, 137.4, 147.2, 150.2 (*Py<u>C</u>6H*), 151.2, 163.7 (*<u>C</u>=O*), 170.8 (*<u>C</u>=O*), 176.9 (*<u>C</u>=O*); *m/z* (MS, ES^+) 492 (100%, MH^+); LCMS (system E) tR 5.7 min (99%); accurate mass: found 514.2059, calc. for $C_{26}H_{29}N_5O_5Na^+$ 514.2061; $[\alpha]_D^{20}$ –0.704 (*c* 1.0 in $CHCl_3$).

[(Cyclopentylcarbonyl)oxy]methyl 2-{1-[(3*R*)-1-benzoylpiperidin-3-yl]-1*H*-1,2,3-triazol-4-yl}isonicotinate 258

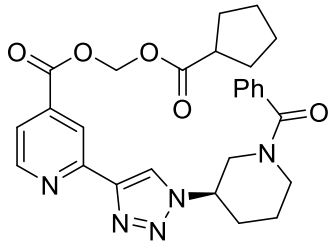

Chloromethyl cyclopentanecarboxylate **248** (26 mg, 0.16 mmol) was added to a solution of 2-{1-[(3*R*)-1-benzoylpiperidin-3-yl]-1*H*-1,2,3-triazol-4-yl}isonicotinic acid hemitrifluoroacetate **227** (50 mg, 0.10 mmol) and triethylamine (41 µL, 0.29 mmol) in *N*,*N*-dimethylformamide (0.5 mL) and the resulting mixture stirred at room temperature for 16 h. The volatile components were removed *in vacuo* and the residue purified by flash column chromatography (50% → 100% ethyl acetate in dichloromethane) to give **258** as a colourless gum (33 mg, 65%). R_f 0.50 (ethyl acetate); ν_{max} (film) 2953 (C–H), 2871 (C–H), 1750 (C=O, amide), 1633 (C=O, ester); δ_H (500 MHz, $CDCl_3$) 1.54–1.76 (4H, m, 2 × *cyclopentyl C<u>H</u>2*), 1.77–2.13 (6H, m, 2 × *cyclopentyl C<u>H</u>2* and *PipC5<u>H</u>2*), 2.20–2.49 (2H, m, *PipC4<u>H</u>2*), 2.82 (1H, quin, *J* 8.0, *cyclopentyl C<u>H</u>*), 3.00–4.32 (4H, m, *PipC2<u>H</u>2* and *PipC6<u>H</u>2*), 4.54–4.76 (1H, m, *PipC3<u>H</u>*), 6.04 (2H, s, *C<u>H</u>2O*), 7.42 (5H, s, *Ph*), 7.81 (1H, dd, *J* 5.0, 1.5, *PyC5<u>H</u>*), 8.11–8.42 (1H, m, *Ar<u>H</u>*), 8.72 (1H, s, *Ar<u>H</u>*), 8.74 (1H, d, *J* 5.0, *PyC6<u>H</u>*); δ_C (125 MHz, $CDCl_3$) 24.4 (*Pip<u>C</u>5H2*), 25.8 (2 × *cyclopentyl <u>C</u>H2*), 29.8 (2 × *cyclopentyl <u>C</u>H2*), 31.0 (*Pip<u>C</u>4H2*), 43.4 (*cyclopentyl <u>C</u>H*), 46.8 and 47.7 (*Pip<u>C</u>2H2* and *Pip<u>C</u>6H2*), 56.6 (*Pip<u>C</u>3H*), 80.2 (*<u>C</u>H2O*), 119.7 (*Ar<u>C</u>H*), 121.6 (*Ar<u>C</u>H*), 122.1 (*Py<u>C</u>5H*), 126.9 (2 × *Ph<u>C</u>H*), 128.6 (2 × *Ph<u>C</u>H*), 130.1 (*Ph<u>C</u>H*), 135.1, 137.5, 147.2, 150.2 (*Py<u>C</u>6H*), 151.2, 163.7 (*<u>C</u>=O*), 170.9 (*<u>C</u>=O*), 175.2 (*<u>C</u>=O*); *m/z* (MS, ES^+) 504 (100%, MH^+); LCMS (system E) tR 5.8 min (100%); accurate mass: found 526.2059, calc. for $C_{27}H_{29}N_5O_5Na^+$ 526.2061; $[\alpha]_D^{20}$ –0.688 (*c* 1.0 in $CHCl_3$).

1-(Acetyloxy)ethyl 2-{1-[(3*R*)-1-benzoylpiperidin-3-yl]-1*H*-1,2,3-triazol-4-yl} isonicotinate 259

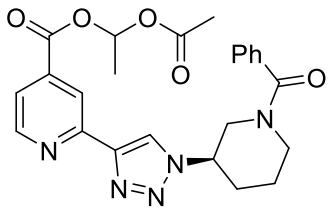

1-Chloroethyl acetate **249** (20 mg, 0.16 mmol) was added to a solution of 2-{1-[(3*R*)-1-benzoylpiperidin-3-yl]-1*H*-1,2,3-triazol-4-yl}isonicotinic acid hemitrifluoroacetate **227** (50 mg, 0.10 mmol) and triethylamine (41 µL, 0.29 mmol) in *N*,*N*-dimethylformamide (0.5 mL) and the resulting mixture stirred at room temperature for 16 h. The volatile components were removed *in vacuo* and the residue purified by flash column chromatography (50% → 100% ethyl acetate in dichloromethane) to give **259** as a colourless gum (11 mg, 64%). R_f 0.40 (ethyl acetate); ν_{max} (film) 2862 (C–H), 1761 (C=O, amide), 1633 (C=O, ester); δ_H (500 MHz, $CDCl_3$) 1.65 (3H, d, *J* 5.5, *C*H$_3$*CHO*), 1.68–1.98 (2H, m, *PipC5*H$_2$), 2.13 (3H, s, *C*H$_3$*CO*$_2$), 2.20–2.52 (2H, m, *PipC4*H$_2$), 2.98–4.33 (4H, m, *PipC2*H$_2$ and *PipC6*H$_2$), 4.51–4.78 (1 H, m, *PipC3*H), 7.14 (1H, d, *J* 5.5, *CH*$_3$*C*H*O*), 7.43 (5H, s, *Ph*), 7.81 (1H, dd, *J* 5.0, 1.5, *PyC5*H), 8.12–8.40 (1H, m, *Ar*H), 8.69 (1H, s, *Ar*H), 8.74 (1H, d, *J* 5.0, *PyC6*H); δ_C (125 MHz, $CDCl_3$) 19.6 (*C*H$_3$*CHO*), 20.8 (*C*H$_3$*CO*$_2$), 24.4 (*PipC5*H$_2$), 31.0 (*PipC4*H$_2$), 46.9 and 47.7 (*PipC2*H$_2$ and *PipC6*H$_2$), 56.6 (*PipC3*H), 89.5 (*CH*$_3$*C*H*O*), 119.6 (*ArC*H), 121.4 (*ArC*H), 122.2 (*PyC5*H), 126.9 (2 × *PhC*H), 128.7 (2 × *PhC*H), 130.1 (*PhC*H), 135.2, 137.8, 147.4, 150.2 (*PyC6*H), 151.2, 163.0 (*C*=*O*), 168.9 (*C*=*O*), 170.9 (*C*=*O*); *m/z* (MS, ES^+) 464 (100%, MH^+); LCMS (system E) tR 5.0 min (99%); accurate mass: found 486.1744, calc. for $C_{24}H_{25}N_5O_5Na^+$ 486.1748; $[\alpha]_D^{20}$ –0.313 (*c* 0.4 in $CHCl_3$).

1-(Propanoyloxy)ethyl 2-{1-[(3*R*)-1-benzoylpiperidin-3-yl]-1*H*-1,2,3-triazol-4-yl} isonicotinate 260

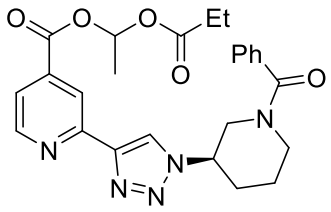

1-Chloroethyl propanoate **250** (22 mg, 0.16 mmol) was added to a solution of 2-{1-[(3*R*)-1-benzoylpiperidin-3-yl]-1*H*-1,2,3-triazol-4-yl}isonicotinic acid hemitrifluoroacetate **227** (50 mg, 0.10 mmol) and triethylamine (41 µL, 0.29 mmol) in *N*,*N*-dimethylformamide (0.5 mL) and the resulting mixture stirred at room temperature for 16 h. The volatile components were removed *in vacuo* and the residue purified by flash column chromatography (50% → 100% ethyl acetate in dichloromethane) to give **260** as a colourless gum (34 mg, 71%). R_f 0.50 (ethyl acetate); ν_{max} (film) 2984 (C–H), 2942 (C–H), 2866 (C–H), 1755 (C=O, amide), 1633 (C=O, ester); δ_H (500 MHz, $CDCl_3$) 1.16 (3H, t, *J* 7.6, *C*H$_3$*CH*$_2$), 1.65 (3H, d, *J* 5.5, *C*H$_3$*CHO*), 1.67–1.99 (2H, m, *PipC5*H$_2$),

2.20–2.50 (4H, m *PipC4H*$_2$ and *CH*$_3$*CH*$_2$), 3.02–4.31 (4H, m, *PipC2H*$_2$ and *PipC6H*$_2$), 4.58–4.76 (1 H, m, *PipC3H*), 7.16 (1H, d, *J* 5.5, *CH*$_3$*CHO*), 7.43 (5H, s, *Ph*), 7.81 (1H, dd, *J* 5.0, 1.5, *PyC5H*), 8.13–8.41 (1H, m, *ArH*), 8.70 (1H, s, *ArH*), 8.74 (1H, d, *J* 5.0, *PyC6H*); δ_C (125 MHz, $CDCl_3$) 8.7 (*CH*$_3$*CH*$_2$), 19.6 (*CH*$_3$*CHO*), 24.4 (*PipC5H*$_2$), 27.3 (*CH*$_3$*CO*$_2$), 31.0 (*PipC4H*$_2$), 46.8 and 47.7 (*PipC2H*$_2$ and *PipC6H*$_2$), 56.6 (*PipC3H*), 89.5 (*CH*$_3$*CHO*), 119.6 (*ArCH*), 122.3 (*ArCH*), 126.9 (*PyC5H*), 128.7 (2 × *PhCH*), 130.1 (2 × *PhCH*), 135.2, 137.9, 147.3, 150.1 (*PyC6H*), 151.1, 163.0 (*C=O*), 170.9 (*C=O*), 172.4 (*C=O*); *m/z* (MS, ES^+) 478 (100%, MH^+); LCMS (system E) tR 5.3 min (100%); accurate mass: found 500.1905, calc. for $C_{25}H_{27}N_5O_5Na^+$ 500.1904; $[\alpha]_D^{20}$ –0.309 (*c* 0.5 in $CHCl_3$).

2-Methyl-1-(propionyloxy)propyl 2-{1-[(3*R*)-1-benzoylpiperidin-3-yl]-1*H*-1,2,3-triazol-4-yl}isonicotinate 261

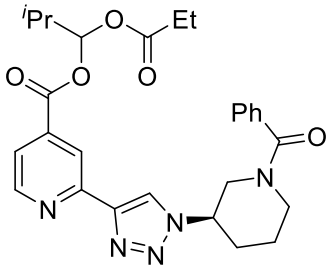

1-Chloro-2-methylpropyl propionate **251** (90 mg, 0.55 mmol) was added to a solution of 2-{1-[(3*R*)-1-benzoylpiperidin-3-yl]-1*H*-1,2,3-triazol-4-yl}isonicotinic acid hemitrifluoroacetate **227** (50 mg, 0.10 mmol) and triethylamine (41 µL, 0.29 mmol) in *N*,*N*-dimethylformamide (0.5 mL) and the resulting mixture stirred at 100 °C for 16 h. The volatile components were removed *in vacuo* and the residue purified by flash column chromatography (50% → 100% ethyl acetate in dichloromethane) to give **261** as a colourless oil (16 mg, 32%). R_f 0.50 (ethyl acetate); ν_{max} (film) 2977 (C–H), 2940 (C–H), 2879 (C–H), 1758 (C=O, amide), 1636 (C=O, ester); δ_H (400 MHz, $CDCl_3$) 1.07 (6H, d, *J* 7.0, *(CH*$_3$*)*$_2$*CHCH*), 1.16 (3H, t, *J* 7.5, *CH*$_3$*CH*$_2$), 1.62–2.07 (2H, m, *PipC5H*$_2$), 2.14–2.50 (5H, m, *PipC4H*$_2$, *(CH*$_3$*)*$_2$*CHCH* and *CH*$_3$*CH*$_2$), 3.02–4.38 (4H, m, *PipC2H*$_2$ and *PipC6H*$_2$), 4.53–4.77 (1H, m, *PipC3H*), 6.92 (1H, d, *J* 5.5, *(CH*$_3$*)*$_2$*CHCH*), 7.42 (5H, s, *Ph*), 7.81 (1H, dd, *J* 5.0, 1.5, *PyC5H*), 8.13–8.40 (1H, m, *ArH*), 8.68 (1H, s, *ArH*), 8.74 (1H, d, *J* 5.0, *PyC6H*); δ_C (125 MHz, $CDCl_3$) 8.8 (*CH*$_3$*CH*$_2$), 16.4 and 16.5 (*(CH*$_3$*)*$_2$*CHCH*), 23.4–24.6 (*PipC5H*$_2$), 27.3 (*CH*$_3$*CH*$_2$), 31.0 (*PipC4H*$_2$), 31.7 (*(CH*$_3$*)*$_2$*CHCH*), 46.6–48.0 (*PipC2H*$_2$ and *PipC6H*$_2$), 56.3–57.4 (*PipC3H*), 93.8 (*(CH*$_3$*)*$_2$*CHCH*), 119.6 (*ArCH*), 121.7 (*ArCH*), 122.3 (*PyC5H*), 126.9 (2 × *PhCH*), 128.6 (2 × *PhCH*), 130.1 (*PhCH*), 135.1, 138.0, 147.2, 150.0 (*PyC6H*), 151.1, 162.5 and 163.1 (*C=O*), 170.9 (*C=O*), 172.6 (*C=O*); *m/z* (MS, ES^+) 506 (100%, MH^+); LCMS (system E) tR 5.9 min (99%); accurate mass: found 528.2228, calc. for $C_{27}H_{31}N_5O_5Na^+$ 528.2217; $[\alpha]_D^{20}$ –0.187 (*c* 0.25 in $CHCl_3$).

2-{1-[(3*R*)-1-(1-Naphthoyl)piperidin-3-yl]-1*H*-1,2,3-triazol-4-yl}isonicotinic acid 262

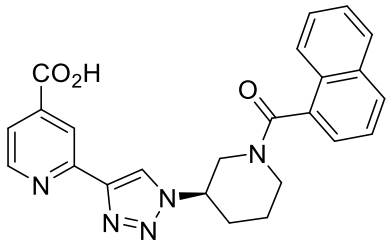

Triethylamine (21 μL, 0.15 mmol) was added to a suspension of methyl 2-{1-[(3*R*)-piperidin-3-yl]-1*H*-1,2,3-triazol-4-yl}isonicotinate **225** (29 mg, 0.10 mmol) and 1-naphthoyl chloride (23 μL, 0.15 mmol) in acetonitrile (1 mL) and the resulting solution stirred at room temperature for 16 h. Lithium hydroxide was added (1 M, aq, 1.0 mL, 1.0 mmol) and the resulting solution stirred at room temperature for 16 h. The reaction mixture was acidified to pH 1 with trifluoroacetic acid then purified by reverse phase chromatography (C18 column, eluting with 0.1% trifluoroacetic acid in water → 0.1% trifluoroacetic acid in 1:1 acetonitrile–water) to give **262** as an off-white solid (18 mg, 42%). mp 295–302 °C; ν_{max} (film) 2952 (C–H), 1711 (CO_2H), 1632 (C=O, amide); δ_H (500 MHz, $(CD_3)_2SO$, 363 K) 1.51–1.83 (2H, m, *PipC5*$\underline{H_2}$), 2.21–2.38 (2H, m, *PipC4*$\underline{H_2}$), 2.81–4.01 (4H, m, *PipC2*$\underline{H_2}$ and *PipC6*$\underline{H_2}$), 4.58–5.02 (1H, m, *PipC3*$\underline{H}$), 7.37–7.59 (4H, m, 4 × *Ar*$\underline{H}$), 7.70–7.83 (2H, m, 2 × *Ar*$\underline{H}$), 7.92–8.00 (2H, m, 2 × *Ar*$\underline{H}$), 8.39–8.50 (1H, m, *Ar*$\underline{H}$), 8.72–8.83 (2H, m, *PyC6*$\underline{H}$ and *Ar*$\underline{H}$); δ_C (125 MHz, $(CD_3)_2SO$, 363 K) 23.7 (*Pip*$\underline{C}$*5H*$_2$), 30.2 (*Pip*$\underline{C}$*4H*$_2$), 45.8–47.3 (*Pip*$\underline{C}$*2H*$_2$ and *Pip*$\underline{C}$*6H*$_2$), 56.6 (*Pip*$\underline{C}$*3H*), 118.9, 122.1, 122.9, 124.1, 125.1, 125.7, 126.8, 127.3, 128.8, 129.3, 129.7, 133.6, 134.6, 139.9, 147.1, 151.1 (*Py*$\underline{C}$*6H*), 151.6, 166.4 (*C*$\underline{=}$*O*), 169.0 (*C*$\underline{=}$*O*); *m/z* (MS, ES^+) 428 (100%, MH^+); LCMS (system E) tR 4.4 min (98%); accurate mass: found 450.1533, calc. for $C_{24}H_{21}N_5NaO_3^+$ 450.1537; $[\alpha]_D^{20}$ −0.252 (*c* 0.5 in CH_3OH).

2-{1-[(3*R*)-1-(2-Naphthoyl)piperidin-3-yl]-1*H*-1,2,3-triazol-4-yl}isonicotinic acid 263

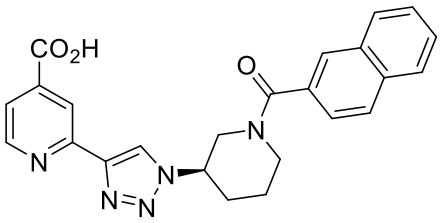

Triethylamine (21 μL, 0.15 mmol) was added to a suspension of methyl 2-{1-[(3*R*)-piperidin-3-yl]-1*H*-1,2,3-triazol-4-yl}isonicotinate (29 mg, 0.10 mmol) and 2-naphthoyl chloride (29 mg, 0.15 mmol) in acetonitrile (1 mL) and the resulting solution stirred at room temperature for 16 h. Lithium hydroxide was added (1 M, aq, 1.0 mL, 1.0 mmol) and the resulting solution stirred at room temperature for 16 h. The reaction mixture was acidified to pH 1 with trifluoroacetic acid, the resulting precipitate filtered then slurried in hot acetonitrile (4 mL), cooled to room temperature and filtered, washing with acetonitrile (2 × 4 mL) to give **263** as an off-white solid (22 mg, 51%). mp 275–278 °C; ν_{max} (film) 2902 (C–H), 2868 (C–H), 1710 (CO_2H), 1619 (C=O, amide); δ_H (500 MHz, $(CD_3)_2SO$) 1.63–2.04 (2H, m, *PipC5*$\underline{H_2}$), 2.20–2.38 (2H, m, *PipC4*$\underline{H_2}$), 3.18–3.73 (4H, m,

PipC2H$_2$ and *PipC6H*$_2$), 4.58–4.90 (1H, m, *PipC3H*), 7.48–7.64 (3H, m, 3 × *ArH*), 7.74–7.78 (1H, m, *ArH*), 7.87–8.07 (4H, m, 4 × *ArH*), 8.35–8.50 (1H, m, *ArH*), 8.65–8.93 (2H, m, *PyC6H* and *ArH*); δ_C (125 MHz, $(CD_3)_2SO$) 22.8–24.0 (*PipC5H*$_2$), 30.0 (*PipC4H*$_2$), 45.9–47.4 (*PipC2H*$_2$ and *PipC6H*$_2$), 56.0 (*PipC3H*), 118.3, 121.8, 122.6, 124.3, 126.3, 126.8, 127.2, 127.7, 128.1, 128.3, 132.2, 133.1, 139.2, 146.5, 150.8 (*PyC6H*), 150.9, 166.0 (*C*=*O*), 169.5 (*C*=*O*); *m/z* (MS, ES^+) 428 (100%, MH^+); LCMS (system E) tR 4.5 min (99%); accurate mass: found 450.1548, calc. for $C_{24}H_{21}N_5NaO_3^+$ 450.1537; $[\alpha]_D^{20}$ −0.471 (*c* 0.5 in *N*,*N*-dimethylformamide).

2-{1-[(3*R*)-1-(Biphenyl-4-ylcarbonyl)piperidin-3-yl]-1*H*-1,2,3-triazol-4-yl}pyridine-4-carboxylic acid 264

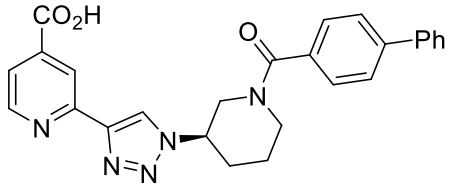

Triethylamine (21 µL, 0.15 mmol) was added to a suspension of methyl 2-{1-[(3*R*)-piperidin-3-yl]-1*H*-1,2,3-triazol-4-yl}isonicotinate **225** (29 mg, 0.10 mmol) and biphenyl-4-carbonyl chloride (33 mg, 0.15 mmol) in acetonitrile (1 mL) and the resulting solution stirred at room temperature for 16 h. Lithium hydroxide was added (1 M, aq, 1.0 mL, 1.0 mmol) and the resulting solution stirred at room temperature for 16 h. The reaction mixture was acidified to pH 1 with trifluoroacetic acid, the resulting precipitate filtered then slurried in hot acetonitrile (4 mL), cooled to room temperature and filtered, washing with acetonitrile (2 × 4 mL) to give **264** as an off-white solid (22 mg, 32%). mp 285–288 °C; ν_{max} (film) 3028 (C–H), 2932 (C–H), 2864 (C–H), 1720 (CO_2H), 1617 (C=O, amide); δ_H (500 MHz, $(CD_3)_2SO$) 1.60–2.02 (2H, m, *PipC5H*$_2$), 2.19–2.38 (2H, m, *PipC4H*$_2$), 3.03–3.77 (4H, m, *PipC2H*$_2$ and *PipC6H*$_2$), 4.52–4.90 (1H, m, *PipC3H*), 7.36–7.43 (1H, m, *ArH*), 7.44–7.57 (4H, m, 4 × *ArH*), 7.62–7.82 (5H, m, 5 × *ArH*), 8.36–8.50 (1H, m, *ArH*), 8.69–8.90 (2H, m, *PyC6H* and *ArH*); δ_C (125 MHz, $(CD_3)_2SO$) 23.7 (*PipC5H*$_2$), 30.0 (*PipC4H*$_2$), 46.0 and 47.1 (*PipC2H*$_2$ and *PipC6H*$_2$), 55.9 (*PipC3H*), 118.3, 121.8, 122.6, 126.7, 126.8, 127.6, 127.9, 129.0, 134.7, 139.3, 141.3, 146.5, 150.8 (*PyC6H*), 150.9, 166.0 (*C*=*O*), 169.2 (*C*=*O*); *m/z* (MS, ES^+) 454 (100%, MH^+); LCMS (system E) tR 4.9 min (98%); accurate mass: found 476.1684, calc. for $C_{26}H_{23}N_5NaO_3^+$ 476.1693; $[\alpha]_D^{20}$ −0.147 (*c* 0.15 in *N*,*N*-dimethylformamide).

2-{1-[(3*R*)-1-(4-Phenoxybenzoyl)piperidin-3-yl]-1*H*-1,2,3-triazol-4-yl}pyridine-4-carboxylic acid 265

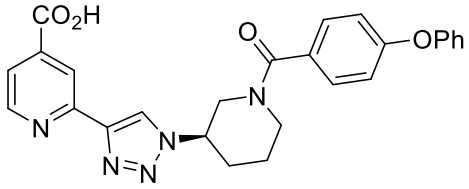

Triethylamine (21 μL, 0.15 mmol) was added to a suspension of methyl 2-{1-[(3*R*)-piperidin-3-yl]-1*H*-1,2,3-triazol-4-yl}isonicotinate **225** (29 mg, 0.10 mmol) and 4-phenoxybenzoyl chloride (35 mg, 0.15 mmol) in acetonitrile (1 mL) and the resulting solution stirred at room temperature for 16 h. Lithium hydroxide was added (1 M, aq, 1.0 mL, 1.0 mmol) and the resulting solution stirred at room temperature for 16 h. The reaction mixture was acidified to pH 1 with trifluoroacetic acid, the resulting precipitate filtered then slurried in hot acetonitrile (4 mL), cooled to room temperature and filtered, washing with acetonitrile (2 × 4 mL) to give **265** as an off-white solid (9 mg, 13%). mp 262–268 °C; ν_{max} (film) 2952 (C–H), 2868 (C–H), 1714 (CO_2H), 1626 (C=O, amide); δ_H (500 MHz, $(CD_3)_2SO$) 1.58–1.96 (2H, m, *PipC5H₂*), 2.18–2.35 (2H, m, *PipC4H₂*), 3.08–3.77 (4H, m, *PipC2H₂* and *PipC6H₂*), 4.44–4.85 (1H, m, *PipC3H*), 6.97–7.04 (2H, m, 2 × *ArH*), 7.06–7.10 (2H, m, 2 × *ArH*), 7.17–7.22 (1H, m, *ArH*), 7.39–7.49 (4H, m, 4 × *ArH*), 7.76 (1H, dd, *J* 5.0, 1.0, *PyC5H*), 8.40–8.47 (1H, m, *ArH*), 8.75–8.84 (2H, m, *PyC6H* and *ArH*); δ_C (125 MHz, $(CD_3)_2SO$) 22.6–24.0 (*PipC5H₂*), 30.0 (*PipC4H₂*), 45.6–47.6 (*PipC2H₂* and *PipC6H₂*), 56.0 (*PipC3H*), 118.3, 119.5, 120.0, 121.8, 122.6, 124.2, 129.2, 130.2, 139.3, 146.4, 150.8 (*PyC6H*), 150.9, 155.1, 155.6, 158.1, 166.0 (*C=O*), 169.0 (*C=O*); *m/z* (MS, ES^+) 470 (100%, MH^+); LCMS (system E) tR 5.0 min (90%); accurate mass: found 492.1631, calc. for $C_{26}H_{23}N_5NaO_4^+$ 492.1642; $[\alpha]_D^{20}$ −0.402 (*c* 0.5 in *N*,*N*-dimethylformamide).

2-{1-[(3*R*)-1-(Phenylsulfonyl)piperidin-3-yl]-1*H*-1,2,3-triazol-4-yl}isonicotinic acid 266

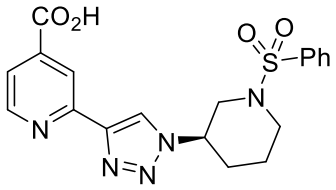

Triethylamine (21 μL, 0.15 mmol) was added to a suspension of methyl 2-{1-[(3*R*)-piperidin-3-yl]-1*H*-1,2,3-triazol-4-yl}isonicotinate **225** (29 mg, 0.10 mmol) and benzenesulfonyl chloride (19 μL, 0.15 mmol) in acetonitrile (1 mL) and the resulting solution stirred at room temperature for 16 h. Lithium hydroxide was added (1 M, aq, 1.0 mL, 1.0 mmol) and the resulting solution stirred at room temperature for 16 h. The reaction mixture was acidified to pH 1 with trifluoroacetic acid, the resulting precipitate filtered then taken up in hot acetonitrile (4 mL), cooled to room temperature and filtered, washing with acetonitrile (2 × 4 mL) to give **266** as an off-white solid (22 mg, 53%). mp 266–270 °C; ν_{max} (film) 2951 (C–H), 2864 (C–H), 1720 (CO_2H); δ_H (400 MHz, $(CD_3)_2SO$) 1.64–1.77 (1H, m, *PipC5H*), 1.80–1.90 (1H, m, *PipC5H*), 1.96–2.07 (1H, m, *PipC4H*),

2.09–2.19 (1H, m, *PipC4H*), 2.54–2.62 (1H, m, *PipC6H*), 2.94–3.01 (1H, m, *PipC2H*), 3.24–3.50 (1H, m, *PipC6H*), 3.78–3.84 (1H, m, *PipC2H*), 4.79–4.89 (1H, m, *PipC3H*), 7.64–7.81 (6H, m, *Ph* and *PyC5H*), 8.43 (1H, dd, *J* 1.5, 1.0, *PyC3H*), 8.79 (1H, dd, *J* 5.0, 1.0, *PyC6H*), 8.81 (1H, s, *TriCH*); δ_C (100 MHz, $(CD_3)_2SO$) 22.7 (*PipC5H₂*), 28.6 (*PipC4H₂*), 45.7 (*PipC6H₂*), 49.9 (*PipC2H₂*), 55.7 (*PipC3H*), 118.3 (*PyC3H*), 121.8 (*PyC5H*), 122.8 (*TriCH*), 127.5 (2 × *PhCH*), 129.6 (2 × *PhCH*), 133.4 (*PhCH*), 135.3, 139.2, 146.4, 150.8 (*PyC6H*), 150.9 (s), 166.0 (*CO₂H*); *m/z* (MS, ES^+) 414 (100%, MH^+); LCMS (system E) tR 4.4 min (93%); accurate mass: found 436.1040, calc. for $C_{19}H_{19}N_5NaO_4S^+$ 436.1050; $[\alpha]_D^{20}$ +0.378 (*c* 0.5 in *N*,*N*-dimethylformamide).

tert-Butyl (3*R*)-3-azidopiperidine-1-carboxylate 271[225]

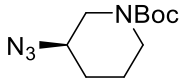

Sodium azide (2.32 g, 35.8 mmol) was added to a solution of *tert*-butyl (3*S*)-3-[(methylsulfonyl)oxy]piperidine-1-carboxylate **223** (1.00 g, 3.58 mmol) in *N*,*N*-dimethylformamide (3.5 mL) and the resulting suspension heated at 90 °C for 16 h then filtered, washing with acetonitrile (2 × 4 mL). The filtrate was concentrated *in vacuo* to give **271** as brown oil that was used in the next step without further purification (768 mg contaminated with 5% w/w *N*,*N*-dimethylformamide, 90%) [*no spectral data reported in the literature*].

tert-Butyl (3*R*)-3-[4-(pyridin-2-yl)-1*H*-1,2,3-triazol-1-yl]piperidine-1-carboxylate 272

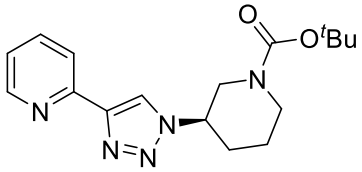

tert-Butyl (3*R*)-3-azidopiperidine-1-carboxylate **271** (237 mg, 95% w/w, 1.00 mmol) was taken up in 4 mL of a 1:1 mixture of *tert*-butanol–water. 2-Ethynyl pyridine (103 mg, 1.00 mmol), copper(II) sulfate pentahydrate (25 mg, 0.10 mmol) and (+)-sodium L-ascorbate (40 mg, 0.20 mmol) were added and the resulting suspension heated at 65 °C for 16 h. The reaction mixture was diluted with water (5 mL) and extracted with dichloromethane (3 × 5 mL). The organic layers were combined, concentrated *in vacuo* and purified by flash column chromatography (15% ethyl acetate in cyclohexane → 30% ethyl acetate in cyclohexane) to give **272** as an off-white solid (235 mg, 71%). R_f 0.25 (2:1 cyclohexane–ethyl acetate); mp 110–112 °C; ν_{max} (film) 2977 (C–H), 2931 (C–H), 2863 (C–H), 1693 (C=O); δ_H (400 MHz, $CDCl_3$) 1.43 (9H, s, *C(CH)₃*), 1.55–1.70 (1H, m, *PipC5H*) and 1.77–1.87 (1H, m, *PipC5H*), 2.05–2.16 (1H, m, *PipC4H*), 2.23–2.34 (1H, m, *PipC4H*), 2.92–3.01 (1H, m, *PipCH*), 3.26–3.40 (1H, m, *PipCH*), 3.87–4.00 (1H, m, *PipCH*), 4.22–4.43 (1H, m, *PipCH*), 4.49–4.60 (1H, m, *PipC3H*), 7.15–7.22 (1H, m, *PyC5H*), 7.70–7.77 (1H, m, *PyC4H*), 8.13 (1H, d, *J* 8.0, *PyC3H*), 8.20 (1H, s, *TriCH*), 8.53 (1H, dd, *J* 4.0, 1.0, *PyC6H*); δ_C (100 MHz, $CDCl_3$) 23.4 (*PipC5H₂*), 28.2 (*C(CH)₃*), 30.7 (*PipC4H₂*), 42.7–44.3 and 47.7–49.3 (*PipC2H₂* and *PipC6H₂*), 56.4 (*PipC3H*), 80.3 (*C(CH)₃*), 120.0 (*PyC3H*), 120.6 (*TriCH*), 122.7 (*PyC5H*), 136.8

(*PyC4H*), 147.9, 149.3 (*PyC6H*), 150.1, 154.3 (*C*=*O*); *m/z* (MS, ES^+) 330 (100%, MH^+); LCMS tR 17.5 min (99%); accurate mass: found 352.1742, calc. for $C_{17}H_{23}N_5NaO_2^+$ 352.1744; $[\alpha]_D^{20}$ −0.706 (*c* 1.0 in $CHCl_3$).

2-{1-[(3*R*)-Piperidin-3-yl]-1*H*-1,2,3-triazol-4-yl}pyridine 273

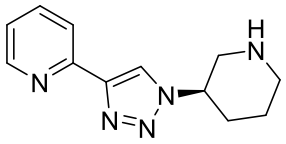

Trifluoroacetic acid (0.5 mL) was added to a solution of *tert*-butyl (3*R*)-3-[4-(pyridin-2-yl)-1*H*-1,2,3-triazol-1-yl]piperidine-1-carboxylate **272** (220 mg, 0.67 mmol) in dichloromethane (1 mL) and the resulting solution stirred at room temperature for 16 h then concentrated *in vacuo* and purified on a 1 g strong cation exchange column, washing with methanol (20 mL) then eluting with methanolic ammonia (2 M, 10 mL) to give **273** as a brown gum (78 mg, 51%). R_f 0.15 (95:5 dichloromethane–methanol); ν_{max} (film) 2946 (C–H), 2860 (C–H); δ_H (400 MHz, $CDCl_3$) 1.47–1.58 (1H, m, *PipC5H*), 1.68–1.77 (1H, m, *PipC5H*), 1.86 (1H, m, *PipC4H*), 2.04 (1H, br. s, *NH*), 2.14–2.23 (1H, m, *PipC4H*), 2.56–2.64 (1H, m, *PipC6H*), 2.87–2.98 (2H, m, *PipC6H* and *PipC2H*), 3.30–3.36 (1H, m, *PipC2H*), 4.44–4.54 (1H, m, *PipC3H*), 7.10 (1H, ddd, *J* 8.0, 5.0, 1.0, *PyC5H*), 7.65 (1H, td, *J* 8.0, 1.5, *PyC4H*), 8.05 (1H, app. d, *J* 8.0, *PyC3H*), 8.19 (1H, s, *TriCH*), 8.46 (1H, ddd, *J* 5.0, 1.5, 1.0, *PyC6H*); δ_C (100 MHz, $CDCl_3$) 24.7 (*PipC5H*$_2$), 30.9 (*PipC4H*$_2$), 45.6 (*PipC6H*$_2$), 51.5 (*PipC2H*$_2$), 57.6 (*PipC3H*), 119.8 (*PyC3H*), 120.4 (*TriCH*), 122.5 (*PyC5H*), 136.6 (*PyC4H*), 147.5, 149.0 (*PyC6H*), 150.1; *m/z* (MS, ES^+) 230 (100%, MH^+); LCMS tR 12.6 min (99%); accurate mass: found 230.1400, calc. for $C_{12}H_{16}N_5^+$ 230.1400; $[\alpha]_D^{20}$ +0. 035 (*c* 0.35 in $CHCl_3$).

Phenyl{(3*R*)-3-[4-(pyridin-2-yl)-1*H*-1,2,3-triazol-1-yl]piperidin-1-yl}methanone 274

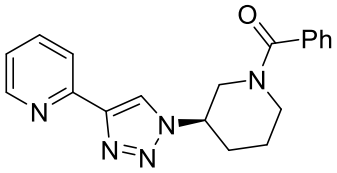

Benzoyl chloride (42 µL, 0.37 mmol) was added to a solution of 2-{1-[(3*R*)-piperidin-3-yl]-1*H*-1,2,3-triazol-4-yl}pyridine **273** (77 mg, 0.34 mmol) and triethylamine (52 µL, 0.37 mmol) in acetonitrile (1 mL) and the resulting solution stirred at room temperature for 16 h. The reaction mixture was diluted with water (5 mL) and extracted with dichloromethane (3 × 5 mL). The organic layers were combined, concentrated *in vacuo* and purified by flash column chromatography (dichloromethane → 4% methanol in dichloromethane) to give **274** as a white gum (122 mg, quant.). R_f 0.50 (95:5 dichloromethane–methanol); ν_{max} (film) 1630 (C=O); δ_H (400 MHz, $CDCl_3$) 1.51–2.04 (2H, m, *PipC5H*$_2$), 2.08–2.43 (2H, m, *PipC4H*$_2$), 2.89–3.85 (2H, m, *PipC6H*$_2$), 4.02–4.25 (2H, m, *PipC2H*$_2$), 4.46–4.70 (1H, m, *PipC3H*), 7.18 (1H, ddd, *J* 8.0, 5.0, 1.5, *PyC5H*), 7.33–7.40 (5H, m, *Ph*), 7.72 (1H, td, *J* 8.0, 1.5, *PyC4H*), 8.11 (1H, app. d, *J* 8.0, *PyC3H*), 8.13–8.31 (1H,

m, *TriC<u>H</u>*), 8.53 (1H, app. d, *J* 5.0, *PyC6<u>H</u>*); δ_C (100 MHz, $CDCl_3$) 23.1–24.6 (*Pip<u>C</u>5H₂*), 30.8 (*Pip<u>C</u>4H₂*), 41.6–42.3 (*Pip<u>C</u>H₂*), 46.3–47.9 (*Pip<u>C</u>H₂*) and 52.0–52.6 (*Pip<u>C</u>H₂*), 56.4 (*Pip<u>C</u>3H*), 120.0 (*Py<u>C</u>3H*), 120.8 (*Tri<u>C</u>H*), 122.8 (*Py<u>C</u>5H*), 126.7 (*Ph<u>C</u>H*), 128.5 (*Ph<u>C</u>H*), 129.9 (*Ph<u>C</u>H*), 135.1, 136.8 (*Py<u>C</u>4H*), 147.9, 149.2 (*Py<u>C</u>6H*), 149.9, 170.6 (*<u>C</u>=O*); *m/z* (MS, ES^+) 334 (100%, MH^+); LCMS tR 11.8 min (100%); accurate mass: found 356.1480, calc. for $C_{19}H_{19}N_5NaO^+$ 356.1482; $[\alpha]_D^{20}$ −0. 785 (*c* 1.0 in CH_3OH).

4-Methoxy-2-[(trimethylsilyl)ethynyl]pyridine 276

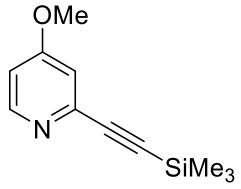

A mixture of 2-chloro-4-methoxypyridine (574 mg, 4.00 mmol), copper(I) iodide (91 mg, 0.48 mmol), triphenylphosphine (210 mg, 0.80 mmol) and tetrakis(triphenylphosphine)palladium (277 mg, 0.24 mmol) was placed in a sealed vial which was evacuated and refilled with nitrogen (× 4) then triethylamine (13 mL, 95 mmol), *N*,*N*-dimethylformamide (6.6 mL) and trimethylsilylacetylene (1.24 mL, 8.80 mmol) were added and the resulting solution heated at 50 °C for 9 h. The reaction mixture was allowed to cool to room temperature then purified by flash column chromatography (cyclohexane → 8% ethyl acetate in cyclohexane) to give a mixture of **276** as an orange gum (132 mg contaminated with 43% w/w triphenylphosphine oxide, 9%) that was taken onto the next step as is.

4-Methoxy-2-{1-[(3*R*)-piperidin-3-yl]-1*H*-1,2,3-triazol-4-yl}pyridine 277

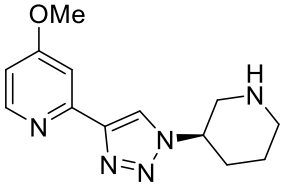

tert-Butyl (3*R*)-3-azidopiperidine-1-carboxylate **271** (184 mg, 95% w/w, 0.77 mmol) was taken up in 4 mL of a 1:1 mixture of *tert*-butanol–water. 4-methoxy-2-[(trimethylsilyl)ethynyl]pyridine **276** (132 mg contaminated with 43% w/w triphenylphosphine oxide, 0.37 mmol) was added followed by copper(II) sulfate pentahydrate (10 mg, 0.04 mmol) and (+)-sodium L-ascorbate (16 mg, 0.08 mmol). A solution of tetrabutylammonium fluoride in tetrahydrofuran (1 M, 0.37 mL, 0.37 mmol) was added dropwise over 5 min and the resulting suspension heated at 65 °C for 16 h. The reaction mixture was diluted with water (30 mL) and extracted with dichloromethane (3 × 15 mL). The organic layers were combined, concentrated *in vacuo* and purified by flash column chromatography (15% ethyl acetate in cyclohexane → 50% ethyl acetate in cyclohexane) to give a green gum that was taken up in dichloromethane (1 mL). Trifluoroacetic acid (1 mL) was added and the resulting solution stirred at room temperature for 16 h then concentrated *in vacuo* and purified on a 1 g strong cation exchange column, washing with methanol (8 mL) then eluting with methanolic ammonia (2

M, 8 mL) to give **277** as a brown gum (56 mg, 58%). R_f 0.15 (95:5 dichloromethane–methanol); ν_{max} (film) 2943 (C–H), 2856 (C–H), 2862 (C–H), 1694 (C=O); δ_H (400 MHz, CD_3OD) 1.23–2.03 (4H, m, 2 × *PipC*$\underline{H_2}$), 2.27–4.56 (8H, m, 2 × *PipC*$\underline{H_2}$, 2 × *PipC*$\underline{H}$ and *OC*$\underline{H_3}$), 7.51–7.59 (2H, m, 2 × *ArC*$\underline{H}$), 7.60–7.68 (2H, m, 2 × *ArC*$\underline{H}$); δ_C (100 MHz, CD_3OD) 25.0 (*PipC*$\underline{H_2}$), 28.8 (*PipC*$\underline{H_2}$), 43.9–45.6 (2 × *PipC*$\underline{H_2}$), 56.8 (*OC*$\underline{H_3}$), 59.6 (*PipC*$\underline{3}$*H*), 130.1 (*ArC*$\underline{H}$), 130.2 (*ArC*$\underline{H}$), 132.3, 133.1 (*ArC*$\underline{H}$), 133.2 (*ArC*$\underline{H}$), 133.9, 156.3; *m/z* (MS, ES^+) 260 (100%, MH^+); LCMS tR 6.8 min (100%); accurate mass: found 260.1509, calc. for $C_{13}H_{18}N_5O_3^+$ 260.1506.

{(3*R*)-3-[4-(4-Methoxypyridin-2-yl)-1*H*-1,2,3-triazol-1-yl]piperidin-1-yl}(phenyl)methanone 278

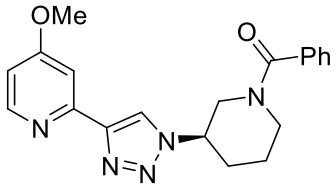

Benzoyl chloride (1.9 µL, 0.017 mmol) was added to a solution of 4-methoxy-2-{1-[(3*R*)-piperidin-3-yl]-1*H*-1,2,3-triazol-4-yl}pyridine **277** (4.0 mg, 0.015 mmol) and triethylamine (2.4 µL, 0.017 mmol) in acetonitrile (1 mL) and the resulting solution stirred at room temperature for 16 h. The reaction mixture was diluted with water (5 mL) and extracted with dichloromethane (3 × 5 mL). The organic layers were combined, concentrated *in vacuo* and purified by flash column chromatography (dichloromethane → 3.5% methanol in dichloromethane) to give **278** as a colourless gum (5 mg, 91%). R_f 0.55 (95:5 dichloromethane–methanol); ν_{max} (film) 1633 (C=O); δ_H (400 MHz, CD_3OD) 1.55–2.12 (2H, m, *PipC5*$\underline{H_2}$), 2.15–2.51 (2H, m, *PipC4*$\underline{H_2}$), 2.93–3.54 (2H, m, *PipC6*$\underline{H_2}$), 3.62–4.33 (5H, m, *PipC2*$\underline{H_2}$ and *OC*$\underline{H_3}$), 4.49–4.78 (1H, m, *PipC3*$\underline{H}$), 6.79 (1H, dd, *J* 6.0, 2.5, *PyC5*$\underline{H}$), 7.36–7.48 (5H, m, *Ph*), 7.74 (1H, app. s, *PyC3*$\underline{H}$), 8.10–8.34 (1H, m, *TriC*$\underline{H}$), 8.38 (1H, d, *J* 6.0, *PyC6*$\underline{H}$); δ_C (125 MHz, $CDCl_3$) 23.3–24.8 (*PipC*$\underline{5}$*H*$_2$), 31.1 (*PipC*$\underline{4}$*H*$_2$), 41.7–42.5 (*PipC*$\underline{H_2}$), 46.4–47.8 (*PipC*$\underline{H_2}$), 52.1–52.9 (*PipC*$\underline{H_2}$), 55.4 (*OC*$\underline{H_3}$), 56.3–57.3 (*PipC*$\underline{3}$*H*), 105.3 (*PyC*$\underline{3}$*H*), 110.3 (*PyC*$\underline{5}$*H*), 121.0 (*TriC*$\underline{H}$), 126.9 (*PhC*$\underline{H}$), 128.7 (*PhC*$\underline{H}$), 130.1 (*PhC*$\underline{H}$), 135.2 (*ipso-Ph*), 147.8, 150.3 (*PyC*$\underline{6}$*H*), 151.6, 166.6, 170.9 (*C*$\underline{=}$*O*); *m/z* (MS, ES^+) 364 (100%, MH^+); LCMS tR 11.8 min (100%); accurate mass: found 364.1761, calc. for $C_{20}H_{22}N_5O_2^+$ 364.1768; $[\alpha]_D^{20}$ −0. 207 (*c* 0.25 in $CHCl_3$).

2-{1-[(3*R*)-Piperidin-3-yl]-1*H*-1,2,3-triazol-4-yl}pyridin-4-ol 279

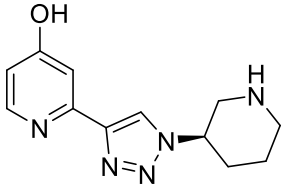

A solution of 4-methoxy-2-{1-[(3*R*)-piperidin-3-yl]-1*H*-1,2,3-triazol-4-yl}pyridine **277** (52 mg, 0.20 mmol) in hydrobromic acid (5 mL of a 55% aq solution) was heated at 90 °C for 3 h. The reaction mixture was concentrated *in vacuo* and purified on a 1 g strong cation exchange column,

washing with methanol (20 mL) then eluting with methanolic ammonia (2 M, 10 mL) to give **279** as a light brown gum (26 mg, 53%). R_f 0.25 (80:20 dichloromethane:2 M methanolic ammonia); ν_{max} (film) 2945 (C–H), 2860 (C–H); δ_H (400 MHz, CD_3OD) 1.65–1.78 (1H, m, *PipC5H*), 1.85–1.95 (1H, m, *PipC5H*), 2.03–2.15 (1H, m, *PipC4H*), 2.28–2.37 (1H, m, *PipC4H*), 2.65–2.74 (1H, m, *PipC6H*), 2.99–3.09 (2H, m, *PipC6H* and *PipC2H*), 3.37–3.44 (1H, m, *PipC2H*), 4.61–4.70 (1H, m, *PipC3H*), 6.49 (1H, dd, *J* 7.0, 2.5, *PyC5H*), 6.92 (1H, d, *J* 2.5, *PyC3H*), 7.87 (1H, d, *J* 7.0, *PyC6H*), 8.64 (1H, s, *TriCH*); δ_C (100 MHz, CD_3OD) 26.0 (*PipC5H*$_2$), 32.1 (*PipC4H*$_2$), 46.3 (*PipC6H*$_2$), 52.0 (*PipC2H*$_2$), 59.4 (*PipC3H*), 113.5 (*PyC3H*), 116.8 (*PyC5H*), 123.6 (*TriCH*), 141.5 (*PyC6H*), 142.6, 143.8, 180.4 (*PyC4*); *m/z* (MS, ES^+) 246 (100%, MH^+); LCMS (system E) tR 3.2 min (82%); accurate mass: found 246.1347, calc. for $C_{12}H_{16}N_5O^+$ 246.1349.

{(3*R*)-3-[4-(4-Hydroxypyridin-2-yl)-1*H*-1,2,3-triazol-1-yl]piperidin-1-yl}(phenyl)methanone 280

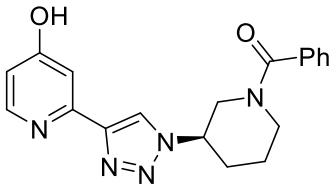

Benzoyl chloride (13.2 µL, 0.12 mmol) was added to a solution of 4-hydroxy-2-{1-[(3*R*)-piperidin-3-yl]-1*H*-1,2,3-triazol-4-yl}pyridine **279** (26.0 mg, 0.11 mmol) and triethylamine (29.5 µL, 0.22 mmol) in acetonitrile (1 mL) and the resulting solution stirred at room temperature for 16 h. The reaction mixture was diluted with water (5 mL) and extracted with dichloromethane (3 × 5 mL). The organic layers were combined, concentrated *in vacuo* and purified on a 1 g strong cation exchange column, washing with methanol (20 mL) then eluting with methanolic ammonia (2 M, 10 mL) to give **280** as a colourless gum (23 mg, 62%). ν_{max} (film) 2941 (C–H), 2864 (C–H), 1632 (C=O); δ_H (400 MHz, CD_3OD) 1.63–2.00 (2H, m, *PipCH*$_2$), 2.05–2.46 (2H, m, *PipCH*$_2$), 3.33–5.06 (5H, m, 2 × *PipCH*$_2$ and *PipC3H*), 6.47–6.53 (1H, m, *ArCH*), 6.83–6.97 (1H, m, *ArCH*), 7.33–7.55 (5H, m, *Ph*), 7.83–7.89 (1H, m, *ArCH*), 8.45–8.73 (1H, m, *ArCH*); δ_C (125 MHz, CD_3OD) 23.8–25.3 (*PipCH*$_2$), 31.4 (*PipC4H*$_2$), 43.3–48.1 (*PipCH*$_2$), 52.6–53.8 (*PipCH*$_2$), 58.1 (*PipC3H*), 113.6 (*ArCH*), 116.9 (*ArCH*), 124.1 (*ArCH*), 128.0 (*PhCH*), 128.8 (*ArCH*), 129.7 (*PhCH*), 129.9 (*PhCH*), 130.6, 131.4 (*PhCH*), 133.1 (s), 135.0, 136.7, 142.6, 173.1 (*C*=*O*); *m/z* (MS, ES^+) 350 (100%, MH^+); LCMS (system E) tR 4.4 min (85%); accurate mass: found 350.1601, calc. for $C_{19}H_{20}N_5O_2^+$ 350.1612; $[\alpha]_D^{20}$ −0.338 (*c* 0.5 in CH_3OH).

[(3*R*)-3-{4-[4-(Hydroxymethyl)pyridin-2-yl]-1*H*-1,2,3-triazol-1-yl}piperidin-1-yl](phenyl)methanone 281

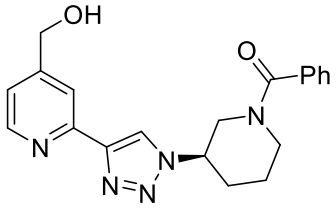

1,1'-Carbonyldiimidazole (28 mg, 89% w/w, 0.16 mmol) was added to a solution of 2-{1-[(3*R*)-1-benzoylpiperidin-3-yl]-1*H*-1,2,3-triazol-4-yl}isonicotinic acid hemitrifluoroacetate **227** (70 mg, 0.14 mmol) and triethylamine (18 µL, 0.13 mmol) in tetrahydrofuran (1 mL). The resulting solution was stirred at room temperature for 45 min then added dropwise to a solution of sodium borohydride (30 mg, 0.78 mmol) in a 1:1 mixture of tetrahydrofuran and water (0.3 mL). The resulting solution was stirred at room temperature for 16 h then acidified to pH1 with hydrochloric acid (1 M, aq), neutralised with sodium hydrogencarbonate (saturated, aq) and extracted with dichloromethane (3 × 5 mL) and ethyl acetate (3 × 5 mL). The organic layers were combined, dried over sodium sulfate then concentrated *in vacuo* to give a white gum which was purified by flash column chromatography (dichloromethane → 8% methanol in dichloromethane) to give **281** as a colourless gum (30 mg, 59%). ν_{max} (film) 3363 (O–H, br), 2947 (C–H), 2864 (C–H), 1614 (C=O); δ_H (400 MHz, $CDCl_3$) 1.43–1.96 (2H, m, *PipC5H₂*), 2.00–2.33 (2H, m, *PipC4H₂*), 2.84–4.19 (4H, m, *PipC2H₂* and *PipC6H₂*), 4.36–4.57 (1H, m, *PipC3H*), 4.62 (2H, s, *CH₂OH*), 7.09 (1H, dd, *J* 5.0, 1.5, *PyC5H*), 7.98 (1H, s, *ArH*), 8.11 (1H, br. s, *ArH*), 8.32 (1H, d, *J* 5.0, *PyC6H*); δ_C (125 MHz, $CDCl_3$) 23.3–24.3 (*PipC5H₂*), 30.9 (*PipC4H₂*), 41.6–42.5 and 46.5–47.7 (*PipC2H₂* and *C6H₂*), 56.6 (*PipC3H*), 63.0 (*CH₂OH*), 117.6 (*ArCH*), 120.5 (*PyC5H*), 121.2 (*ArCH*), 126.8 (*PhCH*), 128.6 (*PhCH*), 130.1 (*PhCH*), 135.0 (*ipso-Ph*), 147.8, 149.2 (*PyC6H*), 149.6, 152.0, 170.9 (*CON*); *m/z* (MS, ES^+) 364 (100%, MH^+); LCMS (system E) tR 4.5 min (99%); accurate mass: found 364.1773, calc. for $C_{20}H_{22}N_5O_2^+$ 364.1768; $[\alpha]_D^{20}$ −0.891 (*c* 1.0 in $CHCl_3$).

2-{1-[(3*R*)-1-Benzoylpiperidin-3-yl]-1*H*-1,2,3-triazol-4-yl}isonicotinaldehyde 282

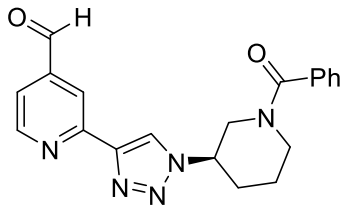

1,1,1-Tris(acetyloxy)-1,1-dihydro-1,2-benziodoxol-3-(1*H*)-one (47 mg, 0.11 mmol) was added to a solution of [(3*R*)-3-{4-[4-(hydroxymethyl)pyridin-2-yl]-1*H*-1,2,3-triazol-1-yl}piperidin-1-yl](phenyl)methanone **281** (20 mg, 0.055 mmol) in chloroform (2 mL) and the resulting suspension stirred at room temperature for 16 h. The reaction mixture was diluted with water (5 mL) and extracted with dichloromethane (3 × 5 mL). The organic layers were combined, concentrated *in vacuo* and purified by flash column chromatography (dichloromethane → 3% methanol in

dichloromethane) to give a colourless gum that was taken up in dichloromethane (5 mL) and washed with 4 mL of a 1:1 mixture of sodium thiosulfate (saturated, aq) and sodium hydrogencarbonate (saturated, aq) and then washed with sodium hydrogencarbonate (saturated, aq, 2 × 4 mL). The aqueous layers were back-extracted with dichloromethane (2 × 5 mL). The organic layers were combined, dried over sodium sulfate then concentrated *in vacuo* to give **282** as a colourless gum (8 mg, 40%). ν_{max} (film) 2926 (C–H), 2856 (C–H), 1706 (C=O, aldehyde), 1631 (C=O, amide); δ_H (500 MHz, $CDCl_3$) 1.18–2.52 (4H, m, *PipC5H*$_2$ and *PipC4H*$_2$), 3.04–5.03 (5H, m, *PipC2H*$_2$, *PipC6H*$_2$ and *PipC3H*), 7.38–7.48 (5H, m, *Ph*), 7.66 (1H, dd, *J* 5.0, 1.5, *PyC5H*), 8.33 (1H, br. s, *Tri*), 8.57 (1H, d, *J* 0.5, *PyC3H*), 8.81 (1H, app. d, *J* 5.0, *PyC6H*), 10.16 (1H, s, *CHO*); δ_C (125 MHz, $CDCl_3$) 23.3–24.8 (*PipC5H*$_2$), 31.0 (*PipC4H*$_2$), 41.4–42.7 and 46.4–48.0 (*PipC2H*$_2$ and *PipC6H*$_2$), 56.2–57.6 (*PipC3H*), 120.0 (*PyC5H* and *PyC3H*), 121.6 (*TriCH*), 126.9 (*PhCH*), 128.7 (*PhCH*), 130.1 (*PhCH*), 135.1, 142.5, 147.2, 150.7 (*PyC6H*), 152.0, 170.9 (*CON*), 191.4 (*CHO*); *m/z* (MS, ES^+) 362 (100%, MH^+); LCMS (system E) tR 5.3 min (100%); accurate mass: found 362.1607, calc. for $C_{20}H_{20}N_5O_2^+$ 362.1612; $[\alpha]_D^{20}$ −0.350 (*c* 0.5 in $CHCl_3$).

(2-{[4-(Phenylsulfonyl)piperazin-1-yl]methyl}pyridin-4-yl)methanol 283

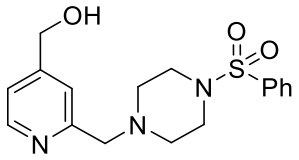

Lithium borohydride (2 mg, 0.08 mmol) was added to a solution of ethyl 2-[(4-(phenylsulfonyl)piperazin-1-yl)methyl]isonicotinate **71** (11 mg, 0.03 mmol) in tetrahydrofuran (0.5 mL). Ethanol (2.5 µL, 0.04 mmol) was added and the resulting suspension heated at 40 °C for 16 h. The reaction mixture was diluted with water (3 mL), neutralised with citric acid (10% w/v, aq) and extracted with ethyl acetate (3 × 3 mL). The organic layers were combined, dried (magnesium sulfate), concentrated *in vacuo* and purified by flash column chromatography (dichloromethane → 9:1 dichloromethane–methanol) to give the title compound as a colourless oil (8 mg, 77% yield). R_f 0.20 (95:5 dichloromethane–methanol); ν_{max} (film) 2894 (C–H), 2854 (C–H), 2822 (C–H); δ_H (400 MHz, $CDCl_3$) 2.57–2.69 (4H, m, 2 × *piperazinyl CH*$_2$), 3.01–3.15 (4H, m, 2 × *piperazinyl CH*$_2$), 3.66 (2H, s, *CH*$_2$*Py*), 4.71 (2H, s, *CH*$_2$*O*), 7.16 (1H, d, *J* 4.5, *PyC5H*), 7.30 (1H, s, *PyC3H*), 7.50–7.64 (3H, m, 3 × *Ph*), 7.72–7.78 (2H, m, 2 × *Ph*), 8.49 (1H, d, *J* 4.5, *PyC6H*); δ_C (100 MHz, $CDCl_3$) 45.7 (2 × *piperazinyl CH*$_2$), 52.2 (2 × *piperazinyl CH*$_2$), 63.3 (*CH*$_2$*O*), 63.8 (*CH*$_2$*Py*), 119.9 (*PyC5H*), 120.8 (*PyC3H*), 127.8 (2 × *PhCH*), 129.0 (2 × *PhCH*), 132.9 (*PhCH*), 135.3 (*ipso-Ph*), 149.4 (*PyC6H*), 154.6, 154.8; *m/z* (MS, ES^+) 370 (100%, MNa^+); LCMS tR 8.2 min (99%); accurate mass: found 370.1187, calc. for $C_{17}H_{21}N_3NaO_3S^+$ 370.1196.

Methyl 3-hydroxyisonicotinate 291[201]

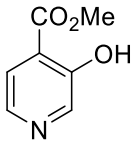

Sulfuric acid (3.5 mL of a concentrated aq. solution) was added to a suspension of 3-hydroxyisonicotinic acid (3.54 g, 25.4 mmol) in methanol (80 mL) and the resulting suspension heated at 65 °C for 16 h. The methanol was removed *in vacuo*, the residue poured into 100 mL ice/water and the resulting solution adjusted to pH 5 by the addition of saturated sodium bicarbonate solution. The resulting suspension was extracted with ethyl acetate (3 × 50 mL). The organic layers were combined, dried over sodium sulfate and concentrated *in vacuo* to give **291** as a yellow solid (3.35 g, 86% yield). mp 79–86 °C [*lit. 80–81* °C]; ν_{max} (film) 3109 (C–H), 3087 (C–H), 2962 (C–H), 1676 (C=O); δ_H (400 MHz, $CDCl_3$) 3.98 (3H, s, *C*$\underline{H}_3$), 7.59 (1H, d, *J* 5.0, *PyC5*$\underline{H}$), 8.20 (1H, d, *J* 5.0, *PyC6*$\underline{H}$), 8.48 (1H, s, *PyC2*$\underline{H}$), 10.27 (1H, s, *O*$\underline{H}$) [*no lit. data*]; δ_C (100 MHz, $CDCl_3$) 52.9 (*C*$\underline{H}_3$), 117.8 (*Py*$\underline{C}$*4*), 121.4 (*Py*$\underline{C}$*5H*), 140.4 (*Py*$\underline{C}$*6H*), 141.9 (*Py*$\underline{C}$*2H*), 155.4 (*Py*$\underline{C}$*3*), 169.1 (*C*$\underline{O}_2$*Me*) [*consistent with lit.*]; *m/z* (MS, ES^+) 154 (100%, MH^+); LCMS (system E) tR 2.4 min (100%).

Methyl 3-{[2-(trimethylsilyl)ethoxy]methoxy}isonicotinate 292

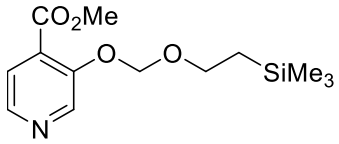

Sodium hydride (40 mg of a 60% dispersion in mineral oil, 1.0 mmol) was added to a solution of methyl 3-hydroxyisonicotinate **291** (153 mg, 1.0 mmol) in tetrahydrofuran (4 mL) and the resulting mixture stirred at room temperature for 5 min. 2-(trimethylsilyl)ethoxymethyl chloride (0.18 mL, 1.0 mmol) was added dropwise and the resulting mixture stirred at room temperature for 2.5 h. The reaction mixture was diluted with water (25 mL) and extracted with ethyl acetate (2 × 25 mL). The organic layers were washed with brine (25 mL) then combined, dried over sodium sulfate and concentrated *in vacuo* to give a brown oil that was purified by flash column chromatography (dichloromethane → 20% ethyl acetate in dichloromethane) to give **292** as a yellow oil (178 mg, 63% yield). R_f 0.50 (15% ethyl acetate in dichloromethane); ν_{max} (film) 2954 (C–H), 2897 (C–H), 1693 (C=O); δ_H (400 MHz, $CDCl_3$) –0.01 (9H, s, *Si(C*$\underline{H}_3$*)*$_3$), 0.93–0.99 (2H, m *SiC*$\underline{H}_2$*CH*$_2$), 3.78–3.84 (2H, m *SiCH*$_2$*C*$\underline{H}_2$), 3.92 (3H, s, *OC*$\underline{H}_3$), 5.34 (2H, s, *OC*$\underline{H}_2$), 7.56 (1H, s, 1H, d, *J* 5.0, *PyC5*$\underline{H}$), 8.36 (1H, d, *J* 5.0, *PyC6*$\underline{H}$), 8.66 (1H, s, *PyC2*$\underline{H}$); δ_C (100 MHz, $CDCl_3$) –1.5 (*Si(*$\underline{C}$*H*$_3$*)*$_3$), 17.9 (*Si*$\underline{C}$*H*$_2$*CH*$_2$), 52.5 (*O*$\underline{C}$*H*$_3$), 66.9 (*SiCH*$_2$$\underline{C}$*H*$_2$), 94.0 (*O*$\underline{C}$*H*$_2$), 123.6 (*Py*$\underline{C}$*5H*), 127.9 (*Py*$\underline{C}$*4*), 140.0 (*Py*$\underline{C}$*2H*), 143.2 (*Py*$\underline{C}$*6H*), 151.5 (*Py*$\underline{C}$*3*), 165.2 (*C*$\underline{O}_2$*Me*); *m/z* (MS, ES^+) 284 (100%, MH^+); LCMS (system E) tR 5.5 min (91%); accurate mass: found 306.1134, calc. for $C_{13}H_{21}NNaO_4Si^+$ 306.1132.

Methyl 3-{[2-(trimethylsilyl)ethoxy]methoxy}isonicotinate 1-oxide 293

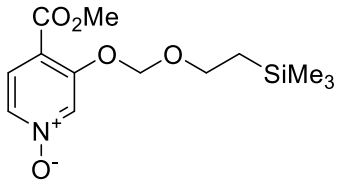

meta-Chloroperbenzoic acid (184 mg, 1.07 mmol) was added to a solution of methyl 3-{[2-(trimethylsilyl)ethoxy]methoxy}isonicotinate **292** (151 mg, 0.53 mmol) in dichloromethane (5 mL) and the resulting solution stirred at room temperature for 72 h. The reaction mixture was diluted with dichloromethane (20 mL), washed with saturated sodium bicarbonate solution (20 mL) then brine (20 mL). The aqueous layers were back-extracted with dichloromethane (20 mL). The organic layers were combined, dried over sodium sulfate and concentrated *in vacuo* to give **293** as a colourless oil (66 mg, 41%). R_f 0.45 (ethyl acetate); ν_{max} (film) 3060 (C–H), 2955 (C–H), 1679 (C=O); δ_H (400 MHz, $CDCl_3$) 0.00 (9H, s, *(C<u>H</u>3)3*), 0.92–0.99 (2H, m, *CH2OCH2C<u>H</u>2Si*), 3.75–3.81 (2H, m, *CH2OC<u>H</u>2CH2Si*), 3.89 (3H, s, *OC<u>H</u>3*), 5.29 (2H, s, *C<u>H</u>2OCH2CH2Si*), 7.71 (1H, d, *J* 7.0, *PyC5<u>H</u>*), 7.90 (1H, dd, *J* 7.0, 1.5, *PyC6<u>H</u>*), 8.32 (1H, d, *J* 1.5, *PyC2<u>H</u>*); δ_C (100 MHz, $CDCl_3$) –1.5 (*(<u>C</u>H3)3*), 17.9 (*CH2OCH2<u>C</u>H2Si*), 52.5 (*O<u>C</u>H3*), 67.5 (*CH2O<u>C</u>H2CH2Si*), 94.3 (*<u>C</u>H2OCH2CH2Si*), 117.7 (s), 127.1 (*Py<u>C</u>5H*), 129.8 (*Py<u>C</u>2H*), 132.9 (*Py<u>C</u>6H*), 155.2 and 163.3 (*Py<u>C</u>3* and *<u>C</u>O2Me*); *m/z* (MS, ES^+) 322 (100%, MNa^+); LCMS (system E) tR 4.8 min (96%); accurate mass: found 322.1086, calc. for $C_{13}H_{21}NNaO_5Si^+$ 322.1081.

Methyl 2-acetoxy-3-hydroxyisonicotinate 294

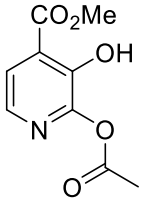

Triethylamine (28 µL, 0.20 mmol) acetic anhydride (0.64 mL, 6.9 mmol) was added to a solution of methyl 3-{[2-(trimethylsilyl)ethoxy]methoxy}isonicotinate 1-oxide **293** (30 mg, 0.10 mmol) in acetic anhydride (0.64 mL) and the resulting solution heated at 140 °C for 16 h. The reaction mixture was diluted with saturated sodium bicarbonate solution (3 mL) and extracted with ethyl acetate (3 × 8 mL). The organic layers were combined and concentrated *in vacuo* to give a brown gum that was purified by flash column chromatography (dichloromethane → ethylacetate) to give **294** as a beige solid (7 mg, 33%). R_f 0.15 (ethyl acetate); δ_H (400 MHz, $CDCl_3$) 2.40 (3H, s, *CC<u>H</u>3*), 3.90 (3H, s, *OC<u>H</u>3*), 6.69 (1H, d, *J* 7.0, *PyC5<u>H</u>*), 7.34 (1H, d, *J* 7.0, *PyC6<u>H</u>*); δ_C (100 MHz, $CDCl_3$) 20.6 (*C<u>C</u>H3*), 52.9 (*O<u>C</u>H3*), 105.8 (*Py<u>C</u>5H*), 131.2 (*Py<u>C</u>6H*), 132.6, 141.3, 160.5 (*Py<u>C</u>2*), 163.3 (*<u>C</u>CH3*), 168.2 (*PyC4<u>C</u>O2Me*); *m/z* (MS, ES^+) 170 (100%, ($[M–Ac]H^+$), 445 (25%, M_2Na^+); LCMS (system E) tR 0.6 min (96%).

2-Bromo-3-methoxyisonicotinic acid 296

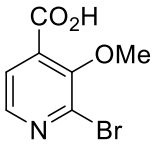

A solution of diisopropylamine (1.54 mL, 11.0 mmol) in tetrahydrofuran (10 mL) was evacuated and refilled with nitrogen (× 3) then cooled to –78 °C. *n*-Butyllithium (4.0 mL of a 2.5 M solution in hexanes, 10.0 mmol) was added dropwise over 5 min and the resulting solution stirred at –78 °C for 30 min. A solution of 2-bromo-3-methoxypyridine (1.88 g, 10.0 mmol) in tetrahydrofuran (5.0 mL) was added dropwise over 50 min and the reaction mixture stirred at –78 °C for 2.5 h. Carbon dioxide (5 g, solid) was added and the reaction mixture allowed to warm to room temperature then diluted with water (50 mL), adjusted to pH 7 with hydrochloric acid (1 M, aq) and then extracted with ethyl acetate (3 × 50 mL). The organic layers were combined, dried over sodium sulfate and concentrated *in vacuo* to give a beige solid that was recrystallised from acetonitrile to give **296** as a beige solid (367 mg). The aqueous layer was acidified to pH 1 with hydrochloric acid (1 M, aq). The resulting precipitate was filtered, washing with hydrochloric acid (0.5 M, aq) to give further **296** as a white solid (116 mg, 21% overall yield). mp 192–200 °C (water); ν_{max} (film) 2944 (C–H), 1726 (C=O); δ_H (400 MHz, CD_3OD) 3.95 (3H, s, *Me*), 7.64 (1H, d, *J* 5.0, *PyC5H*), 8.20 (1H, d, *J* 5.0, *PyC6H*); δ_C (125 MHz, CD_3OD) 63.0 (*C*H_3), 125.2 (*PyC5H*), 137.2, 140.4, 146.2 (*PyC6H*), 153.7, 167.1 (*C*O_2*H*); *m/z* (MS, ES^+) 230 (100%, MH^+); LCMS (system E) tR 2.5 min (100%); accurate mass: found 229.9468, calc. for $C_7H_5BrNO_3^-$ 229.9458.

Methyl 2-bromo-3-methoxyisonicotinate 297

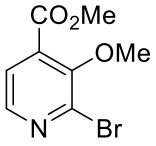

Sulfuric acid (0.27 mL of a concentrated aq. solution, 4.9 mmol) was added to a suspension of 2-bromo-3-methoxyisonicotinic acid **296** (429 mg, 1.85 mmol) in methanol (6 mL) and the resulting suspension heated at 65 °C for 16 h. The methanol was removed *in vacuo*, the residue poured into 25 mL ice/water and the resulting solution neutralised to pH 7 by the addition of saturated sodium bicarbonate solution. The resulting suspension was extracted with ethyl acetate (3 × 25 mL). The organic layers were combined, dried over sodium sulfate and concentrated *in vacuo* to give **297** as a beige oil (416 mg, 91% yield). R_f 0.65 (2:1 cyclohexane–ethyl acetate); ν_{max} (film) 2951 (C–H), 2848 (C–H), 1737 (C=O); δ_H (400 MHz, $CDCl_3$) 3.97 (3H, s, *Me*), 3.98 (3H, s, *Me*), 7.56 (1H, d, *J* 5.0, *PyC5H*), 8.24 (1H, d, *J* 5.0, *PyC6H*); δ_C (100 MHz, $CDCl_3$) 53.0 (*C*H_3), 62.4 (*C*H_3), 123.5 (*PyC5H*), 133.6, 140.0, 144.9 (*PyC6H*), 152.4, 164.2 (*C*O_2*Me*); *m/z* (MS, ES^+) 248 (100%, MH^+); LCMS (system E) tR 4.1 min (95%); accurate mass: found 267.9580, calc. for $C_8H_8BrNNaO_3^+$ 267.9580.

2-Bromo-5-methoxyisonicotinic acid 299

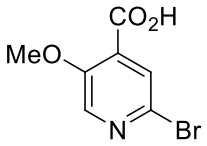

A solution of diisopropylamine (1.54 mL, 11.0 mmol) in tetrahydrofuran (10 mL) was evacuated and refilled with nitrogen (× 3) then cooled to –78 °C. *n*-Butyllithium (4.0 mL of a 2.5 M solution in hexanes, 10.0 mmol) was added dropwise over 5 min and the resulting solution stirred at –78 °C for 30 min. A solution of 2-bromo-5-methoxypyridine (1.88 g, 10.0 mmol) in tetrahydrofuran (5.0 mL) was added dropwise over 50 min and the reaction mixture stirred at –78 °C for 2.5 h. Carbon dioxide (5 g, solid) was added and the reaction mixure allowed to warm to room temperature then diluted with water (50 mL), adjusted to pH 10 with hydrochloric acid (1 M, aq) and then washed with ethyl acetate (3 × 50 mL). The aqueous layer was acidified to pH 1 with hydrochloric acid (1 M, aq). The resulting precipitate was filtered, washing with hydrochloric acid (0.5 M, aq) to give **299** as a white solid (1.30 g, 56% yield). mp 209–214 °C; ν_{max} (film) 2983 (C–H), 2947 (C–H), 2861 (C–H), 1586 (C=O); δ_H (400 MHz, CD_3OD) 3.93 (3H, s, *Me*), 7.08 (1H, s, *PyC3H*), 8.35 (1H, s, *PyC6H*); δ_C (100 MHz, CD_3OD) 54.5 (*CH*$_3$), 109.3, 109.7 (*PyC3H*), 149.7 (*PyC6H*), 154.6, 165.0, 173.2 (*CO*$_2$*H*); *m/z* (MS, ES^+) 230 (100%, MH^+); LCMS (system E) tR 3.0 min (95%); accurate mass: found 229.9467, calc. for $C_7H_5BrNO_3^-$ 229.9458.

Methyl 2-bromo-5-methoxyisonicotinate 300

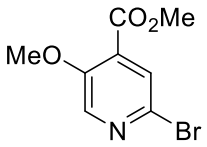

Sulfuric acid (0.83 mL of a concentrated aq. solution, 14.9 mmol) was added to a suspension of 2-bromo-5-methoxyisonicotinic acid **299** (1.28 g, 5.50 mmol) in methanol (19 mL) and the resulting suspension heated at 65 °C for 16 h. The methanol was removed *in vacuo*, the residue poured into 50 mL ice/water and the resulting solution neutralised to pH 7 by the addition of saturated sodium bicarbonate solution. The resulting suspension was extracted with ethyl acetate (3 × 50 mL). The organic layers were combined, dried over sodium sulfate and concentrated *in vacuo* to give **300** as a white solid (1.22 g, 90% yield). R_f 0.80 (2:1 cyclohexane–ethyl acetate); mp 50–53 °C; ν_{max} (film) 2982 (C–H), 2951 (C–H), 2856 (C–H), 1718 (C=O); δ_H (400 MHz, CD_3OD) 3.93 (6H, s, 2 × *Me*), 7.08 (1H, s, *PyC3H*), 8.36 (1H, s, *PyC6H*); δ_C (100 MHz, CD_3OD) 53.6 and 54.8 (2 × *CH*$_3$), 109.8, 113.2 (*PyC3H*), 143.9, 151.4 (*PyC6H*), 165.2 and 166.5 (*PyC5* and *CO*$_2$*Me*); *m/z* (MS, ES^+) 248 (100%, MH^+); LCMS (system E) tR 4.9 min (95%); accurate mass: found 267.9573, calc. for $C_8H_8BrNNaO_3^+$ 267.9580.

Methyl 5-methoxy-2-[(trimethylsilyl)ethynyl]isonicotinate 301

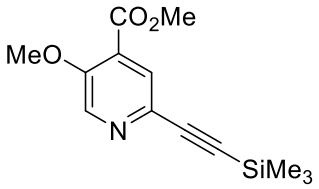

Methyl 2-bromo-5-methoxyisonicotinate **300** (577 mg, 2.34 mmol), copper(I) bromide (42 mg, 0.28 mmol), triphenylphosphine (123 mg, 0.47 mmol) and tetrakis(triphenylphosphine)palladium (169 mg, 0.15 mmol) were placed in a sealed vial which was evacuated and refilled with nitrogen (× 3) then 11 mL of a degassed 2:1 mixture of triethylamine–*N*,*N*-dimethylformamide added followed by trimethylsilylacetylene (3.3 mL, 23.4 mmol) and the resulting mixture heated at 80 °C for 12 h. The triethylamine was removed *in vacuo* and the residue purified by flash column chromatography (cyclohexane → 1:1 dichloromethane–cyclohexane) to give **301** as a yellow oil (519 mg, 84% yield). R_f 0.55 (9:1 cyclohexane–ethyl acetate); ν_{max} (film) 2954 (C–H), 2900 (C–H), 2859 (C–H), 1728 (C=O); δ_H (400 MHz, $CDCl_3$) 0.09 (9H, s, *Si(C<u>H</u>₃)₃*), 3.76 (3H, s, *Me*), 3.79 (3H, s, *Me*), 6.97 (1H, app. s, *PyC3<u>H</u>*), 8.22 (1H, d, *J* 0.5, *PyC<u>6H</u>*); δ_C (100 MHz, $CDCl_3$) –0.1 (*Si(<u>C</u>H₃)₃*), 52.4 (*<u>C</u>H₃*), 54.1 (*<u>C</u>H₃*), 99.7 (*<u>C</u>≡C*), 100.1 (*<u>C</u>≡C*), 111.0 (*PyC<u>3</u>H*), 111.4, 142.0, 153.1 (*PyC<u>6</u>H*), 163.6 and 165.2 (*PyC<u>5</u>* and *<u>C</u>O₂Me*); *m/z* (MS, ES^+) 264 (100%, MH^+); LCMS (system E) tR 6.6 min (99%); accurate mass: found 264.1060, calc. for $C_{13}H_{18}NO_3Si^+$ 264.1050.

Methyl 3-methoxy-2-[(trimethylsilyl)ethynyl]isonicotinate 303

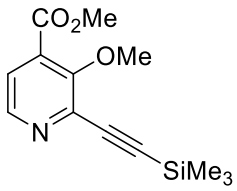

Methyl 2-bromo-3-methoxyisonicotinate **297** (361 mg, 1.47 mmol), copper(I) bromide (26 mg, 0.18 mmol), triphenylphosphine (77 mg, 0.29 mmol) and tetrakis(triphenylphosphine)palladium (106 mg, 0.09 mmol) were placed in a sealed vial which was evacuated and refilled with nitrogen (× 3) then 9 mL of a degassed 2:1 mixture of triethylamine–*N*,*N*-dimethylformamide added followed by trimethylsilylacetylene (2.1 mL, 14.7 mmol) and the resulting mixture heated at 80 °C for 12 h. The triethylamine was removed *in vacuo* and the residue purified by flash column chromatography (cyclohexane → 4:1 cyclohexane–ethyl acetate) to give **303** as a yellow oil (217 mg, 56% yield). R_f 0.45 (3:1 cyclohexane–ethyl acetate); ν_{max} (film) 2956 (C–H), 2900 (C–H), 1737 (C=O); δ_H (400 MHz, $CDCl_3$) 0.28 (9H, s, *Si(C<u>H</u>₃)₃*), 3.93 (3H, s, *Me*), 4.04 (3H, s, *Me*), 7.50 (1H, d, *J* 5.0, *PyC5<u>H</u>*), 8.38 (1H, d, *J* 5.0, *PyC<u>6H</u>*); δ_C (100 MHz, $CDCl_3$) –0.5 (*Si(<u>C</u>H₃)₃*), 52.8 (*<u>C</u>H₃*), 62.1 (*<u>C</u>H₃*), 99.8 (*<u>C</u>≡C*), 101.1 (*<u>C</u>≡C*), 123.3 (*PyC<u>5</u>H*), 132.4, 139.4, 145.0 (*PyC<u>6</u>H*), 156.4, 164.8 (*<u>C</u>O₂Me*); *m/z* (MS, ES^+) 264 (100%, MH^+); LCMS (system E) tR 5.8 min (95%); accurate mass: found 264.1061, calc. for $C_{13}H_{18}NO_3Si^+$ 264.1050.

Methyl 2-{1-[(3*R*)-1-(*tert*-butoxycarbonyl)piperidin-3-yl]-1*H*-1,2,3-triazol-4-yl}-3-methoxyisonicotinate 304

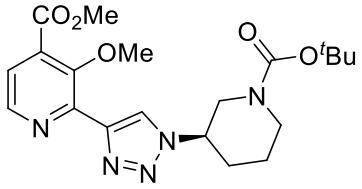

A solution of tetrabutylammonium fluoride in tetrahydrofuran (1 M, 0.92 mL, 0.92 mmol) was added to a solution of methyl 3-methoxy-2-[(trimethylsilyl)ethynyl]isonicotinate **303** (217 mg, 0.82 mmol), *tert*-butyl (3*R*)-3-azidopiperidine-1-carboxylate **271** (224 mg, 0.99 mmol), copper(II) sulfate pentahydrate (21 mg, 0.08 mmol) and (+)-sodium L-ascorbate (33 mg, 0.17 mmol) in 4 mL of a 1:1 mixture of *tert*-butanol–water and the resulting suspension heated at 65 °C for 16 h. The reaction mixture was diluted with water (5 mL) and extracted with dichloromethane (3 × 5 mL). The organic layers were combined, dried over sodium sulfate and concentrated *in vacuo* to give **304** as a yellow gum (310 mg, 78%). ν_{max} (film) 2979 (C–H), 2933 (C–H), 2862 (C–H), 1693 (C=O), 1690 (C=O); δ_H (400 MHz, $CDCl_3$) 1.42 (9H, s, *C(C*<u>*H*</u>*$_3$)$_3$*), 1.55–2.33 (4H, m, *PipC4*<u>*H*</u>*$_2$* and *PipC5*<u>*H*</u>*$_2$*), 2.90–3.79 (3H, m, 3 × *PipC*<u>*H*</u>*), 3.84 (3H, s, *C*<u>*H*</u>*$_3$*), 3.93 (3H, s, *C*<u>*H*</u>*$_3$*), 4.19–4.31 (1H, m, *PipC*<u>*H*</u>*), 4.50–4.63 (1H, m, *PipC3*<u>*H*</u>*), 7.52 (1H, d, *J* 5.0, *PyC5*<u>*H*</u>*), 8.24 (1H, s, *Tri*), 8.53 (1H, d, *J* 5.0, *PyC6*<u>*H*</u>*); δ_C (125 MHz, $CDCl_3$) 23.3 (*Pip*<u>*C*</u>*H$_2$*), 28.2 (*C(*<u>*C*</u>*H$_3$)$_3$*), 30.7 (*Pip*<u>*C*</u>*H$_2$*), 42.6–44.4 and 47.3–49.3 (*Pip*<u>*C*</u>*2H$_2$* and *Pip*<u>*C*</u>*6H$_2$*), 52.7 (*C*<u>*H*</u>*$_3$*), 56.3 (*Pip*<u>*C*</u>*3H*), 62.2 (*C*<u>*H*</u>*$_3$*), 80.4 (*C(CH$_3$)$_3$*), 123.1 (*Py*<u>*C*</u>*5H*), 123.4 (*Tri*<u>*C*</u>*H*), 143.4, 145.2 (*Py*<u>*C*</u>*6H*), 145.6, 151.7, 154.4, 165.0 (2 × *C*<u>*O*</u>*$_2$*); *m/z* (MS, ES^+) 418 (100%, MH^+); LCMS (system E) tR 4.8 min (90%); accurate mass: found 440.1899, calc. for $C_{20}H_{27}N_5NaO_5^+$ 440.1904; $[\alpha]_D^{20}$ +0.113 (*c* 1.0 in $CHCl_3$).

Methyl 2-{1-[(3*R*)-1-(*tert*-butoxycarbonyl)piperidin-3-yl]-1*H*-1,2,3-triazol-4-yl}-5-methoxyisonicotinate 305

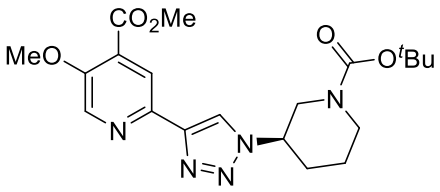

A solution of tetrabutylammonium fluoride in tetrahydrofuran (1 M, 1.6 mL, 1.6 mmol) was added to a solution of methyl 5-methoxy-2-[(trimethylsilyl)ethynyl]isonicotinate **301** (379 mg, 1.44 mmol), *tert*-butyl (3*R*)-3-azidopiperidine-1-carboxylate **271** (393 mg, 1.74 mmol), copper(II) sulfate pentahydrate (36 mg, 0.14 mmol) and (+)-sodium L-ascorbate (57 mg, 0.29 mmol) in 8 mL of a 1:1 mixture of *tert*-butanol and water and the resulting suspension heated at 65 °C for 16 h. The reaction mixture was diluted with water (10 mL) and extracted with dichloromethane (3 × 10 mL). The organic layers were combined, dried over sodium sulfate and concentrated *in vacuo* to give **305** as a yellow gum (394 mg, 66%). ν_{max} (film) 2979 (C–H), 2950 (C–H), 2859 (C–H), 1695 (C=O), 1690 (C=O); δ_H (400 MHz, $CDCl_3$) 1.44 (9H, s, *C(C*<u>*H*</u>*$_3$)$_3$*), 1.57–2.34 (4H, m, *PipC4*<u>*H*</u>*$_2$* and

PipC5H$_2$), 2.96–3.09 (1H, m, *PipCH*), 3.36–3.46 (1H, m, *PipCH*), 3.82 (3H, s, *CH*$_3$), 3.86–3.93 (1H, m, *PipCH*), 3.96 (3H, s, *CH*$_3$), 4.24–4.34 (1H, m, *PipCH*), 4.46–4.58 (1H, m, *PipC3H*), 7.03 (1H, s, *PyC3H*), 7.87 (1H, s, *Tri*), 8.55 (1H, s, *PyC6H*); δ_C (125 MHz, $CDCl_3$) 23.4 (*PipCH*$_2$), 28.3 (*C(CH*$_3$*)*$_3$), 30.7 (*PipCH*$_2$), 42.7–44.6 and 47.3–49.6 (*PipC2H*$_2$ and *PipC6H*$_2$), 52.6 (*CH*$_3$), 53.9 (*CH*$_3$), 56.4 (*PipC3H*), 80.3 (*C(CH*$_3$*)*$_3$), 110.3 (*PyC3H*), 118.0, 121.2 (*TriCH*), 140.0, 142.3, 148.3 (*PyC6H*), 154.4 (*PyC5*), 164.0 and 166.7 (2 × *CO*$_2$); *m/z* (MS, ES^+) 418 (100%, MH^+); LCMS (system E) tR 5.3 min (81%); accurate mass: found 440.1911, calc. for $C_{20}H_{27}N_5NaO_5^+$ 440.1904; $[\alpha]_D^{20}$ +0.204 (*c* 1.0 in $CHCl_3$).

3-Hydroxy-2-{1-[(3*R*)-piperidin-3-yl]-1*H*-1,2,3-triazol-4-yl}isonicotinic acid trifluoroacetate 306

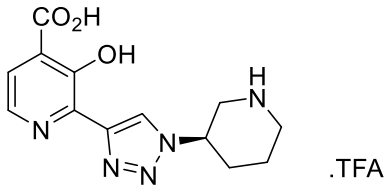

A solution of methyl 2-{1-[(3*R*)-1-(*tert*-butoxycarbonyl)piperidin-3-yl]-1*H*-1,2,3-triazol-4-yl}-3-methoxyisonicotinate **304** (100 mg, 0.24 mmol) in hydrobromic acid (5 mL of a 55% aq solution) was heated at 90 °C for 3 h. The reaction mixture was concentrated *in vacuo* then purified by reverse phase chromatography (C18 column, eluting with 0.1% trifluoroacetic acid in water) to give **308** as a yellow solid (50 mg, 52%). mp 248–250 °C; ν_{max} (film) 1667 (C=O); δ_H (400 MHz, D_2O) 1.89–2.14 (2H, m, *PipC5H*$_2$), 2.23–2.48 (2H, m, *PipC4H*$_2$), 3.19–3.49 (2H, m, *PipC6H*$_2$), 3.69–3.90 (2H, m, *PipC2H*$_2$), 5.08–5.16 (1H, m, *PipC3H*), 7.97 (1H, app. s, *PyC5H*), 8.13 (1H, app. s, *PyC6H*), 8.90 (1H, s, *Tri*); δ_C (100 MHz, D_2O) 19.5 (*PipC5H*$_2$), 27.8 (*PipC4H*$_2$), 43.6 (*PipC6H*$_2$), 46.0 (*PipC2H*$_2$), 54.3 (*PipC3H*), 115.1, 117.4, 125.2 (*PyC5H*), 127.4 (*TriCH*), 130.9 (*PyC6H*), 131.4, 163.1, 169.7 (*CO*$_2$); *m/z* (MS, ES^+) 290 (100%, $[MH]^+$); LCMS (system E) tR 0.4 min (92%); accurate mass: found 312.1074, calc. for $C_{13}H_{15}N_5NaO_3^+$ 312.1067; $[\alpha]_D^{20}$ −0.007 (*c* 0.3 in *N*,*N*-dimethylformamide).

2-{1-[(3R)-1-Benzoylpiperidin-3-yl]-1*H*-1,2,3-triazol-4-yl}-3-hydroxyisonicotinic acid trifluoroacetate 307

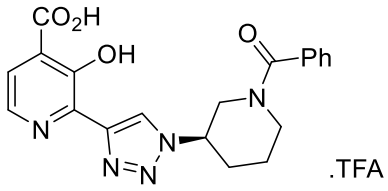

Benzoyl chloride (31 µL, 0.26 mmol) was added to a solution of 3-hydroxy-2-{1-[(3*R*)-piperidin-3-yl]-1*H*-1,2,3-triazol-4-yl}isonicotinic acid trifluoroacetate **306** (97 mg, 0.24 mmol) and triethylamine (134 µL, 0.96 mmol) in dimethyl formamide (2 mL) and the resulting solution stirred at room temperature for 16 h then acidified to pH 1 with trifluoroacetic acid and purified by reverse

phase chromatography (C18 column, eluting with 0.1% trifluoroacetic acid in water → 0.1% trifluoroacetic acid in acetonitrile) to give **307** as a beige solid (54 mg, 44%). mp 197–200 °C; ν_{max} (film) 1681 (C=O), 1615 (C=O); δ_H (400 MHz, $(CD_3)_2SO$) 1.48–2.34 (4H, m, *PipC4*$\underline{H_2}$ and *PipC5*$\underline{H_2}$), 3.12–5.03 (5H, m, *PipC2*$\underline{H_2}$, *PipC6*$\underline{H_2}$ and *PipC3*$\underline{H}$), 7.32–7.65 (5H, m, *Ph*), 7.80–7.89 (1H, m, *ArC*$\underline{H}$), 7.90–7.98 (1H, m, *ArC*$\underline{H}$), 8.96–9.21 (1H, m, *ArC*$\underline{H}$); δ_C (125 MHz, $(CD_3)_2SO$) 25.6–24.0 (*PipC5*H_2), 29.9 (*PipC4*H_2), 45.4–51.7 (*PipC6*H_2 and *PipC2*H_2), 56.2 (*PipC3H*), 124.4 (*ArCH*), 126.3 (*ArCH*), 126.8 (*ArCH*), 128.5 (*ArCH*), 129.3, 129.7, 132.9, 134.4, 135.8, 137.2, 161.6, 167.2 (*CO*$_2$*H*), 169.5 (*CON*); *m/z* (MS, ES^+) 394 (100%, MH^+); LCMS (system E) tR 3.7 min (96%); accurate mass: found 394.1500, calc. for $C_{20}H_{20}N_5O_4^+$ 394.1510; $[\alpha]_D^{20}$ +0.054 (*c* 0.25 in CH_3OH).

5-Hydroxy-2-{1-[(3*R*)-piperidin-3-yl]-1*H*-1,2,3-triazol-4-yl}isonicotinic acid trifluoroacetate 308

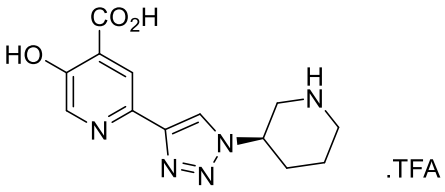

A solution of methyl 2-{1-[(3*R*)-1-(*tert*-butoxycarbonyl)piperidin-3-yl]-1*H*-1,2,3-triazol-4-yl}-5-methoxyisonicotinate **305** (100 mg, 0.24 mmol) in hydrobromic acid (5 mL of a 55% aq solution) was heated at 90 °C for 3 h. The reaction mixture was concentrated *in vacuo* then purified by reverse phase chromatography (C18 column, eluting with 0.1% trifluoroacetic acid in water) to give **308** as an off-white solid (76 mg, 78%). mp 186–189 °C; ν_{max} (film) 2978 (C–H), 2788 (C–H), 1683 (C=O); δ_H (500 MHz, D_2O) 1.76–2.11 (2H, m, *PipC5*$\underline{H_2}$), 2.14–2.39 (2H, m, *PipC4*$\underline{H_2}$), 3.14–3.43 (2H, m, *PipC6*$\underline{H_2}$), 3.61–3.80 (2H, m, *PipC2*$\underline{H_2}$), 4.98–5.04 (1H, m, *PipC3*$\underline{H}$), 6.86 (1H, s, *PyC6*$\underline{H}$), 7.82 (1H, s, *PyC3*$\underline{H}$), 8.17 (1H, s, *Tri*); δ_C (125 MHz, D_2O) 19.3 (*PipC5*H_2), 27.8 (*PipC4*H_2), 43.6 (*PipC6*H_2), 46.0 (*PipC2*H_2), 53.9 (*PipC3H*), 108.7, 118.2 (*PyC6H*), 122.8 (*TriCH*), 136.2 (*PyC3H*), 141.9, 147.1, 163.9, 170.2 (*CO*$_2$); *m/z* (MS, ES^-) 288 (100%, $[M–H]^-$); LCMS (system E) tR 0.4 min (100%); accurate mass: found 312.1058, calc. for $C_{13}H_{15}N_5NaO_3^+$ 312.1067; $[\alpha]_D^{20}$ +0.006 (*c* 0.5 in CH_3OH).

2-{1-[(3R)-1-Benzoylpiperidin-3-yl]-1*H*-1,2,3-triazol-4-yl}-5-hydroxyisonicotinic acid trifluoroacetate 309

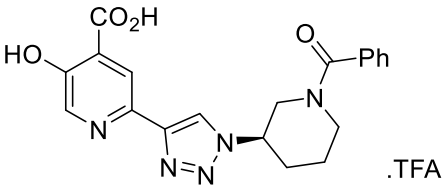

Benzoyl chloride (7 µL, 0.06 mmol) was added to a solution of 5-hydroxy-2-{1-[(3*R*)-piperidin-3-yl]-1*H*-1,2,3-triazol-4-yl}isonicotinic acid trifluoroacetate **308** (22 mg, 0.06 mmol) and

triethylamine (30 μL, 0.22 mmol) in dimethyl formamide (1 mL) and the resulting solution stirred at room temperature for 16 h then acidified to pH 1 with trifluoroacetic acid and purified by reverse phase chromatography (C18 column, eluting with 0.1% trifluoroacetic acid in water → 0.1% trifluoroacetic acid in acetonitrile) to give **309** as a white solid (12 mg, 43%). mp 217–223 °C; ν_{max} (film) 1681 (C=O), 1615 (C=O); δ_H (500 MHz, $(CD_3)_2SO$) 1.55–2.09 (4H, m, *PipC4*$\underline{H_2}$ and *PipC5*$\underline{H_2}$), 3.08–4.66 (4H, m, *PipC2*$\underline{H_2}$ and *PipC6*$\underline{H_2}$), 4.67–4.78 (*PipC3*$\underline{H}$), 6.49–6.55 (1H, m, *PyC6*$\underline{H}$), 7.33–7.52 (5H, m, *Ph*), 7.65–7.74 (1H, m, *Ar*$\underline{H}$), 8.13–8.33 (1H, m, *Ar*$\underline{H}$); δ_C (125 MHz, $(CD_3)_2SO$) 22.5–23.9 (*Pip*$\underline{C}$*5H*$_2$), 30.0 (*Pip*$\underline{C}$*4H*$_2$), 45.8–51.8 (*Pip*$\underline{C}$*6H*$_2$ and *Pip*$\underline{C}$*2H*$_2$), 55.6 (*Pip*$\underline{C}$*3H*), 118.4 (*Py*$\underline{C}$*6H*), 120.6 (*Ar*$\underline{C}$*H*), 126.7 (*Ph*$\underline{C}$*H*), 128.2, 128.5 (*Ph*$\underline{C}$*H*), 129.6 (*Ph*$\underline{C}$*H*), 135.8, 136.2, 141.5, 145.0, 161.4, 167.5 (*C*$\underline{O_2}$*H*), 169.4 (*C*$\underline{O}$*N*); *m/z* (MS, ES^+) 394 (100%, MH^+); LCMS tR 3.1 min (99%); accurate mass: found 392.1363, calc. for $C_{20}H_{18}N_5O_4^-$ 392.1364; $[\alpha]_D^{20}$ –0.133 (*c* 0.3 in CH_3OH).

3-Methoxy-2-{1-[(3*R*)-piperidin-3-yl]-1*H*-1,2,3-triazol-4-yl}isonicotinic acid 310

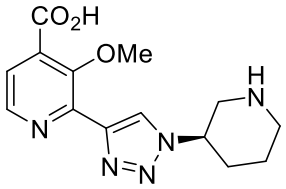

Lithium hydroxide (1 M, aq, 0.5 mL, 0.5 mmol) was added to a solution of methyl 2-{1-[(3*R*)-1-(*tert*-butoxycarbonyl)piperidin-3-yl]-1*H*-1,2,3-triazol-4-yl}-3-methoxyisonicotinate **304** (18 mg, 0.04 mmol) in acetonitrile (0.5 mL) and the resulting solution stirred at room temperature for 30 min. The reaction mixture was acidified to pH 1 with trifluoroacetic acid and the resulting solution stirred at room temperature for 16 h then purified by strong cation exchange chromatography, washing with methanol and eluting with methanolic ammonia (2 M) to give **310** as a yellow gum (7 mg, 54%). ν_{max} (film) 2947 (C–H), 2863 (C–H), 1606 (CO_2H); δ_H (400 MHz, CD_3OD) 1.60–1.97 (2H, m, *PipC4*$\underline{H_2}$), 2.10–2.23 (1H, m, *PipC5*$\underline{H}$), 2.28–2.40 (1H, m, *PipC5*$\underline{H}$), 2.68–2.80 (1H, m, *PipC6*$\underline{H}$), 2.88–3.20 (2H, m, *PipC6*$\underline{H}$ and *PipC2*$\underline{H}$), 3.33–3.47 (1H, m, *PipC2*$\underline{H}$), 3.95 (3H, s, *C*$\underline{H_3}$), 4.62–4.75 (1H, m, *PipC3*$\underline{H}$), 7.34 (1H, d, *J* 5.0, *PyC5*$\underline{H}$), 8.31 (1H, d, *J* 5.0, *PyC6*$\underline{H}$), 8.53 (1H, s, *Tri*); δ_C (125 MHz, CD_3OD) 25.8 (*Pip*$\underline{C}$*4H*$_2$), 32.1 (*Pip*$\underline{C}$*5H*$_2$), 46.2 (*Pip*$\underline{C}$*6H*$_2$), 51.8 (*Pip*$\underline{C}$*2H*$_2$), 58.9 (*Pip*$\underline{C}$*3H*), 61.5 (*C*$\underline{H_3}$), 123.7 (*Py*$\underline{C}$*5H*), 125.5 (*Tri*$\underline{C}$*H*), 143.7, 144.3, 144.5, 145.0 (*Py*$\underline{C}$*6H*), 151.3, 173.8 (*C*$\underline{O_2}$); *m/z* (MS, ES^+) 304 (100%, MH^+); LCMS (system E) tR 2.5 min (90%); accurate mass: found 304.1402, calc. for $C_{14}H_{18}N_5O_3^+$ 304.1404; $[\alpha]_D^{20}$ –0.004 (*c* 0.5 in CH_3OH).

5-Methoxy-2-{1-[(3*R*)-piperidin-3-yl]-1*H*-1,2,3-triazol-4-yl}isonicotinic acid 311

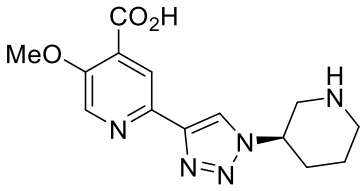

Lithium hydroxide (1 M, aq, 1.0 mL, 1.0 mmol) was added to a solution of methyl 2-{1-[(3*R*)-1-(*tert*-butoxycarbonyl)piperidin-3-yl]-1*H*-1,2,3-triazol-4-yl}-5-methoxyisonicotinate **305** (51 mg, 0.12 mmol)) in acetonitrile (1 mL) and tetrahydrofuran (1 mL) and the resulting solution stirred at room temperature for 30 min. The reaction mixture was acidified to pH 1 with trifluoroacetic acid and the resulting solution stirred at room temperature for 16 h then purified by strong cation exchange chromatography, washing with methanol and eluting with methanolic ammonia (2 M) to give **311** as a yellow gum (10 mg, 27%). ν_{max} (film) 2948 (C–H), 1597 (CO_2H); δ_H (400 MHz, CD_3OD) 1.66–1.81 (1H, m, *PipC5H*), 1.86–2.00 (1H, m, *PipC5H*), 2.06–2.18 (1H, m, *PipC4H*), 2.27–2.37 (1H, m, *PipC4H*), 2.69–2.81 (1H, m, *PipC6H*), 3.03–3.18 (2H, m, *PipC5H* and *PipC6H*), 3.39–3.48 (1H, m, *PipC5H*), 3.95 (3H, s, O*CH*$_3$), 4.54–4.74 (1H, m, *PipC3H*), 6.76 (1H, s, *PyC6H*), 8.20 (1H, s, *Tri*), 8.62 (1H, s, *PyC3H*); δ_C (125 MHz, CD_3OD) 25.5 (*PipC5H*$_2$), 31.8 (*PipC4H*$_2$), 46.1 (*PipC6H*$_2$), 51.5 (*PipC2H*$_2$), 54.5 (O*CH*$_3$), 58.6 (*PipC3H*), 107.9 (*PyC6H*), 117.3, 122.7 (*TriCH*), 144.3, 147.1 (*PyC3H*), 152.4, 165.7, 175.5 (*CO*$_2$); *m/z* (MS, ES^+) 304 (100%, MH^+); LCMS (system E) tR 3.5 min (85%); accurate mass: found 304.1403, calc. for $C_{14}H_{18}N_5O_3^+$ 304.1404; $[\alpha]_D^{20}$ –0.025 (*c* 0.8 in CH_3OH).

2-{1-[(3*R*)-Piperidin-3-yl]-1*H*-1,2,3-triazol-4-yl}isonicotinic acid 312

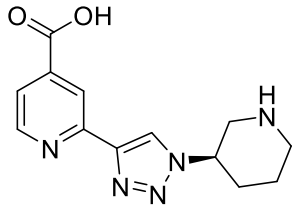

Lithium hydroxide (1 M, aq, 1.0 mL, 1.0 mmol) was added to a solution of methyl 2-{1-[(3*R*)-piperidin-3-yl]-1*H*-1,2,3-triazol-4-yl}isonicotinate **225** (50 mg, 0.17 mmol) in acetonitrile (1 mL) and the resulting suspension stirred at room temperature for 16 h. The reaction mixture was acidified with hydrochloric acid (1 M, aq, 1.1 mL) then purified on a 1 g strong cation exchange column, washing with methanol (50 mL) then eluting with methanolic ammonia (2 M, 50 mL) to give **312** as a white solid (54 mg, quant.). mp 197–200 °C; ν_{max} (film) 3273 (br, OH), 1601 and 1548 (CO_2H); δ_H (400 MHz, CD_3OD) 1.78–1.92 (1H, m, *PipC5H*), 1.94–2.06 (1H, m, *PipC5H*), 2.12–2.26 (1H, m, *PipC4H*), 2.32–2.43 (1H, m, *PipC4H*), 2.87–2.98 (1H, m, *PipC6H*), 3.18–3.27 (1H, m, *PipC6H*), 3.29–3.39 (1H, m, *PipC2H*), 3.57–3.66 (1H, m, *PipC2H*), 4.80–4.91 (1H, m, *PipC3H*), 7.77 (1H, dd, *J* 5.0, 1.5, *PyC5H*), 8.48 (1H, s, *ArH*), 8.54 (1H, s, *ArH*), 8.60 (1H, d, *J* 5.0, *PyC6H*); δ_C (125 MHz, CD_3OD) 24.3 (*PipC5H*$_2$), 31.3 (*PipC4H*$_2$), 45.7 (*PipC6H*$_2$), 50.3

(*Pip*<u>*C*</u>*2H*$_2$), 57.7 (*Pip*<u>*C*</u>*3H*), 121.3 (*Ar*<u>*C*</u>*H*), 123.3 (*Py*<u>*C*</u>*5H*), 123.9 (*Ar*<u>*C*</u>*H*), 148.6, 150.8 (*Py*<u>*C*</u>*6H*), 151.4, 172.5 (<u>*C*</u>*O*$_2$*H*); *m/z* (MS, ES$^-$) 272 (100%, [M–H]$^-$); LCMS tR 7.1 min (100%); accurate mass: found 296.1116, calc. for $C_{13}H_{15}N_5NaO_2^+$ 296.1118; $[\alpha]_D^{20}$ −0.049 (*c* 0.5 in CH_3OH).

2-(1-{(3*R*)-1-[2-(2-Methoxyethoxy)benzoyl]piperidin-3-yl}-1*H*-1,2,3-triazol-4-yl)isonicotinic acid 315

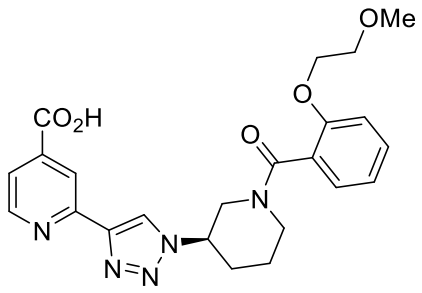

2-(2-Methoxyethoxy)benzoic acid (19.6 mg, 0.10 mmol) was taken up in dichloromethane (0.25 mL). Oxalyl chloride (17 µL, 0.20 mmol) was added followed by dimethyl formamide (1 drop). The reaction mixture was stirred at room temperature for 2 h then concentrated *in vacuo* to give a colourless oil that was taken up in acetonitrile (1 mL). Triethylamine (14 µL, 0.10 mmol) and methyl 2-{1-[(3*R*)-piperidin-3-yl]-1*H*-1,2,3-triazol-4-yl}isonicotinate **225** (29 mg, 0.10 mmol) were added and the resulting solution stirred at room temperature for 16 h. Lithium hydroxide (1 M, aq, 1.0 mL, 1.0 mmol) and water (1.0 mL) were added and the resulting solution stirred at room temperature for 16 h. The reaction mixture was concentrated *in vacuo* then purified on a 1 g strong cation exchange column, washing with methanol (20 mL) then eluting with methanolic ammonia (2 M, 10 mL) to give **315** as a white foam (8 mg, 18%). ν_{max} (film) 1599 (CO_2H); δ_H (400 MHz, CD_3OD) 1.56–2.45 (4H, m, 2 × *PipC*<u>*H*</u>$_2$), 2.93–5.26 (11H, m, *CH*$_2$*CH*$_2$*OC*<u>*H*</u>$_3$, *CH*$_2$*C*<u>*H*</u>$_2$*OCH*$_3$, *C*<u>*H*</u>$_2$*CH*$_2$*OCH*$_3$, 2 × *PipC*<u>*H*</u>$_2$ and *PipC*<u>*H*</u>), 6.95–7.73 (3H, m, 3 × *ArC*<u>*H*</u>), 7.73–7.78 (1H, m, *ArC*<u>*H*</u>), 8.36–8.66 (3H, m, 3 × *ArC*<u>*H*</u>); δ_C (125 MHz, CD_3OD) 24.9 and 31.8 (*Pip*<u>*C*</u>*5H*$_2$ and *Pip*<u>*C*</u>*4H*$_2$), 43.1, 46.8, 47.4 and 53.4 (*Pip*<u>*C*</u>*6H*$_2$ and *Pip*<u>*C*</u>*2H*$_2$), 58.3 (*Pip*<u>*C*</u>*3H*), 59.4 (*CH*$_2$*CH*$_2$*O*<u>*C*</u>*H*$_3$), 69.1 (<u>*C*</u>*H*$_2$*CH*$_2$*OCH*$_3$), 72.4 (*CH*$_2$<u>*C*</u>*H*$_2$*OCH*$_3$), 113.1 (*Ar*<u>*C*</u>*H*), 121.1 (*Ar*<u>*C*</u>*H*), 122.6 (*Ar*<u>*C*</u>*H*), 123.4 (*Ar*<u>*C*</u>*H*), 123.8 (*Ar*<u>*C*</u>*H*), 126.4, 128.6, 129.0 (*Ar*<u>*C*</u>*H*), 132.4 (*Ar*<u>*C*</u>*H*), 144.0, 148.3, 151.2 (*Py*<u>*C*</u>*6H*), 156.0 (*Ar*<u>*C*</u>*O*), 169.5 and 170.5 (<u>*C*</u>*O*$_2$*H* and <u>*C*</u>*ON*); *m/z* (MS, ES$^+$) 452 (100%, MH$^+$); LCMS tR 12.8 min (98%); accurate mass: found 474.1739, calc. for $C_{23}H_{25}N_5NaO_5^+$ 474.1748; $[\alpha]_D^{20}$ −0.334 (*c* 0.5 in CH_3OH).

2-(1-{(3R)-1-[4-(2-Methoxyethoxy)benzoyl]piperidin-3-yl}-1*H*-1,2,3-triazol-4-yl)isonicotinic acid trifluoroacetate 317

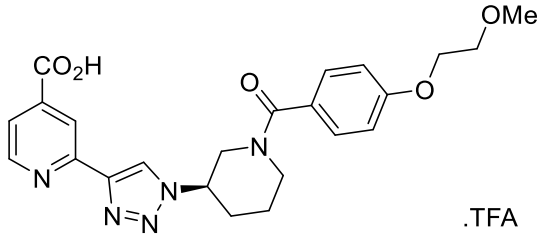

4-(2-Methoxyethoxy)benzoic acid (19.6 mg, 0.10 mmol) was taken up in dichloromethane (0.25 mL). Oxalyl chloride (17 µL, 0.20 mmol) was added followed by dimethyl formamide (1 drop). The reaction mixture was stirred at room temperature for 2 h then concentrated *in vacuo* to give a yellow solid that was taken up in acetonitrile (1 mL). Triethylamine (14 µL, 0.10 mmol) and methyl 2-{1-[(3*R*)-piperidin-3-yl]-1*H*-1,2,3-triazol-4-yl}isonicotinate (29 mg, 0.10 mmol) were added and the resulting solution stirred at room temperature for 16 h. Lithium hydroxide (1 M, aq, 1.0 mL, 1.0 mmol) and water (1.0 mL) were added and the resulting solution stirred at room temperature for 16 h. The reaction mixture was acidified to pH 1 with trifluoroacetic acid then purified by reverse phase chromatography (C18 column, eluting with 0.1% trifluoroacetic acid in water → 0.1% trifluoroacetic acid in 3:7 acetonitrile–water) to give an off-white solid that was taken up in hot acetonitrile (5 mL). The resulting precipitate was filtered, washing with acetonitrile (3 × 0.5 mL) to give **317** as an off-white solid (11 mg, 19%). mp 240–243 °C; ν_{max} (film) 1624 (CO_2H); δ_H (400 MHz, $(CD_3)_2SO$) 1.56–1.91 (2H, m, *PipC5H*$_2$), 2.15–2.35 (2H, m, *PipC4H*$_2$), 2.91–4.67 (11H, m, *CH*$_2$*CH*$_2$*OCH*$_3$, *CH*$_2$*CH*$_2$*OCH*$_3$, *CH*$_2$*CH*$_2$*OCH*$_3$, *PipC2H*$_2$ and *PipC6H*$_2$), 4.73–4.84 (1H, m, *PipC3H*), 6.98 (2H, d, *J* 9.0, *PhC3H* and *PhC5H*), 7.37 (2H, d, *J* 9.0, *PhC2H* and *PhC6H*), 7.76 (1H, dd, *J* 5.0, 1.5, *PyC5H*), 8.42 (1H, s, *ArH*), 8.74–8.80 (2H, m, *ArH* and *PyC6H*); δ_C (125 MHz, $(CD_3)_2SO$) 23.1–24.4 (*PipC5H*$_2$), 30.1 (*PipC4H*$_2$), 45.4–47.8 and 50.4–52.8 (*PipC6H*$_2$ and *PipC2H*$_2$), 56.1 (*PipC3H*), 58.2 (*CH*$_2$*CH*$_2$*OCH*$_3$), 67.1 (*CH*$_2$*CH*$_2$*OCH*$_3$), 70.3 (*CH*$_2$*CH*$_2$*OCH*$_3$), 114.2 (*PhC3H* and *PhC5H*), 118.4 (*ArCH*), 122.0 (*PyC5H*), 122.6 (*ArCH*), 127.8, 129.0 (*PhC2H* and *PhC6H*), 140.0, 146.6, 150.8 (*PyC6H*), 150.9, 159.6, 166.2 (*CO*$_2$*H*), 169.5 (*CON*); *m/z* (MS, ES^+) 452 (100%, MH^+); LCMS tR 11.7 min (100%); accurate mass: found 474.1753, calc. for $C_{23}H_{25}N_5NaO_5^+$ 474.1748; $[\alpha]_D^{20}$ −0.414 (*c* 0.5 in *N*,*N*-dimethylformamide).

Methyl 2-(prop-2-yn-1-yloxy)benzoate 319[211]

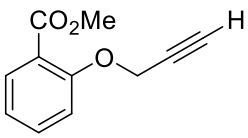

Propargyl bromide (3.0 mL of an 80% w/w solution in toluene, 26.9 mmol) was added dropwise to a suspension of methyl salicylate (1.40 mL, 10.8 mmol) and potassium carbonate (7.44 g, 53.8 mmol) in dimethyl formamide (20 mL) at 0 °C and the resulting suspension stirred at room temperature for 16 h. The reaction mixture was diluted with diethyl ether (50 mL) then washed

with water (75 mL) and brine (2 × 50 mL). The aqueous layers were back-extracted with diethyl ether (50 mL) then the organic layers combined, dried over sodium sulfate and concentrated *in vacuo* to give **319** as a yellow oil (1.85 g, 90%). R_f 0.25 (9:1 cyclohexane–ethyl acetate); ν_{max} (film) 3289 (alkynyl C–H), 2952 (C–H), 2121 (C≡C), 1722 (C=O) [*consistent with lit.*]; δ_H (400 MHz, $CDCl_3$) 2.55 (1H, t, *J* 2.0, *C*≡*C*<u>*H*</u>), 3.91 (3H, s, *C*<u>*H*</u>$_3$), 4.81 (2H, d, *J* 2.0, *C*<u>*H*</u>$_2$*C*≡*C*), 7.06 (1H, app. t, *J* 8.0, *PhC5*<u>*H*</u>), 7.15 (1H, app. d, *J* 8.0, *PhC3*<u>*H*</u>), 7.47–7.52 (1H, m, *PhC4*<u>*H*</u>), 7.83 (1H, dd, *J* 8.0, 2.0, *PhC6*<u>*H*</u>) [*consistent with lit.*]; δ_C (100 MHz, $CDCl_3$) 52.0 (<u>*C*</u>*H*$_3$), 56.8 (<u>*C*</u>*H*$_2$), 76.0 (*C*≡<u>*C*</u>*H*), 78.2 (<u>*C*</u>≡*CH*), 114.4 (*Ph*<u>*C*</u>*3H*), 121.0 (*Ph*<u>*C*</u>*1*), 121.3 (*Ph*<u>*C*</u>*5H*), 131.7 (*Ph*<u>*C*</u>*6H*), 133.2 (*Ph*<u>*C*</u>*4H*), 156.9 (*Ph*<u>*C*</u>*2*), 166.4 (<u>*C*</u>*O*$_2$*Me*); *m/z* (MS, ES^+) 403 (100%, M_2Na^+); LCMS (system E) tR 5.5 min (100%).

2-(Prop-2-yn-1-yloxy)benzoic acid 320[211]

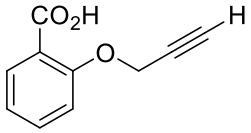

Lithium hydroxide (1 M, aq, 30 mL, 30 mmol) was added to a solution of methyl 2-(prop-2-yn-1-yloxy)benzoate **319** (1.80 g, 9.46 mmol) in a mixture of methanol (10 mL), tetrahydrofuran (20 mL) and water (20 mL) and the resulting solution stirred at room temperature for 16 h. The reaction mixture was acidified to pH 1 with hydrochloric acid (1 M) and the resulting precipitate filtered to give **320** as a white solid (1.34 g, 80%). mp 88–90 °C [*lit. mp 82–83* °C]; ν_{max} (film) 3290 (alkynyl C–H), 2124 (C≡C), 1693 (C=O) [*consistent with lit.*]; δ_H (400 MHz, CD_3OD) 2.98 (1H, s, *C*≡*C*<u>*H*</u>), 4.84 (2H, s, *C*<u>*H*</u>$_2$*C*≡*C*), 7.01–7.09 (1H, m, *PhC3*<u>*H*</u>), 7.21 (1H, d, *J* 7.5, *PhC5*<u>*H*</u>), 7.50 (1H, app. t, *J* 7.5, *PhC4*<u>*H*</u>), 7.82 (1H, d, *J* 7.5, *PhC6*<u>*H*</u>) [*consistent with lit.*]; δ_C (100 MHz, CD_3OD) 57.6 (<u>*C*</u>*H*$_2$), 77.7 (*C*≡<u>*C*</u>*H*), 79.4 (<u>*C*</u>≡*CH*), 115.5 (*Ph*<u>*C*</u>*5H*), 122.2 (*Ph*<u>*C*</u>*1*), 122.4 (*Ph*<u>*C*</u>*3H*), 132.9 (*Ph*<u>*C*</u>*6H*), 134.8 (*Ph*<u>*C*</u>*4H*), 158.4 (*Ph*<u>*C*</u>*2*), 169.6 (<u>*C*</u>*O*$_2$*H*); *m/z* (MS, ES^+) 375 (100%, M_2Na^+); LCMS (system E) tR 3.9 min (100%).

Ethyl 3-(prop-2-yn-1-yloxy)benzoate 322[210]

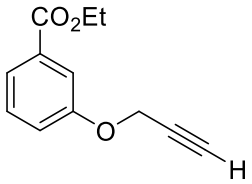

Propargyl bromide (3.0 mL of an 80% w/w solution in toluene, 26.9 mmol) was added dropwise to a suspension of ethyl 3-hydroxybenzoate (1.79 g, 10.8 mmol) and potassium carbonate (7.44 g, 53.8 mmol) in dimethyl formamide (20 mL) at 0 °C and the resulting suspension stirred at room temperature for 16 h. The reaction mixture was diluted with diethyl ether (50 mL) then washed with water (75 mL) and brine (2 × 50 mL). The aqueous layers were back-extracted with diethyl ether (50 mL) then the organic layers combined, dried over sodium sulfate and concentrated *in vacuo* to give **322** as a yellow oil (2.03 g, 92%). R_f 0.40 (9:1 cyclohexane–ethyl acetate); ν_{max} (film)

3294 (alkynyl C–H), 2983 (C–H), 2122 (C≡C), 1714 (C=O); δ_H (400 MHz, $CDCl_3$) 1.41 (3H, t, *J* 7.0, *C*H$_3$*C*H$_2$), 2.57 (1H, t, *J* 2.5, *C*≡*C*H), 4.40 (2H, q, *J* 7.0, *C*H$_3$*C*H$_2$), 4.76 (2H, d, *J* 2.5, *C*H$_2$*C*≡*C*), 7.19 (1H, ddd, *J* 8.0, 2.5, 1.0, *PhC4H*), 7.38 (1H, app. t, *J* 8.0, *PhC5H*), 7.66 (1H, dd, *J* 2.5, 1.5, *PhC2H*), 7.69–7.73 (1H, m, *PhC6H*) [*consistent with lit.*]; δ_C (100 MHz, $CDCl_3$) 14.3 (*C*H$_3$*C*H$_2$), 55.9 (*C*H$_2$*C*≡*C*H), 61.0 (*C*H$_3$*C*H$_2$), 75.8 (*C*≡*C*H), 78.1 (*C*≡*C*H), 115.3 (*PhC2H*), 119.9 (*PhC4H*), 122.8 (*PhC6H*), 129.4 (*PhC5H*), 131.8 (*PhC1*), 157.4 (*PhC3*), 166.2 (*C*O$_2$*Et*); *m/z* (MS, ES$^+$) 227 (100%, MNa$^+$); LCMS (system E) tR 6.4 min (100%).

3-(Prop-2-yn-1-yloxy)benzoic acid 323[210]

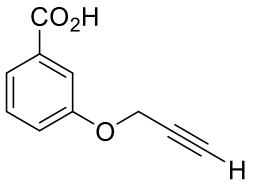

Lithium hydroxide (1 M, aq, 30 mL, 30 mmol) was added to a solution of methyl 3-(prop-2-yn-1-yloxy)benzoate **322** (1.98 g, 9.70 mmol) in a mixture of methanol (10 mL), tetrahydrofuran (20 mL) and water (20 mL) and the resulting solution stirred at room temperature for 16 h. The reaction mixture was acidified to pH 1 with hydrochloric acid (1 M) and the resulting precipitate filtered to give **323** as a white solid (1.70 g, 99%). mp 132–135 °C; ν_{max} (film) 3258 (alkynyl C–H), 1681 (C=O); δ_H (400 MHz, CD_3OD) 2.95 (1H, t, *J* 2.5, *C*≡*C*H), 4.76 (2H, d, *J* 2.5, *C*H$_2$*C*≡*C*), 7.19 (1H, ddd, *J* 8.0, 2.5, 1.0, *PhC4H*), 7.37 (1H, app. t, *J* 8.0, *PhC5H*), 7.60–7.66 (2H, m, *PhC2H* and *PhC6H*) [*consistent with lit.*]; δ_C (100 MHz, CD_3OD) 56.8 (*C*H$_2$), 77.2 (*C*≡*C*H), 79.6 (*C*≡*C*H), 116.8 (*PhC2H*), 121.1 (*PhC4H*), 123.9 (*PhC6H*), 130.7 (*PhC5H*), 133.3 (*PhC1*), 159.1 (*PhC3*), 169.6 (*C*O$_2$*H*); *m/z* (MS, ES$^-$) 175 (100%, [M–H]$^-$); LCMS (system E) tR 4.3 min (100%).

4-(Prop-2-yn-1-yloxy)benzoic acid 325[210]

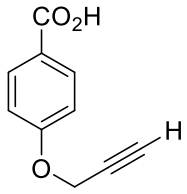

Propargyl bromide (0.56 mL of an 80% w/w solution in toluene, 5.0 mmol) was added dropwise to a suspension of ethyl 4-hydroxybenzoate (831 mg, 5.0 mmol) and potassium carbonate (3.72 g, 26.9 mmol) in dimethyl formamide (10 mL) at 0 °C and the resulting suspension stirred at room temperature for 16 h. Lithium hydroxide (1 M, aq, 60 mL, 60 mmol) was added and the resulting solution stirred at room temperature for 16 h. The reaction mixture was acidified to pH 1 with hydrochloric acid (1 M) and the resulting precipitate filtered, washing with hydrochloric acid (80 mL of a dilute aq solution) to give **325** as a white solid (838 mg, 95%). mp 220–224 °C; ν_{max} (film) 3267 (alkynyl C–H), 1679 (C=O); δ_H (400 MHz, $(CD_3)_2SO$) 3.60 (1H, t, *J* 2.5, *C*≡*C*H), 4.88 (2H, d, *J* 2.5, *C*H$_2$*C*≡*C*), 7.06 (2H, d, *J* 9.0, *PhC3H* and *PhC5H*), 7.91 (2H, d, *J* 9.0, *PhC2H* and *PhC6H*) [*consistent with lit.*]; δ_C (100 MHz, $(CD_3)_2SO$) 55.7 (*C*H$_2$), 78.7 (*C*≡*C*H), 78.8 (*C*≡*C*H), 114.7

(*PhC3H* and *PhC5H*), 123.8 (*PhC1*), 131.4 (*PhC2H* and *PhC6H*), 160.8 (*PhC4*), 167.0 (*CO₂H*); *m/z* (MS, ES⁻) 175 (100%, [M–H]⁻); LCMS (system E) tR 6.8 min (98%).

2-(1-{(3*R*)-1-[2-(Prop-2-yn-1-yloxy)benzoyl]piperidin-3-yl}-1*H*-1,2,3-triazol-4-yl)isonicotinic acid trifluoroacetate 326

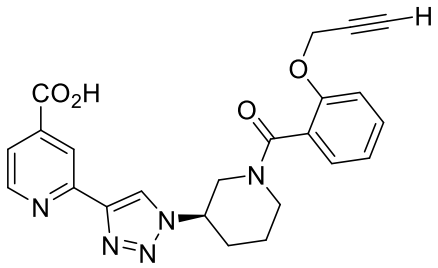

2-(Prop-2-yn-1-yloxy)benzoic acid **320** (17.6 mg, 0.10 mmol) was taken up in dichloromethane (0.25 mL). Oxalyl chloride (17 µL, 0.20 mmol) was added followed by dimethyl formamide (1 drop). The reaction mixture was stirred at room temperature for 2 h then concentrated *in vacuo* to give a yellow solid that was taken up in acetonitrile (1 mL). Triethylamine (14 µL, 0.10 mmol) and methyl 2-{1-[(3*R*)-piperidin-3-yl]-1*H*-1,2,3-triazol-4-yl}isonicotinate **225** (29 mg, 0.10 mmol) were added and the resulting solution stirred at room temperature for 16 h. Lithium hydroxide (1 M, aq, 1.0 mL, 1.0 mmol) and water (1.0 mL) were added and the resulting solution stirred at room temperature for 2 h. The reaction mixture was acidified to pH 1 with trifluoroacetic acid then purified by reverse phase chromatography (C18 column, eluting with 0.1% trifluoroacetic acid in water → 0.1% trifluoroacetic acid in 2:3 acetonitrile–water) to give an off-white solid that was taken up in hot acetonitrile (10 mL). The resulting precipitate was filtered, washing with acetonitrile (2 × 2 mL) to give **326** as an off-white solid (25 mg, 46%). mp 261–263 °C; ν_{max} (film) 3268 (alkynyl C–H), 1632 (CO_2H); δ_H (500 MHz, $(CD_3)_2SO$) 1.46–1.99 (2H, m, *PipC5H₂*), 2.12–2.34 (2H, m, *PipC4H₂*), 2.80–4.66 (5H, m, *C≡CH*, *PipC2H₂* and *PipC6H₂*), 4.69–4.97 (3H, m, *CH₂C≡C* and *PipC3H*), 6.94–7.46 (4H, m, 4 × *ArH*), 7.73–7.80 (1H, m, *ArH*), 8.36–8.48 (1H, m, *ArH*), 8.67–8.89 (2H, m, *PyC6H* and *ArH*); δ_C (125 MHz, $(CD_3)_2SO$) 22.9–23.7 (*PipC5H₂*), 29.8–30.4 (*PipC4H₂*), 44.8–46.3 and 50.8 (*PipC6H₂* and *PipC2H₂*), 55.4–56.6 (*CH₂C≡CH* and *PipC3H*), 78.4–78.9 (*C≡CH* and *C≡CH*), 112.4–112.8 (*PhC3H*), 118.3–118.4 (*ArCH*), 121.4 (*ArCH*), 121.8 (*ArCH*), 122.2–122.7 (*ArCH*), 125.6–126.0, 127.6–128.1 (*ArCH*), 130.2–130.3 (*ArCH*), 139.2, 146.4–146.5, 150.7–150.9 (*PyC6H*), 151.0, 152.6–152.7, 166.0 (*CO₂H*), 166.3–166.9 (*CON*); *m/z* (MS, ES⁺) 432 (100%, MH^+); LCMS (system E) tR 6.0 min (99%); accurate mass: found 454.1469, calc. for $C_{23}H_{21}N_5NaO_4^+$ 454.1486; $[\alpha]_D^{20}$ −0.121 (*c* 0.15 in CH_3OH).

2-(1-{(3*R*)-1-[3-(Prop-2-yn-1-yloxy)benzoyl]piperidin-3-yl}-1*H*-1,2,3-triazol-4-yl)isonicotinic acid trifluoroacetate 327

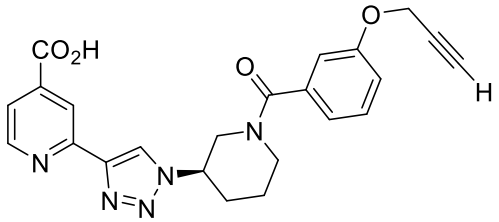

3-(Prop-2-yn-1-yloxy)benzoic acid **323** (17.6 mg, 0.10 mmol) was taken up in dichloromethane (0.25 mL). Oxalyl chloride (17 µL, 0.20 mmol) was added followed by dimethyl formamide (1 drop). The reaction mixture was stirred at room temperature for 2 h then concentrated *in vacuo* to give a yellow solid that was taken up in acetonitrile (1 mL). Triethylamine (14 µL, 0.10 mmol) and methyl 2-{1-[(3*R*)-piperidin-3-yl]-1*H*-1,2,3-triazol-4-yl}isonicotinate **225** (29 mg, 0.10 mmol) were added and the resulting solution stirred at room temperature for 16 h. Lithium hydroxide (1 M, aq, 1.0 mL, 1.0 mmol) and water (1.0 mL) were added and the resulting solution stirred at room temperature for 2 h. The reaction mixture was acidified to pH 1 with trifluoroacetic acid then purified by reverse phase chromatography (C18 column, eluting with 0.1% trifluoroacetic acid in water → 0.1% trifluoroacetic acid in 2:3 acetonitrile–water) to give an off-white solid that was taken up in hot acetonitrile (10 mL). The resulting precipitate was filtered, washing with acetonitrile (2 × 2 mL) to give **327** as an off-white solid (22 mg, 40%). mp 203–206 °C; ν_{max} (film) 1620 (CO_2H); δ_H (500 MHz, $(CD_3)_2SO$) 1.60–1.97 (2H, m, *PipC5H*$_2$), 2.16–2.34 (2H, m, *PipC4H*$_2$), 3.10–4.68 (5H, m, *C*≡*CH*, *PipC2H*$_2$ and *PipC6H*$_2$), 4.73–4.90 (3H, m, *CH*$_2$*C*≡*C* and *PipC3H*), 6.93–7.12 (3H, m, 3 × *ArH*), 7.29–7.44 (1H, m, *ArH*), 7.71–7.80 (1H, m, *ArH*), 8.35–8.51 (1H, m, *ArH*), 8.65–8.92 (2H, m, *PyC6H* and *ArH*); δ_C (125 MHz, $(CD_3)_2SO$) 23.8 (*PipC5H*$_2$), 30.0 (*PipC4H*$_2$), 45.9 and 46.9 (*PipC6H*$_2$ and *PipC2H*$_2$), 55.5 (*CH*$_2$*C*≡*CH*), 55.9 (*PipC3H*), 78.5 (*C*≡*CH*), 79.0 (*C*≡*CH*), 112.9 (*ArCH*), 116.2 (*ArCH*), 118.3 (*ArCH*), 119.5 (*ArCH*), 121.8 (*ArCH*), 122.5 (*ArCH*), 129.8 (*ArCH*), 137.1, 139.2, 146.4, 150.8 (*PyC6H*), 150.9, 157.0 (*PhC3H*), 166.0 (*CO*$_2$*H*), 168.9 (*CON*); *m/z* (MS, ES^+) 432 (100%, MH^+); LCMS (system E) tR 5.7 min (100%); accurate mass: found 454.1466, calc. for $C_{23}H_{21}N_5NaO_4^+$ 454.1486; $[\alpha]_D^{20}$ −0.009 (*c* 0.15 in CH_3OH).

2-(1-{(3*R*)-1-[4-(Prop-2-yn-1-yloxy)benzoyl]piperidin-3-yl}-1*H*-1,2,3-triazol-4-yl)isonicotinic acid trifluoroacetate 328

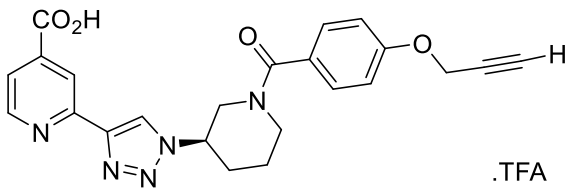

4-(Prop-2-yn-1-yloxy)benzoic acid **325** (17.6 mg, 0.10 mmol) was taken up in dichloromethane (0.25 mL). Oxalyl chloride (17 µL, 0.20 mmol) was added followed by dimethyl formamide (1

drop). The reaction mixture was stirred at room temperature for 2 h then concentrated *in vacuo* to give a yellow solid that was taken up in acetonitrile (1 mL). Triethylamine (14 µL, 0.10 mmol) and methyl 2-{1-[(3*R*)-piperidin-3-yl]-1*H*-1,2,3-triazol-4-yl}isonicotinate **225** (29 mg, 0.10 mmol) were added and the resulting solution stirred at room temperature for 16 h. Lithium hydroxide (1 M, aq, 1.0 mL, 1.0 mmol) and water (1.0 mL) were added and the resulting solution stirred at room temperature for 16 h. The reaction mixture was acidified to pH 1 with trifluoroacetic acid then purified by reverse phase chromatography (C18 column, eluting with 0.1% trifluoroacetic acid in water → 0.1% trifluoroacetic acid in 3:7 acetonitrile–water) to give an off-white solid that was taken up in hot acetonitrile (5 mL). The resulting precipitate was filtered, washing with acetonitrile (3 × 1 mL) to give **328** as an off-white solid (16 mg, 29%). mp 196–199 °C; ν_{max} (film) 3290 (alkynyl C–H), 1606 (CO_2H); δ_H (400 MHz, $(CD_3)_2SO$) 1.57–1.94 (2H, m, *PipC5H₂*), 2.14–2.35 (2H, m, *PipC4H₂*), 3.05–4.66 (5H, m, *C≡CH*, *PipC2H₂* and *PipC6H₂*), 4.74–4.95 (3H, m, *CH₂C≡C* and *PipC3H*), 7.03 (2H, d, *J* 8.5, *PhC3H* and *PhC5H*), 7.41 (2H, d, *J* 8.5, *PhC2H* and *PhC6H*), 7.77 (1H, dd, *J* 5.0, 1.0, *PyC5H*), 8.43 (1H, s, *ArH*), 8.76–8.84 (2H, m, *ArH* and *PyC6H*); δ_C (125 MHz, $(CD_3)_2SO$) 23.5 (*PipC5H₂*), 30.0 (*PipC4H₂*), 46.0–47.3 (*PipC6H₂* and *PipC2H₂*), 55.5 (*CH₂C≡CH*), 56.0 (*PipC3H*), 78.5 (*C≡CH*), 79.0 (*C≡CH*), 114.6 (*PhC3H* and *PhC5H*), 118.3 (*ArCH*), 121.8 (*PyC5H*), 122.6 (*ArCH*), 128.4, 128.8 (*PhC2H* and *PhC6H*), 139.2, 146.4, 150.8 (*PyC6H*), 150.9, 158.2, 166.0 (*CO₂H*), 169.2 (*CON*); *m/z* (MS, ES^+) 432 (100%, MH^+); LCMS tR 12.5 min (99%); accurate mass: found 454.1503, calc. for $C_{23}H_{21}N_5NaO_4^+$ 454.1486; $[\alpha]_D^{20}$ −0.062 (*c* 0.15 in CH_3OH).

Methyl 2-(1-{(3*R*)-1-[2-(prop-2-yn-1-yloxy)benzoyl]piperidin-3-yl}-1*H*-1,2,3-triazol-4-yl)isonicotinate 329

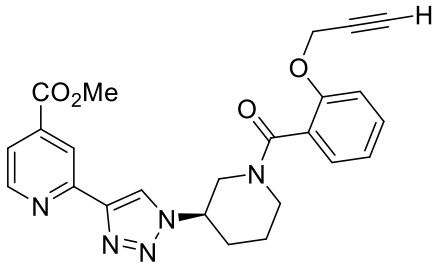

2-(Prop-2-yn-1-yloxy)benzoic acid **320** (148 mg, 0.84 mmol) was taken up in dichloromethane (1.0 mL). Oxalyl chloride (134 µL, 1.60 mmol) was added followed by dimethyl formamide (1 drop). The reaction mixture was stirred at room temperature for 2 h then concentrated *in vacuo* to give a yellow solid that was taken up in acetonitrile (8 mL). Triethylamine (117 µL, 0.84 mmol) and methyl 2-{1-[(3*R*)-piperidin-3-yl]-1*H*-1,2,3-triazol-4-yl}isonicotinate **225** (201 mg, 0.70 mmol) were added and the resulting solution stirred at room temperature for 16 h. The reaction mixture was diluted with water (20 mL) and extracted with dichloromethane (3 × 15 mL). The organic layers were combined, concentrated *in vacuo* and purified by flash column chromatography (dichloromethane → 4% methanol in dichloromethane) to give **329** as a pale yellow gum (279 mg, 90%). ν_{max} (film) 3273 (alkynyl C–H), 1730 (C=O, ester), 1630 (C=O, amide); δ_H (500 MHz,

$(CD_3)_2SO$) 1.46–2.37 (4H, m, *PipC5*$\underline{H_2}$ and *PipC4*$\underline{H_2}$), 2.80–4.07 (8H, m, *C*≡*C*$\underline{H}$, *CO*$_2$*C*$\underline{H_3}$, *PipC2*$\underline{H_2}$ and *PipC6*$\underline{H_2}$), 4.33–5.02 (3H, m, *C*$\underline{H_2}$*C*≡*C* and *PipC3*$\underline{H}$), 6.94–7.46 (4H, m, 4 × *Ar*$\underline{H}$), 7.72–7.79 (1H, m, *Ar*$\underline{H}$), 8.35–8.90 (3H, *PyC6*$\underline{H}$ and 2 × *Ar*$\underline{H}$); δ_C (125 MHz, $(CD_3)_2SO$) 22.7 (*Pip*$\underline{C}$*5H*$_2$), 29.6 (*Pip*$\underline{C}$*4H*$_2$), 44.5–45.0 and 52.2 (*Pip*$\underline{C}$*6H*$_2$, *Pip*$\underline{C}$*2H*$_2$ and *CO*$_2$$\underline{C}$*H*$_3$), 55.7 ($\underline{C}$*H*$_2$*C*≡*CH* and *Pip*$\underline{C}$*3H*), 77.5 and 78.4 ($\underline{C}$≡*CH* and *C*≡$\underline{C}$*H*), 112.8 (*Ar*$\underline{C}$*H*), 117.8 (*Ar*$\underline{C}$*H*), 120.9 (*Ar*$\underline{C}$*H*), 121.1 (*Ar*$\underline{C}$*H*), 121.9 (*Ar*$\underline{C}$*H*), 125.9, 127.4 (*Ar*$\underline{C}$*H*), 129.7 (*Ar*$\underline{C}$*H*), 137.7, 146.0, 150.2 (*Py*$\underline{C}$*6H*), 150.8, 152.6, 164.6 ($\underline{C}$*O*$_2$*H*), 166.3 ($\underline{C}$*ON*); *m/z* (MS, ES^+) 468 (100%, MNa^+); LCMS (system E) tR 5.2 min (99%); accurate mass: found 468.1641, calc. for $C_{24}H_{23}N_5NaO_4^+$ 468.1642; $[\alpha]_D^{20}$ −0.695 (*c* 1.0 in $CHCl_3$).

2-{1-[(3*R*)-1-{2-[(1-{16-Oxo-20-[(3a*S*,4*S*,6a*R*)-2-oxohexahydro-1*H*-thieno[3,4-*d*]imidazol-4-yl]-3,6,9,12-tetraoxa-15-azaicos-1-yl}-1*H*-1,2,3-triazol-4-yl)methoxy]benzoyl}piperidin-3-yl]-1*H*-1,2,3-triazol-4-yl}isonicotinic acid 330

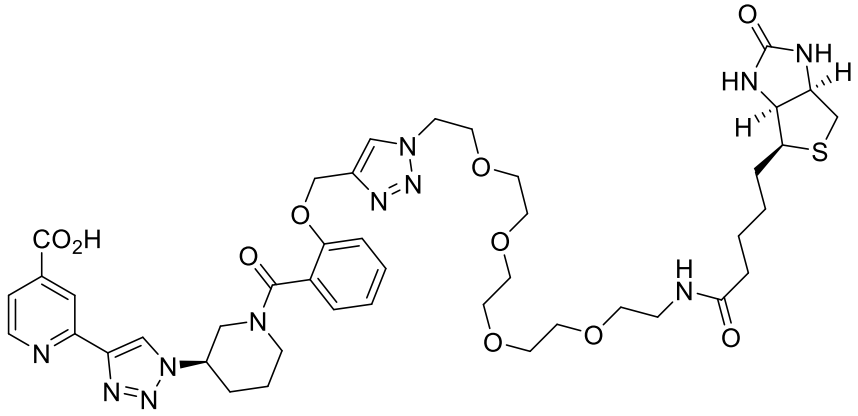

A suspension of methyl 2-(1-{(3*R*)-1-[2-(prop-2-yn-1-yloxy)benzoyl]piperidin-3-yl}-1*H*-1,2,3-triazol-4-yl)isonicotinate **329** (91 mg, 0.20 mmol), *N*-(14-azido-3,6,9,12-tetraoxatetradec-1-yl)-5-[(3a*S*,4*S*,6a*R*)-2-oxohexahydro-1*H*-thieno[3,4-*d*]imidazol-4-yl]pentanamide (100 mg, 0.20 mmol), copper(II) sulfate pentahydrate (5 mg, 0.02 mmol) and (+)-sodium L-ascorbate (12 mg, 0.06 mmol) in *N*,*N*-dimethylformamide (2 mL) was heated at 70 °C for 16 h. The reaction mixture was diluted with water (5 mL) and extracted with dichloromethane (3 × 5 mL). The organic layers were combined, concentrated *in vacuo* and purified by flash column chromatography (dichloromethane → 10% methanol in dichloromethane) to give a colourless gum that was taken up in acetonitrile (1 mL). Lithium hydroxide (1 M, aq, 1.0 mL, 1.0 mmol) and water (1.0 mL) were added and the resulting solution stirred at room temperature for 16 h. The reaction mixture was acidified to pH 1 with trifluoroacetic acid and purified by reverse phase chromatography (C18 column, eluting with 0.1% trifluoroacetic acid in water → 0.1% trifluoroacetic acid in acetonitrile) to give a gum that was purified on a 1 g strong cation exchange column, washing with methanol (20 mL) then eluting with methanolic ammonia (2 M, 10 mL) to give **330** as a colourless gum (16 mg, 38%). R_f 0.45 (7:3 dichloromethane–methanol); ν_{max} (film) 2930 (C–H), 2868 (C–H), 1699 (C=O), 1635 (C=O); δ_H (500 MHz, CD_3OD) 1.32–1.44 (3H, m), 1.51–1.85 (6H, m), 2.15–2.37 (4H, m), 2.64–3.20 (2H, m), 3.28–3.38 (4H, m), 3.46–3.62 (15H, m), 3.67–3.93 (3H, m), 4.25–

4.66 (5H, m), 5.22–5.44 (2H, m), 6.97–7.49 (4H, m, 4 × *ArH*), 7.75–7.81 (1H, m, *ArH*), 8.01–8.23 (1H, m, *ArH*), 8.42–8.66 (3H, m, 3 × *ArH*); δ_C (125 MHz, CD_3OD) 24.6–25.0, 27.0, 29.6, 29.9, 36.9, 40.5, 41.2, 42.9, 43.9, 47.1, 47.4, 50.0, 51.6, 53.2, 55.9, 57.1, 61.7, 63.0, 63.5, 70.7, 71.4, 71.5–71.6, 113.6 (*ArCH*), 114.2, 121.3 (*ArCH*), 122.9 (*ArCH*), 123.3, 123.9 (*ArCH*), 126.8 (*ArCH*), 128.9 (*ArCH*), 129.4 (*ArCH*), 132.4 (*ArCH*), 144.3, 147.8, 148.6, 150.9 (*PyC6H*), 155.4, 166.2 (*CO₂H*), 170.2 (*CON*), 171.6 (*CON*), 176.3 (*CON*); *m/z* (MS, ES^+) 943 (100%, MNa^+); LCMS tR 10.9 min (97%); accurate mass: found 920.42, calc. for $C_{43}H_{57}N_{11}O_{10}S^+$ 920.41; $[\alpha]_D^{20}$ −0.054 (*c* 0.5 in CH_3OH).

2-{1-[(3*R*)-1-{3-[(1-{16-Oxo-20-[(3a*S*,4*S*,6a*R*)-2-oxohexahydro-1*H*-thieno[3,4-*d*]imidazol-4-yl]-3,6,9,12-tetraoxa-15-azaicos-1-yl}-1*H*-1,2,3-triazol-4-yl)methoxy]benzoyl}piperidin-3-yl]-1*H*-1,2,3-triazol-4-yl}isonicotinic acid trifluoroacetate 331

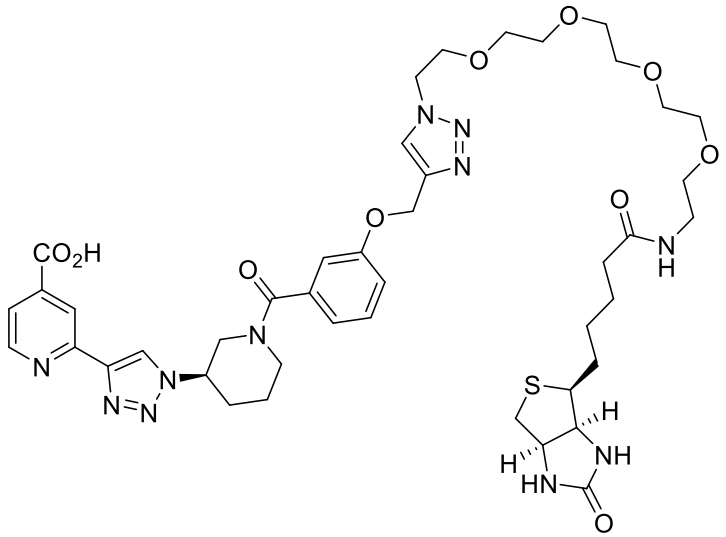

A suspension of 2-(1-{(3*R*)-1-[3-(prop-2-yn-1-yloxy)benzoyl]piperidin-3-yl}-1*H*-1,2,3-triazol-4-yl)isonicotinic acid trifluoroacetate **327** (16 mg, 0.037 mmol), *N*-(14-azido-3,6,9,12-tetraoxatetradec-1-yl)-5-[(3a*S*,4*S*,6a*R*)-2-oxohexahydro-1*H*-thieno[3,4-*d*]imidazol-4-yl]pentanamide (27 mg, 0.056 mmol), copper(II) sulfate pentahydrate (0.9 mg, 0.004 mmol) and (+)-sodium L-ascorbate (2.3 mg, 0.012 mmol) in *N*,*N*-dimethylformamide (2 mL) was heated at 70 °C for 72 h. The reaction mixture was concentrated *in vacuo* and purified by reverse phase chromatography (C18 column, eluting with 0.1% trifluoroacetic acid in water → 0.1% trifluoroacetic acid in acetonitrile) to give **331** as a yellow gum (17 mg, 44%). ν_{max} (film) 2929 (C–H), 2866 (C–H), 1698 (C=O); δ_H (500 MHz, CD_3OD) 1.13–1.90 (9H, m), 1.91–2.58 (4H, m), 2.64–2.73 (1H, m), 2.86–2.96 (1H, m), 3.13–3.24 (1H, m), 3.45–3.70 (18H, m), 3.76–4.01 (4H, m), 4.10–4.79 (4H, m), 5.07–5.36 (2H, m), 6.90–7.23 (4H, m, 4 × *ArH*), 7.25–7.76 (2H, m, 2 × *ArH*), 8.07–8.31 (2H, m, 2 × *ArH*); δ_C (125 MHz, CD_3OD) 13.3, 17.1–19.3, 24.6–25.0, 27.0, 29.6, 29.9, 36.9, 40.5, 41.2, 42.9, 43.9, 47.1, 47.4, 50.0, 51.6, 55.9, 57.1, 61.7, 63.5, 70.7, 71.4, 71.5–71.6, 113.6 (*ArCH*), 114.2, 121.3 (*ArCH*), 122.9 (*ArCH*), 123.3, 123.9 (*ArCH*), 126.8 (*ArCH*), 128.9 (*ArCH*), 129.4 (*ArCH*), 132.4 (*ArCH*), 144.3, 147.8, 148.6, 150.9 (*PyC6H*), 155.4, 166.2 (*CO₂H*),

170.2 (*C*ON), 171.6 (*C*ON), 176.3 (*C*ON); *m/z* (MS, ES^+) 920 (100%, MH^+); LCMS tR 10.9 min (96%); accurate mass: found 942.11, calc. for $C_{43}H_{57}N_{11}NaO_{10}S^+$ 942.39; $[\alpha]_D^{20}$ –0.017 (*c* 0.75 in CH_3OH).

2-{1-[(3*R*)-1-{4-[(1-{16-Oxo-20-[(3a*S*,4*S*,6a*R*)-2-oxohexahydro-1*H*-thieno[3,4-*d*]imidazol-4-yl]-3,6,9,12-tetraoxa-15-azaicos-1-yl}-1*H*-1,2,3-triazol-4-yl)methoxy]benzoyl}piperidin-3-yl]-1*H*-1,2,3-triazol-4-yl}isonicotinic acid trifluoroacetate 332

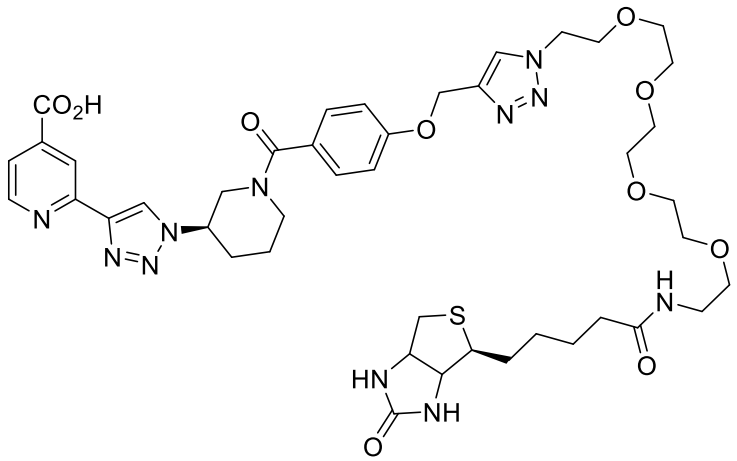

A suspension of 2-(1-{(3*R*)-1-[4-(prop-2-yn-1-yloxy)benzoyl]piperidin-3-yl}-1*H*-1,2,3-triazol-4-yl)isonicotinic acid trifluoroacetate **328** (14 mg, 0.032 mmol), *N*-(14-azido-3,6,9,12-tetraoxatetradec-1-yl)-5-[(3a*S*,4*S*,6a*R*)-2-oxohexahydro-1*H*-thieno[3,4-*d*]imidazol-4-yl]pentanamide (24 mg, 0.049 mmol), copper(II) sulfate pentahydrate (0.8 mg, 0.0032 mmol) and (+)-sodium L-ascorbate (2.3 mg, 0.010 mmol) in *N*,*N*-dimethylformamide (2 mL) was heated at 70 °C for 72 h. The reaction mixture was concentrated *in vacuo* and purified by reverse phase chromatography (C18 column, eluting with 0.1% trifluoroacetic acid in water → 0.1% trifluoroacetic acid in acetonitrile) to give **332** as a yellow gum (40 mg, quant.). ν_{max} (film) 2926 (C–H), 2864 (C–H), 1697 (C=O); δ_H (500 MHz, CD_3OD) 1.34–1.49 (4H, m), 1.50–1.83 (8H, m), 1.94–2.47 (3H, m), 2.64–2.75 (2H, m), 2.86–2.97 (2H, m), 3.13–3.24 (2H, m), 3.45–3.71 (12H, m), 3.84–4.01 (3H, m), 4.24–4.35 (2H, m), 4.42–4.66 (4H, m), 5.16–5.31 (2H, m), 7.02–7.19 (4H, m, 4 × *Ar*H), 7.34–7.54 (2H, m, 2 × *Ar*H), 7.95–8.23 (2H, m, 2 × *Ar*H); δ_C (125 MHz, CD_3OD) 24.4–25.4, 27.0, 29.6, 29.9, 31.5, 36.9, 40.5, 40.5, 41.2, 50.0, 51.7, 51.9, 57.1, 61.8, 62.6, 63.5, 70.4, 70.7, 71.3, 71.4, 71.6, 71.7–71.8, 112.8, 115.1, 115.7, 116.0, 117.3, 119.6, 126.7, 129.2, 130.4, 133.0, 144.7, 159.2, 160.1, 161.4, 166.2 (*C*O_2*H*), 168.6 (*C*ON), 172.9 (*C*ON), 176.3 (*C*ON); *m/z* (MS, ES^+) 920 (100%, MH^+); LCMS tR 10.8 min (95%); accurate mass: found 958.11, calc. for $C_{43}H_{57}N_{11}KO_{10}S^+$ 958.36; $[\alpha]_D^{20}$ +0.008 (*c* 0.5 in CH_3OH).

2-{1-[(3*R*)-1-{2-[(1-{25-Oxo-29-[(3a*S*,4*S*,6a*R*)-2-oxohexahydro-1*H*-thieno[3,4-*d*]imidazol-4-yl]-3,6,9,12,15,18,21-heptaoxa-24-azanonacos-1-yl}-1*H*-1,2,3-triazol-4-yl)methoxy]benzoyl}piperidin-3-yl]-1*H*-1,2,3-triazol-4-yl}isonicotinic acid 333

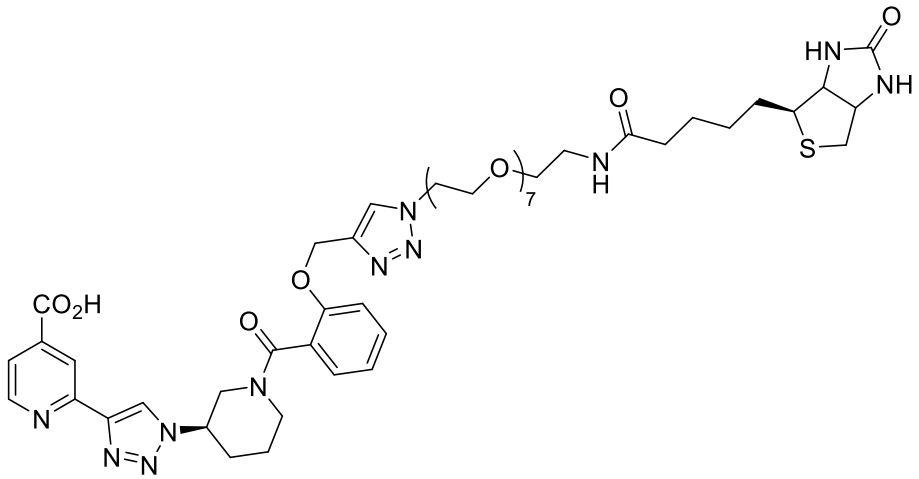

A mixture of methyl 2-(1-{(3*R*)-1-[2-(prop-2-yn-1-yloxy)benzoyl]piperidin-3-yl}-1*H*-1,2,3-triazol-4-yl)isonicotinate **329** (22 mg, 0.048 mmol), *N*-(23-azido-3,6,9,12,15,18,21-heptaoxatricos-1-yl)-5-[(3a*S*,4*S*,6a*R*)-2-oxohexahydro-1*H*-thieno[3,4-*d*]imidazol-4-yl]pentanamide (15 mg, 0.024 mmol), copper(II) sulfate pentahydrate (1.2 mg, 0.0048 mmol) and (+)-sodium L-ascorbate (1.9 mg, 0.0097 mmol) was placed in a sealed vial which was evacuated and refilled with nitrogen (× 3). A 1:1 mixture of *tert*-butanol–water (0.5 mL) was placed in a sealed vial which was evacuated and refilled with nitrogen (× 3) and then added to the other reagents. The resulting suspension was heated at 70 °C for 16 h. The reaction mixture was diluted with water (5 mL) and extracted with dichloromethane (3 × 5 mL). The organic layers were combined, concentrated *in vacuo* and purified by flash column chromatography (dichloromethane → 10% methanol in dichloromethane) to give a colourless gum that was taken up in acetonitrile (1 mL). Lithium hydroxide (1 M, aq, 0.5 mL, 0.5 mmol) and water (0.5 mL) were added and the resulting solution stirred at room temperature for 16 h. The reaction mixture was acidified to pH 1 with trifluoroacetic acid and purified by reverse phase chromatography (C18 column, eluting with 0.1% trifluoroacetic acid in water → 0.1% trifluoroacetic acid in acetonitrile) to give a gum that was purified on a 1 g strong cation exchange column, washing with methanol (10 mL) then eluting with methanolic ammonia (2 M, 5 mL) to give **333** as a colourless gum (15 mg, 59%). ν_{max} (film) 2923 (C–H), 2869 (C–H), 1702 (C=O), 1634 (C=O); δ_H (500 MHz, CD_3OD) 1.26–1.46 (3H, m), 1.54–1.83 (6H, m), 1.95–2.38 (4H, m), 2.66–3.22 (2H, m), 3.28–3.35 (4H, m), 3.46–3.67 (27H, m), 3.79–3.94 (3H, m), 4.26–4.74 (5H, m), 5.20 –5.43 (2H, m), 6.97–7.48 (4H, m, 4 × *ArH*), 7.80–7.86 (1H, m, *ArH*), 7.98–8.22 (1H, m, *ArH*), 8.46–8.76 (3H, m, 3 × *ArH*); δ_C (125 MHz, CD_3OD) 24.5–25.0, 27.0 (s), 28.3 (s), 29.7 (s), 29.9 (s), 31.6 (s), 36.9 (s), 40.5 (s), 41.2 (s), 43.0 (s), 47.0 (s), 47.4 (s), 51.6 (s), 53.1 (s), 55.5 (s), 57.2 (s), 58.4 (s), 61.8 (s), 62.8 (s), 63.5 (s), 70.5 (s), 70.7 (s), 71.4 (s), 71.5–71.7 (s), 113.7 (*ArCH*), 114.2, 120.9 (*ArCH*), 122.9 (*ArCH*), 123.7 (*ArCH*), 123.8 (*ArCH*), 126.5, 126.9 (*ArCH*), 129.3, 129.4 (*ArCH*), 132.4 (*ArCH*), 144.3, 148.4, 151.6

(*PyC6H*), 155.4, 166.3 (*CO₂H*), 168.4 (*CON*), 170.2 (*CON*), 176.3 (*CON*); *m/z* (MS, ES^+) 1074 (100%, MNa^+); LCMS tR 11.3 min (96%); accurate mass: found 1052.4852, calc. for $C_{49}H_{70}N_{11}O_{13}S^+$ 1052.4870; $[\alpha]_D^{20}$ −0. 027 (*c* 0.15 in CH_3OH).

2-{1-[(3*R*)-1-{2-[(1-{15,31-Dioxo-35-[(3a*S*,4*S*,6a*R*)-2-oxohexahydro-1*H*-thieno[3,4-*d*]imidazol-4-yl]-3,6,9,12,20,23,26-heptaoxa-16,30-diazapentatriacont-1-yl}-1*H*-1,2,3-triazol-4-yl)methoxy]benzoyl}piperidin-3-yl]-1*H*-1,2,3-triazol-4-yl}isonicotinic acid 334

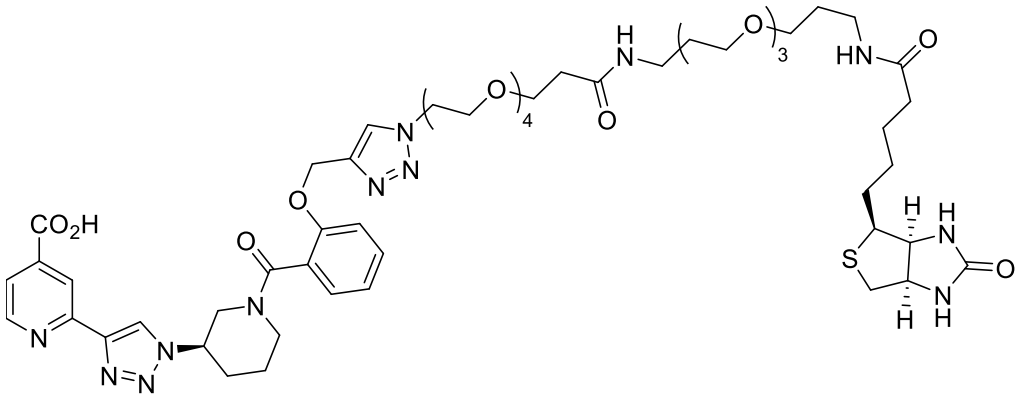

A mixture of methyl 2-(1-{(3*R*)-1-[2-(prop-2-yn-1-yloxy)benzoyl]piperidin-3-yl}-1*H*-1,2,3-triazol-4-yl)isonicotinate **329** (13 mg, 0.029 mmol), 1-azido-*N*-{15-oxo-19-[(3a*S*,4*S*,6a*R*)-2-oxohexahydro-1*H*-thieno[3,4-*d*]imidazol-4-yl]-4,7,10-trioxa-14-azanonadec-1-yl}-3,6,9,12-tetraoxapentadecan-15-amide (15 mg, 0.021 mmol), copper(II) sulfate pentahydrate (1.0 mg, 0.0042 mmol) and (+)-sodium L-ascorbate (1.7 mg, 0.0083 mmol) was placed in a sealed vial which was evacuated and refilled with nitrogen (× 3). A 1:1 mixture of *tert*-butanol–water (0.5 mL) was placed in a sealed vial which was evacuated and refilled with nitrogen (× 3) and then added to the other reagents. The resulting suspension was heated at 70 °C for 16 h. The reaction mixture was diluted with water (5 mL) and extracted with dichloromethane (3 × 5 mL). The organic layers were combined, concentrated *in vacuo* and purified by flash column chromatography (dichloromethane → 10% methanol in dichloromethane) to give a colourless gum that was taken up in acetonitrile (1 mL). Lithium hydroxide (1 M, aq, 0.5 mL, 0.5 mmol) and water (0.5 mL) were added and the resulting solution stirred at room temperature for 16 h. The reaction mixture was acidified to pH 1 with trifluoroacetic acid and purified by reverse phase chromatography (C18 column, eluting with 0.1% trifluoroacetic acid in water → 0.1% trifluoroacetic acid in acetonitrile) to give a gum that was purified on a 1 g strong cation exchange column, washing with methanol (10 mL) then eluting with methanolic ammonia (2 M, 5 mL) to give **334** as a colourless gum (13 mg, 54%). ν_{max} (film) 2923 (C–H), 2868 (C–H), 1702 (C=O), 1640 (C=O); δ_H (500 MHz, CD_3OD) 1.28–1.48 (3H, m), 1.54–1.82 (8H, m), 1.96–2.45 (6H, m), 2.66–2.95 (2H, m), 3.12–3.28 (6H, m), 3.45–3.71 (29H, m), 3.76–3.93 (3H, m), 4.26–4.75 (5H, m), 5.18–5.43 (2H, m), 6.98–7.49 (4H, m, 4 × *ArH*), 7.79–7.85 (1H, m, *ArH*), 7.97–8.22 (1H, m, *ArH*), 8.45–8.76 (3H, m, 3 × *ArH*); δ_C (125 MHz, CD_3OD) 24.5– 25.0, 27.0, 28.3, 29.7, 30.0, 30.6, 31.6, 37.0, 37.9, 37.9, 38.0, 41.2, 42.9, 47.0, 47.4, 51.6, 53.1, 55.4, 57.2, 57.9, 58.1, 58.4, 61.8, 62.8, 63.0, 63.5, 68.4, 70.0, 70.1, 70.5, 71.4, 71.5–71.7,

113.7 (*Ar*<u>*C*</u>*H*), 114.0, 121.0 (*Ar*<u>*C*</u>*H*), 122.9 (*Ar*<u>*C*</u>*H*), 123.3 (*Ar*<u>*C*</u>*H*), 123.7 (*Ar*<u>*C*</u>*H*), 126.4, 126.8 (*Ar*<u>*C*</u>*H*), 128.9, 129.4 (*Ar*<u>*C*</u>*H*), 132.4 (*Ar*<u>*C*</u>*H*), 144.3, 148.4, 151.6 (*Py*<u>*C*</u>*6H*), 155.4, 166.2 (<u>*C*</u>O_2H), 168.9 (<u>*C*</u>*ON*), 170.2 (<u>*C*</u>*ON*), 174.0 (<u>*C*</u>*ON*), 176.1 (<u>*C*</u>*ON*); *m/z* (MS, ES^+) 1152 (100%, MH^+); LCMS tR 11.2 min (95%); accurate mass: found 1151.5541, calc. for $C_{54}H_{79}N_{12}O_{14}S^+$ 1151.5554; $[\alpha]_D^{20}$ −0. 084 (*c* 0.5 in CH_3OH).

2-{1-[(3*R*)-1-{2-[(1-{37-Oxo-41-[(3a*S*,4*S*,6a*R*)-2-oxohexahydro-1*H*-thieno[3,4-*d*]imidazol-4-yl]-3,6,9,12,15,18,21,24,27,30,33-undecaoxa-36-azahentetracont-1-yl}-1*H*-1,2,3-triazol-4-yl)methoxy]benzoyl}piperidin-3-yl]-1*H*-1,2,3-triazol-4-yl}isonicotinic acid 335

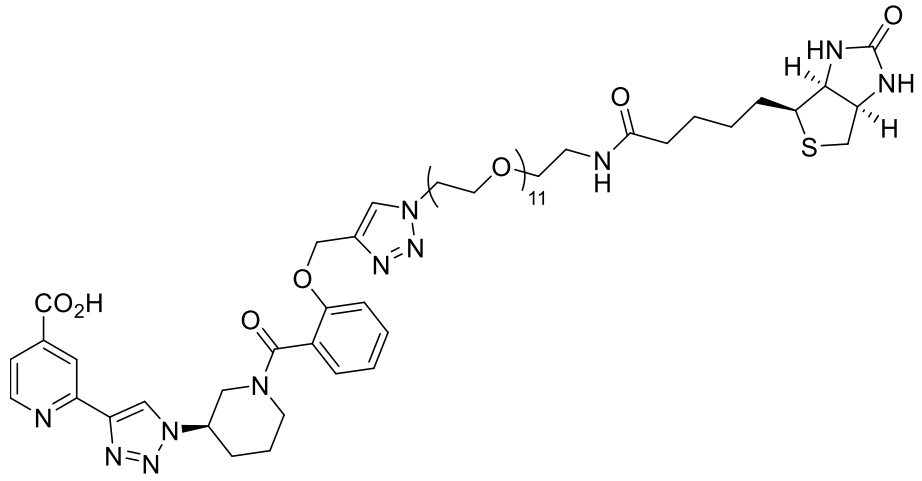

A mixture of methyl 2-(1-{(3*R*)-1-[2-(prop-2-yn-1-yloxy)benzoyl]piperidin-3-yl}-1*H*-1,2,3-triazol-4-yl)isonicotinate **329** (12 mg, 0.026 mmol), *N*-(35-azido-3,6,9,12,15,18,21,24,27,30,33-undecaoxapentatriacont-1-yl)-5-[(3a*S*,4*S*,6a*R*)-2-oxohexahydro-1*H*-thieno[3,4-*d*]imidazol-4-yl]pentanamide (15 mg, 0.019 mmol), copper(II) sulfate pentahydrate (0.94 mg, 0.0038 mmol) and (+)-sodium L-ascorbate (1.5 mg, 0.0075 mmol) was placed in a sealed vial which was evacuated and refilled with nitrogen (× 3). A 1:1 mixture of *tert*-butanol–water (0.5 mL) was placed in a sealed vial which was evacuated and refilled with nitrogen (× 3) and then added to the other reagents. The resulting suspension was heated at 70 °C for 16 h. The reaction mixture was diluted with water (5 mL) and extracted with dichloromethane (3 × 5 mL). The organic layers were combined, concentrated *in vacuo* and purified by flash column chromatography (dichloromethane → 10% methanol in dichloromethane) to give a colourless gum that was taken up in acetonitrile (1 mL). Lithium hydroxide (1 M, aq, 0.5 mL, 0.5 mmol) and water (0.5 mL) were added and the resulting solution stirred at room temperature for 16 h. The reaction mixture was acidified to pH 1 with trifluoroacetic acid and purified by reverse phase chromatography (C18 column, eluting with 0.1% trifluoroacetic acid in water → 0.1% trifluoroacetic acid in acetonitrile) to give a gum that was purified on a 1 g strong cation exchange column, washing with methanol (10 mL) then eluting with methanolic ammonia (2 M, 5 mL) to give **335** as a colourless gum (8 mg, 35%). ν_{max} (film) 2870 (C–H), 1703 (C=O), 1635 (C=O); δ_H (500 MHz, CD_3OD) 1.26–1.48 (3H, m), 1.52–2.07 (6H, m), 2.16–2.38 (4H, m), 2.66–3.23 (2H, m), 3.27–3.38 (4H, m), 3.43–3.68 (43H, m), 3.72–3.93 (3H, m), 4.26–4.73 (5H, m), 5.20–5.43 (2H, m), 6.97–7.49 (4H, m, 4 × *Ar*<u>*H*</u>), 7.80–7.86 (1H, m, *Ar*<u>*H*</u>),

7.98–8.22 (1H, m, *Ar*H), 8.46–8.77 (3H, m, 3 × *Ar*H); δ_C (125 MHz, CD_3OD) 24.5–25.0, 27.0, 28.3, 29.7, 29.9, 31.6, 36.9, 40.5, 41.2, 42.9, 47.0, 47.4, 51.6, 53.1, 55.5, 57.2, 58.4, 61.8, 62.8, 63.0, 63.5, 70.5, 70.7, 71.4, 71.5–71.8, 113.7 (*ArCH*), 114.2, 120.9 (*ArCH*), 122.9 (*ArCH*), 123.7 (*ArCH*), 123.8 (*ArCH*), 126.5, 126.9 (*ArCH*), 129.4 (*ArCH*), 132.4 (*ArCH*), 144.3, 144.5, 148.4, 151.6 (*PyC6H*), 155.5, 166.2 (*CO₂H*), 168.4 (*CON*), 170.2 (*CON*), 176.3 (*CON*); *m/z* (MS, ES^+) 1251 (100%, MNa^+); LCMS tR 11.4 min (97%); accurate mass: found 1228.5900, calc. for $C_{57}H_{86}N_{11}O_{17}S^+$ 1228.5918; $[\alpha]_D^{20}$ −0. 050 (*c* 0.3 in CH_3OH).

2-{1-[(3*R*)-1-{2-[(1-{73-Oxo-77-[(3a*S*,4*S*,6a*R*)-2-oxohexahydro-1*H*-thieno[3,4-*d*]imidazol-4-yl]-3,6,9,12,15,18,21,24,27,30,33,36,39,42,45,48,51,54,57,60,63,66,69-tricosaoxa-72-azaheptaheptacont-1-yl}[138]-1*H*-1,2,3-triazol-4-yl)methoxy]benzoyl}piperidin-3-yl]-1*H*-1,2,3-triazol-4-yl}isonicotinic acid 336

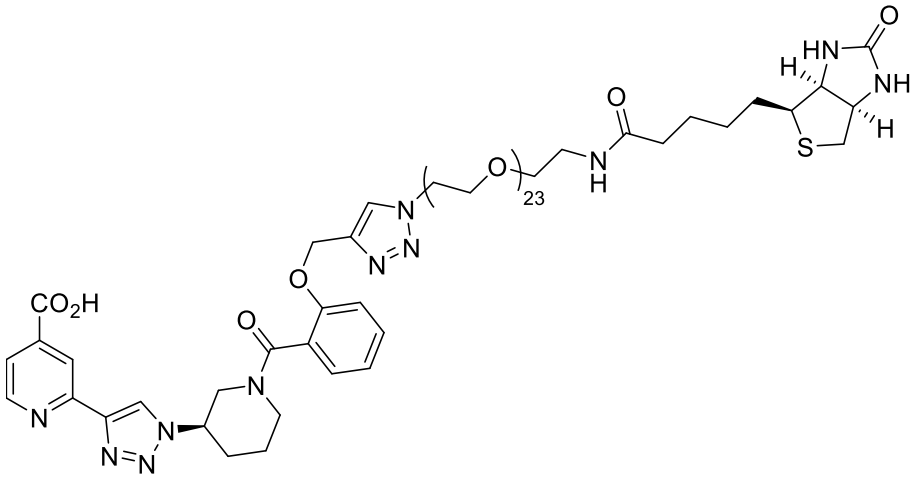

A mixture of methyl 2-(1-{(3*R*)-1-[2-(prop-2-yn-1-yloxy)benzoyl]piperidin-3-yl}-1*H*-1,2,3-triazol-4-yl)isonicotinate **329** (8.5 mg, 0.019 mmol), *N*-(71-azido-3,6,9,12,15,18,21,24,27,30,33,36,39,42,45,48,51,54,57,60,63,66,69-tricosaoxahenheptacont-1-yl)-5-[(3a*S*,4*S*,6a*R*)-2-oxohexahydro-1*H*-thieno[3,4-*d*]imidazol-4-yl]pentanamide (18 mg, 0.014 mmol), copper(II) sulfate pentahydrate (0.68 mg, 0.0027 mmol) and (+)-sodium L-ascorbate (1.1 mg, 0.0054 mmol) was placed in a sealed vial which was evacuated and refilled with nitrogen (× 3). A 1:1 mixture of *tert*-butanol–water (0.5 mL) was placed in a sealed vial which was evacuated and refilled with nitrogen (× 3) and then added to the other reagents. The resulting suspension was heated at 70 °C for 16 h. The reaction mixture was diluted with water (5 mL) and extracted with dichloromethane (3 × 5 mL). The organic layers were combined, concentrated *in vacuo* and purified by flash column chromatography (dichloromethane → 10% methanol in dichloromethane) to give a colourless gum that was taken up in acetonitrile (1 mL). Lithium hydroxide (1 M, aq, 0.5 mL, 0.5 mmol) and water (0.5 mL) were added and the resulting solution stirred at room temperature for 16 h. The reaction mixture was acidified to pH 1 with trifluoroacetic acid and purified by reverse phase chromatography (C18 column, eluting with 0.1% trifluoroacetic acid in water → 0.1% trifluoroacetic acid in acetonitrile) to give a gum that was purified on a 1 g strong cation exchange column, washing with methanol (10 mL) then eluting with methanolic ammonia

(2 M, 5 mL) to give **336** as a colourless gum (14 mg, 59%). ν_{max} (film) 2870 (C–H), 1707 (C=O), 1637 (C=O); δ_H (500 MHz, CD_3OD) 1.24–1.49 (3H, m), 1.52–1.84 (6H, m), 1.85–2.40 (4H, m), 2.67–3.24 (2H, m), 3.26–3.41 (4H, m), 3.44–3.68 (91H, m), 3.73–3.95 (3H, m), 4.27–4.73 (5H, m), 5.19–5.43 (2H, m), 6.96–7.49 (4H, m, 4 × *ArH*), 7.79–7.88 (1H, m, *ArH*), 7.97–8.23 (1H, m, *ArH*), 8.46–8.77 (3H, m, 3 × *ArH*); δ_C (125 MHz, CD_3OD) 24.6–25.0, 27.0, 28.3, 29.7, 29.9, 31.6, 36.9, 40.5, 41.2, 42.9, 47.0, 47.4, 51.6, 53.1, 55.5, 57.2, 57.9, 58.1, 58.4, 59.6, 61.8, 62.8, 63.0, 63.5, 70.5, 70.7, 71.4, 71.5–71.9, 113.7 (*ArCH*), 114.1, 120.9 (*ArCH*), 122.9 (*ArCH*), 123.7 (*ArCH*), 123.8 (*ArCH*), 126.5, 126.8 (*ArCH*), 129.4 (*ArCH*), 132.4 (*ArCH*), 142.1, 144.3, 148.4, 151.7 (*PyC6H*), 155.5, 166.2 (*CO₂H*), 168.2 (*CON*), 170.2 (*CON*), 176.3 (*CON*); *m/z* (MS, MALDI$^+$) 1779 (100%, MNa^+); LCMS tR 11.4 min (97%); accurate mass: found 1756.78, calc. for $C_{81}H_{134}N_{11}O_{29}S^+$ 1756.91; $[\alpha]_D^{20}$ −0. 055 (*c* 0.5 in CH_3OH)

7.3 Assays

7.3.1 General Experimental Details

All reagents were from Sigma Aldrich unless otherwise stated and were of the highest purity. Water was purified using a Millipore Elix® 10 system and then passed through a 0.22 μm filter by a Millipore MilliQ system. Equipment and media were sterilised by autoclaving for 20 minutes at 121 °C. For heat-sensitive solutions, sterilisation was performed using a 0.22 μm filter. Except for Fe(II) and PMSF, all stock solutions were prepared in assay buffer. Fe(II) stocks were prepared by dissolving $(NH_4)_2Fe(SO_4)_2{\cdot}6H_2O$ in 20 mM hydrochloric acid and further diluting in MilliQ water. 100 mM PMSF stocks were prepared by dissolving PMSF in ethanol.

7.3.2 AlphaScreen KDM Assay

Carried out by Dr. Anthony Tumber, Dr. Giuseppe Scozzafava and Dr. Louise Walport.

Bovine serum albumin (BSA) used in the AlphaScreen assays was essentially free from fatty acids and globulin (Sigma A7030). Hydroxyethylpiperazine ethanesulfonic acid (HEPES) buffer was from Life Technologies. Anti-H3K9me1 (ab8896), anti-H3K9me2 (ab1220) and anti-H3K36me1 (ab9048) were from Abcam, anti-H3K27me2 (07-452) was from Millipore and anti-H3K4me2 (9726S) was from Cell Signaling Technology. AlphaScreen General IgG detection kit was from Perkin Elmer. The peptide substrates H3(1–21)K9me3-GGK-biotin (64360, KDM4 substrate), H3(1–21)K4me3-GGK-biotin (64192, KDM5 substrate), H3(1–21)K9me2-GGK-biotin (64359, KDM3A substrate) and H3(21–44)K27me3-GK-biotin (64367, KDM6B substrate) were from Anaspec. H3(1–21)K4me3K9me2-biotin (BP14-122, KDM7B substrate) was from New England Peptide Ltd. For the KDM2A assay the peptide substrates biotin-H3(28–48)K36me2 and H3(28–48)K36me2 were synthesized in house. Stocks of enzyme cofactors were prepared fresh each day.

KDM enzyme assays were performed as previously described.[114, 141] Essentially enzyme assays were carried out in 384-well white proxiplates in 10 μl of assay buffer (50 mM HEPES pH 7.5, 0.1% (w/v) BSA and 0.01% (v/v) polyethylene glycol sorbitan monolaurate, Tween-20). For IC_{50} potency determinations titrations of compound were transferred to dry 384-well proxiplates using an Echo-550 Acoustic Dispenser (Labcyte Technologies). Enzyme (5 μl) was dispensed into each well using a Multidrop (Thermo Scientific) and allowed to incubate with the compounds for 15 min at room temperature. After transfer of substrate (5 μL) the enzyme reaction was progressed for the indicated time period (see **Table 36** for final concentrations and assay parameters). The enzyme reaction was stopped after the indicated time by addition of 5 μL of Stop Solution (30 mM EDTA, 800 mM NaCl in assay buffer). Streptavidin Donor beads (0.08 mg/ml) and Protein-A conjugated acceptor beads (0.08 mg/ml) were pre-incubated for 1 hour with an antibody to the product methyl mark (**Table 36**) and the presence of biotin-H3-product was detected by addition of 5 μL of the pre-incubated AlphaScreen beads (final concentrations of 0.02 mg/ml with respect to acceptor and donor beads). Detection was allowed to proceed for 1 hour at room temperature and the assay plates read in a BMG Labtech Pherastar FS plate reader. Data were normalized to the no enzyme control and the IC_{50} determined from the nonlinear regression curve fit using GraphPad Prism 5.

Table 36 AlphaScreen assay parameters and component concentrations.

	KDM						
	2A	**3A**	**4C**	**4E**	**5C**	**6B**	**7B**
[Enzyme] (nM)	25	0.2	1	1	0.5	1	15
[2-OG] (μM)	10	5	10	10	5	10	20
[(+)-sodium L-ascorbate] (μM)	100	100	100	100	100	100	100
$[(NH_4)_2Fe(SO_4)_2 \cdot 6H_2O]$ (μM)	10	10	1	1	10	10	10
[Peptide] (nM)	100*	60	30	30	100	60	300
Substrate incubation time	30 min	5 min	15 min	10 min	20 min	5 min	10 min

*Blend of biotinylated H3K36me2 (20 nM) and non-biotinylated H3K36me2 (80 nM).

7.3.3 RapidFire KDM Assay

Carried out by Dr. Anthony Tumber and Dr. Giuseppe Scozzafava.

Inhibition assays were performed in a 384-well plate format using polypropylene V-bottom plates (Greiner Bio One). 2-(*N*-Morpholino)ethanesulfonic acid (MES buffer) was from ThermoFisher Scientific. The peptide substrates H3(28–48)K36me2 (KDM2A substrate), H3(1–21)K9me1 (KDM3A substrate), H3(1–21)K9me2 (KDM4 substrate), H3(1–21)K4me2 (KDM5C substrate) were synthesized by Peptide Protein Research Ltd (Hampshire, UK).

Every reaction was performed in assay buffer (50 mM MES pH 7.0). 25.0 μL of assay buffer containing 2 × KDM enzyme (200–600 nM) which was transferred into each well of a 384-well

polypropylene microplate. Titrations of compounds (0.1 μL) were transferred to each well and the enzyme incubated with compound for 15 minutes. 25 μL of a 2 × substrate mix consisting of $(NH_4)_2Fe(SO_4)_2 \cdot 6H_2O$ (20 μM), (+)-sodium L-ascorbate (200 μM), 2OG (10–20 μM) and peptide (20 μM) was dispensed into each well and the enzyme reaction progressed for 50 minutes (see **Table 37** for final concentrations and assay parameters).

Table 37 RapidFire assay parameters and component concentrations.

	KDM			
	2A	**3A**	**4A**	**4C**
[Enzyme] (nM)	150	100	300	150
[2-OG] (μM)	10	5	10	10
[(+)-sodium L-ascorbate] (μM)	100	100	100	100
$[(NH_4)_2Fe(SO_4)_2 \cdot 6H_2O]$ (μM)	10	10	10	10
[Peptide] (μM)	10	10	10	10
Substrate incubation time	50 min	50 min	50 min	50 min
Peptide substrate	H3K36me2	H3K9me1	H3K9me2	H3K9me2
Charge state detected	+4	+5		+3
Peptide product	H3K36me1	H3K9me0	H3K9me	H3K9me
Charge state detected	+4	+5	+3	+3

The enzyme reaction was stopped by addition of 5 μL of 10% formic acid and transferred to a Rapidire RF360 high-throughput sampling robot connected to an Agilent 6530 Accurate-mass Quadrupole Time-of-Flight (Q-TOF) mass spectrometer operated in positive ion mode (Agilent, Wakefield, MA USA). RapidFire technology uses a solid phase extraction (μSPE) cartridge to remove buffer salts from samples before analysis by mass spectrometry and has been successfully applied to screening demethylase targets. A cycle of sample loading, aqueous wash and organic elution onto a mass spectrometer is typically performed in less than 15 sec. Samples were aspirated under vacuum for 400 ms, loaded onto a C4 SPE cartridge and buffer salts were removed by washing the cartridge with 0.1% formic acid in water at a flow rate of 1.5 mL/min for 4.5 sec. Following the aqueous wash peptides were eluted onto the mass spectrometer with 85% acetonitrile, 15% deionised water containing 0.1% formic acid at a flow rate of 1.25 mL/min for 4.5 seconds. The cartridge was re-equilibrated with water for 500 ms. Ion chromatogram data was extracted for the most abundant charge state for the substrate and the product and peak area data for extracted ion chromatograms were integrated using RapidFire Integrator software (Agilent). % conversion of substrate to product was calculated using the equation:

% Conversion = 100 × (area product)/[(area product) + (area substrate)]

IC_{50} data were determined from nonlinear regression curve fit using GraphPad Prism 5.

7.3.4 IF Cell-Based KDM2A Assay

Carried out by Dr. Clarence Yapp and Dr. Stephanie Hatch.

HeLa cells were cultured at 37 °C and 5% CO_2 in RPMI-1640 medium (Sigma Aldrich) and supplemented with 10% FBS (Invitrogen), 1% Glutamax (Invitrogen) and 1% Penicillin-streptomycin (Lonza). HeLa cells were seeded into 96-well clear-bottom optical-grade plates (BD Biosciences) at 8000 cells per well and allowed to settle overnight. The next day, the medium was changed to antibiotics-free medium. For each well, 0.1 µg of plasmid and 0.25 µL of Lipofectamine 2000 (Invitrogen) were each incubated in 25 µL of OptiMEM (Invitrogen) for 5 minutes at room temperature. The two solutions were then combined and mixed gently but thoroughly and incubated for 20 minutes at room temperature. The mixture was then added to the cells. Four hours later, the medium was changed to regular culture medium with antibiotics and dosed with varying concentrations of compound. The amount of DMSO in each well was kept constant throughout the plate. The cells were incubated for a further 24 hours before being fixed for immunostaining.

Cells were fixed in 4% formaldehyde for 20 minutes, permeabilised in 0.5% Triton-X 100 for 6–10 minutes, and blocked in 3% FBS for 1 h with a PBS wash between each step. The primary antibodies anti-H3K36me2 (61019 from Active Motif) and anti-FLAG (F7425 from Sigma Aldrich) were then added to the cells in blocking solution and left overnight. The next day, cells were washed three times in PBS, incubated with secondary antibodies (anti-mouse Alexa488 and anti-rabbit Alexa594 from Invitrogen) for 1 h, washed three times in PBS and counterstained with DAPI before imaging.

Immunostained cells were imaged on the BD Pathway high content analyser (BD Biosciences). The system's autofocus and montage capture features were employed so as to automatically obtain multiple sharp images for each well, thus, increasing the sample size. After image acquisition, the data was imported and analysed in Attovision (BD Biosciences). Measurement of the fluorescence intensity of the FLAG-tag and histone modification staining was restricted to the nucleus of each cell. The nuclei were automatically identified by DAPI staining. Cells expressing low amounts of the exogenous demethylase, where FLAG-tag staining was dim, were omitted from analysis. Finally, the average intensity of the histone modification staining for the remaining cells in each well was exported to BD IDE (BD Biosciences) and GraphPad Prism 5 for plotting.

7.3.5 Cell Transfection for Chemoproteomics Studies

HeLa cells were cultured at 37 °C and 5% CO_2 in Dulbecco's modified Eagle's medium (D5671, Sigma Aldrich) and supplemented with 10% FBS (Invitrogen) and 1% Glutamax (Invitrogen). HeLa cells were seeded into 10 cm dishes (BD Biosciences) at 8.5×10^5 cells per dish or 6 well plates at 1.7×10^5 cells per well and allowed to settle overnight. The next day, the media was changed for 11 mL of fresh media for each 10 cm dish or 1.5 mL of fresh media for each well of a 6 well plate. For each 10 cm dish, 20.4 µg of plasmid and 65 µL of Lipofectamine 2000 (Invitrogen)

were each incubated in 2 mL of OptiMEM (Invitrogen) for 5 minutes at room temperature and for each well of a 6 well plate, 2.5 µg of plasmid and 8 µL of Lipofectamine 2000 (Invitrogen) were each incubated in 250 µL of OptiMEM (Invitrogen) for 5 minutes at room temperature. The two solutions were then combined and mixed gently but thoroughly and incubated for 20 minutes at room temperature. The mixture was then added to the cells. After 5 h, the media was changed for fresh media and the cells incubated overnight before dosing or harvesting.

7.3.6 Cell Dosing for Chemoproteomics Studies

The media was removed from HeLa cells that had been transfected with *KDM2A* in 6 well plates and replaced with 0.6 mL fresh media per well containing varying concentrations of compound in DMSO. The amount of DMSO in each well was kept constant (0.4% v/v). The cells were incubated for 2 h then washed with ice-cold PBS (4 × 1 mL), transferred to fresh Eppendorf vials and lysed (section 7.3.7).

7.3.7 Cell Lysate Preparation for Chemoproteomics Studies

HeLa cells were lysed by the addition of 4 × volume of lysis buffer (4:1 volume:weight of cells). Lysis buffer contains 50 mM HEPES pH 8.0, 500 mM KCl, 0.1% v/v NP-40, 10% v/v glycerol, 1 mM PMSF, 1 mM DTT and 0.02% v/v protease inhibitor cocktail (Merck Set III EDTA free protease inhibitor cocktail, 539134). 2 µL DNAseI (1 mg/mL) was added for each well of a 6-well plate or 16 µL for each 10 cm dish. The resulting mixture was incubated at 4 °C for 1 h and cell debris was pelleted by centrifugation at 14000 rpm for 20 min at 4 °C. The supernatant was either flash frozen in liquid nitrogen and stored at –78 °C or used immediately for incubation with beads. Prior to incubation with beads, the cell lysate was diluted 5-fold with dilution buffer (50 mM HEPES pH 8.0, 0.1% v/v NP-40, 10% v/v glycerol, 1 mM PMSF, 1 mM DTT and 0.02% v/v protease inhibitor cocktail) and $(NH_4)_2Fe(SO_4)_2 \cdot 6H_2O$ (10 µM) and (+)-sodium L-ascorbate (200 µM) added. 200 µL of the diluted cell lysate was used for each 25 µL of beads.

7.3.8 Immobilisation of Biotinylated Compounds

For each condition, 25 µL of streptavidin-coupled MyOne C1 Dynabeads (10 mg/mL, from Life Technologies) were washed three times with a solution of 50 mM HEPES pH 7.5, 50 mM KCl, 10% v/v glycerol then 25 µL of 50 mM HEPES pH 7.5, 50 mM KCl, 10% v/v glycerol containing 1.3 µL of a 1 mM solution of the biotinylated compound in DMSO added and the resulting suspension incubated at room temperature for 1 h. The beads were then washed four times with 50 mM HEPES pH 7.5, 50 mM KCl, 10% v/v glycerol.

7.3.9 Protein Capture

After immobilising the biotinylated compounds, the beads were incubated with a solution containing recombinant protein or cell lysate at 4 °C or room temperature for 2–24 h. The beads

were then washed four times with wash buffer (50 mM HEPES pH 7.5, 100 mM KCl, 0.1% v/v NP-40, 10% v/v glycerol, 1 mM PMSF, 1 mM DTT, 0.02% v/v protease inhibitor cocktail).

7.3.10 Western Blotting

After protein capture, the washed beads were heated in 60 µL LDS loading buffer (141 mM tris(hydroxymethyl)aminomethane (tris base) pH 8.5, 2% w/v lithium dodecyl sulfate, 10% v/v glycerol, 0.51 mM ethylenediaminetetraacetic acid (EDTA), 0.22 mM Brilliant Blue G, 0.175 mM phenolsulfonphthalein, 5 mM DTT) at 95 °C for 3 minutes and polyacrylamide gel electrophoresis was used to separate the bound protein by molecular weight (4–12% polyacrylamide precast gel from Life Technologies, 10 µL of sample loaded per lane). A prestained protein molecular weight ladder was used SeeBlue Plus2 pre-stained protein standard from Life Technologies). Proteins were transferred to a polyvinylidene difluoride membrane and the resulting blot blocked with a solution of 3% bovine serum albumin (BSA) in tris-buffered saline with 0.1% Tween-20 (TBST) and probed with a rabbit anti-KDM2A antibody for 1 h at 4 °C (ab31739 used at 1:1000 dilution in 3% BSA in TBST) and a horseradish peroxidase- (HRP) conjugated goat anti-rabbit antibody for 45 minutes at room temperature (A6154 used at 1:10000 dilution in TBST). After each antibody incubation membranes were washed with TBST (5 × 4 min with shaking). Antibody binding was visualised by incubation with a mixture of luminol and hydrogen peroxide (SuperSignal west pico chemiluminescent substrate from Life Technologies, 34080). HRP-catalysed oxidation of luminol gives an excited version of 3-aminophthalate which decays to the ground state, emitting light which was visualised using a charge-coupled device (CCD) camera. The optical density of bands corresponding to KDM2A was determined using Kodak 1D image analysis software.

7.4 Docking

Compounds were docked into protein crystal structures using the Molsoft ICM-Pro internal coordinate modelling (ICM) methodology.[149] Distance restraints were used to constrain the binding mode to be consistent with the binding mode of closely related ligands.

7.5 Crystallography

Crystallisation experiments and refinement of crystallographic data were carried out by Tobias Krojer.

Crystals of KDM4A were grown as described.[226] The crystals were soaked with compound by mixing 0.5 µL of 10mM compound (in ethylene glycol) with 1.5 µL reservoir solution (0.1 M bis(2-hydroxyethyl)amino-tris(hydroxymethyl)methane pH 5.9, 0.15M ammonium sulfate, 11% PEG3350) and adding it to the crystals. The crystals were directly flash frozen in liquid nitrogen after incubating them for 12 hours. Datasets were collected at the Diamond Light Source, beamline I04-1 with a Pilatus 2M CCD detector at 0.92Å.

References

1. Bunnage, M. E., *Nat. Chem. Biol.*, **2011**, *7*, 335.
2. Paul, S. M., Mytelka, D. S., Dunwiddie, C. T., Persinger, C. C., Munos, B. H., Lindborg, S. R., Schacht, A. L., *Nat. Rev. Drug Discovery*, **2010**, *9*, 203.
3. Arrowsmith, J., Miller, P., *Nat. Rev. Drug Discovery*, **2013**, *12*, 569.
4. Weiss, W. A., Taylor, S. S., Shokat, K. M., *Nat. Chem. Biol.*, **2007**, *3*, 739.
5. Edwards, A. M., Bountra, C., Kerr, D. J., Willson, T. M., *Nat. Chem. Biol.*, **2009**, *5*, 436.
6. Gilbert, L. A., Larson, M. H., Morsut, L., Liu, Z., Brar, G. A., Torres, S. E., Stern-Ginossar, N., Brandman, O., Whitehead, E. H., Doudna, J. A., Lim, W. A., Weissman, J. S., Qi, L. S., *Cell*, **2013**, *154*, 442.
7. Abuin, A., Holt, K. H., Platt, K. A., Sands, A. T., Zambrowicz, B. P., *Trends Biotechnol.*, **2002**, *20*, 36.
8. Lindsay, M. A., *Nat. Rev. Drug Discovery*, **2003**, *2*, 831.
9. Specht, K. M., Shokat, K. M., *Curr. Opin. Cell Biol.*, **2002**, *14*, 155.
10. Workman, P., Collins, I., *Chem. Biol.*, **2010**, *17*, 561.
11. Frye, S. V., *Nat. Chem. Biol.*, **2010**, *6*, 159.
12. Bunnage, M. E., Chekler, E. L. P., Jones, L. H., *Nat. Chem. Biol.*, **2013**, *9*, 195.
13. Tate, P. H., Bird, A. P., *Curr. Opin. Genet. Dev.*, **1993**, *3*, 226.
14. Jenuwein, T., Allis, C. D., *Science*, **2001**, *293*, 1074.
15. Berger, S. L., Kouzarides, T., Shiekhattar, R., Shilatifard, A., *Genes Dev.*, **2009**, *23*, 781.
16. Klose, R. J., Bird, A. P., *Trends Biochem. Sci*, **2006**, *31*, 89.
17. Kriukiene, E., Liutkeviciute, Z., Klimasauskas, S., *Chem. Soc. Rev.*, **2012**, *41*, 6916.
18. Swygert, S. G., Peterson, C. L., *Biochim. Biophys. Acta, Gene Regul. Mech.*, **2014**, *1839*, 728.
19. Rinn, J. L., Kertesz, M., Wang, J. K., Squazzo, S. L., Xu, X., Brugmann, S. A., Goodnough, L. H., Helms, J. A., Farnham, P. J., Segal, E., Chang, H. Y., *Cell*, **2007**, *129*, 1311.
20. Kornberg, R. D., *Annu. Rev. Biochem*, **1977**, *46*, 931.
21. Daxinger, L., Whitelaw, E., *Genome Res.*, **2010**, *20*, 1623.
22. Brykczynska, U., Hisano, M., Erkek, S., Ramos, L., Oakeley, E. J., Roloff, T. C., Beisel, C., Schubeler, D., Stadler, M. B., Peters, A. H. F. M., *Nat. Struct. Mol. Biol.*, **2010**, *17*, 679.
23. Kooistra, S. M., Helin, K., *Nat. Rev. Mol. Cell Biol.*, **2012**, *13*, 297.
24. Luger, K., Mader, A. W., Richmond, R. K., Sargent, D. F., Richmond, T. J., *Nature*, **1997**, *389*, 251.
25. Davey, C. A., Sargent, D. F., Luger, K., Maeder, A. W., Richmond, T. J., *J. Mol. Biol.*, **2002**, *319*, 1097.
26. Ruthenburg, A. J., Allis, C. D., Wysocka, J., *Mol. Cell*, **2007**, *25*, 15.
27. Kouzarides, T., *Cell*, **2007**, *128*, 693.
28. Bannister, A. J., Kouzarides, T., *Cell Res.*, **2011**, *21*, 381.
29. Grunstein, M., *Nature*, **1997**, *389*, 349.
30. Vermeulen, M., Mulder, K. W., Denissov, S., Pijnappel, W. W. M. P., van Schaik, F. M. A., Varier, R. A., Baltissen, M. P. A., Stunnenberg, H. G., Mann, M., Timmers, H. T. M., *Cell*, **2007**, *131*, 58.
31. Dhayalan, A., Rajavelu, A., Rathert, P., Tamas, R., Jurkowska, R. Z., Ragozin, S., Jeltsch, A., *J. Biol. Chem.*, **2010**, *285*, 26114.

32. Otani, J., Nankumo, T., Arita, K., Inamoto, S., Ariyoshi, M., Shirakawa, M., *EMBO Rep.*, **2009**, *10*, 1235.
33. Kim, J., Daniel, J., Espejo, A., Lake, A., Krishna, M., Xia, L., Zhang, Y., Bedford, M. T., *EMBO Rep.*, **2006**, *7*, 397.
34. Musselman, C. A., Lalonde, M.-E., Cote, J., Kutateladze, T. G., *Nat. Struct. Mol. Biol.*, **2012**, *19*, 1218.
35. Tzivion, G., Shen, Y. H., Zhu, J., *Oncogene*, **2001**, *20*, 6331.
36. Taverna, S. D., Li, H., Ruthenburg, A. J., Allis, C. D., Patel, D. J., *Nat. Struct. Mol. Biol.*, **2007**, *14*, 1025.
37. Lee, J.-S., Smith, E., Shilatifard, A., *Cell*, **2010**, *142*, 682.
38. Martin, D. G. E., Grimes, D. E., Baetz, K., Howe, L., *Mol. Cell. Biol.*, **2006**, *26*, 3018.
39. Brauchle, M., Yao, Z., Arora, R., Thigale, S., Clay, I., Inverardi, B., Fletcher, J., Taslimi, P., Acker, M. G., Gerrits, B., Voshol, J., Bauer, A., Schübeler, D., Bouwmeester, T., Ruffner, H., *PLoS One*, **2013**, *8*, e60549.
40. Taunton, J., Hassig, C. A., Schreiber, S. L., *Science*, **1996**, *272*, 408.
41. Ahmad, K., Henikoff, S., *Mol. Cell*, **2002**, *9*, 1191.
42. David Allis, C., Bowen, J. K., Abraham, G. N., Glover, C. V. C., Gorovsky, M. A., *Cell*, **1980**, *20*, 55.
43. Shi, Y., Lan, F., Matson, C., Mulligan, P., Whetstine, J. R., Cole, P. A., Casero, R. A., Shi, Y., *Cell*, **2004**, *119*, 941.
44. Tsukada, Y., Fang, J., Erdjument-Bromage, H., Warren, M. E., Borchers, C. H., Tempst, P., Zhang, Y., *Nature*, **2006**, *439*, 811.
45. Karytinos, A., Forneris, F., Profumo, A., Ciossani, G., Battaglioli, E., Binda, C., Mattevi, A., *J. Biol. Chem.*, **2009**, *284*, 17775.
46. Walport, L. J., Hopkinson, R. J., Schofield, C. J., *Curr. Opin. Chem. Biol.*, **2012**, *16*, 525.
47. Klose, R. J., Kallin, E. M., Zhang, Y., *Nat. Rev. Genet.*, **2006**, *7*, 715.
48. Rose, N. R., McDonough, M. A., King, O. N. F., Kawamura, A., Schofield, C. J., *Chem. Soc. Rev.*, **2011**, *40*, 4364.
49. Hopkinson, R. J., Hamed, R. B., Rose, N. R., Claridge, T. D. W., Schofield, C. J., *ChemBioChem*, **2010**, *11*, 506.
50. Blackledge, N. P., Zhou, J. C., Tolstorukov, M. Y., Farcas, A. M., Park, P. J., Klose, R. J., *Mol. Cell*, **2010**, *38*, 179.
51. Horton, J. R., Upadhyay, A. K., Qi, H. H., Zhang, X., Shi, Y., Cheng, X., *Nat. Struct. Mol. Biol.*, **2010**, *17*, 38.
52. McDonough, M. A., Loenarz, C., Chowdhury, R., Clifton, I. J., Schofield, C. J., *Curr. Opin. Struct. Biol.*, **2010**, *20*, 659.
53. Hanauske-Abel, H. M., Günzler, V., *J. Theor. Biol.*, **1982**, *94*, 421.
54. Zhou, J., Kelly, W. L., Bachmann, B. O., Gunsior, M., Townsend, C. A., Solomon, E. I., *J. Am. Chem. Soc.*, **2001**, *123*, 7388.
55. Hoffart, L. M., Barr, E. W., Guyer, R. B., Bollinger, J. M., Krebs, C., *Proc. Natl. Acad. Sci. U.S.A.*, **2006**, *103*, 14738.
56. Yang, Y., Bedford, M. T., *Nat. Rev. Cancer*, **2013**, *13*, 37.
57. Kawakami, E., Tokunaga, A., Ozawa, M., Sakamoto, R., Yoshida, N., *Mech. Dev.*, **2015**, *135*, 31.
58. Fukuda, T., Tokunaga, A., Sakamoto, R., Yoshida, N., *Mol. Cell. Neurosci.*, **2011**, *46*, 614.
59. Ishimura, A., Minehata, K.-I., Terashima, M., Kondoh, G., Hara, T., Suzuki, T., *Development*, **2012**, *139*, 749.
60. Welstead, G. G., Creyghton, M. P., Bilodeau, S., Cheng, A. W., Markoulaki, S., Young, R. A., Jaenisch, R., *Proc. Natl. Acad. Sci. U.S.A.*, **2012**, *109*, 13004.

61. Tateishi, K., Okada, Y., Kallin, E. M., Zhang, Y., *Nature*, **2009**, *458*, 757.
62. Jensen, L. R., Amende, M., Gurok, U., Moser, B., Gimmel, V., Tzschach, A., Janecke, A. R., Tariverdian, G., Chelly, J., Fryns, J.-P., Van Esch, H., Kleefstra, T., Hamel, B., Moraine, C., Gécz, J., Turner, G., Reinhardt, R., Kalscheuer, V. M., Ropers, H.-H., Lenzner, S., *Am. J. Hum. Genet.*, **2005**, *76*, 227.
63. Laumonnier, F., Holbert, S., Ronce, N., Faravelli, F., Lenzner, S., Schwartz, C. E., Lespinasse, J., Van Esch, H., Lacombe, D., Goizet, C., Phan-Dinh Tuy, F., van Bokhoven, H., Fryns, J.-P., Chelly, J., Ropers, H.-H., Moraine, C., Hamel, B. C. J., Briault, S., *J. Med. Genet.*, **2005**, *42*, 780.
64. Huber, L. C., Brock, M., Hemmatazad, H., Giger, O. T., Moritz, F., Trenkmann, M., Distler, J. H. W., Gay, R. E., Kolling, C., Moch, H., Michel, B. A., Gay, S., Distler, O., Jüngel, A., *Arthritis Rheum.*, **2007**, *56*, 1087.
65. Ito, K., Ito, M., Elliott, W. M., Cosio, B., Caramori, G., Kon, O. M., Barczyk, A., Hayashi, S., Adcock, I. M., Hogg, J. C., Barnes, P. J., *N. Engl. J. Med.*, **2005**, *352*, 1967.
66. De Jager, P. L., Srivastava, G., Lunnon, K., Burgess, J., Schalkwyk, L. C., Yu, L., Eaton, M. L., Keenan, B. T., Ernst, J., McCabe, C., Tang, A., Raj, T., Replogle, J., Brodeur, W., Gabriel, S., Chai, H. S., Younkin, C., Younkin, S. G., Zou, F., Szyf, M., Epstein, C. B., Schneider, J. A., Bernstein, B. E., Meissner, A., Ertekin-Taner, N., Chibnik, L. B., Kellis, M., Mill, J., Bennett, D. A., *Nat. Neurosci.*, **2014**, *17*, 1156.
67. Lunnon, K., Smith, R., Hannon, E., De Jager, P. L., Srivastava, G., Volta, M., Troakes, C., Al-Sarraj, S., Burrage, J., Macdonald, R., Condliffe, D., Harries, L. W., Katsel, P., Haroutunian, V., Kaminsky, Z., Joachim, C., Powell, J., Lovestone, S., Bennett, D. A., Schalkwyk, L. C., Mill, J., *Nat. Neurosci.*, **2014**, *17*, 1164.
68. Dawson, M. A., Kouzarides, T., *Cell*, **2012**, *150*, 12.
69. Filippakopoulos, P., Qi, J., Picaud, S., Shen, Y., Smith, W. B., Fedorov, O., Morse, E. M., Keates, T., Hickman, T. T., Felletar, I., Philpott, M., Munro, S., McKeown, M. R., Wang, Y., Christie, A. L., West, N., Cameron, M. J., Schwartz, B., Heightman, T. D., La Thangue, N., French, C. A., Wiest, O., Kung, A. L., Knapp, S., Bradner, J. E., *Nature*, **2010**, *468*, 1067.
70. Van der Meulen, J., Speleman, F., Van Vlierberghe, P., *Epigenetics*, **2014**, *9*, 658.
71. Wagner, K. W., Alam, H., Dhar, S. S., Giri, U., Li, N., Wei, Y., Giri, D., Cascone, T., Kim, J.-H., Ye, Y., Multani, A. S., Chan, C.-H., Erez, B., Saigal, B., Chung, J., Lin, H.-K., Wu, X., Hung, M.-C., Heymach, J. V., Lee, M. G., *J. Clin. Invest.*, **2013**, *123*, 5231.
72. Cloos, P. A. C., Christensen, J., Agger, K., Maiolica, A., Rappsilber, J., Antal, T., Hansen, K. H., Helin, K., *Nature*, **2006**, *442*, 307.
73. Liu, G., Bollig-Fischer, A., Kreike, B., van de Vijver, M. J., Abrams, J., Ethier, S. P., Yang, Z. Q., *Oncogene*, **2009**, *28*, 4491.
74. Blair, L. P., Cao, J., Zou, M. R., Sayegh, J., Yan, Q., *Cancers*, **2011**, *3*, 1383.
75. Rizwani, W., Schaal, C., Kunigal, S., Chellappan, S., Coppola, D., *PLoS One*, **2014**, *9*, e100888.
76. Csoka, A. B., Szyf, M., *Med. Hypotheses*, **2009**, *73*, 770.
77. Lötsch, J., Schneider, G., Reker, D., Parnham, M. J., Schneider, P., Geisslinger, G., Doehring, A., *Trends Mol. Med.*, **2013**, *19*, 742.
78. Göttlicher, M., Minucci, S., Zhu, P., Krämer, O. H., Schimpf, A., Giavara, S., Sleeman, J. P., Lo Coco, F., Nervi, C., Pelicci, P. G., Heinzel, T., *EMBO J.*, **2001**, *20*, 6969.
79. Deng, C., Lu, Q., Zhang, Z., Rao, T., Attwood, J., Yung, R., Richardson, B., *Arthritis Rheum.*, **2003**, *48*, 746.

80. Kim, Y.-I., Logan, J. W., Mason, J. B., Roubenoff, R., *J. Lab. Clin. Med.*, **1996**, *128*, 165.
81. Dueñas-Gonzalez, A., Coronel, J., Cetina, L., González-Fierro, A., Chavez-Blanco, A., Taja-Chayeb, L., *Expert Opin. Drug Metab. Toxicol.*, **2014**, *10*, 1433.
82. Richon, V. M., *Br. J. Cancer*, **2006**, *95*, S2.
83. Finn, P. W., Bandara, M., Butcher, C., Finn, A., Hollinshead, R., Khan, N., Law, N., Murthy, S., Romero, R., Watkins, C., Andrianov, V., Bokaldere, R. M., Dikovska, K., Gailite, V., Loza, E., Piskunova, I., Starchenkov, I., Vorona, M., Kalvinsh, I., *Helv. Chim. Acta*, **2005**, *88*, 1630.
84. Chun, P., in *Arch. Pharmacal Res.*, Pharmaceutical Society of Korea, **2015**.
85. VanderMolen, K. M., McCulloch, W., Pearce, C. J., Oberlies, N. H., *J. Antibiot.*, **2011**, *64*, 525.
86. Stresemann, C., Bokelmann, I., Mahlknecht, U., Lyko, F., *Mol. Cancer Ther.*, **2008**, *7*, 2998.
87. Stresemann, C., Lyko, F., *Int. J. Cancer*, **2008**, *123*, 8.
88. Arrowsmith, C. H., Bountra, C., Fish, P. V., Lee, K., Schapira, M., *Nat. Rev. Drug Discovery*, **2012**, *11*, 384.
89. Altschul, S. F., Madden, T. L., Schäffer, A. A., Zhang, J., Zhang, Z., Miller, W., Lipman, D. J., *Nucleic Acids Res.*, **1997**, *25*, 3389.
90. Altschul, S. F., Wootton, J. C., Gertz, E. M., Agarwala, R., Morgulis, A., Schäffer, A. A., Yu, Y.-K., *FEBS J.*, **2005**, *272*, 5101.
91. Thinnes, C. C., England, K. S., Kawamura, A., Chowdhury, R., Schofield, C. J., Hopkinson, R. J., *Biochim. Biophys. Acta, Gene Regul. Mech.*, **2014**, *1839*, 1416.
92. Lu, T., Jackson, M. W., Wang, B., Yang, M., Chance, M. R., Miyagi, M., Gudkov, A. V., Stark, G. R., *Proc. Natl. Acad. Sci. U.S.A.*, **2010**, *107*, 46.
93. He, J., Kallin, E. M., Tsukada, Y.-I., Zhang, Y., *Nat. Struct. Mol. Biol.*, **2008**, *15*, 1169.
94. Janzer, A., Stamm, K., Becker, A., Zimmer, A., Buettner, R., Kirfel, J., *J. Biol. Chem.*, **2012**, *287*, 30984.
95. Huang, C., Xiang, Y., Wang, Y., Li, X., Xu, L., Zhu, Z., Zhang, T., Zhu, Q., Zhang, K., Jing, N., Chen, C. D., *Cell Res.*, **2010**, *20*, 154.
96. Liu, W., Tanasa, B., Tyurina, O. V., Zhou, T. Y., Gassmann, R., Liu, W. T., Ohgi, K. A., Benner, C., Garcia-Bassets, I., Aggarwal, A. K., Desai, A., Dorrestein, P. C., Glass, C. K., Rosenfeld, M. G., *Nature*, **2010**, *466*, 508.
97. Wen, H., Li, J., Song, T., Lu, M., Kan, P.-Y., Lee, M. G., Sha, B., Shi, X., *J. Biol. Chem.*, **2010**, *285*, 9322.
98. Yamane, K., Toumazou, C., Tsukada, Y.-I., Erdjument-Bromage, H., Tempst, P., Wong, J., Zhang, Y., *Cell*, **2006**, *125*, 483.
99. Shin, S., Janknecht, R., *Biochem. Biophys. Res. Commun.*, **2007**, *353*, 973.
100. Yang, L., Lin, C., Liu, W., Zhang, J., Ohgi, Kenneth A., Grinstein, Jonathan D., Dorrestein, Pieter C., Rosenfeld, Michael G., *Cell*, **2011**, *147*, 773.
101. Whetstine, J. R., Nottke, A., Lan, F., Huarte, M., Smolikov, S., Chen, Z., Spooner, E., Li, E., Zhang, G., Colaiacovo, M., Shi, Y., *Cell*, **2006**, *125*, 467.
102. Sánchez Fernández, E. M., Tarhonskaya, H., Al Qahtani, K., Hopkinson, R. J., McCullagh, J. S. O., Schofield, C. J., Flashman, E., *Biochem. J.*, **2013**, *449*, 491.
103. Iwase, S., Lan, F., Bayliss, P., de la Torre-Ubieta, L., Huarte, M., Qi, H. H., Whetstine, J. R., Bonni, A., Roberts, T. M., Shi, Y., *Cell*, **2007**, *128*, 1077.
104. Hong, S., Cho, Y.-W., Yu, L.-R., Yu, H., Veenstra, T. D., Ge, K., *Proc. Natl. Acad. Sci. U.S.A.*, **2007**, *104*, 18439.
105. Walport, L. J., Hopkinson, R. J., Vollmar, M., Madden, S. K., Gileadi, C., Oppermann, U., Schofield, C. J., Johansson, C., *J. Biol. Chem.*, **2014**, *289*, 18302.

106. Couture, J.-F., Collazo, E., Ortiz-Tello, P. A., Brunzelle, J. S., Trievel, R. C., *Nat. Struct. Mol. Biol.*, **2007**, *14*, 689.
107. Schofield, C. J., Ratcliffe, P. J., *Nat. Rev. Mol. Cell Biol.*, **2004**, *5*, 343.
108. Hopkinson, R. J., Tumber, A., Yapp, C., Chowdhury, R., Aik, W., Che, K. H., Li, X. S., Kristensen, J. B. L., King, O. N. F., Chan, M. C., Yeoh, K. K., Choi, H., Walport, L. J., Thinnes, C. C., Bush, J. T., Lejeune, C., Rydzik, A. M., Rose, N. R., Bagg, E. A., McDonough, M. A., Krojer, T. J., Yue, W. W., Ng, S. S., Olsen, L., Brennan, P. E., Oppermann, U., Muller, S., Klose, R. J., Ratcliffe, P. J., Schofield, C. J., Kawamura, A., *Chem. Sci.*, **2013**, *4*, 3110.
109. Hamada, S., Kim, T.-D., Suzuki, T., Itoh, Y., Tsumoto, H., Nakagawa, H., Janknecht, R., Miyata, N., *Bioorg. Med. Chem. Lett.*, **2009**, *19*, 2852.
110. Rose, N. R., Ng, S. S., Mecinovic, J., Lienard, B. M. R., Bello, S. H., Sun, Z., McDonough, M. A., Oppermann, U., Schofield, C. J., *J. Med. Chem.*, **2008**, *51*, 7053.
111. Rose, N. R., Woon, E. C. Y., Kingham, G. L., King, O. N. F., Mecinović, J., Clifton, I. J., Ng, S. S., Talib-Hardy, J., Oppermann, U., McDonough, M. A., Schofield, C. J., *J. Med. Chem.*, **2010**, *53*, 1810.
112. Hamada, S., Suzuki, T., Mino, K., Koseki, K., Oehme, F., Flamme, I., Ozasa, H., Itoh, Y., Ogasawara, D., Komaarashi, H., Kato, A., Tsumoto, H., Nakagawa, H., Hasegawa, M., Sasaki, R., Mizukami, T., Miyata, N., *J. Med. Chem.*, **2010**, *53*, 5629.
113. Luo, X., Liu, Y., Kubicek, S., Myllyharju, J., Tumber, A., Ng, S., Che, K. H., Podoll, J., Heightman, T. D., Oppermann, U., Schreiber, S. L., Wang, X., *J. Am. Chem. Soc.*, **2011**, *133*, 9451.
114. Rose, N. R., Woon, E. C. Y., Tumber, A., Walport, L. J., Chowdhury, R., Li, X. S., King, O. N. F., Lejeune, C., Ng, S. S., Krojer, T., Chan, M. C., Rydzik, A. M., Hopkinson, R. J., Che, K. H., Daniel, M., Strain-Damerell, C., Gileadi, C., Kochan, G., Leung, I. K. H., Dunford, J., Yeoh, K. K., Ratcliffe, P. J., Burgess-Brown, N., Von Delft, F., Muller, S., Marsden, B., Brennan, P. E., McDonough, M. A., Oppermann, U., Klose, R. J., Schofield, C. J., Kawamura, A., *J. Med. Chem.*, **2012**, *55*, 6639.
115. King, O. N. F., Li, X. S., Sakurai, M., Kawamura, A., Rose, N. R., Ng, S. S., Quinn, A. M., Rai, G., Mott, B. T., Beswick, P., Klose, R. J., Oppermann, U., Jadhav, A., Heightman, T. D., Maloney, D. J., Schofield, C. J., Simeonov, A., *PLoS One*, **2010**, *5*, e15535.
116. Schiller, R., Scozzafava, G., Tumber, A., Wickens, J. R., Bush, J. T., Rai, G., Lejeune, C., Choi, H., Yeh, T.-L., Chan, M. C., Mott, B. T., McCullagh, J. S. O., Maloney, D. J., Schofield, C. J., Kawamura, A., *ChemMedChem*, **2014**, *9*, 566.
117. Chang, K.-H., King, O. N. F., Tumber, A., Woon, E. C. Y., Heightman, T. D., McDonough, M. A., Schofield, C. J., Rose, N. R., *ChemMedChem*, **2011**, *6*, 759.
118. Suzuki, T., Ozasa, H., Itoh, Y., Zhan, P., Sawada, H., Mino, K., Walport, L., Ohkubo, R., Kawamura, A., Yonezawa, M., Tsukada, Y., Tumber, A., Nakagawa, H., Hasegawa, M., Sasaki, R., Mizukami, T., Schofield, C. J., Miyata, N., *J. Med. Chem.*, **2013**, *56*, 7222.
119. Kruidenier, L., Chung, C.-W., Cheng, Z., Liddle, J., Che, K., Joberty, G., Bantscheff, M., Bountra, C., Bridges, A., Diallo, H., Eberhard, D., Hutchinson, S., Jones, E., Katso, R., Leveridge, M., Mander, P. K., Mosley, J., Ramirez-Molina, C., Rowland, P., Schofield, C. J., Sheppard, R. J., Smith, J. E., Swales, C., Tanner, R., Thomas, P., Tumber, A., Drewes, G., Oppermann, U., Patel, D. J., Lee, K., Wilson, D. M., *Nature*, **2012**, *488*, 404.
120. Kruidenier, L., Chung, C.-W., Cheng, Z., Liddle, J., Che, K., Joberty, G., Bantscheff, M., Bountra, C., Bridges, A., Diallo, H., Eberhard, D., Hutchinson, S.,

Jones, E., Katso, R., Leveridge, M., Mander, P. K., Mosley, J., Ramirez-Molina, C., Rowland, P., Schofield, C. J., Sheppard, R. J., Smith, J. E., Swales, C., Tanner, R., Thomas, P., Tumber, A., Drewes, G., Oppermann, U., Patel, D. J., Lee, K., Wilson, D. M., *Nature*, **2014**, *514*, E2.

121. Wang, L., Chang, J., Varghese, D., Dellinger, M., Kumar, S., Best, A. M., Ruiz, J., Bruick, R., Peña-Llopis, S., Xu, J., Babinski, D. J., Frantz, D. E., Brekken, R. A., Quinn, A. M., Simeonov, A., Easmon, J., Martinez, E. D., *Nat. Commun.*, **2013**, *4*, 2035.
122. WO2014139326 A1, **2014**.
123. WO2012007007 A1, **2012**.
124. WO2014164708 A1, **2014**.
125. US20140275084 A1, **2014**.
126. WO2014151106 A1, **2014**.
127. WO2014089364 A1, **2014**.
128. US20140171432 A1, **2014**.
129. Tachibana, M., Sugimoto, K., Fukushima, T., Shinkai, Y., *J. Biol. Chem.*, **2001**, *276*, 25309.
130. Tachibana, M., Ueda, J., Fukuda, M., Takeda, N., Ohta, T., Iwanari, H., Sakihama, T., Kodama, T., Hamakubo, T., Shinkai, Y., *Genes Dev.*, **2005**, *19*, 815.
131. Upadhyay, A. K., Rotili, D., Han, J. W., Hu, R., Chang, Y., Labella, D., Zhang, X., Yoon, Y.-S., Mai, A., Cheng, X., *J. Mol. Biol.*, **2012**, *416*, 319.
132. Rautio, J., Kumpulainen, H., Heimbach, T., Oliyai, R., Oh, D., Jarvinen, T., Savolainen, J., *Nat. Rev. Drug Discovery*, **2008**, *7*, 255.
133. Huttunen, K. M., Raunio, H., Rautio, J., *Pharmacol. Rev.*, **2011**, *63*, 750.
134. Macarron, R., Banks, M. N., Bojanic, D., Burns, D. J., Cirovic, D. A., Garyantes, T., Green, D. V. S., Hertzberg, R. P., Janzen, W. P., Paslay, J. W., Schopfer, U., Sittampalam, G. S., *Nat. Rev. Drug Discovery*, **2011**, *10*, 188.
135. Hopkins, A. L., Keseru, G. M., Leeson, P. D., Rees, D. C., Reynolds, C. H., *Nat. Rev. Drug Discovery*, **2014**, *13*, 105.
136. Hann, M. M., Oprea, T. I., *Curr. Opin. Chem. Biol.*, **2004**, *8*, 255.
137. Leeson, P. D., Springthorpe, B., *Nat. Rev. Drug Discovery*, **2007**, *6*, 881.
138. Calculated using ACD labs prediction model.
139. Petrauskas, A., Kolovanov, E., *Perspect. Drug Discovery Des.*, **2000**, *19*, 99.
140. Queguiner, G., Pastour, P., *Bull. Soc. Chim. Fr.*, **1969**, *10*, 3678.
141. Kawamura, A., Tumber, A., Rose, N. R., King, O. N. F., Daniel, M., Oppermann, U., Heightman, T. D., Schofield, C., *Anal. Biochem.*, **2010**, *404*, 86.
142. Plant, M., Dineen, T., Cheng, A., Long, A. M., Chen, H., Morgenstern, K. A., *Anal. Biochem.*, **2011**, *419*, 217.
143. Ullman, E. F., Kirakossian, H., Switchenko, A. C., Ishkanian, J., Ericson, M., Wartchow, C. A., Pirio, M., Pease, J., Irvin, B. R., Singh, S., Singh, R., Patel, R., Dafforn, A., Davalian, D., Skold, C., Kurn, N., Wagner, D. B., *Clin. Chem.*, **1996**, *42*, 1518.
144. Ullman, E. F., Kirakossian, H., Singh, S., Wu, Z. P., Irvin, B. R., Pease, J. S., Switchenko, A. C., Irvine, J. D., Dafforn, A., Skold, C. N., *Proc. Natl. Acad. Sci. U.S.A.*, **1994**, *91*, 5426.
145. Peppard, J., Glickman, F., He, Y., Hu, S.-I., Doughty, J., Goldberg, R., *J. Biomol. Screening*, **2003**, *8*, 149.
146. Hutchinson, S. E., Leveridge, M. V., Heathcote, M. L., Francis, P., Williams, L., Gee, M., Munoz-Muriedas, J., Leavens, B., Shillings, A., Jones, E., Homes, P., Baddeley, S., Chung, C.-W., Bridges, A., Argyrou, A., *J. Biomol. Screening*, **2012**, *17*, 39.
147. Milne, H. B., Peng, C.-H., *J. Am. Chem. Soc.*, **1957**, *79*, 639.

148. Krishnan, S., Trievel, R. C., *Structure*, **2013**, *21*, 98.
149. Totrov, M., Abagyan, R., *Proteins: Struct., Funct., Bioinf.*, **1997**, *29*, 215.
150. Hu, X., Manetsch, R., *Chem. Soc. Rev.*, **2010**, *39*, 1316.
151. Lewis, W. G., Green, L. G., Grynszpan, F., Radić, Z., Carlier, P. R., Taylor, P., Finn, M. G., Sharpless, K. B., *Angew. Chem. Int. Ed.*, **2002**, *41*, 1053.
152. Krasiński, A., Radić, Z., Manetsch, R., Raushel, J., Taylor, P., Sharpless, K. B., Kolb, H. C., *J. Am. Chem. Soc.*, **2005**, *127*, 6686.
153. WO2014053491 A1, **2014**.
154. Newkome, G. R., Patri, A. K., Holder, E., Schubert, U. S., *Eur. J. Org. Chem.*, **2004**, *2004*, 235.
155. Fuller, A. A., Hester, H. R., Salo, E. V., Stevens, E. P., *Tetrahedron Lett.*, **2003**, *44*, 2935.
156. Hapke, M., Brandt, L., Lutzen, A., *Chem. Soc. Rev.*, **2008**, *37*, 2782.
157. J. S. Field, J.-A. G., D. Jaganyi, D. R. McMillin, A. Shaira, and D. J. Stewart, *Z. Naturforsch.*, **2010**, *65b*, 1318.
158. Cravotto, G., Beggiato, M., Penoni, A., Palmisano, G., Tollari, S., Lévêque, J.-M., Bonrath, W., *Tetrahedron Lett.*, **2005**, *46*, 2267.
159. Case, F. H., *J. Am. Chem. Soc.*, **1946**, *68*, 2574.
160. Sasse, W. H. F., Whittle, C. P., *J. Chem. Soc.*, **1961**, 1347.
161. Rostovtsev, V. V., Green, L. G., Fokin, V. V., Sharpless, K. B., *Angew. Chem., Int. Ed.*, **2002**, *41*, 2596.
162. Tornøe, C. W., Christensen, C., Meldal, M., *J. Org. Chem.*, **2002**, *67*, 3057.
163. Kolb, H. C., Finn, M. G., Sharpless, K. B., *Angew. Chem. Int. Ed.*, **2001**, *40*, 2004.
164. Hou, J., Liu, X., Shen, J., Zhao, G., Wang, P. G., *Expert Opin. Drug Discovery*, **2012**, *7*, 489.
165. Agalave, S. G., Maujan, S. R., Pore, V. S., *Chem. – Asian J.*, **2011**, *6*, 2696.
166. WO2011058473 A1, **2011**.
167. Nadin, A., Hattotuwagama, C., Churcher, I., *Angew. Chem. Int. Ed.*, **2012**, *51*, 1114.
168. Lipinski, C. A., *Drug Discovery Today: Technol.*, **2004**, *1*, 337.
169. Cooper, T. W. J., Campbell, I. B., Macdonald, S. J. F., *Angew. Chem. Int. Ed.*, **2010**, *49*, 8082.
170. Friscourt, F., Boons, G.-J., *Org. Lett.*, **2010**, *12*, 4936.
171. Loren, J. C., Krasiński, A., Fokin, V. V., Sharpless, K. B., *Synlett*, **2005**, *18*, 2847.
172. Suijkerbuijk, B. M. J. M., Aerts, B. N. H., Dijkstra, H. P., Lutz, M., Spek, A. L., van Koten, G., Klein Gebbink, R. J. M., *Dalton Trans.*, **2007**, *13*, 1273.
173. England, K. S., Tumber, A., Krojer, T., Scozzafava, G., Ng, S. S., Daniel, M., Szykowska, A., Che, K.-H., Von Delft, F., Burgess-Brown, N. A., Kawamura, A., Schofield, C. J., Brennan, P. E., *MedChemComm*, **2014**, *5*, 1879.
174. Chinchilla, R., Nájera, C., *Chem. Rev.*, **2007**, *107*, 874.
175. Dishington, A., Fillery, S., Finlay, M. R. V., *Tetrahedron Lett.*, **2010**, *51*, 4211.
176. Foote, K. M., Blades, K., Cronin, A., Fillery, S., Guichard, S. S., Hassall, L., Hickson, I., Jacq, X., Jewsbury, P. J., McGuire, T. M., Nissink, J. W. M., Odedra, R., Page, K., Perkins, P., Suleman, A., Tam, K., Thommes, P., Broadhurst, R., Wood, C., *J. Med. Chem.*, **2013**, *56*, 2125.
177. Shen, J., Woodward, R., Kedenburg, J. P., Liu, X., Chen, M., Fang, L., Sun, D., Wang, P. G., *J. Med. Chem.*, **2008**, *51*, 7417.
178. Boren, B. C., Narayan, S., Rasmussen, L. K., Zhang, L., Zhao, H., Lin, Z., Jia, G., Fokin, V. V., *J. Am. Chem. Soc.*, **2008**, *130*, 8923.
179. Grundmann, C., Haldenwanger, H., *Angew. Chem.*, **1950**, *62*, 410.
180. Lindsay, R. O., Allen, C. F. H., *Org. Synth.*, **1942**, *22*, 96.

181. Thibault, R. J., Takizawa, K., Lowenheilm, P., Helms, B., Mynar, J. L., Fréchet, J. M. J., Hawker, C. J., *J. Am. Chem. Soc.*, **2006**, *128*, 12084.
182. Meloun, M., Bordovská, S., *Anal. Bioanal. Chem.*, **2007**, *389*, 1267.
183. Juillard, J., *Pure Appl. Chem.*, **1977**, *49*, 885.
184. Grosjean, N., Descorme, C., Besson, M., *Appl. Catal., B*, **2010**, *97*, 276.
185. Kankaanpera, A., Scharlin, P., Kuusisto, I., Kallio, R., Bernoulli, E., *J. Chem. Soc., Perkin Trans. 2*, **1999**, 169.
186. Davis, A. M., Teague, S. J., *Angew. Chem. Int. Ed.*, **1999**, *38*, 736.
187. Kummerow, F. A., *Ann. N.Y. Acad. Sci.*, **1983**, *414*, 29.
188. Kell, D. B., Dobson, P. D., Oliver, S. G., *Drug Discovery Today*, **2011**, *16*, 704.
189. Sugano, K., Kansy, M., Artursson, P., Avdeef, A., Bendels, S., Di, L., Ecker, G. F., Faller, B., Fischer, H., Gerebtzoff, G., Lennernaes, H., Senner, F., *Nat. Rev. Drug Discovery*, **2010**, *9*, 597.
190. Hou, T. J., Zhang, W., Xia, K., Qiao, X. B., Xu, X. J., *J. Chem. Inf. Comput. Sci.*, **2004**, *44*, 1585.
191. Avdeef, A., Tsinman, O., *Eur. J. Pharm. Sci.*, **2006**, *28*, 43.
192. Bundgaard, H., *Adv. Drug Delivery Rev.*, **1989**, *3*, 39.
193. Bundgaard, H., Mørk, N., Hoelgaard, A., *Int. J. Pharm.*, **1989**, *55*, 91.
194. Waranis, R. P., Sloan, K. B., *J. Pharm. Sci.*, **1987**, *76*, 587.
195. Palm, K., Luthman, K., Ungell, A.-L., Strandlund, G., Beigi, F., Lundahl, P., Artursson, P., *J. Med. Chem.*, **1998**, *41*, 5382.
196. Kelder, J., Grootenhuis, P. J., Bayada, D., Delbressine, L. C., Ploemen, J.-P., *Pharm. Res.*, **1999**, *16*, 1514.
197. Ballatore, C., Huryn, D. M., Smith, A. B., *ChemMedChem*, **2013**, *8*, 385.
198. Ertl, P., Rohde, B., Selzer, P., *J. Med. Chem.*, **2000**, *43*, 3714.
199. Alex, A., Millan, D. S., Perez, M., Wakenhut, F., Whitlock, G. A., *MedChemComm*, **2011**, *2*, 669.
200. Girijavallabhan, V., Arasappan, A., Bennett, F., Huang, Y., George Njoroge, F., MacCoss, M., *Tetrahedron Lett.*, **2010**, *51*, 2797.
201. Hansen, P. E., Kamounah, F. S., Ullah, S., *J. Mol. Struct.*, **2007**, *844–845*, 300.
202. Slocum, D. W., Jennings, C. A., *J. Org. Chem.*, **1976**, *41*, 3653.
203. Manteau, B., Genix, P., Brelot, L., Vors, J.-P., Pazenok, S., Giornal, F., Leuenberger, C., Leroux, F. R., *Eur. J. Org. Chem.*, **2010**, *2010*, 6043.
204. Cheng, Z., Cheung, P., Kuo, A. J., Yukl, E. T., Wilmot, C. M., Gozani, O., Patel, D. J., *Genes Dev.*, **2014**, *28*, 1758.
205. Moellering, R. E., Cravatt, B. F., *Chem. Biol.*, **2012**, *19*, 11.
206. Bantscheff, M., Drewes, G., *Biorg. Med. Chem.*, **2012**, *20*, 1973.
207. Sutton, C. W., *Br. J. Pharmacol.*, **2012**, *166*, 457.
208. Green, N. M., *Methods Enzymol.*, **1990**, *184*, 51.
209. Rix, U., Superti-Furga, G., *Nat. Chem. Biol.*, **2009**, *5*, 616.
210. WO200793594 A1, **2007**.
211. Chaudhuri, G., Kundu, N. G., *J. Chem. Soc., Perkin Trans. 1*, **2000**, 775.
212. Mahmood, T., Yang, P.-C., *North Am J Med Sci*, **2012**, *4*, 429.
213. Le Trong, I., Wang, Z., Hyre, D. E., Lybrand, T. P., Stayton, P. S., Stenkamp, R. E., *Acta Crystallogr. Sect. D. Biol. Crystallogr.*, **2011**, *67*, 813.
214. Barsyte-Lovejoy, D., Li, F., Oudhoff, M. J., Tatlock, J. H., Dong, A., Zeng, H., Wu, H., Freeman, S. A., Schapira, M., Senisterra, G. A., Kuznetsova, E., Marcellus, R., Allali-Hassani, A., Kennedy, S., Lambert, J.-P., Couzens, A. L., Aman, A., Gingras, A.-C., Al-Awar, R., Fish, P. V., Gerstenberger, B. S., Roberts, L., Benn, C. L., Grimley, R. L., Braam, M. J. S., Rossi, F. M. V., Sudol, M., Brown, P. J., Bunnage, M. E., Owen, D. R., Zaph, C., Vedadi, M., Arrowsmith, C. H., *Proc. Natl. Acad. Sci. U.S.A.*, **2014**, *111*, 12853.

215. Gassmann, M., Grenacher, B., Rohde, B., Vogel, J., *Electrophoresis*, **2009**, *30*, 1845.
216. Taylor, S. C., Berkelman, T., Yadav, G., Hammond, M., *Mol. Biotechnol.*, **2013**, *55*, 217.
217. Kojima, T., Hayashi, K.-I., Iizuka, S.-Y., Tani, F., Naruta, Y., Kawano, M., Ohashi, Y., Hirai, Y., Ohkubo, K., Matsuda, Y., Fukuzumi, S., *Chem. Eur. J.*, **2007**, *13*, 8212.
218. US20130017194 A1, **2013**.
219. Northrup, A. B., Katcher, M. H., Altman, M. D., Chenard, M., Daniels, M. H., Deshmukh, S. V., Falcone, D., Guerin, D. J., Hatch, H., Li, C., Lu, W., Lutterbach, B., Allison, T. J., Patel, S. B., Reilly, J. F., Reutershan, M., Rickert, K. W., Rosenstein, C., Soisson, S. M., Szewczak, A. A., Walker, D., Wilson, K., Young, J. R., Pan, B.-S., Dinsmore, C. J., *J. Med. Chem.*, **2013**, *56*, 2294.
220. Bénard, C., Mohammad, R., Saraswat, N., Shan, R., Maiti, S. N., Wuts, P. G. M., Stier, M., Lints, T., Bradow, J., Schwarz, J. B., *Synth. Commun.*, **2008**, *38*, 517.
221. US20140056849 A1, **2014**.
222. Peltier, H. M., McMahon, J. P., Patterson, A. W., Ellman, J. A., *J. Am. Chem. Soc.*, **2006**, *128*, 16018.
223. Ellis, E. E., Adkins, C. T., Galovska, N. M., Lavis, L. D., Johnson, R. J., *ChemBioChem*, **2013**, *14*, 1134.
224. Bigler, P., Schönholzer, S., Neuenschwander, M., *Helv. Chim. Acta*, **1978**, *61*, 2059.
225. WO2012058127 A2, **2012**.
226. Ng, S. S., Kavanagh, K. L., McDonough, M. A., Butler, D., Pilka, E. S., Lienard, B. M. R., Bray, J. E., Savitsky, P., Gileadi, O., Von Delft, F., Rose, N. R., Offer, J., Scheinost, J. C., Borowski, T., Sundstrom, M., Schofield, C. J., Oppermann, U., *Nature*, **2007**, *448*, 87.